Design, Synthesis and Application of Small Molecule Acyl Protein Thioesterase Inhibitors

Zur Erlangung des akademischen Grades
eines Doktors des Naturwissenschaften
vom Fachbereich Chemie der
Universität Dortmund angenommen

Dissertation

Von

M.Sc. / Ingénieur

MARION RUSCH

aus Lyon (Frankreich)

1. Gutachter: Prof. Herbert Waldmann
2. Gutachter: Prof. Roger S. Goody
3. Wissenschaftliche Mitarbeiter: Dr. Leif Dehmelt

Tag der mündlichen Prüfung: September 30th 2011

This work was carried out under the supervision of Prof. Dr. Herbert Waldmann at the Faculty of Chemistry of the Technical University of Dortmund and at the Max Planck Institute of Molecular Physiology in Dortmund from September 2007 to September 2011.

Dedicated to my family

and friends for their support.

Acknowledgement

First of all, I would like to thank my Ph.D. supervisor Prof. Dr. Herbert Waldmann for giving me the opportunity to join his research group. I am grateful for the great facilities and nice working environment provided, which allow me to work at the interface between chemistry and biochemistry. This very international group was also a very enriching experience on itself.

I also wish to express my gratitude to Dr. Christian Hedberg for his useful advice and interest in the project, as well as for his motivation to establish numerous collaborations, which have led to real advancements on the project. I would give as an example the collaboration with the Wendtner group, working at the Academic Hospital in Cologne, which allows me to work with relevant patient isolates (CLL).

I would also like to acknowledge the people who have contributed to the Ras/APT1 project, especially Tobias Zimmermann, Dr. Frank Dekker, Dr. Stefan Renner, Dr. Nachiket Vartak, Marco Bürger and Kristina Görmer. I am also grateful to Dr. Ingrid Vetter for sharing her experience in protein structures as well as on docking studies and to the analytical team (Dr. Petra Janning, Andreas Brockmeyer and Chantale Sevenich) for their support regarding proteomic analysis. Many thanks to Dr. Heino Prinz for the very interesting discussion around his recently published book called Numerical Methods for the Life Scientist (Springer edition).

I also would like to thank my "bio-lab" friends and colleagues, not only for introducing me to biochemistry techniques, but also for contributing very largely to a nice and friendly working atmosphere, especially Tuyen Tran, Dr. Verena Pries and Christine Nowak. I would like also to thank the French team of the department (Evelyne Merten, Claude Ostermann and Vincent Eschenbrenner) for the nice time spend together. Additionally, Vincent Eschenbrenner is acknowledged for his helpful comments regarding the construction of this dissertation, as well as Tobias Zimmermann and Marco Bürger for their linguistic support.

I would like to thank all my colleagues at the Department IV who have contributed for a cooperative working environment during the last four years, and in particular people working at the university including Kirtikumar Jadhav, Dr. Hugo Lachance, Hao Tan, Dr. Hongyan Sun, Dr. Debapratim Das, Dr. Remi Martinez, Dr. Victor Vintonyak and Jakub Svenda.

Finally, I would like to express my gratitude to my family for the constant support provided during these four years in Germany.

General introduction

Palmitoylated proteins constitute an important class of signaling components controlling various cellular processes, such as cell proliferation and apoptosis, both frequently deregulated in carcinogenesis. The reversible character of the palmitate lipid anchoring is of utmost importance for maintaining steady-state protein localization and subsequent signaling. Therefore, targeting protein depalmitoylation by inhibiting the depalmitoylating enzymes might be a valid therapeutic strategy for modulating aberrant cell signaling.

Given the importance of Ras mutations in carcinogenesis (33% of all cancers), Ras has been considered as an attractive anti-cancer target. In particular, one strategy developed to affect aberrant Ras signaling, consists in targeting the Ras depalmitoylating enzyme acyl protein thioesterase 1 (APT1). Such APT1 inhibitors could provide a useful tool for studying the biological role of APT1 in vivo. Moreover, employed in activity-based proteome profiling experiments such inhibitors may allow the identification of their cellular target(s), and possibly of additional proteins relevant to the Ras depalmitoylation process. In this context, the first chapter presents the development of potent and selective β-lactone APT1 inhibitors termed palmostatin B and palmostatin M and their use in a chemical proteomic approach.

The second chapter consists in getting a better understanding of the apoptosis resistance characteristic of Chronic Lymphocytic Leukaemia (CLL). Recently, the lipase inhibitor orlistat and later the APT1 inhibitor palmostatin B were shown to restore Fas-mediated apoptotic signaling selectively in CLL cells. With the reported importance of Fas palmitoylation for Fas–mediated death signaling, absence or dysfunction of Fas palmitoylation may account for the accumulation of malignant B-cells characteristic of this disease. To rationalize the observed apoptotic effect, a chemical proteomic approach was developed with human cells from leukaemia and healthy patients in collaboration with Prof. Wendtner's group at the academic hospital in Cologne to address the cellular target(s) of palmostatin B and in particular to identity target protein(s) relevant to Fas depalmitoylation, and therefore possibly involved in CLL pathogenesis.

In order to evaluate the effect of palmostatin B on palmitoylation levels of proteins at global cellular scale, SILAC experiments were subsequently performed in connection to a inert alkynylated palmitate analogue (alkyne-16-C carboxylic acid) in double metabolic labelling experiments. In this context, chapter 3 covers preliminary experiments performed to this goal.

Following the identification of the enzymes catalyzing Ras depalmitoylation, several new Ras depalmitoylation inhibitor candidates were developed, which in contrast to the previous β-lactone inhibitors palmostatin B and M, would be regarded as stable transition state mimics of the deacylation process. In this context, chapter 4 covers the design, synthesis and *in vitro* evaluation of these new inhibitor candidates (α-keto oxazoles, α-keto amides, trifluoromethyl ketones and pentafluoroethyl ketones).

Given that most of the compound class investigated for APT1 inhibition were already reported as Fatty Acid Amide Hydrolase (FAAH) inhibitors, and given the numerous therapeutic applications associated to FAAH inhibition, a global investigation for FAAH inhibition was performed in collaboration with Matthias Lehr from the University of Münster. Chapter 5 is about the discovery of potent sub-micromolar FAAH inhibitors.

Table of contents

Chapter 3: Systematic evaluation of palmostatin B's effect on the human palmitome

Chapter 4: APT1 and APT2 inhibitor candidates as depalmitoylation transition state mimics

Chapter 5: Discovery of potent Fatty Acid Amide Hydrolase (FAAH) inhibitors

CHAPTER 1

TARGETING RAS DEPALMITOYLATION

1 Introduction

1.1 Background cancer

Cancer is a group of over 100 diseases affecting various tissues, characterized by an uncontrolled cell proliferation, generating cell aggregates called tumors. Cancer-related deaths are largely due to the ability of cancer cells to spread, either by invasion to adjacent tissues, or by implantation into distant sites by metastasis. Metastatic tumours trafficking through the bloodstream or lymphatic circulation systems are frequently encountered in the late stages of cancers referred to as generalized cancers therefore associated with significantly reduced prognosis for survival. Today, cancer is an enormous global health problem accounting for one in every eight deaths worldwide - more than HIV/AIDS, tuberculosis and malaria combined. In 2008, the American Cancer Society estimated to 12.4 million the number of diagnosed cancers and to 7.6 million the number of deaths from cancer around the world. This alarming increased number of diagnosed cancers and cancer-related deaths is being driven largely by the adoption of unhealthy lifestyle (ex. tobacco, physical inactivity, obesity, poor nutrition) and population aging. In this context, many efforts have been directed toward the development of more reliable cancer diagnosing and the development of alternative anti-cancer therapies with possibly reduced side effects and increased survival rate.

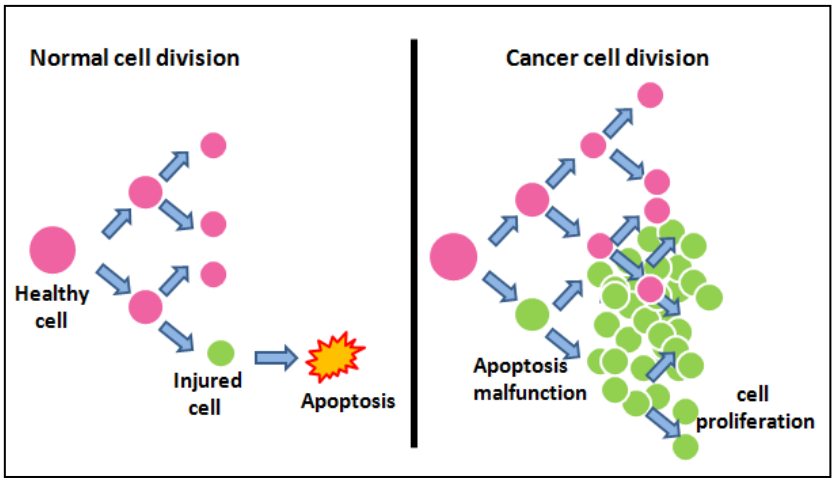

Figure 1.1 Comparison between normal and abnormal cellular behaviours. A) Normal cell division followed by apoptosis of injured cells. B) Cancer cell division leading to uncontrolled cellular growth.

Normal cellular behavior is tightly regulated by complex signaling pathways ensuring balance between cell proliferation and apoptosis (programmed cell death). Mutations of normal cellular

genes, called proto-oncogenes into oncogenes encoding for proteins involved into such signaling pathways inevitably results in altered cell growth characteristic for cancers. One key effector of the signaling pathways controling cell growth is the protein encoded by the Ras gene.

1.2 Ras proteins and cancer

In the 1980s, the Ras oncogene involved in the Harvey virus causing sarcoma tumor in rats was identified[1,2] and therefore named *H*-Ras for Harvey- rat sarcoma. Later, the two additional oncogenic Ras isoforms identified in Kirsten sarcoma viruses[1] and in human Neuroblastoma[3] were respectively named as *K*-Ras and *N*-Ras. The Ras subfamily comprising the *H*-Ras, *N*-Ras, *K*-Ras (*K*-Ras4A and *K*-Ras4B) proteins, forms a family of 21 kDa GTP-regulated molecular switches cycling between an inactive GDP-bound and an active GTP-bound state, characterized by individual conformations (Figure 1.2). Ras activation requires replacement of bound GDP by GTP, an intrinsic process accelerated by nucleotide exchange factors (GEFs), whereas Ras inactivation occurs through the hydrolysis of bound GTP to GDP (GTPase reaction), an intrinsic process accelerated by GTPase activating proteins (GAPs) (Figure 1.2).

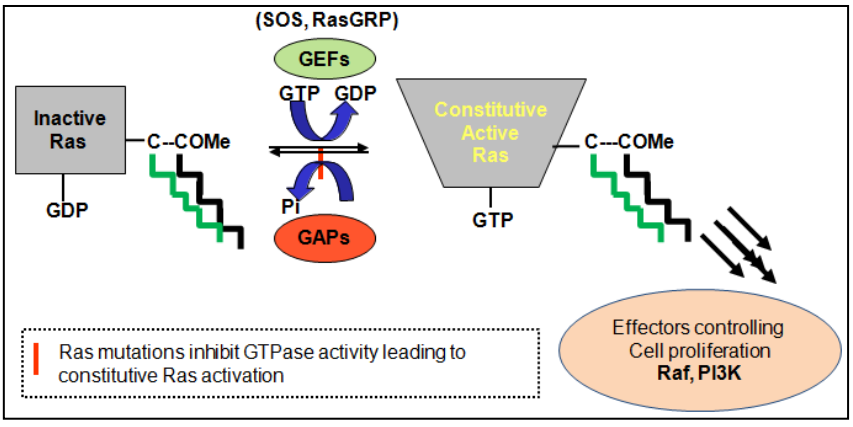

Figure 1.2 Regulation of Ras activity by the regulatory proteins GAPs and GEFs. GAPs inactivate Ras by stimulating the hydrolysis of bound GTP to GDP (GTPase reaction) and GEFs activate Ras by stimulating the replacement of bound GDP by GTP.

Once activated, Ras proteins signal through various cell-signaling pathways involved in cell proliferation (MAPK or PI3K/Akt). This aspect of Ras regulation is frequently disregulated in Ras-related cancers due to Ras mutations located at the interface of the Ras:GTP-GAP complex, typically at the residue Gly 12, Gly 13 and Gln 61. Indeed, mutations at glycine residues Gly 12 and/or Gly 13 were shown to prevent the approach of the regulatory protein GAP through its

"GAP arginine finger" (Arg789)[4](Figure 1.3, A).[4,5] In contrast, mutations on the glutamine residue Gln 61 was shown to affect the catalytic reaction by disrupting important hydrogen-stabilizing interactions (Figure 1.3B).[4,5]

A **B**

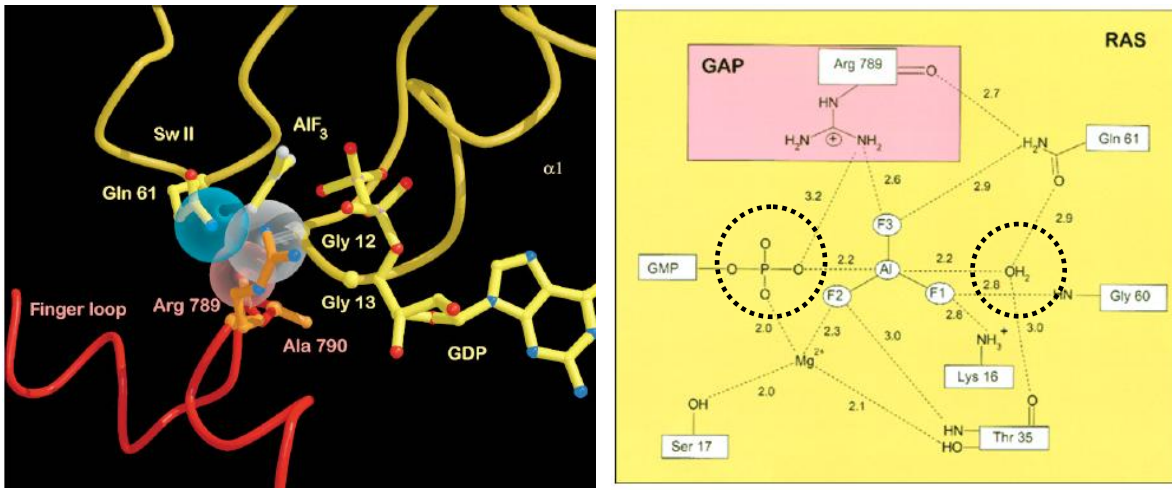

Figure 1.3 Ras mutations preventing Ras inactivation by GAPs. A) Crystal structure of the complex formed between Ras:GTP (in yellow) and GAP (in red) showing the importance of the Ras residue 12,13 and 61 to allow its interaction with the GAP arginine finger (Arg789). B) Hydrogen-stabilizing interactions involved in the GAP-mediated GTP hydrolysis. Figure reproduced from the literature.[4,5]

As a result, such mutations do result in a prolongated Ras activation, thereby leading to cancers. Indeed, Ras gene mutations occur in 30% of all cancers,[6] with *K*-Ras mutations most frequently encountered (85%), followed by *N*-Ras (15%) and *H*-Ras (<1%). Ras–mutations have a significant implication in some cancers, exemplified by *K*-Ras mutations found in 90% of all pancreatic cancers.[6]

1.3 Ras proteins

1.3.1 Ras biosynthesis based on the CAAX motif

In mammals, three Ras genes are expressed encoding for four proteins, *H*-Ras, *N*-Ras, *K*-Ras4A and *K*-Ras4B, ubiquitously expressed at the exception of *K*-Ras4A. For such a reason, *K*-Ras will in the following discussion refer exclusively to the most abundant form *K*-Ras4B. These four Ras isoforms consist in 189 amino acids with high sequence conservation over their 165 N-terminal residues (>90% identity) contrasting with significant divergences (10-15% identity) over their C-terminal 24 residues therefore referred as their C-terminal hypervariable region (HVR). The HVR can be divided into two domains: the linker domain and the membrane-targeting domain.[7] The

membrane-targeting domain was shown to contain two cooperating signal recognition sequences sufficient for Ras trafficking and anchoring to the plasma membrane (PM), a process that is necessary for its biological activity (Figure 1.4A).

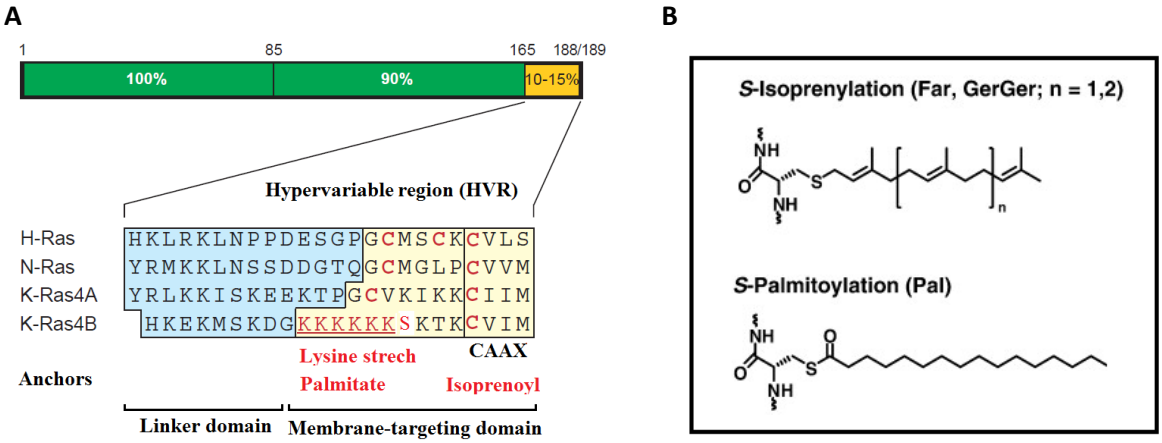

Figure 1.4 Schematic representations of *H*-Ras, *N*-Ras, *K*-Ras4A and *K*-Ras4B isoforms. A) Divergence of Ras isoforms in their HVR, containing the two signal recognition sequences necessary for their stable membrane anchoring. B) Structure of palmitoyl and isoprenyl (geranylgeranyl and farnesyl) moieties. Figure reproduced from the literature.[7]

The first signal recognition sequence is the C-terminal CAAX motif (C stand for cysteine, A for aliphatic amino acid and X for any amino acid).[8,9] Irreversible *S*-isoprenylation of the CAAX motif by attachment of a isoprenyl group (either C_{15}-farnesyl or C_{20}-geranylgeranyl) on its cysteine residue provide Ras proteins with a weak membrane affinity, with geranylgeranylated proteins generally more tightly bound to membranes than farnesylated proteins presumably due to their longer anchors. *H*-Ras was found to be exclusively farnesylated in contrast to *K*-Ras and *N*-Ras, which can be either farnesylated or geranylgeranylated. Isoprenylation[10] of cytosolic Ras precursors is the first step in a series of post-translational modifications allowing Ras anchoring in the endoplasmic reticulum (ER), where the three terminal amino-acids residues (AAX) are removed by the endoprotease RCE1 (Ras converting enzyme1).[11-13] The carboxyl group of the terminal cysteine is subsequently esterified (methyl ester) on the ER by ICMT (isoprenylcysteine carboxymethyltransferase).[14,15] Correct processing of the CAAX motif was found to be essential for the efficient transport of Ras to the PM given that mutations of the CAAX motif[9] or deletion of RCE1 or ICMT[11,12,16-18] were shown to result in Ras mislocalization in the cytosol, associated with a complete loss of biological activity. After post-translational modifications of the CAAX motif, stable membrane anchoring of Ras to the PM is ensured by a second recognition signal

sequence also located in the membrane-targeting domain consisting either in one or two *S*-palmitoylation sites, or in a polybasic domain of six consecutive lysine residues (Lys175 to Lys180). After methyl esterification, solely prenylated *H*-Ras and *N*-Ras proteins are reversibly[19] *S*-palmitoylated at the Golgi by attachment of palmitate group(s) respectively at Cys 181,184 for *H*-Ras and at Cys 181 for *N*-Ras. Although their absolute identification is still lacking, Golgi-localized palmitoyltransferase(s) (PATs) are suspected to be involved in the palmitoyl transfer from Palmitoyl-CoA (Pal-CoA). After *S*-Palmitoylation, fully processed *H*- and *N*-Ras proteins enter the secretory pathway[20] trafficking from the Golgi to the PM, resulting in stable PM anchoring ensured by their isoprenyl and palmitate moieties. In contrast, isoprenylated *K*-Ras proteins do not require palmitoylation for their stable PM anchoring given their positively charged polybasic lysine-rich sequence which allows electrostatic stabilizing interactions with negatively charged phospholipids constituting the plasma membrane. *K*-Ras directy and quickly traffic from the ER to the PM through a poorly characterized transport differing from the secretory pathway[20,21] (Figure 1.5).

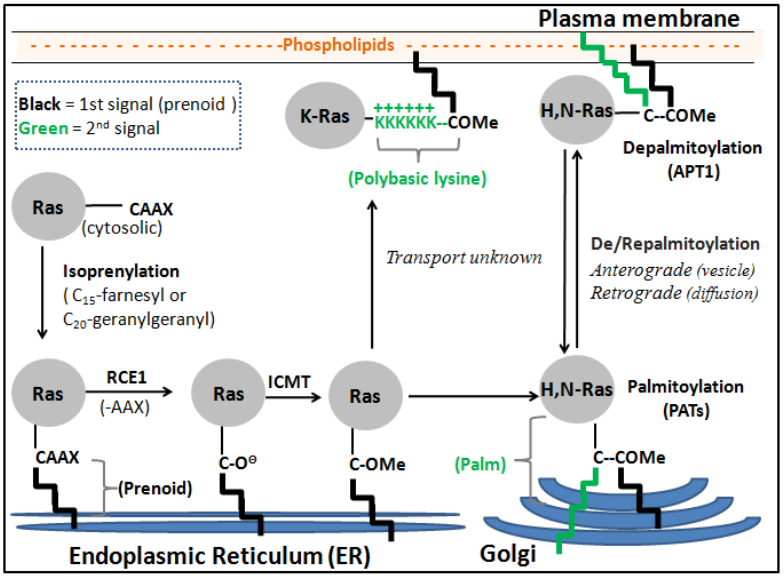

Figure 1.5 Schematic overview of Ras post-translational modifications. After biosynthesis, cytosolic Ras proteins undergo isoprenylation (prenyl group in black) followed by cleavage of AAX tripeptide by RCE1 and carboxymethylation by ICMT at the ER. Palmitoylation of *H*- and *N*-Ras at the Golgi (palmitate tail in green) allow their transport to the PM through the secretory pathway. *K*-Ras bypasses the Golgi and reaches the PM directly by a yet uncharacterized pathway. Figure adapted from the literature.[22]

1.3.2 Spatiotemporal Ras distribution

Dynamic Ras isoform localization

Once fully processed, PM-bound *H*- and *N*-Ras isoforms were shown to traffic within the cell due to the reversible nature of their palmitate moiety. Indeed, recent studies[23] on semi-synthetic Ras proteins, have pointed out a dynamic de/repalmitoylation cycle regulating *H*-Ras and *N*-Ras trafficking to ensure their correct spatiotemporal distribution between PM, endosomes, endoplasmic reticulum and Golgi. In this model, depalmitoylation detaches *H*- and *N*-Ras isoforms from the PM and rapidly repartitions solely isoprenylated proteins randomly to any cellular membrane by cytosolic diffusion until their new and reversible stable membrane trapping by repalmitoylation occurs at the Golgi (Δt = 14 sec). Only after a longer time (Δt = 173 sec), palmitoylated Ras proteins exit the Golgi and access the PM via the secretory pathway. [20] The importance of the de/repalmitoylation cycle for correct Ras localization was demonstrated either by preventing Ras palmitoylation using 2-bromopalmitate (2-BP),[24,25] or by preventing Ras depalmitoylation using Ras proteins modified by non-cleavable thioether palmitate-like groups.[26,27] Both experiments resulted in an incorrect non-specific Ras localization to all membrane compartments, when targeting Ras palmitoylation or depalmitoylation respectively (Figure 1.6).

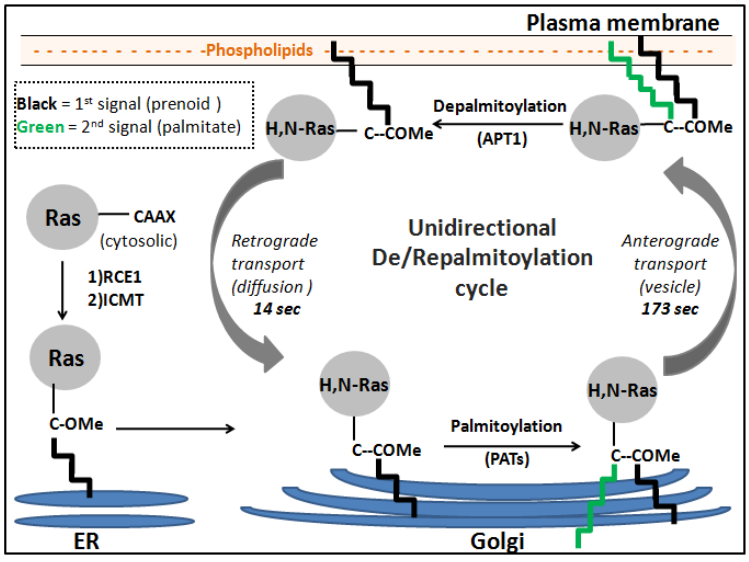

Figure 1.6 Schematic illustration of the dynamic and unidirectional de/repalmitoylation cycle. A dynamic cycle regulates *H*- and *N*-Ras isoform distribution between the Golgi and the PM through palmitoylation on the Golgi and depalmitoylated at the PM. Figure adapted from the literature.[28]

In contrast, *K*-Ras partitions rapidly and transiently to various non-specific cellular membranes (endoplasmic reticumum, Golgi, Mitochondria) by a dynamic process of PM absorption/desorption. Two different repulsion mechanisms for *K*-Ras desorption from the PM have been proposed consisting either in a Ca^{2+}/calmodulin-mediated *K*-Ras solubilisation[29,30] or in a PKC–mediated *K*-Ras phosphorylation at a serine group adjacent to its polybasic stretch.[31] Both proposed mechanisms involved the neutralisation of electrostatic stabilizing interactions between the positively charged polybasic lysine-rich sequence of *K*-Ras and the negatively charged phospholipids constituting the PM (Figure 1.7).

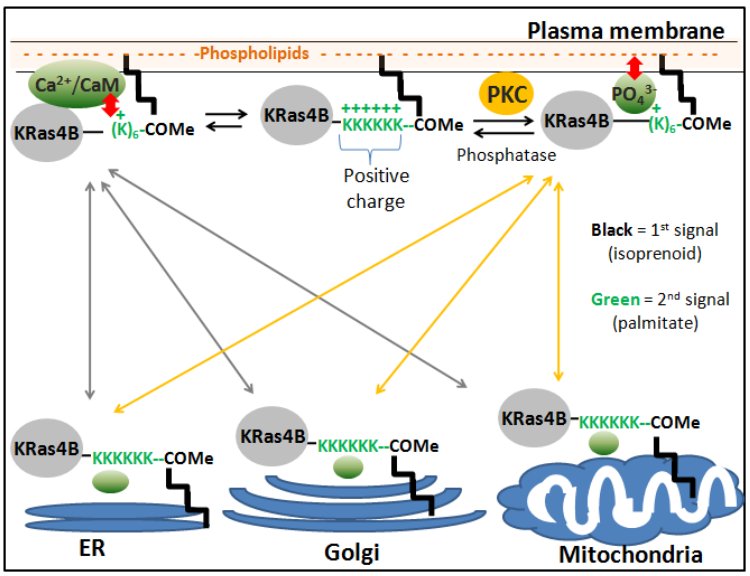

Figure 1.7 Proposed dynamic *K*-Ras absorption/desorption mechanisms. A rapid and transient *K*-Ras partitioning to different endomembranes (ER, Golgi, Mitochondria) was proposed to occur either by Ca^{2+}/calmodulin-mediated *K*-Ras solubilisation or by PKC–mediated *K*-Ras phosphorylation. Electrostatic repulsions are shown by red arrows. PKC = Protein kinase C. Figure adapted from the literature.[28]

Steady-state Ras cellular localization

As a result of the de/repalmitoylation cycle, *H*-Ras and *N*-Ras are mainly localized at the PM and at the Golgi,[28] with *H*-Ras principally localized at the PM given its dually palmitoylation pattern. In contrast, *N*-Ras is predominantly found at the Golgi. Given the predominant *K*-Ras localization at the PM visible in Figure 1.8, the dynamic absorption/desorption mechanism presented above in Figure 1.7 may only be occasional or minor. However, the absence of *K*-Ras at the Golgi is consistent with the model described previously in Figure 1.5, in which *K*-Ras bypasses the Golgi to reach directly the PM. These experiments clearly show the importance of the second membrane anchor (either palmitate moiety or polybasic stretch) for Ras isoform localization given that solely prenylated Ras isoforms (*H*-, *N*-and *H*-Ras) localize unspecifically to all cellular membranes, without any distinction (Figure 1.8)

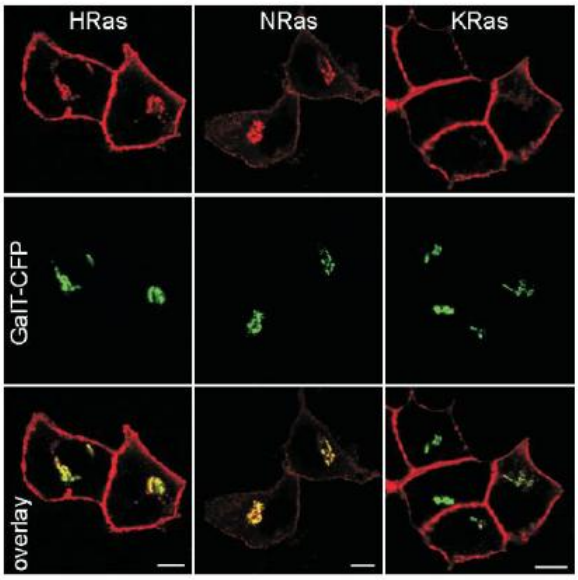

Figure 1.8 Subcellular Ras localization. Observation of the cellular localisation of *H*-Ras, *N*-Ras and *K*-Ras in MDCK cells cotransfected with the Golgi marker GaIT-CFP and YFP fusion of the Ras proteins. YFP = yellow fluorescent protein. Figure reproduced from the literature.[27]

1.3.3 Ras signaling from distinct locations and pathways

Over the past, cell signaling in general, including Ras signaling, was thought to be restricted to the plasma membrane. Recent work employing live cell imaging with genetically encoded fluorescent probes to visualize GTP-bound Ras, have pointed out that Ras signaling indeed is not limited to the PM, with signals generated from the Golgi as well as from various additional signaling platforms (endosomes, mitochondria and endoplasmic reticulum).[28,32-38] Recently, Ras signaling from the PM was shown to be coupled to Ras signaling events occurring at the Golgi through the Ras de/repalmitoylation cycle.

Signaling on the PM through the MAPK pathway

Upon external epidermal growth factor (EGF) stimulus, EGF receptors (EGRF) undergo conformational changes leading to their dimerization and finally to the transphosphorylation of their cytoplasmic tyrosine residues. Receptor phosphorylation in turn generate binding sites necessary for the formation of the SHC/GRB2 complex which further order the PM recruitment of the Ras guanine nucleotide exchange factor (RasGEFs) called SOS[39] (son of sevenless). As described previously, subsequent SOS-mediated Ras activation occurs by stimulating the replacement of bound-GDP by GTP. Activated Ras:GTP finally recruit the serine-threonine kinase Raf to the PM whose activation by phosphorylation further activate a cascade of downstream

serine-threonine kinases such as MEK followed by ERK. Through the successive activation of the three in-line kinases Raf/MEK/ERK referred to as MAP kinases (MAPK, mitogen activated protein kinase),[40] emitted signals access the nucleus and order the phosphorylation of transcription factors which further activate banks of genes required for cell proliferation (Figure 1.9).

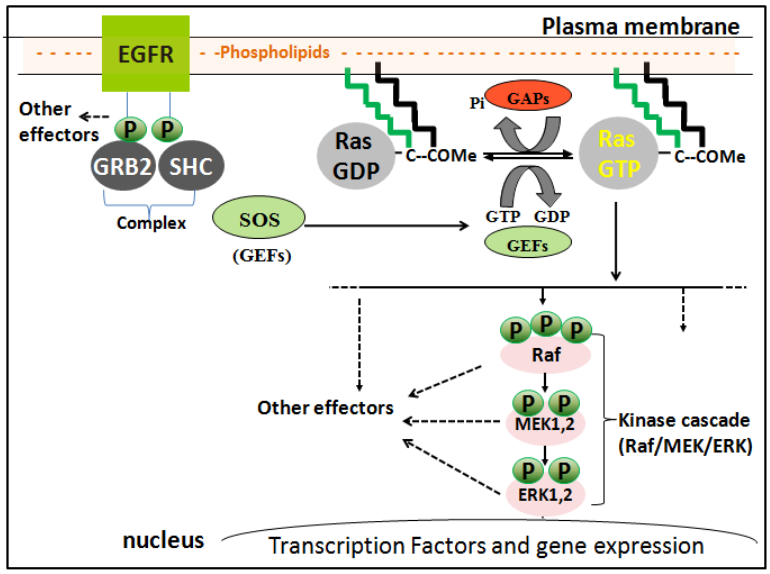

Figure 1.9 Schematic illustration of the MAPK signaling pathway. Upon EGF activation, PM-localized Ras isoforms signal through the activation of the three in-line kinases Raf, MEK and ERK. GRB2 = *growth-factor receptor-bound protein-2* and SHC = Src homology/collagen *proteins.* Figure adapted from the literature.[41]

Signaling on the Golgi apparatus

Following the rapid and transient Ras signaling occurring at the PM upon growth factor stimulus ($t_{1/2}$ = 2.9+/- 0.6 min), a delayed and sustained Ras signaling activity was observed at the Golgi by Chiu et al.[32] ($\Delta t_{1/2}$ = 13.6+/- 4.0 min). Ras activity at the Golgi is dependent on Ras retrograde trafficking (from the PM to the Golgi) given that inhibiting Ras depalmitoylation was associated to PM-restricted Ras signaling.[25] To explain such signaling coupling events, EGFR activation was proposed[42] not only to activate MAPK signaling at the PM, but also to activate phospholipase Cγ (PLCγ) involved in the degradation of phosphatidylinositols (PI) into diacylglycerol (DAG) and inositol trisphosphate ($InsP_3$). In turn, $InsP_3$ liberates calcium (Ca^{2+}) necessary to activate in combination with DAG, the Ras GEF GRP1 (Ras guanine nucleotide-releasing protein 1). Upon activation, GRP1 translocates to the Golgi to activate Golgi-localized Ras proteins finally signaling through the MAPK Pathway. The calcium release is also responsible for the recruitment of the Ras GAP CAPRI (Calcium-promoted Ras inactivator) to the PM in order to inactivate Ras signaling occurring from the PM (Figure 1.10).

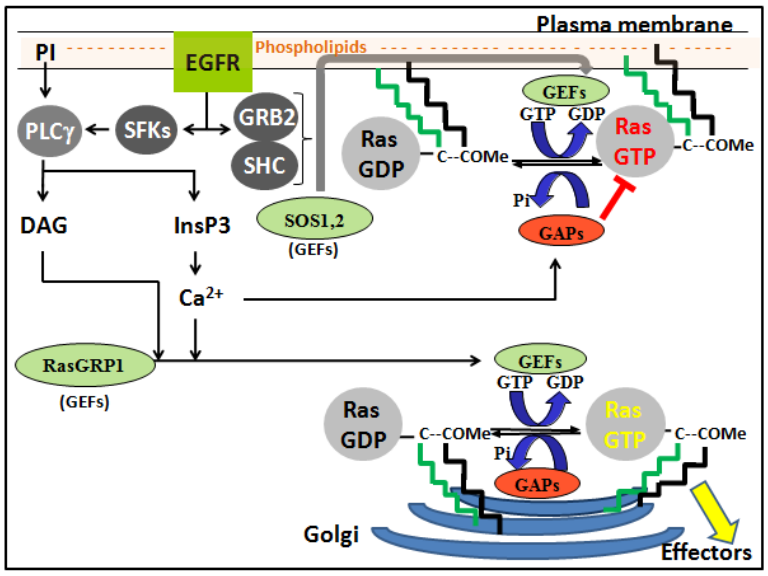

Figure 1.10 Schematic illustration of coupled PM and Golgi Ras signaling events. Model proposed for the delayed and sustained Ras-signaling occurring at the Golgi upon growth factor stimulus. Figure adapted from the literature.[38]

1.3.4 Ras microlocalization at the plasma membrane

Ras isoforms are localized into distinct microdomains[38] or "signaling platforms" within the PM consisting either in lipid raft (liquid-ordered) and non-lipid raft (liquid-disordered) domains. Lipid raft membranes, rich in cholesterols and sphingolipids, contain essentially proteins harboring palmitate chains allowing their insertion into such liquid-ordered structures, whereas isoprenylated proteins were found essentially in disordered non-raft fractions.[43] *K*-Ras with an isoprenyl lipid anchor was found predominantly localized in non-raft fractions (85% approx.) independently of its activation state. However, the PM microlocalization of *N*-Ras and *H*-Ras anchored by palmitoyl and isoprenyl moieties is much harder to predict. PM-localized *N*-Ras were shown[44] to be preferably localized in non-raft fractions, independently of their lipid anchors and of their activation state. In contrast, a dynamic equilibrium has been proposed for *H*-Ras,[7] cycling between lipid raft and non-lipid raft fractions regulated by GTP loading. *H*-Ras distributes equally between raft and non-raft domains when GDP-loaded and is essentially localized in non-lipid raft membranes when GTP-loaded (Figure 1.11A).

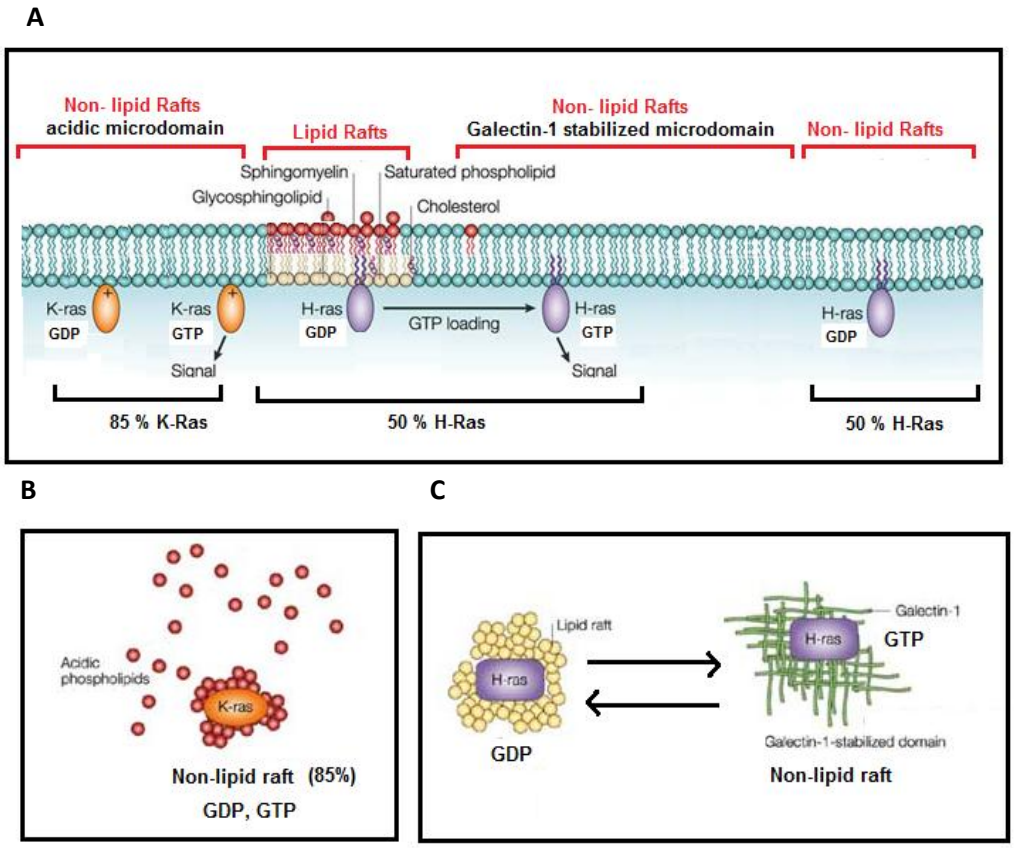

Figure 1.11 Ras isoforms microlocalization within the PM. A) *H*-Ras and *K*-Ras microlocalization within the plasma membrane depending of their activation state. B) Schematic representation of *K*-Ras acidic microdomains generated through an electrostatic-induced phospholipids accumulation. C) Schematic representation of the dynamic equilibrium of *H*-Ras cycling between lipid raft membranes and Galectin1-stabilized non-lipid raft membranes regulated by GTP loading. Figure modified from the literature.[38]

Additionally, GTP-bound Ras isoforms are thought to be localized into distinct microdomains within liquid-disordered fractions.[7] *K*-Ras is believed to generate an acidic microdomain by attracting phospholipids composing the PM through electrostatic interactions with its polybasic stretch (Figure 1.11B). *H*-Ras is thought instead to generate a Galectin 1 enriched microdomain upon activation thereby stabilizing Ras active form (Figure 1.11C). Such segregation within the plasma membrane is likely to complexify Ras signaling occurring at the PM by the generation of various and distinct signals.

1.4 Ras as a molecular target for antitumor drugs

Ras has been regarded as an attractive anti-cancer target given its central role in cell signaling pathways controlling cell proliferation (MAPK or Ras/PI3K/Akt), often disregulated in cancer due to activating mutations of constituting effectors. For example, Ras mutations are responsible for 33% of all cancers. Therefore, many approaches regarded as “signal transduction therapies”

were developed.[45] Among such approaches presented in Figure 1.12, targeting Ras membrane anchoring and localization for example represent an attractive approach to affect aberrant oncogenic Ras signaling.

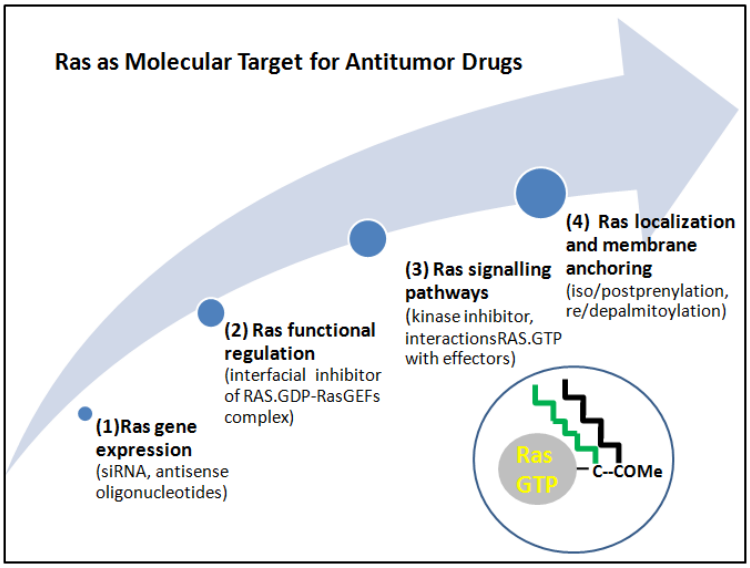

Figure 1.12 Targeting Ras as an attractive anti-cancer approach. Overview of the four principal approaches developed to target oncogenic Ras signaling, consisting in targeting either Ras gene expression, Ras functional regulation, Ras signaling or Ras localisation & anchoring.

1.4.1 Targeting mutated-RAS gene expression

Knocking down or silencing specifically mutant Ras genes may also represent a safe and effective anti-cancer therapy.[46,47] Several methods interfering on mRNA[48] to knockdown (down regulate) a gene have been developed such as the antisense oligonucleotides (ODNs) and the small interfering RNAs technology (siRNA). The first ODNs drug to enter clinical trials was the 20-base antisense oligonucleotide ISIS 2503 targeting *H*-Ras gene; however its application as anti-cancer agent remained limited due to toxicity. In contrast, the gene silencing method siRNA demonstrated many advantages over the use of antisense oligonucleotides such as a higher efficiency, stability and reduced toxicity[49,50] and is therefore considered as a promising strategy for the treatment of cancers involving Ras mutations. Recently, siRNA knockdown of oncogenic *Ras-gene* (*K-*,*H-*,*N-RAS*) revealed of therapeutic interest, exemplified by a reduced human ovarian cancer growth[51] when targeting *H*-Ras, a reduced pancreatic[52] and lung[53] cancer growth when targeting *K*-Ras or an induced apoptosis in human melanoma cells[54] when targeting *N*-Ras. Although improvements in delivery methods have provided cell permeability to negatively charge macromolecules, the development of gene cancer therapy remained challenging and therefore limited.

1.4.2 Targeting Ras functional regulation

An alternative approach to selectively block oncogenic Ras signaling may be to target Ras functional regulation. Ras proteins regarded as molecular switches offer the possibility to be artificially turned “off” either by stimulating Ras GTPase activity or by inhibiting their activation by GEFs. The first approach consisting in developing GTPase inducers remain challenging given the difficulty to create in a possibly reduced active site (due to possible mutations on Gly12 and/or Gly13) suitable hydrogen-stabilizing interactions to allow the GTPase reaction. Therefore, a more feasible approach has consisted in the development of interfacial inhibitors to prevent the formation of the Ras:GDP–RasGEFs complex necessary for an efficient Ras activation. Recently, the crystal structure of Ras in complex with the RasGEFs SOS was solved by Boriack-Sjodin et al.,[55] highlighting regions in the interface essential for the complex assembly called 'hot spot', which therefore constitute excellent target for the development of such molecule (Figure 1.13A). To date, no interfacial inhibitor targeting any Ras:GDP-RasGEFs complex has been reported, however the proof of concept was provided with Brefeldin A (BFA) shown to inhibit Arf activation by binding at the Arf:GDP - ArfGEFs complex interface (Figure 1.13B).[56,57]

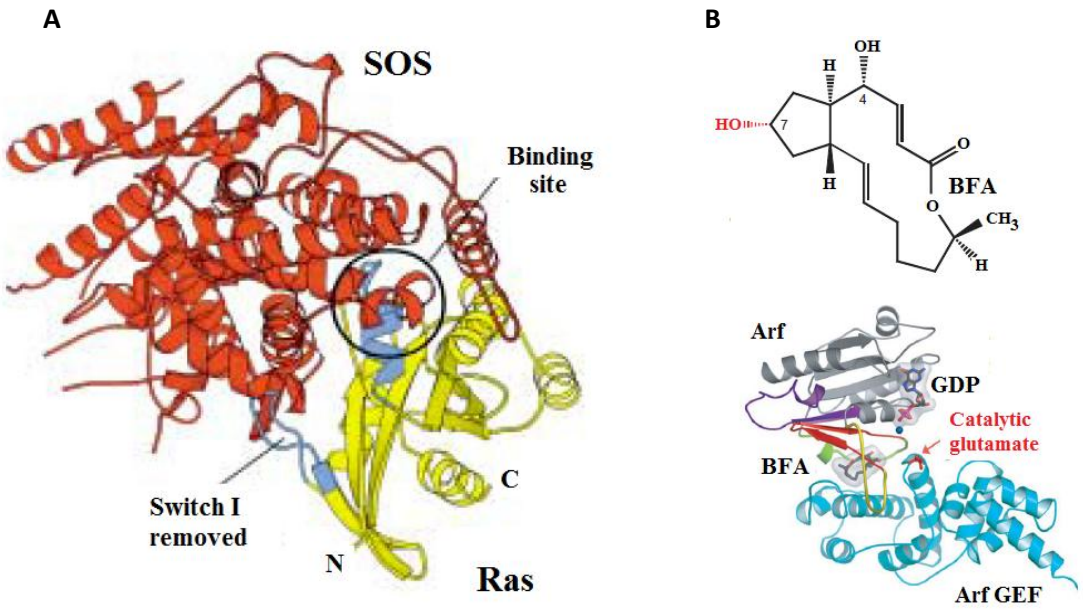

Figure 1.13. **Targeting Ras functional regulation for the treatment of Ras-related cancers.** A) Representation of Ras in complex with SOS showing interfacial regions essential for the complex assembly ('hot spot'), and the binging site for GTP (circled region). B) Structure of the interfacial inhibitor Brefeldin A (BFA), binding at the interface of the Arf:GDP–ArfGEFs complex. Figure modified from the literature.[5 56,57]

1.4.3 Targeting Ras signaling pathways

Given the central role of Ras signaling in the control of cell growth, differentiation and apoptosis, effort have been focused in targeting aberrant Ras signaling by two distinct approaches consisting either in the inhibition of specific kinase receptors/effectors involved in such pathways or in disrupting interactions of activated Ras with its downstream effectors.

Inhibitors of kinase receptors/effectors

Various inhibitors of kinases involved in Ras signaling pathways have entered clinical trials, exemplified by inhibitors targeting both upstream regulators of Ras, such as growth-factor receptor, and downstream effectors, such as the components of the MAPK pathway. The number of kinase receptor/effector drug candidate developed attests on the excitement surrounding the inhibition of the signaling cascades controlled by Ras such as the MAPK and Ras/PI3K/Akt pathways, frequently altered in cancers (Figure 1.14).

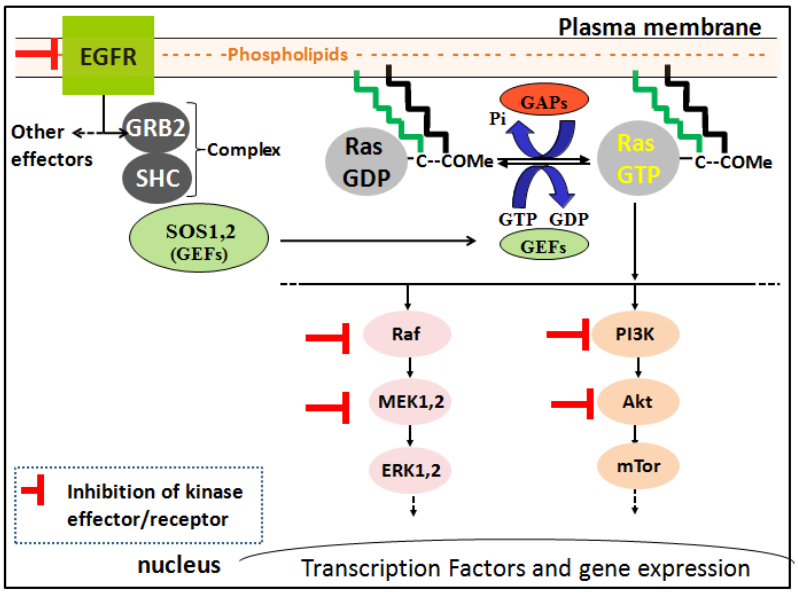

Figure 1.14 Targeting oncogenic Ras signaling by inhibition of kinase receptors/effectors. Development of kinase inhibitors to block respectively the MAPK and Ras/PI3K/Akt pathways frequently altered in cancers. *PI3K*= phosphatidylinositol 3-kinase. Figure adapted from the literature. [58]

Epidermal growth factor receptor (EGFR) overexpression or mutational activations are commonly seen in various cancers, thus resulting in a persistent Ras activation. In this context, a number of EGFR kinase inhibitors were developed,[59] such as Gefitinib (Iressa®, ZD1839, AstraZeneca Inc), FDA-approved in 2005 for the treatment of non-small cell lung cancer (NSCLC) leading to its worldwide commercialization. In addition, several antibody drugs were developed

exemplified by the fully humanized monoclonal antibody Panitumumab (Vectibix®, ABX-EGF, Abgenix Inc) FDA-approved in 2006 for the monotherapy treatment of chemotherapy-refractory metastatic colorectal cancer. By binding to the EGFR extracellular domain, such anti-body inhibit EGFR activation by EGF thereby promoting receptor internalization and down regulation. Despite their considerable success, the use of anti-bodies remains limited given their high production cost compared to small-molecule inhibitors, which complicate their clinical evaluation.

Many drugs targeting Ras downstream effectors were developed including various MEK inhibitors such as PD 98059[60] and U0126, which have been extensively used to study the MAPK pathway. In this context, PD184352 renamed CI-1040 was discovered as the first MEK inhibitor with an *in-vivo* activity in cancer mouse model[61] and as the first MEK inhibitor to enter clinical trials (clinical trials terminated in phase II for solubility and degradation issue).[62,63] Subsequently, additional MEK inhibitors were developed such as PD325901[64], optimized from CI-1040 with several polar hydroxylamine side chains which enter clinical trials for the treatment of advanced breast cancer, colon cancer and melanoma, but failed in phase II due to toxicity. Additionally, the Raf kinase has been regarded as an attractive therapeutic target given the strong implication of B-Raf mutations in carcinogenesis. In this context, the Raf kinase inhibitor BAY 43-9006 was shown to prevent tumor growth by inhibiting not only the MAPK pathway, but also angiogenesis (blood vessel growth) by targeting the receptor tyrosine kinases VEGFR (Vascular Endothelial Growth Factor Receptor) and PDGFR (Platelet Derived Growth Factor Receptor). As a result, the tosyl salt derived from BAY 43-9006 called Sorafenib Tosylate (Nexavar®, Bayer Pharmaceuticals Inc.) was FDA-approved for the treatment of advanced kidney cancers in 2005 and for liver cancer treatments in 2007 (Figure 1.15)

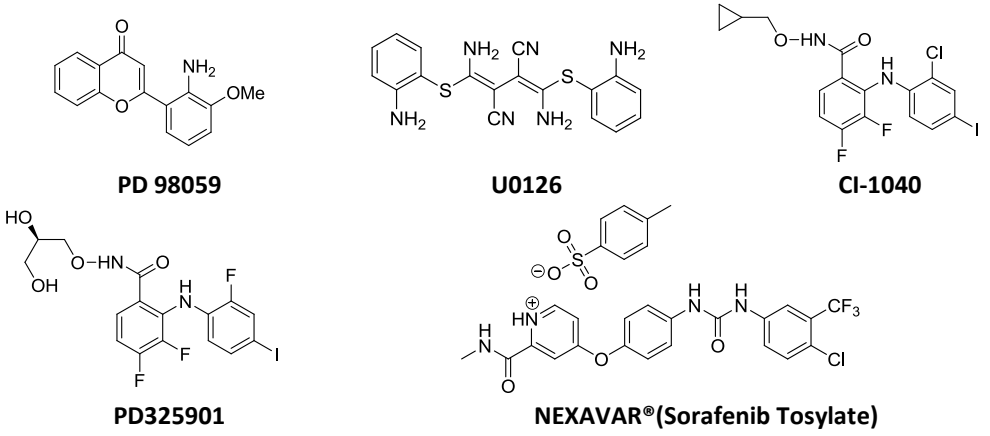

Figure 1.15 Example of MEK and ERK inhibitors developed to affect oncogenic Ras signaling. Kinase inhibitors used to block the MAPK and Ras/PI3K/Akt pathways which are frequently altered in cancers.

Given the role of the Ras/PI3K/Akt signaling pathway in cell growth and in particularly its frequent activation in human cancers such as in multiple myeloma,[65] targeting kinase effectors PI3K or Akt may as well offer a valuable anti-cancer approach, including for cancers involving Ras mutations.

Interfering with RAS:GTP – effector protein interactions

Given the direct interaction of activated Ras with the downstream effectors Raf and PI3K, and the essential role of MAPK and PI3K/Akt signaling pathways for cell proliferation, disruption of such protein–protein interactions has been regarded as an alternative anti-cancer approach (Figure 1.16).

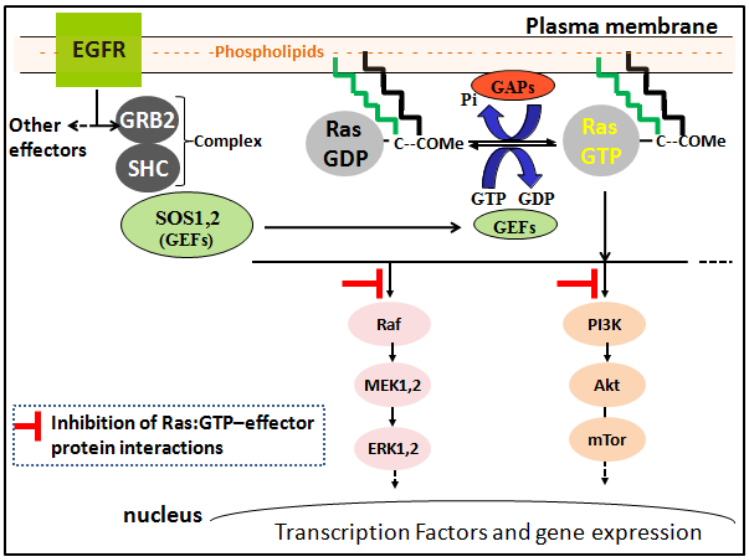

Figure 1.16 Disrupting the interaction of activated Ras with its direct effector as an anti-cancer strategy. Targeting the interaction of Ras:GTP with Raf or PI3K as a relevant approach to affect MAPK and Ras/PI3K/Akt signaling pathways, frequently altered in cancers.

Classically, designing interfacial inhibitors was referred as challenging given a typically large (1000 – 5000 Å^2) and flat interface without well-defined binding pockets as found in enzyme active sites. However, X-Ray crystallography has allowed the detection of small region of residues in the complex interface crucial for the complex assembly referred to as 'hot spot', suggesting the possibility to inhibit specifically protein/protein interactions with relatively small molecules. Given a close homology between Ras and Rap1A, with a strictly conserved effector region (residue 32-40) at their interface with RafRBD,[66,67] the Rap1A-RafRBD complex[68] was used as a mimic of the Ras-RafRBD complex to design Ras:GTP-Raf interfacial inhibitors (Figure 1.17A).

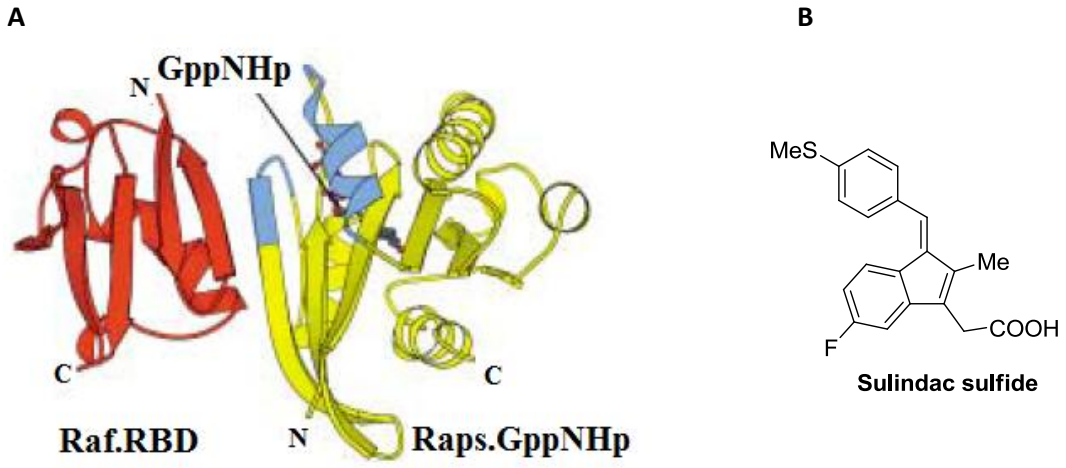

Figure 1.17 Guideline for the development of Ras:GTP-Raf interfacial inhibitors. A) Representation of the Rap1A-RafRBD complex used as a mimic of the Ras-RafRBD complex. B) Structure of Sulindac sulfide, an interfacial inhibitor of the Ras-RafRBD complex. RBD=Ras binding domain. Figure modified from the literature.[5]

In this context, several small peptides[69,70] derived from the Ras binding domain of Raf were designed and were shown *in-vitro* to inhibit the association of Ras:GTP with Raf (IC_{50} = 7µM) thereby inhibiting Ras-induced signaling. To overcome solubility issues encountered with peptide-drugs, efforts to develop small molecules instead have lead to Sulindac sulfide (Figure 1.17B),[71] a weak interfacial inhibitor of the Ras:GTP-Raf complex. More recently, the small molecule MCP1[72] was shown to inhibit Ras signaling through the inhibition of Ras/Raf interactions in human cancers and to reverse Ras-transformed phenotypes in HT1080 and Ras-transformed NIH 3T3 cells. MCP1 was also found highly active in human cancers harboring *K*-Ras mutations thereby providing a real proof of concept. In addition, disrupting the Ras:GTP-PI3K complex by creating mutation points into PI3K gene was shown to reduce significantly Ras-induced lung tumor formation.[73]

1.4.4 Targeting Ras localization and membrane anchoring

Given the importance of Ras correct localization and membrane anchoring for its biological function, targeting either Ras post-translational modifications (isoprenylation, post-isoprenylation, palmitoylation) or Ras de/repalmitoylation cycle at the level of depalmitoylation, may represent an attractive approach to disrupt aberrant oncogenic Ras signaling (Figure 1.18).

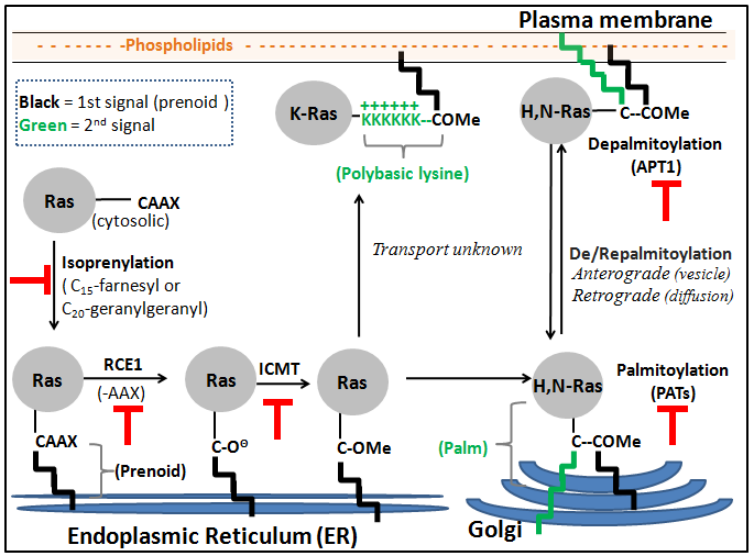

Figure 1.18 Targeting Ras localization and membrane anchoring to affect oncogenic Ras signaling. Developed strategies consisting either in targeting Ras isoprenylation, Ras post-isoprenylation, Ras palmitoylation or Ras depalmitoylation. RCE1= Ras Converting Enzyme 1, ICMT= isoprenylcysteine carboxyl methyltransferase, APT1=acyl-protein thioesterase 1, PATs= protein acyl transferases.

Isoprenylation inhibition

Given the importance of the isoprenyl group (farnesyl or geranylgeranyl group) for Ras biological activity through its membrane anchoring, targeting isoprenylation either by inhibiting the synthesis of the isoprenylation substrates or by inhibiting the enzymes involved in such lipidation process (farnesyltransferase/ geranylgeranyltransferase) represent an attractive anti-cancer approach. One strategy has consisted in the inhibition of the mevalonate pathway essential for the synthesis of the prenylation substrates farnesyl diphosphate (FPP) and geranylgeranyl diphosphate (GGPP). In this context, statins were first developed as HMG-CoA reductase inhibitors. Given their excessive toxicity, aminobisphosphonates were subsequently developed to inhibit the two enzymes isopentenyl diphosphate isomerase (IPPI) and farnesyl diphosphate synthase (FPP synthase), however, anti-cancer applications revealed very limited.

Subsequently, FTase inhibitors (FTIs) and GGTase inhibitors (GGTIs) were developed either as substrate mimetics, as CAAX peptidominetics or as combined substrate/CAAX mimetics. The significant FTIs–induced inhibition of *H*-Ras farnesylation without apparent toxicity, have lead to the development of various FTIs inhibitors. However, FTIs treatments were found to be ineffective on *N*-Ras and *K*-Ras given their ability to cross-prenylate (alternative prenylation) leading to their persistent membrane anchoring and therefore signaling. Given the strong implication of *K*-Ras and *N*-Ras in carcinogenesis (>99% of all Ras-mutated tumors), alternative

approaches were investigated such as the use of GGTI's either as single agent or in association with FTIs for toxicity issues. Finally, dual prenylation inhibitors (DPIs) consisting in simultaneous GGTase inhibitors (GGTIs) and FTase inhibitors (FTIs) were developed such as AZD3409 shown to inhibit tumor growth *in-vivo* without any toxicity. Although farnesylation is an obligatory first step in Ras post-translational modification, to date, success of therapies targeting Ras isoprenylation are very modest (Figure 1.19).

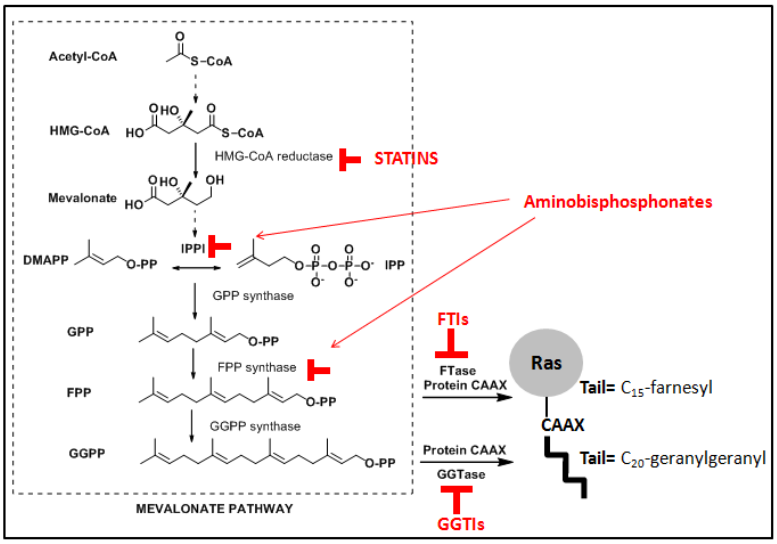

Figure 1.19 Targeting Ras isoprenylation. Two main strategies developed consisting either in targeting the Mevalonate pathway involved in the synthesis of the isoprenyl substrate (GPP and GGPP) or in targeting the enzymes FTase or GGTase catalysing Ras isoprenylation. HMG-CoA=3-hydroxy-3-methylglutaryl coenzyme A, DMAPP= Dimethylallyl diphosphate, IPP= Isopentenyl diphosphate, IPPI= Isopentenyl diphosphate isomerase, GPP= Geranyl diphosphate, FPP= Farnesyl diphosphate, GGPP= Geranygeranyl diphosphate, FTase = Farnesyltransferase, GGTase= Geranylgeranyl transferase. Figure modified from the literature.[74]

Post-isoprenylation inhibition (ICMT, RCE1)

Given an induced cytosolic Ras mislocalization with a complete loss of activity upon RCE1 or ICMT delection, targeting post-isoprenylation has emerged as an attractive strategy to affect oncogenic-Ras signaling, especially given that such approach by affecting both geranylgeranylated and farnesylated Ras proteins would overcome Ras cross-prenylation problem encountered with FTIs. However, RCE1 inhibition revealed to have even weaker effects than FTI's monotherapies and ICMT inhibition was found to affect multiple pathways besides Ras. Although several ICMT inhibitors entered clinical trials, their evaluation was generally confronted to their excessive toxicity due to their low selectivity.

Palmitoylation inhibition

Given the importance of the palmitate lipid anchor for the correct Ras cellular localization and signaling, targeting Ras palmitoylation may define a new class of anti-cancer agents. In this context, a first approach has consisted in a global inhibition of protein palmitoylation by inhibiting palmitic acid biosynthesis. Such strategy was shown to induce Ras mislocalization and loss of activity with a severe toxicity due to various off targets.[75] The alternative approach consisting in targeting the enzyme(s) catalysing Ras palmitoylation referred to as protein acyltransferases (PATs), has been rarely investigated given the high controversy and questioning around such enzymes. To date only two Ras protein acyltransferase inhibitors have been reported (Figure 1.20).

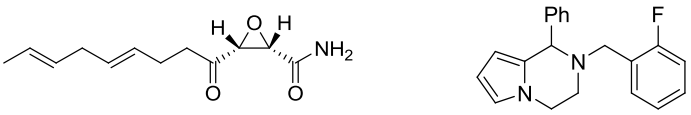

CERULENIN

Figure 1.20 Targeting Ras palmitoylation. Structure of the two reported PAT inhibitors developed in order to inhibit protein acyltransferases involved into Ras palmitoylation. Cerulenin as a well established PAT inhibitor.

Cerulenin was the first established palmitoylation inhibitor of Ras proteins and since recently of several additional proteins.[76] The Cerulenin-induced antiproliferative effect was shown to be exclusively due to its ability to inhibit Ras palmitoylation (IC_{50}= 4.5 µM) and not to its ability to inhibit fatty acid synthase (fas) given that some Cerulenin analogues presenting an antiproliferative effect were inactive against fas.[77] The second PAT inhibitor presented in Figure 1.20 inhibits the MAKP signaling pathway thereby inducing a significant anti-proliferative effect in various human cancer cell lines (with IC_{50} values typically in the low µM range).[78]

Depalmitoylation inhibition

Targeting the Ras acylation cycle at the level of depalmitoylation, may offer a viable alternative to PAT inhibitors, as signaling down regulation rather than full inhibition would allow cell viability. To date, only three depalmitoylating enzymes have been described consisting in protein palmitoylthioesterase-1 (PPT1), acyl protein thioestease 1 (APT1) and acyl protein thioesterase 2 (APT2). In this context, a large effort has been devoted to address their relevance to Ras depalmitoylation.

- *Protein palmitoylthioesterase-1 (PPT1)*

This enzyme was isolated[79] from bovine brain extract and cloned[80] based on its ability to depalmitoylate *H*-Ras *in-vitro*. Later, it was found irrelevant to the Ras cycle due to its involvement in the lysosomal[81] protein degradation by depalmitoylation,[26] exemplified by PPT1 mutations causing fatal lysosomal storage diseases such as infantile neuronal ceroid lipofuscinosis (INCL).[82,83]

- *Acyl protein thioesterase 1 (APT1) or lysophospholipase 1 (LYPA1)*

This enzyme is a 25-kDa cytosolic[84] acylhydrolase lysophospholipase 1 (LYPA1), isolated from rat liver [85] and pig stomach.[86] First described as a lysophospholipase,[85,87] LYPA1 was subsequently renamed as acyl protein thioesterase-1 (APT1) given its stronger depalmitoylation activity over lysophospholipase activity demonstrated by Duncan and Gilman.[84] In 2000, the crystal structure of human acyl protein thioesterase 1 (hAPT1) was solved[88] showing a catalytic triad consisting in Ser114, His203 and Asp169, with Ser114 as the nucleophilic residue (Figure 1.21A). Moreover, hAPT1 appears to be dimeric with its active site occluded by the dimer interface suggesting the necessity of enzyme dissociation to interact with its substrates. Human APT1 is characterized by a negative potential surrounding its active site, which is a common feature among esterases and lipases to facilitate the expulsion of the negatively charged hydrolysis product like palmitic acid in the present case (Figure 1.21B).

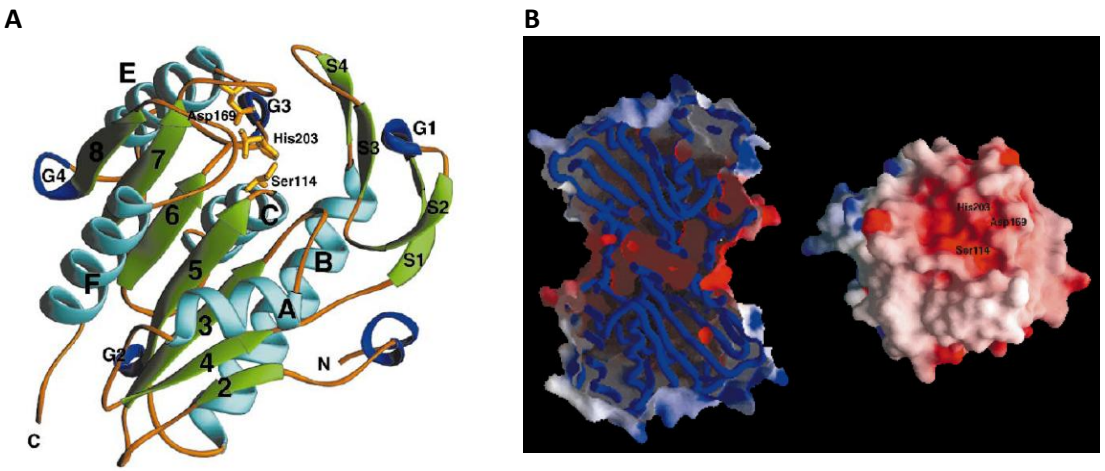

Figure 1.21 Crystal structure and electrostatic potential of human APT1. A) Representation of the secondary structure elements of APT1 with the catalytic triad (Ser114, His203 and Asp169). B) View of the electrostatic potential surface of the APT1 dimer and monomer showing the negatively charged catalytic site occluded in the dimeric form. Positively charged regions are shown in blue and negative regions in red. Figure modified from the literature.[88]

APT1 depalmitoylates *in-vitro* a wide variety of substrates such as *H*-Ras proteins,[84,89] various heterotrimeric G protein α subunits,[84,90] eNOs,[89] RGS4,[84] SNAP-23,[91] Ghrelin[92] and platelets.[76] This wide substrate tolerance commonly encountered with acylating and deacylating enzymes, is consistent with the absence of primary consensus sequences surrounding the thioacyl group for its recognition by APT1. APT1 seems to depalmitoylate *in-vitro* structurally different proteins from soluble proteins like eNOs to transmembrane proteins like SNAP-23. However, APT1 does not depalmitoylate without any discrimination, exemplified by the protein Caveolin[89] not affected by APT1 in the conditions used for eNOs deacylation.[93] Although APT1 was shown to depalmitoyate *H*-Ras *in-vitro,* experimental proof of its involvement in Ras depalmitoylation *in-vivo* have been lacking until very recently.

- *Acyl protein thioesterase 2 or lysophospholipase 2 (LYPA2)*

This enzyme was purified from pig stomach[86] and subsequently cloned.[94] Human acyl protein thioesterase 2 revealed 66% sequence identity with hAPT1, with in particular a conserved catalytic triad. In analogy to APT1, its close homologue APT2 has a highly conserved amino acid sequence between various species (mouse, rat, human).[95] The crystal structure of APT2 is very similar to the structure of APT1 as shown by the superposition of their respective crystal structures (Figure 1.22A). In addition, APT2 like APT1 is dimeric with its catalytic site occluded by the dimer interface (Figure 1.22B)

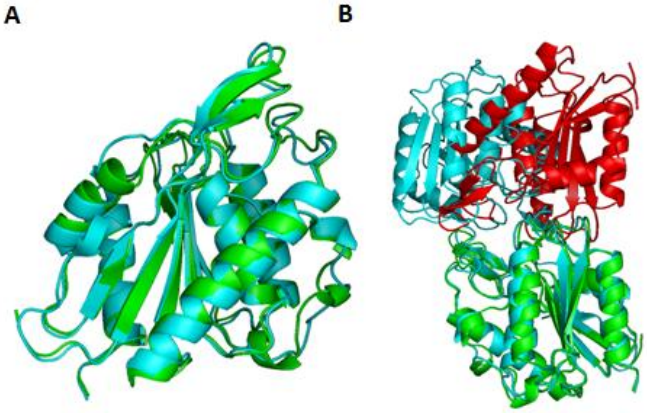

Figure 1.22 Superposition of human APT1 and human APT2 crystal structures. A) Crystal structure overlay of APT1 and APT2 monomers. Green = hAPT2, blue = hAPT1 B) Crystal structure overlay of APT1 and APT2 dimers, showing their catalytic site occluded by the dimer interface. Green/red = hAPT2, blue = hAPT1. Work by Marco Bürger.

In contrast, significant differences are visible between APT1 and APT2 in their electrostatic potentials at the proximity of their active sites, with APT2 significantly more hydrophobic in comparison to APT1 (work by Marco Bürger, Figure 1.23).

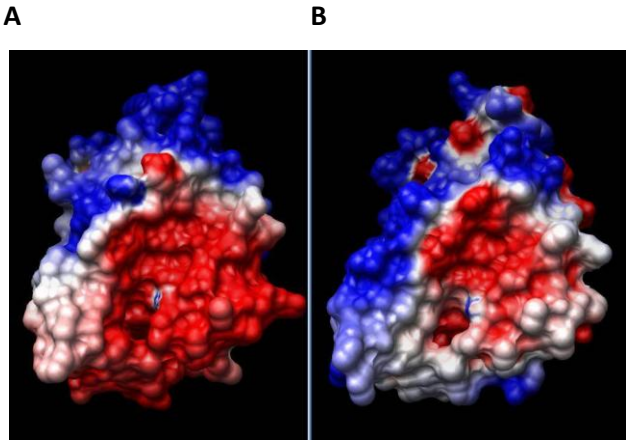

Figure 1.23 Comparison of human APT1 and human APT2 electrostatic surface potentials. A) View of the electrostatic potential surface of the hAPT1 monomer. B) View of the electrostatic potential surface of the hAPT2 monomer. Positively charged regions are shown in blue and negative regions in red. Work by Marco Bürger.

Recently, an increased depalmitoylation rate of GAP-43 (growth-associated protein 43) was observed in cells overexpressing APT2, suggesting that APT2 may be involved in GAP-43 depalmitoylation whereas no effect was observed in cells overexpressing APT1.[96] Using the same approach, the authors suggested the involvement of APT2 in *H*-Ras depalmitoylatation.[96] Earlier experiments already suggested the involvement of second enzyme in Ras depalmitoylation given that *H*-Ras depalmitoylation proceeded normally in yeast strains where the APT1 gene was disrupted.[90] However, experimental proof of the involvement of APT2 in Ras depalmitoylation *in vivo*, are still lacking.

1.5 APT1 as a Ras depalmitoylating enzyme *in vivo*

1.5.1 Palmostatin B as a potent APT1 inhibitor

Given the widely conserved character of APT1,[84] the 'Protein Structure Similarity Clustering' (PSSC) approach[97,98] was used to develop APT1 inhibitors as tools to investigate the biological role of APT1 and in particular its relevance to Ras depalmitoylation. The PSSC approach has permitted the identification of gastric lipase as structurally similar to APT1 in their binding sites, especially in terms of subfold and in the orientation of their catalytic residues (Figure 1.24A). The known gastric lipase inhibitor tetrahydrolipstatin (generic name Orlistat)[99] was therefore used for the design of APT1 inhibitor candidates harboring an electrophilic β-lactone core for the nucleophilic attack of APT1 in analogy to gastic lipase inhibition (Figure 1.24B).

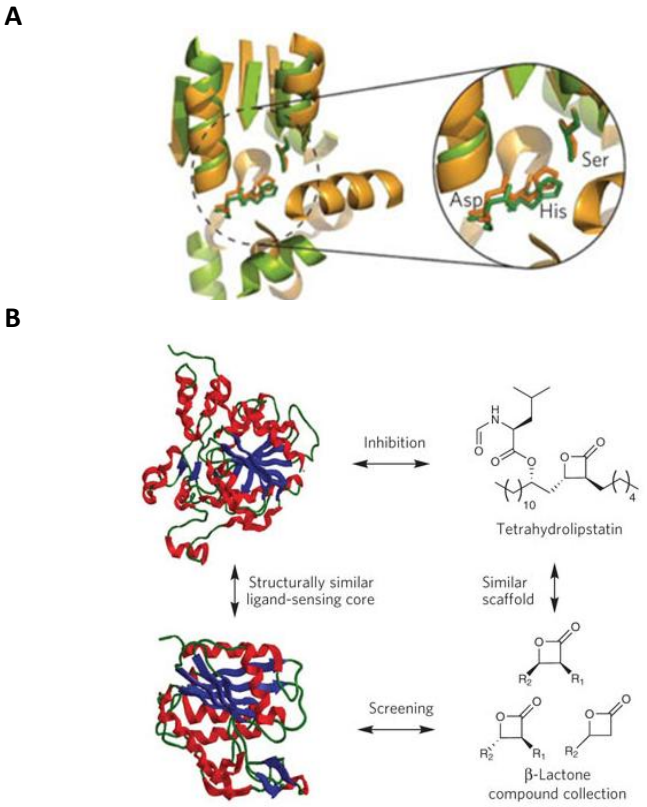

Figure 1.24 Design of palmostatin B based on a PSSC approach. A) Overlay of the ligand-sensing cores of gastric lipase (orange) and APT1 (green) with a similar orientation of their catalytic residues. B) Design of β-lactone APT1 inhibitors based on the gastric lipase inhibitor tetrahydrolipstatin (orlistat) containing a β-lactone core. Figure reproduced from the literature.[25]

In-vitro screening for APT1 inhibition using a colorimetric assay have led to the development of potent β-lactone APT1 inhibitors termed palmostatins comprising palmostatins A, B, C and D, among which the (*S,S*)-*trans* configured inhibitor palmostatin B was the most potent (Figure 1.25).[25] The advantage of the PSSC approach is clearly shown here given that classical approaches would not have allowed a correlation between gastric lipase and APT1 given their low sequence identity.

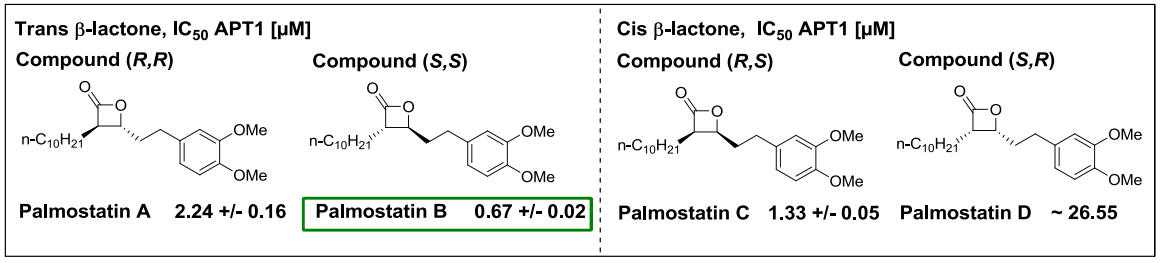

Figure 1.25 Evaluation of palmostatin A,B,C and D as APT1 inhibitors. IC_{50} values were obtained by employing a colorimetric assay using para-nitrophenyl octanoate (PNPO) as substrate (APT1 = 75nM, PNPO= 600μM, 30 min. inhibitor pre-incubation).

1.5.2 Investigation of the biological role of APT1 *in-vivo*

Recently, the first *in-vivo* evidence of APT1 as a Gα13 depalmitoylating enzyme was provided by studies conducted in neurons.[100] To address the biological role of APT1 in Ras depalmitoylation, *in-cellulo* experiments were performed with the cell permeable palmostatin B.[25] Palmostatin B induces a random redistribution of palmitoylated Ras isoforms to all cellular membranes comparable to that of solely farnesylated Ras proteins. Moreover, by inhibiting Ras depalmitoylation, Ras retrograde trafficking from the PM to the Golgi was affected thereby resulting in a quasi PM restricted Ras signaling. Palmostatin B uncouples Ras signaling events occurring normally between the PM and the Golgi. Additionally, upon palmostatin B treatment, a partial phenotypic reversion was induced in *H*-RasG12V-transformed MDCK-F3 cells with restoration of E-cadherin expression at the cell-cell interfaces, whereas *K*-RasG12V-transformed MDCK-F3 cells were unaffected. Recent proteomic analyses have suggested that the cytosolic APT1 is itself palmitoylated therefore providing a means for it to access its membrane-localized substrates.[101] This model was further completed by a prolyl isomerase FKBP12 which may promote *H*-Ras depalmitoylation through the formation of a complex with PM-localized palmitoylated Ras isoforms thereby rendering the thioester bond more accessible for the membrane associated thioesterase APT1. [102] However, this model well may be modified in the future when addressing the relevance of APT2 to Ras depalmitoylation *in vivo* (Figure 1.26).

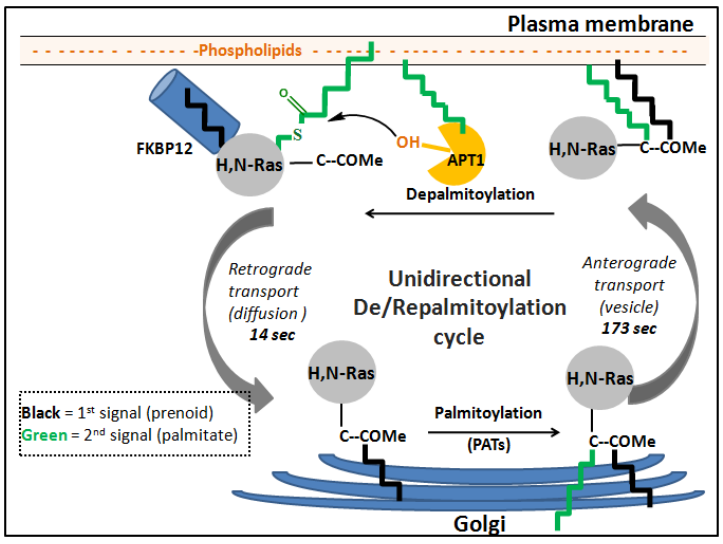

Figure 1.26 Ras depalmitoylation possibly facilitated by APT1 palmitoylation and FKBP12. Recently proposed model of the de/repalmitoylation cycle with FKBP12 binding to PM-localized Ras isoforms to facilitate their depalmitoylation by plasma membrane anchored APT1proteins. Figure modified from the literature. [102]

2 Results and discussion

2.1 Fluorescent enzymatic assay for APT1 inhibition

2.1.1 Fluorescent coumarin reporter dyes

Extensive efforts in targeting the Ras depalmitoylating enzyme APT1 have led to the development of a colorimetric assay measuring the release of para-nitrophenolate from para-nitrophenyl octanoate (PNPO), used as mimic of palmitic acid thioesters.[25] However, with the development of highly potent β-lactone APT1 inhibitors, a more sensitive fluorometric assay was developed allowing an accurate inhibitor characterization with reduced enzyme and substrate amounts. 7-Hydroxy-4-methyl coumarin **1** (4-methylumbelliferone; MU) for example constitutes an important fluorogenic substrate used to monitor phosphatases,[103,104] proteases[105,106] and glycosidases.[107-109] Its fluorinated analogue 6,8-difluoro-7-hydroxy-4-methylcoumarin **2** (6,8-difluoro-4-methylumbelliferone; DiFMU) display improved properties, exemplified by a lower pK_a value at 4.7 vs. 7.8, resulting in maximum fluorescence of the cleavage product over a much broader pH range, a higher quantum yield (0.89 vs. 0.63) and an increased photostability (5% bleaching vs. 22% bleaching after 33 min. of illumination at the wavelength of maximal absorption).[110] Encouraged by the use of 6,8-difluoro-4-methyl umbelliferyl octanoate **3** (DiFMUO) to monitor lipase activity (*Candida antarctica* Lipase B and its mutants),[111] DiFMUO was chosen as substrate for a new fluorescent enzymatic assay for APT1 inhibition (Figure 1.27).

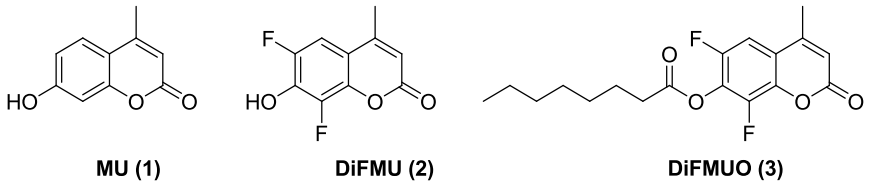

Figure 1.27 Coumarins used as fluorogenic substrates or as reporter system. 4-methylumbelliferone (MU), 6,8-difluoro-4-methylumbelliferone (DiFMU) and 6,8-difluoro-4-methylumbelliferyl octanoate (DiFMUO).

2.1.2 Synthesis of the fluorescent coumarin substrate DiFMUO

The synthesis of DiFMUO commenced with the conversion of fluorinated nitrobenzene **4** into 3,5-difluoro-2,4-dimethoxynitrobenzene **5** using sodium methoxide (2.4 eqv.) in methanol.[112] The *ortho* and *para* directing nitro group in compound **5** accounting for the efficient fluorine displacement was subsequently removed in a two step sequence involving nitro group reduction

by hydrogenation on Pd/C leading to 1-amino-3,5-difluoro-2,4-dimethoxy benzene **6** followed by hydrodediazoniation with HNO_2/H_3PO_2 leading to 1,3-dimethoxy-2,4-difluorobenzene **7** in 84% yield.[112] Finally, compound **7** was demethylated using BBr_3 in DCM for 28 hours leading to 2,4-difluororesorcinol **8** in 92% yield.[112] Fluorinated phenol derivative **8** was subsequently involved in a Pechmann condensation[113] consisting in a acid catalysed condensation of a phenol derivative with a β-ketoester to access the coumarin skeleton. Although several alternative coumarin syntheses have been reported[114] (Perkin, Knoevenagel, Reformatsky and Wittig), the Pechmann condensation, regarded as one of the simplest and most straightforward methods, was first investigated. Reactions between 2,4-difluororesorcinol **8** and freshly distilled ethylacetoacetate have led to a relatively poor yield (10%) when performed in sulfuric acid (22 eqv.),[115] but proceeded smoothly in methanesulfonic acid (25 eqv. CH_3SO_3H)[110,116] leading to coumarin **2** in 84% yield. The lipophilic tail mimicking palmitic acid was subsequently attached to the coumarin by esterification[117] leading to DiFMUO **3** in 64% yield over 6 steps (Scheme 1.1).

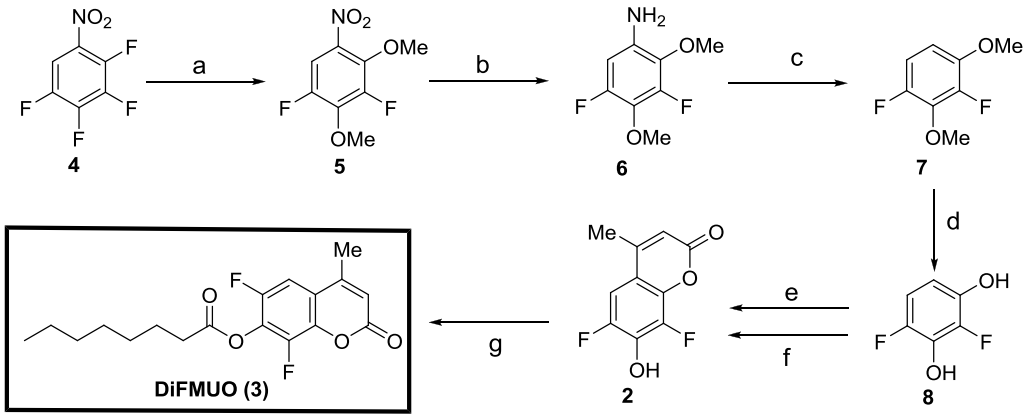

Scheme 1.1 Synthesis of fluorescent DiFMUO substrate **3**. Reagents and conditions: a) NaOMe (2.4 eqv.), MeOH, rt, 18h, quantitative. b) 10% Pd(C), H_2 (10 Bar), EtOAc/EtOH 1/1, rt, 18h, quantitative. c) $NaNO_2$ (1.05 eqv.), H_3PO_2 (20 eqv.), HCl/H_2O 1/2, 4°C, 21h, then rt 2h, 84% yield. d) BBr_3 (3.0 eqv.), DCM, rt, 28h, 92% yield. e) CH_3COCH_2COOEt (1.0 eqv.), $MeSO_3H$ (25 eqv.), rt, 28h, 84% yield. f) CH_3COCH_2COOEt (1.0 eqv.), H_2SO_4 (22 eqv.), rt, 20h, 10% yield. g) n-$C_7H_{15}COCl$ (1.1 eqv.), NEt_3 (1.5 eqv.), DCM, rt, 8h, 95% yield.

2.2 Additional experiments with the APT1 inhibitor palmostatin B

2.2.1 Synthesis of palmostatin B and fluorescently labeled analogue

Encouraged by the effect of the APT1 inhibitor palmostatin B on oncogenic Ras signaling and to perform additional experiments, two grams of palmostatin B (**14**) were first prepared following a strategy previously established involving an *anti*-selective aldol reaction.[118] The synthesis started

with the acylation of compound **9** (synthesized in 76 % from norephedrine by mesitylation, followed by N-alkylation[119]) with dodecanoyl chloride leading to *O*-dodecylated ephedrine auxiliary **10.**[120] β-Hydroxyester **12** was obtained by reaction of ephedrine auxiliary **10** with aldehyde **11** in the presence of freshly prepared dicyclohexylborontriflate (c-Hex_2BOTf).[121] Hydrogenolysis of β-hydroxyester **12** to β–hydroxyacid **13** followed by cyclization using phenylsulfonyl chloride in pyridine concluded the synthesis of palmostatin B (**14**) (Scheme 1.2).[122,123]

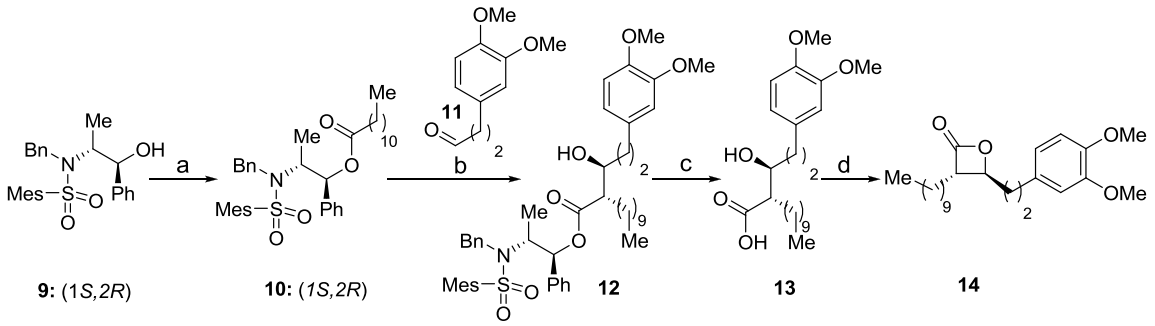

Scheme 1.2 Scale-up synthesis of palmostatin B **14**. Reagents and conditions: a) pyridine (1.3 eqv.), dodecanoyl chloride (1.0 eqv.), CH_2Cl_2, rt, 15h, 87% yield. b) Aux **10** (1.2 eqv.), NEt_3 (2.5 eqv.), c-Hex_2BOTf (2.2 eqv.), CH_2Cl_2, -78°C, 2h then aldehyde **11** (1.0 eqv.), -78°C (1h) then 0°C (1h) and rt (1h), 63% yield. c) $Pd(OH)_2/C$, H_2, MeOH, 40°C (30h), 72.5% yield .d) $PhSO_2Cl$ (3.0 eqv.), pyridine, 0°C, over night, 75% yield (2 grams obtained).

Subsequently, in order to study intracellular processes, and in particular the interaction between palmostatin B (**14**) and APT1 in cells using fluorescence lifetime imaging microscopy (FLIM), a TAMRA-labeled palmostatin B analogue (**25**) was synthesized by a $Cu^{(I)}$-catalyzed [3+2] dipolar cycloaddition[124] between acetylene tagged palmostatin B (**23**) and the azide functionalized rhodamine **24**. Compound **23** was prepared from aldehyde **11** in a conceptually similar strategy as for the synthesis of palmostatin B (**14**) involving an *anti*-selective aldol reaction[118] with an *O*-dodecylated acetylene tagged ephedrine auxiliary **20.** The obtained β-hydroxyester **21** was subsequently hydrogenolysed to β-hydroxyacid **22,** which was subsequently cyclized to β-lactone **23** using phenylsulfonyl chloride in pyridine.[122,123] The synthesis of acetylenic ephedrine auxiliary **20** started from 11-bromo-1-undecene **15** which was converted into 11-dodecanoic acid **16** by a Grignard reaction.[125] 11,12-Dibromododecanoic acid **17,** obtained by bromination of compound **16**,[126] was subsequently used to access to the terminal alkyne **18** by double elimination. Using a large excess of base such as potassium hydroxide (10 eqv. in refluxing ethylene glycol or water or water/ethanol 1:2 or toluene) or potassium tert-butoxide (4.0 eqv. in dry THF at 70°C), the reaction did not lead to the desired terminal alkyne **18** but rather to various internal alkyne side products. However, the use of sodium amide in liquid ammonia

furnished 11-dodecynoic acid **18** in 96% yield, without any purification necessary**.**[126] Treatment of carboxylic acid **18** with thionyl chloride in refluxing benzene furnished 11- dodecynoyl chloride **19** in 97% yield,[127] subsequently used for the acylation of alcohol **9** leading to acetylenic ephedrine auxiliary **20.**[118] Rhodamine derivative **24** was synthesized in 83% yield by treatment of commercially available 5/6 TAMRA SE with 3-azidopropyl-1-amine[128] (prepared in 73% yield from 3-chloropropyl-1-amine hydrochloride and NaN_3[129]) in the presence of triethylamine (Scheme 1.3).

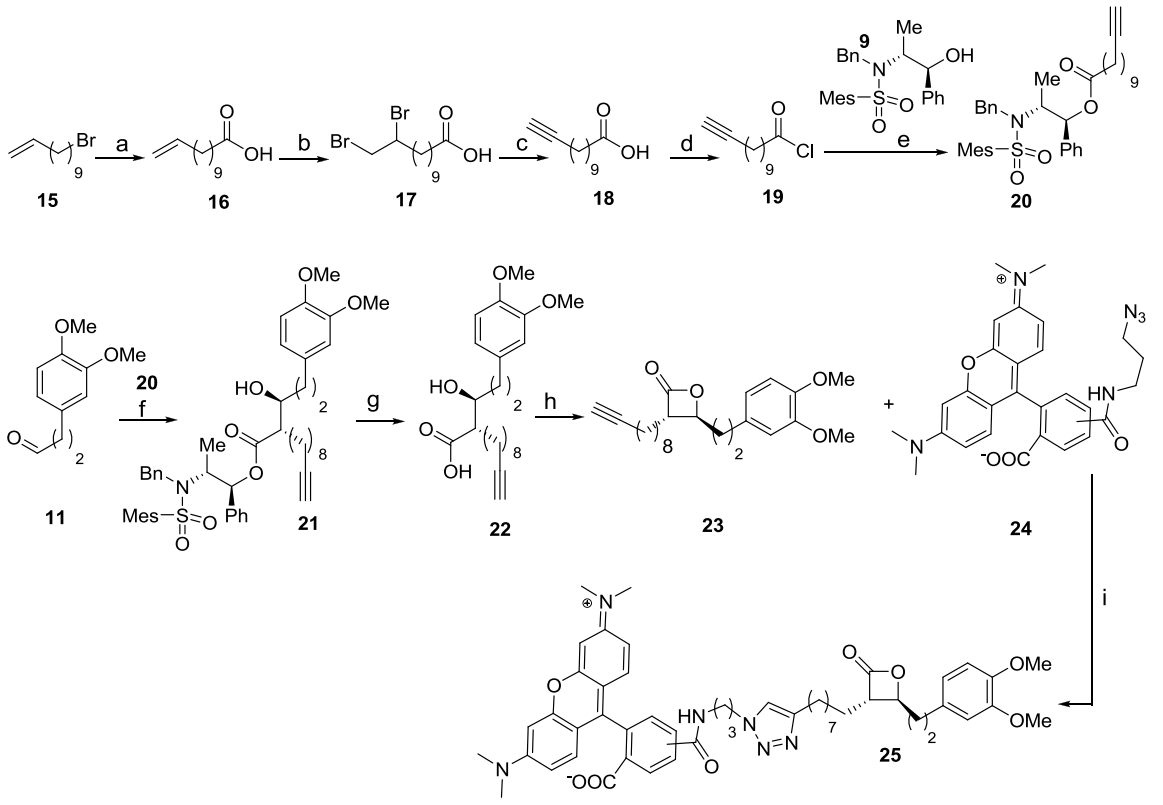

Scheme 1.3 Synthesis of tetramethylrhodamine palmostatin B analogue **25**. Reagents and conditions: a) Mg (2.85 eqv.), Et_2O, reflux, 5h then CO_2, -40°C (2h), 56% yield. b) Br_2 (1.2 eqv.), Et_2O, -5°C (2h), quantitative. c) $NaNH_2$ (5.5 eqv.), liq. NH_3, THF, -45°C (4h) then -35°C (1h), 96% yield. d) $SOCl_2$ (1.5 eqv.), benzene, reflux, 3h, 97% yield. e) Pyridine (1.3 eqv.), alcohol **9** (1.0 eqv.), rt (15h), 67% yield. f) Aux **20** (1.2 eqv.), NEt_3 (2.5 eqv.), c-Hex_2BOTf (2.2 eqv.), DCM, -78°C, 2h then aldehyde **11** (1.0 eqv.), -78°C (1h) then 0°C (1h), and rt (1h), 76% yield. g) $LiOH.H_2O$ (9.0 eqv.), dioxane/H_2O 4/1, 40°C (90h), 87% yield. h) $PhSO_2Cl$ (3.0 eqv.), pyridine, 0°C, over night, 89% yield. i) Alkynylated β-lactone **23** (1.2 eqv.), rhodamine azide **24** (1.0 eqv.), sodium ascorbate (1.5 eqv.), $CuSO_4$ (0.9 eqv.), EtOH/H_2O degased, rt (16h), dark, 83% yield.

2.2.2 APT1 as a cellular target of palmostatin B

The attachment of the bulky TAMRA fluorescent group to palmostatin B (**14**) may affect the resulting inhibitory activity due to steric hindrance. However, the chosen attachment point of the dye turned out to be appropriated with a weaker but still potent inhibitory effect for compound **25** compared to palmostatin B (IC_{50} (**25**) = 300nM, IC_{50} (**14**) = 5.37+/- 0.38 nM, fluorometric assay employing 5nM of enzyme). The cell permeable TAMRA-palmostatin B analogue **25** was employed by the Bastiaens group (Nachiket Vartak) to demonstrate the direct interaction between palmostatin B and APT1 in cells. Fluorescence lifetime imaging microscopy (FLIM) in MDCK cells expressing APT1 tagged with green fluorescent protein (APT1-GFP), permitted to observe a significant reduction of GFP fluorescence lifetime due to Foerster Resonance Energy Transfer (FRET) from APT1 tagged with green fluorescent protein (APT1-GFP) to the TAMRA acceptor **25.**[25] This distance-dependent transfer of energy proves the molecular proximity of the two dyes and therefore revealed APT1 as a cellular target of palmostatin B (Figure 1.28).

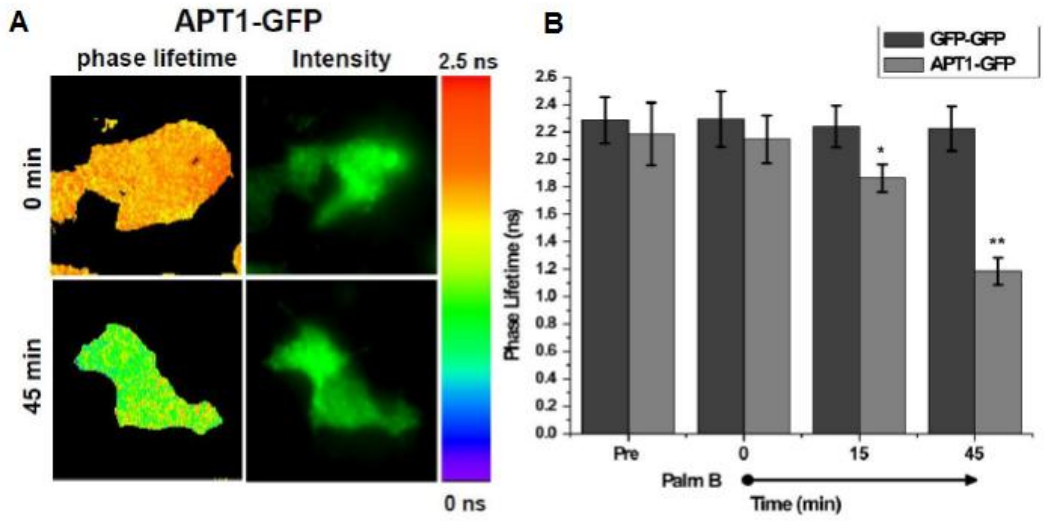

Figure 1.28 APT1 as a cellular target of palmostatin B. Fluorescence lifetime imaging (FLIM) in MDCK cells expressing GFP-APT1 (donor) after incubation with palmostatin B analogue **25** (acceptor). A) Significant reduction of APT1-GFP lifetime. B) Reduction of APT1-GFP lifetime compared to a GFP-GFP control upon incubation with compound **25**. Data from Nachiket Vartak.

2.2.3 Investigation on palmostatin B selectivity

Further experiments were performed to investigate the selectivity of palmostatin B (**14**) for APT1 by studying its inhibitory effect on additional phospholipases potentially relevant to Ras signaling. No inhibition of phospholipase Cβ (PLCβ) could be observed in a cellular assay at 50 μM palmostatin B concentration.[25] However, the effect of palmostatin B on cytosolic phospholipase A2 (cPLA2), phospholipase D (PLD) and phospholipase A1 (PLA1) had to be addressed in relevant biochemical assays.

Cytosolic phospholipase A2 (cPLA2)

The evaluation of cytosolic phospholipase A2 (cPLA2) inhibition was performed using an HPLC assay with UV spectrometric detection as reported in the literature.[130] In the assay, the final reaction mixture contained 0.2 mM phospholipid substrate 1-stearoyl-2-arachidonoyl-*sn*-glycero-3-phosphocholine (SAPC) and 0.1 mM 1,2-dioleoyl-*sn*-glycerol as substrate. After incubation of the substrate with palmostatin B for 5 min at 37°C, cPLA2 (isolated from human platelets by anion exchange chromatography) was added and the mixture was incubated at 37°C for 60 min. The enzymatic reaction was terminated and 4-un-decyloxybenzoic acid was added to the sample as internal standard (IStd). Samples were measured by reverse-phase HPLC with UV detection at 200 nm to determine the quantity of arachidonic acid (AA, retention time at 11.7 min) released from SAPC by cPLA2. The comparison of the peak area obtained for arachidonic acid (AA) in the control (no inhibitor), with the peak area of arachidonic acid (AA) in the palmostatin B treated sample permit to evaluate the inhibitory effect of palmostatin B on cPLA2. No inhibition was observed at 1 μM and 10 μM palmostatin B (**14**) concentrations. A known cPLA2 inhibitor was used to validate the assay and all activity measurements were performed in triplicate (Figure 1.29).

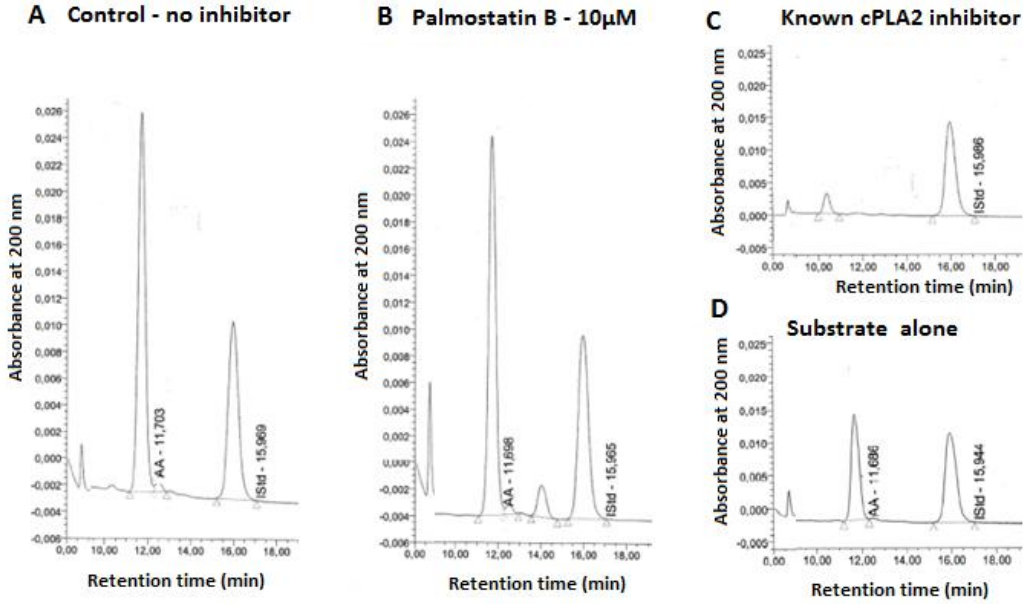

Sample name	AA Area	IStd Area	Average (AA/IStd)	Std (AA/IStd)	cPLA2 residual
Negative	687673	476703	1,430579	0,076071	**100+/- 5%**
PALMB 10 µM	699027	490699	1,434876	0,038552	**100+/- 2%**
PLA2 inhibitor	392885	479828	0,818803	-	**56.6 %**

Figure 1.29 Investigation of cytosolic phospholipase A2. HPLC analysis showing the amount of arachidonic acid (AA) released from 1-stearoyl-2-arachidonoyl-*sn*-glycero-3-phosphocholine (SAPC) by cPLA2. A) In absence of inhibitor (negative control). B) In presence of palmostatin B (10 µM). C) In presence of a known cPLA2 inhibitor at 33 nM (positive control). D) HPLC analysis of the substrate SAPC used in the assay ensuring the absence of disturbing peak in the area of the AA peak (t = 11.7 min). E) Evaluation of cPLA2 remaining activity by comparison of the ratio AA/IStd between positive controls (no inhibitor), and in presence of 10 µM palmostatin B (**14**). Std = Standard deviation.

Phospholipase A1 (PLA1)

PLA1 inhibition was monitored directly using the EnzChek® Phospholipase A1 substrate (PED-A1) which is a dye-labeled glycerophosphoethanolamine with BODIPY® FL dye-labeled acyl chain at the *sn*-1 position and dinitrophenyl quencher-modified head group. The BODIPY® FL pentanoic acid entity is released by cleavage of the substrate by PLA1 in the *sn*-1 position leading to an increased fluorescence. The assay developed with MDCK-F3 cell lysates as PLA1-containing sample, was validated by using a bacterial recombinant PLA1 enzyme. After incubation of the inhibitor/DMSO with MDCK-F3 cell lysate for 2 min. at 37°C, PLA1 substrate (PED-A1) was added and the increase of fluorescence measured over time. The remaining PLA1 activity after palmostatin B treatment (1 µM, 10 µM and 50 µM) was determined by linear regression analyses ($r^2 \geq 0.98$) of the fluorescence emission increase over time. The background reaction

rate with no enzyme present was subtracted and reaction rates were normalized to the reaction rate with no inhibitor present (100%). Figure 1.30 shows the curves obtained for PLA1 inhibition showing 75+/-4% PLA1 remaining activity at 50 µM palmostatin B, 88+/-3% PLA1 remaining activity at 10 µM palmostatin B, and no inhibition at 1 µM palmostatin B (Z' = 0.90).

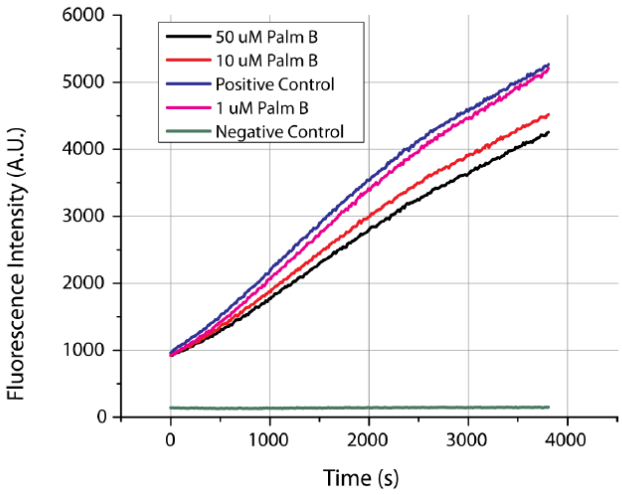

Figure 1.30 Investigation of phospholipase A1. Typical activity curves obtained for PLA1 activity respectively at 1 µM, 10 µM and 50 µM palmostatin B concentration.

Phospholipase D (PLD)

PLD inhibition was monitored indirectly using the Amplex Red reagent (10-acetyl-3,7-dihydrophenoxazine), a sensitive fluorogenic probe for H_2O_2. First, PLD cleaves the phosphatidylcholine (lecithin) substrate yielding choline and phosphatidic acid. Second, choline is oxidized by choline oxidase to betaine and H_2O_2. Finally, H_2O_2 in the presence of horseradish peroxidise reacts with Amplex Red reagent in a 1:1 stoechiometry to generate the fluorescent product, resorufin. The assay was developed with MDCK-F3 cell lysates as PLD-containing sample and was validated by using a bacterial recombinant PLD enzyme. H_2O_2 was used as second positive control of the reporter system. After incubation of the inhibitor/DMSO with MDCK-F3 cell lysate for 2 min. at 37°C, Amplex Red reagent was added as a solution in buffer containing HRP, choline oxidase and lecithin and the formation of fluorescent resorufin was recorded over time. The remaining PLD activity after palmostatin B treatment (50 µM) was determined by linear regression analyses ($r^2 \geq 0.98$) of the fluorescence emission increase over time. The background reaction rate with no enzyme present was subtracted and reaction rates were normalized to the reaction rate with no inhibitor present (100%). No inhibition of PLD was observed at 50 µM palmostatin B (Figure 1.31).

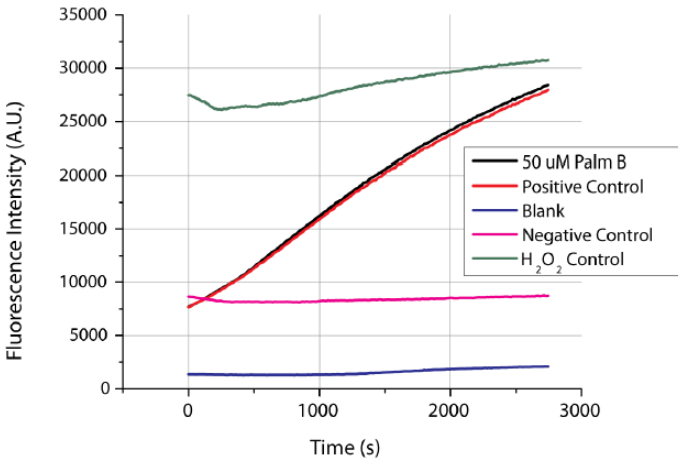

Figure 1.31 Investigation of phospholipase D. No inhibition of PLD by palmostatin B at 50 µM. Typical curves for PLD activity at 50 µM palmostatin B. Data based on three independent experiments (Z'= 0.95).

2.3 2nd generation of β-lactone APT1 inhibitors based on natural substrates

2.3.1 Design based on natural substrate considerations

Subsequently to the discovery of palmostatin B, a 2nd generation of *trans* β-lactone inhibitors was designed based on structural similarity with the native APT1 substrates lysophospholipid and *H*-Ras C-terminus presenting common recognition motifs such as an electronegative group at a distance of five to six bonds from a (thio)ester functionality and an electropositive tail at ten to twelve bonds distance (Figure 1.32A). These considerations led to a proposed assembly consisting in a (thio)ester, phosphate and dimethylamino group subsequently replaced by a β-lactone, sulfone and dimethylamino group preferred for convenient synthesis. The sulfone and amino group containing fragment was fused using a variable spacer to a *trans* β-lactone core and a lipophilic tail mimicking palmitic acid, which served well for palmostatin B (**14**), was introduced on the opposite side of the β-lactone core to create affinity for the enzyme lipid-binding pocket. The inhibitor design was further evaluated *in silico* (Steffen Renner), showing strong hydrogen bond stabilizing interactions in the APT1 active site at polar residues glutamine Q114 and leucine L25, with the inhibitor covalently bound to the nucleophilic residue serine S114. Moreover, polar head groups (sulfone and dimethylamino groups) were shown to create additional electrostatic stabilizing interactions with the threonine T28 and histidine H203 residue of two different APT1 monomers. Such interactions were therefore thought to enhance the inhibitory activity by stabilizing APT1 under a dimerized inactive form with an active site no longer accessible (Figure 1.32B). Based on these criteria, a small focussed library of three series of inhibitors denoted A-C

was synthesized by C. Hedberg and F. Dekker with variation in spacer length for optimal hydrogen bond stabilizing interactions in the enzyme active site.

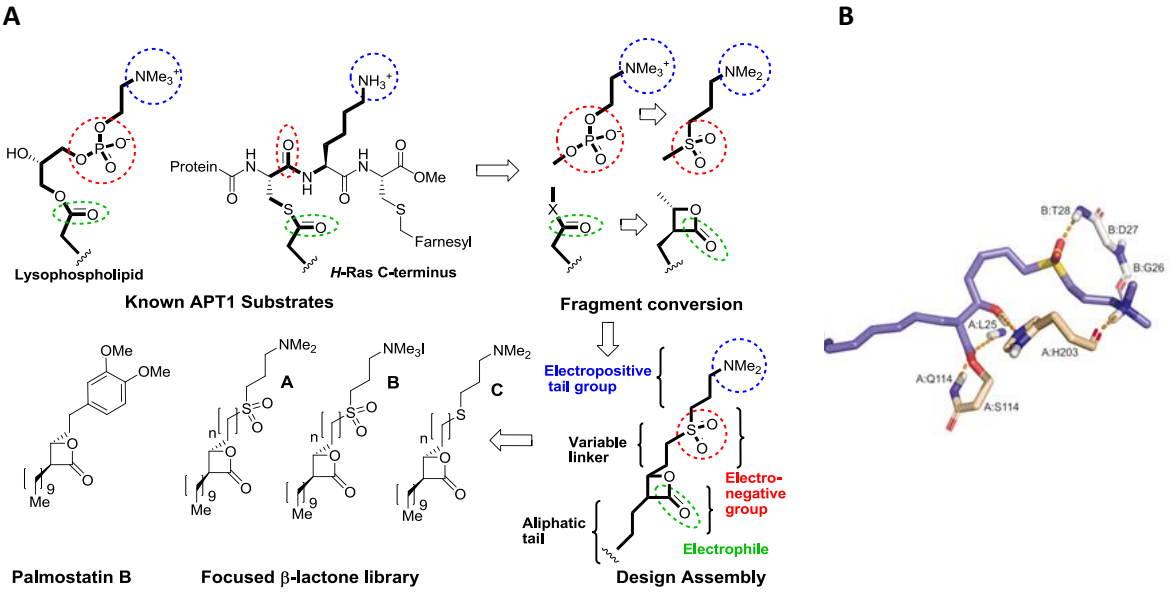

Figure 1.32 Design of 2nd generation β-lactone inhibitors. A) Design based on natural substrate considerations. B) Docking studies showing the postulated importance of polar head groups (-SO_2 and –NMe_2) to stabilize APT1 under an inactive dimerized form via hydrogen bond stabilizing interactions at residue T28 and H203.

2.3.2 IC_{50} re-evaluation of the β-lactone library

The complete β-lactone library, previously screened for APT1 inhibition by C. Hedberg and F. Dekker using the colorimetric assay after 30 min pre-incubation, revealed a significantly higher inhibitory effect of (*S,S*) β-lactone inhibitors over (*R,R*) β-lactone inhibitors. IC_{50} values of the more potent (*S,S*) β-lactone inhibitors were subsequently re-evaluated employing the developed fluorometric assay after 2 min. incubation time, revealing a slow enzyme reactivation. The maximal APT1 inhibition was visualized typically after 5 min. measurement time, after which the enzyme starts to be reactivated. The slope after 5 min. measurement was used for the calculation leading to significantly improved IC_{50} values generally 100 folds lower as the values determined earlier (Figure 1.33). Results obtained using the two assays were consistent as shown by the comparison of Figure 1.33A with Figure 1.33B, with an invariable superiority of lactones with a spacer length of 4-5 carbons and a sulfone moiety (as pointed out by docking studies). Some IC_{50} values are below half of the enzyme concentration, thereby suggesting the stabilization of the enzyme in a dimerized form, as predicted by docking studies. Subsequently,

the more potent APT1 inhibitor compound **28** (IC_{50} = 2.13+/-0.31 nM) was chosen for additional *in-cellulo* experiments and named palmostatin M.

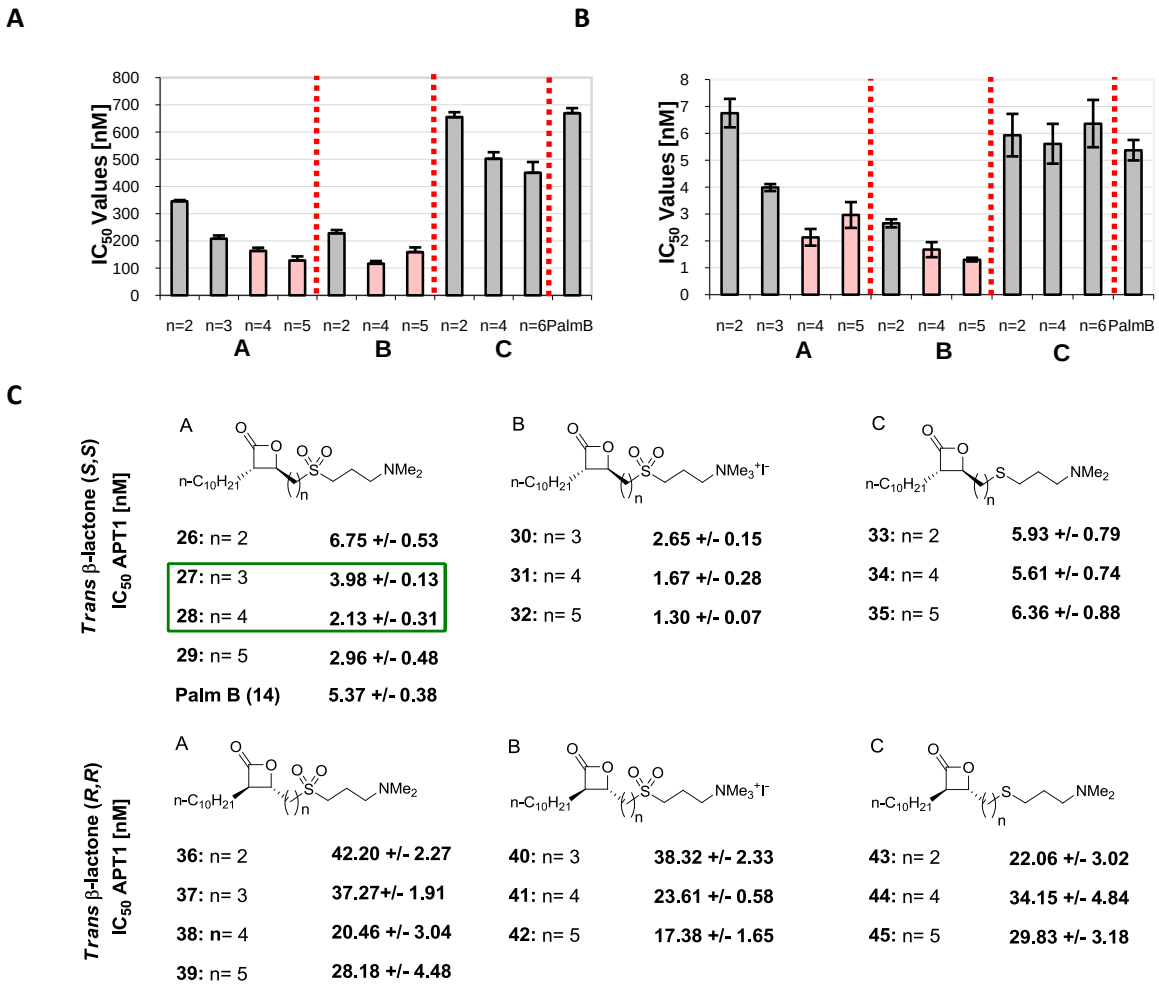

Figure 1.33 IC_{50} re-evaluation of the β-lactone library. A) Graphical representation of IC_{50} values obtained for the *trans* β-lactone (*S,S*) of series A, B and C (**26-45**) using the colorometric assay compared with palmostatin B (APT1 = 75 nM, PNPO= 600 µM, 30 min inhibitor pre-incubation). B) Graphical representation of IC_{50} values obtained for *trans* β-lactone (*S,S*) of series A, B and C using the fluorometric assay compared with palmostatin B (APT1= 5 nM, DiFMUO= 15 µM, Ex/Emi.= 358/455 nm, gain= 100, 2 min inhibitor pre-incubation time). C) Table displaying IC_{50} values for APT1 inhibition obtained for the complete *trans* β-lactone library employing the fluorometric assay described above. Z' factors were in all cases higher than 0.75. Data based on three independent experiments.

2.3.3 Enzyme reactivation over time

In order to monitor the enzyme reactivation, after complete APT1 inhibition ensured by a large excess of inhibitor, the consumption of the fluorogenic substrate DiFMUO by reactivated APT1 was recorded over time. The enzyme reactivation occurs through the hydrolysis of the covalently bound inhibitor-APT1 complex, associated with the conversion of the inhibitor to the

β-hydroxy acid (Figure 1.34A). As a result, a significant fluorescence increase was observed over time in the developed biochemical assay (Figure 1.34B).

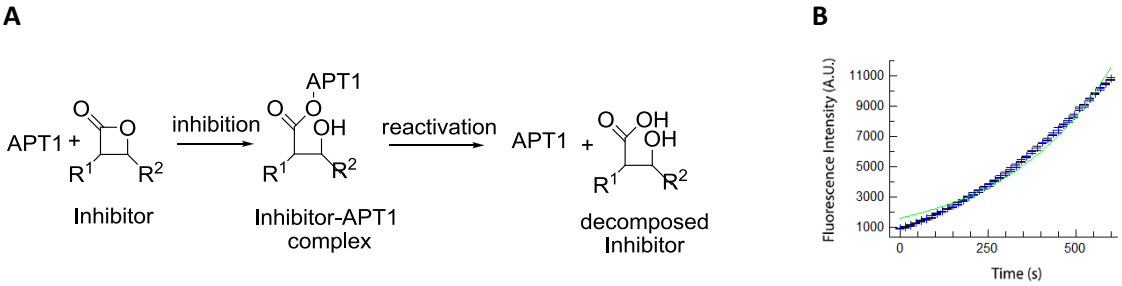

Figure 1.34 APT1 reactivation over time. A) Inhibition of APT1 by β-lactone inhibitors followed by the enzyme reactivation through the hydrolysis of the inhibitor-APT1 complex. B) APT1 reactivation curve observed after complete enzyme inhibition with an excess of palmostatin B (**14**).

Investigation on (*S,S*) β-lactone inhibitors from series A, B and C (**26 - 35**) revealed half life ($t_{1/2}$) values for APT1 reactivation in the range of 2 to 3 minutes. Palmostatin B (**14**) is also affected with a $t_{1/2}$ value in a similar range (Table 1.1).

Compound (*S,S*)	Reactivation rate [sec $^{-1}$]	$t_{1/2}$ [min]
A 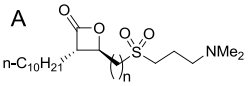		
26: n= 2	$4{,}39*10^{-3}$ +/- $1{,}41*10^{-4}$	2,6 +/- 0.1
27: n= 3	$3{,}97*10^{-3}$ +/- $1{,}02*10^{-4}$	2,9 +/- 0.1
28: n= 4	$3{,}27*10^{-3}$ +/- $8{,}69*10^{-5}$	3,5 +/- 0.1
29: n= 5	$4{,}23*10^{-3}$ +/- $1{,}12*10^{-4}$	2,7 +/- 0.1
B 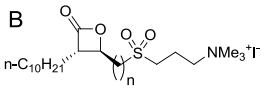		
30: n= 3	$3{,}85*10^{-3}$ +/- $1{,}16*10^{-4}$	3,0 +/- 0.1
31: n= 4	$3{,}51*10^{-3}$ +/- $8{,}98*10^{-5}$	3,3 +/- 0.0
32: n= 5	$3{,}89*10^{-3}$ +/-$1{,}09*10^{-4}$	3,0 +/- 0.1
C 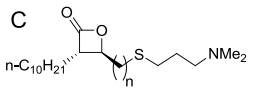		
33: n= 2	$5{,}39*10^{-3}$ +/- $1{,}86*10^{-4}$	2,1 +/- 0.1
34: n= 4	$4{,}31*10^{-3}$ +/- $1{,}27*10^{-4}$	2,7 +/- 0.0
35: n= 5	$4{,}26*10^{-3}$ +/- $1{,}27*10^{-4}$	2,7 +/-0.1
PalmB (14)	$3{,}30*10^{-3}$ +/- $8{,}22*10^{-5}$	3,5 +/- 0.1

Table 1.1 Evaluation of APT1 reactivation. Reactivation characteristics determined for (*S,S*) β-lactone inhibitors (**26-35**) and their comparison with palmostatin B (**14**), with reactivation rates given in sec^{-1} and half-life $t_{1/2}$ in minutes.

2.3.4 Resynthesis of the most potent inhibitors (27, Palm M 28)

To further characterize the β-lactone inhibitors in cell-based assays, the two most potent APT1 inhibitors **27** and palmostatin M (**28**) were chosen and re-synthesized. The synthesis commenced with the conversion of commercially available *N,N*-dimethylamino-1-propyl chloride hydrochloride **46** into *N,N*-(dimethylamino)propyl thioacetate **47** in 82% yield using thioacetic acid and triethylamine. Subsequent S-alkylation using iodo esters **48-49** (prepared from the corresponding bromo ester through a Finkelstein reaction)[131] and Cs_2CO_3 furnished amino ethyl esters **50-51**. Reduction of esters **50-51** to alcohols **52-53** followed by Swern oxidation yielded aldehydes **54-55** (Scheme 1.4).

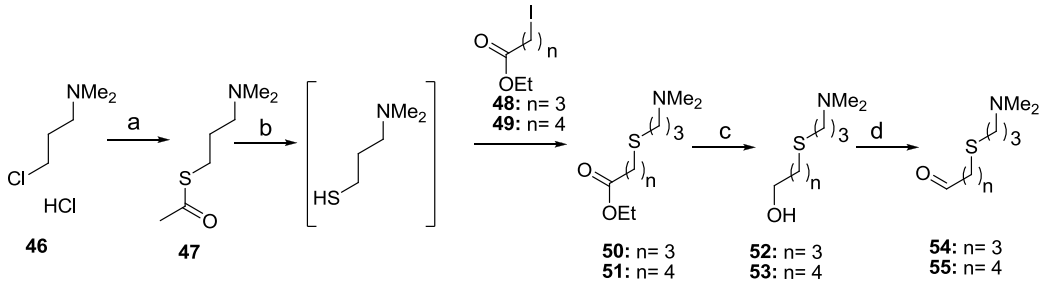

Scheme 1.4 Synthesis of aldehyde spacers **54** (n= 3) and **55** (n=4). Reagents and conditions: a) AcSH (1.2 eqv.), NEt_3 (3.0 eqv.), $CHCl_3$, reflux, 18h, 82%. b) Cs_2CO_3 (1.1 eqv.), EtOH, reflux, 2.5h, iodoester **48** or **49** (1.1 eqv.), 40°C (18h), 92% (**50**, n=3), 97% (**51**, n=4). c) $LiAlH_4$ (1.25 eqv.), THF, 0°C (1h) then rt (2h), 91% (**52**, n=3), 93% (**53**, n=4). d) DMSO (2.4 eqv.), oxalyl chlorid (1.1 eqv.), NEt_3 (3.65 eqv.), CH_2Cl_2, 73% (**54**, n=3), 85% (**55**, n=4).

Aldehydes **54-55** were involved into an *anti*-selective aldol reaction[118] with *O*-dodecylated ephedrine auxiliary **10** in presence of dicyclohexylborontriflate and triethylamine leading to the aldol reaction products **56-57**, subsequently oxidized to sulfone**s 58-59** using oxone®.[132] Auxiliary removal from **58-59** by hydrogenolysis furnished β-hydroxyacids **60-61**, subsequently cyclized using phenylsulfonyl chloride in pyridine[122,123] leading to compound **27** and **28** (Scheme 1.5).

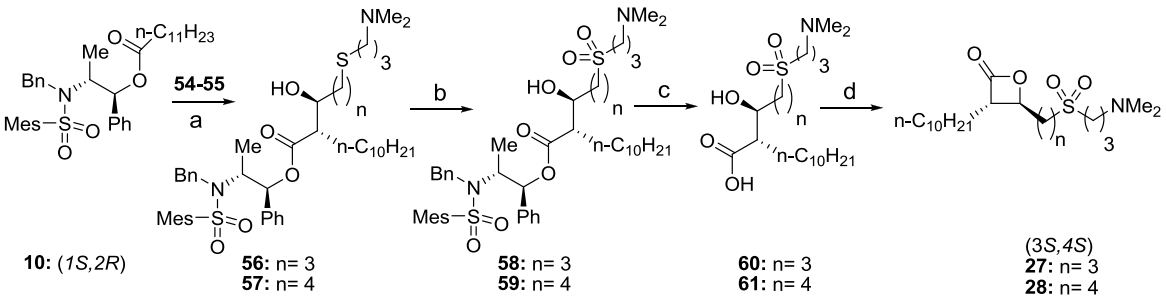

Scheme 1.5 Synthesis of *trans* β–lactone inhibitors palmostatin M (**28**) and **27**. Reagents and conditions: a) Aux **10** (1.2 eqv.), NEt_3 (2.5 eqv.), c-Hex_2BOTf (2.2 eqv.), CH_2Cl_2, -78°C, 2h then aldehyde **54**-**55** (1.0 eqv.), -78°C (1h), 0°C (2h) and rt (1h), 40% (**56**, n=3), 33% (**57**, n=4). b) Oxone® (3.0 eqv.), MeOH/H_2O, rt (8h), 91% (**58**, n=3), Quant. (**59**, n=4). c) $Pd(OH)_2$/C, H_2, MeOH, 40°C (6h), 65% (**60**, n=3), 77% (**61**, n=4). d) $PhSO_2Cl$ (3.0 eqv.), pyridine, 0°C, overnight, 98% (**27**, n=3), 92% (**28**, n=4).

2.3.5 Investigation of *cis* β-lactone inhibitors

To confirm the superiority of *trans* β-lactones already pointed out with the palmostatins, *cis* β-lactone inhibitors derived from the two more potent *trans* β-lactones palmostatin M (**28**) and **27** were synthesized. Therefore, *O*-dodecylated ephedrine auxiliary **63** was synthesized by analogy to its enantiomer **10** by acylation of (*1R,2S*)-norephedrine derived alcohol **62** with dodecanoyl chloride. Both *O*-dodecylated ephedrine auxiliary enantiomers **10** and **63** were subsequently involved into a *cis*-selective aldol reaction with the two previously synthesized aldehydes **54**-**55** in the presence of dibutylborontriflate (*n*-Bu_2BOTf) and diisopropylethylamine (DIPEA) leading to *cis*-aldol reaction products **64-67**. β-Hydroxyesters **64-67** were subsequently oxidized to sulfones **68-71** employing oxone®[132] and the chiral auxiliary was removed by hydrogenolysis leading to β–hydroxyacids **72-75**. Cyclization of **72-75** using phenylsulfonyl chloride in pyridine concluded the synthesis of *cis* β-lactone inhibitors **76-79** (Scheme 1.6).

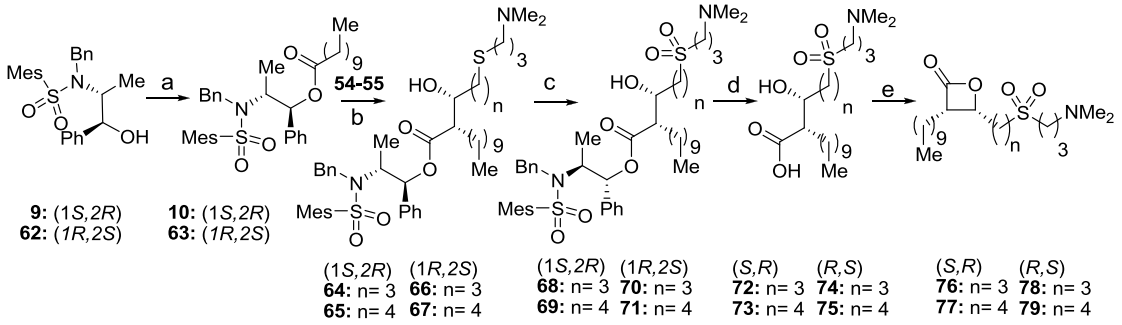

Scheme 1.6 Synthesis of *cis* β-lactone inhibitors **76**-**79**. Reagents and conditions: a) pyridine (1.3 eqv.), dodecanoyl chloride (1.0 eqv.), CH_2Cl_2, rt (15h), 87% yield for **10**, 80% yield for **63**. b) Aux **10** or **63** (1.0 eqv.), DIPEA (2.5 eqv.), n-Bu_2BOTf (2.2 eqv.), CH_2Cl_2, -78°C (2h) then aldehyde **54** or **55** (1.2 eqv.), -78°C (1h), 0°C (1h), rt (1h), 36-55% yield. c) Oxone® (3.0 eqv.), MeOH/H_2O, rt (8h), 92-81% yield. d) $Pd(OH)_2$/C, H_2, MeOH, rt (90h), 29-79% yield. e) $PhSO_2Cl$ (3.0 eqv.), pyridine, 0°C, overnight, 13-55% yield.

For a comparison with their *trans*-homologues palmostatin M (**28**) and **27**, *cis* β-lactones **76-79** were screened for APT1 inhibition under strictly identical conditions using the fluorometric assay. In conclusion, and consistent with IC_{50} values evaluated for the palmostatins, (*R,S*)-*cis* β-lactones **78**-**79** were slightly less potent compared to their (*S,S*)-*trans* diastereoisomers **27** -**28**, but far more potent than (*R,R*)-*trans* β–lactones **37-38** and (*S,R*)-*cis* β-lactone inhibitors **76-77.** This observation is in full agreement with the stereochemistry of the β-lactone core chosen for the design of the 2nd generation of inhibitors using preliminary results for palmostatin A-D as guiding arguments. Moreover, the configuration of the tail holding the polar residues allowing hydrogen bond stabilizations in the enzyme active site, was shown to be important for the

inhibitory activity. In contrast, the orientation of the lipid tail seems to be much more flexible as shown by a similar potency of compounds **27**-**28** and compounds **78**-**79** (Figure 1.35)**.**

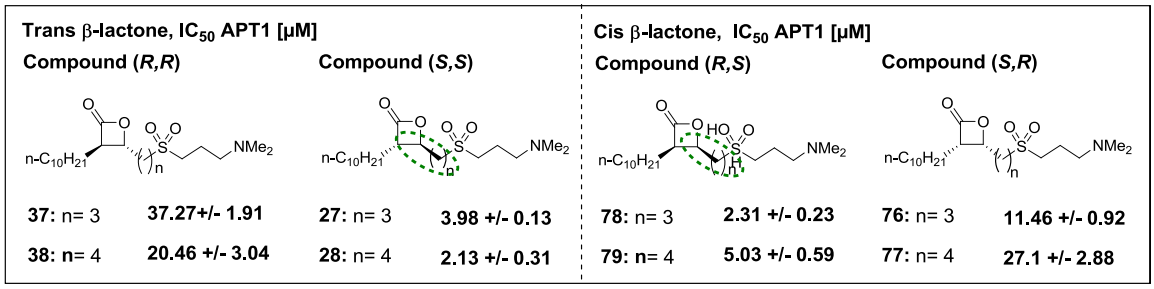

Figure 1.35 Evaluation of the cis β-lactones for APT1 inhibition. IC_{50} values for APT1 inhibition obtained for the *cis* β-lactone inhibitors **76-79** compared to their *trans*-homoloques using the fluorometric assay (APT1= 5nM, DiFMUO= 15μM, Ex/Emi.= 358/455nm, gain= 100, 2 min inhibitor pre-incubation time), Z' factors were in all cases higher than 0.75.

2.3.6 Cellular evaluation of palmostatin M and B

Phenotypic reversion in transformed MDCK-F3 cells

(S,S) trans β-lactones from sub-libraries A,B and C (**26-35**) were subjected to a back-transformation assay (data from Claas Gerding-Reimers) in which *H*-RasG12V-transformed MDCK-F3 cells were subjected to chronic overnight incubation with a high, but non-cytotoxic inhibitor concentration (30 μM) to ensure that—despite inhibitor consumption through hydrolysis—the inhibitor concentration remained high enough to fully suppress APT1 activity. *H*-RasG12V-transformed MDCK-F3 cells are characterized by a long and spindle-like phenotype with reduced cell-cell contact, thereby allowing their clear distinction from untransformed MDCK cells. Down-regulation of oncogenic Ras signaling would result in a partial phenotypic reversion,[25] characterized by change in cell morphology (from spindle-shaped to more round-shaped) and by the restoration of cell adhesion and cadherin expression at the cell-cell contact sites. Compounds from cationic sub-library B (**30-32**), which proved to be potent APT1 inhibitors in the biochemical assay, had none or minor activity in cells, possibly due their poor cell permeability. Nevertheless, compounds from sub-library A (**26-29**) and C (**33-35**) induce a partial phenotypic reversion in transformed MDCK-F3 cells among which palmostatin M (**28**) turned out to be the most potent compound. Palmostatin M was clearly superior to palmostatin B (**14**) judging by E-cadherin expression at the cell surface. Moreover, the phenoptypic reversion induced by Palmostatin M was comparable to the effect observed when using the MEK inhibitor U0126,[133] a known inhibitor of the Raf/MEK/ERK signaling pathway downstream of Ras (Figure 1.36).

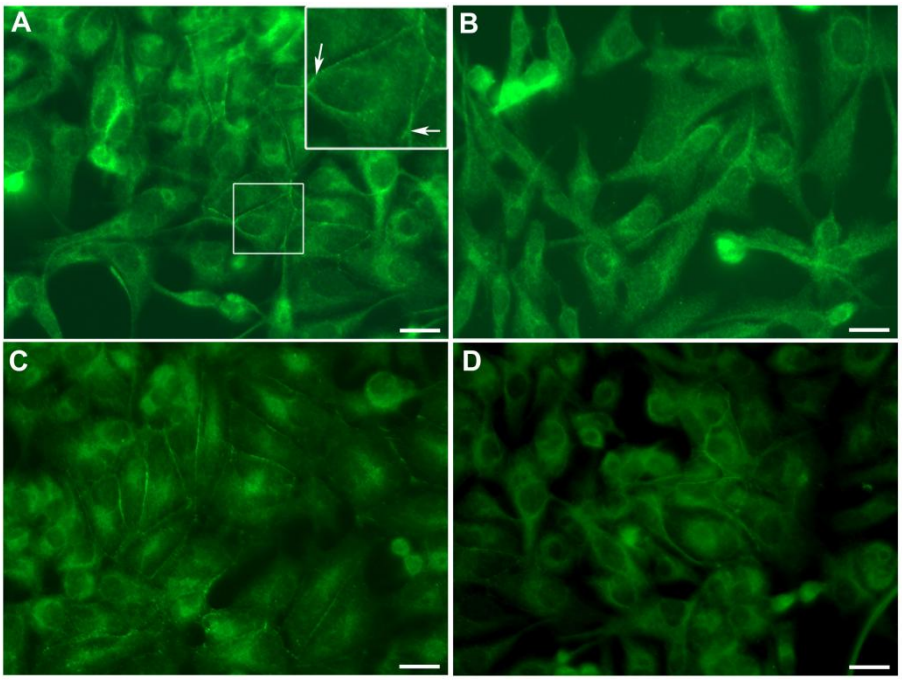

Figure 1.36 Palmostatin M-induced phenotypic reversion of MDCK-F3 cells. A) E-cadherin immuno staining of HRasG12V-transformed MDCK-F3 cells showing the restoration of E-cadherin expression at the cell-cell interfaces (arrow-heads) after treatment with 10 μM palmostatin M (**28**), compared to a DMSO control (B). C) HRasG12V-transformed MDCK-F3 cells treated with palmostatin B (**14**) at 50 μM showing a similar, but weaker effect on the phenotype. D) HRasG12V-transformed MDCK-F3 cells treated with the known MEK-inhibitor U0126 (30 μM) used as positive control. Scale bars represent 20 μm. Data from Claas Gerding-Reimers.

Influence on the MAPK signaling pathway

To demonstrate that oncogenic *H*-Ras maintains the transformed phenotype through the Raf/MEK/ERK signaling pathway, the influence of palmostatin M (**28**) was further investigated *in-cellulo* by Western blotting experiments to visualize ERK phosphorylation. Upon epidermal growth factor (EGF) activation, Ras is activated as Ras:GTP mediated by SHC-GRB2-SOS, thereby activating the MAPK signaling pathway through phosphorylation of Raf, MEK followed by ERK. Therefore, Ras delocalization induced by palmostatin M (**28**), due to APT1-inhibition, is expected to affect EGF-induced Ras activity, thus leading to a visible attenuation of downstream $ERK_{1/2}$ phosphorylation. To validate this hypothesis, several Western blotting experiments were performed in HeLa and MDCK-F3 cells to monitor $ERK_{1/2}$ activation after treatment with various palmostatin M (**28**) concentrations. A known inhibitor of the MAPK signaling pathway, U0126 (MEK inhibitor) was used as positive control.

ERK blots for HeLa cells

After EGF activation, the influence of palmostatin M (**28**) on $ERK_{1/2}$ phosphorylation was investigated at several inhibitor concentrations and compared to a sample treated with DMSO. Signals for phospho $ERK_{1/2}$ (Figure 1.37A) and total $ERK_{1/2}$ (Figure 1.37B) were subsequently quantified and the ratio phospho $ERK_{1/2}$/total $ERK_{1/2}$ normalized to 100% using the sample treated with DMSO (Figure 1.37C). A non-EGF activated sample was used as negative control, showing as expected no induced $ERK_{1/2}$ phosphorylation. A concentration-dependent effect of palmostatin M (**28**) on $ERK_{1/2}$ phosphorylation was observed with an approximate 50% reduction of $ERK_{1/2}$ phosphorylation observed at 5 µM palmostatin M concentration. The MEK inhibitor U0126 used as additional positive control surprisingly did not reduce $ERK_{1/2}$ phosphorylation at 30 µM concentration. Confronted with reproducibility problems and to confirm the results, similar experiments were subsequently performed using MDCK-F3 cells with mutated H-Ras (Figure 1.37).

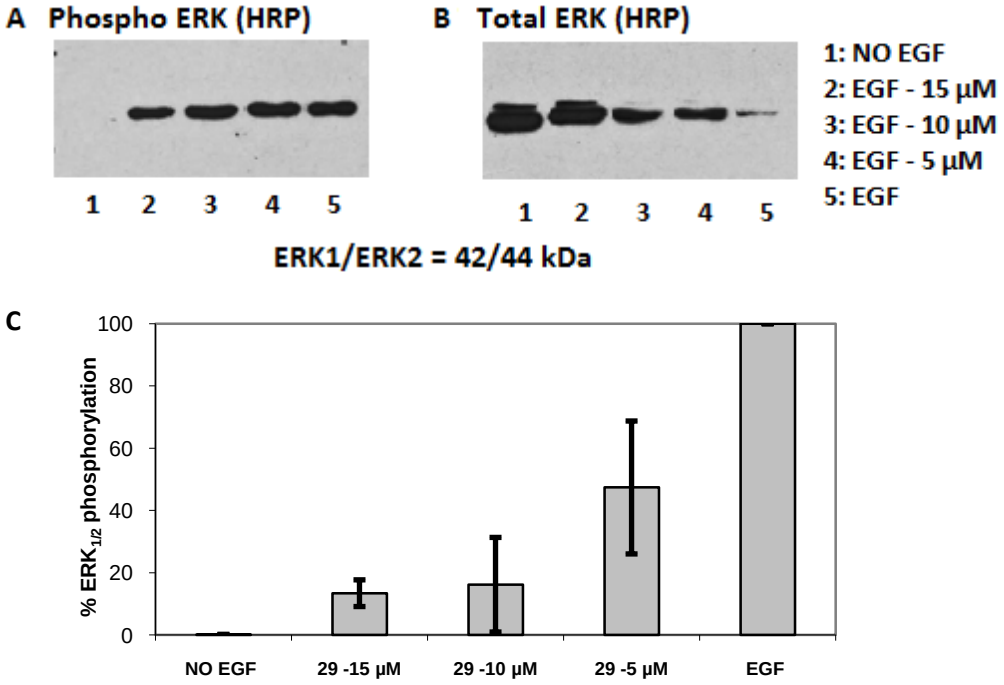

Figure 1.37 Palmostatin B affects MAPK signaling in HeLa cells. Western blotting experiments for $ERK_{1/2}$ phosphorylation in HeLa cells (HRP detection system) at various palmostatin M (**28**) concentrations (15 µM, 10 µM, 5 µM). A) Phospho-$ERK_{1/2}$ Western blotting using Supersignal® West Pico Chemiluminescent substrate after 2h exposure. Phospho-$ERK_{1/2}$ antibody (1/10 000) in TBST 2% chocolate slimfast (overnight at 4°C), IgG mouse (1/20 000) in TBST (1h, rt). B) Total-ERK Western blotting using Supersignal® West Pico Chemiluminescent substrate after overnight exposure. Total-ERK antibody (1/1 000) in TBST 2% BSA (over night at 4°C), IgG rabbit (1/10 000) in TBST (1h, rt). C) Graphical representation of the effect of palmostatin M (**28**) and U0126 at various concentrations, on $ERK_{1/2}$ phosphorylation. Data based on two independent experiments.

ERK blots for MDCK-F3 cells

A similar protocol was followed to investigate the influence of palmostatin M (**28**) on MDCK-F3 cells with mutated H-Ras. Consistent with earlier results, a concentration-dependent effect was observed with 50% reduction of $ERK_{1/2}$ phosphorylation at 10 µM palmostatin M (**28**), a value in a similar range as observed for HeLa cells. However, due to the constitutively active character of Ras in this cell line, a higher reproducibility of the results was observed compared to earlier experiments performed in HeLa cells. $ERK_{1/2}$ phosphorylation was normalized to 100% corresponding to the sample treated with DMSO which, given the characteristic of the cell line, was similar to the inactivated sample (no EGF-treated sample). Unlike in HeLa cells, the MEK inhibitor U0126 used as positive control reduces the Raf/MEK/ERK signaling by 30% at 30 µM concentration (Figure 1.38).

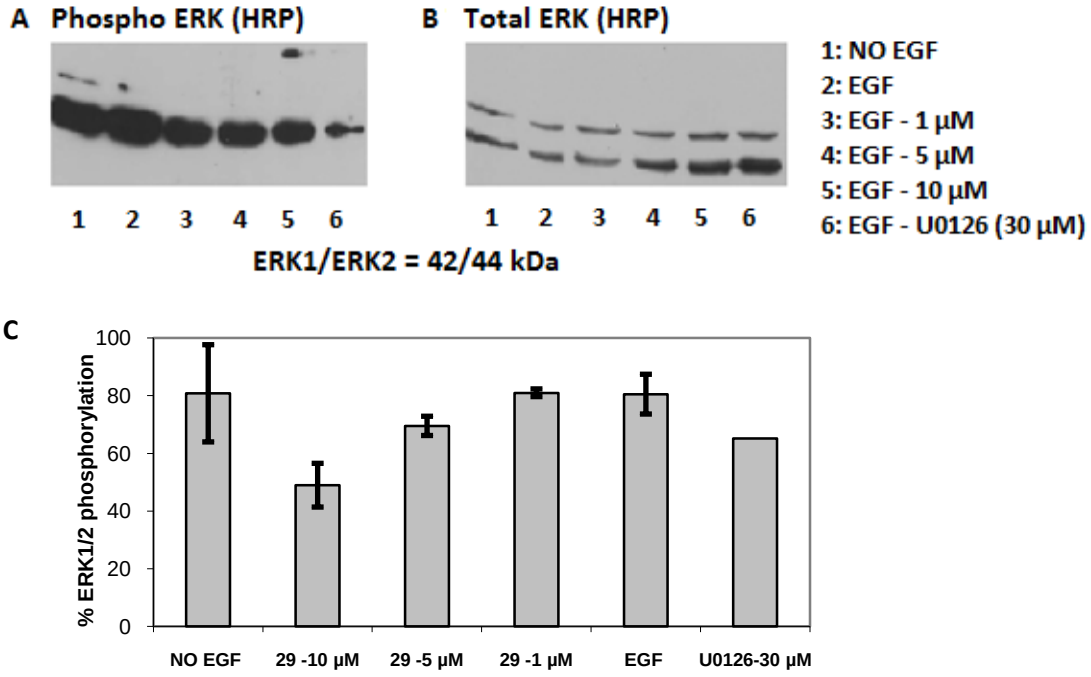

Figure 1.38 Palmostatin B affects MAPK signaling in MDCK-F3 cells. Western blotting experiments for $ERK_{1/2}$ phosphorylation in MDCK-F3 cells (HRP detection system) at various palmostatin M (**28**) concentrations (1 µM, 5 µM, 10 µM) and U0126 (30 µM, MEK inhibitor) as positive control. A) Phospho-$ERK_{1/2}$ Western blotting using Supersignal® West Femto Chemiluminescent substrate after 15 minutes exposure. Phospho-$ERK_{1/2}$ antibody (1/10 000) in TBST 2% chocolate slimfast (overnight at 4°C), IgG mouse (1/20 000) in TBST (1h, rt). B) Total-ERK Western blotting using Supersignal® West Pico Chemiluminescent substrate after 10 min exposure. Total-ERK antibody (1/1 000) in TBST 2% BSA (overnight at 4°C), IgG rabbit (1/10 000) in TBST (1h, rt). C) Graphical representation of the effect of palmostatin M (**28**) and U0126 at various concentrations, on $ERK_{1/2}$ phosphorylation. Data are based on three independent experiments.

Disruption of Ras trafficking between the Golgi and the plasma membrane

Palmostatin M (**28**) would be expected to interrupt the dynamic trafficking of *H*- and *N*-Ras between the Golgi and the plasma membrane (PM), whereas unpalmitoylated *K*-Ras should not be affected. To validate this hypothesis, MDCK cells expressing the fluorescent protein fusion constructs mCitrine-*N*-Ras, mCitrine-*H*-Ras or mCitrine-*K*-Ras, together with an unpalmitoylatable mutant mCherry-*H*-RasC181S,C184S and a Golgi marker, were treated with palmostatin M (1 μM) for 3 hours (work by Nachiket Vartak). The influence of palmostatin M on *N*-, *H*- and *K*-Ras redistribution was evaluated by comparison with the solely prenylated unpalmitoylable *H*-RasC181S,C184S, known to distribute non-specifically to all membranes.[134] Palmostatin M (**28**) leads to a complete *N*-Ras mislocalization after 1 hour treatment, whereas *H*-Ras enrichment at the PM was not affected on this timescale. Instead, a complete depletion of *H*-Ras from the Golgi was observed (Figure 1.39).

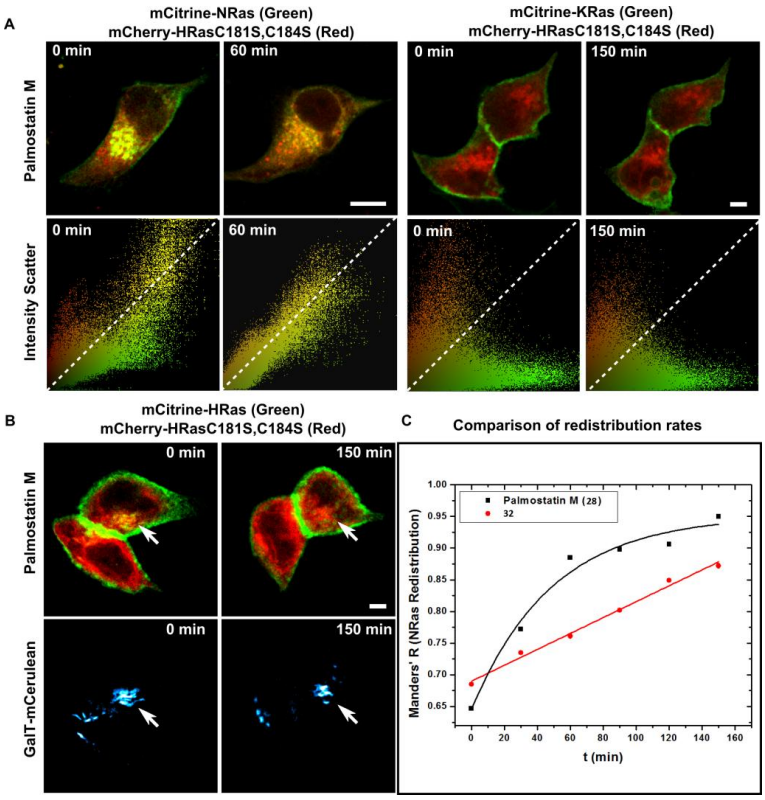

Figure 1.39 Disruption of Ras trafficking between Golgi and PM by palmostatin M. A)left: Co-localization of mCitrine-*N*-Ras and mCherry-*H*-RasC181S,C184S showing palmostatin M-induced mislocalization of mCitrine-*N*-Ras after 60 min. Right: similar experiments with mCitrine-*K*-Ras showing no effect on mCitrine-*K*-Ras localisation after 150 min. B) Similar experiments with mCitrine-*H*-Ras showing a minimal effect on *H*-Ras localisation at the plasma membrane after 150 min, but a complete depletion of mCitrine *H*-Ras on the Golgi (arrows), GalT-mCerulean is a Golgi marker. C) Graph showing a faster mCitrine-*N*-Ras aspecific redistribution upon treatment with palmostatin M (**28**) (black) compared to treatment with **32** (red). Data from Nachiket Vartak.

In addition, *K*-Ras localization was not affected, thereby demonstrating a specific effect of palmostatin M (**28**) on the acylation cycle. Consistent with earlier cellular evaluations, compound **32** from cationic sub-library B, which proved as potent as palmostatin M (**28**) *in-vitro*, was less effective than palmostatin M. Compound **32** induces a complete unspecific distribution of *N*-Ras after 3 hours, whereas only 1 hour is required for palmostatin M at similar 1µM concentration.

2.4 Identification of additional Ras depalmitoylating enzymes

2.4.1 Principle of activity-based proteome profiling (ABPP)

To confirm APT1 as a cellular target and to potentially identify additional target proteins relevant to the Ras cycle, *in-cellulo* activity-based proteome profiling (ABPP) experiments were performed using cell permeable ABPP pull down probes derived from palmostatin B and palmostatin M. In ABPP experiments, reactive chemical probes derived from active small molecules are employed to covalently bind to a nucleophilic residue of inhibited enzymes via an electrophilic group, thereby allowing the identification of target proteins. β-lactone ABPP probes have already served as useful tools for ABPP experiments conducted on bacterial,[135,136] plant,[137] as well as mammalian proteomes.[138] Figure 1.38 describes the chemical proteomic strategy employed for i*n-cellulo* labeling experiments. Cells were first incubated with cell permeable alkyne probes allowing their covalent binding to their target proteins through their reactive β-lactone groups. After cell lysis, target proteins were tagged through $Cu^{(I)}$-catalyzed Huisgen [3+2]-cycloaddition with a trifunctional fluorescent reporter group such as a biotin-rhodamine-azide construct allowing their enrichment using biotin/streptavidin affinity. After separation by SDS-gel electrophoresis, target proteins were detected by fluorescence read-out and were digested with trypsin to allow their identification by mass spectrometry (Figure 1.40).

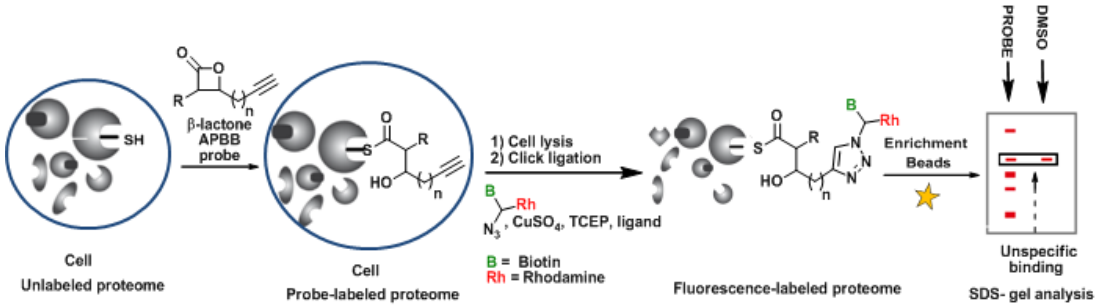

Figure 1.40 Principle of *in-cellulo* ABPP labeling experiments. After incubation with a cell permeable β-lactone probe, cells are lysed and target proteins subsequently fluorescently tagged by click ligation. In-gel fluorescence scanning, allow the visualization of the target proteins, subsequently identified by mass-spectrometry. Ligand = tris((1-benzyl-1H-1,2,3-triazol-4-yl)methyl)amine.

2.4.2 Design of cell permeable ABPP probes

Given the improved efficiency of alkyne-ABPP probes over azide-ABPP probes pointed out by Sieber and co-workers, several cell permeable ABPP-alkyne probes derived from palmostatin B and M were designed and synthesized. Subsequently, *in cellulo* labeling experiments were performed to clarify whether APT1 is the only Ras depalmitoylating enzyme or whether palmostatin B and M target additional proteins relevant to the Ras cycle, in particular the closely related isoenzyme APT2. The palmostatin B analogue **23** with an alkyne functionality embedded in its lipid chain, previously used for the synthesis of fluorescently labeled palmostatin B (**25**) was an obvious ABPP probe candidate. The compound **23** was subsequently validated as suitable pull down probe given its APT1 inhibitory activity similar to that of palmostatin B (Scheme 1.7A). An attractive approach for the synthesis of a palmostatin M derived probe could be the attachment of the alkyne functionality directly on palmostatin M through quarterisation of the amino functionality. However given that compounds from cationic sub-library B (**30-32)**, which were potent APT1 inhibitors *in-vitro*, had only weak activity in cellular assays, such probes may therefore be inappropriate for *in-vivo* labeling experiments, possibly due cell permeability issues. Instead, two regioisomeric palmostatin M-derived ABPP probes (**83** and **94**) were designed and synthesized with an alkyne group introduced at opposing sites of the molecule to maximize the accessibility of the alkyne group for the $Cu^{(I)}$-catalysed [3+2]-cycloaddition, when covalently bound into enzyme active sites. The two ABPP probes **83** and **94** turned out to be as potent as palmostatin M (**28**) for APT1 inhibition using the fluorometric assay, therefore constituting suitable pull down probes to target APT1 *in cellulo* (Scheme 1.7).

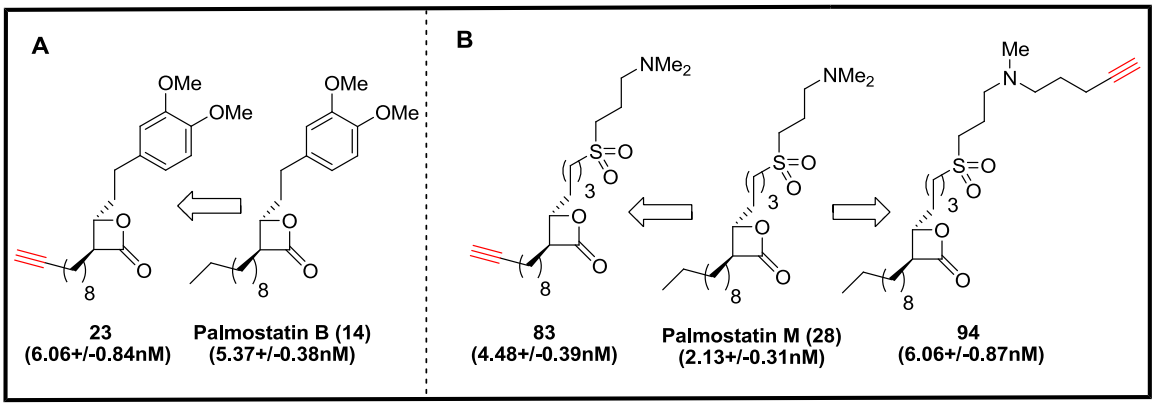

Scheme 1.7 Design of suitable ABPP alkyne probes. A) Design of palmostatin B-derived probe **23** showing a quasi-similar APT1 inhibitory activity as palmostatin B (**14**). B) Design of palmostatin M-derived probes **83** and **94,** showing a quasi-similar APT1 inhibitory activity as palmostatin M (**28**). IC_{50} values obtained using the APT1 fluorometric assay (APT1= 5 nM, DiFMUO= 15 µM, Ex/Emi.= 358/455 nm, gain= 100, 2 min inhibitor pre-incubation time). Data based on three independent measurements with Z'> 0.85.

2.4.3 Synthesis of palmostatin M-derived probes

A conceptually similar strategy as for the synthesis of the *trans* β-lactone library was used for the synthesis of palmostatin M-derived probe **83**. The synthesis of compound **83** commenced with a dicyclohexyl-borontriflate-mediated *anti* aldol-reactionbetween aldehyde **55** and *O*-dodecylated ephedrine derivative **20**.[120] Subsequent *S*-oxidationof compound **80** with an excess of Oxone® in aqueous methanol yielded sulfone **81**.[132] Auxiliary removal from β-hydroxy ester **81** by hydrolysis provided β-hydroxy acid **82** without epimerization. Subsequent β-lactonization with phenylsulfonyl chloride in pyridine concluded the synthesis of the ABPP probe **83** (Scheme 1.8).[21,22]

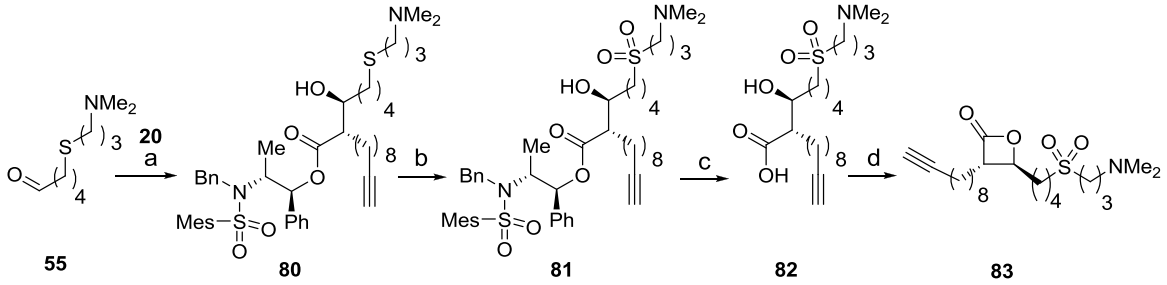

Scheme 1.8 Synthesis of palmostatin M-derived probe **83**. Reagents and conditions: a) Aux **20** (1.2 eqv.), NEt_3 (2.5 eqv.), c-Hex_2BOTf (2.2 eqv.), CH_2Cl_2, -78°C, 2h then aldehyde **55** (1.0 eqv.), -78°C (1h), 0°C (1h), then rt (1h), 66% yield. b) Oxone® (3.0 eqv.), MeOH/H_2O 2/1, rt (8h), quantitative. c) LiOH.H_2O (4.3 eqv.), Dioxane/H_2O 4/1, 40°C (48 h), 85% yield. d) $PhSO_2Cl$ (3.0 eqv.), pyridine, 0°C, overnight, 31% yield.

The synthesis of the regioisomeric probe **94** started with the preparation of alkynylated aldehyde **90**. Conversion of commercially available pent-4-yn-1-ol **84** into the corresponding tosylated alcohol[139] **85** followed by nucleophilic substitution using 3-(methylamino)propan-1-ol[140] furnished compound **86**. Chlorination of alcohol **86** followed by treatment with thioacetic acid/NEt_3 furnished thioacetate derivative **87** which was then S-alkylated using ethyl 5-iodopentanoate **49** and t-BuOK leading to ethyl ester **88** in 90% yield.[141] Reduction of ethyl ester **88** to alcohol **89** followed by Swern oxidation yielded aldehyde **90.** Subsequent *anti*-selective aldol reaction between aldehyde **90** and *O*-dodecylated ephedrine auxiliary **10** furnished β-hydroxyester **91**,[118] which was finally S-oxidizedto compound **92** using oxone®.[132] Saponification of β-hydroxyester **92** to β-hydroxyacid **93** followed by cyclization[122,123] using $PhSO_2Cl$/pyridine completed the synthesis of palmostatin M-derived probe **94** (Scheme 1.9).

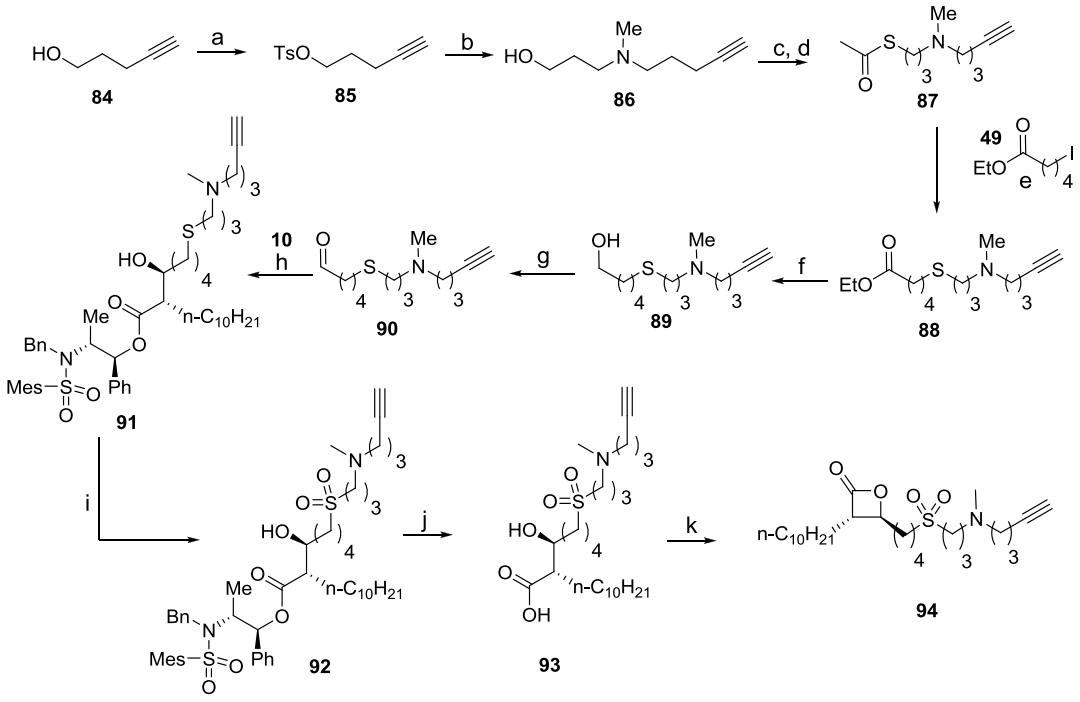

Scheme 1.9 Synthesis of palmostatin M-derived probe **94**. Reagents and conditions: a) NEt_3 (1.1 eqv.), TsCl (1.1 eqv.), CH_2Cl_2, rt, 20h, 71% yield. b) **85** (1.1 eqv.), $MeNH(CH_2)_3OH$ (1.0 eqv.), K_2CO_3 (1.1 eqv.), CH_3CN, 80°C (20h), 81% yield. c) $SOCl_2$ (1.2 eqv.), CH_2Cl_2, rt (4h). d) AcSH (1.2 eqv.), NEt_3 (3.0 eqv.), $CHCl_3$, 60°C (18h), 80% yield over two steps. e) t-BuOK (1.05 eqv.), EtOH, rt (30 min.) then ester **49** (1.0 eqv.), rt (20h), 90% yield. f) $LiAlH_4$ (1.05 eqv.), Et_2O, 0°C (1h) then rt (2h), 73% yield. g) Oxalyl chloride (1.1 eqv.), DMSO (2.3 eqv.), NEt_3 (3.65 eqv.), CH_2Cl_2, -78°C then rt, 45 min., 91% yield. h) Aux **10** (1.2 eqv.), NEt_3 (2.5 eqv.), c-Hex_2BOTf (2.2 eqv.), CH_2Cl_2, -78°C (2h) then aldehyde **90** (1.0 eqv.), -78°C (1h), 0°C (1h), then rt (1h), 68% yield. i) Oxone® (3.0 eqv.), MeOH/H_2O 2/1, rt (8h), 90% yield. j) LiOH.H_2O (5.5 eqv.), Dioxane/H_2O 4/1, 40°C (24h), 30% yield. k) $PhSO_2Cl$ (3.0 eqv.), pyridine, 0°C, over night, 30% yield.

2.4.4 Synthesis of trifunctional fluorophore reporter dye (TrifN_3)

Rhodamine-biotin-azide dye TrifN_3 (**103**) was synthesized following a modified protocol from the literature[128] using a standard 9-fluorenylmethoxycarbonyl (Fmoc) solid phase synthesis on Sieber amide resin (**95**), chosen for its relatively mild cleavage conditions (1% TFA). After removal of the Fmoc protecting group using 20% piperidine/N-methylpyrrolidinone, unprotected resin **96** (0.7 mmol/g) was coupled with Fmoc-L-Lys(4-azidobenzoyl)-OH **97**, synthesized in solution from Fmoc-LysOH and 4-azidobenzoyl chloride.[142,143] Optimized coupling conditions employed HATU (2.0 eqv.), HOBT (2.0 eqv.) and DIPEA (4.0 eqv.) in DMF for 1 hour at rt to decrease the resin loading (0.5 mmol/g), initially probably too high for the synthesis of such a bulky molecule. Unreacted free amino groups were subsequently protected as *N*-acetamide using pyridine/acetic anhydride in DCM and Fmoc protecting groups were finally removed from azide-functionalized resin **98** using 4% DBU in DMF leading to unprotected resin **99**. Subsequently, the strategy shown in Scheme 1.10 consisting in a coupling reaction with orthogonally protected Fmoc-

Lys(Alloc)-OH was investigated as it would offer the possibility to introduce a biotin modified lysine and only in the last step the fluorescent dye.

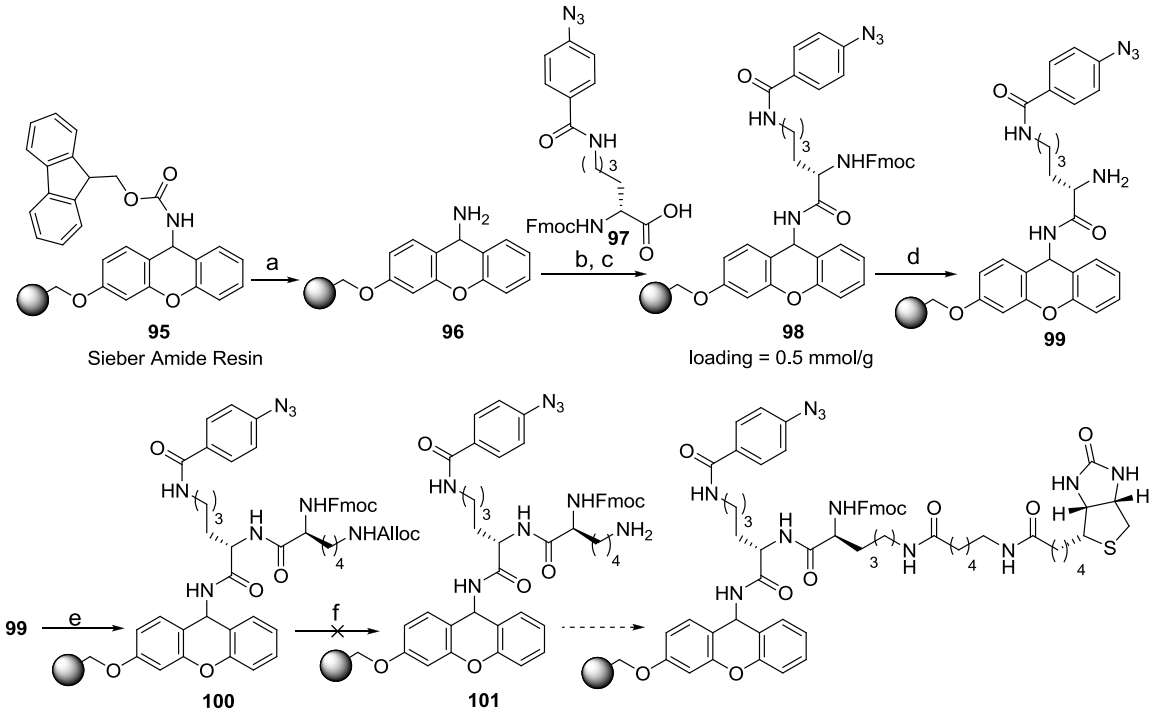

Scheme 1.10 First strategy for the trifunctional dye synthesis (**103**). Reagents and conditions: a) 20% piperidine/NMP (3 times, 5 ml, 5 min). b) Fmoc-L-Lys(4-azidobenzoyl)-OH **97** (2.0 eqv.), HATU (2.0 eqv.), HOBT (2.0 eqv.), DIPEA (4.0 eqv.), DMF, 1h, rt. c) Pyridine/acetic anhydride/DCM 1:1:4, 30 min, rt. d) 4% DBU/DMF (6 times, 5 ml, 10min). e) Fmoc-Lys(Alloc)-OH (4.0 eqv.), HATU (4.0 eqv.), HOBT (4.0 eqv.), DIPEA (8.0 eqv.), DMF, 3h, rt. f) various unsuccessful attempts to remove the Alloc protecting group.

Unfortunately, after attachment of protected Fmoc-Lys(Alloc)-OH onto resin **99**, Alloc removal from resin **100** was problematic when using tetrakis(triphenylphosphine) palladium due to the formation of the Staudinger reduction side product **S1**. Reduction of catalyst loading and optimization of the solvent system permitted a significant reduction in side product **S1**, but the reaction efficiency was also dramatically affected with largely incomplete reactions even after several days. Alternative palladium sources such as 30 mol% $Pd_2(dba)_3$ subsequently investigated were also unsuccessful with incomplete reactions and the formation of the side product **S2**, possibly by reduction of the azido group (Figure 1.41).

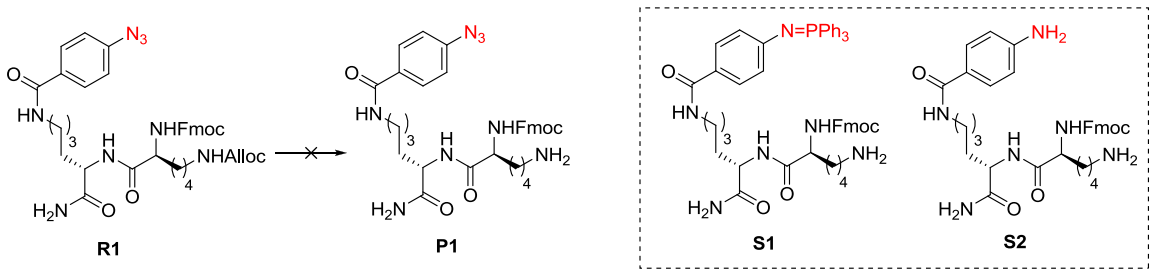

Figure 1.41 Optimization for the Alloc protecting group removal. Structure of the two side products generated during the alloc deprotection, Staudinger side product **S1** and primary amide **S2**.

Given the crucial role of the azido group in the TrifN_3 construct (**103**), the strategy presented in Scheme 1.11 was investigated in order to overcome such degradation problems. The coupling reaction of intermediate **99** with commercially available Fmoc-Lys(biotinyl-ε-aminocaproyl)-OH, permitted after subsequent Fmoc removal (4% DBU in DMF) to attach a rhodamine to the free amine upon reaction with 5-(and-6)-carboxytetramethylrhodamine succinimidyl ester (5/6 TAMRA-SE, 1.35 eqv.) in the presence of triethylamine (6.0 eqv.). Subsequent cleavage from the resin using 1% TFA in DCM, followed by purification on reverse phase C_{18} column, furnished the trifunctional dye TrifN_3 (**103**) as a dark red solid in 60% overall yield (Scheme 1.11).

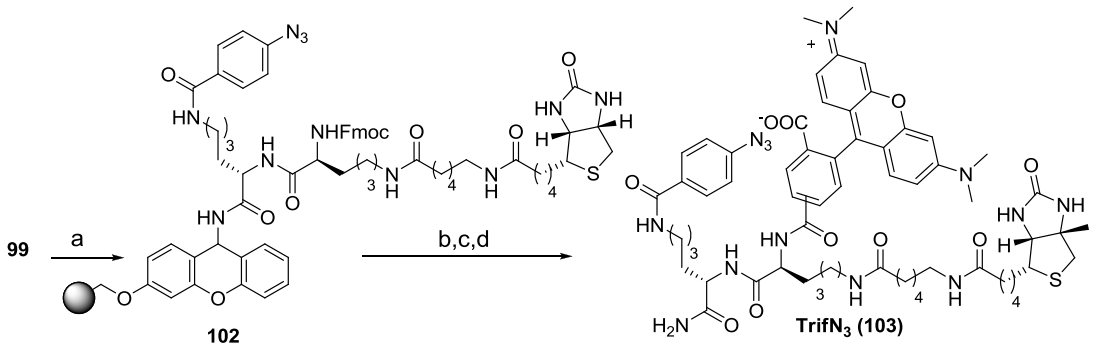

Scheme 1.11 New strategy for the trifunctional dye synthesis (**103**). Reagents and conditions: a) Fmoc-Lys(biotinyl-ε-aminocaproyl)-OH (2.0 eqv.), HATU (2.0 eqv.), HOBT (2.0 eqv.), DIPEA (4.0 eqv.), DMF, 22h, rt. b) 4% DBU/DMF (6 times, 5 ml, 10min). c) 5/6-TAMRA SE (1.5 eqv.), NEt_3 (6.0 eqv.), NMP, rt, dark, 60h. d) Cleavage from the resin using 1% TFA/DCM (5*3ml, 10 min).

2.4.5 Confirmation of the β-lactone binding mode

The two cell permeable palmostatin M-derived probes **83** and **94** were first subjected to analogous activity-based profiling experiments to allow the comparison of their labeling profiles after 20 minutes incubation with identical numbers of HeLa cells, at various probe concentrations (50/ 10/ 1 µM). In-gel fluorescence detection revealed significantly different labeling profiles for the two regioisomeric probes (Figure 1.42A). Labeling experiments

conducted with probe **83**, embedding the alkyne group in its lipid chain, were characterized by three major intense fluorescent bands compared to the negative control, whereas weaker bands were detected when using regioisomeric probe **94**. To compare their labeling efficiency for APT1, the gel was scanned by fluorescence, transferred to a PVDF membrane and used for Western blotting analysis for APT1 visualization using a know amount of recombinant hAPT1 as reference and internal standard (Figure 1.42B). Probe **83** was several-fold more efficient to label APT1 compared to probe **94,** although the two probes were displaying similar APT1 inhibitory activity in the biochemical assay (IC_{50} = 4.48 +/- 0.39nM vs. 6.06 +/- 0.87nM respectively for probe **83** and **94**). The observed discrimination between the two regioisomeric probes indicated a preferred orientation of the β-lactone into the APT1 active site with its polar head groups (SO_2 and NMe_2) penetrating the active site (Figure 1.42C). This suggested binding mode for the β-lactone inhibitors is in accordance with their substrate-based design. Given the accessibility of its alkyne group for the fluorescent labeling by [3+2]-cyloaddition when covalently bound to the APT1 active site, palmostatin M-derived probe **83** was chosen for further investigation, especially for its comparison with palmostatin B-derived probe **23**.

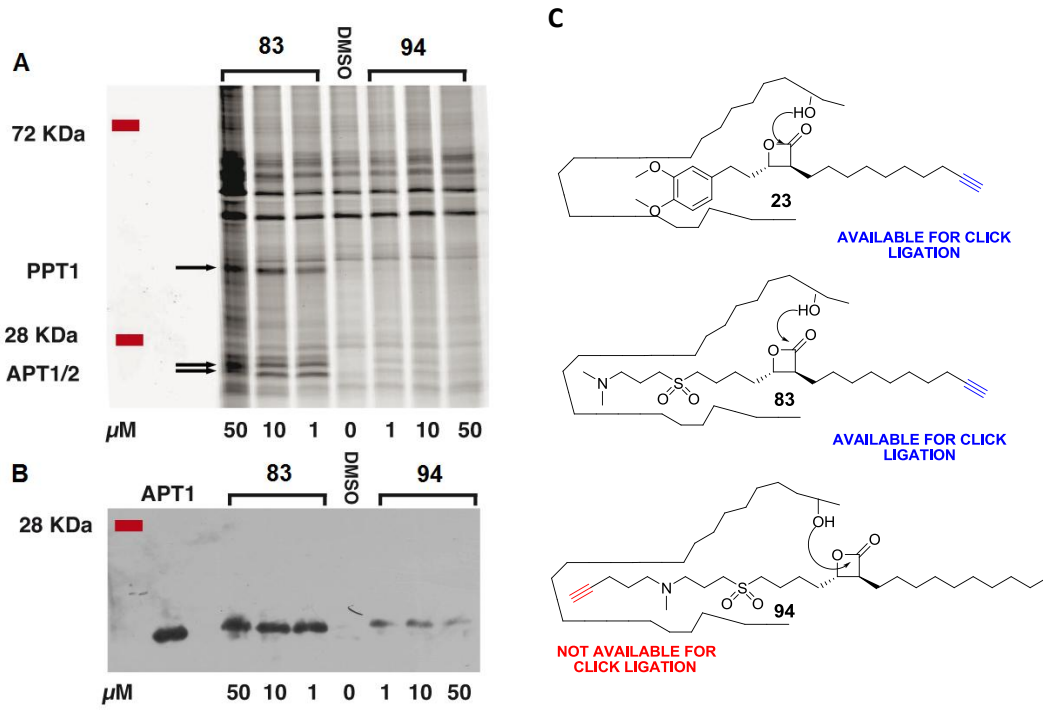

Figure 1.42 Confirmation of the β–lactone binding mode. Cellular proteome labeling profile for palmostatin M-derived probes **83** and **94** after 20 minutes incubation at various probe concentrations (50 /10 / 1 μM). A) Fluorescent gel highlighting three major bands corresponding to PPT1 (MW=34.193 kDa), APT1 (MW= 24.67 kDa) and APT2 (MW = 24.73 kDa) Conditions: $TrifN_3$ (**103**) = 20 μM, TCEP:HCl = 0.5 mM, ligand = 50 μM, $CuSO_4$ = 0.5 mM, HeLa cells = $2*10^6$. B) Corresponding Western blotting for APT1 visualization using polyclonal rabbit APT1 antibody showing a stronger affinity of probe **83** compared to probe **94** for APT1. Recombinant hAPT1 (25 ng) used as reference. C) Binding mode accounting for the observed APT1-labeling efficiency based on the accessibility of the alkyne group for the click ligation.

2.4.6 Stronger APT1 inhibition by palmostatin M over palmostatin B

To rationalize the stronger phenotypic reversion induced by palmostatin M over palmostatin B, *In cellulo* ABPP experiments were subsequently performed using the two probes **83** and **23** respectively derived from palmostatin M and B and their labeling efficiency for APT1 were compared under similar conditions. To this end, probe **83** and probe **23** were compared by means of activity based profiling experiments performed with identical cell number, after 20 minutes probe pre-incubation with concentrations varying from 10 µM to 60 nM. Although their fluorescent labeling profiles were quite similar (Figure 1.43A), palmostatin M-derived probe **83** was several fold more efficient than palmostatin B-derived probe **23** to label APT1. For probe **83**, detection of labeled APT1 by Western blotting was possible down to 60 nM concentration whereas probe **23** required at least 100 nM concentration to observe detectable levels of APT1 (Figure 1.43B). In conclusion, these results have provided the first cellular proof of a cause-effect relationship between a stronger APT1 inhibitory efficiency and a stronger phenotypic reversion of palmostatin M (**28**) as compared to palmostatin B (**14**).

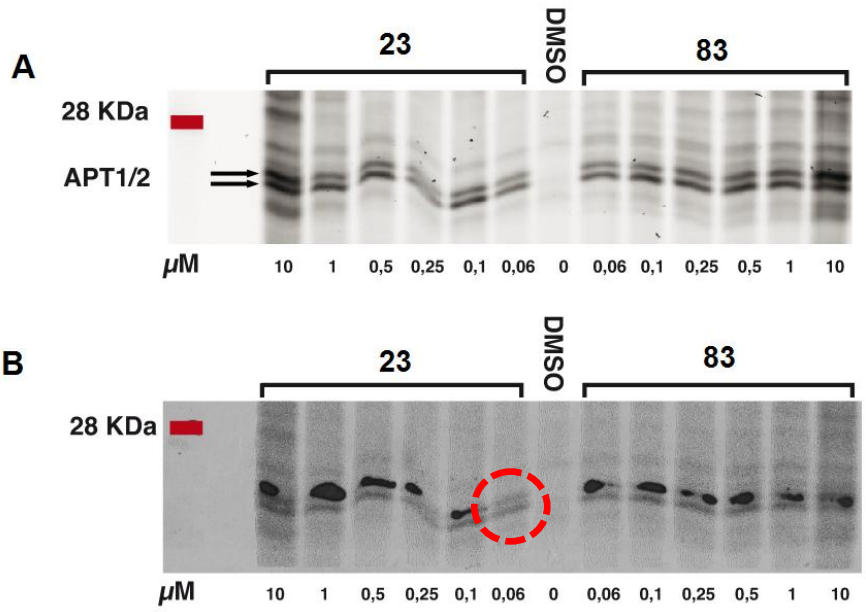

Figure 1.43 Stronger APT1 inhibition by palmostatin M over palmostatin B. Labeling profile comparison between palmostatin B-derived probe **23** and palmostatin M-derived probe **83** after 20 minutes incubation with probe concentrations from 10 µM to 60 nM. A) Fluorescent gel highlighting the bands corresponding to APT1 (MW= 24.67 kDa) and APT2 (MW = 24.73 kDa). Conditions: $TrifN_3$ (**103**) = 10 µM, TCEP:HCl = 0.5 mM, Ligand = 50 µM, $CuSO_4$ = 0.5 mM, HeLa cells = $7*10^5$. B) Corresponding Western blotting for APT1 visualization (polyclonal Rabbit APT1 antibody) showing a stronger APT1 affinity of probe **83** compared to probe **23**.

2.4.7 Identification of APT2 as Ras depalmitoylating enzyme

Although Western blotting analysis confirmed APT1 as one of the cellular targets of palmostatin B and M, the identification of all fluorescently labeled proteins covalently bound to β-lactone probes **23** and **83**, and especially those relevant to Ras depalmitoylation remained to be addressed. Therefore, palmostatin B-derived probe **23** and palmostatin M-derived probe **83** were subjected to three independent labeling experiments performed at 50 µM. After fluorescent scanning and/or silver staining, bands corresponding to fluorescently labeled proteins were isolated from the gel and digested with trypsin. Peptide fragments were subsequently separated, analyzed by nano-HPLC-MS/MS and finally compared to the SwissProt database for protein identification. Only proteins, for which at least two protein specific peptides were identified, were chosen for further validation and only those identified in at least two out of three independent pull down experiments but not in control pull downs (DMSO treated sample) were considered as hits. Table 1.2 display the list of proteins identified by proteomic analysis respectively using probe **83** or probe **23** with the probability threshold P <0.01.

Proteins	Probe 83	Probe 23	MW (kDa)	Protein function
ADRM1_HUMAN	No	yes	42412	Proteasomal ubiquitin receptor ADRM1 OS=Homo sapiens GN=ADRM1 PE=1 SV=2
ATRX_HUMAN	yes	yes	284801	Transcriptional regulator ATRX OS=Homo sapiens GN=ATRX PE=1 SV=4
BPNT1_HUMAN	yes	yes	33713	3'(2'),5'-bisphosphate nucleotidase 1 OS=Homo sapiens GN=BPNT1 PE=2 SV=1
CDC2_HUMAN	yes	no	34131	Cell division control protein 2 homolog OS=Homo sapiens GN=CDC2 PE=1 SV=1
CEBPZ_HUMAN	yes	yes	121540	CCAAT/enhancer-binding protein zeta OS=Homo sapiens GN=CEBPZ PE=1 SV=2
CHRD1_HUMAN	yes	yes	38264	Cysteine and histidine-rich domain-containing protein 1 OS=Homo sapiens GN=CHORDC1 PE=1 SV=2
CLP1L_HUMAN	yes	yes	62531	Cleft lip and palate transmembrane protein 1-like protein OS=Homo sapiens GN=CLPTM1L PE=2 SV=1
CLPT1_HUMAN	yes	no	76277	Cleft lip and palate transmembrane protein 1 OS=Homo sapiens GN=CLPTM1 PE=1 SV=1

CYBP_HUMAN	yes	yes	26308	Calcyclin-binding protein OS=Homo sapiens GN=CACYBP PE=1 SV=2
DUT_HUMAN	yes	yes	26975	Deoxyuridine 5'-triphosphate nucleotidohydrolase, mitochondrial OS=Homo sapiens GN=DUT PE=1 SV=3
EGFR_HUMAN	yes	yes	137612	Epidermal growth factor receptor OS=Homo sapiens GN=EGFR PE=1 SV=2
ERF1_HUMAN	no	yes	49228	Eukaryotic peptide chain release factor subunit 1 OS=Homo sapiens GN=ETF1 PE=1 SV=3
ERP29_HUMAN	yes	yes	29032	Endoplasmic reticulum protein ERp29 OS=Homo sapiens GN=ERP29 PE=1 SV=4
FADS1_HUMAN	yes	no	52216	Fatty acid desaturase 1 OS=Homo sapiens GN=FADS1 PE=1 SV=1
GBF1_HUMAN	yes	yes	208367	Golgi-specific brefeldin A-resistance guanine nucleotide exchange factor 1 OS=Homo sapiens GN=GBF1 PE=1 SV=2
GDIR1_HUMAN	yes	yes	23250	Rho GDP-dissociation inhibitor 1 OS=Homo sapiens GN=ARHGDIA PE=1 SV=3
HELC1_HUMAN	yes	yes	252898	Activating signal cointegrator 1 complex subunit 3 OS=Homo sapiens GN=ASCC3 PE=1 SV=3
HINT2_HUMAN	yes	yes	17208	Histidine triad nucleotide-binding protein 2 OS=Homo sapiens GN=HINT2 PE=1 SV=1
LYPA1_HUMAN	**yes**	**yes**	**24996**	**Acyl-protein thioesterase 1 OS=Homo sapiens GN=LYPLA1 PE=1 SV=1**
LYPA2_HUMAN	**yes**	**yes**	**25063**	**Acyl-protein thioesterase 2 OS=Homo sapiens GN=LYPLA2 PE=2 SV=1**
MOSC1_HUMAN	yes	yes	37989	MOSC domain-containing protein 1, mitochondrial OS=Homo sapiens GN=MOSC1 PE=2 SV=1
MRCKB_HUMAN	yes	yes	196189	Serine/threonine-protein kinase MRCK beta OS=Homo sapiens GN=CDC42BPB PE=1 SV=2
MRP1_HUMAN	yes	yes	172877	Multidrug resistance-associated protein 1 OS=Homo sapiens GN=ABCC1 PE=1 SV=2
NOC2L_HUMAN	yes	yes	85707	Nucleolar complex protein 2 homolog OS=Homo sapiens GN=NOC2L PE=1 SV=3
OLA1_HUMAN	yes	No	44943	Obg-like ATPase 1 OS=Homo sapiens GN=OLA1 PE=1 SV=2
OTUB1_HUMAN	yes	yes	31492	Ubiquitin thioesterase OTUB1 OS=Homo sapiens GN=OTUB1 PE=1 SV=2

PININ_HUMAN	yes	yes	81679	Pinin OS=Homo sapiens GN=PNN PE=1 SV=4
PPT1_HUMAN	Yes*	Yes*	34627	Palmitoyl-protein thioesterase 1 OS=Homo sapiens GN=PPT1 PE=1 SV=1
RAC1_HUMAN	yes	yes	21835	Ras-related C3 botulinum toxin substrate 1 OS=Homo sapiens GN=RAC1 PE=1 SV=1
RHOG_HUMAN	yes	yes	21751	Rho-related GTP-binding protein RhoG OS=Homo sapiens GN=RHOG PE=1 SV=1
RISC_HUMAN	No	yes	51083	Retinoid-inducible serine carboxypeptidase OS=Homo sapiens GN=SCPEP1 PE=1 SV=1
RRMJ3_HUMAN	yes	yes	96972	Putative rRNA methyltransferase 3 OS=Homo sapiens GN=FTSJ3 PE=1 SV=1
RTN3_HUMAN	yes	No	113169	Reticulon-3 OS=Homo sapiens GN=RTN3 PE=1 SV=2
SCAM3_HUMAN	yes	yes	38661	Secretory carrier-associated membrane protein 3 OS=Homo sapiens GN=SCAMP3 PE=1 SV=3
SPEE_HUMAN	yes	No	34373	Spermidine synthase OS=Homo sapiens GN=SRM PE=1 SV=1
SPRE_HUMAN	yes	yes	28316	Sepiapterin reductase OS=Homo sapiens GN=SPR PE=1 SV=1
SYNE2_HUMAN	yes	yes	801817	Nesprin-2 OS=Homo sapiens GN=SYNE2 PE=1 SV=3
TM9S4_HUMAN	yes	yes	75211	Transmembrane 9 superfamily member 4 OS=Homo sapiens GN=TM9SF4 PE=1 SV=2
TPM4_HUMAN	yes	yes	28619	Tropomyosin alpha-4 chain OS=Homo sapiens GN=TPM4 PE=1 SV=3
TYSY_HUMAN	yes	yes	35978	Thymidylate synthase OS=Homo sapiens GN=TYMS PE=1 SV=3

Table 1.2 Proteins identified by proteomic analysis. Labeling experiments performed in HeLa cells using 50 µM palmostatin B-derived probe **23** or palmostatin M-derived probe **83.** Table showing Protein ID, molecular weight (MW) and function of identified proteins. *****Protein identified not convincingly.

Consistent with Western blotting results, APT1 (or LYPL1) was found among the target proteins using both probes. Proteomic analysis also identified among the target proteins, the close homologue of APT1 called APT2 (or LYPA2) and with a weaker probability palmitoyl protein thioesterase 1 (PPT1). The clear distinction of APT2 from APT1 was possible by nano-LCMS/MS based on significantly different peptide signals exemplified by the $[M+2H]^{2+}$ ion of

TYPGVMHSSCPQEMAAVK for LYPA2 and the $[M+2H]^{2+}$ ion of TYEGMMHSSCQQEMMDVK for LYPA1 (Figure 1.44).

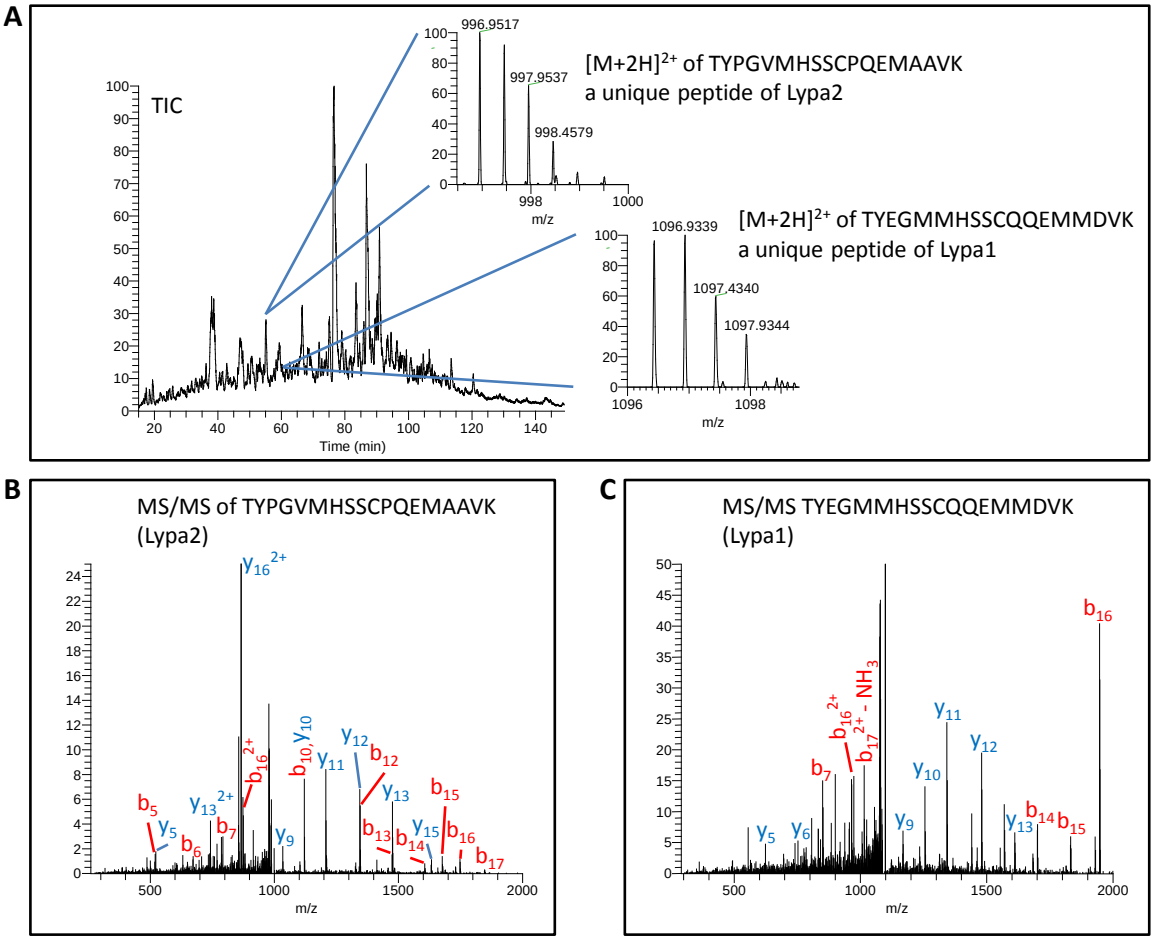

Figure 1.44 Distinction of APT1 from APT2 by nano-LCMS/MS. A) Example showing the total ion chromatogram from which the $[M+2H]^{2+}$ signals of the peptides TYPGVMHSSCPQEMAAVK for LYPA2 or TYEGMMHSSCQQEMMDVK for LYPA1 were obtained. B) MS/MS-spectrum of the $[M+2H]^{2+}$ ion of TYPGVMHSSCPQEMAAVK (LYPA2). C) MS/MS-spectrum of the $[M+2H]^{2+}$ ion of TYEGMMHSSCQQEMMDVK (LYPA1).

Given its lysosomal localization, PPT1 is unlikely to be involved *in-vivo* in the Ras depalmitoylation process, but rather in lipidated protein degradation in lysosomal compartments. In contrast, APT2 or lysophospholipase II (LYPL2) sharing 65% sequence identify with APT1 and already reported to have an activity against several lipid substrates[94] may potentially be involved in the Ras de/reacylation cycle. Encouraged by these promising results, the APT2 inhibitory activity for palmostatin B-derived probe **23** and palmostatin M-derived probe **83** was further investigated *in-vitro* by means of a biochemical assay.

2.5 Confirmation of the results

2.5.1 β-lactones as *in vitro* APT2 inhibitors

In order to monitor APT2 inhibition, the fluorometric assay previously developed for APT1 inhibition was adapted (work by Tobias Zimmermann) by adjusting the enzyme quantity to 50 nM keeping the concentration of substrate DiFMUO constant (15 µM). Recombinant human APT2 protein was expressed by Marco Bürger in analogy to APT1. Consistent with the proteomic results, palmostatin M and their corresponding pull down probes **23** and **83** were found as potent APT2 inhibitors. To explore differences in substrate specificity between APT1 and APT2, the complete *trans* β-lactone library **26-45** was subsequently screened for APT2 inhibition leading to the IC_{50} values presented in Table 1.3.

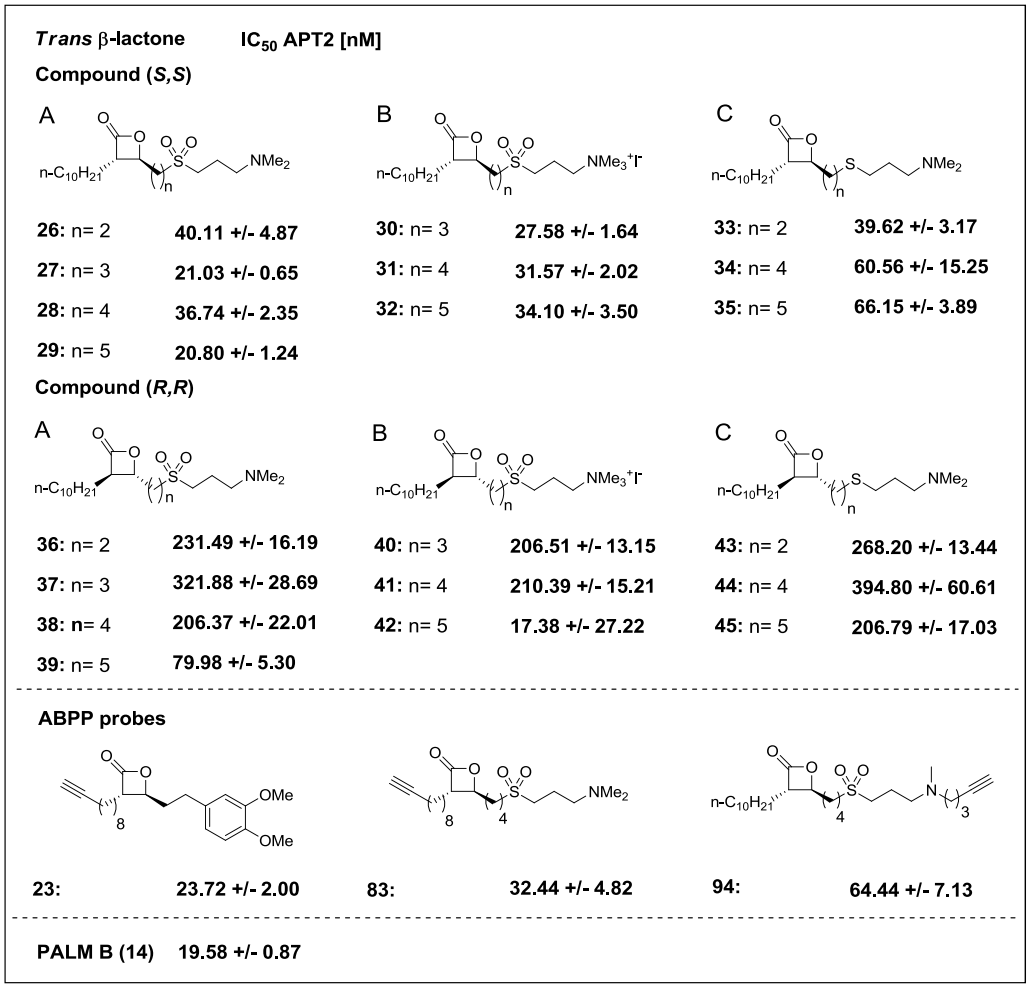

Table 1.3 β-lactone as potent APT2 inhibitors. IC_{50} values for APT2 inhibition obtained for the *trans* β-lactone inhibitors **26-45** and for ABPP probes derived from palmostatin B (**23**) and palmostatin M (**83** and **94**) using the fluorometric assay (APT2= 50nM, DiFMUO= 15µM, Ex/Emi.= 358/455nm, gain= 100, 2 min inhibitor pre-incubation time), Z' factors were in all cases higher than 0.75. Data based on three independent experiments.

In analogy to APT1, (*S,S*)-*trans* β-lactones were several fold more potent APT2 inhibitors compared to (*R,R*)-*trans* β-lactones. In general, a strong correlation between APT1 and APT2 potency was noticed. However, palmostatin M (**28**) and the two pull down probes **23** and **83** were significantly more potent APT2 than APT1 inhibitors judging from IC_{50} values obtained using 5 nM APT1 and 50 nM APT2 respectively (Figure 1.45).

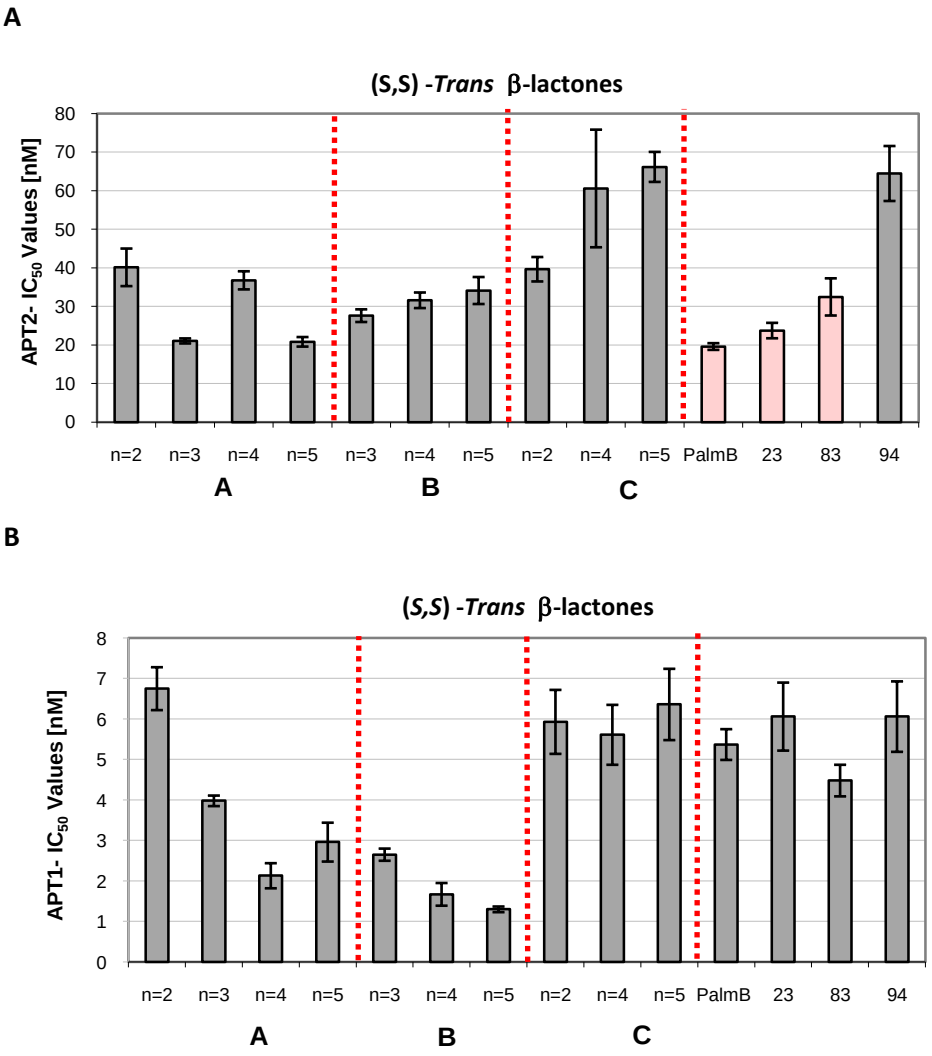

Figure 1.45 Strong correlation between APT1 and APT2 activity for the β-lactones. Graphical representation of IC_{50} values obtained for (*S,S*)-*trans* β-lactone (series A, B and C), for palmostatin B, for palmostatin B-derived probe **23** and for palmostatin M-derived probe (**83**, **94**). A) For APT2 inhibition using the APT2 fluorometric assay (APT2 = 50 nM, DiFMUO= 15 µM, 2 min inhibitor pre-incubation). B) For APT1 inhibition using the APT1 fluorometric assay (APT1 = 5 nM, DiFMUO= 15 µM, 2 min inhibitor pre-incubation). Data based on three independent experiments with Z'>0.85.

2.5.2 APT2 as *in vitro* Ras depalmitoylating enzyme

To address the relevance of APT2 for the Ras cycle, the ability of APT2 to depalmitoylate Ras proteins was evaluated *in vitro* by mean of an AcryloDated Intestinal Fatty Acid Binding protein (ADIFAB) assay using biologically active semi-synthetic *N*-Ras proteins as substrate (work by Kristina Goermer). ADIFAB is an established fluorescent assay for the detection and the measurement of released or unbound palmitic acids and is therefore suitable to monitor *in vitro* Ras depalmitoylation.[144] The principle of this assay is described in Figure 1.46 A-B. In the absence of unbound palmitic acid, the ADIFAB probe gives a fluorescent signal at 432 nm, whereas the emission shifts to 505 nm in the presence of unbound palmitic acid.

By the evaluation of the fluorescence intensity ratio F_{505nm}/F_{432nm} , the concentration of unbound palmitic acid as well as the depalmitoylation rate can be calculated for various *N*-Ras concentrations by keeping the other parameters constant (APT1/APT2= 50 nM, ADIFAB= 200 nM). Finally, the curve presented in Figure 1.46C can be obtained, allowing the determination of the maximum velocity (Vmax) and the Michaelis constant (Km), respectively for APT1 or APT2-mediated depalmitoylation. As a result, APT1 and APT2 were shown to depalmitoylate semi-synthetic *N*-Ras proteins *in-vitro* with a similar affinity for the *N*-Ras substrate, given their comparable K_M values (K_M = 1.16+/-0.02 µmol/L for APT1 and K_M = 1.43+/-0.28 µmol/L for APT2). However, APT2 was shown to depalmitoylate Ras faster than APT1, given a V_{max} value for APT2 two fold higher to that of APT1 under identical conditions (V_{max}= 0.29 +/- 0.00 nM/s for APT1 and V_{max}=0.48 +/- 0.02 nM/s for APT2) as shown in Figure 1.46.

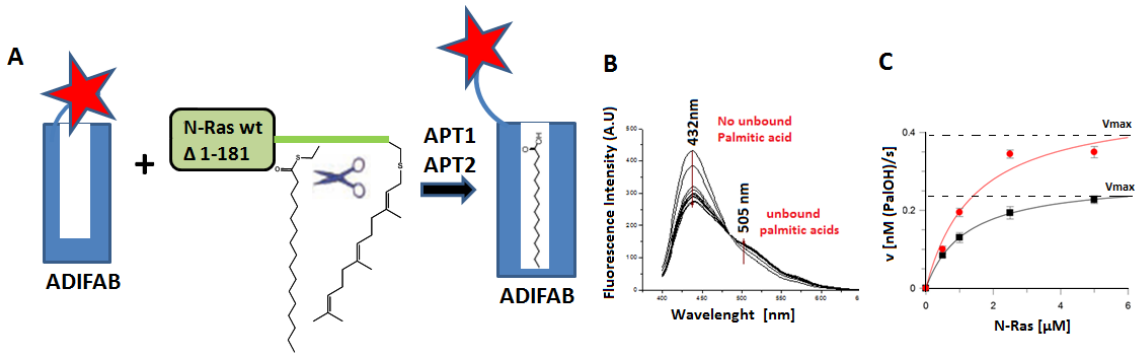

Figure 1.46 Depalmitoylation of semi-synthetic *N*-Ras by APT1 and APT2. A) Principle of the ADIFAB assay. B) Shift in the fluorescence signal (from 432 nm to 505 nm) when unbound palmitic acids are generated. C) *In-vitro* depalmitoylation of semi-synthetic *N*-Ras proteins at different concentration respectively by APT1 (black curve) and APT2 (red curve) using 50 nM APT1/APT2, 200 nM ADIFAB. Release of palmitic acids is monitored by measuring the fluorescence specta (400-650 nm) over time. Data from Kristina Goermer.

3 Conclusion

In conclusion, potent acyl protein thioesterases inhibitors were developed based on substrate similarity design principles. Pull down experiments showed that they effectively target APT1 and APT2 in cells. These inhibitors attenuate Ras signaling by interfering with the dynamic Ras de/repalmitoylation cycle and induce phenotypic reversal in *H*-Ras transformed cells. The data provide the first experimental proof that both APT1 and APT2 are thioesterases relevant to Ras depalmitoylation and signaling. Notably, β-lactone inhibitors do not inhibit additional esterases relevant to Ras signaling which proves their high selectivity. Taken as a whole, these findings suggest that no further hydrolases in general are involved in Ras-depalmitoyation in cells. Recently, the APT1/APT2 homologue LPLYP1 (APT3) expressed and purified by Marco Bürger was shown to exhibit a different electrostatic surface in the proximity of its active site. It is largely positive, in contrast to APT1 and APT2 found highly negative in the same area. This negative potential is thought to facilitate the elimination of negatively charged palmitic acids once the enzymatic cleavage accomplished thereby suggesting that APT3 may not have a thioesterase activity like APT1 and APT2. This hypothesis was subsequently confirmed by Kristina Goermer using the ADIFAB assay, showing the inability of APT3 to depalmitoylate biologically active semi-synthetic *N*-Ras proteins *in vitro*. With the discovery of APT1 and APT2 as relevant proteins for Ras depalmitoylation, targeting both proteins may constitute a viable anti-cancer approach to interfere with aberrant *H*- and *N*-Ras signaling.

4 References

(1) Ellis, R. W.; DeFeo, D.; Shih, T. Y.; Gonda, M. A.; Young, H. A.; Tsuchida, N.; Lowy, D. R.; Scolnick, E. M. *Nature* **1981**, *292*, 506.
(2) Parada, L. F.; Tabin, C. J.; Shih, C.; Weinberg, R. A. *Nature* **1982**, *297*, 474.
(3) Ireland, C. M. *Cancer Res*. **1989**, *49*, 5530.
(4) Scheffzek, K.; Ahmadian, M. R.; Kabsch, W.; Wiesmuller, L.; Lautwein, A.; Schmitz, F.; Wittinghofer, A. *Science* **1997**, *277*, 333.
(5) Wittinghofer, A.; Waldmann, H. *Angew. Chem., Int. Ed.* **2000**, *39*, 4192.
(6) Downward, J. *Nat. Rev. Cancer* **2003**, *3*, 11.
(7) Prior, I. A.; Hancock, J. F. *J. Cell Sci.* **2001**, *114*, 1603.
(8) Hancock, J. F.; Magee, A. I.; Childs, J. E.; Marshall, C. J. *Cell* **1989**, *57*, 1167.
(9) Willumsen, B. M.; Christensen, A.; Hubbert, N. L.; Papageorge, A. G.; Lowy, D. R. *Nature* **1984**, *310*, 583.
(10) Reiss, Y.; Goldstein, J. L.; Seabra, M. C.; Casey, P. J.; Brown, M. S. *Cell* **1990**, *62*, 81.
(11) Boyartchuk, V. L.; Ashby, M. N.; Rine, J. *Science* **1997**, *275*, 1796.
(12) Kim, E.; Ambroziak, P.; Otto, J. C.; Taylor, B.; Ashby, M.; Shannon, K.; Casey, P. J.; Young, S. G. *J. Biol. Chem.* **1999**, *274*, 8383.
(13) Otto, J. C.; Kim, E.; Young, S. G.; Casey, P. J. *J. Biol. Chem.* **1999**, *274*, 8379.

(14) Hrycyna, C. A.; Sapperstein, S. K.; Clarke, S.; Michaelis, S. *EMBO J.* **1991**, *10*, 1699.
(15) Dai, Q.; Choy, E.; Chiu, V.; Romano, J.; Steitz, S. R.; Steitz, S. A.; Michaelis, S.; Philips, M. R. *J. Biol. Chem.* **1998**, *273*, 15030.
(16) Bergo, M. O.; Ambroziak, P.; Gregory, C.; George, A.; Otto, J. C.; Kim, E.; Nagase, H.; Casey, P. J.; Balmain, A.; Young, S. G. *Mol. Cell. Biol.* **2002**, *22,* 171.
(17) Bergo, M. O.; Leung, G. K.; Ambroziak, P.; Otto, J. C.; Casey, P. J.; Gomes, A. Q.; Seabra, M. C.; Young, S. G. *J. Biol. Chem.* **2001**, *276*, 5841.
(18) Bergo, M. O.; Leung, G. K.; Ambroziak, P.; Otto, J. C.; Casey, P. J.; Young, S. G. *J. Biol. Chem.* **2000**, *275,* 17605.
(19) Magee, A. I.; Gutierrez, L.; McKay, I. A.; Marshall, C. J.; Hall, A. *EMBO J.* **1987**, *6*, 3353.
(20) Apolloni, A.; Prior, I. A.; Lindsay, M.; Parton, R. G.; Hancock, J. F. *Mol. Cell. Biol.* **2000**, *20*, 2475.
(21) Choy, E.; Chiu, V. K.; Silletti, J.; Feoktistov, M.; Morimoto, T.; Michaelson, D.; Ivanov, I. E.; Philips, M. R. *Cell* **1999**, *98*, 69.
(22) Rajalingam, K.; Schreck, R.; Rapp, U. R.; Albert, S. *Biochim. Biophys. Acta, Mol. Cell Res.* **2007**, *1773*, 1177.
(23) Goodwin, J. S.; Drake, K. R.; Rogers, C.; Wright, L.; Lippincott-Schwartz, J.; Philips, M. R.; Kenworthy, A. K. *J. Cell Biol.* **2005**, *170*, 261.
(24) Jennings, B. C.; Nadolski, M. J.; Ling, Y.; Baker, M. B.; Harrison, M. L.; Deschenes, R. J.; Linder, M. E. *J. Lipid Res*. **2009**, *50*, 233.
(25) Dekker, F. J.; Rocks, O.; Vartak, N.; Menninger, S.; Hedberg, C.; Balamurugan, R.; Wetzel, S.; Renner, S.; Gerauer, M.; Schoelermann, B.; Rusch, M.; Kramer, J. W.; Rauh, D.; Coates, G. W.; Brunsveld, L.; Bastiaens, P. I. H.; Waldmann, H. *Nat. Chem. Biol*. **2010**, *6,* 449.
(26) Linder, M. E.; Deschenes, R. J. *Nat. Rev. Mol. Cell Biol.* **2007**, *8*, 74.
(27) Rocks, O.; Peyker, A.; Kahms, M.; Verveer, P. J.; Koerner, C.; Lumbierres, M.; Kuhlmann, J.; Waldmann, H.; Wittinghofer, A.; Bastiaens, P. I. H. *Science* **2005**, *307*, 1746.
(28) Rocks, O.; Peyker, A.; Bastiaens, P. I. H. *Curr. Opin. Cell Biol.* **2006**, *18*, 351.
(29) Villalonga, P.; Lopez-Alcala, C.; Bosch, M.; Chiloeches, A.; Rocamora, N.; Gil, J.; Marais, R.; Marshall, C. J.; Bachs, O.; Agell, N. *Mol. Cell. Biol.* **2001**, *21*, 7345.
(30) Sidhu, R. S.; Clough, R. R.; Bhullar, R. P. *Biochem. Biophys. Res. Commun.* **2003**, *304*, 655.
(31) Bivona, T. G.; Quatela, S. E.; Bodemann, B. O.; Ahearn, I. M.; Soskis, M. J.; Mor, A.; Miura, J.; Wiener, H. H.; Wright, L.; Saba, S. G.; Yim, D.; Fein, A.; Perez, d. C. I.; Li, C.; Thompson, C. B.; Cox, A. D.; Philips, M. R. *Mol. Cell* **2006**, *21*, 481.
(32) Chiu, V. K.; Bivona, T.; Hach, A.; Sajous, J. B.; Silletti, J.; Wiener, H.; Johnson, R. L.; Cox, A. D.; Philips, M. R. *Nat. Cell Biol.* **2002**, *4*, 343.
(33) Arozarena, I.; Matallanas, D.; Berciano, M. T.; Sanz-Moreno, V.; Calvo, F.; Munoz, M. T.; Egea, G.; Lafarga, M.; Crespo, P. *Mol. Cell. Biol.* **2004**, *24*, 1516.
(34) Sobering, A. K.; Romeo, M. J.; Vay, H. A.; Levin, D. E. *Mol. Cell. Biol.* **2003**, *23*, 4983.
(35) Sobering, A. K.; Watanabe, R.; Romeo, M. J.; Yan, B. C.; Specht, C. A.; Orlean, P.; Riezman, H.; Levin, D. E. *Cell* **2004**, *117*, 637.
(36) Plowman, S. J.; Hancock, J. F. *Biochim. Biophys. Acta, Mol. Cell Res.* **2005**, *1746*, 274.
(37) Mor, A.; Philips, M. R. *Annu. Rev. Immunol.* **2006**, *24*, 771.
(38) Hancock, J. F. *Nat. Rev. Mol. Cell Biol.* **2003**, *4*, 373.
(39) Aronheim, A.; Engelberg, D.; Li, N.; Al-Alawi, N.; Schlessinger, J.; Karin, M. *Cell* **1994**, *78*, 949.
(40) Kyriakis, J. M.; App, H.; Zhang, X. F.; Banerjee, P.; Brautigan, D. L.; Rapp, U. R.; Avruch, J. *Nature* **1992**, *358*, 417.
(41) Egan, S. E.; Weinberg, R. A. *Nature* **1993**, *365*, 781.
(42) Bivona, T. G.; Perez, d. C. I.; Ahearn, I. M.; Grana, T. M.; Chiu, V. K.; Lockyer, P. J.; Cullen, P. J.; Pellicer, A.; Cox, A. D.; Philips, M. R. *Nature* **2003**, *424*, 694.

(43) Melkonian, K. A.; Ostermeyer, A. G.; Chen, J. Z.; Roth, M. G.; Brown, D. A. *J. Biol. Chem.* **1999**, *274*, 3910.
(44) Weise, K.; Triola, G.; Brunsveld, L.; Waldmann, H.; Winter, R. *J. Am. Chem. Soc.* **2009**, *131*, 1557.
(45) Levitzki, A. *Eur. J. Biochem.* **1994**, *226*, 1.
(46) Johnson, L.; Greenbaum, D.; Cichowski, K.; Mercer, K.; Murphy, E.; Schmitt, E.; Bronson, R. T.; Umanoff, H.; Edelmann, W.; Kucherlapati, R.; Jacks, T. *Genes Dev.* **1997**, *11*, 2468.
(47) Corey, D. R. *Nat Chem Biol* **2007**, *3*, 8.
(48) Braasch, D. A.; Corey, D. R. *Biochemistry* **2002**, *41*, 4503.
(49) Bertrand, J.-R.; Pottier, M.; Vekris, A.; Opolon, P.; Maksimenko, A.; Malvy, C. *Biochem. Biophys. Res. Commun.* **2002**, *296,* 1000.
(50) Miyagishi, M.; Hayashi, M.; Taira, K. *Antisense Nucleic Acid Drug Dev.* **2003**, *13*, 1.
(51) Yang, G.; Thompson, J. A.; Fang, B.; Liu, J. *Oncogene* **2003**, *22,* 5694.
(52) Brummelkamp, T. R.; Bernards, R.; Agami, R. *Cancer Cell* **2002**, *2*, 243.
(53) Zhang, Z.; Jiang, G.; Yang, F.; Wang, J. *Cancer Biol. Ther.* **2006**, *5*, 1481.
(54) Eskandarpour, M.; Kiaii, S.; Zhu, C.; Castro, J.; Sakko, A. J.; Hansson, J. *Int. J. Cancer* **2005**, *115*, 65.
(55) Boriack-Sjodin, P. A.; Margarit, S. M.; Bar-Sagi, D.; Kuriyan, J. *Nature* **1998**, *394*, 337.
(56) Mossessova, E.; Corpina, R. A.; Goldberg, J. *Mol. Cell* **2003**, *12*, 1403.
(57) Renault, L.; Guibert, B.; Cherfils, J. *Nature* **2003**, *426*, 525.
(58) Saxena, N.; Lahiri, S. S.; Hambarde, S.; Tripathi, R. P. *Cancer Invest*. **2008**, *26*, 948.
(59) Mendelsohn, J.; Baselga, J. *Oncogene* **2000**, *19*, 6550.
(60) Dudley, D. T.; Pang, L.; Decker, S. J.; Bridges, A. J.; Saltiel, A. R. *Proc. Natl. Acad. Sci. U. S. A.* **1995**, *92*, 7686.
(61) Sebolt-Leopold, J. S.; Dudley, D. T.; Herrera, R.; Van, B. K.; Wiland, A.; Gowan, R. C.; Tecle, H.; Barrett, S. D.; Bridges, A.; Przybranowski, S.; Leopold, W. R.; Saltiel, A. R. *Nat. Med.* **1999**, *5*, 810.
(62) LoRusso, P. M.; Adjei, A. A.; Varterasian, M.; Gadgeel, S.; Reid, J.; Mitchell, D. Y.; Hanson, L.; DeLuca, P.; Bruzek, L.; Piens, J.; Asbury, P.; Van, B. K.; Herrera, R.; Sebolt-Leopold, J.; Meyer, M. B. J. *Clin. Oncol.* **2005**, *23*, 5281.
(63) Rinehart, J.; Adjei, A. A.; LoRusso, P. M.; Waterhouse, D.; Hecht, J. R.; Natale, R. B.; Hamid, O.; Varterasian, M.; Asbury, P.; Kaldjian, E. P.; Gulyas, S.; Mitchell, D. Y.; Herrera, R.; Sebolt-Leopold, J. S.; Meyer, M. B. J. *Clin. Oncol.* **2004**, *22*, 4456.
(64) Barrett, S. D.; Bridges, A. J.; Dudley, D. T.; Saltiel, A. R.; Fergus, J. H.; Flamme, C. M.; Delaney, A. M.; Kaufman, M.; LePage, S.; Leopold, W. R.; Przybranowski, S. A.; Sebolt-Leopold, J.; Van, B. K.; Doherty, A. M.; Kennedy, R. M.; Marston, D.; Howard, W. A., Jr.; Smith, Y.; Warmus, J. S.; Tecle, H. *Bioorg. Med. Chem. Lett.* **2008**, *18*, 6501.
(65) Vara, J. A. F.; Casado, E.; de, C. J.; Cejas, P.; Belda-Iniesta, C.; Gonzalez-Baron, M. *Cancer Treat. Rev.* **2004**, *30*, 193.
(66) Pizon, V.; Chardin, P.; Lerosey, I.; Olofsson, B.; Tavitian, A. *Oncogene* **1988**, *3*, 201.
(67) Nassar, N.; Horn, G.; Herrmann, C.; Block, C.; Janknecht, R.; Wittinghofer, A. *Nat. Struct. Biol.* **1996**, *3*, 723.
(68) Nassar, N.; Horn, G.; Herrmann, C.; Scherer, A.; McCormick, F.; Wittinghofer, A. *Nature* **1995**, *375*, 554.
(69) Barnard, D.; Diaz, B.; Hettich, L.; Chuang, E.; Zhang, X.-f.; Avruch, J.; Marshall, M. *Oncogene* **1995**, *10*, 1283.
(70) Barnard, D.; Sun, H.; Baker, L.; Marshall, M. S. *Biochem. Biophys. Res. Commun.* **1998**, *247*, 176.
(71) Herrmann, C.; Block, C.; Geisen, C.; Haas, K.; Weber, C.; Winde, G.; Moroy, T.; Muller, O. *Oncogene* **1998**, *17*, 1769.

(72) Kato-Stankiewicz, J.; Hakimi, I.; Zhi, G.; Zhang, J.; Serebriiskii, I.; Guo, L.; Edamatsu, H.; Koide, H.; Menon, S.; Eckl, R.; Sakamuri, S.; Lu, Y.; Chen, Q.-Z.; Agarwal, S.; Baumbach, W. R.; Golemis, E. A.; Tamanoi, F.; Khazak, V. *Proc. Natl. Acad. Sci. U. S. A*. **2002**, *99*, 14398.
(73) Gupta, S.; Ramjaun, A. R.; Haiko, P.; Wang, Y.; Warne, P. H.; Nicke, B.; Nye, E.; Stamp, G.; Alitalo, K.; Downward, J. *Cell* **2007**, *129*, 957.
(74) Kirby, J.; Keasling, J. D. *Annu. Rev. Plant Biol.* **2009**, *60*, 335.
(75) Resh, M. D. *Methods* **2006**, *40*, 191.
(76) Sim, D. S.; Dilks, J. R.; Flaumenhaft, R. *Arterioscler., Thromb., Vasc. Biol.* **2007**, *27*, 1478.
(77) Lawrence, D. S.; Zilfou, J. T.; Smith, C. D. *J. Med. Chem.* **1999**, *42*, 4932.
(78) Ducker, C. E.; Griffel, L. K.; Smith, R. A.; Keller, S. N.; Zhuang, Y.; Xia, Z.; Diller, J. D.; Smith, C. D. *Mol. Cancer Ther.* **2006**, *5*, 1647.
(79) Camp, L. A.; Hofmann, S. L. *J. Biol. Chem.* **1993**, *268*, 22566.
(80) Camp, L. A.; Verkruyse, L. A.; Afendis, S. J.; Slaughters, C. A.; Hofmann, S. L. *J. Biol. Chem.* **1994**, *269*, 23212.
(81) Verkruyse, L. A.; Hofmann, S. L. *J. Biol. Chem.* **1996**, *271*, 15831.
(82) Schriner, J. E.; Yi, W.; Hofmann, S. L. *Genomics* **1996**, *34,* 317.
(83) Hellsten, E.; Vesa, J.; Olkkonen, V. M.; Jalanko, A.; Peltonen, L. *EMBO J*. **1996**, *15*, 5240.
(84) Duncan, J. A.; Gilman, A. G. *J. Biol. Chem.* **1998**, *273*, 15830.
(85) Sugimoto, H.; Hayashi, H.; Yamashita, S. *J. Biol. Chem.* **1996**, *271*, 7705.
(86) Sunaga, H.; Sugimoto, H.; Nagamachi, Y.; Yamashita, S. *Biochem. J.* **1995**, *308*, 551.
(87) Wang, A.; Deems, R. A.; Dennis, E. A. *J. Biol. Chem.* **1997**, *272*, 12723.
(88) Devedjiev, Y.; Dauter, Z.; Kuznetsov, S. R.; Jones, T. L. Z.; Derewenda, Z. S. *Structure* **2000**, *8*, 1137.
(89) Yeh, D. C.; Duncan, J. A.; Yamashita, S.; Michel, T. *J. Biol. Chem.* **1999**, *274*, 33148.
(90) Duncan, J. A.; Gilman, A. G. *J. Biol. Chem.* **2002**, *277*, 31740.
(91) Flaumenhaft, R.; Rozenvayn, N.; Feng, D.; Dvorak, A. M. *Blood* **2007**, *110*, 1492.
(92) Satou, M.; Nishi, Y.; Yoh, J.; Hattori, Y.; Sugimoto, H. *Endocrinology* **2010**, *151*, 4765.
(93) Dietzen, D. J.; Hastings, W. R.; Lublin, D. M. *J. Biol. Chem.* **1995**, *270*, 6838.
(94) Toyoda, T.; Sugimoto, H.; Yamashita, S. *Biochim. Biophys. Acta, Mol. Cell Biol. Lipids* **1999**, *1437*, 182.
(95) http://www.uniprot.org
(96) Tomatis, V. M.; Trenchi, A.; Gomez, G. A.; Daniotti, J. L. *PLoS One* **2010**, *5*, 15045.
(97) Koch, M. A.; Wittenberg, L.-O.; Basu, S.; Jeyaraj, D. A.; Gourzoulidou, E.; Reinecke, K.; Odermatt, A.; Waldmann, H. *Proc. Natl. Acad. Sci. U. S. A.* **2004**, *101*, 16721.
(98) Dekker, F. J.; Koch, M. A.; Waldmann, H. *Curr. Opin. Chem. Biol.* **2005**, *9*, 232.
(99) Hadvary, P.; Sidler, W.; Meister, W.; Vetter, W.; Wolfer, H. *J. Biol. Chem.* **1991**, *266*, 2021.
(100) Siegel, G.; Obernosterer, G.; Fiore, R.; Oehmen, M.; Bicker, S.; Christensen, M.; Khudayberdiev, S.; Leuschner, P. F.; Busch, C. J. L.; Kane, C.; Huebel, K.; Dekker, F.; Hedberg, C.; Rengarajan, B.; Drepper, C.; Waldmann, H.; Kauppinen, S.; Greenberg, M. E.; Draguhn, A.; Rehmsmeier, M.; Martinez, J.; Schratt, G. M. *Nat. Cell Biol.* **2009**, *11*, 705.
(101) Yang, W.; Di, V. D.; Kirchner, M.; Steen, H.; Freeman, M. R. Mol. Cell. *Proteomics* **2010**, *9*, 54.
(102) Ahearn, I. M.; Tsai, F. D.; Court, H.; Zhou, M.; Jennings, B. C.; Ahmed, M.; Fehrenbacher, N.; Linder, M. E.; Philips, M. R. *Mol. Cell* **2010**, *41*, 173.
(103) Fernley, H. N.; Walker, P. G. *Biochem. J.* **1965**, *97*, 95.
(104) Robinson, D.; Willcox, P. *Biochim. Biophys. Acta, Enzymol.* **1969**, *191*, 183.
(105) Steven, F. S.; Al-Ahmad, R. K. *Eur. J. Biochem.* **1983**, *130*, 335.
(106) Krishnaswamy, S.; Vlasuk, G. P.; Bergum, P. W. *Biochemistry* **1994**, *33*, 7897.
(107) Maiden, M. F.; Tanner, A.; Macuch, P. J. *J Clin Microbiol* **1996**, *34*, 376.

(108) Yano, S.; Kawata, Y.; Delbarre, S.; Kojima, H. *Biosci., Biotechnol., Biochem.* **1992**, *56*, 1310.
(109) Villari, P.; Iannuzzo, M.; Torre, I. *Lett. Appl. Microbiol.* **1997**, *24*, 286.
(110) Sun, W.-C.; Gee, K. R.; Haugland, R. P. *Bioorg. Med. Chem. Lett.* **1998**, *8,* 3107.
(111) Qian, Z.; Lutz, S. *J. Am. Chem. Soc.* **2005**, *127*, 13466.
(112) Sun, W.-C.; Gee, K. R.; Klaubert, D. H.; Haugland, R. P. *J. Org. Chem*. **1997**, *62*, 6469.
(113) von, P. H.; Duisberg, C. *Ber., 16*, 2119.
(114) Sethna, S. M.; Shah, N. M. *Chem. Rev.* **1945**, *36*, 1.
(115) Russell, A.; Frye, J. R. *Org. Synth*. **1941**, *21*, 22.
(116) Brun, M.-P.; Bischoff, L.; Garbay, C. *Angew. Chem., Int. Ed.* **2004**, *43*, 3432.
(117) Khatyr, A.; Maas, H.; Calzaferri, G. *J. Org. Chem.* **2002**, *67*, 6705.
(118) Inoue, T.; Liu, J.-F.; Buske, D. C.; Abiko, A. *J. Org. Chem*. **2002**, *67*, 5250.
(119) Abiko, A.; Liu, J.-F.; Masamune, S. *J. Am. Chem. Soc.* **1997**, *119*, 2586.
(120) Inoue, T.; Liu, J.-F.; Buske, D. C.; Abiko, A. *J. Org. Chem*. **2002**, *67*, 5250.
(121) Abiko, A. *Org. Synth.* **2002**, *79*, No pp. given.
(122) Black, T. H.; DuBay, W. J., III; Tully, P. S. *J. Org. Chem*. **1988**, *53*, 5922.
(123) Yadav, J. S.; Reddy, M. S.; Prasad, A. R. *Tetrahedron Lett.* **2006**, *47,* 4995.
(124) Ritschel, J.; Sasse, F.; Maier, M. E. *Eur. J. Org. Chem.* **2007**, *78*.
(125) Csuk, R.; Niesen, A. Z. *Naturforsch., B: Chem. Sci.* **2004***, 59*, 934.
(126) Zakhrkin, L. I.; Churilova, I. M. *Izv. Akad. Nauk SSSR, Ser. Khim.* **1984**, 2635.
(127) Bergel'son, L. D.; Molotkovskii, Y. G.; Shemyakin, M. M. *Zh. Obshch. Khim.* **1962**, *32*, 58.
(128) Speers, A. E.; Cravatt, B. F. *Chem. Biol.* **2004**, *11*, 535.
(129) Vercillo, O. E.; Andrade, C. K. Z.; Wessjohann, L. A. *Org. Lett.* **2008**, *10*, 205.
(130) Schmitt, M.; Lehr, M. *J. Pharm. Biomed. Anal.* **2004**, *35*, 135.
(131) Sparks, S. M.; Chow, C. P.; Zhu, L.; Shea, K. J. *J. Org. Chem.* **2004**, *69*, 3025.
(132) Veleiro, A. S.; Pecci, A.; Monteserin, M. C.; Baggio, R.; Garland, M. T.; Lantos, C. P.; Burton, G. *J. Med. Chem*. **2005**, *48*, 5675.
(133) Duncia, J. V.; Santella, J. B.; Higley, C. A.; Pitts, W. J.; Wityak, J.; Frietze, W. E.; Rankin, F. W.; Sun, J.-H.; Earl, R. A.; Tabaka, A. C.; Teleha, C. A.; Blom, K. F.; Favata, M. F.; Manos, E. J.; Daulerio, A. J.; Stradley, D. A.; Horiuchi, K.; Copeland, R. A.; Scherle, P. A.; Trzaskos, J. M.; Magolda, R. L.; Trainor, G. L.; Wexler, R. R.; Hobbs, F. W.; Olson, R. E. *Bioorg. Med. Chem. Lett.* **1998**, *8*, 2839.
(134) Rocks, O.; Gerauer, M.; Vartak, N.; Koch, S.; Huang, Z.-P.; Pechlivanis, M.; Kuhlmann, J.; Brunsveld, L.; Chandra, A.; Ellinger, B.; Waldmann, H.; Bastiaens, P. I. H. *Cell* **2010**, *141*, 458.
(135) Boettcher, T.; Sieber, S. A. *J. Am. Chem. Soc.* **2008**, *130*, 14400.
(136) Boettcher, T.; Sieber, S. A. *Angew. Chem., Int. Ed.* **2008**, *47*, 4600.
(137) Wang, Z.; Gu, C.; Colby, T.; Shindo, T.; Balamurugan, R.; Waldmann, H.; Kaiser, M.; van, d. H. R. A. L. *Nat. Chem. Biol.* **2008***, 4,* 557.
(138) Yang, P.-Y.; Liu, K.; Ngai, M. H.; Lear, M. J.; Wenk, M. R.; Yao, S. Q. *J. Am. Chem. Soc.* **2010**, *132*, 656.
(139) Tashima, T.; Toriumi, Y.; Mochizuki, Y.; Nonomura, T.; Nagaoka, S.; Furukawa, K.; Tsuru, H.; Adachi-Akahane, S.; Ohwada, T. *Bioorg. Med. Chem.* **2006**, *14*, 8014.
(140) Boyle, G. A.; Kruger, H. G.; Maguire, G. E. M.; Singh, A. *Struct. Chem.* **2007**, *18*, 633.
(141) Pettersson, L.; *Innoventus Project AB, Swed.* **2005**, p 80 pp.
(142) Mehlmann, H.; Olschewski, D.; Olschewski, A.; Feigel, M. Z. *Naturforsch., B: Chem. Sci.* **2002**, *57*, 343.
(143) Lanza, T.; Leardini, R.; Minozzi, M.; Nanni, D.; Spagnolo, P.; Zanardi, G. *Angew. Chem., Int. Ed.* **2008**, *47,* 9439.
(144) Richieri, G. V.; Ogata, R. T.; Kleinfeld, A. M. *J. Biol. Chem.* **1992**, *267*, 23495.

CHAPTER 2

TARGETING FAS DEATH RECEPTOR DEPALMITOYLATION

1 Background Chronic Lymphocytic Leukaemia (CLL)

Leukaemia is a group a several diseases affecting white blood cells and accounting for 0.8% of all cancer deaths. Chronic lymphocytic leukaemia (CLL) is the most common diagnosed form of leukaemia, representing nearly 30% of all leukaemia related deaths.[1,2] CLL is characterized by an aberrant accumulation of long lived malignant B cells or B-CLL cells[3] due to dysfunction in normal apoptotic signaling pathways resulting instead in the activation of non-apoptotic pathways.[4] This uncurable disease affects mainly aged people,[1] and is characterized by low chances of self–remission.[5] Moreover, attempts to treat CLL patients employing DNA-damaging chemotherapy[6] had only minor effects thereby resulting in a low survival prognosis, typically 5 years.[1] Over 15 years numerous research groups have been focusing on understanding the mechanisms of this age-related disease and in particular the apoptosis resistance characteristic for CLL, in order to develop new therapeutic approaches.

2 Fas-mediated signaling pathways in healthy cells

2.1 Fas receptors as key regulators of cell death signaling

Ubiquitously expressed, Fas receptors (also known as CD95 or APO-1) are one of the most studied plasma membrane cell death receptors involved in apoptotic cell signaling pathways. Like other well-studied members of the TNFR (tumor necrosis factor receptor) superfamily (TNFR1, TRAIL DR4 and TRAIL DR5), Fas receptors are characterized by the presence of a death domain binding motif (DD = 80 amino acids). Moreover, Fas receptors are constitutively palmitoylated in their transmembrane domains (TM) with a palmitoylation site located at the cysteine residue Cys 199 in human Fas.[7,8] Post-translational lipid modifications together with their death domains (DD) are essential for the initiation of Fas-mediated apoptotic signaling.[9] A simplified representation of Fas receptor proteins is provided in Figure 2.1, showing their segmentation into three distinct domains respectively extracellular, transmembrane and cytoplasmic domains.

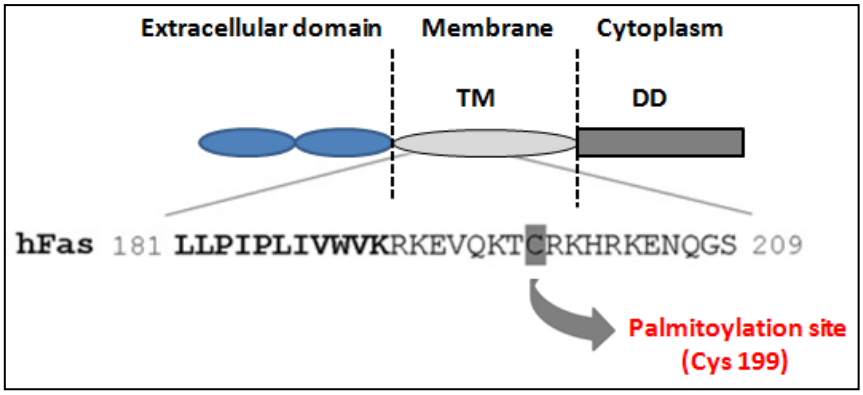

Figure 2.1 Simplified Fas receptor structure. Death domain and palmitoylation site of Fas receptors reported to be essential for Fas-induced apoptotic cell signaling. TM = transmembrane domain, DD = death domain. Figure adapted from the literature.[10]

2.2 Fas palmitoylation initiates Fas trimerization in lipid rafts

S-palmitoylation is a post-translational lipid modification commonly found among signaling proteins. Fas palmitoylation is essential for Fas translocation to lipid rafts (liquid ordered plasma membrane microdomains)[7] as well as for Fas-induced apoptotic signaling.[7] Indeed, lipid-raft localized and palmitoylated Fas receptors form non covalent pre-assembled trimers by self association, with their Fas death domains hindered.[11,12] Upon binding to their homotrimeric Fas ligands (FasL or CD95L), pre-assembled Fas receptors undergo conformational changes allowing homotypic interactions with their death domains, thus resulting in Fas trimerization (Figure 2.2).[12-15]

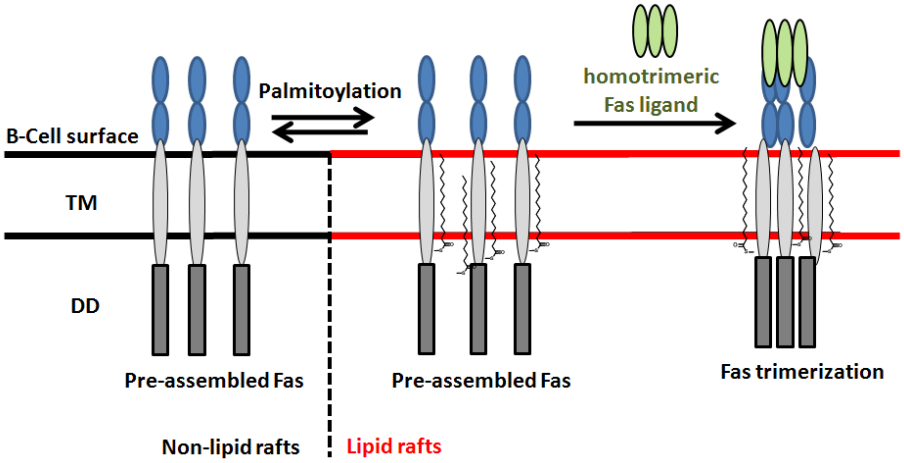

Figure 2.2 Fas palmitoylation initiates Fas trimerization in lipid rafts. Fas palmitoylation induces Fas pre-assembly in lipid rafts, followed by Fas receptor trimerization upon activation by homotrimeric Fas ligands. TM = trans membrane domain, DD = death domain. Figure modified from the literature.[16]

2.3 Fas palmitoylation facilitates Fas internalization

S-palmitoylation is not only essential for Fas trimerization in lipid rafts, but also for Fas association with the actin cytoskeleton, which plays an important role in Fas internalization,[17] an obligatory step for Fas-mediated cell death signaling.[7,18] Artificial disruption of Fas palmitoylation by mutations, as wells as by competition with palmitic acid analogues, inhibit Fas internalization thereby inhibiting Fas-induced apoptosis.[7] Fas receptor internalization occurs through endocytosis[18] to facilitate the assembly of ternary DISC signaling complexes (Death–Inducing Signaling Complex) in endosomal compartments.[19] Recently, two distinct Fas-mediated apoptosis signaling pathways were described referred to as type I or type II, depending on Fas internalization efficiency (Figure 2.3).[20-22]

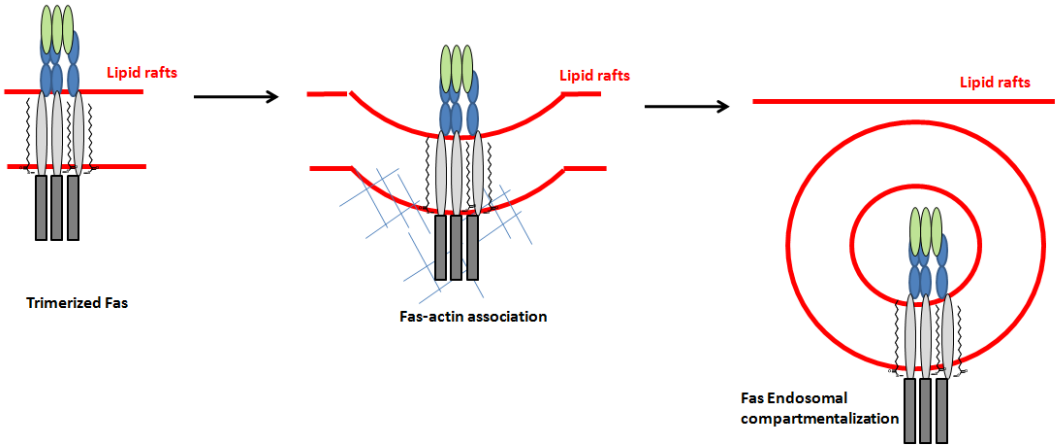

Figure 2.3 Fas palmitoylation facilitates Fas internalization. Fas internalization occurs by endocytocis through Fas - actin association. Figure addapted from literature.[7]

2.4 Distinct Fas signaling depending on Fas internalization

2.4.1 Fas-mediated apoptotic cell signaling pathway type I

In Fas-mediated apoptotic signaling pathway type I, Fas internalization allows the efficient recruitment of the cytoplasmic adaptor molecule FADD (Fast Associated Death Domain) through a homotypic interaction between FAS and FADD's respective death domains (DD).[13,14,23] Subsequently, FAS-bound FADD forms a DISC complex[23] through an homotypic interaction between FADD and procaspase-8's respective death effector domains (DED).[24-26] Such ternary complexes are mainly assembled in endosomal compartments after internalization.[18] The sufficient amount of DISC generated finally allows the direct activation of caspase-8 by autoproteolysis due to the close proximity of the two procaspases-8 involved in the DISC

complex.[27,28] Activated caspase-8 subsequently activates the caspase effector 3 thereby triggering Fas-mediated (or extrinsic) apoptotic signals in the cell (Figure 2.4).

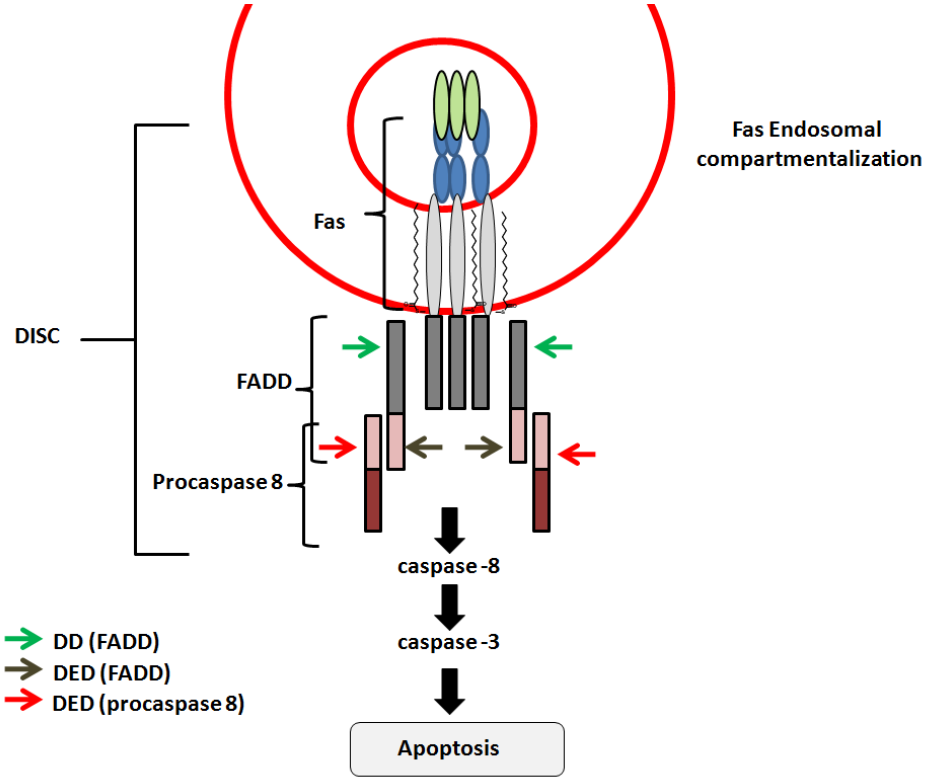

Figure 2.4 Fas-mediated apoptotic cell signaling pathway type I (extrinsic death signaling pathway). The efficent Fas internalization permits an efficent caspase-8 activation resulting in caspase-3 activation and finally to apoptosis. DD= death domain, DED= death effector domain. Figure adapted from the literature. [9]

2.4.2 Fas-mediated apoptotic cell signaling pathway type II

In Fas-mediated apoptotic signaling pathway type II, Fas internalization is significantly less effective leading to considerably reduced DISC formation and, in consequence, to less activated caspase-8 rendering the direct activation of effector caspase-3 through the extrinsic death signaling pathway impossible. Instead, activated caspase-8 triggers the apoptotic signal by activation of the intrinsic death signaling from the mitochondria functioning as an apoptosis activation loop.[29,30] After caspase 8–induced proteolytic activation of BID proteins, active t-BID proteins translocate to the mitochondria and induce Bak protein oligomerization. As a result, released cytochrome C (CytC) finally triggers cell death signals via caspase-9 followed by caspase-3 activation (Figure 2.5).

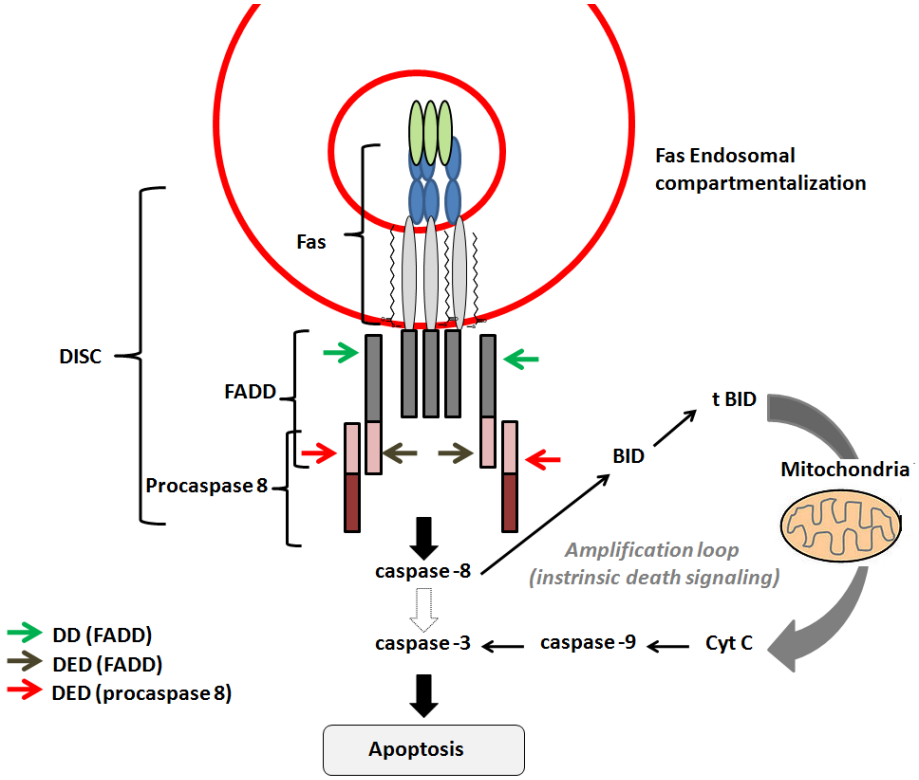

Figure 2.5 Fas-mediated apoptotic cell signaling pathway type II. The inefficent Fas internalization prevent the direct activation of caspase-3 by caspase-8. Instead, caspase-8 activates caspase-3 through the intrinsic death signaling pathway at the mitochondria, regarded as an apoptosis amplification loop. DD= death domain, DED= death effector domain. Figure adapted from the literature.[31]

2.4.3 Fas-mediated non-apoptotic cell signaling pathways

Originaly, Fas receptors were exclusively related to apoptotic signaling pathways (type I or II). However recently, various non-apoptotic Fas-mediated signaling pathways were identified such as the nuclear factor κB (NF-κB) signaling pathway and three major MAPK signaling pathways ($Erk_{1/2}$, $JNK_{1/2}$, P38) controling cell proliferation, motility and invasion.[18,32-38] In contrast to Fas-mediated apoptotic signaling pathways which require Fas internalization, non-apoptotic signaling pathways occur without Fas receptor internalization[18] through the formation of DISC complexes at the cell surface.[16,39] In case of absence/dysfunction of Fas palmitoylation, Fas receptors may be redirected and self-assembled into non-lipid rafts where such non-apoptotic signaling may occur as replacement of internalization-dependant apoptotic signaling. This hypothesis is consistent with the exclusive dependancy on FasL and Fas extracellular domains for Fas trimerization (Figure 2.6).[40]

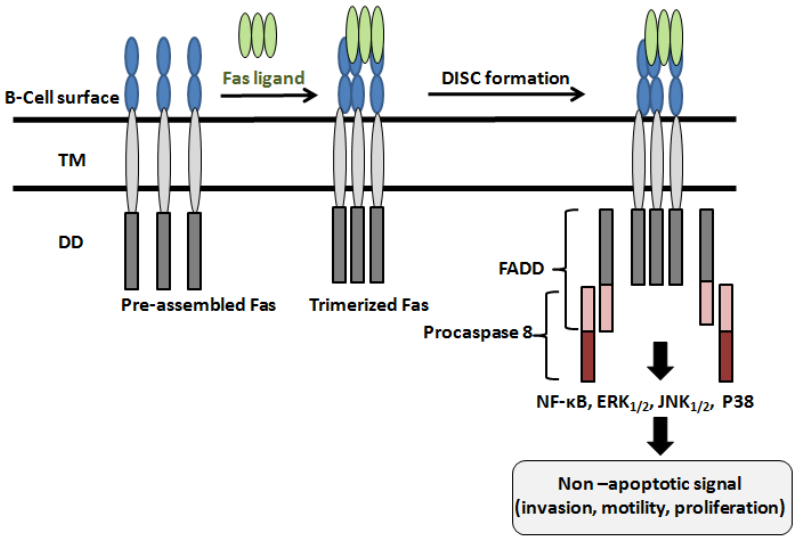

Figure 2.6 Fas-mediated non-apoptotic cell signaling pathways. Signaling occuring in absence of Fas internalization through the formation of DISC complexes at the cell surface. DD= death domain, DED= death effector domain. Figure modified from the literature. [16,33,39]

3 Fas as molecular target for CLL treatment

Given that Fas receptors need to internalize to trigger apoptotic signals, and that Fas internalization is facilitated by Fas palmitoylation, absence/dysfunction of Fas palmitoylation may account for the accumulation of mature B-cells characteristic for CLL disease. Recently, gene expression profiling experiments performed by Wendtner and co-workers[41] have demonstrated that 21 genes with a phospholipase activity were overexpressed in CLL B-cells in comparison with healthy B-cells. Among these genes, seven genes were associated to the activity of phospholipase A2, five genes to phospholipase C, two genes to phospholipase D, and one gene to phospholipase A1, lipoprotein lipase (LPL) and APT1 respectively. Notably, LPL was shown as the gene presenting the more significant overexpression. The cause-effect relationship between the lipase overexpression in CLL cells and the aberrant B-cell accumulation observed in CLL disease was further demonstated by Wendtner et al.[41] employing the lipase inhibitor orlistat. Upon orlistat treatment, an induced apoptosis was observed selectively in CLL cells, whereas no apoptosis was observed in healthy B-cells (hPMBCs, human peripheral blood mononuclear cells) under similar conditions. Given the strong structural similarity between the APT1/APT2 inhibitor palmostatin B (**14**) and orlistat, identical experiments were performed by Wendtner and co-workers using palmostatin B. This have shown that not only orlistat but also palmostatin B was inducing apoptosis selectively in CLL cells, with a several fold stronger effect of palmostatin B compared to orlistat. Given the involvement of APT1 in Ras depalmitoylation,[42] its possible

involvement in Fas depalmitoylation would be consistent with the importance of Fas palmitoylation for Fas-mediated cell death signaling (Figure 2.7).

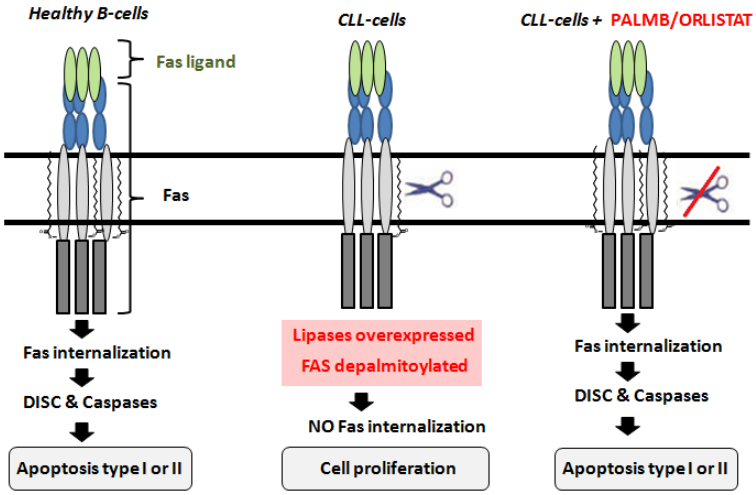

Figure 2.7 Possible explanation for palmostatin B / orlistat-induced apoptosis in B-CLL cells. Palmostatin B/orlistat may inhibit enzymes involved in Fas depalmitoylation therefore allowing Fas internalization, which is required to trigger Fas-mediated death signaling type I or type II.

4 Investigation on palmostatin B's targets in B-CLL cells

4.1 APT1 as a cellular target of palmostatin B

In order to identify the enzyme(s) targeted by palmostatin B in CLL cells, and to identify enzymes possibly involved in Fas depalmitoylation, palmostatin B-derived pulldown probe **23** was used to perform ABPP experiments in B-CLL cells and healthy hPMBC cells in collaboration with the Wendtner group. In this context, primary CLL and hPMBC cells collected from leukaemic and healthy patients, respectively, were incubated for 20 minutes in PBS buffer containing either the cell permeable palmostatin-B derived probe **23** at 50 µM concentration or DMSO. After subsequent washing followed by cell lysis, samples were frozen and were further processed in Dortmund. After evaluation of the sample protein concentration, all samples were adjusted to ~ 1-1.2 mg/ml protein concentration by dilution with PBS to ensure an optimal $Cu^{(I)}$- [3+2] cycloaddition. Indeed, experience in pulldown experiments revealed a significantly impaired click ligation when using concentrated lysates. By analogy to previous labeling experiments, target proteins were tagged by reaction with the rhodamine-azide-biotin construct $TrifN_3$ (**103**). After subsequent enrichment using streptavidin beads, an equal amount of sample was loaded on a 12% SDS-PAGE gel, allowing the comparison of the fluorescent labeling profile obtained

respectively using primary CLL and hPMBC cells (Figure 2.8A). As expected, *in gel* fluorescence detection revealed significant differences in the labeling profile obtained with probe **23** in CLL and PMBC cells, exemplified by two major intense fluorescent bands in CLL samples compared to significantly weaker bands in hPMBC samples. Interestingly, one of these major bands was located in the area where APT1/APT2 would be expected to be localized. Therefore, to confirm the presence of APT1 among the target proteins and to potentially detect a higher amount of labeled APT1 in CLL samples over PMBCs samples, the gel previously scanned for fluorescence was subsequently transferred to a PVDF membrane and used for Western blotting analysis for APT1 visualization. As a result, APT1 was confirmed as one of the target proteins in both samples with a slightly higher amount of labeled APT1 in CLL samples compared to hPMBC samples (Figure 2.8B).

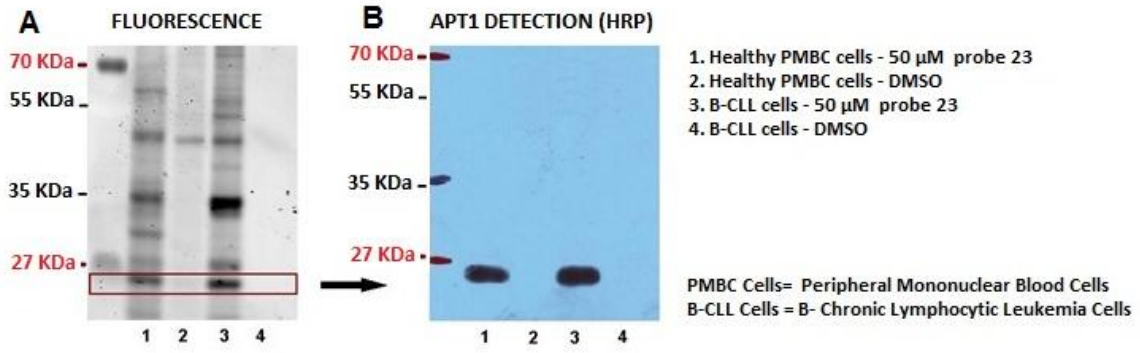

Figure 2.8 Comparison of the labeling profile using palmostatin B-derived probe 23 in CLL and hPMBC cells. B-CLL cells and hPMBCs cells were incubated for 20 minutes with palmostatin-B derived probe **23** (50 µM) and compared to their respective DMSO treated control. A) *In gel* fluorescence scanning highlighting several major bands including APT1 (MW= 24.67 kDa). Conditions for healthy PMBC samples: $TrifN_3$ (**103**) = 10 µM, TCEP:HCl = 0.5 mM, ligand = 50 µM, $CuSO_4$ = 0.5 mM, lysate 1.5 mg/ml, 500 µM bead suspension, 1/10 of the sample loaded on the gel. Condition for B-CLL samples: $TrifN_3$ (**103**) = 10 µM, TCEP:HCl = 0.5 mM, ligand = 50 µM, $CuSO_4$ = 0.5 mM, lysate 1.2 mg/ml, 500 µM bead suspension, 1/10 of the sample loaded on the gel. B) Corresponding Western blotting analysis for APT1 visualization using polyclonal rabbit APT1 antibody. Condition: proteins blocked in TBST 2% chocolate slimfast for 1h at rt, then primary APT1 antibody (anti-hAPT1 from rabbit, custom-raised from BioGenes Gmbh as a 0.26 mg/ml suspension) applied in 1/50 dilution in TBST 2% chocolate slimfast (overnight at 4°C), then secondary antibody (ImmunoPure® antibody, goat anti-rabbit IgG (H+L), horseradish peroxidase, # 31460, Thermo Scientific) in a 1/10 000 dilution in PBST for 1h at rt. Final detection using *Supersignal ® West Pico Chemiluminescent substrat* after 30 seconds exposure.

4.2 Toward palmostatin B cellular targets - proteomic analysis

Although Western blotting analysis could clearly identify APT1 as one cellular target of palmostatin B, proteomic analyses were subsequently performed to identify all proteins covalently bound to the β-lactone probe **23** and especially those potentially relevant to Fas depalmitoylation. In this context, three independent labeling experiments were performed using cells from three different healthy and leukaemic patients. After silver staining, fluorescent bands corresponding to labeled proteins were isolated and digested with trypsin. Peptide fragments were subsequently separated, analyzed by nano-HPLC-MS/MS and finally compared with the SwissProt database for protein identification. Only proteins, for which at least two protein specific peptides were identified, were chosen for further validation and only those identified at least in two out of three independent pulldown experiments but not in control pulldowns (DMSO treated sample) were considered as hits**.** Table 2.1 displays the list of lipases/hydrolases identified by proteomic analysis either in hPMBC and/or CLL samples with the probability threshold $p < 0,01$.

Proteins	CLL cells	hPMBC cells	MW (kDa)	Protein function
ABHDA_HUMAN	**yes**	**yes**	33.933	Ab-hydrolase domain-containing protein 10, mitochondrial OS=Homo sapiens GN=ABHD10 PE=1 SV=1
ABHDB_HUMAN	no	yes	34.690	Ab-hydrolase domain-containing protein 11 OS=Homo sapiens GN=ABHD11 PE=2 SV=1
ABHEB_HUMAN	**yes**	**No****	22.346	Ab-hydrolase domain-containing protein 14B OS=Homo sapiens GN=ABHD14B PE=1 SV=1
AT2A2_HUMAN	no	yes	114.757	Sarcoplasmic/endoplasmic reticulum calcium ATPase 2 OS=Homo sapiens GN=ATP2A2 PE=1 SV=1 (ATP hydrolase)
AT2A3_HUMAN	no	yes	113.977	Sarcoplasmic/endoplasmic reticulum calcium ATPase 3 OS=Homo sapiens GN=ATP2A3 PE=1 SV=2 (ATP hydrolase)
ACOT1_HUMAN	no	yes	46.277	Acyl-coenzyme A thioesterase 1 OS=Homo sapiens GN=ACOT1 PE=2 SV=1
BAT5_HUMAN	no	yes	63.243	Abhydrolase, Protein BAT5 OS=Homo sapiens GN=BAT5 PE=1 SV=3
CATB_HUMAN	no	yes	37.822	Cathepsin B OS=Homo sapiens GN=CTSB PE=1 SV=3 (peptidase)

CPVL_HUMAN	no	yes	54.164	Probable serine carboxypeptidase CPVL OS=Homo sapiens GN=CPVL PE=1 SV=2
ESTD_HUMAN	**yes**	**yes**	31.463	S-formylglutathione hydrolase OS=Homo sapiens GN=ESD PE=1 SV=2
F18A1_HUMAN	no	yes	33.990	Abhydrolase domain-containing protein FAM108A1 OS=Homo sapiens GN=FAM108A1 PE=2 SV=1
FAS_HUMAN	no	yes	273.427	Fatty acid synthase OS=Homo sapiens GN=FASN PE=1 SV=2
LYPA1_HUMAN	**yes**	**yes**	24.670	Acyl-protein thioesterase 1 OS=Homo sapiens GN=LYPLA1 PE=1 SV=1
LYPA2_HUMAN	**Yes***	**yes**	24.637	Acyl-protein thioesterase 2 OS=Homo sapiens GN=LYPLA2 PE=2 SV=1
MGLL_HUMAN	no	yes	33.261	Monoglyceride lipase OS=Homo sapiens GN=MGLL PE=2 SV=2
PAFA2_HUMAN	no	yes	44.036	Platelet-activating factor acetylhydrolase 2, cytoplasmic OS=Homo sapiens GN=PAFAH2 PE=1 SV=1
PLBL1_HUMAN	no	yes	63.255	Putative phospholipase B-like 1 OS=Homo sapiens PE=1 SV=1
PLPL6_HUMAN	no	yes	149.995	Neuropathy target esterase OS=Homo sapiens GN=PNPLA6 PE=1 SV=2
PPGB_HUMAN	no	yes	54.466	Lysosomal protective protein OS=Homo sapiens GN=CTSA PE=1 SV=2 (peptidase)
PPT1_HUMAN	no	yes	34.193	Palmitoyl-protein thioesterase 1 OS=Homo sapiens GN=PPT1 PE=1 SV=1
SAMH1_HUMAN	no	yes	72.201	SAM domain and HD domain-containing protein 1 OS=Homo sapiens GN=SAMHD1 PE=1 SV=2 (hydrolase)
EST1_HUMAN	no	yes	62.521	Liver carboxylesterase 1 OS=Homo sapiens GN=CES1 PE=1 SV=2

Table 2.1 List of lipases/hydrolases identified by mass spectrometry in hPMBC and CLL samples. Labeling experiments performed using 50 µM palmostatin B-derived probe **23**. Table showing Protein ID, molecular weight (MW) of proteins together with their respective function.*****Protein identified twice in the positive control and once in the negative control with the high probability threshold p <0,01, and identified only in the positive control (twice) with the lower probability p <0,001. ** Protein identified once in the positive control and not in the negative control with the high probability threshold p <0,01. Data based on three distinct cell samples respectively healthy PMBC cells and CLL-B cells.

As expected, a larger variety of proteins were identified in healthy hPMBC samples given that hPMBC samples not only contain healthy B-cells but also various additional blood cells. Proteins identified exclusively in CLL samples or simultaneously in hPMBC and CLL samples may potentially be involved in CLL pathogenesis such as ABHDA, ABHEB, ESTD, LYPA1 and LYPA2. Interestingly, phospholipases shown to be overexpressed in CLL cells at the gene expression level, were not identified among the cellular target of palmostatin B at the exception from APT1. In addition, proteomic analysis showing APT1 as a cellular target of palmostatin B in primary hPMBC and CLL cells, were found to be consistent with Western blotting experiments. Although proteomic analysis could only identify the hydrolase ABHEB in CLL cells and not in hPMBC cells, its unique implication in CLL disease is very unlikely. Instead, a CLL overexpression of one (or several) protein(s) targeted by palmostatin B is more likely. This hypothesis would indeed be consistent with the reported lipase overexpression in CLL cells over healthy B-cells.[41] The relevance of the proteomic data was confirmed by the strong correlation observed when assigning the five proteins with a fluorescent labeling profile obtained previously under similar conditions (Figure 2.9).

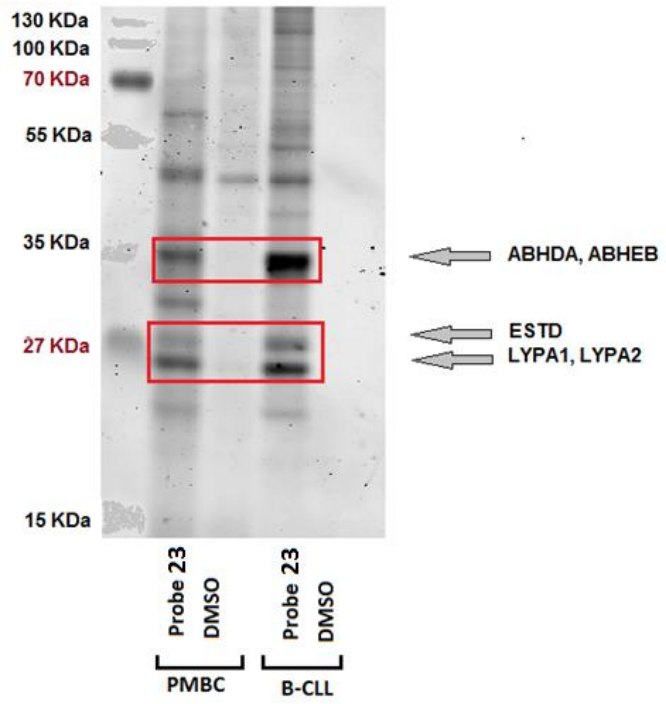

Figure 2.9 Assignment of the proteins identified by proteomic analysis to the fluorescence labeling profile. Fluorescent labeling profile using palmostatin B-derived probe **23** after 20 minutes incubation with healthy hPMBC cells or B-CLL cells at 50 µM concentrations compared to their respective negative control treated with DMSO. The major fluorescent bands were correlated to hydrolase/lipases identified by mass spectrometry either exclusively in the CLL sample or simultaneously in CLL and hPMBC samples. Data based on three independent experiments.

APT1 (or LYPA1) and APT2 (or LYPA2) proteins found in both healthy and CLL cells as a strong fluorescent band at approximately 25 kDa, constitute possible Fas depalmitoylating enzyme given that both were already shown as Ras depalmitoylating enzymes, and that APT1 was shown to be overexpressed in CLL cells by gene expression profiling experiments.[41] Moreover, palmostatin B inhibit APT1 and APT2 *in vitro* with a higher efficiency over orlistat (IC_{50} (APT1, Orlistat) = 549 +/-171 nM , IC_{50} (APT2, Orlistat) = 408 +/- 211 nM, IC_{50} (APT1, PalmB) = 5.37+/- 0.38 nM , IC_{50} (APT2, PalmB) = 19.58 +/- 0.87 nM; values obtained with the DiFMUO fluorescent assay for APT1 and APT2) which would be consistent with the stronger induced apoptosis observed upon palmostatin B treatment compared to orlistat.

Additional Fas depalmitoylation enzyme candidates are the α,β–hydrolases ABHDA and ABHEB found in both healthy and B-CLL samples as a strong fluorescent band at approximately 35 kDa. Although these two proteins have a Ser-Asp-His catalytic triad necessary for their hydrolase activity, no depalmitoylating activity is reported. However, given the mitochondrial localization of the protein ABHDA, relevance to Fas depalmitoylation is unlikely. In contrast, the protein ABHEB which mainly localized in the cytoplasm, and which has a reported hydrolase activity toward the ester p-nitrophenyl butyrate *in vitro*,[43] would require additional investigation to address its eventual relevance to Fas depalmitoylation. Given its S-formylglutathione hydrolase activity,[44] the cytosolic serine esterase ESTD presenting a Ser-Asp-His catalytic triad, would also require further investigation.

5 Conclusion

In conclusion, we have succeeded in identifying a number of proteins, whose overexpression in CLL cells may potentially be involved in CLL pathogenesis. Wendtner and co-workers are currently performing additional experiments in order to address their possible involvement in Fas depalmitoylation. In particular, a large effort is spent on APT2 to demonstrate its overexpression in CLL cells over healthy B-cells**.** Although no depalmitoylating activity was reported for ABHDA, ABHEB and ESTD, further investigation would also be required given the strong intensity of their corresponding bands in the fluorescent labeling profile. In addition, given that orlistat was identified as an effective inhibitor of LPL[45] and PLA2[46] (both overexpressed in CLL cells) and that both enzymes were not identified among the cellular target of palmostatin B, it would be interesting to perform similar labeling experiments using an ABPP-probe derived from orlistat, in order to know if both compounds are having different target(s) both possibly involved in CLL pathogenesis or rather similar target(s) but with different affinity.

6 References

(1) www.seer.cancer.gov
(2) Kipps, T. J. *Curr Opin Hematol* **2000**, *7*, 223.
(3) Caligaris-Cappio, F.; Hamblin, T. J. *J Clin Oncol* **1999**, *17*, 399.
(4) Messmer, B. T.; Messmer, D.; Allen, S. L.; Kolitz, J. E.; Kudalkar, P.; Cesar, D.; Murphy, E. J.; Koduru, P.; Ferrarini, M.; Zupo, S.; Cutrona, G.; Damle, R. N.; Wasil, T.; Rai, K. R.; Hellerstein, M. K.; Chiorazzi, N. *J. Clin. Invest*. **2005**, *115*, 755.
(5) Bernard, M.; Drenou, B.; Pangault, C.; Dauriac, C.; Fauchet, R.; LePrise, P. Y.; Lamy, T. *Br J Haematol* **1999**, *107,* 213.
(6) Frenzel, L. P.; Patz, M.; Pallasch, C. P.; Brinker, R.; Claasen, J.; Schulz, A.; Hallek, M.; Kashkar, H.; Wendtner, C.-M. *Br. J. Haematol.* **2011**, *152*, 191.
(7) Chakrabandhu, K.; Herincs, Z.; Huault, S.; Dost, B.; Peng, L.; Conchonaud, F.; Marguet, D.; He, H.-T.; Hueber, A.-O. *EMBO J*. **2007**, *26*, 209.
(8) Feig, C.; Tchikov, V.; Schuetze, S.; Peter, M. E. *EMBO J.* **2007**, *26*, 221.
(9) Ashkenazi, A.; Dixit, V. M. *Science* **1998**, *281*, 1305.
(10) Rossin, A.; Derouet, M.; Abdel-sater, F.; Hueber, A.-O. *Biochem. J.* **2009**, *419*, 185.
(11) Papoff, G.; Hausler, P.; Eramo, A.; Pagano, M. G.; Di, L. G.; Signore, A.; Ruberti, G. *J. Biol. Chem.* **1999**, *274,* 38241.
(12) Siegel, R. M.; Frederiksen, J. K.; Zacharias, D. A.; Chan, F. K.-M.; Johnson, M.; Lynch, D.; Tsien, R. Y.; Lenardo, M. J. *Science* **2000**, *288*, 2354.
(13) Chinnaiyan, A. M.; O'Rourke, K.; Tewari, M.; Dixit, V. M. *Cell* **1995**, *81*, 505.
(14) Boldin, M. P.; Varfolomeev, E. E.; Pancer, Z.; Mett, I. L.; Camonis, J. H.; Wallach, D. *J. Biol. Chem.* **1995**, *270*, 7795.
(15) Itoh, N.; Nagata, S. *J. Biol. Chem.* **1993**, *268*, 10932.
(16) Muppidi, J. R.; Tschopp, J.; Siegel, R. M. *Immunity* **2004**, *21*, 461.
(17) Parlato, S.; Giammarioli, A. M.; Logozzi, M.; Lozupone, F.; Matarrese, P.; Luciani, F.; Falchi, M.; Malorni, W.; Fais, S. *EMBO J*. **2000**, *19*, 5123.
(18) Lee, K.-H.; Feig, C.; Tchikov, V.; Schickel, R.; Hallas, C.; Schuetze, S.; Peter, M. E.; Chan, A. C. *EMBO J*. **2006**, *25*, 1009.
(19) Miaczynska, M.; Pelkmans, L.; Zerial, M. *Curr. Opin. Cell Biol.* **2004**, *16*, 400.
(20) Scaffidi, C.; Fulda, S.; Srinivasan, A.; Friesen, C.; Li, F.; Tomaselli, K. J.; Debatin, K.-M.; Krammer, P. H.; Peter, M. E. *EMBO J*. **1998**, *17*, 1675.
(21) Barnhart, B. C.; Alappat, E. C.; Peter, M. E. *Semin. Immunol.* **2003**, *15*, 185.
(22) Algeciras-Schimnich, A.; Pietras, E. M.; Barnhart, B. C.; Legembre, P.; Vijayan, S.; Holbeck, S. L.; Peter, M. E. *Proc. Natl. Acad. Sci. U. S. A*. **2003**, *100*, 11445.
(23) Kischkel, F. C.; Hellbardt, S.; Behrmann, I.; Germer, M.; Pawlita, M.; Krammer, P. H.; Peter, M. E. *EMBO J.* **1995**, *14*, 5579.
(24) Peter, M. E.; Krammer, P. H. *Cell Death Differ.* **2003**, *10*, 26.
(25) Boldin, M. P.; Goncharov, T. M.; Goltsev, Y. V.; Wallach, D. *Cell* **1996**, *85,* 803.
(26) Muzio, M.; Chinnaiyan, A. M.; Kischkel, F. C.; O'Rourke, K.; Shevchenko, A.; Ni, J.; Scaffidi, C.; Bretz, J. D.; Zhang, M.; et, a. *Cell* **1996**, *85*, 817.
(27) Chen, M.; Wang, J. *Apoptosis* **2002**, *7*, 313.
(28) Salvesen, G. S.; Dixit, V. M. *Proc. Natl. Acad. Sci. U. S. A.* **1999**, *96,* 10964.
(29) Scaffidi, C.; Schmitz, I.; Zha, J.; Korsmeyer, S. J.; Krammer, P. H.; Peter, M. E. J. *Biol. Chem.* **1999**, *274*, 22532.
(30) Wei, M. C.; Zong, W.-X.; Cheng, E. H. Y.; Lindsten, T.; Panoutsakopoulou, V.; Ross, A. J.; Roth, K. A.; MacGregor, G. R.; Thompson, C. B.; Korsmeyer, S. J. *Science* **2001**, *292*, 727.
(31) Krammer, P. H. *Nature* **2000**, *407*, 789.
(32) Barnhart, B. C.; Legembre, P.; Pietras, E.; Bubici, C.; Franzoso, G.; Peter, M. E. *EMBO J.* **2004**, *23*, 3175.

(33) Peter, M. E.; Legembre, P.; Barnhart, B. C. *Biochim. Biophys. Acta, Rev. Cancer* **2005**, *1755*, 25.
(34) Legembre, P.; Barnhart, B. C.; Zheng, L.; Vijayan, S.; Straus, S. E.; Puck, J.; Dale, J. K.; Lenardo, M.; Peter, M. E. *EMBO Rep.* **2004**, *5*, 1084.
(35) Ahn, J.-H.; Park, S.-M.; Cho, H.-S.; Lee, M.-S.; Yoon, J.-B.; Vilcek, J.; Lee, T. H. *J. Biol. Chem*. **2001**, *276*, 47100.
(36) Qin, Y.; Camoretti-Mercado, B.; Blokh, L.; Long, C. G.; Ko, F. D.; Hamann, K. J. *J. Immunol.* **2002**, *169*, 3536.
(37) Peter, M. E.; Budd, R. C.; Desbarats, J.; Hedrick, S. M.; Hueber, A.-O.; Newell, M. K.; Owen, L. B.; Pope, R. M.; Tschopp, J.; Wajant, H.; Wallach, D.; Wiltrout, R. H.; Zornig, M.; Lynch, D. H. *Cell* **2007**, *129*, 447.
(38) Wajant, H.; Pfizenmaier, K.; Scheurich, P. *Cytokine Growth Factor Rev.* **2003**, *14*, 53.
(39) Kreuz, S.; Siegmund, D.; Rumpf, J.-J.; Samel, D.; Leverkus, M.; Janssen, O.; Haecker, G.; Dittrich-Breiholz, O.; Kracht, M.; Scheurich, P.; Wajant, H. *J. Cell Biol.* **2004**, *166,* 369.
(40) Henkler, F.; Behrle, E.; Dennehy, K. M.; Wicovsky, A.; Peters, N.; Warnke, C.; Pfizenmaier, K.; Wajant, H. *J. Cell Biol.* **2005**, *168*, 1087.
(41) Pallasch, C. P.; Schwamb, J.; Koenigs, S.; Schulz, A.; Debey, S.; Kofler, D.; Schultze, J. L.; Hallek, M.; Ultsch, A.; Wendtner, C. M. *Leukemia* **2008**, *22*, 585.
(42) Rusch, M.; Zimmermann, T.J.; Bürger, M.; Dekker, F.J.; Görmer, K.; Triola, G.; Brockmeyer, A.; Janning, P.; Böttcher, T.; Sieber, S.A.; Vetter, I.R.; Hedberg, C., Waldmann, H. *Angew. Chem. Int. Ed.,* **2011,** *in press*
(43) http://www.uniprot.org/uniprot/Q96IU4
(44) http://www.uniprot.org/uniprot/P10768
(45) Lookene, A.; Skottova, N.; Olivecrona, G. Eur. *J. Biochem*. **1994**, *222*, 395.
(46) Filippatos, T. D.; Gazi, I. F.; Liberopoulos, E. N.; Athyros, V. G.; Elisaf, M. S.; Tselepis, A. D.; Kiortsis, D. N. *Atherosclerosis* **2007**, *193*, 428.

CHAPTER 3

SYSTEMATIC EVALUATION OF PALMOSTATIN B'S EFFECT ON THE HUMAN PALMITOME

1 Metabolic labeling of palmitoylated proteins

1.1 Principle of the metabolic labeling

Given that palmitoylated proteins control various cellular processes, the effect of palmostatin B (**14**) on palmitoylated proteins was investigated to potentially discover new applications of thioesterase inhibition within the global palmitome. In this context, a metabolic labeling strategy based on the reversibility of *S*-palmitoylation, already reported for the visualization of the human palmitome was applied.[1] Palmitoylated proteins contained in HeLa cells were metabolically labeled by incorporation of the inert palmitate analogue ω16-alkynyl fatty acid **106** (100 µM). For the metabolic labeling, the cell medium was complemented with 5% of bovine serum albumin (BSA) in replacement to fetal bovine serum (FBS), in order to facilitate the solubilization of the fatty acid. Subsequently, cells were lysed and alkynylated proteins were tagged through a $Cu^{(I)}$-catalyzed Huisgen [3+2]-cycloaddition using the rhodamine reporter dye $TriN_3$ **103**. After separation by SDS-gel electrophoresis, *in gel* fluorescence scanning allows for the detection of labeled palmitoylated proteins by comparison with a sample treated with DMSO (Figure 3.1).

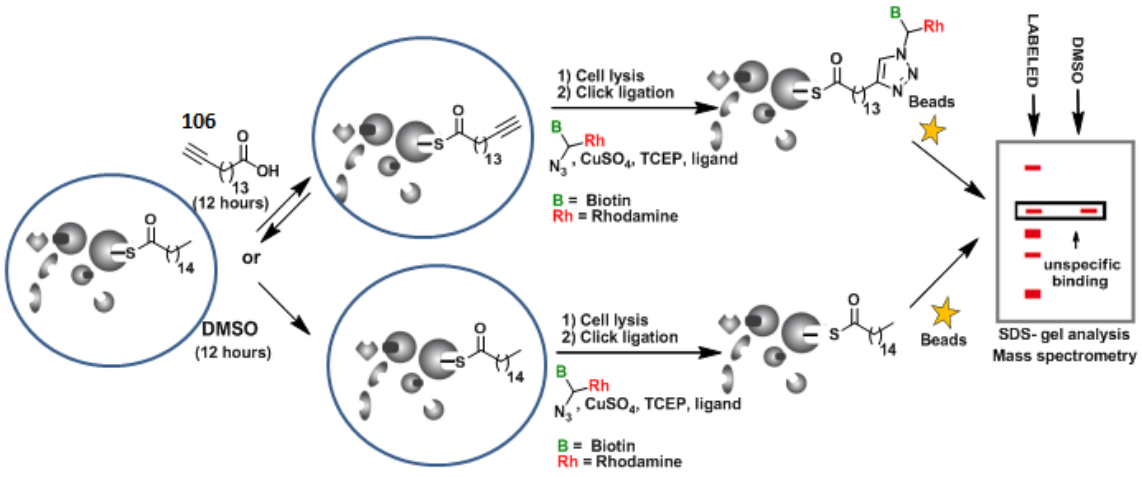

Figure 3.1 Principle of palmitome labeling experiments. After incubation with ω16-alkynyl fatty acid (**106**) /DMSO for 12 hours, HeLa cells are lysed and alkynytated proteins are subsequently tagged through $Cu^{(I)}$-catalyzed Huisgen [3+2]-cycloaddition. After separation by SDS-gel electrophoresis, fluorescence scanning allows the visualization of fluorescently labeled palmitoylated proteins as well as unspecific binding (DMSO sample). Mass spectrometry subsequently allows the identification of the labeled palmitoylated proteins.

1.2 Synthesis of ω16-alkynyl fatty acid 106

ω16-Alkynyl fatty acid **106** (15-hexadecyn-1-oic acid) was synthesized according to the literature[1] from commercially available 7-hexadecyn-1-ol **104** in two steps consisting in a zipper reaction or base-catalyzed isomerization of an internal alkyne to a terminal alkyne employing sodium hydride and 1,3-diaminopropane (DAP). Terminal alkyne **105** was subsequently oxidized to carboxylic acid **106** using the Jones reagent (Scheme 3.1).

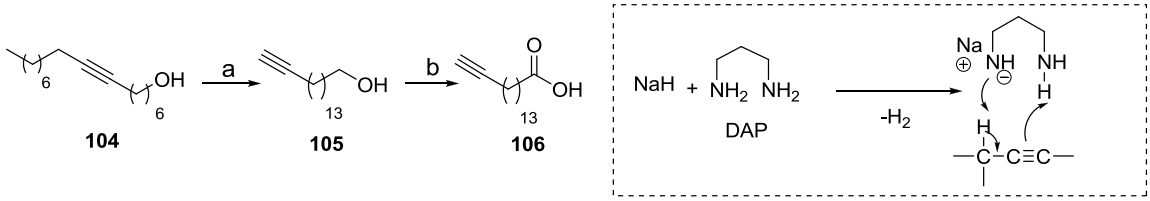

Scheme 3.1 Synthesis of ω16-alkynyl fatty acid 106. Reagents and conditions: a) NaH (8.0 eqv.), 70°C in DAP, then alkyne (1.0 eqv.), 55°C, overnight, 90% yield. b) Jones oxidation ($CrO_3/H_2SO_4/H_2O$) in acetone, 94% yield.

1.3 Optimization of the labeling conditions

For the optimization of the metabolic labeling experiments, it was chosen to use a relatively large amount of HeLa cells ($1.5*10^6$ cells) to ensure the visualization of palmitoylated proteins which are generally present in low abundance. *S*-palmitoylated proteins were originally postulated to be enriched in lipid rafts due to their palmitate moieties, and therefore their solubilization from these detergent resistant membranes would require specific treatments such as the use of methyl-β-cyclodextrin. However, a recent global analysis of palmitoylated proteins in membrane domains,[2] revealed a considerable amount of *S*-acylated proteins contained in non-raft membranes including palmitoylated Ras proteins. Therefore, several mild lysis conditions were investigated to solubilize a maximal amount of palmitoylated proteins from membranes. After metabolic incorporation of ω16-alkynyl fatty acid **106** (100 µM, 5 hours, 37°C), HeLa cells were lysed either by sonication in PBS buffer or using detergent-containing lysis buffers (1% NP40). After click ligation followed by sample enrichment using streptavidin magnetic beads, target proteins were separated by SDS-gel electrophoresis allowing to observe the influence of the lysis conditions on the fluorescent labeling profile by comparison with a control treated with DMSO.

In gel fluorescence scanning revealed a similar labeling profile when using PBS or a phosphate buffer containing 1% NP40 (referred to as buffer B), with several strong fluorescent bands compared to the negative DMSO control. In particular, one band was located at 21 kDa which may correspond to palmitoylated Ras isoforms (~21 KDa for *H*-Ras, *N*-Ras and *K*-Ras4A). In contrast, employing the detergent-containing lysis buffer referred to as buffer A, no fluorescent bands was observed due to the cleavage of the rhodamine reporter group by mercaptoethanol contained in the buffer. However, the labeling profile is likely to be similar to the two previous conditions. In addition, given that gels were typically run over night in a DTT-containing loading buffer, decrease in fluorescent labeling is also possible. As exclusion of reducing reagent from the loading buffer usually results in smearing bands,[3] the use of a TCEP-containing loading buffer could be an alternative to denaturate proteins. Finally, gel staining techniques allowing the use of N_3-(azidopropyl)-biotinamide were preferred for protein visualization and were used in all newly performed labeling experiments (Figure 3.2).

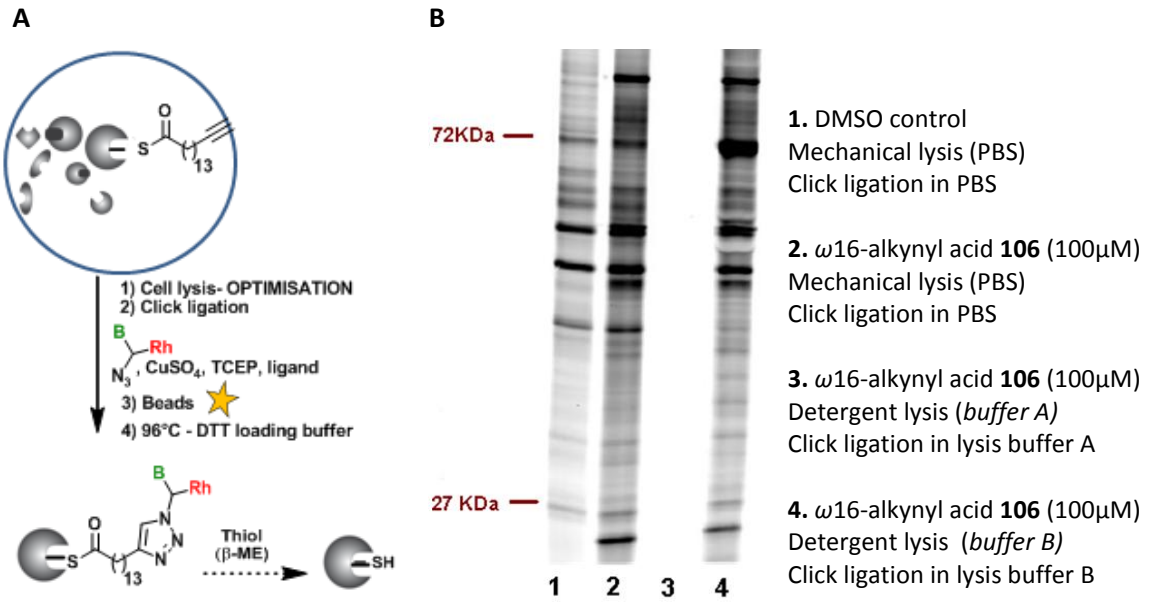

Figure 3.2 Comparison of the fluorescent labeling profile obtained using different lysis conditions. A) Principle of the metabolic labeling and explanation for the loss of rhodamine reporter group using thiols (β-mercaptoethanol (β-ME) or DTT). B) Fluorescent gel highlighting few bands not present in the DMSO – treated control using various lysis conditions. Condition: HeLa cells= 1.5*10 ^{6}, ω16-alkynyl fatty acid (**106**) /DMSO= 100 µM (in a 5% BSA-containing media, 5 hours), lysis, click ligation (TrifN_3 (**103**) = 15 µM, TCEP:HCl = 0.5 mM, ligand = 50 µM, $CuSO_4$ = 0.5 mM). Buffer A: 50mM PIPES, 50mM NaCl, 5mM $MgCl_2.6H_2O$,1% NP40, pH 7.4, mercaptoethanol (0.1%), protease inhibitor cocktail Mini. Buffer B: 150mM NaCl, 100mM phosphate buffer pH 7.5, 1% NP40, protease inhibitor cocktail Mini.

1.4 Proteomic analyses

Before SILAC quantification, two similar experiments performed either in PBS buffer or in 1% NP40 containing PBS buffer, were submitted to proteomic analyses in order to compare their labeling efficiency. Importantly, neither the use of BSA nor the use of the detergent-containing lysis buffer was a problem; however protein identification was extremely difficult given a high number of proteins present in both samples treated with ω16-alkynyl fatty acid and with DMSO respectively. Given a relatively simple fluorescent labeling profile similar to Figure 3.2B, unspecific binding due to the protein carrier BSA is likely to occur, generating protein aggregates which may unspecifically attached to streptavidin beads. One alternative to avoid such a problem, would consist in releasing first *S*-palmitoylated proteins from streptavidin beads by employing hydroxylamine (0.32M at pH= 6.8, for 1 hour at 37°C)[44] to cleave thioester bonds and in a second step to thermo-detach unspecifically bound proteins from the beads consisting in non-fluorescently labeled proteins. Therefore, experiences developed to evaluate the effect of palmostatin B on palmitoylated proteins will be performed using the hydroxylamine-based strategy to limit protein identification problems, and cells will be mechanically lysed in PBS buffer for practical reason.

2 Quantification of palmostatin B's effect on the human palmitome

2.1 Principle of the double metabolic labeling

To quantify the effect of palmostatin B (**14**) on relative levels of palmitoylated proteins, the SILAC (stable isotope labeling with amino acids in cell culture) method was applied to HeLa cells, given that such method would permit to avoid risk of quantification errors due to for example unequal sampling. Two different cell populations were grown in SILAC media complemented either with heavy (isotopic, ^{13}C) or light (normal, ^{12}C) arginine and lysine. The use of both amino acid permits to ensure the isotopic labeling of all peptides given that protein digestion with trypsin cleaves proteins after lysine and arginine residues. After five cell duplication cycles, the amino acid incorporation should be completed. This allows the metabolic labeling of the distinct cell populations by incubation of the cells with ω16-alkynyl fatty acid (**106**) for 12 hours at 100 µM, in their respective SILAC media in which FBS was replaced by 5% BSA. Subsequently, isotopically labeled cells were treated for 3 hours with palmostatin B at a non-cytotoxic concentration of 30 µM, whereas the other cell population was treated with DMSO (cell incubation in their respective SILAC media). Cells from the obtained populations were finally

washed with PBS buffer, treated with trypsin and lysed by sonication in 1 ml PBS, respectively. Once their correct and complete amino acid incorporation was determined by mass spectrometry, the two resulting cell populations were mixed in a 1:1 ratio based on their respective cell concentration, typically more accurate compared to protein concentration. Finally, a 1 ml volume of cell lysate containing $5*10^5$ cells taken from each cell populations (10^6 cells/ml in total) was tagged through a $Cu^{(I)}$-catalyzed Huisgen [3+2]-cycloaddition with N_3-(azidopropyl)-biotinamide. After click ligation followed by sample enrichment using streptavidin beads, palmitoylated proteins were released using hydroxylamine and beads were subsequently boiled 5 min in SDS-loading buffer to detach proteins binding unspecifically to the beads. Finally, the hydroxylamine cleavage solution containing released *S*-palmitoylated proteins was concentrated to be fully loaded on a 12 % SDS gel to be compared with proteins released by boiling the beads, applied on the gel as a distinct band. A sample of the initial cell lysate mixture (taken before initiating the click ligation) was additionally loaded on the gel in order to quantify the effect of palmostatin B (**14**) on the palmitoylation level of proteins. In parallel, the two isotopically distinct cell populations were treated only with DMSO, mixed in a 1:1 ratio and proceed like previously leading to the three corresponding samples referred to as NH_2OH, Lysate and Δ used as negative control. After separation by SDS-gel electrophoresis, the gel containing all six samples was silver stained revealing a significantly weaker amount of proteins in samples obtained after hydroxylamine treatment compared to samples obtained by boiling the beads, thereby confirming unspecific binding. After band isolation followed by protein digestion, mass spectrometry analysis was performed to compare the relative peak intensity of isotopic peptide pairs in all six different samples, with peptide pairs distinguishable by a +6 Da mass difference. Given that proteins collected using hydroxylamine are palmitoylated, they may be affected upon palmostatin B treatment. For example, *H*- and *N*-Ras proteins, whose depalmitoylation is inhibited by the APT1/APT2 inhibitor palmostatin B, should present significant differences in the relative intensity between their peptide pairs, consistent with a higher Ras palmitoylation level in cells treated with palmostatin B compared to control cells treated with DMSO. In contrast, the relative intensity between peptide pairs from proteins unspecifically binding to streptavidin beads should remain identical to the ratio evaluated for the cell lysate mixture employed. In addition, the negative control experiment employing DMSO in both cell populations would be expected to lead to identical peptide pair ratios after and before double metabolic labeling pulldown experiments (Figure 3.3B).

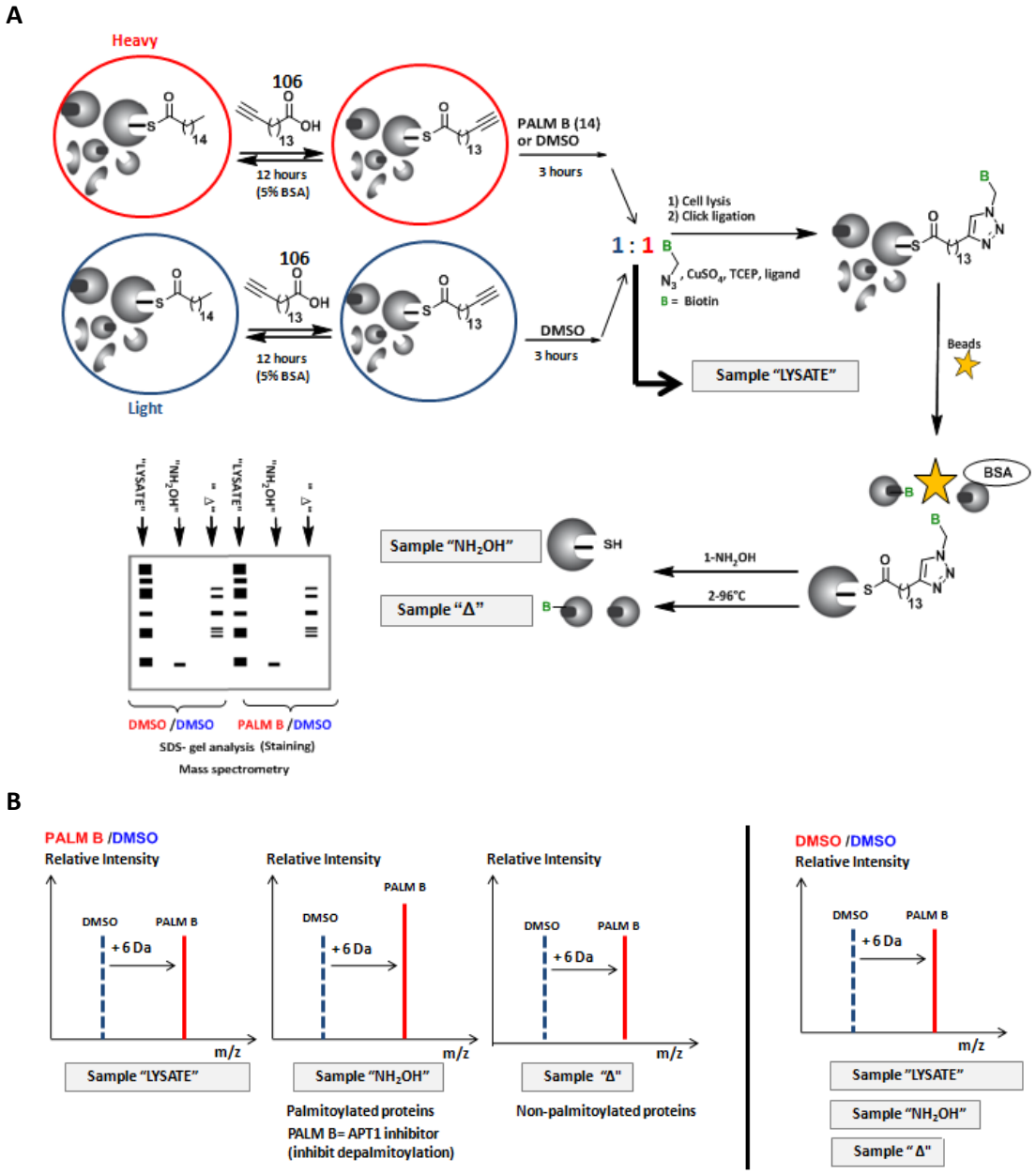

Figure 3.3 Double metabolic labeling experiments to quantify palm B's effect on palmitoylated proteins. A) Principle of the experiment. After metabolic labeling of two cell populations with ω 16—alkynyl fatty acid **106** (100 µM), palmostatin B (C=30 µM) and DMSO are added respectively to the two cell populations (isotopically labeled and normal). After cell lysis, cell lysates are mixed in a ratio 1:1 (10^6 total cells/ml) and alkynylated proteins are tagged by click ligation (conditions: Biotin-N_3 = 30µM, TCEP:HCl = 0.5 mM, ligand = 50 µM, $CuSO_4$ = 0.5 mM). After enrichment with streptavidin magnetic beads, thioester linkages are cleaved off employing hydroxylamine (0.32M, pH=6.8, 1h, 37°C, sample referred to as NH_2OH). Proteins remaining on the beads are finally released by boiling the sample in SDS loading buffer (5 min, 96°C, sample referred to as Δ). After protein separation by SDS-gel electrophoresis, silver staining allow the visualization of proteins contained in the different samples referred to as LYSATE, NH_2OH and Δ respectively. Bands isolation followed by protein digestion finally allow the evaluation of the relative peak intensity of isotopic peptide pairs in all samples. B) Relative peak intensity of isotopic peptide pairs. In theory, a 1:1 ratio should be visible for proteins contained in the initial lysate. Proteins obtained using hydroxylamine should be affected by palmostatin B in contrast to proteins thermo-detached from the beads which should not be affected. In the DMSO control experiment, the relative peak intensity of isotopic peptide pairs should not be affected, with ratios identical before and after pulldown experiments.

2.2 Result and discussion

In order to limit identification problem, proteins of interested were first released by hydroxylamine treatment. In addition, protein digestion was performed on smaller gel pieces in order to help for protein identification (typical area of 10 mm^2 instead of 1 cm^2). Therefore, only a restricted part of the gel comprising proteins below 35 kDa was digested, given that the APT1/2 inhibitor palmostatin B should influence at least the palmitoylation level of *N*-and *H*-Ras isoforms (~ 21 KDa). For optimal quantitative proteomic analyses, several points are of utmost importance. First, absolute peak intensities need to be sufficient to distinguish between signal peaks from background peaks. Second, relative peak intensities of isotopic peptide pairs have to be fixed as closed as possible to a ratio of heavy/light labeled peptides (H/L) of 1:1 in order to limit quantification errors. Relative ratios of peptide pairs in initial cell lysate mixtures treated with palmostatin B/DMSO or only with DMSO were found to vary from H/L = 0.97 to H/L = 1.7 and from H/L = 0.69 to H/L = 1.70 respectively. In this context, accurate proteomic quantifications should be possible. Therefore, in order to evaluate the effect of palmostatin B on protein palmitoylation level, relative ratios of isotopic peptide pairs after pulldown were compared to initial ratios (in cell lysate). In the condition of the experiment, the inhibition of protein depalmitoylation by palmostatin B should be visible by a H/L ratio above 1, whereas the inhibition of protein palmitoylation should lead to a H/L ratio below 1. Relative ratios of isotopic peptide pairs in the sample containing palmitoylated proteins, referred to as the NH_2OH sample were evaluated leading to H/L ratios varying from 0.1 to values largely above 10 (~33). Note: H/L ratio values which are not contained in the range [0.1-10] have typically a large statistical variability and are therefore too uncertain to be considered. Surprisingly, relative ratios of isotopic peptide pairs contained in the sample referred to as Δ, containing in theory only (or largely) unspecifically bound proteins were also significantly different from initial ratios, with H/L ratios between 0.25 and ~12. In order to rationalize these observations, the control experiment performed employing the two cell populations in combination with DMSO was analysed. Relative peak intensities of isotopic peptide pairs contained in sample after pulldown experiments were also largely modified from initial ratios with H/L ratios varying from values below 0.1 to values largely above 10 (~93), and from 0.18 to ~11 in samples referred to as NH_2OH and Δ respectively. Given that both experiments performed with palmostatin B and DMSO respectively, were influenced with a similar magnitude, such effects are therefore very likely not due to palmostatin B. Moreover, unspecific binding to streptavidin beads may not explain this effect given that proteins would be expected to be enrolled in protein aggregates without any distinction between isotopically labeled or normal proteins. Although further investigations

would be required, several explanations could be proposed. First, the metabolic labeling with ω16-fatty acid **106** may differ between normal and isotopically labeled proteins. Alternatively, the availability of the alkyne functionality for the click ligation may be affected by changes in protein structures potentially induced by the double labeling (isotopic follow by metabolic labelings).

3 Conclusion and outlook

In conclusion, conditions for the metabolic labeling and the visualization of palmitoylayed proteins contained in HeLa cells were successfully optimized, allowing notably the detection of an intense fluorescent band at approximately 21 kDa which may correspond to palmitoylated Ras isoforms. Subsequently, SILAC experiments employing an inert alkynylated palmitate analogue in double metabolic labelling experiments were developed in order to evaluate the influence of palmostatin B on the complete palmitome. Although, these experiments did not so far permit any quantification, these experiments permitted to stress some points which would need further investigation. In particular, relative ratios of isotopic peptide pairs were largely modified after pulldown experiments in the DMSO control for an unclear reason. Tentative to reproduce this control experiment failed due to bacterial contaminations. However, it would be worth to clarify this point before performing any new quantification experiments. After further investigations and optimizations, this strategy may allow the systematic evaluation of the effect of palmostatin B on the human palmitome, and may lead to the discovery of new interesting applications for the β–lactones in general and of thioesterase-mediated processes in particular.

4 References

(1) Hannoush, R. N.; Arenas-Ramirez, N. *ACS Chem. Biol.* **2009**, *4*, 581.
(2) Yang, W.; Di, V. D.; Kirchner, M.; Steen, H.; Freeman, M. R. *Mol. Cell. Proteomics* **2010**, *9*, 54.
(3) Martin, B. R.; Cravatt, B. F. *Nat. Methods* **2009**, *6*, 135.
(4) Mack, D.; Kruppa, J. *Biochem. J.* **1988**, *256*, 1021.

CHAPTER 4

APT1/2 INHIBITOR CANDIDATES AS DEPALMITOYLATION TRANSITION STATE MIMICS

1 Design of stable APT1/2 inhibitor candidates

Subsequently to the discovery of APT1 and APT2 as Ras depalmitoylating enzymes and given that targeting these enzymes may constitute a viable approach to interfere with aberrant Ras signaling, various new APT1/2 inhibitor candidates were designed, which in contrast to the previous β-lactone inhibitors, would be regarded as stable transition state mimics of the deacylation process. Therefore, the β–lactone core was replaced by new electrophilic motifs such as α-keto oxazole, α-keto amide and trifluoromethyl ketone, chosen for their steric hindrance comparable to the β–lactone core, which may limit additional strain due to steric repulsions with the enzyme. In this context, and in analogy to previous work, functional groups allowing stabilizing binding interactions in the enzyme active site (SO_2 and NMe_2) which served well for the inhibitory activity of β–lactone inhibitors were introduced in the inhibitor side chain (R in blue), and their optimal position in the enzyme active site was investigated. When possible, a lipophilic tail (in red) mimicking palmitic acid was also introduced on the opposite site of the molecule to create affinity for the enzyme lipid-binding pocket (Scheme 4.1).

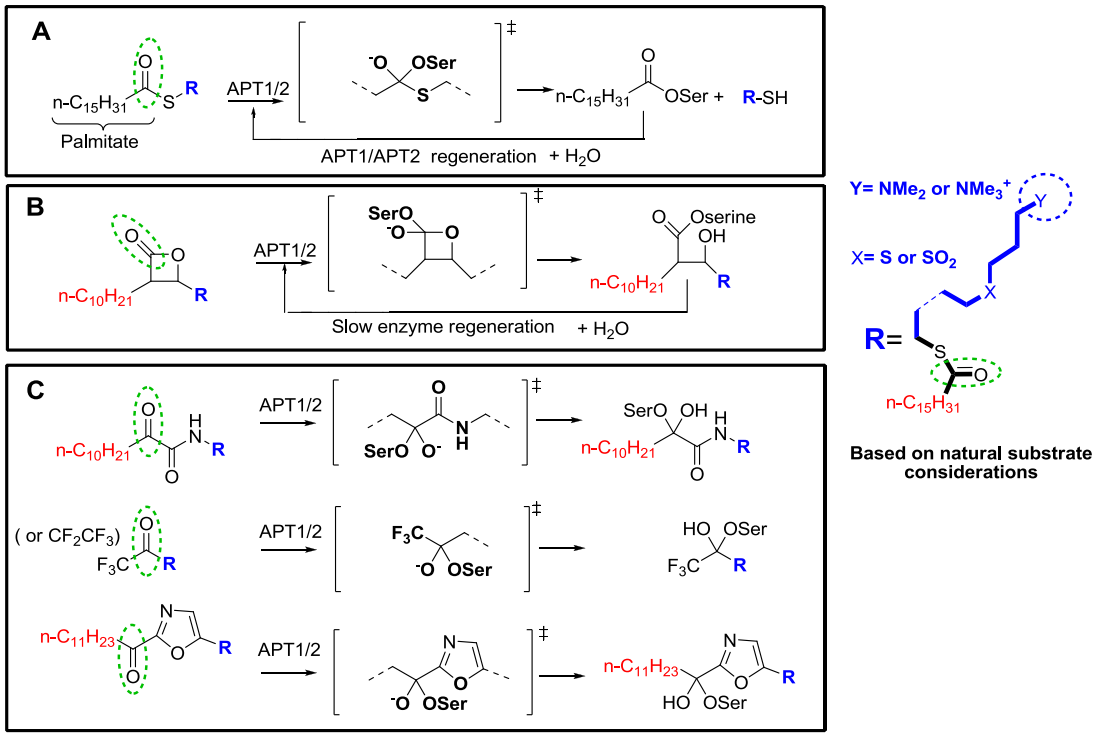

Scheme 4.1 Design of stable APT1/APT2 inhibitor candidates based on structural similarities with native APT1 substrates. A) Depalmitoylation mechanism by the serine hydrolases APT1/APT2, regenerated by hydrolysis. B) Designed β-lactone APT1/APT2 inhibitors as transition state mimic of the deacylation process leading to the slow enzyme regeneration or reactivation. C) Newly designed APT1/APT2 inhibitors (α-Keto-amide, α–Keto-CF_3/CF_2CF_3 and α-Keto oxazole) as stable transition state mimics of the deacylation process.

2 α-Keto amide inhibitor candidates

2.1 Synthesis of the α–keto amide library

Synthesis of the amine spacer

Regarding the amine spacer synthesis, a one step approach consisting in a Mitsunobu[1] reaction was first investigated for alcohol **109**, obtained in 75% through reduction of ester **108**. Conversion of alcohol **109** into *N*-Boc protected amine **110** followed by *in-situ* deprotection using TFA, only permits to obtain amine spacer **111** in 14% yield. Attempts to first isolate the less polar di-tert butyl carbamate protected amine **110** to perform in a second step the BOC deprotection, was also disappointing with compound **110** obtained in a moderate 42% yield (Scheme 4.2).

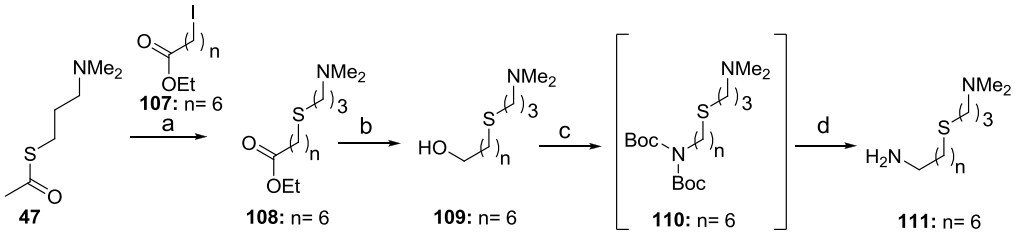

Scheme 4.2 Synthesis of amino spacer **111** via a Mitsunobu reaction. Reagents and conditions: a) Cs_2CO_3 (1.1 eqv.), EtOH, reflux, 2.5h, iodoester **107** (1.1 eqv.), 40°C, 18h, 75%. b) $LiAlH_4$ (1.25 eqv.), THF, 0°C, 1h then rt, 2h, 87% yield. c) PPh_3 (4.0 eqv.), DBAD (3.0 eqv.), Di-t-butyliminodicarboxylate (4.0 eqv.), 0°C (30 min), dry CH_2Cl_2, 42% yield. d) TFA, 0°C, 1h30, 14% yield (over two steps c and d).

As an alternative, a two step procedure was preferred involving the *in-situ* formation of a brominated intermediate, which reacts with sodium azide through a nucleophilic substitution leading to the corresponding azido derivatives.[2,3] Reduction of purified azido derivatives **118-121** by hydrogenation[4] completed the synthesis of amine spacers (n= 2, 3, 5, 6) obtained in a good overall yield as no additional purification step on the amine was required (Scheme 4.3).

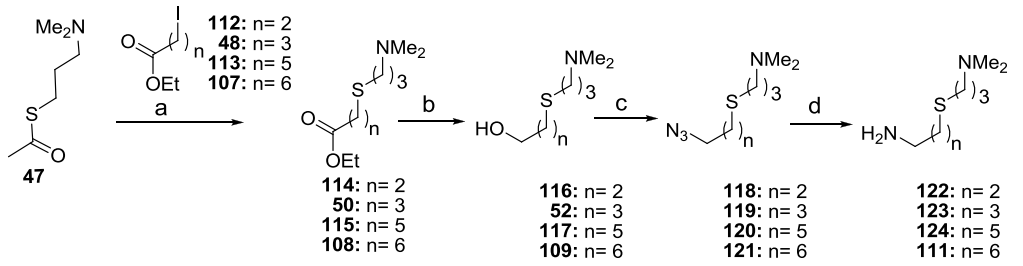

Scheme 4.3 Synthesis of amino spacers through the formation of azido-intermediates. Reagents and conditions: a) Cs_2CO_3 (1.1 eqv.), EtOH, reflux, 2.5h, iodoester (1.1 eqv.), 40°C, 18h, 75-97% yield. b) $LiAlH_4$ (1.3 eqv.), dry THF, 0°C (1h), rt (2h), 87-93% yield. c) PPh_3 (2.0 eqv.), dry DMF, NBS (2.0 eqv.), 55°C (2h), NaN_3 (7.0 eqv.), 85°C (13h), 54-68% yield. d) 10% Pd(C), dry MeOH, H_2, rt (21h), 86-99% yield.

Amide coupling reactions with α– hydroxy acids

The importance of protecting groups for coupling reactions with α-hydroxy acids was first investigated. Therefore, α-hydroxy acid **126** was synthesized by the reaction of commercially available α-brominated carboxylic acid **125** with sodium hydroxide.[5] TBDMS-protected α-hydroxy acid **127** was subsequently obtained from **126** in 76% yield using imidazole/TBDMSCl.[5,6] Protected as well as unprotected α-hydroxy acids were subsequently investigated for optimal coupling conditions with the amine **123** (n=3). Reactions performed using HOBT (1.2 eqv.) and EDC:HCl (3.3 eqv.) as coupling agent with an excess of unprotected α-hydroxy acid **126** (1.25 eqv.) were optimal leading to **129** in 76% yield, whereas the use of NMM/ isobutylchloroformate was optimal for reactions with protected α-hydroxy acid **127** leading to **128** in 56% yield. Although TBDMS deprotection of compound **128** with TBAF was performed in 68% yield,[5,6] the approach starting directly from unprotected α-hydroxy acids was more straightforward with a higher overall yield. Subsequently, a Swern oxidation was performed on compound **129** to obtain keto-amide **130**. However the reaction generated many decomposition products (Scheme 4.4).

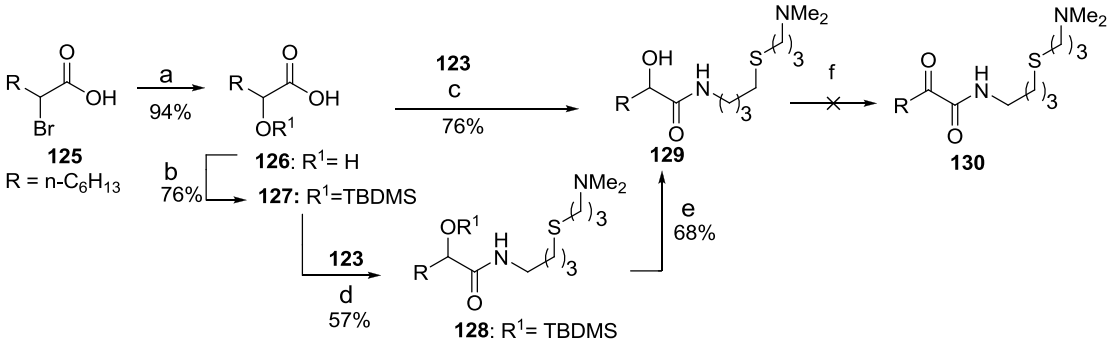

Scheme 4.4 Synthesis of α–keto amide **130** from protected and unprotected α-hydroxy acids. Reagents and conditions: a) NaOH (8.0 eqv.), H_2O, 80°C, 24h, 94% yield. b) imidazole (2.0 eqv.), DMF, 0°C, TBDMSCl (4.0 eqv.), 24h, rt, 76% yield. c) Amine **123** (1.0 eqv.), unprotected α-hydroxy acid (1.25 eqv.), HOBT (1.2 eqv.), EDC.HCl (3.3 eqv.), rt, overnight, 76% yield. d) N-Methylmorpholine (0.8 eqv.), Isobutylchloroformate (0.8 eqv.), Amine **123** (1.2 eqv.), THF, -10°C (1h), rt overnight, 57%. e) TBAF (6.0 eqv.), THF, rt, overnight, 68% yield. f) DMSO (2.4 eqv.), oxalyl chlorid (1.1 eqv.), NEt_3 (3.65 eqv.), CH_2Cl_2, failed.

Amide coupling reactions with α– keto acids

Aware of the relative instability of α-keto acids and the possibility of side reactions, coupling reactions directly with α-keto acids have been regarded as challenging. However, given the disappointing results obtained with unprotected or protected α-hydroxy acids, coupling reactions directly with α- keto acids were reconsidered. The synthesis of α-keto acid **134** started with the α-methylenation of the commercially available aldehyde **131** using aqueous formalin

and dimethylamine hydrochloride, leading to compound **132** in 76% yield.[7] α-Methylenated aldehyde **132** was subsequently oxidized to carboxylic acid **133** in 86% yield using sodium chlorite ($NaClO_2$), sodium phosphate (NaH_2PO_4) and 2-methyl-2-butene as HCl scavenger.[8] After unsuccessful attempts to perform ozonolysis of compound **133,**[8] the oxidative cleavage of the alkene was finally performed via a Lemieux-Johnson oxidation,[9-11] involving catalytic amounts of osmium tetroxide and sodium periodate in aqueous dioxane, leading finally to α-keto acid **134** in 87% yield (Scheme 4.5).

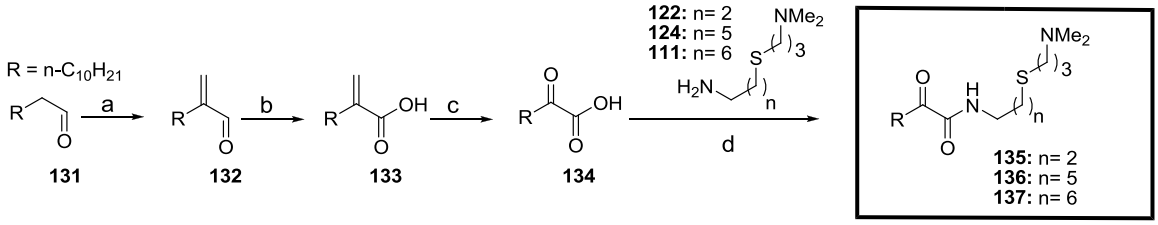

Scheme 4.5 Synthesis of α-keto amides (**135-137**) from α-keto acid **134**. Reagents and conditions: a) $NMe_2H.HCl$ (1.2 eqv.), 37% aqueous formalin (1.2 eqv.), 70°C, 24h, 76% yield. b) $NaClO_2$ (2.3 eqv.), NaH_2PO_4 (2.0 eqv.), 2-methyl-2-butene (3.0 eqv.), t-BuOH/H_2O (3:1), rt, 4h, 86% yield. c) 6 mol% OsO_4, $NaIO_4$ (3.0 eqv.), Dioxane/H_2O (3:1), rt, overnight, 87% yield. d) Various coupling conditions investigated between α-keto acid **134** and various amine spacers.

Several coupling conditions were subsequently tested using an excess of α-keto acid **134** to investigate the possibility to perform coupling reactions directly with α-keto acids. Although low yields were obtained for this one-step approach, the use of isobutylchloroformate/N-methyl morpholine or EDC:HCl as coupling reagents led to a small set of α-keto amides, used to evaluate their *in-vitro* APT1 and APT2 inhibitory activity, before considering an alternative synthetic route (Table 4.1).

ENTRY	Amine	Condition	Yield
1	**111**: n=6 (1 eqv.)	HATU (1.5 eqv.), DIPEA (2 eqv.), CH_2Cl_2, rt , overnight	DC
2	**111**: n=6 (1 eqv.)	HBTU (1.5 eqv.), DIPEA (2 eqv.), CH_2Cl_2, rt , overnight	DC
3	**111**: n=6 (1 eqv.)	NMM(1eqv.), Isobutylchloroformate (1 eqv.), THF, rt, 16h	33%
4	**124**: n=5 (1 eqv.)	EDC.HCl (3 eqv.), CH_2Cl_2, rt , overnight	40%
5	**122**: n=2 (1 eqv.)	EDC.HCl (3 eqv.), CH_2Cl_2, rt , overnight	22%

Table 4.1 Optimisation coupling reactions with α-keto-acids. Table showing the coupling reactions investigated using an excess of α-keto acid **134** (1.2 eqv.). DC= decomposition products.

Derivatization to the sulfone using Oxone®

To investigate the effect of a sulfone on the inhibitory activity, α-keto amide **136** was converted to its oxidized form **138** using an excess of potassium hydrogen monoperoxysulfate (Oxone®)[12] in aqueous methanol at room temperature. The reaction proceeded through the formation of a sulfoxide intermediate, which subsequently converted to the sulfone as single product after 24 hours. α-Keto amide **138** was isolated in 52% yield after reverse phase C_{18} column chromatography (Scheme 4.6).

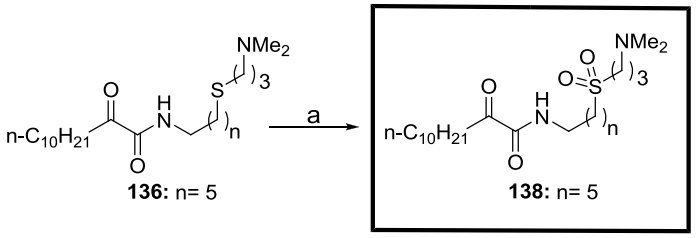

Scheme 4.6 Oxidation of α-keto amide **136** into sulfone **138** using Oxone®. Reagents and conditions: a) Oxone® (3.0 eqv.), MeOH:H_2O (3:2), 24h, rt, 52% yield.

2.2 *In vitro* evaluation for APT1/2 inhibition

The small α-keto amide library (**135-138**) was subsequently screened for APT1 inhibition using the colorimetric assay based on PNPO after 30 min pre-incubation. The APT1 activity remaining at 50 µM was evaluated for each compound based on three independent experiments. No promising APT1 inhibitory activity was detected, with a maximal of 25 % APT1 inhibition observed using 50 µM of compound **137**. Potency for APT1 inhibition is therefore largely below that of the β-lactone inhibitors under similar conditions. In order to investigate their inhibitory effect on APT2, α-keto amides were screened using the fluorescent assay based on DiFMUO. APT2 activities remaining at 50 µM were evaluated for each compound based on three independent experiments. With an activity remaining between 30-50 %, α-keto amides were significantly weaker APT2 inhibitors (IC_{50} values slightly below 50 µM) compared to β-lactone inhibitors, characterized by low nanomolar IC_{50} values under similar conditions (Table 4.2).

Keto Amide	APT1 activity remaining (50 µM, PNPO assay)	APT2 activity remaining (50 µM, DiFMUO assay)
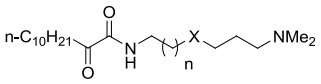		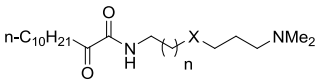
135: n= 2, X= S	**108 +/- 3 %**	**135:** n= 2, X= S **48 +/- 2 %**
136: n= 5, X= S	**107 +/- 5 %**	**136:** n= 5, X= S **26 +/- 2 %**
137: n= 6, X= S	**75 +/- 2 %**	**137:** n= 6, X= S **36 +/- 2 %**
138: n= 5, X= SO_2	**93 +/- 1 %**	**138:** n= 5, X= SO_2 **58 +/- 2 %**

Table 4.2 Evaluation of the α-keto amide library for APT1/APT2 inhibition. Residual APT1 and APT2 activity in percentage obtained for α-keto amides (**135-138**) at 50 µM concentration using respectively the colorimetric assay (PNPO = 600 µM, APT1 = 75 nM, 30 min inhibitor pre-incubation) and the fluorometric assay (DiFMUO = 15 µM, APT2 = 50 nM, 2 min inhibitors pre-incubation). Z' factors were in all cases higher than 0.80. Data based on three independent experiments.

3 α-Keto CF_2CF_3/CF_3 inhibitor candidates

3.1 Synthesis of the α-keto CF_2CF_3/CF_3 library

The synthesis of α- keto CF_2CF_3/CF_3 inhibitor candidates started with ethyl esters hydrolysis into their corresponding carboxylic acids **139-143**, followed by their conversion in a single step to trifluoromethyl ketones **144-148** and pentafluoroethyl ketones **149-153** using respectively ethyl trifluoroacetate and ethyl pentafluoroacetate.[13] Treatment of carboxylic acids **139-143** with LDA generated an enediolate dianion, which was subsequently trifluoro/pentafluoro acetylated. After decarboxylation by acidic treatment, trifluoromethyl ketones **145-148** and pentafluoroethyl ketones **150-153** were obtained. Reactions proceeded in moderate yield (46-53% over two steps), but failed when using carboxylic acid **139** (n=2), probably due the enediolate instability leading into lithium acrylate and lithium 3-(dimethylamino)propane-1-thiolate. In order to investigate the effect of sulfone polar head groups on the inhibitory activity, compound **148** was further oxidized to compound **154** in 35 % yield, using an excess of oxone® in aqueous methanol (Scheme 4.7).[12]

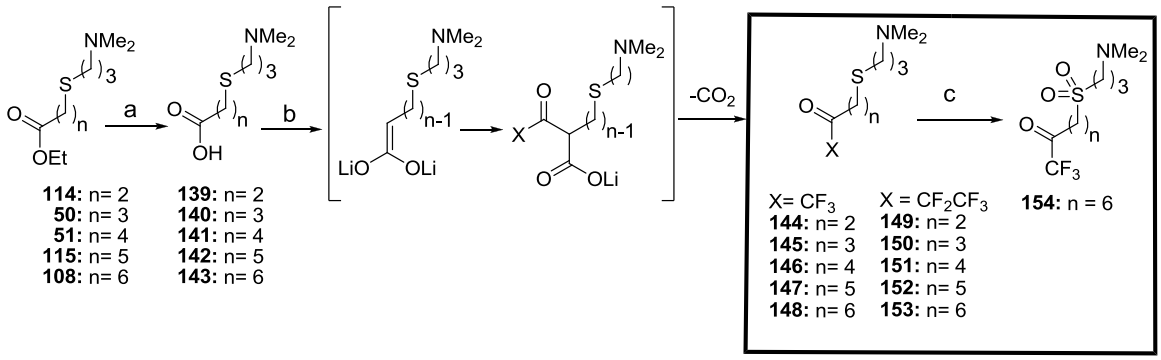

Scheme 4.7 Synthesis of α-keto-CF_3 and α-keto-CF_2CF_3 libraries. Reagents and conditions: a) NaOH (1.0 eqv.), H_2O:EtOH, rt, 2h. b) Diisopropylamine (3.5 eqv.), n-Buli (3.4 eqv.), -78°C, carboxylic acid **139-143** (1.0 eqv.), THF, rt (4h), XCOOEt (3.0 eqv., X= CF_3 or CF_2CF_3), -78°C (15 min), 6N HCl, 45-53 % yield (over two steps). c) Oxone® (3.0 eqv.), MeOH/H_2O (3/2), overnight, rt, 24h, 35% yield. Reactions with carboxylic acid **139** (n=2) failed in leading to compound **144** and **149.**

3.2 *In vitro* evaluation for APT1/2 inhibition

By analogy to α-keto amides, trifluoromethyl ketones and pentafluoroethyl ketones were first screened for APT1 inhibition using the colorimetric assay to evaluate the APT1 activity remaining at 50 µM compound concentration. All compound tested were shown to be at best weak APT1 inhibitors (Table 4.3).

Keto CF_3/CF_2CF_3
APT1 activity remaining (50 µM, PNPO assay)

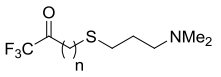

145: n= 3	**107 +/- 1 %**	**150:** n= 3	**86 +/- 2 %**	**154:** n= 6	**83 +/- 2 %**
146: n= 4	**106 +/- 2 %**	**151:** n= 4	**99 +/- 3 %**		
147: n= 5	**91 +/- 2 %**	**152:** n= 5	**93 +/- 1 %**		
148: n= 6	**101 +/- 1 %**	**153:** n= 6	**103 +/- 2 %**		

Table 4.3 Evaluation of α-keto CF_2CF_3/CF_3 libraries for APT1 inhibition. Residual APT1 activity in percentage obtained for α-keto CF_2CF_3/CF_3 compounds at 50 µM concentration using the colorimetric assay (PNPO = 600 µM, APT1 = 75 nM, 30 min inhibitor pre-incubation). Z'factors were in all cases higher than 0.80. Data based on three independent experiments.

The APT2 activity remaining at 50 µM compound concentration was evaluated using the APT2 fluorescent assay. No APT2 inhibitory activity was detected among this family of compound at 50 µM concentration (Table 4.4).

Keto CF_3/CF_2CF_3
APT2 activity remaining (50 µM, DiFMUO assay)

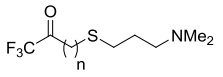

145: n= 3	**99 +/- 3 %**	**150:** n= 3	**98 +/- 2 %**	**154:** n= 6	**107 +/- 3 %**
146: n= 4	**127 +/- 3 %**	**151:** n= 4	**109 +/- 3 %**		
147: n= 5	**98 +/- 2 %**	**152:** n= 5	**109 +/- 3 %**		
148: n= 6	**118 +/- 3 %**	**153:** n= 6	**96 +/- 2 %**		

Table 4.4 Evaluation of α-keto CF_2CF_3/CF_3 libraries for APT2 inhibition. Residual APT2 activity in percentage obtained for α-keto CF_2CF_3/CF_3 compounds at 50 µM concentration using the fluorometric assay (DiFMUO = 15 µM, APT2 = 50 nM, 2 min inhibitors pre-incubation). Z' factors were in all cases higher than 0.80. Data based on three independent experiments.

4 α-Keto oxazole inhibitor candidates

4.1 Synthesis of the α-keto oxazole library

Synthesis of C5-functionalized Oxazoles

Tosylmethyl isocyanide (TosMIC) is a widely used and versatile building block for many organic reactions such as for the van Leusen oxazole synthesis consisting in a base-catalysed cycloaddition of TosMIC with aldehydes leading to C5-substituted oxazoles.[14] Such reactions occur through the formation of a 4-tosyl-oxazoline intermediate, which after β-elimination of a tosyl leaving group (TsH) furnishes the oxazole core (Scheme 4.8).

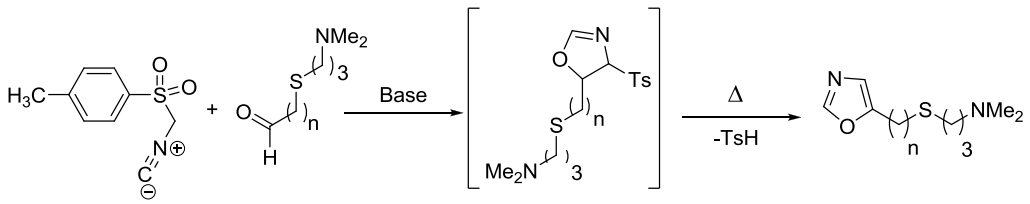

TosMIC **54:** n= 3 **155:** n= 3 **156:** n= 3

Scheme 4.8 Synthesis of C5-substituted oxazoles using Van Leusen oxazole synthesis. Reaction employing the TosMIC reagent to generate the 4-tosyl-oxazoline intermediate **155** undergoing subsequently a tosyl group β–elimination leading to oxazole **156**.

For obvious handling reasons, the TosMIC reagent is regarded as an attractive alternative to the odorous methyl isocyanide. Therefore, given the numerous TosMIC-mediated reactions reported in the literature to access 5-aryl substituted oxazoles, the Van Leusen strategy was first

investigated with aldehyde **54.** After various reactions with organic and inorganic bases, oxazole **156** was finally obtained in 16% yield by the successive addition of K_2CO_3 (1 eqv.) followed by KOH (14 eqv.) in refluxing methanol[15] or in 30% yield using NaOMe (6 eqv.) in methanol (110°C). Subsequently, tosyl-oxazoline intermediate **155** was isolated in 45% yield using potassium carbonate (3.0 eqv.) in refluxing acetonitrile (85°C). Attempt to generate oxazole **156** from intermediate **155** using various solvent\base combinaisons (DBU, KOH, t-BuOK[16,17]) failed, leading to decomposition products.

Alternatively, the Schöllkopf oxazole synthesis was investigated consisting in a base-mediated reaction of methyl isocyanide ($CH_3N{\equiv}C$) with an ethyl ester[18] leading to a transient β-keto-isocyanide, which after rearrangement into its enolic form, cyclize to generate the oxazole ring. In contrast to the Van Leusen synthesis mainly applied to aryl aldehydes, numerous C5-alkyl substituted oxazoles were already reported in literature with generally good yields.[19-21] In this context, methyl isocyanide **157** was prepared[22] from *N*-methylformamide in 76% yield and was successfully used for the synthesis of C5-substituted oxazoles with various spacer length (n=2-6), obtained in 84-94 % yields (Scheme 4.9).

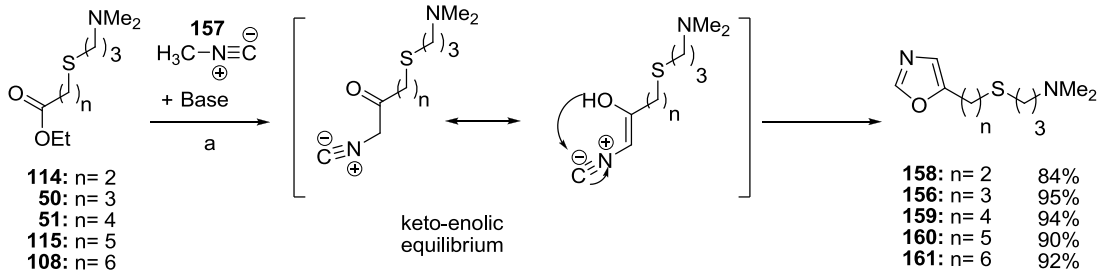

Scheme 4.9 Synthesis of C5-substituted oxazoles using Schöllkopf synthesis. Reagents and conditions: a) MeNC (1.34 eqv.), n-Buli (1.5 eqv.), dry THF, -78°C (2h), then ethyl ester (1.0 eqv.), -78°C (3h) then rt (3h).

Oxazole C2-functionalization

Although C2-metalated oxazoles have been well documented as existing in equilibrium between ring-opened and ring-closed forms depending on the nature of the metal, 2-magnesiated oxazoles are known to exist predominantly as a ring-closed system allowing their C2-functionalization. After an optimized 2 hours deprotonation time using isopropylmagnesium chloride,[23,24] reaction of C2-metalated oxazoles with Weinreb amides **162**-**163** (prepared from N,O-dimethylhydroxylamine hydrochloride and the corresponding acid chlorides[23,25]) permitted the synthesis of sub-library A (**164-173**) in moderate yields (24-37%) consistent with the literature. Moreover, such low yields were not due to isolation problems given that isolated

yields were identical to yields evaluated directly from the crude mixture using DMF as internal standard (Scheme 4.10).

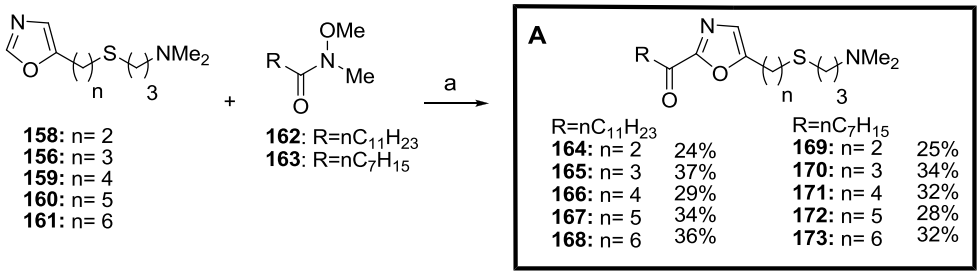

Scheme 4.10 Oxazole *C2*-fonctionalization using Weinreb amides. Reaction occurring through the formation of 2-magnesiated oxazole intermediates, reacting with Weinreb amides **162-163** to furnish 2,5-disubstituted oxazoles **164-173**. Reagents and conditions: a) i-PrMgCl (1.4 eqv.), dry THF, -15°C (2H15), Weinreb amide **162** or **163** (1.0 eqv.), -20°C (30 min) then rt (25 h), Yield = 24-37%.

Derivatization to the sulfone

To investigate the effect of sulfone groups on the inhibitory activity, oxazoles **164-173** were oxidized using Oxone®[12] leading to α-keto-oxazoles **174-183** denoted sub-library B. Purification by reverse phase C_{18} chromatography (RPC_{18}) permitted to significantly increase the yield of the reaction, exemplified by compound **180** (n=3, nC_7H_{15}) obtained either in 69% or 30% using RPC_{18} or silica gel, respectively. Finally, after RPC_{18} purification compounds **174-183** were obtained in good yields between 70-84% (Scheme 4.11).

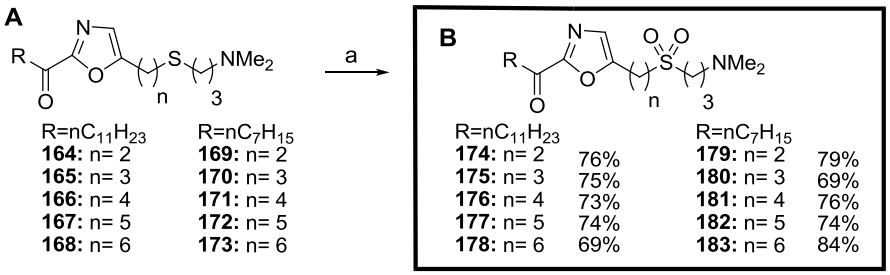

Scheme 4.11 Derivatization to the sufone using Oxone. Synthesis of sub-library B (**174-183**) by oxidation of sub-library A (**164-173**). Reagents and conditions: a) Oxone® (3.0 eqv.), MeOH:H_2O (3:2), 60 h, rt, 69-84% yield after RPC_{18} column.

Quaternization of the amino group using methyl iodide

Sub-library A and sub-library B were quaternized at the dimethylamino functionality by treatment with an excess of methyl iodide in acetonitrile,[26] yielding cationic sub-library C (**184-189**) and D (**190-199**) respectively. At the exception of oxazole **199** obtained as traces, yields were generally good given that products isolation by precipitation was rendered difficult by the relatively low reaction scale, typically from 0.052 to 0.105 mmol. (Scheme 4.12)

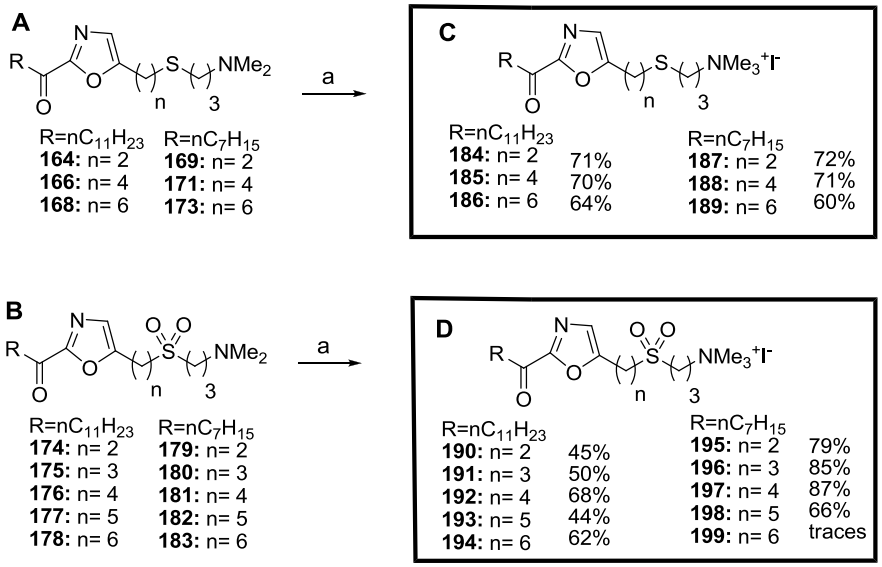

Scheme 4.12 Derivatization by quaternization. Synthesis of cationic sub-library C **(184-189**) and sub-library D (**190-199**) by amino group quarternization. Reagents and conditions: **a)** MeI (1.16 eqv.), CH_3CN, rt, 5 h, precipitation in Et_2O. Yield = 44-87% excepted for compound **199** (n= 6, X= SO_2, n-C_7H_{15}) obtained as traces.

4.2 *In vitro* evaluation for APT1/2 inhibition

The α-keto oxazole library was screened to evaluate the residual APT1 activity at 50 µM compound concentration. Judging from the obtained values, no promising APT1 inhibitory activity was detected. With an activity remaining of 59 %, α-keto oxazole **191** was found as a weak APT1 inhibitor (IC_{50} value slightly above 50 µM) compared to β-lactone inhibitors, characterized by low nanomolar IC_{50} values under similar conditions (Table 4.5).

APT1 activity remaining (50µM, PNPO assay)

R = n-$C_{11}H_{23}$

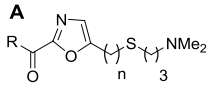

A		B		C		D	
164: n= 2	**126 +/- 1.5 %**	**174:** n= 2	**109 +/- 3 %**	**184:** n= 2	**150 +/- 2 %**	**190:** n= 2	**155 +/- 2 %**
165: n= 3	**122 +/- 1 %**	**175:** n= 3	**108 +/- 3 %**	**185:** n= 4	**115+/- 1.5 %**	**191:** n= 3	**59 +/- 0.5 %**
166: n= 4	**128 +/- 14 %**	**176:** n= 4	**115 +/- 4 %**	**186:** n= 6	**107 +/- 1 %**	**192:** n= 4	**101 +/- 1 %**
167: n= 5	**119 +/- 1 %**	**177:** n= 5	**105 +/- 7 %**			**193:** n= 5	**147 +/- 2 %**
168: n= 6	**115 +/- 2 %**	**178:** n= 6	**108 +/- 7 %**			**194:** n= 6	**187 +/- 10 %**

R = n-C_7H_{15}

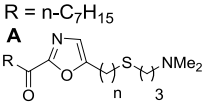

A		B		C		D	
169: n= 2	**111 +/- 1%**	**179:** n= 2	**104 +/- 1 %**	**187:** n= 2	**84.5 +/- 2 %**	**195:** n= 2	**90.5 +/- 3 %**
170: n= 3	**112 +/- 3 %**	**180:** n= 3	**105 +/- 5 %**	**188:** n= 4	**88 +/- 2 %**	**196:** n= 3	**83 +/- 1 %**
171: n= 4	**103 +/- 16 %**	**181:** n= 4	**101 +/- 6 %**	**189:** n= 6	**91 +/- 1.5 %**	**197:** n= 4	**89 +/- 1.5 %**
172: n= 5	**103 +/- 3 %**	**182:** n= 5	**105 +/- 4 %**			**198:** n= 5	**85 +/- 1.5 %**
173: n= 6	**105 +/- 2 %**	**183:** n= 6	**93 +/- 8 %**			**199:** n= 6	**-**

Table 4.5 Evaluation of the α-keto oxazole library for APT1 inhibition. Residual APT1 activity in percentage obtained for α-keto oxazoles (**164-199**) at 50 µM concentration using the colorimetric assay (PNPO = 600 µM, APT1 = 75 nM, 30 min inhibitor pre-incubation). Z' factors were in all cases higher than 0.80. Data based on three independent experiments.

Oxazole sub-libraries A, B, C and D were subsequently investigated for APT2 inhibition using the fluorescent assay based on DiFMUO. The APT2 activity remaining at 50 µM was evaluated for each compound based on three independent experiments. However, although α-keto oxazoles inhibit at best 70-75% of APT2 activity at 50 µM concentration, their potency still remain largely inferior to that of the β-lactone inhibitors (Table 4.6).

APT2 activity remaining (50µM, DiFMUO assay)

R = n-$C_{11}H_{23}$

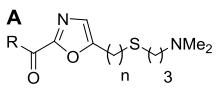

A		B		C		D	
164: n= 2	**66 +/- 3 %**	**174:** n= 2	**60 +/- 2 %**	**184:** n= 2	**40 +/- 2 %**	**190:** n= 2	**52 +/- 1 %**
165: n= 3	**57 +/- 1 %**	**175:** n= 3	**60 +/- 3 %**	**185:** n= 4	**44 +/- 2 %**	**191:** n= 3	**25 +/- 2 %**
166: n= 4	**55 +/- 3 %**	**176:** n= 4	**52 +/- 2 %**	**186:** n= 6	**39 +/- 1 %**	**192:** n= 4	**54 +/- 1 %**
167: n= 5	**66 +/- 3 %**	**177:** n= 5	**56 +/- 2 %**			**193:** n= 5	**40 +/- 1 %**
168: n= 6	**60 +/- 4 %**	**178:** n= 6	**52 +/- 1 %**			**194:** n= 6	**39 +/- 3 %**

R = n-C_7H_{15}

A		B		C		D	
169: n= 2	**86 +/- 3 %**	**179:** n= 2	**78 +/- 5 %**	**187:** n= 2	**84 +/- 1 %**	**195:** n= 2	**72 +/- 1 %**
170: n= 3	**90 +/- 2 %**	**180:** n= 3	**82 +/- 4 %**	**188:** n= 4	**70 +/- 3 %**	**196:** n= 3	**86 +/- 3 %**
171: n= 4	**84 +/- 2 %**	**181:** n= 4	**90 +/- 2 %**	**189:** n= 6	**26 +/- 1 %**	**197:** n= 4	**71 +/- 2 %**
172: n= 5	**54 +/- 4 %**	**182:** n= 5	**78 +/- 2 %**			**198:** n= 5	**31 +/- 1 %**
173: n= 6	**38 +/- 3 %**	**183:** n= 6	**58 +/- 1 %**			**199:** n= 6	**-**

Table 4.6 Evaluation of the α-keto oxazole library for APT2 inhibition. Residual APT2 activity in percentage obtained for α-keto oxazoles (**164-199**) at 50 µM concentration using the fluorometric assay (DiFMUO = 15 µM, APT2 = 50 nM, 2 min inhibitors pre-incubation). Z' factors were in all cases higher than 0.80. Data based on three independent experiments.

5 Conclusion

Although the effort spent to develop α-keto-oxazoles, α-keto-CF_3, α- keto-CF_2CF_3 and α–keto-amide APT1/APT2 inhibitors, no or substantially weaker inhibitory activities were obtained in comparison to the activity of the β-lactone inhibitors under similar conditions. Therefore, a small representative set of compounds containing α-keto-oxazoles, α-keto-CF_3, α- keto-CF_2CF_3 and α-keto-amides were investigated on additional serine hydrolases such as cytosolic phospholipase A2 (cPLA2) and fatty acid amide hydrolase (FAAH) in collaboration with Matthias Lehr. As a result, none of the compounds tested were shown to inhibit cPLA2. However, α-keto oxazoles revealed as potent FAAH inhibitors and are the object of the last chapter.

6 References

(1) Sun, W.; Pelletier, J. C. *Tetrahedron Lett.* **2007**, *48*, 7745.

(2) Al-Masoudi, N.; Al-Soud, Y.; Schuppler, T. *J. Carbohydr. Chem.* **2005**, *24*, 237.

(3) Hanessian, S.; Ducharme, D.; Masse, R.; Capmau, M. L. *Carbohydr. Res.* **1978**, *63*, 265.

(4) Koshi, Y.; Nakata, E.; Miyagawa, M.; Tsukiji, S.; Ogawa, T.; Hamachi, I. *J. Am. Chem. Soc.* **2008**, *130*, 245.

(5) Masuda, Y.; Yoshida, M.; Mori, K. Biosci., *Biotechnol., Biochem.* **2002**, *66*, 1531.

(6) Diez, E.; Dixon, D. J.; Ley, S. V.; Polara, A.; Rodriguez, F. *Helv. Chim. Acta* **2003**, *86*, 3717.

(7) Nakatsuji, Y.; Nakamura, T.; Yonetani, M.; Yuya, H.; Okahara, M. *J. Am. Chem. Soc.* **1988**, *110*, 531.

(8) Hon, Y.-S.; Liu, Y.-W.; Hsieh, C.-H. *Tetrahedron* **2004**, *60*, 4837.

(9) Pappo, R.; Allen, D. S., Jr.; Lemieux, R. U.; Johnson, W. S. *J. Org. Chem.* **1956**, *21*, 478.

(10) Iwata, C.; Takemoto, Y.; Doi, M.; Imanishi, T. *J. Org. Chem.* **1988**, *53*, 1623.

(11) Mori, Y.; Kohchi, Y.; Suzuki, M.; Carmeli, S.; Moore, R. E.; Patterson, G. M. L. *J. Org. Chem.* **1991**, *56*, 631.

(12) Veleiro, A. S.; Pecci, A.; Monteserin, M. C.; Baggio, R.; Garland, M. T.; Lantos, C. P.; Burton, G. *J. Med. Chem.* **2005**, *48*, 5675.

(13) Reeves, J. T.; Song, J. J.; Tan, Z.; Lee, H.; Yee, N. K.; Senanayake, C. H. *J. Org. Chem.* **2008**, *73*, 9476.

(14) van, L. D.; van, L. A. M. *Org. React*. **2001**, *57,* 417.

(15) Lee, J. C.; Cha, J. K. *J. Am. Chem. Soc.* **2001**, *123*, 3243.

(16) Krishna, P. R.; Reddy, V. V. R.; Sharma, G. V. M. *Synlett* **2003**, 1619.

(17) Wei, Z.-L.; Xiao, Y.; George, C.; Kellar, K. J.; Kozikowski, A. P. *Org. Biomol. Chem.* **2003**, *1*, 3878.

(18) Schoellkopf, U.; Schroeder, R. *Angew. Chem., Int. Ed. Engl.* **1971**, *10*, 333.

(19) Wenkert, D.; Chen, T.-F.; Ramachandran, K.; Valasinas, L.; Weng, L.-l.; McPhail, A. T. *Org. Lett.* **2001**, *3*, 2301.

(20) Vedejs, E.; Naidu, B. N.; Klapars, A.; Warner, D. L.; Li, V.-s.; Na, Y.; Kohn, H. *J. Am. Chem. Soc.* **2003**, *125*, 15796.

(21) Ohba, M.; Izuta, R.; Shimizu, E. *Tetrahedron Lett.* **2000**, *41*, 10251.

(22) Schuster, R. E.; Scott, J. E., Jr.; Casanova, J., *Jr. Org. Synth.* **1966**, *46,* No pp. given.

(23) Nahm, S.; Weinreb, S. M. *Tetrahedron Lett.* **1981**, *22*, 3815.

(24) Pippel, D. J.; Mapes, C. M.; Mani, N. S. *J. Org. Chem.* **2007**, *72*, 5828.

(25) Trost, B. M.; Lee, C. *J. Am. Chem. Soc.* **2001**, *123*, 12191.

(26) Tamayo, A.; Lodeiro, C.; Escriche, L.; Casabo, J.; Covelo, B.; Gonzalez, P. *Inorg. Chem.* **2005**, *44*, 8105

CHAPTER 5

DISCOVERY OF POTENT FATTY ACID AMIDE HYDROLASE (FAAH) INHIBITORS

1 FAAH as a degradating enzyme of the endocannabinoid system

A well-established function of the endogenous cannabinoid system (ECS) is its role in various physiological processes, including brain neuromodulation (learning, memory[1], motor coordination) but also in the regulation of anxiety[2], cell proliferation[3,4], inflammation[5] and appetite. In contrast to classical neuronal signals, travelling from pre- to post-synaptic neurons, retrograde endocannabinoid signals travel within the brain from post- to pre-synaptic neurons. Recently, a model for retrograde ECS signaling has been proposed.[6-8] In this model, when an action potential reaches the extremity of the pre-synaptic neuron, neurotransmitters such as glutamate are released by the pre-synaptic neuron. Released neurotransmitters bind to post-synaptic glutamate receptors (AMPA or NMPA), which allows calcium ion channels to open, leading to a calcium accumulation in post-synaptic neurons. In turn, calcium activates N-acetyl transferase (NAT) and phospholipase C (PLC) involved in arachidonoylethanolamide (AEA, anandamide) and 2-arachidonoylglycerol (2-AG) biosynthesis from membrane phospholipids phosphatidylethanolamine (PE) and phosphatidyl choline (PC) respectively. After biosynthesis, endocannabinoids AEA and 2-AG diffuse out of the post-synaptic neuron to bind and activate CB1 receptors (CB1R) located on the pre-synaptic neuron. Activated CB1 receptors couple to G-proteins to regulate calcium and potassium influx and inhibit the release of neurotransmitters.[9] Once the signal is transmitted, endocannabinoids are redirected in the neuron by an unknown mechanism to be enzymatically degraded by two well-characterized serine hydrolases, fatty acid amide hydrolase (FAAH)[2,10-12] and monoacylglycerol lipase (MAGL). FAAH is located in post-synaptic neurons and cleaves anandamide (AEA) into arachidonic acid (AA) and ethanolamine, whereas MAGL is essentially found in pre-synaptic neurons to hydrolyse 2-AG leading to arachidonic acid (AA) and glycerol (Figure 5.1).

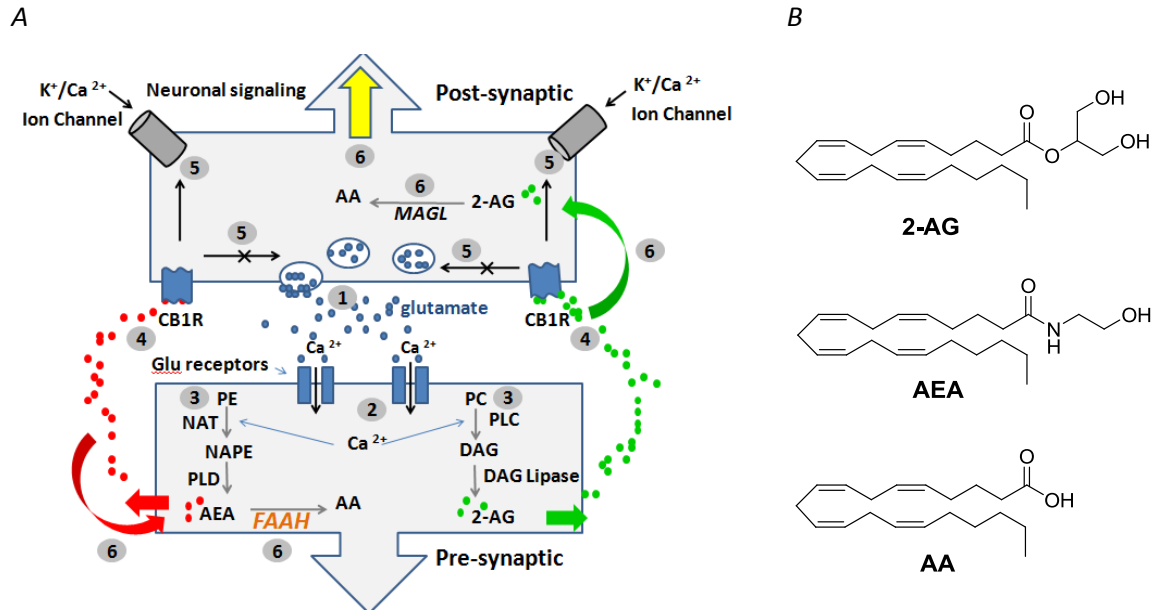

Figure 5.1 **Overview of the endocannabinoid system.** A) General model for the retrograde endocannabinoid signaling occurring in the brain from post-synaptic to pre-synaptic neurons. 1- Release of neurotransmitter glutamate upon action potential arrival, 2- Glutamate-mediated activation of post-synaptic receptors (AMPA, NMDA) allowing Ca^{2+} accumulation in the pre-synaptic neuron, 3- Calcium-mediated activation of NAT and PLC leading to the biosynthesis of AEA and 2-AG from phospholipids, 4- CB1R activation by endocannabinoids AEA and 2-AG, 5- Activation of calcium/potassium ion channels and interruption of neurotransmitter releasing, 6- Retrograde signal transmitted and enzymatic degradation of endocannabinoids AEA and 2-AG respectively by FAAH and MAGL. B) Structure of the two endocannabinoids anandamide (AEA), 2-arachidonoylglycerol (2-AG) and of the hydrolysis product arachidonic acid (AA). PC = phosphatidylcholine, PLC= phospholipase C, DAG= Diacylglycerol, DAGL = DAG lipase, NAT= N-acetyl transferase, PE= phosphatidyl ethanolamine, NAPE= N-acetyl PE, FAAH= fatty acid amide hydrolase, MAGL = monoacylglycerol lipase, CB1R= cannabinoid receptor CB1. Figure adapted from the literature.[6]

2 FAAH as an attractive therapeutic target

The biological role of FAAH in the degradation of the endocannabinoid AEA was confirmed by an increased AEA brain level in mice with FAAH genetically inactivated (so called FAAH (-/-) mice).[10] Moreover, FAAH knockdown in mice is associated with various therapeutic effects such as analgesic,[10] anti-inflammatory[10] and anxiolytic effects.[10] A positive effect on depression[13,14] as well as an improvement in sleep[15] or in memory acquisition and extinction[16] was also later discovered in knockout FAAH (-/-) mice. Given such promising effects observed in animal models, an extensive effort was spent to modulate the ECS by developing FAAH inhibitors[17-19] for the treatment of various important diseases (neurodegenerative disorders, eating disorders, metabolic disorders, and emotional disorders).[20-23]

2.1 First generation FAAH inhibitors

Originally identified in rat[24] and porcine brain[25] as an anandamide (AEA) amidase, the enzyme was subsequently renamed in 1996 as fatty acid amide hydrolase (FAAH) when Cravatt et al.[26] reported a plurality of fatty acid amides hydrolysed by the enzyme purified and cloned from rat liver. Given a constant preference of FAAH for anandamide (AEA) over its additionally discovered substrates (lauroylethanolamide (C12), myristoylethanolamide (C14), palmitoylethanolamide (C16, PEA) and oleoylethanolamide (OAE)), early developed FAAH inhibitors were derived from anandamide (AEA). Not surprisingly, the first generation of FAAH inhibitors were poor drug candidates due to their ability to bind to CB1 receptors.[17] For example, the AEA-derived FAAH inhibitor MAFP has an IC_{50} value of 20 nM for FAAH and an IC_{50} value of 304 nM for CB1 receptors. Although this lack of selectivity, MAPF has been successfully used for FAAH co-crystallization[27] revealing an unusual catalytic site consisting in Ser241 –Ser217- Lys142 differing from the more commonly seen Asp-His-Ser hydrolase catalytic triad. Subsequently, a new approach have consisted in developing inhibitors derived from the FAAH substrates oleoylethanolamide (OAE) and palmitoylethanolamide (PEA) instead, given their inability to activate CB1 receptors. For example, the OEA-derived FAAH inhibitor EOFP was useful for the identification of Ser241 as the nucleophilic residue of FAAH catalytic machinery (Figure 5.2).[28]

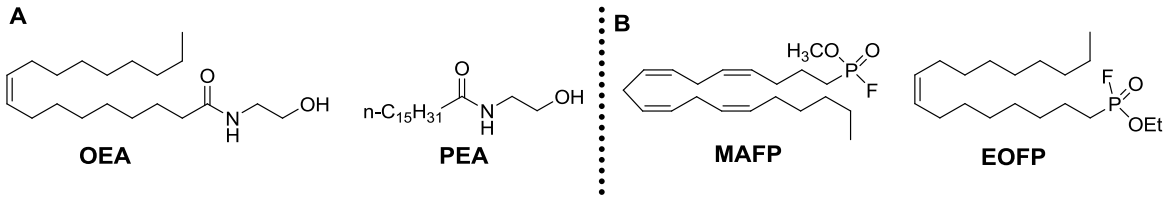

Figure 5.2 First generation FAAH inhibitors. A) Structure of the two FAAH substrate extensively used for the design of FAAH inhibitors: oleoylethanolamide (OAE) and palmitoylethanolamide (PAE). B) Example of 1st generation FAAH inhibitors methoxy arachidonoyl fluorophosphonate (MAFP) and ethoxyoleyl fluorophosphonate (EOFP) derived from anandamide (AEA) and oleoylethanolamide (OAE) respectively.

2.2 Selective second generation FAAH inhibitors

Subsequently, FAAH inhibitors lacking completely substrate-like structure were discovered. In 2003, Piomelli and coworkers reported[2] the arylcarbamate URB-597 to inhibit FAAH by irreversible carbamoylation of the nucleophilic serine residue (Ser241) leading to anxiolytic and analgesic activities. In 2004, α-keto oxazole FAAH inhibitors were published by Cravatt et al.[29] among which OL-135 turned out to be highly potent and selective[29] and to promote analgesia *in*

vivo.[11] As a result, OL-135 has become the starting point for two Structure-Activity Relationships studies (SARs) exploring successively the C2-acyl side chain[30] and the C5-position of the oxazole ring.[31] The crystal structure of h/rFAAH[32] in complex with OL-135 has allowed to determine an enzyme inhibition mode involving the reversible formation of an hemiketal with the nucleophilic Ser241 residue. To date, various structurally different FAAH inhibitors were discovered, exemplified by the α–keto heterocycle PHOP[33] and the arylcarbamate ML987[34] (Figure 5.3)

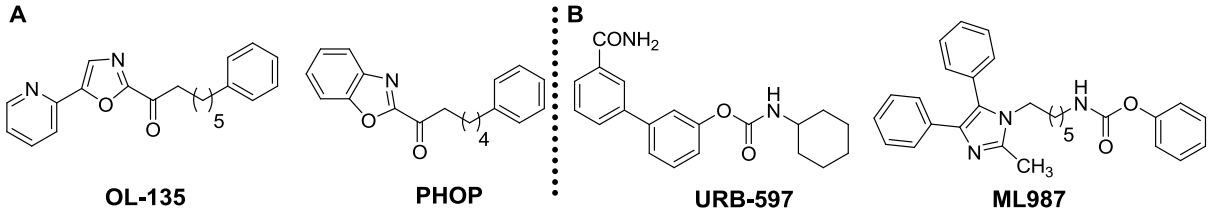

Figure 5.3 Selective second generation FAAH inhibitors. A) α-keto heterocycle PHOP (Ki = 0.2 nM (Rat) and Ki= 0.094 nM (human)) and OL-135 (IC_{50} = 4.6 nM (brain membrane) and IC_{50} = 0.5 nM (intact neurons)). B) Carbamate URB597 (Ki= 4.7 nM) and ML987 (IC_{50} = 5.3 +/- 1.6 nM).

3 *In vitro* evaluation of α–keto-oxazoles for FAAH inhibition

3.1 Principle of the HPLC-based FAAH inhibition assay

Given the fact that α–keto oxazoles were reported as FAAH inhibitors,[29-31] the complete α–keto oxazole library (**164-199**) was investigated for FAAH inhibition in collaboration with Matthias Lehr using microsomes from rat brain as enzyme source and a fluorogenic ethanolamide as substrate (Figure 5.4).[35] Inhibitory potencies were determined by comparing the amount of carboxylic acid (4-pyren-1-ylbutanoic acid) released from the substrate in the presence and in the absence of compound after 60 min incubation time. The quantity of fluorescent carboxylic acid was measured by reversed-phase HPLC with fluorescence detection (excitation: 340 nm, emission: 380 nm) and was quantified using 6-pyren-1-ylhexanoic acid as internal standard (IStd). To estimate the inhibitory potency of the tested α–keto oxazoles, the known FAAH inhibitors URB-597, ML987 and PHOP presented in Figure 5.3, were used as references.

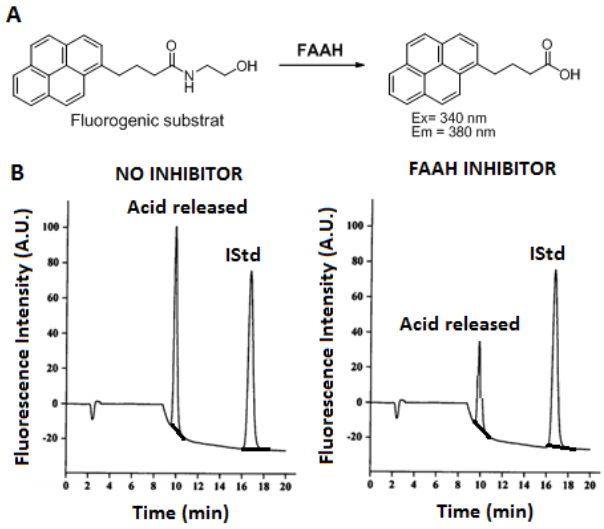

Figure 5.4 Principle of the HPLC-based assay for FAAH inhibition. A) Fluorometric assay used to evaluate the α-keto oxazole library (**164-199**) using 100 µM fluorogenic substrate, FAAH enzyme as crude microsome preparation from rat brain after 60 minutes incubation either with DMSO or with the tested compound at 37°C. Evaluation of the acid released from the substrate by C_{18} HPLC measurement using 6-pyren-1-ylhexanoic acid as internal standard. B) C_{18} HPLC spectra of the reaction mixture after incubation with DMSO or with an FAAH inhibitor.

3.2 α–Keto oxazoles as potent FAAH inhibitors

The complete α–keto oxazole library (**164-199**) was screened for FAAH inhibition. FAAH activity remaining at 10 µM compound concentration was evaluated based on two independent experiments leading to relatively low standard deviations, therefore ensuring the reliability of the values. Some of the investigated compounds were potent FAAH inhibitors. The graphical representation of the residual enzyme activity obtained for the two series of α–keto-oxazole inhibitors (respectively R=*n*-$C_{11}H_{23}$ or R=*n*-C_7H_{15}) at 10 µM concentration, revealed the crucial role of a short spacer (n=2 to 3 carbons) for the inhibitory activity. A beneficial effect was also observed for compounds substituted at C2 position with long acyl chains (R = *n*-$C_{11}H_{23}$), as replacement by the shorter chain (R= *n*-C_7H_{15}) resulted generally in a decreased activity. This observation was consistent with the reduced activity observed by Boger et al.[36] for 1,1,1-trifluorononan-2-one (R= *n*-C_7H_{15}, Ki= 1.2 µM) compared to the four-carbon longer homologue (R=*n*-$C_{11}H_{23}$, Ki= 0.14µM) or by Jonsson et al.[37] for octanoylethanolamide (R= *n*-C_7H_{15}) compared to lauroylethanolamide (R=*n*-$C_{11}H_{23}$). Moreover, an increased number of polar heteroatoms in the oxazole C5-side chain resulted in a significant increase in inhibitory potency, with sulfones generally more potent than their non-oxidized homologues. At last, the substitution of the terminal dimethylamino group (located in the oxazole C5-side chain) by a terminal quaternary amino group turned out to affect the inhibitory efficiency negatively (Figure 5.5A).

A

FAAH activity remaining (10 µM, HPLC assay)

R = n-$C_{11}H_{23}$

A		B		C		D	
164: n= 2	**27 +/- 2 %**	**174:** n= 2	**3 +/- 1 %**	**184:** n= 2	**78 +/- 1 %**	**190:** n= 2	**11 +/- 3 %**
165: n= 3	**40 +/- 2 %**	**175:** n= 3	**2 +/- 1 %**	**185:** n= 4	**78 +/- 9 %**	**191:** n= 3	**13 +/- 0 %**
166: n= 4	**49 +/- 1 %**	**176:** n= 4	**32 +/- 3 %**	**186:** n= 6	**71 +/- 6 %**	**192:** n= 4	**49 +/- 1 %**
167: n= 5	**64 +/- 2 %**	**177:** n= 5	**53 +/- 3 %**			**193:** n= 5	**57 +/- 1 %**
168: n= 6	**72 +/- 6 %**	**178:** n= 6	**51 +/- 0 %**			**194:** n= 6	**31 +/- 5 %**

R = n-C_7H_{15}

A		B		C		D	
169: n= 2	**34 +/- 3%**	**179:** n= 2	**23 +/- 6 %**	**187:** n= 2	**No activity**	**195:** n= 2	**61 +/- 11 %**
170: n= 3	**64 +/- 3 %**	**180:** n= 3	**22 +/- 1 %**	**188:** n= 4	**68 +/- 6 %**	**196:** n= 3	**53 +/- 5 %**
171: n= 4	**48 +/- 10 %**	**181:** n= 4	**59 +/- 7 %**	**189:** n= 6	**82 +/- 6 %**	**197:** n= 4	**83 +/- 5 %**
172: n= 5	**78 +/- 11 %**	**182:** n= 5	**73 +/- 8 %**			**198:** n= 5	**70 +/- 7 %**
173: n= 6	**78 +/- 2 %**	**183:** n= 6	**62 +/- 4 %**			**199:** n= 6	**-**

B

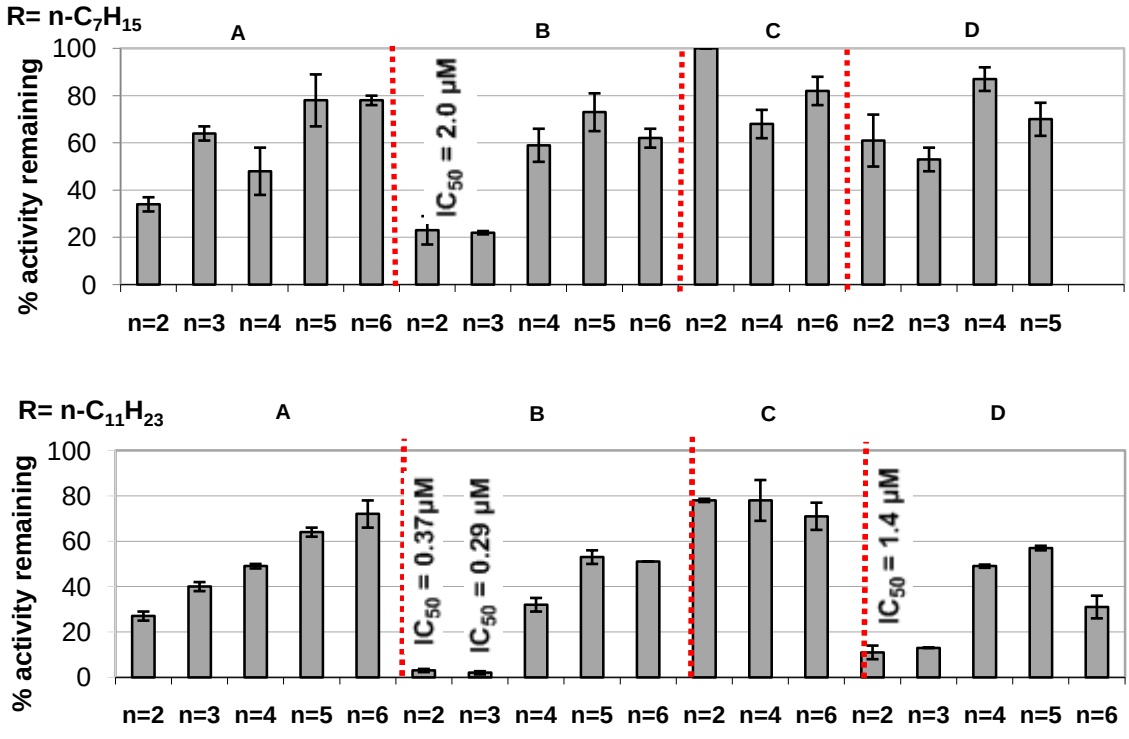

Figure 5.5 Evaluation of the α-keto oxazole library for FAAH inhibition. A) Residual enzyme activity in percentage obtained for α-keto-oxazole inhibitors **164-199** at 10 µM concentration (HPLC assay).B) Graphical representation of the residual enzyme activity for the two series of α-keto oxazole inhibitors (respectively R=*n*-$C_{11}H_{23}$ or R=*n*-C_7H_{15}) at 10 µM concentration, IC_{50} values of the more potent oxazoles are also provided. Values obtained based on two independent measurements.

IC_{50} values for the more potent compounds were determined, revealing few compounds with low or submicromolar IC_{50} values (Figure 5.5B). The FAAH inhibitory activity of the more potent inhibitor **175** (n=3, SO_2, R=n-$C_{11}H_{15}$, NMe_2) was subsequently compared with structurally different known FAAH inhibitors screened under similar conditions (PHOP, URB597 and ML987). α–Keto oxazole **175** with an IC_{50} of 290 nM, is slightly more potent than ML987 (IC_{50}= 340 nM) but also significantly less potent than URB597 (IC_{50}= 61 nM) and PHOP (IC_{50}= 2.9 nM). However, given that such compounds were initially designed as APT1 inhibitors, their FAAH inhibitory activities remain acceptable.

4 Rationalization of the results by docking studies

Using FAAH crystal structure in complex with OL-135,[32] docking studies were subsequently performed by Ingrid Vetter (MPI Dortmund) on the more potent compound **175** in order to rationalize the crucial role of a relatively short spacer (n= 2 or 3 carbons) for the activity and the beneficial effect observed with long C2-acyl side chains, or by introducing polar heteroatoms (SO_2, NMe_2) into the C5-oxazole side chain. The electrophilic carbonyl group of the oxazole **175** was fixed at the serine 241. The importance of a rather short spacer for the FAAH inhibitory activity was suggested given that the close homologue with a one carbon longer spacer **176** (n=4, SO_2, NMe_2, n-$C_{11}H_{23}$) was suffering from steric repulsions with the enzymatic pocket. Moreover, the reported[36,37]enzyme preference for inhibitors substituted with long aliphatic side chains may be explained by an increased binding affinity in the rather deep and hydrophobic acyl binding pocket.[27] In order to rationalize the increased activity observed when introducing H-bond acceptor groups into the C5-oxazole side chain such as SO_2 and NMe_2, H-donor residues provided by the enzyme, and located in a close proximity to the inhibitor were investigated. No particular candidates for hydrogen bonding interactions with SO_2 and NMe_2 groups were identified. However, given the positively charged character of the enzyme in the cavity containing the sulfone group (in blue), electrostatic stabilizing interactions with SO_2 may contribute to the inhibitory activity. Following the same idea, stabilizing electrostatic interactions between negatively charged enzyme regions (in red) and positively charged groups, should contribute to the inhibitor affinity with the enzyme. However, steric repulsions with the NMe_3^+ group are likely to occur, thereby explaining the decrease in inhibitory potency observed with cationic inhibitors compared to inhibitors with NMe_2 groups (Figure 5.6).

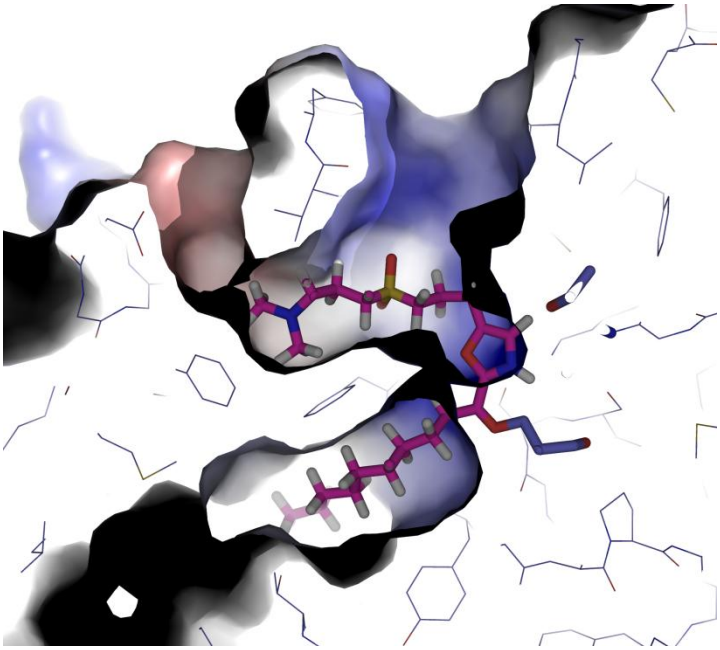

Figure 5.6 Covalent docking studies. Docking of the more potent α-keto oxazole inhibitor **175** in FAAH active site with the oxazole carbonyl group connected to the nucleophilic serine residue (Ser 241). The electrostatic potential surface of the enzyme in the proximity of the C5-side chain of the inhibitor, possibly accounts for stabilizing interactions respectively with SO_2 and NMe_2 groups. Positively charged regions are shown in blue and negative regions in red. Figure performed using the Pymol software (Ingrid Vetter).

5 Conclusion

Originally designed as APT1 inhibitors, some of the α–keto oxazoles turned out to be potent FAAH inhibitors with lowmicromolar or submicromolar IC_{50} values although lacking an heteroaromatic group in C5-position of the oxazole ring, reported to be important for FAAH inhibition.[31] Importantly, to date only few C5-substituted oxazoles with small non-aromatic substituents were reported.[31] Our α–keto oxazole library have permitted to point out the importance of short C5-side chains (n=2 or 3 carbons maximum), as well as the importance of electrostatic stabilizing interactions for the inhibitory activity. Moreover, the reported[36,37] significance of long C2-acyl chains could also be confirmed, although an improved inhibitory effect could very likely be obtained by introducing a C2-acyl side chain terminated by a phenyl group (typically located at 6 carbons from the carbonyl group[30]) like in OL-135. Additionally, the α–keto oxazole library did not inhibit additional serine hydrolases investigated such as APT1, APT2 and cPLA2.

6 References

(1) Mallet, P. E.; Beninger, R. J. *Psychopharmacology* **1998**, *140*, 11.

(2) Kathuria, S.; Gaetani, S.; Fegley, D.; Valino, F.; Duranti, A.; Tontini, A.; Mor, M.; Tarzia, G.; La, R. G.; Calignano, A.; Giustino, A.; Tattoli, M.; Palmery, M.; Cuomo, V.; Piomelli, D. *Nat. Med.* **2003**, *9*, 76.

(3) Melck, D.; Rueda, D.; Galve-Roperh, I.; De, P. L.; Guzman, M.; Di, M. V. *FEBS Lett.* **1999**, *463*, 235.

(4) Yamaji, K.; Sarker, K. P.; Kawahara, K.; Iino, S.; Yamakuchi, M.; Abeyama, K.; Hashiguchi, T.; Maruyama, I. *Thromb. Haemostasis* **2003**, *89,* 875.

(5) Massa, F.; Marsicano, G.; Hermann, H.; Cannich, A.; Monory, K.; Cravatt, B. F.; Ferri, G.-L.; Sibaev, A.; Storr, M.; Lutz, B. *J. Clin. Invest.* **2004**, *113*, 1202.

(6) Ahn, K.; McKinney, M. K.; Cravatt, B. F. *Chem. Rev.* **2008**, *108*, 1687.

(7) Piomelli, D. *Nat. Rev. Neurosci.* **2003**, *4,* 873.

(8) Chevaleyre, V.; Takahashi, K. A.; Castillo, P. E. *Annu. Rev. Neurosci.* **2006**, *29*, 37.

(9) Mackie, K. *Annu. Rev. Pharmacol. Toxicol*. **2006**, *46*, 101.

(10) Cravatt, B. F.; Demarest, K.; Patricelli, M. P.; Bracey, M. H.; Giang, D. K.; Martin, B. R.; Lichtman, A. H. *Proc. Natl. Acad. Sci. U. S. A*. **2001**, *98*, 9371.

(11) Lichtman, A. H.; Leung, D.; Shelton, C. C.; Saghatelian, A.; Hardouin, C.; Boger, D. L.; Cravatt, B. F. *J. Pharmacol. Exp. Ther.* **2004**, *311*, 441.

(12) Fegley, D.; Gaetani, S.; Duranti, A.; Tontini, A.; Mor, M.; Tarzia, G.; Piomelli, D. J. *Pharmacol. Exp. Ther*. **2005**, *313*, 352.

(13) Naidu, P. S.; Varvel, S. A.; Ahn, K.; Cravatt, B. F.; Martin, B. R.; Lichtman, A. H. *Psychopharmacology* **2007**, *192*, 61.

(14) Moreira, F. A.; Kaiser, N.; Monory, K.; Lutz, B. *Neuropharmacology* **2007**, *54*, 141.

(15) Huitron-Resendiz, S.; Sanchez-Alavez, M.; Wills, D. N.; Cravatt, B. F.; Henriksen, S. J. *Sleep* **2004**, *27,* 857.

(16) Varvel, S. A.; Wise, L. E.; Niyuhire, F.; Cravatt, B. F.; Lichtman, A. H. *Neuropsychopharmacolog*y **2007**, *32*, 1032.

(17) Vandevoorde, S. *Curr. Top. Med. Chem*. **2008**, *8*, 247.

(18) Deng, H. *Expert Opin. Drug Discovery* **2010**, *5*, 961.

(19) Seierstad, M.; Breitenbucher, J. G. *J. Med. Chem.* **2008**, *51*, 7327.

(20) Lambert, D. M.; Fowler, C. J. *J. Med. Chem.* **2005**, *48*, 5059.

(21 Jhaveri, M. D.; Richardson, D.; Chapman, V. *Br. J. Pharmacol.* **2007**, *152*, 624.

(22) Labar, G.; Michaux, C. *Chem. Biodiversity* **2007**, *4*, 1882.

(23) Cravatt, B. F.; Lichtman, A. H. *Curr. Opin. Chem. Biol.* **2003**, *7*, 469.

(24) Desarnaud, F.; Cadas, H.; Piomelli, D. *J. Biol. Chem.* **1995**, *270*, 6030.

(25) Ueda, N.; Kurahashi, Y.; Yamamoto, S.; Tokunaga, T. *J. Biol. Chem.* **1995**, *270*, 23823.

(26) Cravatt, B. F.; Giang, D. K.; Mayfield, S. P.; Boger, D. L.; Lerner, R. A.; Gilula, N. B. *Nature* **1996**, *384*, 83.

(27) Bracey, M. H.; Hanson, M. A.; Masuda, K. R.; Stevens, R. C.; Cravatt, B. F. *Science* **2002**, *298*, 1793.

(28) Patricelli, M. P.; Lovato, M. A.; Cravatt, B. F. *Biochemistry* **1999***, 38*, 9804.

(29) Boger, D. L.; Miyauchi, H.; Du, W.; Hardouin, C.; Fecik, R. A.; Cheng, H.; Hwang, I.; Hedrick, M. P.; Leung, D.; Acevedo, O.; Guimaraes, C. R. W.; Jorgensen, W. L.; Cravatt, B. F. *J. Med. Chem*. **2005**, *48*, 1849.

(30) Hardouin, C.; Kelso, M. J.; Romero, F. A.; Rayl, T. J.; Leung, D.; Hwang, I.; Cravatt, B. F.; Boger, D. L. *J. Med. Chem.* **2007**, *50*, 3359.

(31) Romero, F. A.; Du, W.; Hwang, I.; Rayl, T. J.; Kimball, F. S.; Leung, D.; Hoover, H. S.; Apodaca, R. L.; Breitenbucher, J. G.; Cravatt, B. F.; Boger, D. L. *J. Med. Chem.* **2007**, *50*, 1058.

(32) Mileni, M.; Garfunkle, J.; DeMartino, J. K.; Cravatt, B. F.; Boger, D. L.; Stevens, R. C. *J. Am. Chem. Soc.* **2009**, *131*, 10497.
(33) Boger, D. L.; Sato, H.; Lerner, A. E.; Hedrick, M. P.; Fecik, R. A.; Miyauchi, H.; Wilkie, G. D.; Austin, B. J.; Patricelli, M. P.; Cravatt, B. F. *Proc. Natl. Acad. Sci. U. S. A*. **2000**, *97*, 5044.
(34) Sit, S. Y.; Conway, C.; Bertekap, R.; Xie, K.; Bourin, C.; Burris, K.; Deng, H. *Bioorg. Med. Chem. Lett.* **2007**, *17*, 3287.
(35) Forster, L.; Schulze, E. A.; Lehr, M. *Anal. Bioanal. Chem.* **2009**, *394*, 1679.
(36) Boger, D. L.; Sato, H.; Lerner, A. E.; Austin, B. J.; Patterson, J. E.; Patricelli, M. P.; Cravatt, B. F. *Bioorg. Med. Chem. Lett*. **1999**, *9*, 265.
(37) Jonsson, K.-O.; Vandevoorde, S.; Lambert, D. M.; Tiger, G.; Fowler, C. J. *Br. J. Pharmacol.* **2001**, *133*, 1263.

General conclusions

Following the discovery of the β-lactones palmostatin B and M as the first APT1 inhibitors able to prevent Ras depalmitoylation in cells and to induce phenotypic reversal in *H*-Ras transformed cells, various cellular experiments using these cell permeable inhibitors allowed the identification of the thioesterases involved in Ras depalmitoylation. First, FLIM experiments performed using a fluorescently labeled palmostatin B analogue confirmed APT1 as a cellular target of palmostatin B. Second, activity-based proteome profiling (ABPP) experiments using alkynylated probes derived from the two inhibitors revealed APT1 and APT2 as unique cellular targets of palmostatin M and B. These results were subsequently confirmed by an enzymatic assay, showing that β-lactones are potent APT2 inhibitors, with an inhibitory potency comparable to APT1 inhibition. Finally, APT1 and APT2 were both shown to depalmitoylate semi-synthetic *N*-Ras proteins *in-vitro*. Taken together these findings provide the first experimental proof that no further hydrolases employing a similar mechanism of catalysis and possibly no further hydrolases in general are involved in Ras depalmitoylation. For these reasons, inhibition of the Ras depalmitoylating enzymes APT1 and APT2, may constitute a viable approach to interfere with aberrant oncogenic *H*- and *N*-Ras signaling.

A chemical proteomic approach developed using a palmostatin B-derived probe and human cells from leukaemic and healthy patients, allowed the identification of proteins possibly involved in the restoration of Fas-mediated apoptotic signaling observed upon palmostatin B treatment in Chronic Lymphocytic Leukaemia (CLL). Among the target proteins, several lipases were identified whose overexpression may prevent Fas palmitoylation and thereby attenuate Fas-mediated apoptotic signaling in CLL. Among them, APT1 and APT2 are representing good Fas depalmitoylating enzyme candidates given their Ras depalmitoylating activity and the overexpression of APT1 in CLL cells. Although more experiments are needed to address their possible involvement in Fas depalmitoylation, these first experiments are encouraging and may lead to a better understanding of the apoptosis resistance characteristic for CLL.

SILAC experiments employing an inert alkynylated palmitate analogue in double metabolic labelling were performed in order to evaluate the effect of palmostatin B on the complete palmitome. Although, these experiments did not so far permit any quantification, this strategy may allow the systematic evaluation of the effect of palmostatin B on all palmitoylated proteins. This would permit to discover new interesting applications for β-lactones in general and thioesterase-mediated processes in particular.

A major effort was devoted to the design, synthesis and evaluation of new APT1/APT2 inhibitor candidates which would in contrast to the previous β-lactone inhibitors, be regarded as stable transition state mimics of the deacylation process. Although no interesting APT1/APT2 inhibitory activity was discovered, some of the designed α-keto oxazoles turned out to be sub-micromolar fatty acid amide hydrolase (FAAH) inhibitors. In particular, this work revealed the importance of a short C5-side chain, of a long aliphatic chain, and of electrostatic stabilizing interactions for the FAAH inhibitory activity of α-keto oxazoles substituted at the C5 position with non-aromatic substituents.

Abbreviations

AA	Arachidonic acid
ABPP	Activity based proteome profiling
AcOH	Acetic acid
AcSH	Thioacetic acid
ADIFAB	AcryloDated Intestinal Fatty Acid Binding protein
AEA	Anandamide
2-AG	2-Arachidonoylglycerol
APT1	Acyl protein thioesterase 1
APT2	Acyl protein thioesterase 1
Bn	Benzyl
Boc	Tert-butyl carboxycarbonyl
BSA	Bovine serum albumin
Calc.	Calculated
CAPRI	Calcium-promoted Ras inactivator
CB1R	Cannabinoid receptor CB1
c-Hex	Cyclohexyl
CLL	Chronic Lymphocytic Leukemia
Da	Dalton
DAP	1,3-diaminopropane
DAG	Diacylglycerol
DBAD	di-tert-butyl azodicarboxylate
DBU	1,8-Diazabicyclo[5.4.0]undecene-7
DCM	Dichloromethane
DD	Death domain
DED	Death effector domain
DiFMUO	6,8-difluoro-4-methylumbelliferyl octanoate
DIPEA	N,N-diisopropylethylamine
DISC	Death -inducing signaling complex
DMF	N,N-dimethylformamide
DMSO	Dimethyl sulfoxide
DPI	Dual prenylation inhibitor
ECS	Endocannabinoid system

EGF	Epidermal growth factor
EGFR	Epidermal growth factor receptor
Eqv.	Equivalent
ER	Endoplasmic reticulum
ESI	Electron spray ionization
FAAH	Fatty acid amide hydrolase
FAB	Fast atom bombardment
FADD	Fast associated death domain
FAS	Fatty acid synthase
Fas	Fas cell death receptor
FBS	Fetal bovine serum
FLIM	Fluorescence lifetime imaging microscopy
Fmoc	9-Fluorenylmethyloxycarbonyl
FPP	Farnesyl diphosphate
FRET	Foerster Resonance Energy Transfer
FTase	Farnesyl transferase
FTI	Farnesyl transferase inhibitor
GAP	GTPase activating
GC-MS	Gas chromatography -mass spectrometry
GDP	Guanosine 5'-diphosphate
GFP	Green fluorescent protein
GGPP	Geranylgeranyl diphosphate
GGTase	Geranylgeranyl transferase
GGTI	Geranylgeranyl transferase inhibitor
Golgi	Golgi apparatus
GPP	Geranyl diphosphate
GRP1	Ras guanine nucleotide-releasing protein 1
GTP	Guanosine5'-triphosphate
GEF	Guanine nucleotide exchange factor
HATU	2-(1H-7-Azabenzotriazol-1-yl)-1,1,3,3-tetramethyl uronium hexafluorophosphate Methanaminium
HBTU	O-Benzotriazole-N,N,N',N'-tetramethyl-uronium-hexafluoro-phosphate
HOBT	Hydroxybenzotriazole
HPLC	High performance liquid chromatography
HRP	Horseradish peroxidase

HVR	Hyper variable region
IC_{50}	Concentration corresponding to 50% inhibition
ICMT	Isoprenylcysteine carboxyl methyltransferase
InsP3	Inositol triphosphate
IPP	Isopentenyl diphosphate
IPPI	Isopentenyl diphosphate isomerase
Km	Michaelis constant
LC-MS	Liquid chromatography mass spetrometry
LDA	Lithium diisopropylamide
MAGL	Monoacylglycerol lipase
MALDI	Matrix assisted laser desorption ionization
MAPK	Mitogen activated protein kinase
NAT	N-acetyl transferase
NBS	N-bromosuccinimide
NMM	N-methyl morpholine
NMP	N-methyl pyrrolidine
NMR	Nuclear magnetic resonance
MTBE	Methyl tert-butyl ether
ODNs	Oligonucleotides
OEA	oleoylethanolamide
Oxone®	Potassium hydrogen monoperoxysulfate
PAT	Protein acyl transferase
PC	Phosphatidylcholine
PDGFR	Platelet derived growth factor receptor
PE	Phosphatidyl ethanolamine
PM	Plasma membrane
PMBCs	Peripheral mononuclear blood cells
PNPO	Paranitro phenyl octanoate
PPT1	Palmitoylthioesterase 1
PSSC	Protein Structure Similarity Clustering
RBD	Ras binding domain
RCE1	Ras Converting enzyme 1
Rf	Retention factor
RPC_{18}	Reverse phase C_{18} chromatography
rt	Room temperature

SDS	Sodium dodecylsulfate
SE	Succinimidyl ester
SILAC	Stable isotope labeling by/with amino acids in cell culture
siRNA	Small interfering RNA
SOS	Son of sevenless
$T_{1/2}$	Half life
TAMRA	Tetramethylrhrodamine
TBDMS	tert-butyldimethylsilyl
TBAF	Tetrabutylammonium fluoride
TFA	Trifluoro acetic acid
Tf	Triflate
TLC	Thin layer chromatography
THF	Tetrahydrofuran
TNFR	Tumor necrosis factor receptor
TM	Transmembrane domain
TosMIC	Tosyl methyl isocyanide
Ts	Tosyl group
VEGFR	Vascular endothelial growth factor receptor
V_{max}	Maximun velocity
$[\alpha]_D^{20}$	Optical rotation at 20°C

EXPERIMENTAL PART

1 Materials and methods

1.1 Laboratory devices and materials

Laboratory Name	Name given by the company	Company
Autoklav	Varioklav®400	Thermo scientific, USA
Sterile bench Microflow	Hera Safe type HS12	Kendro laboratory, D
	NUAIRE, class II	Integra Biosciences, D
CO_2- incubator	NUAIRE IR Autoflow and NUAIRE DHD Autoflow	Integra Biosciences, D
Ice machine	AF80	Scotsman, USA
Fluorescence scanner	Typhoon TRIO + ^{TM} variable Mode Imager	GE Healthcare
LI-COR scanner	Odyssey Infrared Imaging System	LI-COR Biosciences, D
pH- meter	Mettler Toledo FiveEasy	Mettler Toledo
Semi-dry transfer device	Trans-Blot ® SD	BioRad, USA
Power supply device	Power PAC 1000	BioRad, USA
Ultrasonic bath	EMMI® 30HC	AMAG, D
Vacuum concentrator	Concentrator 5301	Eppendorf, D
UV spectrometer	Biophotometer	Eppendorf, D
Vortex devices	Vortex Genie 2	Carl Roth, D
Centrifuge	Centrifuge 5415R	Eppendorf, D
Balance	BP301S	Sartorius, D
PVDF-transfer membrane	Immobilon®-FL	Millipore, USA
Film for WB development	CL-Xposure ^{TM} film (#34091)	Thermo scientific, USA

Cell culture flask	BD Falcon ™ 175 cm^2 (#353045)	BD Biosciences, USA
	BD Falcon ™ 75 cm^2 (#353135)	BD Biosciences, USA
Falcon tubes	50 ml falcon tube (# 5044455)	Sarstedt, D
	15 ml falcon tube (#5044452)	Sarstedt, D
Eppendorf tubes	Safe lock tube 2 ml	Eppendorf, D
Cell culture dish	BD Falcon ™ Easy grip tissue culture dish (#353004)	BD Biosciences, USA
Microscope	Leitz , Labovert type 090-122.012	ERNST LEITZ WETZLAR, D
Shaker	VIBRAX VXR Basic	IKA
Thermo shaker	Thermomixer comfort	Eppendorf, D
Plate reader	Infinite M200	TECAN
Sonicator for cell lysis	Sonoplus HD2070	BANDELIN
96 well plate for absorbance	353072-microtest ™ 96, sterile, flat bottom	Becton Dickinson labware, USA
96 well plate for fluorescence	Costar®Assay plate, sterile, flat bottom, black (#3616)	Corning Incorporated, USA
Commercial SDS- gel 12%	12% precise ™ protein gels (10 wells, #25202)	Thermoscientific, USA
Commercial SDS- gel 4-20 %	4-20 % precise ™ protein gels (10 wells, #25204)	Thermoscientific, USA
Device to run large gel	PROTEAN II xi 20 cm Cell	BioRad, hercules, USA
Device to run precast gel	Cell –Surelock ™ Novex Mini-cell	Invitrogen
Cell counting chamber	Neubauer Cell counting chamber	Carl Roth, D
Cell scrapers	BD Falcon ™ Cell scrapers (#353085)	BD Biosciences, USA
Scalpel	B-Braun, Surgical Disposable Scalpel	Aesculap, D

1.2 Chemical and reagents

Product Name	Company
DMEM high glucose (4.5g/l) mit L-glutamin	PAA, Pasching, A
Penicillin (10. 000U/ml) –Streptomycin (10 mg/ml) in 0.9% NaCl	Sigma Aldrich, D
Sodium pyruvate solution (100 mM)	Sigma Aldrich, D
Trypsin-EDTA (1*) – cell culture laboratory	PAA, Pasching, A; and GIBCO-Invitrogen, D
Recombinante trypsin-proteomic analysis (#03 708 969 001)	Roche
Acetic acid (CAS = 64-19-7)	J.T. Baker, Holland
Developing solution for Western blot (#100296)	TETENAL-Eukobrom , D
Fixing solution for Western blot (#102762)	TETENAL-Eukobrom , D
NaF (CAS= 7681-49-4, MW = 41.99)	Sigma Aldrich, D
Ethanol absolute (CAS = 64-17-5)	Sigma Aldrich, D
Na_3VO_4 (CAS= 13721-39-6, MW= 183.91)	Sigma Aldrich, , D
$Na_2S_2O_3$ anhydrous (CAS = 7772-98-7, MW = 158.11)	Alfa Aesar
$AgNO_3$ (CAS = 7761-88-8, MW = 169.87)	Sigma Aldrich, D
Na_2CO_3 (CAS = 497-19-8, MW = 105.99)	Riedel-deHäen ®, Sigma Aldrich, D
Formaldehyde 37%, for molecular biology, CAS= 7732-18-5	Fischer Sicentific (BP531-500)
EDTA. disodium (CAS = 6381-92-6, MW= 372.34)	Gerbu Biotechnik, D
Concentrated 37% HCl (CAS = 7647-01-0)	J.T. Baker, Holland
TFA for peptid synthesis (CAS= 76-05-1)	Carl Roth, D

Acetonitrile HPLC grade (CAS= 75-05-8)	Fisher Scientific
Methanol (CAS = 67-64-1)	J.T. Baker, Holland
t-butanol (CAS = 75-65-0)	Sigma Aldrich, D
Bradford Reagent - Bio-Rad-protein assay (#500-0006)	Bio-Rad laboratories, D
Acetone reagent ACS (CAS = 67-56-1)	Sigma Aldrich, D
Acrylamid 4K- solution 30%	AppliChem , D
Complete Mini EDTA-free protease inhibitor	Roche Diagnostics, D
Dimethylsulfoxyde research grade (DMSO)	Serva, D
1,4-Dithio-D,L-threitol hight purity (DTT) (CAS = 3483-12-3, MW = 154.25)	Gerbu Biotechnik, D
Sodium HEPES salts (CAS = 75277-39-3, MW = 260.3, #25249)	Serva, D
Recombinant human epidermal Growth Factor (EGF) , #PHGO315	Invitrogen, USA
Ethylenglycol-bis(2-Aminoethylether)-N,N,N',N'-tetraacetic acid (EGTA), (CAS = 67-42-5, MW = 380.35)	Sigma Aldrich, D
Glycerol 99% (CAS = 56-81-5)	Riedel-deHäen ®, Sigma Aldrich, D
Glycin 99% (CAS= 56-40-6, MW = 75.07)	Carl Roth, D
TRIS·HCl (CAS= 1185-53-1, MW = 121.14)	Carl Roth, D
Sodium HEPES (CAS = 75277-39-3, MW= 260.29)	Serva, D
Bromophenol blue-Na salt	Serva, D
NaCl (CAS = 7647-14-5, MW = 58.44)	Sigma Aldrich, D
Iodoacetamide (CAS = 144-48-9, MW= 184.96)	Sigma Aldrich, USA
Fetal bovine serum (FBS) (#10270)	GIBCO-Invitrogen, D

KCl (CAS = 7447-40-7, MW = 74.55)	J.T. Baker , Holland
Na_2HPO_4 ; $2H_2O$ (CAS= 10028-24-7, MW = 177.99)	Merck, D
KH_2PO_4 (CAS= 7778-77-0, MW = 136.09)	J.T. Baker Holland
N,N,N', N'-tetramethylethylendiamine, electrophoresis reagent (TEMED, CAS = 110 – 18-9, MW= 116.21)	Sigma Aldrich, D
NP-40 Alternative (CAS = 9016-45-9, #492016)	CalBiochem , D
Tween 20 (CAS= 9005-64-5)	Serva, D
Triton X-100 (CAS= 9002-93-1)	Serva, D
Chocolate powder	Slim fast
Streptavidin magnetic beads (4 mg/ml), #S1420S	New england Biolabs
Super Signal ® West Pico Chemiluminescence substrate	Thermo Scientific, USA
Super Signal ® West femto Chemiluminescence substrate	Thermo Scientific, USA
U0126 (CAS= 109511-58-2, MW= 380.50, #662005)	CalBiochem, USA
BSA –fatty acid free (CAS = 9048-46-8)	Sigma Aldrich, D
$CuSO_4$; 5 H_2O (CAS= 7758-99-8, MW =249.68)	Sigma Aldrich, D
TCEP·HCl (CAS = 51805-45-9, MW= 286.65, #20490)	Thermo Scientific, USA
Urea 99%, ACS Reagent, (CAS= 57-13-6, MW=60.06)	Sigma Aldrich, D
Amonium persultate analytical grade (CAS= 7727-54-0, MW = 228.2, #13375)	Serva, D
Dodecylsulfate sodium (SDS-b, CAS= 151-21-3, MW = 288.38)	Gerbu Biotechnik, D

PageRuler ^{TM} prestained protein ladder plus (#SM1811)	Fermentas
Tryptan blue solution (CAS = 72-57-1, #93595)	Fluka, D
Guanidine hydrochloride (CAS= 50-01-1, MW= 95.53, #369079)	CalBiochem, USA
TBTA 97%, Tris[(1-benzyl-1H-1,2,3-triazol-4-yl)methyl] amine (CAS= 510758-28-8 , MW= 530.63)	Sigma Aldrich, D
SILAC kit (MS10030)	Invitrogen
Light lysine (# 32462)	Invitrogen
Heavy lysine (# 32457)	Invitrogen
Light arginine (#32460)	Invitrogen
Heavy arginine (#MS10009)	Invitrogen

1.3 Buffers and solutions

Buffer	**Composition**
5 * SDS-PAGE – loading buffer	0.225 M TRIS·HCl pH=6.8 50% glycerol 5% SDS-b 0.05% Bromophenol Blue 0.25M DTT
10* SDS- PAGE - running buffer (big gel)	2.5 M Glycine 0.25 M TRIS·HCl 35 mM SDS-b
1* Running buffer (small commercial gel)	1M TRIS·HCl 0.9 M HEPES.Na 35 mM SDS-b

10* PBS (10* phosphate buffered saline)	1.37 M NaCl 27 mM KCl 0.1 M Na_2HPO_4 20 mM KH_2PO_4 pH= 7.4
10* TBS	0.2 M TRIS·HCl 1.5 M NaCl pH = 7.4
PBST	PBS + 0.1% Tween 20
TBST	TBS + 0.1% Tween 20
Transfer or blotting buffer	25 mM TRIS·HCl 0.2 M Glycine MeOH / H_2O = 1/4
Ripa buffer	50 mM TRIS·HCl pH= 7.4 1% NP40 150 mM NaCl 1mM EDTA 1mM Na_3VO_4
Membrane stripping buffer	6M guanidine Hydrochloride

1.4 Antibodies

1.4.1 Primary antibodies

Antigen	**Type**	**Organism**	**Company (concentration)**
APT1	Polyclonal	Rabbit	BioGenes Gmbh - 0.26 mg/ml
Phospho-$ERK_{1/2}$	Monoclonal	Mouse	Sigma Aldrich (#M8159)
Total $ERK_{1/2}$	Monoclonal	Rabbit	Cell signalling (#M4695)

1.4.2 Secondary antibodies

Antigen	Description	Company
HRP rabbit	ImmunoPure® antibody, goat anti-rabbit IgG (H+L)	Thermo Scientific (# 31460)
HRP mouse	ImmunoPure® antibody, goat anti-mouse IgG (H+L)	Pierce (# 31430)

1.5 Growth medias for cell culture

Media	Composition
MDCK-F3 cells (normal media)	500 ml DMEM 25 ml FBS 5ml non essential amino acid 5 ml sodium pyruvate 3 ml penicilium/streptomycin
HeLa cells (normal media)	500 ml DMEM 50 ml FBS 5ml non essential amino acid 5 ml sodium pyruvate 3 ml penicilium/streptomycin
HeLa cells (palmitome experiments)	500 ml DMEM 5% BSA (fatty acid free) 5ml non essential amino acid 5ml sodium pyruvate 3 ml penicilium/streptomycin
Starving media (ERK phosphorylation)	500 ml DMEM 5ml non-essential amino acids 5ml sodium pyruvate 3ml penicillium /streptomycin

HeLa SILAC media heavy or light (for 100 ml media)	80.6ml DMEM-Flex Medium (kit) 2.25ml glucose (kit) 2ml L-glutamine (kit) 10 ml FBS 1ml penicillium /streptomycin 1 ml non essential amino acid 1 ml sodium pyruvate 10 mg lysine (light or heavy) 10 mg arginine (light or heavy) 150 µl phenol red (kit)
HeLa SILAC starving media (heavy or light)	80.6ml DMEM-Flex Medium (kit) 2.25ml glucose (kit) 2ml L-glutamine (kit) 1ml penicillium /streptomycin 1 ml non essential amino acid 1 ml sodium pyruvate 10 mg lysine (light or heavy) 10 mg arginine (light or heavy) 150 µl phenol red (kit)

1.6 Cell culture methods

1.6.1 Counting cells

The cell number can be evaluated using a Neubauer cell counting chamber. To limit the risk of error, the cell suspension is first diluted with tryptan blue, by a factor 4, chosen for simplicity reason. The use of tryptan blue permits to distinguish living cells from dead cells, with dead cells stained in blue. After proper cell re-suspension in tryptan blue to ensure the absence of cell aggregates, the diluted cell suspension is placed in the counting chamber and living cells located into the counting grid consisting in 4 large outer squares (holding 16 small squares in each) were counted. The number of cell contained in 1 ml of the initial cell suspension can subsequently be obtained by multiplying this number by factor 10^4.

1.6.2 Splitting cells

When cells are confluent (no space anymore for a new cell duplication cycle), cells need to be splitted. Splitting cells consist in detaching cells from their previous cell culture flask and in seeding some of them into a new cell culture flask. Splitting cells should be performed regularly, typically twice a week with HeLa cells and slightly more often with MDCK-F3 cells. After discarding the old growing media, cells are washed twice with PBS and are incubated for 2-5 min at 37°C, 5% CO_2 with some trypsin/EDTA solution (typically 1 ml for a 75 cm^2 cell culture flask, and 2 ml for a 175 cm^2 cell culture flask) to, allow their complete detachment (visualization under microscope). Cells are subsequently diluted with new cell growing media (typically 1/9 dilution) and incubated at 37°C before repeating the operation.

1.6.3 Freezing cells

After cells trypsination, a volume of cell suspension corresponding to 10^6 cells is centrifuged (5 min, $1.2*10^3$ rpm) and the cell pellet is washed twice by centrifugation followed by re-suspension in PBS. After the last centrifugation step, PBS is discarded and 0.25 ml of DMEM media containing 10% DMSO and 10% FBS, is added to the cells, which are subsequently frozen at -80°C, before being placed in liquid nitrogen for long term storage.

1.6.4 Thawing cells

Thawing cells consist in defrosting cells in order to place them under culture. A cell aliquot is carefully defrosted by keeping it for few minutes into a 37°C water bath and the content is quickly transferred into a 75 cm^2 cell culture flask, containing 10 ml of pre-warmed cell growing media. After incubation of the cells at 37°C for one day, the media is subsequently replaced by fresh media in order to remove the DMSO originally contained into the aliquot.

1.7 Proteins methods

1.7.1 Preparation of cell lysate

Cell lysis consists in the cell disruption leading to a free protein suspension. Two different methods are commonly used to lyse cells either by mechanical cell disruption using a sonicator (3*10 sec, 30% power, on ice) or by using a lysis buffer containing 1-2% detergent such as NP-40, Tween 20, Triton-X100. Typically, 30 minutes incubation in a detergent-containing buffer are sufficient to ensure complete cell destruction. For pull down experiments, and in particular for

proteomic analysis, the sonication method is preferred in order to avoid detergent contamination problem which may complicate proteins identification by mass spectrometry.

1.7.2 Determination of protein concentration

Protein concentrations are commonly evaluated by means of a Bradford assay. The Bradford solution is first titrated by measuring the absorbance of several known protein containing samples used in quantity ensuring an absorbance value below 1. Typically the measurement of the absorbance at 595nm of BSA used in a range varying from 0 to 5 µg (in the Bradford solution) permit to determine the linear relation between protein quantity and absorbance, which can be used to evaluate the protein concentration of unknown sample. To get reliable values, measurements need to be performed in an absorbance range below 1, typically the addition of 1-2 µl of the unknown sample into 1 ml of Bradford solution is sufficient.

1.7.3 Proteins separation on SDS-PAGE

SDS- gel PAGE preparation

Two glass plates (inner and outer) are first assembled. The interspace between the two glass plates is ¾ filled with the chosen resolving gel preparation and the remaining interspace subsequently filled with ethanol to get a flat base line. After complete polymerization (typically 30 minutes for a small gel, and 1 hour for a large gel), the ethanol layer is removed and the remaining interspace is completely filled with a gel stacking preparation and a comb is rapidly added. After complete polymerisation of the second layer of the gel, the gel can be assembled into the running chamber (typically after an additional 30 minutes for a small gel or 1 hour for a large gel).

- Composition for 10 ml of 12% resolving gel preparation:
    - 3.3 ml H_2O
    - 4.0 ml 30% acrylamide mix
    - 2.5 ml 1.5M TRIS·HCl, pH= 8.8
    - 0.1 ml 10% SDS
    - 0.1 ml 10% ammonium persulfate
    - 0.01 ml TEMED

- Composition for 10 ml of 11% resolving gel preparation:
    - 3.45 ml H_2O
    - 3.45 ml 30% acrylamide mix
    - 2.5 ml 1.5M TRIS·HCl, pH= 8.8
    - 0.1 ml 10% SDS
    - 0.1 ml 10% ammonium persulfate
    - 0.01 ml TEMED
- Composition for 1 ml stacking gel preparation:
    - 0.68 ml H_2O
    - 0.17 ml 30% acrylamide mix
    - 0.13 ml 1M TRIS·HCl, pH= 6.8
    - 0.01 ml 10% SDS
    - 0.01 ml 10% ammonium persulfate
    - 1 µl TEMED
- Volume require for one small gel (1 mm thickness, size: 8 cm * 8 cm, 10 pockets):
    - 5 ml resolving gel preparation
    - 1 ml stacking gel preparation
- Volume require for one large gel (1 mm thickness, size: 20 cm*20 cm, 15 pockets):
    - 25 ml resolving gel preparation
    - 5 ml stacking gel preparation

Sodium Dodecyl Sulfate Poly Acrylamide Gel Electrophoresis or SDS–PAGE electrophoresis is commonly used to separate proteins according to their size. Since different proteins with similar molecular weight may migrate differently on the gel, due to their differences in secondary, ternary or quaternary structure, the anionic detergent SDS is added to the running buffer and in the gel to reduce proteins to their primary (linearized) structure and coat them with uniform negative charges. Additional reducing reagents such as TEMED also enter in the composition of the gel in order to reduce disulfide bonds present in the proteins. After dilution into 5*SDS loading buffer, proteins containing sample are boiled at 96°C for 5 min to denaturate proteins. Once the gel is properly assembled and the apparatus filled with SDS-running buffer, the comb is removed and the samples are loaded onto the different pockets of the gel. Typically, 25 µl can

be loaded on a small gel (10 pockets, 1 mm thickness) whereas up to 200 µl can be loaded onto a large gel (15 pockets, 1 mm thickness) without any risk of contamination within the different pocket of the gel. A prestained protein ladded is also usually applied in one gel pocket in order to estimate the molecular weight of proteins given their localization in the gel. Typically 3 µl of ladder is sufficient for a small gel, whereas large gels require 10 µl of ladder. Once the different sample properly loaded onto the gel, a suitable amperage is applied to make proteins moved into the gel. For a small gel, 30 mA is typically applied for 45 min (60 mA for 2 gels), whereas large gels are usually run overnight by convenience using 12 mA for 12 hours for one gel (24 mA for 2 gels). Large gels require the use of a cooling system to avoid any overheating of the system that might affect the quality of the gel. Once the run is completed, the two glass plates are removed carefully, and the gel is either transferred into a PVDF membrane for Western blotting analysis or trypsin-digested for proteomic analysis after proteins detection (*in-gel* fluorescence scanning or silver staining).

1.8 Western blotting methods

1.8.1 Semi- dry protein transfer

In semi-dry blotting, the electrodes are placed directly in contact with the gel/membrane sandwich to allow an efficient proteins transfer. Usually PVDF-membranes are preferred given their possibility to be stripped to remove bound antibody thereby allowing multiple uses. PVDF membranes are first activated by immersion for 5 min in methanol, and are subsequently pre-incubated together with the gel and 4 pieces of blotting paper into blotting buffer for 5-10 min. Note: the size of the membrane and blotting papers should be adjusted to the size of the gel for an optimal protein transfer. The sandwich gel/membrane can subsequently be assembled in the transfer device, by disposing first two blotting papers, recovered by the membrane, followed by the gel. Two additional blotting papers are then added to recover the gel and a particular attention is then given to ensure the absence of air bubble which may affect the quality of the protein transfer. Usually the voltage or time needed for the transfer is evaluated depending on the surface of the membrane. Typically 5 mA are applied for 30 min to transfer proteins contained in 1 cm^2 of gel. For more information, refer to the manual of the transfer device. Typically, the transfer of a small gel (8cm*4cm) require approximately 45 minutes at 25 Volts. A correct evaluation of the time require for the transfer is crucial given that an over estimation would lead to a partial or to a complete protein transfer into the blotting papers. A short control

of the transfer of the prestained ladder, by detaching carefully one corner of the gel from the membrane, is therefore a good way to follow the protein transfer.

1.8.2 Specific protein visualization

After protein transfer, specific proteins can be visualized by Western blotting analysis. The membrane is first blocked by incubation for 1 hour at rt in a suitable blocking buffer and the primary antibody is subsequently applied to the membrane in an appropriate dilution, typically overnight at 4°C. The membrane is washed with PBST or TBST (3 times, 10 min) to remove unbound antibodies before applying a secondary antibody for HRP detection in an appropriate dilution, typically for 1 hour at rt. After new PBST or TBST washing steps (3 times, 10 min), the membrane can be developed using the *Supersignal ® West Pico Chemiluminescent substrat* or *Supersignal ® West Femto Chemiluminescent substrat* from Thermo Scientific. **Table 1** contained the specific antibody dilution optimized for APT1, phosphor-$ERK_{1/2}$ and total-$ERK_{1/2}$ visualization.

APT1 (HeLa pull down)	**Solution**	**Composition**
	Blocking buffer	PBST + 2% chocolate slim fast
	Primary antibody (BioGenes)	1/50 dilution in blocking buffer
	Secondary antibody (# 31460)	1/10 000 dilution in PBST
	Detection Kit	Pico (few minutes)
APT1 (CLL pull down)	Blocking buffer	PBST + 2% chocolate slim fast
	Primary antibody (BioGenes)	1/50 dilution in blocking buffer
	Secondary antibody (# 31460)	1/10 000 dilution in PBST
	Detection Kit	Pico (few minutes)
Phospho-$ERK_{1/2}$ (MDCKF3 cells)	Blocking buffer	TBST + 2% chocolate slim fast
	Primary antibody (#M8159)	1/1000 dilution in blocking buffer
	Secondary antibody (# 31430)	1/20 000 dilution in TBST
	Detection kit	Femto (few minutes)
Total-$ERK_{1/2}$ (MDCKF3 cells)	Blocking buffer	TBST + 2% chocolate slim fast
	Primary antibody (#M4695)	1/1000 dilution in TBST + 2% BSA

	Secondary antibody (# 31460)	1/10 000 dilution in TBST
	Detection kit	Pico (few minutes)
Phospho-$ERK_{1/2}$ (HeLa cells)	Blocking buffer	TBST + 2% chocolate slim fast
	Primary antibody (#M8159)	1/10 000 dilution in blocking buffer
	Secondary antibody (# 31430)	1/20 000 dilution in TBST
	Detection kit	Pico (2 hours)
Total-$ERK_{1/2}$ (HeLa cells)	Blocking buffer	TBST + 2% chocolate slim fast
	Primary antibody (#M4695)	1/1000 dilution in TBST + 2% BSA
	Secondary antibody (# 31460)	1/10 000 dilution in TBST
	Detection kit	Pico (overnight)

Table 1: Summary of the Western blotting conditions used for the detection of APT1, phospho-$ERK_{1/2}$ and total-$ERK_{1/2}$respectively.

1.8.3 Stripping PVDF- membranes

As already mentioned PVDF-membranes offer the possibility to be used several times which is very appreciable when investigating different Western blotting conditions. Immersion of the membrane into stripping buffer until complete transparency (few sec to 1 minute) permits to wash away bound antibodies. After being washed several time with PBST or TBST (3 times, 10 min), the membrane recover its original aspect, and needs to be blocked before to be re-used. This process can usually be performed 2 to 3 times without affecting the emitted signal.

1.9 Target identification methods

1.9.1 General protocol for target identification in HeLa cells

Pull down experiments were performed using a protocol modified from the literature.[1] After removal of the HeLa cells growing media, HeLa cells were washed twice with PBS and trypsinized according to a standard protocol (2-3 min incubation at 37°C). After complete detachment, HeLa cells were re-suspended in their growing media and the cell suspension was washed 3 times by centrifugation (1500 rpm, 5 min, rt) followed by re-suspension in PBS. The obtained cell pellet was finally re-suspended into PBS to achieve a suspension containing $2*10^6$ cells/ml. Experiments for enrichment were carried out in 947 µl cell suspension volume, such as when the click chemistry reagents were added, the total reaction was 1 ml. 947 µl of the $2*10^6$ cells/ml

suspension was incubated 20 minutes at rt with the pull down probe (**23** or **83** or **94**) by addition of 1 µl of a suitable DMSO stock solution. Subsequently, the probe excess was removed by three successive centrifugation (4000 rpm, 5 min, 4°C) / ice-cold PBS washing steps. After re-suspension into 948 µl of PBS, cells were lysed by sonication at 0°C (3 times, 10 sec, 30% power) and the click ligation was initiated by addition of the rhodamine-biotin-azide dye **103** (10 to 30 µM final concentration, as a 10 mM stock DMSO solution), followed by the addition of a 0.5 mM aqueous TCEP reducing reagent solution and 50 µM ligand TBTA (as a DMSO/t-BuOH 1/4 solution). After addition of 0.5 mM aqueous $CuSO_4$ solution, the reaction was gently vortexed and incubated at rt for 1 hour. Proteins were subsequently precipitated by addition of an equal volume of cold acetone (1 ml) to the reaction, which was kept at -20°C for approximately 30 min. After centrifugation (13000 rpm, 10 min, 4°C), the supernatant was discarded and precipitated proteins were washed 3 times by successive centrifugation (13 000 rpm, 4°C)/ ice-cold MeOH (0.6 ml) washing steps. For an higher efficiency, proteins were re-suspended by sonication (1 time, 5 sec, 30% power) between all washing steps. For such experiments, samples were prepared in duplicate and were finally combined before enrichment with streptavidin magnetic beads so as the quantity of proteins contained in each aliquot correspond to $4*10^6$ cells. After a new centrifugation step (13 000 rpm, 10 min, 4°C), proteins were re-suspended in 1 ml of PBS containing 0.2% SDS by sonication (10 sec, 30% power, rt). Note: The sample should not be cooled while sonificating into PBS buffer containing 0.2% SDS as proteins should not precipitate. Subsequently, the sample was incubated at rt for 1 hour with 250 µl of streptavidin magnetic beads suspension (prewashed twice with PBS) under rotatory stirring. After enrichment, beads were washed successively with PBS buffer containing 0.2% SDS (3 times, 1 ml), with 6M urea aqueous solution (2 times, 1 ml) and with PBS (3 times, 1 ml). Target proteins were subsequently released from the beads by boiling the sample in 30 µl of 5* SDS loading buffer (96°C, 5 min). After centrifugation (13 000 rpm, 5 min, rt), beads were discarded and the sample fully loaded on a 12% SDS-PAGE gel (PROTEAN II xi 20 cm Cell from BioRad, 1 mm spacer, 15 wells comb), which was then scanned for fluorescence using a Typhoon TRIO + ^{TM} variable Mode Imager from GE Healthcare (fluorescence measurement, grey scale, emission filter 580BP 30 Cy3, TAMRA, AlexaFluor 546, PMT: 600, laser: green 532, sensibility normal). Data were analysed using the software *ImageQuant™ TL* from GE Healthcare. After fluorescence scanning, the gel was either used for proteomic analyses or for Western blotting experiments for specific protein visualization. Note: for proteomic analyses, each sample was fully loaded onto 2 different pockets of a small commercially available 12% gel, which were subsequently digested together.

The use of commercial gel is preferred for proteomic analyses in order to avoid contamination problem especially with PEG.

1.9.2 General protocol for target identification in PMBC and CLL cells

Protocol for fluorescence detection and Western blotting analysis Primary PMBC and CLL cells were collected from healthy and leukemia patients respectively. The blood from patients was first treated with the antibody complex *RosetteSep*® capable to bind to all non B-cells. Subsequent centrifugation over the Ficoll densient medium permits to pellet complexes together with red blood cells and to isolate purified B-CLL cells. Subsequently, B-CLL cells were washed with PBS and re-suspended in IMDM Medium containing 10% FCS and 1% penicilium/ streptomycin. A similar procedure was used for the isolation of PMBC cells, at the exception from antibody complexes which were omitted. PMBC and CLL cells were subsequently incubated for 20 minutes either with probe **23** (50 µM) or with DMSO in IMDM medium containing 10% FCS and 1% penicilium/streptomycin. After removal *of* excess probe*,* cells were re-suspended into 1 ml of PBS, lysed and frozen to be further processed in Dortmund. Usually ~10^8 cells were contained in each aliquot to ensure a sufficient protein concentration. Samples were subsequently adjusted to 1.2-1.5 mg protein/ml by dilution with PBS to ensure an optimal $Cu^{(I)}$-catalyzed Huisgen [3+2]-cycloaddition. Labeling experiments were subsequently performed following the protocol decribed above with $TrifN_3$ (**103**) = 10 µM, TCEP= 0.5 mM, TBTA ligand= 50 µM, $CuSO_4$ =0.5 mM and 750 µl beads. For these experiments, PMBC and CLL samples were prepared in duplicate and were combined two by two before enrichment with streptavidin magnetic beads. Finally, proteins were released from the beads in 5*SDS loading buffer, and 1/10 of each sample was loaded on a 12% SDS-PAGE gel (PROTEAN II xi 20 cm Cell from BioRad, 1 mm spacer, 15 wells comb). The gel was then used for *in gel* fluorescence scanning and Western blotting analysis for APT1 visualization. All the experiments were performed using cells from different patients.

- CLL cells (10013), treated with probe **23** / DMSO
- PBMC cells (10081), treated with probe **23** / DMSO

Protocol for proteomic analysis:

A similar protocol was followed for proteomic analysis with the exception that the dye **103** was used at 30 µM final concentration and that each reaction was performed in quadruplet to be

combined before sample enrichment with 750 µl streptavidin beads. Finally PMBC cells samples were fully loaded on a 12% commercially available gel as two bands, which were digested together. In contrast, only half of the final CLL sample was loaded as two bands on the gel, which was then used for proteomic analyses. All the experiments were performed in triplicate using cells from different patients.

- PMBC cells (10353/10354), treated with probe **23** / DMSO
- PMBC cells (10080/10084), treated with probe **23** /DMSO
- PMBC cells (10081), treated with probe **23** / DMSO
- CLL cells (10293), treated with probe **23** /DMSO
- CLL cells (10245), treated with probe **23** /DMSO
- CLL cells (10012), treated with probe **23** /DMSO

1.9.3 General protocol for palmitome experiments

Protocol for visualization of the palmitome by fluorescence

Pull down experiments were performed using a protocol modified from the literature.[2] Approximately 10^6 HeLa cells were seeded in a 10 cm diameter dish for 12 hours. After removal of the HeLa growing media, cells were washed twice with PBS and were incubated with 100 µM ω16-alkynyl fatty acid **106** in 5% BSA containing starving media for 5 hours at 37°C. Subsequently, cells were washed three times with PBS before being collected (typically $1.5*10^6$ cells are obtained from one 10 cm diameter dish) either by trypsination or using a cell scraper in the presence of various lysis buffers. Cells were finally obtained in 1 ml total volume (PBS or lysis buffer) corresponding to a suspension containing approximately $1.5*10^6$ cells /ml. Cells were lysed by sonication at 0°C (3 times, 10 sec, 30% power) and the experiment was subsequently performed using a similar protocol as described above using $TrifN_3$ (**103**) = 15 µM, TCEP= 0.5 mM, TBTA ligand= 50 µM, $CuSO_4$ =0.5 mM, 500 µl streptavidin beads. For such experiments, samples were prepared in duplicate and were finally combined before enrichment with streptavidin magnetic beads such that the quantity of proteins contained in each aliquot corresponds to approx. $3*10^6$ cells. Proteins were released from the beads in 5*SDS loading buffer, and the sample was fully loaded on a 12% SDS-PAGE gel (PROTEAN II xi 20 cm Cell from BioRad, 1 mm spacer, 15 wells comb). Finally, *in gel* fluorescence scanning allowed the visualization of labeled palmitoylated proteins.

Protocol for SILAC proteomic quantification

HeLa cells were grown in SILAC media complement either with heavy (isotopic, ^{13}C) or light (normal, ^{12}C) arginine and lysine amino acids respectively for 5 cell duplication cycles, with the media exchanged once. Subsequently, cells treated with isotopic amino acids were seeded in two 75 cm^2 flasks (A,B), and cells treated with normal amino acids were seeded in two 75 cm^2 flasks (C,D) in their respective SILAC growing media. After 6 hours incubation, the growing media was removed, cells were washed three times with PBS, and treated for 12 hours with ω16-alkynyl fatty acid **106** at 100µM final concentration in their growing media respectively, in which FBS was replaced by 5% BSA. Cells were subsequently washed with PBS (3 times) and were incubated for 3 hours with DMSO or palmostatin B **14** (30 µM final concentration) in their respective media containing 5% BSA. After trypsination, cells were washed three times by centrifugation (1500 rpm, 5 min, rt) followed by re-suspension into PBS. The four distinct cell pellets were finally re-suspended in 1 ml PBS leading to sample A= $5*10^5$cells/ml (ω16-alkynyl fatty acid **106**, isotopic labeled cells, DMSO), B= $8*10^5$cells/ml (ω16-alkynyl fatty acid **106**, isotopic labeled cells, palmostatin B), C= $1.9*10^6$ cells/ml (ω16-alkynyl fatty acid **106**, non-isotopic labeled cells, DMSO), D= $2.1*10^6$ cells/ml (ω16-alkynyl fatty acid **106**, non-isotopic labeled cells, DMSO). The incorporation of isotopic or normal amino acids (arginine, lysine) was determined by mass spectrometry for the four cell populations leading to a complete absence of isotopic labeled peptides in sample C and D as expected, whereas sample A and B were found to have respectively 97% and 92% of isotopic labeled peptides. Therefore, 1 ml of each 1:1 mixture of B/C (296 µl of C + 703 µl of B) and A/D (192µl of D + 808 µl of A) were prepared to be used like previously for pull down experiments using using $TrifN_3$ (**103**) = 30 µM, TCEP= 0.5 mM, TBTA ligand= 50 µM, $CuSO_4$ =0.5 mM, 750 µl streptavidin beads. For such experiment, only 1 ml of each cell mixture B/C and A/D were used for the complete experiment and the ratio 1:1 was evaluated based on cell concentration more accurate compared to protein concentrations. Finally, proteins presenting thioester linkages were released from the beads using hydroxylamine (0.32M, pH 6.8, for 1 hour at 37°C). After concentration to dryness, samples were resuspended in SDS loading buffer and were loaded on a 12% SDS gel as two distinct bands corresponding to the sample referred to as "NH_2OH B/C" and "NH_2OH A/D" respectively. Streptavidin magnetic beads were subsequently boiled in SDS loading buffer for 5 min at 96°C to collect remaining proteins leading to two samples referred to as "Δ B/C" and "Δ A/D". A small aliquot of each initial lysate mixure (referred to as "LYSATE B/C" and sample "LYSATE A/D") was collected before initiating the click ligation, in order to check the initial ratio of isotopic peptide pairs which should be close to 1:1. The six different samples referred to as sample "NH_2OH B/C",

sample "NH_2OH A/D", sample "Δ B/C", sample "Δ A/D", sample "LYSATE B/C" and sample "A/D LYSATE", were subsequently fully loaded on a commercially available 12% small SDS-PAGE gel (PROTEAN II xi 20 cm Cell from BioRad, 1 mm spacer, 15 wells comb). After silver staining, bands were cut and proteins were digested with trypsin to be submitted for proteomic analyses.

1.10 Proteomic analysis protocols

1.10.1 Silver staining protocol

Gels were usually silver stained using the following protocol prior to the protein digestion. The gel was first fixed for 1 hour at rt using EtOH/AcOH/H_2O (4/1/5) and was washed with EtOH/H_2O 3/7 (2 times, 10 minutes) followed by H_2O (1 time, 10 minutes). The gel was subsequently treated with aqueous 0.02% w/v $Na_2S_2O_3$ solution for 1 minute and was washed with water (3*20 sec). A cold 0.1% w/v $AgNO_3$ aqueous solution was added to the gel, subsequently stored for 20 minutes at 0°C. The gel was washed with water (6*20 sec) and a developing solution consisting in 3% w/v Na_2CO_3, 0.05% v/v formaldehyde in water was added to the gel until bands with a suitable intensity were visible. Note: The developing solution should be replaced by a fresh solution when turning yellow. Once satisfying bands were obtained, the solution was discarded and the gel was washed for 1 minute with water before termination of the reaction by adding 0.05 M aqueous EDTA solution. Bands can subsequently be isolated using a scalpel and transferred as small gel pieces into a 1.5 ml Eppendorf tube, and the protein content can be subsequently digested using trypsin.

1.10.2 Trypsin-digestion protocol

Gel pieces were first washed with buffer A (50 mM NH_4HCO_3 in water) for 10 min at 37°C (450 rpm) followed by buffer B (50% buffer A, 50% MeCN) for 10 min at 37°C (450 rpm). Two additional washing steps were performed like previously successively with buffer A and B. Proteins were subsequently reduced at 56°C (450 rpm) for 30 minutes using 10 mM DTT as a solution in buffer A. The solution was discarded and replaced by 5 mM iodoacetamide as a solution in buffer A. The alkylation reaction was performed at room temperature for 30 min (450 rpm). Samples were subsequently washed like previously at 37°C (450 rpm) for 10 min successively with buffer A, B, A and B. After the last washing step, the washing solution was discarded and the gel pieces were dried using a vacuum concentrator for 10 min. Subsequently, 100 µl of a 100 µg/ml trypsin solution in 1 mM HCl, were dissolved in 900 µl buffer A. Finally, 70

µl of the obtained trypsin solution were added to the gel pieces which were subsequently incubated at 37°C (450 rpm) for 15 min. After addition of buffer A (100 µl), the gel pieces were incubated at 30°C (450 rpm) for 15 hours. After digestion, the liquid was transferred into a new 1.5 ml Eppendorf tube and peptides were extracted by incubation of the gel pieces with 1% TFA in water at 37°C (450 rpm) for 15 min. The extract was combined to the previously collected one and the operation repeated one time with 1% TFA aqueous solution followed by a last extraction step using 2% TFA in H_2O/CH_3CN (1/1). Combined extracts were finally concentrated to dryness using a vacuum concentrator and submitted to mass spectrometry analysis.

1.10.3 Mass spectrometry analysis

For protein identification, tryptic peptides were separated and analyzed by nano-HPLC-MS/MS. The separations were carried out on an Ultimate 3000 nano-HPLC (Dionex, Idstein, Germany) equipped with one analytical pump connected to a nano flow splitter, a flow manager, an autosampler and a variable two wavelength UV detector. MS and MS/MS experiments were carried out on an Orbitrap mass spectrometer equipped with a LTQ XL linear ion trap (Thermo Electron Corporation, Dreieich, Germany). All solvents were LC-MS grade. Lyophilized tryptic peptides were dissolved in 25 µl 0.1 % TFA, and 10 µl were injected and enriched onto a C18 PepMap 100 column (3 µm, 100 Å, 300 µm ID * 5 mm, Dionex, Idstein, Germany) using 0.1 % TFA and a flow rate of 30 µl/min for 5 min. Peptides were separated on a C18 PepMap 100 column (3 µm, 100 Å, 75 µm ID * 150 mm) using a linear gradient starting with 96.8 % solvent A / 3.2 % solvent B and increasing to 62.0 % solvent A / 38.0 % solvent B in 145 min with a flow rate of 300 nl/min (solvent A: water containing 0.1 % formic acid; solvent B: acetonitrile containing 0.1 % formic acid). The nano-HPLC was online coupled to the Orbitrap mass spectrometer using a standard coated Pico Tip (ID 20 µm, Tip-ID 10 µM, New Objective, Woburn, MA, USA). Precursor scans were carried out in the Orbitrap with a resolution of 60000. MS/MS data of the 5 most intense and at least two-fold charged ions were simultaneously recorded in the linear trap. For protein identification, data was analyzed using SwissProt database (version 56.7) using the MOWSE algorithmn brief, a MS/MS ion search was performed for full enzymatic trypsin cleavages allowing one miscleavage. The taxonomy was set to Homo sapiens (human). For protein modifications carbamidomethylation was chosen as fixed modification and oxidation of methionine as variable. The mass accuracy was set to 5 ppm for peptide masses and 0.5 Da for MS/MS data. The significance threshold was set to $P < 0.01$. Only proteins for which at least two protein specific peptides were identified are chosen for further validation and only those

identified in at least two out of three independent pull down experiments, but not identified in the control pull downs (DMSO treated sample) were considered hits.

1.11 Erk phosphorylation protocol

Cells were seeded on a 6 cm diameter dish (3-7*10^5 cells/dish) and were incubated at 37°C for approximately 18 hours. After being washed with PBS (3 times), cells were treated with palmostatin M (**28**)/ DMSO as a solution in starving media. After 1 hour incubation at 37°C, cells were washed with PBS (3 times) and EGF was subsequently added to the cells as a solution into starving media (final concentration 200 ng/µl). After 10 min EGF-activation, cells were washed twice with ice-cold PBS buffer and subsequently lysed with 60 µl RIPA buffer on ice. Sodium fluoride (NaF, 50mM final concentration), sodium vanadate (Na_3VO_4, 1mM final concentration), 10 µl mercaptoethanol and one complete Mini EDTA-free protease inhibitor tablet were freshly added to 10 ml of RIPA buffer. Cells were scrapped on ice and transferred into a 1.5 ml Eppendorf tube which was maintained on ice at least for 20 min and were subsequently sonicated (ultrasonic bath, 3x10 min) to ensure complete cell destruction. Samples were centrifuged (13 000 rpm, 4°C, 15 min) and the protein concentration of the supernatant (previously transferred into a new 1.5 ml Eppendorf tube) was determined by a Bradford assay. An equal amount of proteins (approx. 30 µg proteins) was boiled in 5*SDS loading buffer and was loaded as one band on a 11% SDS-PAGE gel. The gel was subsequently run for maximal separation, transferred on a PVDF membrane and used for Western blotting analysis for phospho-$ERK_{1/2}$ detection. The membrane was subsequently stripped and re-used for total $ERK_{1/2}$ detection, allowing the determination of the ratio phosphor-$ERK_{1/2}$ / total $ERK_{1/2}$ for the tested compound which was normalized to 100% using a control treated with DMSO after EGF activation. As negative control, a NON-EGF activated DMSO sample was used, whereas the known MEK inhibitor U0126 was used as additional positive control at 30 µM concentration.

1.12 Determination of phospholipase A1, A2, D inhibition

Assay for cytosolic phospholipase A2 (cPLA2) activity

Materials: 1-stearoyl-2-arachidonoyl-*sn*-glycero-3-phosphocholine (SAPC), 1,2-dioleoyl-sn-glycerol, arachidonic acid (AA), EDTA-Na_2, 4-undecyloxybenzoic acid, nor-dihydroguaiaretic acid (NDGA)

Development of the assay: The evaluation of cytosolic phospholipase A2 (cPLA2) inhibition was performed using an HPLC assay with UV spectrometric detection as reported in literature.[3] The final reaction mixture contained 0.2 mM phospholipid substrate 1-stearoyl-2-arachidonoyl-*sn*-glycero-3-phosphocholine (SAPC) and 0.1 mM 1,2-dioleoyl-*sn*-glycerol as enzyme substrate. After incubation of the substrate with palmostatin B (**14**) at 10 µM final concentration for 5 min at 37°C, cPLA2 (isolated from human platelets by anion exchange chromatography) was added to the mixture subsequently incubated at 37°C for 60 min. The enzyme reaction was terminated by addition of a mixture of acetonitrile, methanol and 3 mM aqueous EDTA-Na_2, which contained 4-undecyloxybenzoic acid as internal standard (IStd) and nor-dihydroguaiaretic acid (NDGA) as oxygen scavenger. After addition of dilute NaOH, the sample was cleaned up by solid phase extraction using reverse-phase C_{18} column. Samples were subsequently analysed by reverse-phase HPLC with UV detection at 200 nm to determine the quantity of arachidonic acid (AA, retention time at 11.7 min) released by cPLA2. The comparison of the peak area obtained for arachidonic acid (AA) in the control (no inhibitor), with the peak area of arachidonic acid (AA) in the palmostatin B-treated sample allow the evaluation of the cPLA2 inhibitory activity of palmostatin B at 10 µM. A known cPLA2 inhibitor was used as positive control and all activity measurements were performed in triplicate.

Assay for phospholipase A1 (PLA1) activity

Materials: The evaluation of phospholipase A1 (PLA1) inhibition was performed using the assay kit EnzChek® Phospholipase A1 purshased from Invitrogen. Phospholipase A1 substrate (PED-A1), dioleoylphosphatidylchlorine (DOPC), phospholipase A1 (Lecitase® Ultra, bacterial recombinant enzyme), dioleoylphosphatidylglycerol (DOPG), dimethylsulfoxyde (DMSO), and 5*Phospholipase A1 reaction buffer (250 mM Tris-HCl, 0.7M NaCl, 10 mM $CaCl_2$, pH 7.4) were provided in the kit. The protease-inhibitor cocktail was purchased from Roche.

MDCK-F3 cell lysate preparation: MDCK-F3 cells were trypsinized accordingly to a standard protocol and were washed three times by successive centrifugation (1500 rpm, 5 min, rt) followed by re-suspension into PBS. The cell pellet was subsequently re-suspended into 0.6 ml of cold aqueous lysis-buffer (50 mM Tris·HCl, 150 mM NaCl, 5 µM DTT, pH 8.0) containing freshly added protease-inhibitor cocktail solution (obtained by dissolving 1 tablet into 1 ml of d-H_20) in a ratio buffer/ protease-inhibitor 10/1. Cells were disrupted by sonication (5 times, 5 sec, 30% power) at 0°C and then stored at -80°C.

Development of the assay: MDCK-F3 cell lysates (PLA1-containing sample) were diluted with 1* PLA1 Reaction buffer leading to a 1.59 mg/ml protein concentration. The enzyme activity was monitored directly using the EnzChek® Phospholipase A1 substrate (PED-A1) which is a dye-labeled glycerophosphoethanolamines with BODIPY® FL dye-labeled acyl chain at the *sn*-1 position and dinitrophenyl quencher-modified head group. The BODIPY® FL pentanoic acid entity is released by cleavage of the substrate by PLA1 in the *sn*-1 position leading to an increased fluorescence. The enzyme activity was determined by measuring the release of fluorescence using a Tecan Infinite M200 microplate reader in a 96 well format. Reactions were carried out into a 100 µl reaction volume. The assay developed on MDCK-F3 cell lysates (PLA1-containing sample) was validated by using a bacterial recombinant PLA1 enzyme. In the assay, 1 µL of inhibitor DMSO stock solutions with different concentrations (C stock= 5 mM leading to a final concentration of 50 µM, C stock= 1 mM leading to a final concentration of 10 µM, C stock= 0.1 mM leading to a final concentration of 1µM) was mixed with 49 µl of cell lysate (1.59 mg/ml) and the mixture was incubated for 2 min. at 37°C. The same quantity of DMSO (1 µl) was also added to the controls. A substrate solution was subsequently prepared by adding 30 µl of 10 mM of DOPC in Ethanol, 30 µl 10 mM of DOPG in Ethanol, 30 µl 1mM of PLA1 substrate in 1* reaction buffer to 9 ml of 1* PLA1 reaction buffer. Subsequently, 50 µl of the prepared substrate solution was added to each reaction (sample and controls) and after 2 min. lag time the formation of fluorescence was recorded (λ_{ex} = 470 nm, λ_{em} = 515 nm, Gain = 100) over 1 hour at 15 sec. intervals at 37°C. During the incubation and in between measurements the reaction mixture was shaken. The residual PLA1 activity at 50 µM palmostatin B was determined by linear regression analyses ($r^2 \geq 0.98$) of the fluorescence emission increase over time. The background reaction rate with no enzyme present was subtracted and the reaction rates were normalized to the reaction rate with no inhibitor present (100%). Experiments were preformed in triplicate and the linear regression analysis was performed with Microsoft Excel.

Assay for phospholipase D (PLD) activity

Materials: The PLD evaluation was performed using the assay kit Amplex® Red Phospholipase D purshased from Invitrogen. Amplex Red reagent (10-acetyl-3,7-dihydrophenoxazine), dimethysulfoxide (DMSO), horseradish peroxidase (HRP), hydrogen peroxide (H_2O_2), 5* Reaction buffer (250 mM Tris·HCl, 25 mM $CaCl_2$, pH 8.0), Choline oxidase from *Alcaligenes sp*. and L-α-Phosphatidylcholine (lecithin) were provided in the kit. Phospholipase D from *Streptomyces Chromofuscus* was purchased from Sigma.

MDCK-F3 cell lysate preparation: prepared like above for PLA1 assay.

Development of the assay: MDCK-F3 cell lysates (PLD-containing sample) were diluted with 1* PLD Reaction buffer leading to a 1.79 mg/ml protein concentration. The enzyme activity was monitorated indirectly using the Amplex Red reagent, a sensitive fluorogenic probe for H_2O_2. First, PLD cleaves the phosphatidylcholine (lecithin) substrate to yield choline and phosphatidic acid. Second, Choline is oxidized by choline oxidase to betaine and H_2O_2. Finally, H_2O_2 in presence of horseradish peroxidase, reacts with Amplex Red reagent in a 1:1 stoechiometry to generate the highly fluorescent product, resorufin. The enzyme activity was evaluated by measuring the release of fluorescent resorufin using a Tecan Infinite M200 microplate reader in a 96 well format. Reactions were carried out into a 200 µl reaction volume. The assay developed on MDCK-F3 cell lysates (PLD-containing sample) was validated by using a bacterial recombinant PLD enzyme, and 99 µl of a 10 µM H_2O_2 solution in 1*reaction buffer was used as second positive control. 1 µl of 10 mM inhibitor DMSO stock solution (final concentration = 50 µM in V total = 200 µl) was mixed with 99 µl of the MDCK-F3 cell lysate (1.79 mg/ml by Bradford test) and the mixture was subsequently incubated for 2 min. at 37°C. The same quantity of DMSO (1 µl) was also added to the controls. Subsequently, a 100 µM of Amplex Red reagent solution in 1*PLD reaction buffer was prepared containing 2U/ml HRP, 0.2U/ml choline oxidase and 0.5 mM lecithin. Finally, 100 µl of the prepared substrate solution was added to each reaction (sample and controls) and after 2 min. lag time the formation of fluorescence was recorded (λ_{ex} = 540 nm, λ_{em} = 590 nm, Gain = 90) over 1 hour at 15 sec. intervals at 37°C. During the incubation and in between measurements the reaction mixture was shaken. The residual PLD activity at 50 µM palmostatin B was determined by linear regression analyses ($r^2 \geq 0.98$) of the fluorescence emission increase over time. The background reaction rate with no enzyme present was subtracted and the reaction rates were normalized to the reaction rate with no inhibitor present (100%). Experiments were performed in triplicate and the linear regression analysis was performed with Microsoft Excel.

1.13 Enzymatic assays for APT1 and APT2

1.13.1 Molecular cloning, expression and purification of APT1/2

Human acyl protein thioesterase 1 (APT1) was expressed and purified as described previously.[4] APT2 was produced under the same conditions as already described for APT1, with the following changes: the *apt2* gene (cDNA clone IRATp970G0114D, imaGenes, Berlin) was Gateway cloned

into a pGEX expression vector, modified to contain a PreScission protease recognition sequence between the *apt2* and the *gst* gene. The construct was then expressed as GST-APT2 fusion protein in *E. coli* BL21 (DE3) Codon+ RIL cells at 20 °C for 16 hours. The fusion protein was loaded on a GSH column and APT2 was separated from GST by overnight incubation of the column with PreScission protease, and finally purified to homogeneity by gel filtration.

1.13.2 Biochemical assay protocols

Colorimetric enzymatic assay for APT1[5]

The enzyme activity was determined by measuring the release of para-nitrophenolate (PNP) from para-nitrophenyl octanoate (PNPO) by absorbance employing 75 nM of enzyme and 600 µM of substrate PNPO. The assay was developed in a 96 well format on a TECAN plate reader. The assay was performed in buffer containing 20 mM HEPES, 150 mM NaCl, which was titrated to pH 7.52-7.55 using concentrated HCl solution (37%). In the assay, 50 µl inhibitor solutions (with varying concentration) in HEPES buffer with 0.01% (v/v) Triton-X100 was mixed with 30 µl APT1 solution (240 nM) in HEPES buffer with 0.01% (v/v) Triton-X100. The mixture was incubated for 30 min at 37 °C. Subsequently, 20 µl of an emulsion of PNPO (3.0 mM) in HEPES buffer containing 0.25% (v/v) Triton-X100 was added to the reaction mixture and after 2 min. lag time. The extinction at 401 nm was subsequently measured over 40 min. with 1 min. intervals at 37 ^{o}C. The substrate emulsion was prepared by vigorous stirring of PNPO in buffer containing 10% (v/v) Triton-X100 and subsequent dilution to give an emulsion with 3.0 mM PNPO and 0.25% (v/v) Triton-X100. During the incubation and in between measurements, the reaction mixture was shaken for 10 sec with 30 sec intervals with 600 rpm.

Fluorescent enzymatic assay for APT1:

The enzyme activity was determined by measuring the release of fluorescent 6,8-difluoro-4-methylumbelliferone (DiFMU, **2**) from 6,8-difluoro-4-methylumbelliferyl octanoate (DiFMUO, **3**) by fluorescence (λ_{ex} = 358 nm, λ_{em} = 455 nm) employing 5 nM of enzyme and 15 µM of substrate DiFMUO. The assay was developed in a 96 well format on a TECAN plate reader. The assay was performed in buffer containing 20 mM HEPES, 150 mM NaCl, which was titrated to pH 7.52-7.55 using concentrated HCl solution (37%). In the assay, 50 µl inhibitor solutions (with varying concentration) in HEPES buffer with 0.01% (v/v) Triton-X100 was mixed with 30 µl APT1 solution (16.6 nM) in HEPES buffer with 0.01% (v/v) Triton-X100. The mixture was incubated for 2 min at 37 °C. Subsequently, 20 µl of a solution of DiFMUO (75 µM) in HEPES buffer containing 0.09%

(v/v) Triton-X100 was added to the reaction mixture. The substrate solution was prepared by dissolving 2.4 mg of DiFMUO in 100 µl DMSO. Then, 900 µl HEPES buffer containing 10% (v/v) Triton-X100 was added and the mixture was vigorously stirred. 200 µl of the resulting mixture were subsequently dissolved into 19.8 ml of HEPES buffer to afford a solution containing 75 µM DiFMUO and 0.09% (v/v) Triton-X100. After 2 min. lag time, the formation of fluorescent DiFMU was recorded (λ_{ex} = 358 nm, λ_{em} = 455 nm) over 35 min. at 35 sec. intervals at 37 ^{o}C. During the incubation and in between measurements, the reaction mixture was shaken for 10 sec with 30 sec intervals with 600 rpm.

Fluorescent enzymatic assay for APT2:

The enzyme activity was determined as described previously for APT1, at the exception that 50 nM of APT2 was used. The preparation of the substrate DiFMUO solution remained unchanged from the one previously described for the APT1 fluorometric assay. 50 µl of inhibitor solutions (with varying concentrations) in HEPES buffer with 0.01% (v/v) Triton-X100 was first mixed with 30 µl of APT2 solution (166 nM) in HEPES buffer with 0.01% (v/v) Triton-X100. After 2 min incubation at 37°C, 20 µl of a solution of DiFMUO (75 µM) in HEPES buffer containing 0.09% (v/v) Triton-X100 was subsequently added to the reaction , and the formation of DiFMU recorded over time by analogy to the fluorometric APT1 assay.

1.13.3 Enzyme activity remaining- determination

Linear regression was performed using the Microsoft Excel software. The reaction rate was determined by linear regression analyses ($r^2 \geq 0.98$) of the fluorescence\extinction increase over time. The background reaction rate with no enzyme present was substracted and reaction rates were normalized to the reaction rate with no inhibitor present (100%) leading to the enzyme activity remaining in percent.

1.13.4 IC_{50}-determination

Linear regression was performed using the Microsoft Excel software and nonlinear curve fitting was performed using the Excel-fit plug-in software. For IC_{50} determination, 12 concentrations around the IC_{50} value were measured in triplicate. Inhibition plots were fitted to **Equation 1** in which y is the reaction rate at concentration of the inhibitor x, A_1 is the minimum reaction rate (no enzyme present), A_2 the maximum reaction rate (no inhibitor present), p is the Hill-slope and x_0 is the IC_{50}.

$$y = \frac{(A_1 - A_2)}{1 + (x / x_0)^p} + A_2$$

Equation 1: Equation used for IC_{50} evaluation.

1.13.5 Enzyme reactivation - $t_{1/2}$ determination

Conditions to monitor APT1 reactivation were optimised as follows using 5 nM enzyme and 15 µM DiFMUO. The assay was developed in a 96 well format on a TECAN plate reader. The assay was performed in a buffer containing 20 mM HEPES, 150 mM NaCl, which was titrated to a pH 7.52-7.55 using concentrated HCl solution (37%). In the assay, 5 µl APT1 solution (100 nM) in HEPES buffer with 0.01% (v/v) Triton-X100 was incubated for 4 min at 37°C with an excess of inhibitor (5 µl of a 200 nM inhibitor solution in HEPES buffer with 0.01% (v/v) Triton-X100, leading to a final concentration of 10 nM). After 4 minutes incubation (corresponding to the complete enzyme inactivation), 90 µl of a solution of DiFMUO (16.6 µM) in HEPES buffer containing 0.09% (v/v) Triton-X100 was added to the reaction mixture. The substrate solution was prepared by dissolving 0.53 mg of DiFMUO in 100 µl DMSO. Then, 900 µl HEPES buffer containing 10% (v/v) Triton-X100 was added and the mixture was vigorously stirred. 200 µl of the resulting mixture were subsequently dissolved into 19.8 ml of HEPES buffer to afford a solution containing 16.6 µM DiFMUO and 0.09% (v/v) Triton-X100. After 2 min. lag time, the formation of fluorescent DiFMU was recorded (λ_{ex} = 358 nm, λ_{em} = 455 nm) over 1 hour at 15 sec. intervals at 37°C. During the incubation and in between measurements the reaction mixture was shaken (600 rpm) for 5 sec with 30 sec intervals. The reaction rate was determined by linear regression analyses ($r^2 \geq 0.98$) of the fluorescence emission increase over time. The background reaction rate with no enzyme present was substracted and reaction rates were normalized to the reaction rate with no inhibitor present (100%). Linear regression was performed using Microsoft Excel software and nonlinear curve fitting was performed using the Excel-fit plug-in software. For $t_{1/2}$ (half-life) determination, values were measured in triplicate. The fluorescence emission increase over time plots were fitted to the first order Equation 2 in which y is the reactivation rate, A_o is the initial fluorescence and K the rate constant for reactivation. The half-life value ($t_{1/2}$) is then given by the following relation $t_{1/2} = \ln(2)/K$.

$$y = A_o \exp(-Kt)$$

Equation 2: Equation used for $t_{1/2}$ determination.

2 Chemical Synthesis

2.1 General methods and procedures

All chemicals were obtained from Aldrich, Acros or Novabiochem, and were used without further purification except when noted. Triethylamine was distilled over calcium hydride and stored over potassium hydroxide. Solvents were used as received or passed over a drying column (DCM, THF, DMF). Flash chromatography was performed using silica gel for chromatography 0.035-0.070 mm, 60Å purchased from Acros Organic. ^{1}H spectra were recorded on a *Varian Mercury*- 400 Oxford NMR spectrometer. Chemical shifts are reported in δ values relative to tetramethylsilane and coupling constants *J* are reported in Hz. Melting points were recorded on a Büchi Melting point B-540. IR spectra were recorded on a Bruker Tensor 27 and specific optical rotation ($[\alpha]_D^{20}$) on a Polartronic HH8 from Schmidt and Haensch. HPLC-MS measurements were performed using an Agilent 1100 Series instrument. GC-MS spectra were recorded on a Hewlett Packard, HP6890 series GC system, equiped with a Hewlett Packard, HP5973 series mass selective detector.

2.1.1 Spacer synthesis

General procedure for Finkelstein reaction.[6] Bromoethylester (56 mmol, 1.0 eqv.) and NaI (67 mmol, 1.2 eqv.) were dissolved into acetone (35 ml), and the reaction mixture was heated under reflux for 15-20 hours (T = 85°C). NaBr salts were subsequently filtered on a sintered funnel containing 5-10 cm silica gel and the silica washed with 50% EtOAc/cyclohexane. After concentration of the filtrate, iodoethylester was obtained and used in the next step.

General procedure for *S*-alkylation. To a two neck round bottom flask equipped with a large egg-shape stirring bar, containing a solution of *N,N*-(dimethylamino)propyl thioacetate **47** (26.5 mmol, 1.0 eqv.) in absolute ethanol (40 ml) was added Cs_2CO_3 (29 mmol, 1.1 eqv.) in one portion. A reflux condenser was mounted and the apparatus was flushed with argon and kept under positive argon pressure for the further manipulations. The mixture was refluxed for 2 hours, until TLC analysis indicated the complete disappearance of **47** and the formation of a much more polar thiol intermediary product (TLC eluent EtOAc/cylohexane 1/2). The mixture was cooled to 0°C and a solution of iodoethylester (29 mmol, 1.1 eqv.) in absolute ethanol (10 ml) was added dropwise to the mixture which was stirred at rt for 1 hour and then kept at 40°C until TLC indicated the disappearance of the thiol intermediary product (approx. 12 hours, TLC

system as above). After concentration to dryness, the residue was diluted with EtOAc/H_2O 1/2 (200ml) and was stirred until all solids dissolved. The phases were separated and the aqueous layer was extracted with EtOAc (2x50 ml). The combined organic extracts were washed with water (50 ml), brine (100 ml) and subsequently dried over anhydrous $MgSO_4$. Filtration and evaporation under reduced pressure lead to the coresponding *S*-alkylated compound which was used without any further purification step.

General procedure for Reduction. To an oven dried 250 ml round bottom flask was added $LiAlH_4$ (29.5 mmol, 1.25 eqv.), followed by a large egg-shaped stirring bar. The flask was flushed with argon, set under positive argon pressure and subsequently cooled to 0°C. Dry THF (50 ml) was added under rapid stirring and the resulting suspension was stirred at 0°C for 15 min. A solution of ethylester derivative (23.6 mmol, 1.0 eqv.) in dry THF (10 ml) was added dropwise over 10 min to the reaction mixture at such a rate that the temperature was kept around 0°C. The mixture was stirred for 1 hour at 0°C followed by 2 hours at rt and was quenched at 0°C by dropwise addition of H_2O (1.1 ml) (caution, gas evolution), followed by 1N NaOH (2.2 ml) and 1.1 ml H_2O. The thick suspension gets thinner upon aging and was diluted with further 50 ml THF. Two spoons of Celite were added and the mixture was allowed to age for another 30 min at rt. The resulting free running suspension was filtered over Celite in a sintered funnel. The filter cake was re-suspended in THF/MeOH 10/1 (50 ml) and was refluxed for 10 min in order to dissolve all products. After hot filtration over Celite, the combined organic extracts were evaporated under reduced pressure. Al-salt traces remaining were removed by suspending the residue in 6 N NaOH (20 ml) and CH_2Cl_2 (100 ml). The organic layer was separated and extracted with CH_2Cl_2 (3x30 ml), washed with brine and dried over Na_2SO_4. After concentration under reduced pressure, the corresponding alcohol was obtained, which was used directly in the next step.

General procedure for Swern oxidation. To a -78°C (dry-ice) cold oxalyl chloride solution (14.4 mmol, 1.1 eqv.) in dry CH_2Cl_2 (10 ml) was added dropwise over 10 minutes DMSO (31.4 mmol, 2.4 eqv.) as a solution in dry CH_2Cl_2 (10 ml). After 20 minutes at -78°C, the alcohol (13.1 mmol, 1.0 eqv.) was added dropwise (over 10 minutes) to the reaction as a solution in dry CH_2Cl_2 (10 ml). The mixture was subsequently stirred for 20 minutes at -78°C. Et_3N (47.7 mmol, 3.65 eqv.) was added over 10 minutes to the mixture which was stirred for 10 minutes at -78° followed by 45 minutes at rt. The reaction was quenched with water (50 ml) and phases were separated. The aqueous layer was extracted with CH_2Cl_2 (3x20 ml) and the combined organic extracts were washed with H_2O (20 ml), brine (2x50 ml) and dried over Na_2SO_4. After evaporation under reduced pressure, the corresponding aldehyde was obtained and used directly in the next step.

2.1.2 β-lactone synthesis

Aldol reactions

General procedure for ephedrine auxiliary synthesis.[7,8] In a round bottom flask was added (*1S,2R*) or (*1R,2S*)-Norephedrine (52.9 mmol, 1.0 eqv.) and NEt_3 (63.4 mmol, 1.2 eqv.) in dry DCM (200 ml). Mesilylenesulfonyl chloride (52.5 mmol, 1.0 eqv.) was added dropwise at 0°C to the reaction which was stirred at 0°C for 2 hours. The reaction was diluted with diethylether (200 ml), and subsequently washed with water, 1M HCl, Water, saturated $NaHCO_3$ and brine. Combined organic layers were finally dried and concentrated under reduced pressure. Recrystallized from DCM and hexane finally lead to mesylated intermediate compound which was alkylated using benzylbromide (63.4 mmol, 1.2 eqv.) and K_2CO_3 (78.5 mmol, 1.5 eqv.) in refluxing CH_3CN (230 ml) for 10 hours. The reaction was subsequently was filtered over silica in a sintered funnel to remove K_2CO_3 salts and the silica was washed with several portion of EtOAc/cyclohexane 50:50. The organic phases were concentrated under reduced pressure and the ephedrine auxiliary (**9** or **62**) finally recrystalized from Et_2O and Petrolum.

General procedure for *O*-dodecylated ephedrine auxiliary synthesis.[7] To a solution of *(1S,2R)* or *(1R,2S)* 2-(*N*-benzyl-*N*-mesitylene-sulfonyl)amino-1-phenyl-1-propanol (19.5 mmol, 1.0 eqv.) and pyridine (25.4 mmol, 1.3 eqv.) in dry CH_2Cl_2 (80 ml) was added dropwise dodecanoyl chloride (19.5 mmol, 1.0 eqv.) at 0°C. The reaction was stirred at rt until completion (15-30 hours) and diluted with diethylether. The mixture was washed successively with water, 1N HCl, water, saturated $NaHCO_3$ solution and brine. The organic extracts were dried over anhydrous $MgSO_4$, concentrated under reduced pressure and purified by flash chromatography (accordingly to each case) leading to the corresponding *O*-dodecylated ephedrine auxiliary (**10** or **63**)**.**

General procedure for *anti*-selective aldol reaction. Protocol modified from the literature.[7-10] An oven dried Schlenk-vessel under argon pressure was charged with (*1S,2R*) or (*1R,2S*) *O*-dodecylated ephedrine auxiliary **10** or **63** (17.4 mmol, 1.2 eqv.) and dry CH_2Cl_2 (56 ml). The reaction was cooled to -78 ^{o}C with acetone/dry ice, and Et_3N (43.5 mmol, 2.5 eqv.) was subsequently added followed by a dropwise addition (over 20 min) of freshly prepared c-Hex_2BOTf (1 M in hexane, 38.3 mmol, 2.2 eqv.). The resulting mixture was stirred at -78 ^{o}C for 2 hours and the aldehyde (16.5 mmol, 1.0 eqv.) was subsequently added dropwise (over 10 min) as a solution in dry CH_2Cl_2 (14 ml). The resulting mixture was stirred at -78 ^{o}C for 1 hour followed by 1 hour at 0 ^{o}C and 1 hour at rt. The reaction was quenched at 0°C by slow addition of methanol (80 ml), 50% H_2O_2 (1.2 eqv. compared to boron triflate) and 1M phosphate buffer pH

7.0 (58 ml). CAUTION: hydrogen peroxide generates a strong gas formation. The mixture was stirred vigorously at rt overnight, and concentrated under reduced pressure. The residue was diluted with CH_2Cl_2 (200 ml) and H_2O (100 ml) and the organic layer was extracted with H_2O (2x100 ml) followed by brine (100 ml) and finally dried over anhydrous $MgSO_4$. After evaporation to dryness, the residue was co-evaporated with several portions of mesitylene (at 40°C, under 1 mbar) to remove the cyclohexanol formed during the reaction. The residue was then purified by flash column chromatography (5 -25 % ETOAc/cyclohexane) leading to the corresponding *trans* β-hydroxyester.

General procedure for *cis*-selective aldol reaction. [7] An oven-dried 100 ml round bottom flask, was charged with (*1S,2R*) or (*1R,2S*) *O*-dodecylated ephedrine auxiliary **10** or **63** (1.0 eqv.) and dry CH_2Cl_2 (0.3M) under argon. The reaction was cooled to -78°C with acetone/dry ice, and freshly distilled DIPEA (2.5 eqv.) was subsequently added followed by a dropwise addition (over 20 min) of *n*-Bu_2BOTf (1M in DCM, 2.2 eqv.). The resulting mixture was stirred at -78°C for 2 hours and the aldehyde (1.2 eqv.) was subsequently added dropwise (over 10 min) as a solution in dry CH_2Cl_2 (0.9M). The reaction was subsequently stirred at -78°C for 1hour followed by 1 hour at 0°C and 1 hour at rt. The reaction was quenched at 0°C by slow addition of methanol (80 ml), 50% H_2O_2 (1.2 eqv. compared to boron triflate) and 1M phosphate buffer pH 7.0 (58 ml). CAUTION: hydrogen peroxide generates a strong gas formation. The mixture was stirred vigorously at rt overnight, and concentrated under reduced pressure. The residue was diluted with CH_2Cl_2 (200 ml) and H_2O (100 ml) and the organic layer was extracted with H_2O (2x100 ml) followed by brine (100 ml) and finally dried over anhydrous $MgSO_4$. After evaporation to dryness, the residue was co-evaporated with several portions of mesitylene (at 40°C, under 1 mbar) to remove the cyclohexanol formed during the reaction. The residue was then purified by flash column chromatography accordingly to each case leading to the corresponding *cis* β-hydroxyester.

O-dodecylated ephedrine auxiliary removal

General procedure for hydrogenolysis. In a round bottom flask was added the β-hydroxyester (1.8 mmol, 1.0 eqv.) together with $Pd(OH)_2$ on carbon (1.8 g) under argon. Subsequently, dry MeOH (30 ml) was added and the reaction mixture was flushed under H_2. The resulting mixture was stirred at 40°C until completion, monitored by TLC (eluent: 10% MeOH/DCM). The reaction was then filtered over Celite in a sintered funnel to remove the palladium and the celite was washed with sereval portions of methanol. After concentration under reduced pressure, the

obtained residue was subsequently purified by flash chromatography accordingly to each case leading to the corresponding β-hydroxyacid.

General procedure for saponification. In a round bottom flask was added the β-hydroxyester (3.85 mmol, 1 eqv.) and $LiOH.H_2O$ (5-9 eqv.) in dioxane/ H_2O (4/1) The resulting mixture was stirred at 40°C-45°C until completion. After completion, glacial acetic acid (5-9 eqv.) was added at 0°C to the reaction mixture which was stirred for 30 min at 0°C and subsequently concentrated under reduced pressure. Purification of the residue flash chromatography (accordingly to each case) finally lead to the corresponding β-hydroxyacids.

β-Lactonization

General procedure for β-lactonization.[11,12] A 100 ml round bottom flask, was charged with β-hydroxyacid (7.07 mmol, 1.0 eqv.) and anhydrous pyridine (100 ml) under argon. The reaction was cooled to 0°C benzenesulfonyl chloride (14.15 mmol, 2.0 eqv.) was added dropwise to the reaction as a solution in dry pyridine (10 ml). The reaction mixture was subsequently stirred at 0 °C for 3 hours and then stored without stirring at 0°C for 24 hours. The mixture was diluted with DCM (250 ml) and the organic layer was extracted with saturated Na_2CO_3 (100 ml), water (100 ml), brine (100 ml) and was finally dried over anhydrous $MgSO_4$. After evaporation to dryness, the residue was purified by flash chromatography accordingly to each case leading to the corresponding β-lactone.

2.1.3 Keto amide synthesis

Generale procedure for azide formation.[13,14] To a ice-cold solution of alcohol (1.12 mmol, 1.0 eqv.) and PPh_3 (2.25 mmol, 2.0 eqv.) in dry DMF (6.5 ml) was added N-bromosuccinimide (2.25 mmol, 2.0 eqv.). The mixture was heated for 2 hours at 55°C under argon. The avancement of the reaction was monitorated by TLC (eluent MeOH/DCM 2/8) showing the formation of a less polar compound. After completion, MeOH (0.5 ml) was added at 0°C to the mixture (to decompose the excess of NBS) followed by NaN_3 (7.84 mmol, 7.1 eqv.). The mixture was heated under argon for 5 hours at 80°C under vigorous stirring. The reaction was concentrated under reduced pressure and the DMF removed by coevaporation with several portions of n-Butanol. The residue was dissolved in $CHCl_3$/water and the layers separated. The aqueous phase was basified using 2M NaOH and extracted with $CHCl_3$ (3*50 ml). The combined organic layers were dried over anhydrous $MgSO_4$, concentrated under reduced pressure and purified by flash

chromatography (eluent: gradient 1-10% MeOH/DCM) leading to the corresponding azide substate.

Generale procedure for reduction azide into amine.[15] In a round bottom flask was added the azido derivative (0.46 mmol, 1.0 eqv.) together with 10 mol% Pd on carbon under argon. Subsequently, dry MeOH (20 ml) was added and the reaction mixture was flushed under H_2. The resulting mixture was stirred at rt until completion (TLC system 10%MeOH/DCM), typically 21 hours. The reaction was then filtered over Celite in a sintered funnel to remove the palladium and the celite was washed with sereval portions of methanol. After concentration under reduced pressure, the corresponding amine was obtained and used directly in the next step.

Generale procedure for amide formation.

Method A.[16] In a round bottom flask was added α-keto acid (1.4 mmol, 1.2 eqv.), amine (1.2 mmol, 1.0 eqv.) and EDC.HCl (3.5 mmol, 3.0 eqv.) in dry DCM (20 ml). The reaction mixture was subsequently stirred at rt for 16-24 hours. The mixture was then poured into DCM (50 ml) and the organic layer was washed with 1M NaOH followed by brine and finally dried over anhydrous $MgSO_4$. After concentrated under reduced pressure, the residue was purified by flash chromatography (eluent: 1-5% MeOH/DCM) leading to the corresponding α-ketoamide.

Method B.[17] To α- keto acid (0.26 mmol, 1.2 eqv.) in dry THF (1 ml) was added dropwise at -10°C, N-Methylmorpholine (0.21 mmol, 1.0 eqv.) followed by isobutylchloroformate (0.21 mmol, 1.0 eqv.). The reaction mixture was stirred for 10 min at -10°C and the amine (0.21 mmol, 1.0 eqv.) was added to the reaction mixture as a solution in dry THF (1ml). The reaction mixture was subsequently stirred for 1 hour at -10°C followed by 16 hours at rt. After concentration under reduced pressure, the residue was dissolved in EtOAc and was washed with brine. After drying over anhydrous $MgSO_4$, the organic layer was concentrated under reduced pressure and purified by flash chromatography (eluent: 1-5% MeOH/DCM) leading to the α-ketoamide.

2.1.4 Trifluoromethy ketone and pentafluoroethyl ketone synthesis.

Generale procedure for ester saponification. To a solution of ethy ester (0.38 mmol, 1.0 eqv.) in EtOH (0.5 ml) was added 2M NaOH (0.38 mmol, 1.0 eqv.) to the reaction mixture which was stirred at rt for 2 hours. The reaction was monitorated by TLC using MeOH/DCM 2/8. After completion, the reaction mixture was extracted with Et_2O and the organic layer discarded.The aqueous layer was acidified to approx. pH 3.0 using concentrated HCl and was lyophilised leading to the carboxylic acid which was used directly in the next step (contain some NaCl salts).

Generale procedure for α-keto-CF_3 or α-keto-CF_2CF_3 formation.[18] Carboxylic acid (0.38 mmol, 1.0 eqv.) was resuspended in dry THF (0.9 ml) at -20°C. In parallele, a LDA solution was prepared *in-situ* by dropwise addition of n-Buli (2.5 M in hexane, 1.29 mmol, 3.4 eqv.) at -78°C to a solution of freshly distilled diisopropylamine (1.33 mmol, 3.5 eqv.) in dry THF (0.7 ml). The prepared LDA solution was subsequently added dropwise over 10 min to the previous reaction which was subsequently stirred at rt for 4 hours. In a separate flask, the enediolate solution was added dropwise at -78°C to a solution of CF_3CO_2Et or $CF_3CF_2CO_2Et$ (1.14 mmol, 3.0 eqv.) in dry THF (0.4 ml). After complete addition, the mixture was aged for 15 min at -78°C and was quenched with 6N HCl (0.7 ml). The reaction mixture was subsequently diluted with EtOAc, the layers were separated and the organic phase was dried over anhydrous $MgSO_4$. After concentration under reduced pressure, the residue was purified by flash chromatography (gradient 1-8 % MeOH/DCM) leading to the keto-CF_3 or keto-CF_2CF_3 derivative respectively.

2.1.5 Keto- oxazole synthesis

General procedure for *C5*-substituted oxazole formation.[19-21] To a solution of methyl isocyanide (5.8 mmol, 1.34 eqv.) in anhydous THF (13.5 ml) was added dropwise at -78°C nBuLi (2.5M in hexane, 6.5 mmol, 1.5 eqv.) to the reaction mixture which was then stirred at -78°C for 2 hours. A solution of ethyl ester (4.3 mmol, 1.0 eqv.) in dry THF (3 ml) was added dropwise (over 30 min) to the reaction mixture which was then stirred for 3 hours at -78°C followed by 3 hours at rt. The mixture was quenched with brine (100ml) and extracted with Et_2O (3* 100 ml). The combined organic extracts were subsequently dried over anhydrous $MgSO_4$, concentrated under reduced pressure and purified by flash chromatography (gradient 1-4 % MeOH/DCM using NEt_3 pre-treated column) leading to the corresponding C5-substituted oxazole.

General procedure for Weinreb amide synthesis.[22,23] To a solution of *N,O*-dimethylhydroxyl amine hydrochloride (3.9 g, 39 mmol, 1.1 eqv.) and pyridine (82 mmol, 2.2 eqv.) in dry CH_2Cl_2 (55 ml), was added dropwise the acid chloride (36.5 mmol, 1.0 eqv.) at 0°C over 15 min. The mixture was allowed to warm to rt and was stirred for 5 hours at rt. The mixture was then diluted with EtOAc (200 ml), washed with 1N HCl (100 ml*2), saturated aqueous $NaHCO_3$ (50 ml*2) and brine (50 ml). The organic layer was dried over anhydrous $MgSO_4$ and concentrated under reduced pressure leading to the corresponding Weinreb amide which was used directly in the next step.

General procedure for oxazole *C2*-functionalization.[23,24]To a 100 ml round bottom flask equipped with a stirring bar, argon inlet, was added C5-substituted oxazole (8.7 mmol, 1 eqv.) as a solution in freshly distilled THF (20ml). *I*-PrMgCl (2 M in THF, 11.3 mmol, 1.4 eqv.) was added over 10 min to the mixture previously cooled to -15°C which was then stirred for 2 hours between -15°C to -20°C. A solution of Weinreb amide (8.65 mmol, 1.0 eqv.) as a solution in distilled THF (15ml) was added dropwise to the reaction mixture at such a rate that the temperature was kept between -20°C and -25°C (addition over 25 min). The reaction was stirred at -20°C for 10 min and at rt for 25 hours. The mixture was quenched with water (25ml) and extracted with EtOAc (4*150 ml) and brine (100 ml). Saturated NH_4Cl solution was added to the aqueous layer which was extracted with EtOAc. The combined organics layers were dried over anhydrous $MgSO_4$, concentrated under reduced pressure and purified by flash chromatography (eluent: gradient 1-2% MeOH/DCM) leading to the C2-functionalized oxazoles.

2.1.6 Library diversification

General procedure for oxidation into sulfone.[25] To a solution of thioether derivative (5.05 mmol, 1.0 eqv.) in MeOH (130 ml) was added at 0°C oxone® (15.13 mmol, 3 eqv.) as a suspension in water (80 ml). The reaction mixture was stirred at rt for 8-24 hours before being quenched with saturated $Na_2S_2O_3$ solution and diluted with EtOAc (100 ml). The two layers were separated and the aqueous layer was basified to approx. pH 12.0 using saturated $NaHCO_3$. After extraction of the aqueous layer with several portions of EtOAc, the combined organic layers were dried over $MgSO_4$, filtered and concentrated under reduced pressure leading to the corresponding sulfone which was used directly in the next step.

General procedure for amine quaternization.[26] To a solution of oxazole (0.074 mmol, 1.0 eqv.) in CH_3CN (0.8 ml) was added dropwise at 0°C methyl iodide (0.085 mmol, 1.16 eqv.) as a solution in CH_3CN (0.3 ml). The reaction mixture was stirred at rt for 5 hours and the quaternized ammonium salt was finally precipatated with Et_2O, filtered and washed with Et_2O.

2.2 Synthesis of the fluorescent Substrate DiFMUO (3)

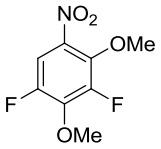

3,5-Difluoro-2,4-dimethoxynitrobenzene (**5**).[27] To a solution of 2,3,4,5-tetrafluoronitrobenzene **4** (5 g, 25.4 mmol, 1.0 eqv.) in 70 ml MeOH under argon at 4°C, was added a freshly prepared sodium methoxide solution (27.6% wt in MeOH, 61.0 mmol, 2.4 eqv.) obtained by refluxing for 4 hours Sodium (1.41 g) into MeOH (12 ml). The yellow mixture was stirred at rt for 18 hours and was monitored by TLC (EtOAc/cyclohexane 1/6). The reaction was quenched with 1M citric acid (2.53 mmol, 0.1 eqv.) and the reaction was concentrated under reduced pressure. The residue was taken up in Et_2O, washed with 1M citric acid (2x100 ml), brine (100 ml), dried over anhydrous $MgSO_4$, concentrated under reduced pressure and purified by flash chromatography (EtOAc/cyclohexane 1/40) leading to 3,5-difluoro-2,4-dimethoxynitrobenzene **5** as a pale yellow solid in a quantitative yield. R_f = 0.53 (EtOAc /cyclohexane 1/6). mp = 32.2 - 32.6°C. IR: 1532cm^{-1} (N-O stretch), 1361 cm^{-1} (N-O stretch). **^{1}H NMR** (400 MHz, $CDCl_3$): δ 7.50 (dd, *J* = 2.3, 11.0, 1H, Haro), 4.12 (t, *J* = 2.0, 3H, OC*H*$_3$), 4.01 (d, *J* = 1.1, 3H, OC*H*$_3$). **^{19}F NMR** (377 MHz, $CDCl_3$): δ 142.2 (d, *J* = 6.5, 1F), 132.3 – 132.4 (m, 1F). **^{13}C NMR** (100 MHz, $CDCl_3$): δ 149.4 (dd, *J* = 6.3, 249.6, *C*F), 246.2 (dd, *J* = 5.3, 246.2, *C*F), 142.0 (dd, *J* = 11.6, 13.7, *C*OMe), 140.9 (dd, *J* = 3.7, 13.6, *C*OMe), 136.6 (dd, *J* = 2.1, 7.3, *C*NO_2), 108.2 (dd, *J* = 3.3, 26.4, *C*H), 62.9 (dd, *J* = 1.0, 4.5, O*C*H_3), 61.8 (t, *J* = 4.2, O*C*H_3). HRMS (ESI) calc. for $C_8H_7F_2NO_4$ $[M+H]^+$ 220.0416, found 220.0417. GCMS found 219 for $[M]^{+\cdot}$.

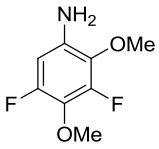

1-Amino-3,5-difluoro-2,4-dimethoxybenzene (**6**).[27] To an autoclave flask was added a large egg-shaped stirring bar followed by a solution of 3,5-difluoro-2,4-dimethoxynitrobenzene **5** (5.46 g, 24.9 mmol, 1.0 eqv.) in EtOAc/EtOH 1/1 (14 ml) and catalytic 10 mol% Pd on carbon (0.55g). The hydrogenation was performed at 10 bar, at rt for 18 hours with progress monitored by TLC (EtOAc/Cyclohexane 1/9). After completion of the reaction, the catalyst was collected on Celite over a glass frit via filtration. The filtrate was concentrated under reduced pressure, leading to 1-amino-3,5-difluoro-2,4-dimethoxybenzene **6** in a quantitative yield as a pale brown oil. R_f = 0.18 (EtOAc/cyclohexane 1/9). IR: 3550-3270 cm^{-1} (amino group). **^{1}H NMR** (400 MHz, $CDCl_3$): δ 6.24 (dd, *J* = 2.3, 12.0, 1H, Haro), 3.85 (t, *J* = 2.0, 3H, OC*H*$_3$), 3.84 (d, *J* = 1.0, 3H, OC*H*$_3$), 3.79 (brs, 2H, N*H*$_2$). **^{19}F NMR** (377 MHz, $CDCl_3$): δ 135.7 (dd, *J* = 4.6, 12.0, 1F), 147.2 (s, 1F). **^{13}C NMR** (100 MHz, $CDCl_3$): δ 152.1 (dd, *J* = 6.6, 239.5,*C*F), 150.1 (dd, *J* = 7.9, 243.7, *C*F), 135.8 (dd, *J* = 5.5, 11.9, *C*OMe), 131.7 (dd, *J* = 3.5, 12.1, *C*NH_2), 128.5 (dd, *J* = 13.4, 15.9, *C*OMe), 97.5 (dd, *J* = 2.8, 23.4, *C*H), 62.3 (t, *J* = 2.6, O*C*H_3), 60.9 (dd, *J* = 1.1, 4.7, O*C*H_3). HRMS (ESI) calc. for $C_8H_9F_2NO_2$ $[M+H]^+$ 190.0674, found 190.0670. GCMS found 189 for $[M]^{+\cdot}$.

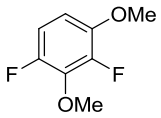

1,3-Dimethoxy-2,4-difluorobenzene (**7**).[27] To a 250 ml round bottom flask was added a large egg-shaped stirring bar followed by a solution of 1-amino-3,5-difluoro-2,4-dimethoxybenzene **6** (4.25 g, 22.47 mmol, 1.0 eqv.) in 75 ml of conc. HCl/ H_2O (1/2). The mixture was cooled to 0°C and treated with a cold 6 M aqueous sodium nitrite $NaNO_2$ solution (4 ml, 23.65 mmol, 1.05 eqv.). The mixture was stirred for 15 min at 0°C and H_3PO_2 (50% wt in water, 50 ml, 449.35 mmol, 20.3 eqv.) was added over 5 min. The resulting mixture was kept at 4°C for 21 hours under argon followed by 2 hours at 20°C. The mixture was diluted with water and extracted with Et_2O (3x150 ml). After concentration under reduced pressure, the residue was dissolved into Et_2O, washed with water (1x150 ml), brine (1x150ml) and dried over anhydrous $MgSO_4$. After filtration and evaporation to dryness, the residue was purified by flash column chromatography (cyclohexane/EtOAc 95/5) leading to 1,3-dimethoxy-2,4-difluoro benzene **7** as a colorless oil. Yield = 84%. R_f = 0.44 (EtOAc/cyclohexane 5/95). **^{1}H NMR** (400 MHz, $CDCl_3$): δ 6.78 (ddd, *J* = 4.0, 9.3, 10.5, 1H, Haro), 6.57 (ddd, *J* = 4.4, 9.0, 9.0, 1H, Haro), 3.99 (t, *J* = 1.2, 3H, OC*H*$_3$), 3.84 (s, 3H,

OC*H*$_3$). **^{19}F NMR** (377 MHz, $CDCl_3$): δ 138.9 -139.0 (m, 1F), 150.3 (d, *J* = 8.4, 1F). **^{13}C NMR** (100 MHz, $CDCl_3$): δ 150.0 (dd, *J* = 3.6, 239.2*, C*F), 146.0 (dd, *J* = 5.4, 251.3*, C*F), 145.1 (dd, *J* = 2.9, 9.3*,C*OMe), 137.3 (dd, *J* = 12.0, 26.6*,C*OMe), 109.9 (dd, *J* = 4.2, 20.3, *C*H), 106.2 (dd, *J* = 2.0, 8.5*,C*H), 61.7 (t, *J* = 3.4, O*C*H$_3$), 56.7 (s, O*C*H$_3$). HRMS (EI) calc. for $C_8H_8F_2O_2$ [$M^{+\cdot}$] 174.0487, found 174.0489. GCMS found 174 for [$M^{+\cdot}$].

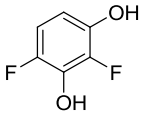

2,4-Difluororesorcinol (**8**).[27] A solution of 1,3-dimethoxy-2,4-difluorobenzene **7** (3.14 g, 18.05 mmol, 1.0 eqv.) in anhydrous CH_2Cl_2 (60 ml) at 20°C under argon was treated with BBr_3 (1M in CH_2Cl_2, 54 ml, 54 mmol, 3.0 eqv.) via syringe over 5 min. The reaction was monitored by TLC, EtOAc/cyclohexane 1/3, showing a complete conversion after 28 hours. The reaction was carefully quenched with water and the mixture subsequently stirred until all precipitate dissolved. The suspension was extracted with Et_2O and the organic layer was washed with brine (1x100 ml), dried over anhydrous $MgSO_4$, concentrated under reduced pressure and purified by flash column chromatography (EtOAc/cyclohexane 30/70) to afford 2,4-difluororesorcinol **8** as a colorless crystalline solid. Yield = 92%. R_f = 0.14 (EtOAc /cyclohexane 25/75). mp = 101.6-102.3°C. **^{1}H NMR** (400 MHz, DMSO): δ 10.08 - 9.79 (brs, 1H, O*H*), 9.69 - 9.42 (brs, 1H, O*H*), 6.76 (ddd, *J* = 2.3, 9.2, 10.7, 1H, Haro), 6.34 (ddd, *J* = 5.0, 9.2, 9.2, 1H, Haro). **^{19}F NMR** (377 MHz, DMSO): δ 144.8 -144.9 (m, 1F), 155.0 -155.1 (m, 1F). **^{13}C NMR** (100 MHz, DMSO): δ 145.5 (dd, *J* = 4.1, 230.1*, C*F), 142.1 (dd, *J* = 2.2, 10.2*, C*OH), 141.8 (dd, *J* = 6.0, 236.1*, C*F), 134.4 (dd, *J* = 13.5, 17.0*, C*OH), 109.7 (dd, *J* = 3.7, 19.2, *C*H), 105.6 (dd, *J* = 1.7, 7.8, *C*H). HRMS (EI) calc. for $C_6H_4F_2O_2$ [$M^{+\cdot}$] 146.0174, found 146.0178. GCMS found 146 for [$M^{+\cdot}$]

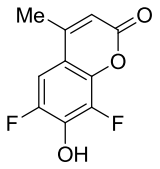

6,8-Difluoro-7-hydroxy-4-methyl-*2H*-chromen-2-one (**2**).[28] In a 10 ml round-bottom flask, equipped with a stirring bar and a septum, was added concentrated sulfuric acid (2.59 g, 24.8 mmol, 18.1 eqv.) followed by a dropwise addition of a solution of 2,4-difluororesorcinol **8** (200.9 mg, 1.37 mmol, 1.0 eqv.) in freshly distillated ethyl acetoacetate (179.5mg, 1.38 mmol, 1.0 eqv.). The temperature of the reaction was keept below -10°C during the addition. After 20 min at -

10°C, the reaction mixture was allowed to warm at rt for 20 hours, and the advancement of the reaction was monitorated by TLC using as eluent EtOAc/cyclohexane 2/5. After completion, the reaction mixture was diluted with water and extracted with several portions of EtOAc. The combined organic layers were dried over anhydrous $MgSO_4$ and concentrated under reduced pressure leading to a low mass recovery (25 mg crude). Subsequenty the aqueous layer was extracted with various solvent such as DCM, benzene and 1-fluorobenzene to improve the compound recovery. Finaly, compound **2** was obtained in 10% yield. Identical characterization as when the reaction was performed in methane sulfonic acid.

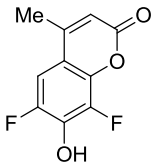

6,8-Difluoro-7-hydroxy-4-methyl-*2H*-chromen-2-one (**2**).[29,30] In a 250 ml round-bottom flask, equipped with a stirring bar and a septum was placed 2,4-difluororesorcinol **8** (2.04 g, 13.97 mmol, 1.0 eqv.) and freshly distilled ethyl acetoacetate (1.83 g, 14.06 mmol, 1.0 eqv.). $MeSO_3H$ (23 ml, 351 mmol, 25.1 eqv.) was added dropwise to the reaction mixture keeping the temperature at 0°C. The mixture was stirred 20 min at 0°C and at rt for 28 hours (reaction monitored by TLC, eluent EtOAc/cyclohexane 2/5). The mixture was cooled to 0°C and was quenched with water (25 ml). The precipitate formed was collected on a filter and washed with cold water (3x20ml).The crude product was dissolved with 1M sodium hydroxide (60 ml) and the resulting solution was filtered. The coumarin was reprecipitated from the filtrate by slow additon of H_2SO_4 until approx. pH 1.0. After filtration, the solid was washed with 3 portions of cold water (20 ml) and subsequently dried under reduced pressure leading to coumarine **2** as a white solid. Yield = 84%. R_f = 0.17 (EtOAc/cyclohexane 1/1). mp = 154 -155°C (conform with literature). IR: 1682 cm^{-1} (ester group). **^{1}H NMR** (400 MHz, DMSO): δ 11.45 (brs, 1H, O*H*), 7.47 (dd, *J* = 2.0, 11.4, 1H, *H*-C=CF), 6.30 (s, 1H, -C*H*CO), 2.36 (d, *J* = 1.0, 3H, -CH_3). **^{19}F NMR** (377 MHz, DMSO): δ 136.6 (t, *J* = 9.9, 1F), 154.3 (d, *J* = 8.3, 1F). **^{13}C NMR** (100 MHz, DMSO): δ 158.6 (s, CO), 152.9 (t, *J* = 2.6, -*C*Me), 148.3 (dd, *J* = 5.2, 237.7, *C*F), 139.2 (dd, *J* = 2.0, 9.4, -*C*(OCOR)), 139.2 (dd, *J* = 6.6, 242.4*, C*F), 137.4 (dd, *J* = 12.8, 17.9*, C*OH), 112.2 (s*, C*H), 110.7 (d, *J* = 9.0, C_{IV}), 106.1 (dd, *J* = 3.2, 21.3*, C*H), 18.1 (s, *C*H_3). HRMS (ESI) calc. for $C_{10}H_6F_2O_3$ $[M+H]^+$ 213.0358, found 213.0357. GCMS found 212 for $[M^{+\cdot}]$.

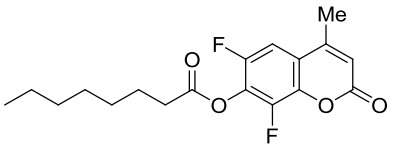

6,8-Difluoro-4-methyl-2-oxo-*2H*-chromen-7-yl octanoate (**3**).[31] To a suspension of 6,8-difluoro-7-hydroxy-4-methyl-2H-chromen-2-one **2** (52.1 mg, 0.245 mmol, 1.0 eqv.) in CH_2Cl_2 (4 ml) was added NEt_3 (38.4 mg, 0.375 mmol, 1.5 eqv.). Subsequnetly, octanoyl chloride (44 mg, 0.268 mmol,1.1 eqv.) was added to the reaction mixture which was stirred for 8 hours at rt (reaction monitored by TLC EtOAc/cyclohexane 1/1). The reaction was quenched with water (25 ml) and extracted with CH_2Cl_2 (4x15 ml). The combined organic extracts were dried over anhydrous $MgSO_4$, filtered, concentrated under reduced pressure and the residue purified by flash column chromatography (EtOAc/cyclohexane 1/5) leading to DiFMUO subtrate (**3**) as a white solid. Yield = 95%. R_f = 0.78 (EtOAc/cyclohexane 1/1). mp = 86.2 - 86.6°C. IR: 1777 cm^{-1}, 1745 cm^{-1}, 1724cm^{-1} (ester groups). **^{1}H NMR** (400 MHz, $CDCl_3$): δ 7.18 (dd, *J* = 2.3, 9.7, 1H, *H*-C=CF), 6.36 (d, *J* = 1.2, 1H, -C*H*CO coumarine), 2.68 (t, *J* = 7.4, 2H, -C*H*$_2$COOR), 2.41 (d, *J* = 1.3, 3H, -C*H*$_3$ coumarine), 1.83 – 1.75 (m, 2H), 1.57 - 1.28 (m, 8H), 0.90 (t, *J* = 6.9, 3H, -C*H*$_3$). **^{19}F NMR** (377 MHz, $CDCl_3$): δ 130.1 (d, *J* = 9.4, 1F), 142.9 (s, 1F). **^{13}C NMR** (100 MHz, $CDCl_3$): δ 169.7 (s, CO lipid tail), 158.4 (s, CO coumarine), 151.0 (t, *J* = 2.6, -*C*Me), 150.9 (dd, *J* = 2.9, 246.6, *C*F), 142.9 (dd, *J* = 4.8, 255.0, *C*F), 139.2 (dd, *J* = 3.1, 9.8, -*C*(OCOR)), 130.0 (dd, *J* = 13.1, 17.8, -*C*(OCOR)), 118.1 (dd, *J* = 1.4, 8.5, C_{IV}), 116.2 (s, *C*H), 105.5 (dd, *J* = 4.0, 21.5, *C*H), 33.4 (s), 31.5 (s), 28.8 (s), 28.7 (s), 24.7 (s), 22.5 (s), 18.7 (s, *C*H_3 coumarine), 13.9 (s, *C*H_3 terminal). HRMS (ESI) calc. for $C_{18}H_{20}F_2O_4$ $[M+H]^+$ 339.1402, found 339.1403. GCMS found 338 for $[M^{+\cdot}]$.

2.3 Synthesis of palmostatin B (14)

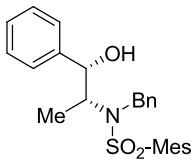

***N*-benzyl-*N*-((*1S,2R*)-1-hydroxy-1-phenylpropan-2-yl)-2,4,6-trimethylbenzenesulfonamide** (**9**). Compound **9** was synthesized following the general procedure for ephedrine auxiliary synthesis using 52.9 mmol of (*1S,2R*)-Norephedrine. The mesylated intermediate was obtained in 96% yield as a white solid. R_f =0.61 (EtOAc/cyclohexane 1/1). **^{1}H NMR** (400 MHz, $CDCl_3$): δ 7.34 - 7.20 (m, 5H, Haro), 6.93 (s, 2H, Haro), 4.96 (d, *J* = 8.8, 1H, -C*H*(OH)), 4.74 (d, J = 2.8, 1H, -N*H*), 3.54-

3.40 (m, 1H, -C*H*NHR), 2.63 (s, 6H, 2*-C$H_{3,\,Mes}$), 2.27 (s, 3H, -C$H_{3,\,Mes}$), 0.83 (d, *J* = 6.8, 3H, -CH_3). **^{13}C NMR** (100 MHz, $CDCl_3$): δ 142.2, 140.3, 138.9 (2C), 134.2, 131.9 (2C), 128.3 (2C), 127.6, 125.9 (2C), 75.6, 54.5, 22.9 (2C), 20.9, 14.6. (NMR analysis consistent with the literature[8]). Alcohol **9** was obtained in 82% as a white solid. R_f =0.46 (EtOAc/cyclohexane 2/8). mp= 122-123°C. **^{1}H NMR** (400 MHz, $CDCl_3$): δ 7.36 - 7.15 (m, 8H, Haro), 7.09 – 7.04 (m, 2H, Haro), 6.91 (s, 2H, Haro), 4.97 (brs, 1H,- C*H*(OH)), 4.77 (d, *J* = 16, 1H, -CH_2Bn), 4.54 (d, *J* = 16, 1H, -CH_2Bn), 3.82 (dq, *J* = 1.6, 7.0, 1H, -C*H*NSO_2Mes(Bn)), 2.63 (s, 6H, 2*-C$H_{3,\,Mes}$), 2.28 (s, 3H, -C$H_{3,\,Mes}$), 1.03 (d, *J* = 6.8, 3H, -CH_3). **^{13}C NMR** (100 MHz, $CDCl_3$): δ 142.6, 142.1, 140.1 (2C), 138.6, 133.4, 132.1 (2C), 128.5 (2C), 128.1 (2C), 127.7 (2C), 127.3, 127.2, 125.5 (2C), 76.5, 59.6, 49.0, 22.9 (2C), 20.8, 9.9. (NMR analysis consistent with the literature[8]).

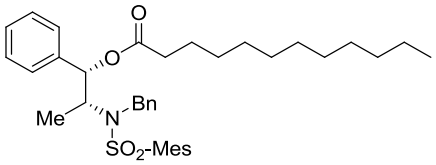

(*1S,2R*)-2-(*N*-benzyl-*N*-mesitylenesulfonyl)amino-1-phenyl-1-propyldodecanoate (**10**). Compound **10** was synthesized following the general procedure for *O*-dodecylated ephedrine auxiliary synthesis using 19.5 mmol of dodecanoyl chloride. Reaction time 30 hours at rt. Purification by flash chromatography (eluent 10-15% EtOAc/cyclohexane) lead to compound **10** (m= 10.5 g). Yield = 87% (white solid). R_f =0.61 (EtOAc/cyclohexane 2/8). $[\alpha]_D^{20}$ = - 20.5 (c = 0.2, $CHCl_3$). mp = 59.9 - 60.2°C (recrystallisation from EtOAc/hexane). IR: 1734 cm^{-1} (ester, C=O stretch). **^{1}H NMR** (400 MHz, $CDCl_3$): δ 7.36 - 7.15 (m, 8H, Haro), 6.92 - 6.84 (m, 4H, Haro), 5.82 (d, *J* = 4.0, 1H, -C*H*OCOR), 4.73 (d, *J* = 16. 4, 1H, -C*H*Ph), 4.58 (d, *J* = 16. 8, 1H, -C*H*Ph), 4.08 - 3.99 (m, 1H, C*H*N(Bn)Mes), 2.51 (s, 6H, CH_3 (Mes)), 2.27 (s, 3H, CH_3 (Mes)), 2.21 - 2.01 (m, 2H), 1.52 - 1.42 (m, 2H), 1.35 - 1.14 (m, 16H), 1.11 (d, *J* = 6.8, 3H, -CH_3), 0.87 (t, *J* = 6.8, 3H, -CH_3). **^{13}C NMR** (100 MHz, $CDCl_3$): δ 172.0, 142.5, 140.2, 138.7, 138.5 133.3, 132.1, 128.4, 128.3, 127.7, 127.3, 127.0, 125.9, 77.9, 56.6, 48.1, 34.2, 31.9, 29.6, 29.4, 29.3, 29.2, 29.0, 24.6, 22.9, 22.7, 20.9, 14.1, 12.8. HRMS (ESI) calc. for $C_{37}H_{51}NO_4S$ $[M+H]^+$ 606.3612, $[M+Na]^+$ 628.3431, found $[M+H]^+$ 606.3607, $[M+Na]^+$ 628.3424. LCMS (ESI) found 605.82 for $[M+H]^+$, found 622.93 for $[M+NH_4]^+$, found 628.20 for $[M+Na]^+$, found 1227.98 for $[2M+NH_4]^+$.

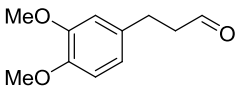

3-(3,4-Dimethoxyphenyl)propanal (**11**). Compound **11** was synthesized following the general procedure for Swern oxidation using 17.2 mmol of 3-(3,4-dimethoxyphenyl)propan-1-ol. Yield = 94% (m= 3.28g, yellow oil). R_f = 0.61 (MeOH/CH_2Cl_2 1/9) or R_f = 0.21 (EtOAc/cyclohexane 2/8). IR: 1721 cm^{-1} (C=O). **^{1}H NMR** (400 MHz, $CDCl_3$): δ 9.82 (t, *J* = 1.6, 1H, -C*H*O), 6.82-6.70 (m, 3H, Haro), 3.87 (s, 3H, -OCH_3), 3.85 (s, 3H, -OCH_3), 2.91 (t, *J* = 7.4, 2H), 2.79 - 2.73 (m, 2H, -CH_2CHO). **^{13}C NMR** (100 MHz, $CDCl_3$): δ 201.5, 148.9, 147.4, 132.8, 120.0, 111.6, 111.3, 55.8, 55.7, 45.4, 27.6. HRMS (EI) calc. for $C_{11}H_{14}O_3$ [$M^{+\cdot}$] 194.0937, found 194.0933. GCMS found 194 for [$M^{+\cdot}$].

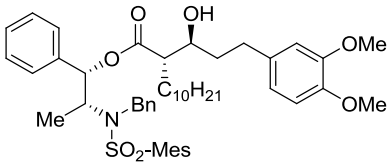

(*S*)-((*1S,2R*)-2-(N-benzyl-2,4,6-trimethylphenylsulfonamido)-1-phenylpropyl)2-((S)-3-(3,4-dimethoxyphenyl)-1-hydroxypropyl)dodecanoate (**12**). Compound **12** was synthesized following the general procedure for *anti*-selective aldol reaction using 17.42 mmol of *O*-dodecylated ephedrine auxiliary **10**. Purifiaction by flash chromatography (5-25 % EtOAc/cyclohexane) yield β-hydroxyester **12** (m = 2.6 g). Yield = 63 % (yellow oil). R_f =0.40 (EtOAc/cyclohexane 30/70). $[\alpha]_D^{20}$= - 26.1 (c = 2.0, $CHCl_3$). IR: 1736 cm^{-1} (ester, C=O stretch). **^{1}H NMR** (400 MHz, $CDCl_3$): 7.24 - 7.11 (m, 8H, Haro), 6.90 - 6.66 (m, 7H, Haro), 5.85 (d, *J* = 5.6, 1H, -C*H*OCOR), 4.69 (d, *J* = 16.4, 1H, -C*H*Ph), 4.46 (d, *J* = 16.4, 1H, -C*H*Ph), 4.23 - 4.13 (m, 1H, -C*H*N(Bn)Mes), 3.85 (s, 3H, -OCH_3), 3.84 (s, 3H, -OCH_3), 3.71 - 3.63 (m, 1H, -C*H*OH), 2.81 - 2.54 (m, 2H), 2.48 - 2.32 (m, 1H, -C*H*COOR), 2.41 (s, 6H, CH_3 (Mes)), 2.27 (s, 3H, CH_3 (Mes)), 1.81 - 1.45 (m, 4H), 1.35 - 0.92 (m, 19H), 0.88 (t, *J* = 6.8, 3H, -CH_3). **^{13}C NMR** (100 MHz, $CDCl_3$): δ 174.5, 148.9, 147.2, 142.4, 140.3 (2C), 138.1, 137.8, 134.4, 133.2, 132.0 (2C), 128.3 (2C), 128.2 (2C), 128.1, 127.9 (2C), 127.2, 126.6 (2C), 120.2, 111.8, 111.3, 78.2, 71.5, 56.4, 55.9, 55.8, 51.2, 48.1, 37.3, 31.9, 31.6, 29.7, 29.5, 29.5, 29.4, 29.3, 29.2, 27.0, 26.9, 22.8, 22.7, 20.8, 14.3, 14.1. HRMS (ESI) calc. for $C_{48}H_{65}NO_7S$ $[M+H]^+$ 800.4554, $[M+NH_4]^+$ 817.4820, $[M+Na]^+$ 822.43740, found $[M+H]^+$ 800.4559, $[M+NH_4]^+$ 817.48247, $[M+Na]^+$ 822.43728. LCMS (ESI) found 816.79 for $[M+NH_4]^+$.

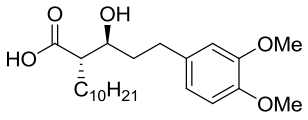

(*S*)-2-((*S*)-3-(3,4-dimethoxyphenyl)-1-hydroxypropyl)dodecanoic acid (**13**). Compound **13** was synthesized following the general procedure for hydrogenolysis using 10.41 mmol of β-hydroxyester **12** and approximately 12 g of $Pd(OH)_2$. After 30 hours reaction at 40°C, purification by flash chromatography using 1% MeOH/DCM to remove the unpolar impurities, then gradient 2-5% MeOH/DCM to collect β-hydroxyacid **13** (m= 2.97 g). Yield = 73% (colorless oil). R_f = 0.30 (EtOAc/cyclohexane 1/1). $[\alpha]_D^{20}$= - 10.4 (c = 0.13, $CHCl_3$). IR: 1705 cm^{-1} (acid, C=O stretch). **^{1}H NMR** (400 MHz, $CDCl_3$): δ 6.79 - 6.67 (m, 3H, Haro), 3.84 (s, 3H, -OC*H*$_3$), 3.83 (s, 3H, -OC*H*$_3$), 3.76 - 3.68 (m, 1H, -C*H*OH), 2.83 - 2.55 (m, 2H), 2.50 - 2.34 (m, 1H,-C*H*COOR), 1.90 - 1.50 (m, 4H), 1.41 - 1.16 (m, 16H), 0.86 (t, *J* = 6.8, 3H, -C*H*$_3$). **^{13}C NMR** (100 MHz, $CDCl_3$): δ 180.2, 148.8, 147.2, 134.2, 120.2, 111.8, 111.3, 71.4, 55.8, 55.7, 51.1, 37.1, 31.8, 31.5, 29.5 (2C), 29.4, 29.3 (2C), 29.2, 27.2, 22.6, 14.0. HRMS (ESI) calc. for $C_{23}H_{38}O_5$ $[M+H]^+$ 395.27920, found $[M+H]^+$ 395.27894. LCMS (ESI) found 411.87 for $[M+NH_4]^+$.

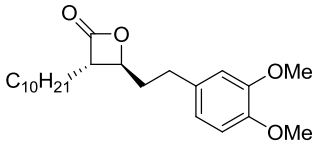

(*3S,4S*)-3-decyl-4-(3,4-dimethoxyphenethyl)oxetan-2-one (**Palmostatin B, 14**). Compound **14** was synthesized following the general procedure for β-lactonization using 7.07 mmol of β-hydroxyacid **13**. Purification by flash chromatography (gradient 2-5% EtOAc/toluene) lead to β-lactone **14** (m= 2.0 g). Yield=75% (white solid). R_f = 0.5 (EtOAc/cyclohexane 30/70). mp = 45.8-46°C (after recrystallisation from hexane). $[\alpha]_D^{20}$ = - 29.4 (c = 0.15, $CHCl_3$). IR: 1801 cm^{-1} (β-lactone, C=O stretch). **^{1}H NMR** (400 MHz, $CDCl_3$): δ 6.83 - 6.79 (m, 1H, Haro), 6.75 - 6.69 (m, 2H, Haro), 4.22 (ddd, *J* = 4.0, 5.3, 8.0, 1H, -C*H*OCOR), 3.87 (s, 3H, -OC*H*$_3$), 3.86 (s, 3H, -OC*H*$_3$), 3.19 (ddd, *J* = 4.0, 6.8, 8.5, 1H, -C*H*CO), 2.80 -2.60 (m, 2H), 2.19 - 1.99 (m, 2H), 1.84 - 1.61 (m, 2H), 1.46 - 1.20 (m, 16H), 0.88 (t, *J* = 7.0, 3H, -C*H*$_3$). **^{13}C NMR** (100 MHz, $CDCl_3$): δ 171.4, 149.0, 147.6, 132.7, 120.2, 111.6, 111.4, 77.1, 56.2, 55.9, 55.8, 36.4, 31.8, 30.9, 29.5, 29.4, 29.3, 29.3, 29.2, 27.8, 26.9, 22.7, 14.1. HRMS (ESI) calc. for $C_{23}H_{36}O_4$ $[M+H]^+$ 377.26864, $[M+NH_4]^+$ 394.29519, $[M+Na]^+$ 399.25058, found $[M+H]^+$ 377.26858, $[M+NH_4]^+$ 394.29495, $[M+Na]^+$ 399.25012. LCMS (ESI) found 393.90 for $[M+NH_4]^+$

2.4 Synthesis of palmostatin B-derived pull down probe (23)

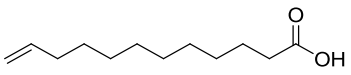

11-Dodecanoic acid (**16**).[32,33] In a two neck-round bottom flask was added freshly crushed Mg (5 g, 200 mmol, 2.85 eqv.) followed by dry Et_2O (27 ml). 11-Bromo-1-undecene **15** (15 ml, 70 mmol, 1.0 eqv.) as a solution in dry Et_2O (45 ml) was slowly added to the reaction mixture which was subsequently heated under reflux for 5 hours. The excess of magnesium was removed by transferring the solution via syringe into a new flask. The obtained Grignard solution was cooled to -40°C and CO_2 gas was bubbled through the solution for 2 hours (CO_2 source: dry-ice placed into a separated flask connected via a tubing system to avoid humidity). The reaction was quenched with water and subsequently basified to pH 12.0 using NaOH. The two phases were separated and the organic layer discarded. The aqueous layer was acidify using 18% HCl and extracted with several portion of EtOAc. The combined organic extracts were dried over anhydrous $MgSO_4$ and concentrated under reduced pressure leading to compound **16**, which was used directly in the next step without further purification. Yield = 56% (yellow oil). R_f = 0.61 (EtOAc/cyclohexane 1/1). IR: 1708 cm^{-1} (acid, C=O stretch). **^{1}H NMR** (400 MHz, $CDCl_3$): δ 5.81 (ddt, *J* = 6.8, 10.4, 17.2, 1H, -C*H*=CH_2), 4.99 (ddt, *J* = 1.6, 2.4, 17.0, 1H, -C=C*H*$_2$), 4.92 (ddt, *J* = 1.2, 2.0, 10.2, 1H, -C=C*H*$_2$), 2.34 (t, *J* = 7.4, 2H, -C*H*$_2$COOH), 2.03 (dt, *J* = 6.8, 8.0, 2H, -C*H*$_2$-CH=CH_2), 1.71 – 1.59 (m, 2H), 1.42 - 1.23 (m, 12H). **^{13}C NMR** (100 MHz, $CDCl_3$): δ 180.2, 139.1, 114.1, 34.0, 33.8, 29.4, 29.3, 29.2, 29.1, 29.0, 28.9, 24.6. HRMS (ESI) calc. for $C_{12}H_{22}O_2$ $[M+H]^+$ 199.1692, found 199.1692. GCMS found 198 for $[M^{+\cdot}]$.

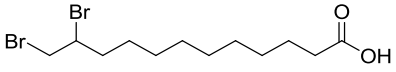

11,12-Dibromododecanoic acid (**17**).[34] To a solution of 11-dodecanoic acid **16** (5.9 g, 29.7 mmol, 1.0 eqv.) in dry Et_2O (50 ml) was added Br_2 (1.9 ml, 36 mmol, 1.2 eqv.) at -5°C. The mixture was stirred at -5°C for an additional 2 hours and was quenched using saturated $Na_2S_2O_3$ aqueous solution. The organic layer was dried over anhydrous $MgSO_4$ and concentrated under reduced pressure leading to compound **17**, which was used directly in the next step. Yield = quantitative (yellow viscous oil). R_f = 0.61 (EtOAc/cyclohexane 1/1). IR: 1706 cm^{-1} (acid, C=O stretch). **^{1}H NMR** (400 MHz, $CDCl_3$): δ 4.15 (ddt, *J* = 3.4, 4.3, 9.3, 1H, -C*H*BrCH_2Br), 3.83 (dd, *J* = 4.4, 10.4, 1H, -C*H*$_2$Br), 3.62 (dd, *J* = 10.0, 9.4, 1H, -C*H*$_2$Br), 2.35 (t, *J* = 7.4, 2H, -C*H*$_2$COOH), 2.16 - 2.06 (m, 1H, -C*H*$_2$-CHBrCH_2Br), 1.83 - 1.72 (m, 1H, -C*H*$_2$-CHBrCH_2Br), 1.68 – 1.58 (m, 2H), 1.47 - 1.22 (m, 12H).

^{13}C NMR (100 MHz, $CDCl_3$): δ 178.7, 53.1, 36.3, 35.9, 33.8, 29.3, 29.2, 29.1, 29.0, 28.7, 26.7, 24.6. HRMS (ESI) calc. for $C_{12}H_{22}Br_2O_2$ $[M-H]^-$ 354.9914, found 354.9918.

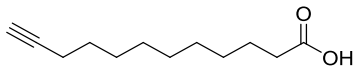

11- Dodecynoic acid (**18**).[34,35] In a round bottom flask containing $NaNH_2$ (commercial quality, Aldrich, 0.602 g, 15.4 mmol, 5.5 eqv.) was condensed liquid NH_3 (10 ml) at - 60°C. A solution of 11,12-dibromododecanoic acid **17** (1 g, 2.8 mmol, 1.0 eqv.) in dry THF (4 ml) was added dropwise to the reaction mixture which was subsequently stirred at -45°C for 4 hours followed by 1 hour at -35°C. The reaction was quenched by addition of NH_4Cl (1g) and the ammonia was evaporated. Water was added dropwise to the mixture which was then acidified with concentrated HCl and diluted with ice-cold water. After several extractions with Et_2O, combined organic layers were washed with brine, dried over anhydrous $MgSO_4$ and concentrated under reduced pressure leading to compound **18**, which was used directly in the next step. Yield =96% (yellow oil). R_f = 0.41 (EtOAc/cyclohexane 1/1). IR: 3306 cm^{-1} (C≡C-H stretch), 2118 cm^{-1} (-C≡C- stretch), 1706 cm^{-1} (acid, C=O stretch). **^{1}H NMR** (400 MHz, $CDCl_3$): δ 2.32 (t, *J* = 7.4, 2H, -C*H*$_2$COOH), 2.16 (dt, *J* = 2.8, 7.2, 2H, -C*H*$_2$-C≡C), 1.91 (t, *J* = 2.8, 1H, -C≡C*H*), 1.66 – 1.56 (m, 2H), 1.54 - 1.46 (m, 2H), 1.43 - 1.23 (m, 10H). **^{13}C NMR** (100 MHz, $CDCl_3$): δ 180.3, 84.6, 68.0, 34.0, 29.2, 29.1, 28.9, 28.6, 28.4, 24.6, 18.3. HRMS (ESI) calc. for $C_{12}H_{20}O_2$ $[M-H]^-$ 195.1390, found 195.1392. GCMS found 196 for $[M^{+\cdot}]$.

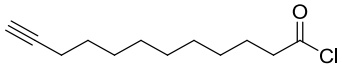

11- Dodecynoyl chloride (**19**).[36] To a solution of 11- dodecynoic acid **18** (3.5 g, 17.8 mmol, 1.0 eqv.) in dry benzene (21 ml) was added thionyl chloride (2 ml, 26.7 mmol, 1.5 eqv.). After 3 hours under reflux, the mixture was concentrated under reduced pressure leading to compound **19** which was used directly in the next step. Yield = 97% (brown oil). IR: 3306 cm^{-1} (C≡C-H stretch), 2117 cm^{-1} (-C≡C- stretch), 1795 cm^{-1} (C=O stretch). **^{1}H NMR** (400 MHz, $CDCl_3$): δ 2.86 (t, *J* = 7.4, 2H, -C*H*$_2$COCl), 2.16 (dt, *J* = 2.8, 7.2, 2H, -C*H*$_2$-C≡C), 1.91 (t, *J* = 2.8, 1H, -C≡C*H*), 1.74 – 1.64 (m, 2H), 1.55 - 1.45 (m, 2H), 1.42 - 1.22 (m, 10H). **^{13}C NMR** (100 MHz, $CDCl_3$): δ 173.7, 84.6, 68.0, 47.0, 29.0, 28.9, 28.8, 28.6, 28.4, 28.3, 24.7, 18.3.

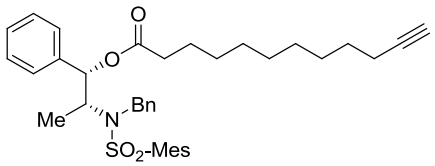

(*1S,2R*)-2-(*N*-benzyl-*N*-mesitylenesulfonyl)amino-1-phenyl-1-propyldodec-11-ynoate (20). Compound **20** was synthesized following the general procedure for *O*-dodecylated ephedrine auxiliary synthesis using 16.3 mmol of limiting reagent, reaction time 15 hours. Purification using a gradient 1-5% EtOAc/cyclohexane for the flash chromatography leads to compound **20**. Yield = 67% (yellow oil). R_f = 0.66 (EtOAc/cyclohexane 20/80). $[\alpha]_D^{20}$= – 30.7 (c = 0.16, $CHCl_3$). IR: 3304 cm^{-1} (C≡C-H stretch), 2116 cm^{-1} (-C≡C- stretch), 1741 cm^{-1} (ester, C=O stretch). **^{1}H NMR** (400 MHz, $CDCl_3$): δ 7.34 - 7.15 (m, 8H, Haro), 6.92 - 6.86 (m, 4H, Haro), 5.81 (d, *J* = 4.0, 1H, -C*H*OCOR), 4.73 (d, *J* = 16.8, 1H, -C*H*Ph), 4.57 (d, *J* = 16.4, 1H, C*H*Ph), 4.08 - 4.01 (m, 1H, C*H*N(Bn)Mes), 2.50 (s, 6H, CH_3 (Mes)), 2.27 (s, 3H, CH_3 (Mes)), 2.17 (dt, *J* = 2.8, 7.2, 2H, -CH_2-C≡C), 1.93 (t, *J* = 2.8, 1H, -C≡C*H*), 1.55 - 1.44 (m, 6H), 1.40 - 1.31 (m, 2H), 1.29 - 1.17 (m, 8H), 1.12 (d, *J* = 6.8, 3H, -CH_3). **^{13}C NMR** (100 MHz, $CDCl_3$): δ 171.9, 142.4, 140.2, 138.6, 138.6, 133.4, 132.1, 128.4, 128.3, 127.8, 127.4, 127.1, 125.9, 84.7, 77.9, 68.0, 56.7, 48.1, 34.1, 29.2, 29.1, 29.0, 28.9, 28.7, 28.4, 24.6, 22.9, 20.9, 18.4, 12.9. HRMS (ESI) calc. for $C_{37}H_{47}NO_4S$, $[M+H]^+$ 602.3298, $[M+Na]^+$ 624.3118, $[M+NH_4]^+$ 619.3564, found $[M+H]^+$ 602.3296, $[M+Na]^+$ 624.3111, $[M+NH_4]^+$ 619.3563. LCMS (ESI) found 618.93 for $[M+NH_4]^+$.

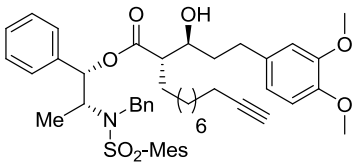

(*S*)-((*1S,2R*)-2-(*N*-benzyl-2,4,6-trimethylphenylsulfonamido)-1-phenylpropyl)2-((*S*)-3-(3,4-dimethoxy phenyl)-1-hydroxypropyl)dodec-11-ynoate (**21**). Compound **21** was synthesized following the general procedure for the *anti*-selective aldol reaction using 5.20 mmol of limiting reagent. Purification using a gradient 5-7% EtOAc/cyclohexane for the flash chromatography leads to compound **21**. Yield =76% (yellow oil). R_f = 0.3 (EtOAc/cyclohexane 30/70). $[\alpha]_D^{20}$= -33.3 (c = 0.27, $CHCl_3$). IR: 3291 cm^{-1} (C≡C-H stretch), 2115 cm^{-1} (-C≡C- stretch), 1736 cm^{-1} (ester, C=O stretch). **^{1}H NMR** (400 MHz, $CDCl_3$): δ 7.24 - 7.11 (m, 8H, Haro), 6.88 - 6.67 (m, 7H, Haro), 5.86 (d, *J* = 5.6, 1H, -C*H*OCOR), 4.69 (d, *J* = 16.4, 1H, -C*H*Ph), 4.46 (d, *J* = 16.4, 1H, -C*H*Ph), 4.23 - 4.15 (m, 1H, -C*H*N(Bn)Mes), 3.85 (s, 3H, -OCH_3), 3.84 (s, 3H, -OCH_3), 3.71 - 3.62 (m, 1H, -C*H*OH), 2.83 - 2.55 (m, 2H), 2.48 - 2.38 (m, 7H, -C*H*COOR, CH_3 (Mes)), 2.27 (s, 3H, CH_3 (Mes)), 2.16 (dt, *J* = 2.8, 6.8, 2H, -CH_2-C≡C), 1.93 (t, *J* = 2.8, 1H, -C≡C*H*), 1.80 - 1.61 (m, 2H), 1.58 – 1.40 (m, 4H), 1.37 –

0.94 (m, 13H). **^{13}C NMR** (100 MHz, $CDCl_3$): δ 174.5, 148.9, 147.2, 142.5, 140.3, 138.1, 137.8, 134.3, 133.1, 132.0, 128.3, 128.3, 128.1, 127.9, 127.2, 126.7, 120.2, 111.8, 111.3, 84.7, 78.1, 71.5, 68.1, 56.4, 55.9, 55.8, 51.3, 48.1, 37.3, 31.6, 29.7, 29.4, 29.1, 28.9, 28.6, 28.4, 27.0, 26.9, 22.8, 20.9, 18.4, 14.4. HRMS (ESI) calc. for $C_{48}H_{61}NO_7S$ $[M+H]^+$ 796.4241, $[M+Na]^+$ 818.4061, $[M+NH_4]^+$ 813.4507, found $[M+H]^+$ 796.4248 $[M+Na]^+$ 818.4057, $[M+NH_4]^+$ 813.4510. LCMS (ESI) found 813.04 for $[M+NH_4]^+$.

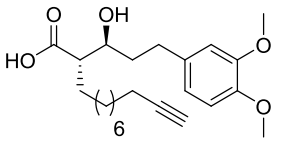

(*S*)-2-((*S*)-3-(3,4-dimethoxyphenyl)-1-hydroxypropyl)dodec-11-ynoic acid (**22**). Compound **22** was synthesized following the general procedure for saponification on 3.85 mmol of β-hydroxyester **21** by reaction with 9.0 eqv. $LiOH{\cdot}H_2O$ at 40-45°C for 90 hours. Purification by chromatography using 1% $MeOH/CH_2Cl_2$ to remove unpolar impurities, then gradient 2-5% $MeOH/CH_2Cl_2$ to collect compound **22** (separation monitored by TLC using eluent EtOAc/cyclohexane 1/1). Yield = 87% (yellow oil). R_f = 0.71 ($MeOH/CH_2Cl_2$ 10/90). $[\alpha]_D^{20}$= - 29.0 (c = 0.1, $CHCl_3$). IR: 3291 cm^{-1} (C≡C-H stretch), 2115 cm^{-1} (-C≡C- stretch), 1704 cm^{-1} (acid, C=O stretch). **^{1}H NMR** (400 MHz, $CDCl_3$): δ 6.79 - 6.67 (m, 3H, Haro), 3.84 (s, 3H, -OC*H*$_3$), 3.83 (s, 3H, -OC*H*$_3$), 3.76 - 3.68 (m, 1H, -C*H*OH), 2.83 - 2.55 (m, 2H), 2.50 - 2.34 (m, 1H, -C*H*COOH), 2.15 (dt, *J* = 2.8, 7.0, 2H, -C*H*$_2$-C≡C), 1.91 (t, *J* = 2.8, 1H, -C≡C*H*), 1.87 - 1.42 (m, 6H), 1.39 - 1.17 (m, 10H). **^{13}C NMR** (100 MHz, $CDCl_3$): δ 180.5, 148.9, 147.3, 134.1, 120.2, 111.8, 111.3, 84.6, 71.6, 68.1, 55.9, 55.8, 37.6, 31.6, 29.5, 29.3, 29.0, 28.7, 28.4, 27.3, 18.3. HRMS (ESI) calc. for $C_{23}H_{34}O_5$ $[M+H]^+$ 391.2479, $[M+Na]^+$ 413.2298, $[M+NH_4]^+$ 408.2744, found $[M+H]^+$ 391.2485, $[M+Na]^+$ 413.2300, $[M+NH_4]^+$ 408.2749. LCMS (ESI) found 407.98 for $[M+NH_4]^+$.

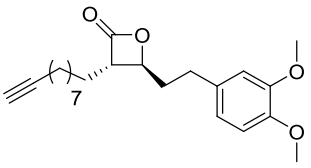

(3*S*,4*S*)-3-(dec-9-ynyl)-4-(3,4-dimethoxyphenethyl)oxetan-2-one (**23**). Compound **23** was synthesized following the general procedure for β-lactonization using 3.32 mmol of compound **22** (reaction monitored by TLC using EtOAc/cyclohexane 3/7). Purification by flash chromatography using gradient 2-5% EtOAc/toluene followed by recrystallisation into EtOAc/pentane to remove the remaining traces of the *cis*-β-lactone. Yield=89% (white solid). R_f =

0.50 (EtOAc/cyclohexane 30/70). mp= 33.2-33.5°C (after recrystallisation from EtOAc/pentane). $[\alpha]_D^{20}$ = – 51.9 (c = 0.21, $CHCl_3$). IR: 3244 cm^{-1} (C≡C-H stretch), 2115 cm^{-1} (-C≡C- stretch), 1795 cm^{-1} (β-lactone, C=O stretch). **^{1}H NMR** (400 MHz, $CDCl_3$): δ 6.83 - 6.79 (m, 1H, Haro), 6.75 - 6.69 (m, 2H, Haro), 4.21 (ddd, *J* = 4.1, 5.2, 8.1, 1H, -C*H*OCOR), 3.87 (s, 3H, -OCH_3), 3.86 (s, 3H, -OCH_3), 3.18 (ddd, *J* = 4.0, 6.9, 8.4, 1H, -C*H*CO), 2.81 - 2.59 (m, 2H), 2.17 (dt, *J* = 2.6, 7.0, 2H, -CH_2-C≡C), 2.15 - 1.98 (m, 2H), 1.93 (t, *J* = 2.6, 1H, -C≡C*H*), 1.84 - 1.61 (m, 2H), 1.55 - 1.47 (m, 2H), 1.45 - 1.22 (m, 10H). **^{13}C NMR** (100 MHz, $CDCl_3$): δ 171.4, 148.9, 147.5, 132.7, 120.1, 111.5, 111.3, 84.7, 77.1, 68.1, 56.2, 55.9, 55.8, 36.4, 30.9, 29.2, 29.1, 28.9, 28.6, 28.4, 27.7, 26.9, 18.3. HRMS (ESI) calc. for $C_{23}H_{32}O_4$ $[M+H]^+$ 373.2373, $[M+Na]^+$ 395.2193, found $[M+H]^+$ 373.2376, $[M+Na]^+$ 395.2194. LCMS (ESI) found 373.07 for $[M+H]^+$.

2.5 Synthesis of TAMRA-labeled palmostatin B analogue (25)

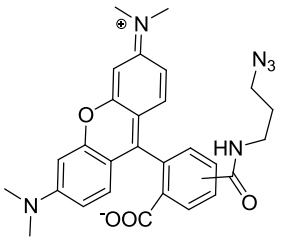

Rhodamine-azide (**24**).[37] In a 1 ml glass vial was added 5/6-TAMRA-SE (9 mg, 0.0167 mmol, 1.0 eqv.) into MeOH (0.3 ml). Then 3-azido propylamine [38] (20.1 mg, 0.201 mmol, 12.0 eqv.) followed by NEt_3 (12µl, 0.085 mmol, 5.0 eqv.) were added to the reaction mixture, which was stirred at rt for 20 hours (in the dark). After concentrated under reduced pressure, the residue was subsequently diluted with 1% citric acid (10 ml), and the aqueous layer extracted with several portion of DCM (5* 10 ml). The combined organic layer was finally extracted with brine (10 ml), and concentrated without being dried with any deshydrating reagents to avoid the strong absorption problem occuring with $MgSO_4$ or Na_2SO_4. The crude was finally purified by RPC_{18} column (2g) using a CH_3CN/H_2O gradient (0- 100% CH_3CN) leading to compound **24** in 81% yield (m = 6.9 mg) as a dark red solid. R_f = 0.48 (EtOAc/AcOH/MeOH/H_2O 5/2/2/1, fluorescent single spot). **^{1}H NMR** (400 MHz, $CDCl_3$, assignment includes both isomers): δ 8.43 (brs, 0.5H), 8.19 (d, *J* = 7.6, 0.5H), 8.07 (d, *J* = 8.0, 0.5H), 8.01 (d, *J* = 8.0, 0.5H), 7.85 - 7.69 (m, 0.5H), 7.63 (brs, 1H), 7.22 (d, *J* = 8.0, 0.5H), 6.79 (d, *J* = 8.8, 1H), 6.75 (d, *J* = 8.8, 1H), 6.56 - 6.49 (m, 4H), 3.57 (q, *J* = 6.4, 1H), 3.47 - 3.40 (m, 2H), 3.34 (t, *J* = 6.8, 1H), 3.07 (s, 6H), 3.06 (s, 6H), 1.93 (m, 1H),

1.84 (m, 1H). HRMS (ESI) calc. for $C_{28}H_{28}N_6O_4$, $[M+H]^+$ 513.2245, found $[M+H]^+$ 513.2238. LCMS (ESI) found 513.07 for $[M+H]^+$.

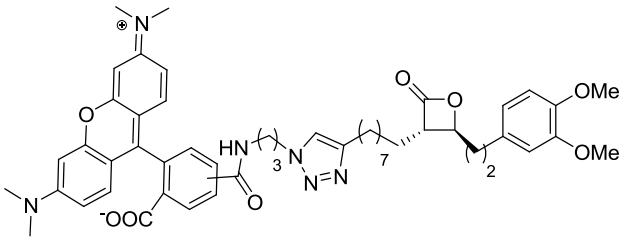

TAMRA- palmostatin B derived compound (**25**)[39]**.** In a round bottom flask was added rhodamine-azide **24** (0.0169 mmol, 1.0 eqv.) and the corresponding alkynylated β-lactone **23** (7.8 mg, 0.0209 mmol, 1.2 eqv.) into degassed EtOH (0.7 ml). Subsequently 1M degassed $CuSO_4$ aqueous solution (15 µl, 0.01521 mmol, 0.9 eqv.) was added to the reaction mixture followed by 2 M degassed aqueous sodium ascorbate solution (13 µl, 0.02535 mmol, 1.5 eqv.). The reaction mixture was then stirred at rt in the dark for 16 hours. The avancement of the reaction was monitorated by LCMS analysis. After concentration under reduced pressure, the crude was purified by RPC_{18} column (2g) using a CH_3CN/H_2O gradient (0- 100% CH_3CN) leading to compound **25** in 83% yield (m = 10 mg) as a dark red solid. The purification was monitorated by the MALDI analysis of each fraction collected. R_f = 0.48 (EtOAc/AcOH/MeOH/H_2O 5/2/2/1, fluorescent single spot). IR: 1814.91 cm^{-1} (β-lactone, C=O stretch). **^{1}H NMR** (400 MHz, $CDCl_3$, assignment includes both isomers): δ 8.44 (brs, 0.5H), 8.14 (d, *J* = 8.0, 0.5H), 8.01 (brs, 1H), 7.58 (s, 0.5H), 7.48 - 7.31 (m, 1.5H), 7.24 (d, *J*= 7.6, 0.5H), 7.10 - 6.95 (m, 0.5H), 6.81 - 6.78 (m, 1H), 6.74 - 6.68 (m, 2H), 6.65 - 6.59 (m, 2H), 6.51 - 6.46 (m, 2H), 6.44 - 6.38 (m, 2H), 4.43 (t, *J* = 6.4, 1H), 4.47 (t, *J* = 6.4, 1H), 4.21 (ddd, *J* = 3.3, 7.8, 7.8, 1H), 3.86 (s, 3H, -OCH_3), 3.85 (s, 3H, -OCH_3), 3.50 (q, *J* = 5.8, 1H), 3.39 (q, *J* = 5.8, 1H), 3.18 (ddd, *J* = 3.6, 7.6, 11.1, 1H), 3.00 (s, 6H), 2.99 (s, 6H), 2.80 - 2.57 (m, 4H), 2.27 - 1.97 (m, 4H), 1.83 - 1.53 (m, 4H), 1.45 - 1.19 (m, 10H). HRMS (ESI) calc. for $C_{51}H_{60}N_6O_8$, $[M+H]^+$ 885.4545, found $[M+H]^+$ 885.4547. LCMS (ESI) found 885.26 for $[M+H]^+$.

2.6 Synthesis *trans* β-lactone inhibitors 27 and palmostatin M (28)

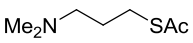

***N,N*-(Dimethylamino)propyl thioacetate** (**47**). To a 500 ml round bottom flask equipped with a large egg-shaped stirring bar, argon inlet, reflux condenser and pressure equalized dropping

funnel was added *N,N*-dimethylamino-1-propyl chloride hydrochloride **46** (20.0 g, 126.6 mmol, 1.0 eqv.), followed by 200 ml $CHCl_3$. After the apparatus had been flushed with argon, the resulting suspension was cooled to 0°C and NEt_3 (52.57 ml, 379 mmol, 3.0 eqv.) was added dropwise at such a rate that the temperature of the reaction mixture kept at approx. 10°C. The dropping funnel was rinsed with $CHCl_3$ (2*5 ml) and refilled with thioacetic acid (10.8 ml, 151.9 mmol, 1.2 eqv.) which was added dropwise to the reaction mixture at such a rate that the temperature was kept below 20°C. The addition was completed in 30 min and the dropping funnel was rinsed with $CHCl_3$ (2*5 ml) and replaced by a stopper. The ice-bath was removed and the resulting homogeneous mixture was heated to gentle reflux for 20 hours. The reaction mixture was allowed to cool to rt and was extracted with ice-cold 1N NaOH (3x90 ml), followed by H_2O (100 ml). Combined aqueous layers were extracted with $CHCl_3$ (2x100 ml) and combined $CHCl_3$ extracts were washed with brine (200 ml), allowed to separate completely (some formation of emulsion) over 30 min and subsequently dried twice over anhydrous $MgSO_4$ (2x30g, stirring with the drying agent for 30 min each time). After filtration over Celite and concentration under reduced pressure, the crude was purified by distillation under reduced pressure (8 mm Hg) through a short Vigreux column (150 mm), yielding compound **47** as slight yellow oil. bp 73-76°C at 8.0 mm Hg. Yield = 82% **Note:** It is important that the crude product is dry (water-free) before attempting distillation. If not dry, heating of the material will result in formation of a tar-like residue and low yield of impure material. IR 1689 cm^{-1} (C=O stretch). **^{1}H NMR** (400 MHz, $CDCl_3$): δ 2.90 (t, *J* = 7.2, 2H, -C*H*$_2$S), 2.31 (t, *J* = 7.2, 2H, -C*H*$_2$N), 2.32 (s, 3H, -COC*H*$_3$), 2.21 (s, 6H, N(C*H*$_3$)$_2$), 1.74 (p, *J* = 7.2, 2H). **^{13}C NMR** (125 MHz, $CDCl_3$): δ 195.7, 58.5, 45.5, 30.7, 27.8, 27.1. HRMS (ESI) calc. for $C_7H_{15}NOS$ $[M+H]^+$ 162.0947, found 162.0946. GCMS found 161 for $[M^{+\cdot}]$.

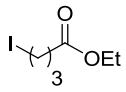

Ethyl-4-iodobutanoate (**48**). Compound **48** was synthesized following the general procedure for Finkelstein reaction on 67 mmol ethyl-4-bromobutanoate. Yield = 96% (yellow oil). R_f = 0.43 (EtOAc/cyclohexane 5/95). IR: 1729 cm^{-1} (ester, C=O stretch). **^{1}H NMR** (400 MHz, $CDCl_3$): δ 4.12 (q, *J* = 7.0, 2H, -C*H*$_2$CH$_3$), 3.22 (t, *J* = 6.8, 2H, -C*H*$_2$COOR), 2.41 (t, *J* = 7.2, 2H, -C*H*$_2$I), 2.1 (dd, *J* = 6.8, 7.2, 2H), 1.24 (t, *J* = 7.0, 3H, -CH$_2$C*H*$_3$).**^{13}C NMR** (125 MHz, $CDCl_3$): δ 172.2, 60.4, 34.8, 28.5, 14.2, 5.4. HRMS (ESI) calc. for $C_6H_{11}IO_2$ $[M+H]^+$ 242.9877, found $[M+H]^+$ 242.9879. GCMS found 197 for $[M\text{-}OEt^{+\cdot}]$.

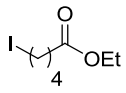

Ethyl-5-iodopentanoate (**49**). Compound **49** was synthesized following the general procedure for Finkelstein reaction on 119 mmol ethyl-5-bromopentanoate. Yield = 92% (yellow oil). R_f = 0.41 (EtOAc/cyclohexane 5/95). IR: 1729 cm^{-1} (ester, C=O stretch). **^{1}H NMR** (400 MHz, $CDCl_3$): δ 4.11 (q, *J* = 7.2, 2H, -C*H*$_2$CH$_3$), 3.17 (t, *J* = 6.8, 2H, -C*H*$_2$COOR), 2.31 (t, *J* = 7.4, 2H, -C*H*$_2$I), 1.85 (dd, *J* = 6.8, 7.4, 2H), 1.72 (p, *J* = 7.4, 2H), 1.24 (t, *J* = 7.2, 3H, -CH$_2$C*H*$_3$). **^{13}C NMR** (125 MHz, $CDCl_3$): δ 173.0, 60.3, 33.1, 32.7, 25.7, 14.2, 5.8. HRMS (ESI) calc. for $C_7H_{13}IO_2$ $[M+Na]^+$ 278.9852, found $[M+Na]^+$ 278.9856. GCMS found 211 for $[M\text{-}OEt^{+\cdot}]$.

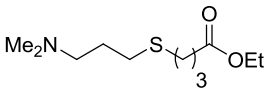

Ethyl 4-(3-(dimethylamino)propylthio)butanoate (**50**). Compound **50** was synthesized following the general procedure for *S*-alkylation using 68.7 mmol of thioacetate **47** (no purification needed). Yield = 92% (slight yellow oil). R_f = 0.48 (AcOH/ EtOAc/MeOH/H_2O 3/3/3/2). IR: 1732 cm^{-1} (ester, C=O stretch). **^{1}H NMR** (400 MHz, $CDCl_3$): δ 4.01 (q, *J* = 7.2, 2H, -COC*H*$_2$CH$_3$), 2.43 (t, *J* = 7.2, 2H, -C*H*$_2$S), 2.41 (t, *J* = 7.4, 2H, -C*H*$_2$S), 2.30 (t, *J* = 7.2, 2H, -C*H*$_2$COOEt), 2.22 (t, 2H, *J* = 7.4, -C*H*$_2$NMe$_2$), 2.09 (s, 6H, N(C*H*$_3$)$_2$), 1.83 – 1.74 (m, 2H), 1.66 – 1.56 (m, 2H), 1.12 (t, *J* = 7.2, 3H, -COCH$_2$C*H*$_3$). **^{13}C NMR** (125 MHz, $CDCl_3$): δ 172.8, 60.1, 58.4, 45.2, 32.8, 31.2, 29.5, 27.5, 24.5, 14.0. HRMS (ESI) calc. for $C_{11}H_{23}NO_2S$ $[M+H]^+$ 234.1522, found 234.1521. GCMS found 233 for $[M^{+\cdot}]$.

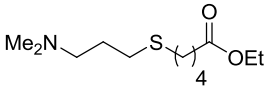

Ethyl 5-(3-(dimethylamino)propylthio)pentanoate (**51**). Compound **51** was synthesized following the general procedure for *S*-alkylation using 40.3 mmol of thioacetate **47** (no purification needed). Yield = 97% (slighlt yellow oil). R_f = 0.50 (AcOH/EtOAc/MeOH/H_2O 3/3/3/2). IR: 1733 cm^{-1} (ester, C=O stretch). **^{1}H NMR** (400 MHz, $CDCl_3$): δ 4.05 (q, *J* = 7.2, 2H, -COC*H*$_2$CH$_3$), 2.47 (t, *J* = 7.2, 2H, -C*H*$_2$S), 2.45 (t, *J* = 7.2, 2H, -C*H*$_2$S), 2.32 (t, *J* = 7.4, 2H, -C*H*$_2$COOEt), 2.24 (t, *J* = 7.4, 2H, -C*H*$_2$NMe$_2$), 2.19 (s, 6H, (N(C*H*$_3$)$_2$), 1.74 - 1.60 (m, 4H), 1.59 - 1.49 (m, 2H), 1.18 (t, *J* = 7.2, 3H, -COCH$_2$C*H*$_3$). **^{13}C NMR** (125 MHz, $CDCl_3$): δ 173.2, 60.1, 58.4, 45.2, 33.7, 31.6, 29.7, 28.9, 27.4, 24.0, 14.1. HRMS (ESI) calc. for $C_{12}H_{25}NO_2S$ $[M+H]^+$ 248.1679, found 248.1678. GCMS found 247 for $[M^{+\cdot}]$.

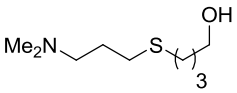

4-(3-(Dimethylamino)propylthio)butan-1-ol (**52**). Compound **52** was synthesized following the general procedure for ester reduction using 21 mmol of ethylester **50**. Yield = 91% (colorless oil). R_f = 0.28 (AcOH/EtOAc/MeOH/ H_2O 3/3/3/2). **^{1}H NMR** (400 MHz, $CDCl_3$): δ 3.43 (t, *J* = 6.2, 2H, -C*H*$_2$OH), 2.39 (t, *J* = 7.2, 2H, -C*H*$_2$S), 2.38 (t, *J* = 7.0, 2H, -C*H*$_2$S), 2.23 – 2.20 (m, 2H, -C*H*$_2$NMe$_2$), 2.07 (s, 6H, N(C*H*$_3$)$_2$), 1.64 – 1.55 (m, 2H), 1.54 - 1.43 (m, 4H). **^{13}C NMR** (125 MHz, $CDCl_3$): δ 61.3, 58.2, 45.0 (2C), 31.6, 31.6, 29.5, 27.1, 25.7. HRMS (ESI) calc. for $C_9H_{21}NOS$ $[M+H]^+$ 192.1416, found 192.1413. GCMS found 191 for $[M^{+\cdot}]$.

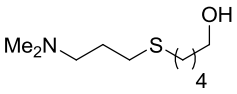

5-(3-(Dimethylamino)propylthio)pentan-1-ol (53). Compound **53** was synthesized following the general procedure for ester reduction using 40.3 mmol of ethylester **51**. Yield = 93% (slight yellow oil). R_f = 0.33 (AcOH/EtOAc/ MeOH/H_2O 3/3/3/2). **^{1}H NMR** (400 MHz, $CDCl_3$): δ 3.58 (t, *J* = 6.6, 2H, -C*H*$_2$OH), 2.50 (t, *J* = 7.4, 2H, -C*H*$_2$S), 2.49 (t, *J* = 7.2, 2H, -C*H*$_2$S), 2.32 (t, *J* = 7.2, 2H, C*H*$_2$NMe$_2$), 2.19 (s, 6H, N(C*H*$_3$)$_2$), 1.77 – 1.65 (m, 2H), 1.63-1.50 (m, 4H), 1.46-1.38 (m, 2H). **^{13}C NMR** (125 MHz, $CDCl_3$): δ 62.3, 58.6, 45.3 (2C), 32.2, 32.0, 29.9, 29.3, 27.5, 25.0. HRMS (ESI) calc. for $C_{10}H_{23}NOS$ $[M+H]^+$ 206.1573, found 206.1571. LC-MS (ESI) found 205.99 for $[M+H]^+$.

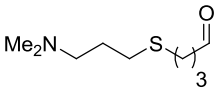

4-(3-(Dimethylamino)propylthio)butanal (**54**). Compound **54** was synthesized following the general procedure for Swern oxidation using 6.27 mmol of alcohol **52**. Yield = 73% (slight yellow oil). R_f = 0.54 (EtOAc/AcOH/ MeOH/H_2O 3/3/3/2). IR: 1722 cm^{-1} (C=O). **^{1}H NMR** (400 MHz, $CDCl_3$): δ 9.76 (t, *J* = 1.2, 1H, -C*H*O), 2.55 (dt, *J* = 1.2, 7.2, 2H, -C*H*$_2$CHO), 2.52 (t, *J* = 7.2, 2H, -C*H*$_2$S), 2.50 (t, *J* = 7.4, 2H, -C*H*$_2$S), 2.32 (dd, *J* = 7.4, 2H, -C*H*$_2$NMe$_2$), 2.19 (s, 6H, N(C*H*$_3$)$_2$), 1.89 (dd, *J* = 7.2, 7.4, 2H), 1.71 (p, *J* = 7.4, 2H). **^{13}C NMR** (125 MHz, $CDCl_3$): δ 201.7, 58.8, 45.6, 42.8, 31.6, 29.9, 27.8, 22.0. HRMS (ESI) calc. for $C_9H_{19}NOS$ $[M+H]^+$ 190.1260, found 190.1258. GCMS found 189 for $[M^{+\cdot}]$.

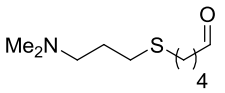

5-(3-(Dimethylamino)propylthio)pentanal (**55**). Compound **55** was synthesized following the general procedure for Swern oxidation using 15.6 mmol of alcohol **53**. Yield = 85% (yellow oil). R_f = 0.50 (AcOH/EtOAc/MeOH/H_2O 3/3/3/2). IR: 1721 cm^{-1} (C=O). **^{1}H NMR** (400 MHz, $CDCl_3$): δ 9.76 (t, *J* = 1.6, 1H, -C*H*O), 2.54 (t, *J* = 7.4, 2H, -CH_2S), 2.53 (t, *J* = 7.2, 2H, -CH_2S), 2.45 (dt, *J* = 1.6, 7.2, 2H, -CH_2CHO), 2.38 (t, *J* = 7.4, 2H, -CH_2NMe_2), 2.25 (s, 6H, N(CH_3)$_2$), 1.80 - 1.69 (m, 4H), 1.66 - 1.57 (m, 2H). **^{13}C NMR** (125 MHz, $CDCl_3$): δ 202.1, 58.5, 45.3, 43.3, 31.8, 29.9, 28.9, 27.5, 21.2. HRMS (ESI) calc. for $C_{10}H_{21}NOS$ $[M+H]^+$ 204.1416, found 204.1413. GCMS found 203 for $[M^{+\cdot}]$.

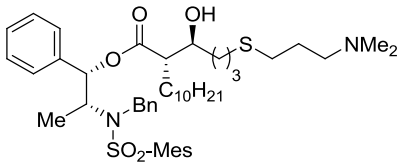

(*2S*)-(*1S,2R*)-2-((*N*-benzyl-*N*-mesitylsulfonyl)amino)-1-phenylpropyl-2-((*S*)-4-(3-(dimethylamino) propylthio)-1-hydroxybutyl) dodecanoate (**56**). Compound **56** was synthesized following the general procedure for *anti*-selective aldol reaction using 4.6 mmol of aldehyde **54**. After purification by column chromatography (1-3% MeOH/CH_2Cl_2), compound **56** is obtained as colorless oil in 40% yield, as a single diastereoisomer. R_f = 0.44 (10% MeOH/CH_2Cl_2). $[\alpha]_D^{20}$ = -28.3 (c = 1.0, $CHCl_3$). **^{1}H NMR** (500 MHz, $CDCl_3$): δ 7.29 - 7.13 (m, 8H, Haro), 6.85 - 6.82 (m, 4H, Haro), 5.83 (d, *J* = 5.7, 1H, -C*H*OCOR), 4.75 (d, *J* = 16.5, 1H, -C*H*Ph), 4.52 (d, *J* = 16.5, 1H, -C*H*Ph), 4.19 - 4.13 (m, 1H, -C*H*N(Bn)Mes), 3.70 - 3.65 (m, 1H, -C*H*OH), 2.55 - 2.50 (m, 4H), 2.44 (s, 6H), 2.42 - 2.36 (m, 4H), 2.28 (s, 3H), 2.24 (s, 6H), 1.80 - 1.40 (m, 8H), 1.32 - 0.96 (m, 19H), 0.89 (t, *J* = 6.7, 3H, -CH_3). **^{13}C NMR** (125 MHz, $CDCl_3$): δ 174.7, 142.7, 140.5, 138.5, 138.1, 133.4, 132.2, 128.5, 128.4, 128.2, 128.1, 127.4, 126.8, 78.3, 71.9, 58.7, 56.6, 51.6, 48.3, 45.5, 34.3, 32.1, 32.0, 29.9, 29.8, 29.7, 29.6, 29.5, 29.4, 27.6, 27.2, 25.7, 23.0, 22.8, 21.0, 14.5, 14.3. HRMS (ESI) calc. for $C_{46}H_{71}N_2O_5S_2$ $[M+H]^+$ 795.4799, found 795.4798. LC-MS (ESI) found 795.47 for $[M+H]^+$.

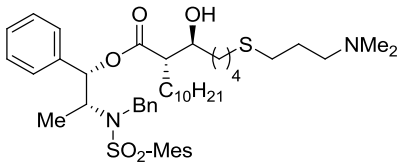

(*2S*)-(*1S,2R*)-2-((*N*-benzyl-*N*-mesitylsulfonyl)amino)-1-phenylpropyl-2-((*S*)-5-(3-(dimethylamino) propylthio)-1-hydroxypentyl) dodecanoate (**57**). Compound **57** was

synthesized following the general procedure for *anti*-selective aldol reaction using 4.7 mmol of aldehyde **55**. After purification by column chromatography (1-3% MeOH/CH_2Cl_2), compound **57** is obtained as colorless oil in 33% yield, as a single diastereoisomer. R_f = 0.30 (8% MeOH/CH_2Cl_2). $[\alpha]_D^{20}$ = -27.4 (c = 1.0, $CHCl_3$). **^{1}H NMR** (500 MHz, $CDCl_3$): δ 7.29 - 7.13 (m, 8H, Haro), 6.85 - 6.82 (m, 4H, Haro), 5.83 (d, *J* = 5.5, 1H, -C*H*OCOR), 4.75 (d, *J* = 16.2, 1H, -C*H*Ph), 4.52 (d, *J* = 16.5, 1H, -C*H*Ph), 4.19 - 4.13 (m, 1H, -C*H*N(Bn)Mes), 3.68 - 3.63 (m, 1H, -C*H*OH), 2.58 - 2.46 (m, 4H), 2.45 - 2.39 (m, 10H), 2.30 - 2.27 (m, 7H), 1.80 - 1.74 (m, 2H), 1.60 - 1.33 (m, 8H), 1.32 - 0.96 (m, 21H), 0.89 (t, *J* = 7.0, 3H, -CH_3). **^{13}C NMR** (125 MHz, $CDCl_3$): δ 174.7, 142.7, 140.5, 138.5, 138.0, 133.4, 132.2, 128.5, 128.4, 128.2, 128.1, 127.4, 126.8, 78.2, 72.2, 58.7, 56.5, 51.5, 48.3, 45.4, 34.9, 32.2, 32.0, 31.1, 30.1, 29.8, 29.7, 29.6, 29.5, 29.4, 27.5, 27.3, 25.0, 23.0, 22.8, 21.0, 14.5, 14.3. HRMS (ESI) calc. for $C_{47}H_{73}O_5N_2S_2$ $[M+H]^+$ 809.4955, found 809.4956. LCMS (ESI) found 809.52 for $[M+H]^+$.

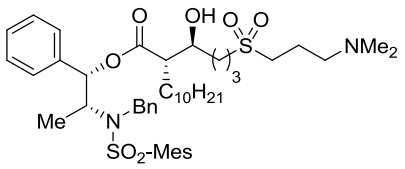

(*S*)-((*1S,2R*)-2-(*N*-benzyl-2,4,6-trimethylphenylsulfonamido)-1-phenylpropyl)2-((*S*)-4-(3-(dimethyl amino)propylsulfonyl)-1-hydroxybutyl) dodecanoate (**58**). Compound **58** was synthesized following the general procedure for oxidation into sulfone using 2.0 mmol of sulfide derivative **56,** reaction time 8 hours. Yield = 91% (white semi-solid). R_f = 0.26 (10% MeOH/DCM). $[\alpha]_D^{20}$ = - 30.6 (c = 0.31, $CHCl_3$). IR: 1734 cm^{-1} (ester, C=O stretch), 1312 cm^{-1} (SO_2 asym. stretch), 1149cm^{-1} (SO_2 sym. Stretch). **^{1}H NMR** (400 MHz, $CDCl_3$): δ 7.28 - 7.11 (m, 8H, Haro), 6.90 - 6.79 (m, 4H, Haro), 5.85 (d, *J* = 5.2, 1H, -C*H*OCOR), 4.64 (d, *J* = 16.2, 1H, -C*H*Ph), 4.47 (d, *J* = 16.3, 1H, -C*H*Ph), 4.25 - 4.09 (m, 1H, -C*H*N(Bn)Mes), 3.77 - 3.65 (m, 1H, -C*H*OH), 3.11 (t, *J* = 7.4, 2H, -C*H*SO_2), 3.02 (t, *J* = 8.0, 2H, -C*H*SO_2), 2.85 (t, *J* = 7.2, 2H, -CH_2N(Me)$_2$), 2.54 (s, 6H, CH_3 (Mes)), 2.43 (s, 7H, N(CH_3)$_2$, -C*H*COOR), 2.27 (s, 3H, CH_3 (Mes)), 2.22 -1.85 (m, 4H), 1.69 - 1.37 (m, 4H), 1.35 - 0.94 (m, 19H), 0.88 (t, *J* = 7.0, 3H, CH_3). **^{13}C NMR** (125 MHz, $CDCl_3$): δ 174.2, 142.5, 140.2 (2C), 138.3, 137.9, 133.1, 132.1 (2C), 128.3 (2C), 128.2 (2C), 128.1, 127.9 (2C), 127.2, 126.6 (2C), 78.2, 71.3, 56.7, 56.5, 52.9, 51.8, 49.2, 48.1, 43.9 (2C), 33.2, 31.9 (2C), 29.5 (2C), 29.5, 29.4, 29.3, 29.3, 27.1, 22.9, 22.7, 20.9, 18.8, 18.4, 14.2, 14.1. HRMS (ESI) calc. for $C_{46}H_{70}N_2O_7S_2$ $[M+H]^+$ 827.46972, found $[M+H]^+$ 827.46967. LCMS (ESI) found 827.18 for $[M+H]^+$.

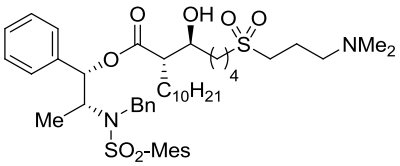

(*S*)-((*1S,2R*)-2-(*N*-benzyl-2,4,6-trimethylphenylsulfonamido)-1-phenylpropyl)2-((*S*)-5-(3-(dimethyl amino)propylsulfonyl)-1-hydroxypentyl) dodecanoate (**59**). Compound **59** was synthesized following the general procedure for oxidation into sulfone using 1.79 mmol of sulfide derivative **57,** reaction time 8 hours. Yield = quantitative (yellow semi-solid). R_f = 0.22 (10% MeOH/DCM). $[\alpha]_D^{20}$ = - 30.0 (c = 0.25, $CHCl_3$). IR: 1735 cm^{-1} (ester, C=O stretch), 1314 cm^{-1} (SO_2 asym. stretch), 1150 cm^{-1} (SO_2 sym. stretch). **^{1}H NMR** (400 MHz, $CDCl_3$): δ 7.27 - 7.11 (m, 8H, Haro), 6.90 - 6.81 (m, 4H, Haro), 5.86 (d, *J* = 5.6, 1H, -C*H*OCOR), 4.67 (d, *J* = 16.4, 1H, -C*H*Ph), 4.46 (d, *J* = 16.4, 1H, -C*H*Ph), 4.24 - 4.11 (m, 1H, -C*H*N(Bn)Mes), 3.69 - 3.61 (m, 1H, -C*H*OH), 3.04 (t, *J* = 7.8, 2H, -CH_2SO_2), 2.95 (t, *J* = 8.0, 2H, -CH_2SO_2), 2.58 (t, *J* = 6.8, 2H, -CH_2N(Me)$_2$), 2.42 (s, 7H, CH_3 (Mes), -C*H*COOR), 2.35 (s, 6H, N(CH_3)$_2$), 2.27 (s, 3H, CH_3 (Mes)), 2.11 - 2.01 (m, 2H), 1.90 - 1.75 (m, 2H), 1.67 - 1.44 (m, 4H), 1.42 - 0.96 (m, 21H), 0.88 (t, *J* = 7.0, 3H, -CH_3). **^{13}C NMR** (125 MHz, $CDCl_3$): δ 174.4, 142.5, 140.3 (2C), 138.3, 137.9, 133.2, 132.1 (2C), 128.3 (2C), 128.2 (2C), 128.1, 127.9 (2C), 127.2, 126.6 (2C), 78.1, 71.6, 58.8, 56.5, 53.1, 51.6, 49.8, 48.1, 44.1 (2C), 34.2, 31.9 (2C), 29.7, 29.5, 29.5, 29.5, 29.3, 29.3, 27.1, 24.5, 22.9, 22.7, 21.9, 20.8, 18.6, 14.2, 14.1. HRMS (ESI) calc. for $C_{47}H_{72}N_2O_7S_2$ $[M+H]^+$ 841.4854, found $[M+H]^+$ 841.4854. LCMS (ESI) found 841.21 for $[M+H]^+$.

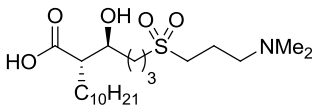

(*S*)-2-((*S*)-4-(3-(dimethylamino)propylsulfonyl)-1-hydroxybutyl)dodecanoic acid (**60**). Compound **60** was synthesized following the general procedure for hydrogenolysis on 1.82 mmol of β-hydroxyester **58,** reaction time 6 hours. Purification by column chromatography using MeOH/CH_2Cl_2 4/96 to first remove unpolar impurities followed by Et_3N/MeOH/CH_2Cl_2 2/10/88 to elute compound **60**. Yield = 65% (white semi-solid). R_f = 0.62 (AcOH/EtOAc /MeOH/H_2O 3/3/3/2). $[\alpha]_D^{20}$ = -8.2 (c = 1.0, MeOH/CH_2Cl_2 1/4). IR: 1615 cm^{-1} (acid, C=O stretch), 1279 cm^{-1} (SO_2 asym. stretch), 1135 cm^{-1} (SO_2 sym. stretch). **^{1}H NMR** (400 MHz, $CDCl_3$): δ 3.63 - 3.53 (m, 1H, -C*H*OH), 3.18 - 3.01 (m, 4H, -CH_2SO_2), 2.93 (t, *J* = 7.4, 2H, -CH_2N(Me)$_2$), 2.60 (s, 6H, -N(CH_3)$_2$), 2.25 - 2.17 (m, 1H, -C*H*COOH), 2.12 - 2.09 (m, 2H), 2.01 - 1.83 (m, 2H), 1.69 - 1.17 (m, 20H), 0.81 (t, *J* = 6.8, 3H, -CH_3). **^{13}C NMR** (100 MHz, $CDCl_3$): δ 181.1, 71.6, 55.9, 52.9, 52.2, 49.2,

42.9 (2C), 34.2, 31.7, 30.1, 29.6, 29.5, 29.5, 29.4, 29.2, 27.7, 22.5, 18.9, 18.0, 13.9. HRMS (ESI) calc. for $C_{21}H_{43}O_5NS$ $[M+H]^+$ 422.2935, found 422.2929. LCMS (ESI) found 422.37 for $[M+H]^+$.

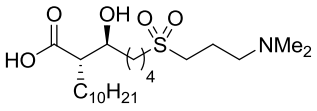

(*S*)-2-((*S*)-5-(3-(dimethylamino)propylsulfonyl)-1-hydroxypentyl)dodecanoic acid (**61**). Compound **61** was synthesized following the general procedure for hydrogenolysis on 1.81 mmol of β-hydroxyester **59,** reaction time 6 hours. Purification by column chromatography using $MeOH/CH_2Cl_2$ 10/90 to first remove unpolar impurities followed by $Et_3N/MeOH/CH_2Cl_2$ 2/10/88 to elute compound **61**. Yield= 77% (white semi-solid). R_f = 0.59 ($AcOH/EtOAc/MeOH/H_2O$ 3/3/3/2). $[\alpha]_D^{20}$= -6.4 (c = 1.0, $MeOH/CH_2Cl_2$ 1/4). IR: 1648 cm^{-1} (acid, C=O stretch), 1270 cm^{-1} (SO_2 asym. stretch), 1134 cm^{-1} (SO_2 sym. stretch). **^{1}H NMR** (400 MHz, $CDCl_3$): δ 3.64 - 3.55 (m, 1H, -C*H*OH), 3.12 – 2.95 (m, 4H, -CH_2SO_2), 2.95-2.83 (m, 2H, -CH_2N(Me)$_2$), 2.55 (s, 6H, -N(CH_3)$_2$), 2.30 - 2.22 (m, 1H, -C*H*COOH), 2.17 (p, *J* = 7.6, 2H), 1.91 - 1.77 (m, 2H), 1.75 - 1.39 (m, 6H), 1.37 - 1.14 (m, 16H), 0.86 (t, *J* = 6.8, 3H). **^{13}C NMR** (100 MHz, $CDCl_3$): δ 181.1, 71.8, 55.9, 52.6, 52.0, 49.6, 43.1 (2C), 35.4, 31.8, 30.2, 29.7, 29.6, 29.6, 29.5, 29.3, 27.8, 24.2, 22.6, 22.2, 18.6, 14.1. HRMS (ESI) calc. for $C_{22}H_{45}O_5NS$ $[M+H]^+$ 436.3091, found 436.3086. LCMS (ESI) found 436.42 for $[M+H]^+$.

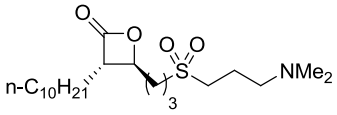

(*3S,4S*)-4-(3-(3-(dimethylamino)propylsulfonyl)propyl)-3-decyloxetan-2-one (**27**). Compound **27** was synthesized following the general procedure for β-lactonization on 1.06 mmol of β-hydroxyacid **60**. Purification by column chromatography (1-5% MeOH/DCM) yield compound **27** as a white solid in 98% yield. R_f = 0.36 ($MeOH/CH_2Cl_2$ 1/9). mp = 85.2- 85.5°C (after recrystallisation from EtOAc/hexane). $[\alpha]_D^{20}$ = -28.2 (c = 0.11, $CHCl_3$). IR: 1798 cm^{-1} (β-lactone, C=O stretch), 1252 cm^{-1} (SO_2 asym. stretch), 1121 cm^{-1} (SO_2 sym. stretch). **^{1}H NMR** (400 MHz, $CDCl_3$): δ 4.20 (ddd, *J* = 4.1, 5.4, 7.5, 1H, -C*H*OCOR), 3.16 (ddd, *J* = 4.0, 6.7, 8.5, 1H, -C*H*CO), 3.06 - 2.94 (m, 4H, -CH_2SO_2), 2.36 (t, *J* = 6.6, 2H, -CH_2NMe$_2$), 2.17 (s, 6H, -N(CH_3)$_2$), 2.02 - 1.61 (m, 8H), 1.45 - 1.13 (m, 16H), 0.82 (t, *J* = 7.0, 3H, -CH_3). **^{13}C NMR** (100 MHz, $CDCl_3$): δ 170.6, 76.9, 57.2, 56.3, 51.9, 50.6, 44.9 (2C), 32.9, 31.7, 29.4, 29.3, 29.1, 29.1 (2C), 27.5, 26.7, 22.5, 19.7, 18.1, 13.9. HRMS (ESI) calc. for $C_{21}H_{41}O_4NS$ $[M+H]^+$ 404.2829, found $[M+H]^+$ 404.2817. LCMS (ESI) found 404.22 for $[M+H]^+$.

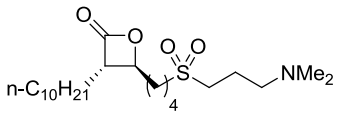

(*3S,4S*)-4-(4-(3-(dimethylamino)propylsulfonyl)butyl)-3-decyloxetan-2-one (palmostatin M, 28). Compound **28** was synthesized following the general procedure for β-lactonization on 0.091 mmol of β-hydroxyacid **61**. Purification by column chromatography (1-5% MeOH/DCM) yield compound **28** as a white solid in 92 % yield. R_f = 0.33 (MeOH/CH_2Cl_2 1/9). mp = 69.1- 69.4°C (after recrystallisation from EtOAc/hexane). $[\alpha]_D^{20}$ = -18.7 (c = 0.2, $CHCl_3$). IR: 1799 cm^{-1} (β-lactone, C=O stretch), 1266 cm^{-1} (SO_2 asym. stretch), 1120 cm^{-1} (SO_2 sym. stretch).**^{1}H NMR** (400 MHz, $CDCl_3$): δ 4.19 (ddd, *J* = 4.0, 5.6, 7.4, 1H, -C*H*OCOR), 3.16 (ddd, *J* = 3.9, 6.7, 8.7, 1H, -C*H*CO), 3.02 - 2.98 (m, 4H, -C$H_2$$SO_2$), 2.40 (t, *J* = 6.6, 2H, -C$H_2$$NMe_2$), 2.21 (s, 6H, -N(C$H_3$)$_2$), 2.02 - 1.49 (m, 8H), 1.44 - 1.16 (m, 18H), 0.85 (t, *J* = 7.0, 3H, -CH_3). **^{13}C NMR** (100 MHz, $CDCl_3$): δ 171.0, 77.3, 57.3, 56.2, 52.4, 50.6, 45.0 (2C), 33.8, 31.8, 29.5, 29.4, 29.2, 29.2 (2C), 27.7, 26.8, 24.2, 22.5, 21.5, 19.7, 14.0. HRMS (ESI) calc. for $C_{22}H_{43}O_4NS$ $[M+H]^+$ 418.2986, found $[M+H]^+$ 418.2981. LCMS (ESI) found 418.27 for $[M+H]^+$.

2.7 Synthesis of *cis* β-lactone inhibitors derived from 27 and 28

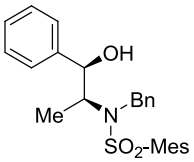

***N*-benzyl-N-((*1R,2S*)-1-hydroxy-1-phenylpropan-2-yl)-2,4,6-trimethylbenzenesulfonamide (62).** Compound **62** was synthesized following the general procedure for ephedrine auxiliary synthesis using 52.9 mmol of (*1R,2S*)-Norephedrine. The mesylated intermediate was obtained in 90% yield as a white solid. R_f =0.53 (EtOAc/cyclohexane 1/1). **^{1}H NMR** (400 MHz, $CDCl_3$): δ 7.34 - 7.20 (m, 5H, Haro), 6.93 (s, 2H, Haro), 4.96 (d, *J* = 8.8, 1H, -C*H*(OH)), 4.74 (d, J = 2.8, 1H, -N*H*), 3.54-3.40 (m, 1H, -C*H*NHR), 2.63 (s, 6H, 2*-C$H_{3,\,Mes}$), 2.27 (s, 3H, -C$H_{3,\,Mes}$), 0.83 (d, *J* = 6.8, 3H, -CH_3). **^{13}C NMR** (100 MHz, $CDCl_3$): δ 142.2, 140.3, 138.9 (2C), 134.2, 131.9 (2C), 128.3 (2C), 127.6, 125.9 (2C), 75.6, 54.5, 22.9 (2C), 20.9, 14.6. (NMR analysis consistent with the literature[8]). Alcohol **62** was obtained in 79 % as a white solid. R_f =0.45 (EtOAc/cyclohexane 2/8). mp= 121-122°C. **^{1}H NMR** (400 MHz, $CDCl_3$): δ 7.36 - 7.15 (m, 8H, Haro), 7.09 – 7.04 (m, 2H, Haro), 6.91 (s, 2H, Haro), 4.97 (brs, 1H,- C*H*(OH)), 4.77 (d, *J* = 16, 1H, -CH_2Bn), 4.54 (d, *J* = 16, 1H, -CH_2Bn), 3.82 (dq, *J* = 1.6,

7.0, 1H, -C*H*NSO$_2$Mes(Bn)), 2.63 (s, 6H, 2*-C$H_{3,\ Mes}$), 2.28 (s, 3H, -C$H_{3,\ Mes}$), 1.03 (d, *J* = 6.8, 3H, -CH_3). **^{13}C NMR** (100 MHz, $CDCl_3$): δ 142.6, 142.1, 140.1 (2C), 138.6, 133.4, 132.1 (2C), 128.5 (2C), 128.1 (2C), 127.7 (2C), 127.3, 127.2, 125.5 (2C), 76.5, 59.6, 49.0, 22.9 (2C), 20.8, 9.9. (NMR analysis consistent with the literature[8]).

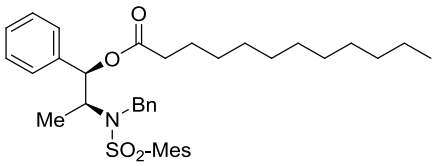

(*1R,2S*)-2-(*N*-benzyl-*N*-mesitylenesulfonyl)amino-1-phenyl-1-propyl dodecanoate (63). Compound **63** was synthesized following the general procedure for *O*-dodecylated ephedrine auxiliary synthesis using 12.0 mmol of compound **62**, reaction time 15 hours. Purification using 2,5% EtOAc/cyclohexane as eluent for the flash chromatography lead to compound **63** in 80% yield (white solid). R_f =0.61 (EtOAc/cyclohexane 2/8). $[\alpha]_D^{20}$ = +22.5 (c = 0.2, $CHCl_3$). mp = 59.9 - 60.2°C (recrystallisation from EtOAc/hexane). IR: 1734 cm^{-1} (ester, C=O stretch). **^{1}H NMR** (400 MHz, $CDCl_3$): δ 7.36 - 7.15 (m, 8H, Haro), 6.92 - 6.84 (m, 4H, Haro), 5.82 (d, *J* = 4.0, 1H, -C*H*OCOR), 4.73 (d, *J* = 16. 4, 1H, -C*H*Ph), 4.58 (d, *J* = 16. 8, 1H, -C*H*Ph), 4.08 - 3.99 (m, 1H, C*H*N(Bn)Mes), 2.51 (s, 6H, CH_3 (Mes)), 2.27 (s, 3H, CH_3 (Mes)), 2.21 - 2.01 (m, 2H), 1.52 - 1.42 (m, 2H), 1.35 - 1.14 (m, 16H), 1.11 (d, *J* = 6.8, 3H, -CH_3), 0.87 (t, *J* = 6.8, 3H, -CH_3). **^{13}C NMR** (100 MHz, $CDCl_3$): δ 172.0, 142.5, 140.2, 138.7, 138.5 133.3, 132.1, 128.4, 128.3, 127.7, 127.3, 127.0, 125.9, 77.9, 56.6, 48.1, 34.2, 31.9, 29.6, 29.4, 29.3, 29.2, 29.0, 24.6, 22.9, 22.7, 20.9, 14.1, 12.8. HRMS (ESI) calc. for $C_{37}H_{51}NO_4S$ $[M+H]^+$ 606.3612, $[M+Na]^+$ 628.3431, found $[M+H]^+$ 606.3607, $[M+Na]^+$ 628.3424. LCMS (ESI) found 605.82 for $[M+H]^+$, found 622.93 for $[M+NH_4]^+$, found 628.20 for $[M+Na]^+$, found 1227.98 for $[2M+NH_4]^+$.

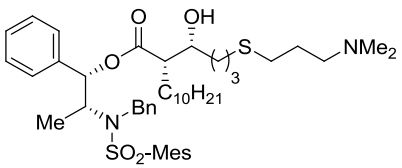

(*2S*)-(*1S,2R*)-2-((*N*-benzyl-*N*-mesitylsulfonyl)amino)-1-phenylpropyl-2-((*R*)-4-(3-(dimethylamino) propylthio)-1-hydroxybutyl) dodecanoate (**64**). Compound **64** was synthesized following the general procedure for *cis*-selective aldol reaction using 4.95 mmol of *O*-dodecylated ephedrine auxiliary **10** followed by purification by flash chromatography using 1-3% MeOH/DCM. Yield = 43 % (slight yellow oil). R_f = 0.41 (10% MeOH/DCM). $[\alpha]_D^{20}$ = +23.4 (c = 1.03, $CHCl_3$). IR: 1735 cm^{-1} (ester, C=O stretch). **^{1}H NMR** (400 MHz, $CDCl_3$): δ 7.30 - 7.11 (m, 8H, Haro),

6.91 - 6.82 (m, 4H, Haro), 5.85 (d, *J* = 5.2, 1H, -C*H*OCOR), 4.69 (d, *J* = 16.4, 1H, -C*H*Ph), 4.48 (d, *J* = 16.4, 1H, -C*H*Ph), 4.18 - 4.09 (m, 1H, -C*H*N(Bn)Mes), 3.70 - 3.62 (m, 1H, -C*H*OH), 2.57 - 2.23 (m, 22H), 1.84 - 1.02 (m, 27H), 0.88 (t, *J* = 7.0, 3H, -CH_3). **^{13}C NMR** (100 MHz, $CDCl_3$): δ 174.2, 142.5, 140.3 (2C), 138.2, 137.9, 133.1, 132.1 (2C), 128.4 (2C), 128.3 (2C), 128.0, 127.7 (2C), 127.2, 126.5 (2C), 78.2, 71.2, 58.4, 56.5, 50.9, 48.2, 45.1 (2C), 33.1, 31.9, 31.8, 29.7, 29.6, 29.6, 29.5, 29.4, 29.3 27.7, 27.2, 27.1, 26.1, 22.9 (2C), 22.7, 20.9, 14.1, 13.9. HRMS (ESI) calc. for $C_{46}H_{70}N_2O_5S_2$ $[M+H]^+$ 795.4799, found $[M+H]^+$ 795.4797. LCMS (ESI) found 795.46 for $[M+H]^+$.

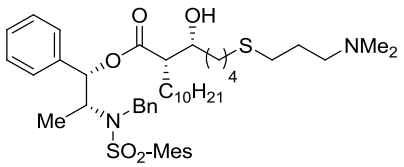

(*2S*)-(*1S,2R*)-2-((*N*-benzyl-*N*-mesitylsulfonyl)amino)-1-phenylpropyl-2-((*R*)-5-(3 (dimethylamino) propylthio)-1-hydroxypentyl) dodecanoate (**65**). Compound **65** was synthesized following the general procedure for *cis*-selective aldol reaction using 4.95 mmol of *O*-dodecylated ephedrine auxiliary **10** followed by purification by flash chromatography using 1-3% MeOH/DCM. Yield = 55 % (slight yellow oil). R_f = 0.41 (10% MeOH/DCM). $[\alpha]_D^{20}$ = -22.7 (c = 1.2, $CHCl_3$). IR: 1734 cm^{-1} (ester, C=O stretch). **^{1}H NMR** (400 MHz, $CDCl_3$): δ 7.29 - 7.20 (m, 8H, Haro), 6.92 - 6.81 (m, 4H, Haro), 5.84 (d, *J* = 5.2, 1H, -C*H*OCOR), 4.69 (d, *J* = 16.4, 1H, -C*H*Ph), 4.48 (d, *J* = 16.4, 1H, -C*H*Ph), 4.23 - 4.08 (m, 1H, -C*H*N(Bn)Mes), 3.72 - 3.57 (m, 1H, -C*H*OH), 2.75 - 2.67 (m, 2H, -CH_2N(Me)$_2$), 2.54 (t, *J* = 6.8, 2H, -CH_2S), 2.51 - 2.47 (m, 8H, -CH_2S, CH_3 (Mes)), 2.44 (s, 6H, N(CH_3)$_2$), 2.34 -2.26 (m, 1H, -C*H*COOR), 2.26 (s, 3H, CH_3 (Mes)), 1.88 (p, *J* = 7.4, 2H), 1.63 - 1.02 (m, 27H), 0.87 (t, *J* = 7.0, 3H, -CH_3). **^{13}C NMR** (100 MHz, $CDCl_3$): δ 174.2, 142.5, 140.2 (2C), 138.2, 137.9, 133.0, 132.0 (2C), 128.3 (2C), 128.2 (2C), 128.0, 127.6 (2C), 127.2, 126.5 (2C), 78.1, 71.5, 58.4, 56.4, 50.9, 48.1, 45.2 (2C), 33.6, 32.0, 31.8, 29.8, 29.5, 29.5, 29.4, 29.3, 29.3, 29.2, 27.7, 27.3, 27.1, 25.2, 22.9 (2C), 22.6, 20.8, 14.1, 13.9. HRMS (ESI) calc. for $C_{47}H_{72}N_2O_5S_2$ $[M+H]^+$ 809.4955, found $[M+H]^+$ 809.4953. LCMS (ESI) found 809.50 for $[M+H]^+$.

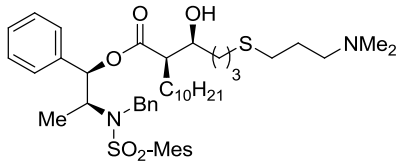

(*2R*)-(*1R,2S*)-2-((*N*-benzyl-*N*-mesitylsulfonyl)amino)-1-phenylpropyl-2-((*S*)-4-(3-(dimethylamino) propylthio)-1-hydroxybutyl) dodecanoate (**66**). Compound **66** was synthesized following the general procedure for *cis*-selective aldol reaction using 4.78 mmol of *O*-

dodecylated ephedrine auxiliary **63** followed by purification by flash chromatography using 1-3% MeOH/DCM. Yield = 36 % (slight yellow oil). R_f = 0.41 (10% MeOH/DCM). $[\alpha]_D^{20}$ = +22.4 (c = 1.3, $CHCl_3$). IR: 1734 cm^{-1} (ester, C=O stretch). **^{1}H NMR** (400 MHz, $CDCl_3$): δ 7.28 - 7.13 (m, 8H, Haro), 6.92 - 6.81 (m, 4H, Haro), 5.85 (d, *J* = 5.2, 1H, -C*H*OCOR), 4.69 (d, *J* = 16.4, 1H, -C*H*Ph), 4.48 (d, *J* = 16.4, 1H, -C*H*Ph), 4.18 - 4.09 (m, 1H, C*H*N(Bn)Mes), 3.70 - 3.62 (m, 1H, -C*H*OH), 2.66 - 2.49 (m, 4H), 2.49 - 2.37 (m, 14H), 2.33 - 2.24 (m, 4H), 1.84 (p, *J* = 7.4, 2H), 1.77 - 1.03 (m, 25H), 0.88 (t, *J* = 6.8, 3H, -CH_3). **^{13}C NMR** (100 MHz, $CDCl_3$): δ 174.2, 142.6, 140.3 (2C), 138.2, 137.9, 133.1, 132.1 (2C), 128.4 (2C), 128.3 (2C), 128.0, 127.7 (2C), 127.2, 126.5 (2C), 78.2, 71.3, 58.1, 56.5, 51.1, 48.2, 44.7 (2C), 33.1, 31.9, 31.8, 29.6, 29.6, 29.5, 29.4, 29.3, 29.2, 27.7, 27.3, 26.3, 26.0, 22.9 (2C), 22.7, 20.9, 14.1, 13.8. HRMS (ESI) calc. for $C_{46}H_{70}N_2O_5S_2$ $[M+H]^+$ 795.4799, found $[M+H]^+$ 795.4797. LCMS (ESI) found 795.44 for $[M+H]^+$.

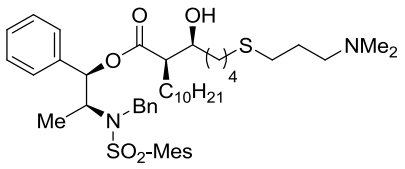

(*2R*)-(*1R,2S*)-2-((*N*-benzyl-*N*-mesitylsulfonyl)amino)-1-phenylpropyl-2-((*S*)-5-(3-(dimethylamino) propylthio)-1-hydroxypentyl) dodecanoate (**67**)**.** Compound **67** was synthesized following the general procedure for *cis*-selective aldol reaction using 4.78 mmol of *O*-dodecylated ephedrine auxiliary **63** followed by purification by flash chromatography using 1-3% MeOH/DCM. Yield = 47 % (slight yellow oil). R_f = 0.41 (10% MeOH/DCM). $[\alpha]_D^{20}$ = +20.2 (c = 1.2, $CHCl_3$). IR: 1732 cm^{-1} (ester, C=O stretch). **^{1}H NMR** (400 MHz, $CDCl_3$): δ 7.27 - 7.12 (m, 8H, Haro), 6.92 - 6.82 (m, 4H, Haro), 5.85 (d, *J* = 4.8, 1H, -C*H*OCOR), 4.69 (d, *J* = 16.4, 1H, -C*H*Ph), 4.48 (d, *J* = 16.4, 1H, -C*H*Ph), 4.19 - 4.10 (m, 1H, -C*H*N(Bn)Mes), 3.70 - 3.62 (m, 1H, -C*H*OH), 3.11-3.02 (m, 2H, -CH_2N(Me)$_2$), 2.78 (s, 6H, CH_3 (Mes)), 2.57 (t, *J* = 6.8, 2H, -CH_2S), 2.49 (t, *J* = 7.0, 2H, -CH_2S), 2.45 (s, 6H, N(CH_3)$_2$), 2.35 - 2.29 (m, 1H, -C*H*COOR), 2.27 (s, 3H, CH_3 (Mes)), 2.04 - 1.95 (m, 2H), 1.62 - 1.01 (m, 27H), 0.88 (t, *J* = 7.0, 3H, -CH_3). **^{13}C NMR** (100 MHz, $CDCl_3$): δ 174.3, 142.7, 140.3 (2C), 138.2, 137.9, 133.1, 132.1 (2C), 128.4 (2C), 128.3 (2C), 128.0, 127.6 (2C), 127.2, 126.4 (2C), 78.3, 71.6, 57.7, 56.6, 51.1, 48.2, 43.9 (2C), 33.5, 31.9, 31.8, 29.6, 29.6, 29.5, 29.4, 29.3, 29.1, 28.6, 27.7, 27.3, 25.1, 24.6, 22.9 (2C), 22.6, 20.8, 14.1, 13.8. HRMS (ESI) calc. for $C_{47}H_{72}N_2O_5S_2$ $[M+H]^+$ 809.4955, found $[M+H]^+$ 809.4953. LCMS (ESI) found 809.48 for $[M+H]^+$.

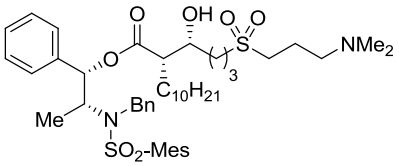

(*S*)-((*1S,2R*)-2-((*N*-benzyl-*N*-mesitylsulfonyl)amino)-1-phenylpropyl)-2-((*R*)-4-(3-(dimethylamino) propylsulfonyl)-1-hydroxybutyl) dodecanoate (**68**)**.** Compound **68** was synthesized following the general procedure for oxidation into sulfone using 1.69 mmol of sulfide derivative **64**, reaction time 8 hours (no purification). Yield = 96 % (slight yellow oil). R_f = 0.41 (10% MeOH/DCM). $[\alpha]_D^{20}$ = - 15.8 (c = 1.1, $CHCl_3$). IR: 1734 cm^{-1} (ester, C=O stretch), 1314 cm^{-1} (SO_2 asym. stretch), 1150 cm^{-1} (SO_2 sym. Stretch). **^{1}H NMR** (400 MHz, $CDCl_3$): δ 7.26 - 7.13 (m, 8H, Haro), 6.95 - 6.80 (m, 4H, Haro), 5.89 (d, *J* = 5.2, 1H, -C*H*OCOR), 4.69 (d, *J* = 16.4, 1H, -C*H*Ph), 4.48 (d, *J* = 16.4, 1H, -C*H*Ph), 4.23 - 4.08 (m, 1H, -C*H*N(Bn)Mes), 3.71 - 3.62 (m, 1H, -C*H*OH), 3.04 - 2.84 (m, 4H, -C$H_2$$SO_2$), 2.50 (t, *J* = 7.0, 2H, -CH_2N(Me)$_2$), 2.45 (s, 6H, CH_3 (Mes)), 2.29 (s, 6H, N(CH_3)$_2$), 2.28 -2.24 (m, 4H, CH_3 (Mes), -C*H*COOR), 2.09 – 0.99 (m, 27H), 0.88 (t, *J* = 7.0, 3H, -CH_3). **^{13}C NMR** (100 MHz, $CDCl_3$): δ 173.9, 142.6, 140.2 (2C), 138.0, 137.8, 132.9, 132.1 (2C), 128.4 (2C), 128.3 (2C), 128.1, 127.6 (2C), 127.3, 126.5 (2C), 78.1, 70.9, 57.1, 56.5, 52.5, 51.1, 49.9, 48.1, 44.7 (2C), 32.3, 31.9 (2C), 29.6 (2C), 29.5, 29.4, 29.3, 27.7, 27.3, 22.9, 22.7, 20.9, 19.3, 19.1, 14.1, 13.9. HRMS (ESI) calc. for $C_{46}H_{70}N_2O_7S_2$ $[M+H]^+$ 827.4697, $[M+Na]^+$ 849.4516, found $[M+H]^+$ 827.4696, $[M+Na]^+$ 849.4508. LCMS (ESI) found 827.43 for $[M+H]^+$.

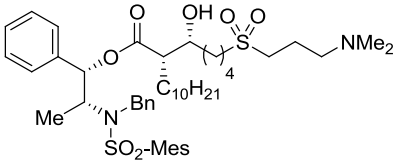

(*S*)-((*1S,2R*)-2-((*N*-benzyl-*N*-mesitylsulfonyl)amino)-1-phenylpropyl)-2-((*R*)-5-(3-(dimethylamino) propylsulfonyl)-1-hydroxypentyl) dodecanoate (**69**). Compound **69** was synthesized following the general procedure for oxidation into sulfone using 1.31 mmol of sulfide derivative **65**, reaction time 8 hours (no purification). Yield = 92 % (slight yellow oil). R_f = 0.39 (10% MeOH/DCM). $[\alpha]_D^{20}$ = - 16.4 (c = 1.0, $CHCl_3$). IR: 1734 cm^{-1} (ester, C=O stretch), 1315 cm^{-1} (SO_2 asym. stretch), 1151 cm^{-1} (SO_2 sym. Stretch). **^{1}H NMR** (400 MHz, $CDCl_3$): δ 7.28 - 7.12 (m, 8H, Haro), 6.93 - 6.81 (m, 4H, Haro), 5.88 (d, *J* = 5.2, 1H, -C*H*OCOR), 4.69 (d, *J* = 16.4, 1H, -C*H*Ph), 4.48 (d, *J* = 16.4, 1H, -C*H*Ph), 4.20 - 4.08 (m, 1H, -C*H*N(Bn)Mes), 3.68 - 3.61 (m, 1H, -C*H*OH), 3.10 - 2.90 (m, 4H, -C$H_2$$SO_2$), 2.60 (t, *J* = 7.0, 2H, -CH_2N(Me)$_2$), 2.45 (s, 6H, CH_3 (Mes)), 2.36 (s, 6H, N(CH_3)$_2$), 2.30 - 2.24 (m, 4H, CH_3 (Mes), -C*H*COOR), 2.13 – 1.01 (m, 29H), 0.88 (t, *J* = 7.0, 3H, -CH_3). **^{13}C NMR** (100 MHz, $CDCl_3$): δ 174.1, 142.6, 140.2 (2C), 138.1, 137.8, 132.9, 132.1

(2C), 128.4 (2C), 128.3 (2C), 128.1, 127.6 (2C), 127.2, 126.5 (2C), 78.1, 71.2, 57.1, 56.4, 52.9, 50.9, 49.9, 48.1, 44.6 (2C), 33.2, 31.8 (2C), 29.6, 29.5, 29.5, 29.4, 29.3, 27.7, 27.2, 25.0, 22.9, 22.6, 21.7, 20.9, 19.1, 14.1, 13.9. HRMS (ESI) calc. for $C_{47}H_{72}N_2O_7S_2$ $[M+H]^+$ 841.4854, $[M+Na]^+$ 863.4673, found $[M+H]^+$ 841.4853, $[M+Na]^+$ 863.4663. LCMS (ESI) found 841.46 for $[M+H]^+$.

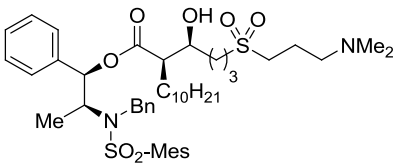

(*R*)-((*1R,2S*)-2-((*N*-benzyl-*N*-mesitylsulfonyl)amino)-1-phenylpropyl)-2-((*S*)-4-(3-(dimethylamino) propylsulfonyl)-1-hydroxybutyl) dodecanoate (**70**). Compound **70** was synthesized following the general procedure for oxidation into sulfone using 1.73 mmol of sulfide derivative **66**, reaction time 8 hours (no purification). Yield = 98 % (slight yellow oil). R_f = 0.40 (10% MeOH/DCM). $[\alpha]_D^{20}$ = + 15.7 (c = 1.05, $CHCl_3$). IR: 1733 cm^{-1} (ester, C=O stretch), 1313 cm^{-1} (SO_2 asym. stretch), 1150 cm^{-1} (SO_2 sym. Stretch). **^{1}H NMR** (400 MHz, $CDCl_3$): δ 7.27 - 7.13 (m, 8H, Haro), 6.96 - 6.81 (m, 4H, Haro), 5.89 (d, *J* = 4.8, 1H, -C*H*OCOR), 4.69 (d, *J* = 16.4, 1H, -C*H*Ph), 4.48 (d, *J* = 16.4, 1H, -C*H*Ph), 4.23 - 4.09 (m, 1H, -C*H*N(Bn)Mes), 3.68 - 3.61 (m, 1H, -C*H*OH), 3.08 - 2.85 (m, 4H, -C$H_2$$SO_2$), 2.61 (t, *J* = 7.0, 2H, -CH_2N$(Me)_2$), 2.45 (s, 6H, CH_3 (Mes)), 2.37 (s, 6H, N(CH_3)$_2$), 2.31 - 2.24 (m, 4H, CH_3 (Mes), -C*H*COOR), 2.18 - 1.01 (m, 27H), 0.88 (t, *J* = 7.0, 3H, -CH_3). **^{13}C NMR** (100 MHz, $CDCl_3$): δ 173.9, 142.6, 140.2 (2C), 138.0, 137.8, 132.9, 132.1 (2C), 128.4 (2C), 128.3 (2C), 128.1, 127.6 (2C), 127.3, 126.5 (2C), 78.1, 70.9, 57.0, 56.5, 52.5, 51.1, 49.8, 48.1, 44.6 (2C), 32.3, 31.9 (2C), 29.6 (2C), 29.5, 29.4, 29.3, 27.7, 27.3, 22.9, 22.7, 21.4, 20.9, 19.1, 14.1, 13.9. HRMS (ESI) calc. for $C_{46}H_{70}N_2O_7S_2$ $[M+H]^+$ 827.4697, found $[M+H]^+$ 827.4695. LCMS (ESI) found 827.43 for $[M+H]^+$.

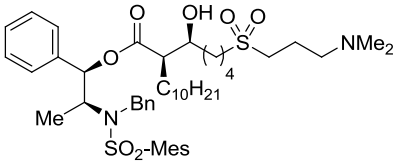

(*R*)-((*1R,2S*)-2-((*N*-benzyl-*N*-mesitylsulfonyl)amino)-1-phenylpropyl)-2-((*S*)-5-(3-(dimethylamino) propylsulfonyl)-1-hydroxypentyl) dodecanoate (**71**). Compound **71** was synthesized following the general procedure for oxidation into sulfone using 2.24 mmol of sulfide derivative **67**, reaction time 8 hours (no purification). Yield = 81% (slight yellow oil). R_f = 0.39 (10% MeOH/DCM). $[\alpha]_D^{20}$ = +18.3 (c = 1.3, $CHCl_3$). IR: 1733 cm^{-1} (ester, C=O stretch), 1315 cm^{-1} (SO_2 asym. stretch), 1150 cm^{-1} (SO_2 sym. Stretch). **^{1}H NMR** (400 MHz, $CDCl_3$): δ 7.27 - 7.11

(m, 8H, Haro), 6.91 - 6.81 (m, 4H, Haro), 5.88 (d, *J* = 5.2, 1H, -C*H*OCOR), 4.69 (d, *J* = 16.4, 1H, -C*H*Ph), 4.48 (d, *J* = 16.4, 1H, -C*H*Ph), 4.22 - 4.11 (m, 1H, -C*H*N(Bn)Mes), 3.68 - 3.61 (m, 1H, -C*H*OH), 3.10 - 2.96 (m, 4H, -C$H_2$$SO_2$), 2.57 (t, *J* = 6.8, 2H, -CH_2N(Me)$_2$), 2.45 (s, 6H, CH_3 (Mes)), 2.34 (s, 6H, N(CH_3)$_2$), 2.30 - 2.24 (m, 4H, CH_3 (Mes), -C*H*COOR), 2.04 (p, *J* = 7.4, 2H), 1.90 – 1.02 (m, 27H), 0.88 (t, *J* = 7.0, 3H, -CH_3). **^{13}C NMR** (100 MHz, $CDCl_3$): δ 174.1, 142.6, 140.2 (2C), 138.1, 137.8, 132.9, 132.1 (2C), 128.4 (2C), 128.3 (2C), 128.1, 127.6 (2C), 127.2, 126.5 (2C), 78.2, 71.2, 57.2, 56.4, 52.9, 50.9, 50.1, 48.1, 44.8 (2C), 33.2, 31.8 (2C), 29.6, 29.5, 29.5, 29.4, 29.3, 27.7, 27.1, 25.0, 22.9, 22.6, 21.7, 20.8, 19.2, 14.1, 13.8. HRMS (ESI) calc. for $C_{47}H_{72}N_2O_7S_2$ $[M+H]^+$ 841.4854, found $[M+H]^+$ 841.4853. LCMS (ESI) found 841.46 for $[M+H]^+$.

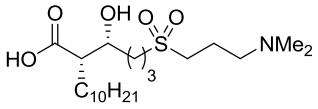

(*S*)-2-((*R*)-4-(3-(dimethylamino)propylsulfonyl)-1-hydroxybutyl)dodecanoic acid (72). Compound **72** was synthesized following the general procedure for hydrogenolysis using 1.61 mmol substrate **68**, reaction time 90 hours at rt. Purification by flash chromatography using 10% MeOH/DCM to first remove unpolar impurities, then MeOH/ DCM /NEt_3 10/88/2 to elute compound **72** (Column monitored by TLC using EtOAc/AcOH/MeOH/H_2O 3/3/3/2 as eluent). Yield = 29% (white solid). R_f = 0.72 (EtOAc/AcOH/MeOH/H_2O 6/3/3/2). $[\alpha]_D^{20}$ = - 2.9 (c = 1.06, $CHCl_3$/MeOH 1/1). IR: 1600 cm^{-1} (acid, C=O stretch), 1273 cm^{-1} (SO_2 asym. stretch), 1134 cm^{-1} (SO_2 sym. stretch). **^{1}H NMR** (400 MHz, $CDCl_3$): δ 3.84 - 3.77 (m, 1H, -C*H*OH), 3.18 - 3.01 (m, 4H, -C$H_2$$SO_2$), 2.95 - 2.83 (m, 2H, -CH_2N(Me)$_2$), 2.58 (s, 6H, -N(CH_3)$_2$), 2.45 - 2.37 (m, 1H, -C*H*COOH), 2.24 - 2.12 (m, 2H), 2.09 - 1.90 (m, 2H), 1.76 - 1.17 (m, 20H), 0.87 (t, *J* = 6.8, 3H, -CH_3). **^{13}C NMR** (100 MHz, $CDCl_3$): δ 180.0, 71.7, 56.0, 52.9, 52.2, 49.6, 43.2 (2C), 31.9, 31.8, 29.8, 29.6, 29.6, 29.5, 29.3, 28.1, 27.9, 22.6, 19.4, 18.5, 14.1. HRMS (ESI) calc. for $C_{21}H_{43}NO_5S$ $[M+H]^+$ 422.2935, found $[M+H]^+$ 422. 2929. LCMS (ESI) found 422.28 for $[M+H]^+$.

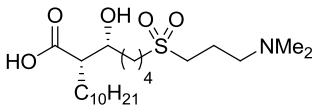

(*S*)-2-((*R*)-5-(3-(dimethylamino)propylsulfonyl)-1-hydroxypentyl)dodecanoic acid (**73**)**.** Compound **73** was synthesized following the general procedure for hydrogenolysis using 1.20 mmol substrate **69**, reaction time 90 hours at rt. Purification by flash chromatography using 10% MeOH/DCM to first remove unpolar impurities, then MeOH/ DCM /NEt_3 10/88/2 to elute compound **73** (Column monitored by TLC using EtOAc/AcOH/MeOH/H_2O 3/3/3/2 as eluent).Yield

= 79% (white solid). R_f = 0.46 (EtOAc/AcOH/MeOH/H_2O 6/3/3/2). $[\alpha]_D^{20}$ = + 3.6 (c = 1.04, $CHCl_3$). IR: 1615 cm^{-1} (acid, C=O stretch), 1277 cm^{-1} (SO_2 asym. stretch), 1130cm^{-1} (SO_2 sym. stretch). **^{1}H NMR** (400 MHz, $CDCl_3$): δ 3.76 - 3.69 (m, 1H, -C*H*OH), 3.10 - 2.96 (m, 4H, -CH_2SO_2), 2.93 -2.78 (m, 2H, -CH_2N(Me)$_2$), 2.53 (s, 6H, -N(CH_3)$_2$), 2.40 - 2.34 (m, 1H, -C*H*COOH), 2.20 - 2.07 (m, 2H), 1.98 - 1.75 (m, 2H), 1.71 - 1.17 (m, 22H), 0.87 (t, *J* = 7.0, 3H, -CH_3). **^{13}C NMR** (100 MHz, $CDCl_3$): δ 180.2, 71.9, 55.9, 52.3 (2C), 49.6, 43.2 (2C), 32.9, 31.9, 29.8, 29.7, 29.6, 29.6, 29.3, 28.1, 27.7, 24.3, 22.7, 22.1, 19.0, 14.1. HRMS (ESI) calc. for $C_{22}H_{45}NO_5S$ $[M+H]^+$ 436.3091, found $[M+H]^+$ 436.3085. LCMS (ESI) found 436.31 for $[M+H]^+$.

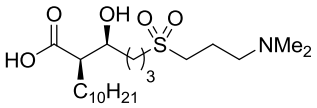

(*R*)-2-((*S*)-4-(3-(dimethylamino)propylsulfonyl)-1-hydroxybutyl)dodecanoic acid (**74**). Compound **74** was synthesized following the general procedure for hydrogenolysis using 1.69 mmol substrate **70**, reaction time 90 hours at rt. Purification by flash chromatography using 10% MeOH/DCM to first remove unpolar impurities, then MeOH/ DCM /NEt_3 10/88/2 to elute compound **74** (Column monitored by TLC using EtOAc/AcOH/MeOH/H_2O 3/3/3/2 as eluent). Yield = 65% (white solid). R_f = 0.63 (EtOAc/AcOH/MeOH/H_2O 6/3/3/2). $[\alpha]_D^{20}$ = + 1.7 (c = 1.04, $CHCl_3$/MeOH 1/1). IR: 1599 cm^{-1} (acid, C=O stretch), 1280 cm^{-1} (SO_2 asym. stretch), 1111 cm^{-1} (SO_2 sym. stretch). **^{1}H NMR** (400 MHz, $CDCl_3$): δ 3.83 - 3.78 (m, 1H, -C*H*OH), 3.18 - 3.01 (m, 4H, -CH_2SO_2), 2.95 - 2.83 (m, 2H, -CH_2N(Me)$_2$), 2.57 (s, 6H, -N(CH_3)$_2$), 2.37 - 2.30 (m, 1H, -C*H*COOH), 2.19 - 2.09 (m, 2H), 2.07 - 1.83 (m, 2H), 1.68 - 1.17 (m, 20H), 0.84 (t, *J* = 6.8, 3H, -CH_3). **^{13}C NMR** (100 MHz, $CDCl_3$): δ 180.1, 71.5, 56.0, 52.8, 52.4, 49.5, 43.2 (2C), 32.0, 31.9, 29.8, 29.6, 29.6, 29.5, 29.3, 28.0, 28.0, 22.6, 19.2, 18.4, 14.0. HRMS (ESI) calc. for $C_{21}H_{43}NO_5S$ $[M+H]^+$ 422.2935, found $[M+H]^+$ 422.2929. LCMS (ESI) found 422.29 for $[M+H]^+$.

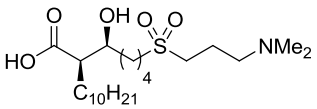

(*R*)-2-((*S*)-5-(3-(dimethylamino)propylsulfonyl)-1-hydroxypentyl)dodecanoic acid (**75**). Compound **75** was synthesized following the general procedure for hydrogenolysis using 1.81 mmol substrate **71**, reaction time 90 hours at rt. Purification by flash chromatography using 10% MeOH/DCM to remove unpolar impurities, then MeOH/DCM/NEt_3 10/88/2 to elute compound **75** (Column monitored by TLC using EtOAc/AcOH/MeOH/H_2O 3/3/3/2 as eluent). Yield = 74% (white solid). R_f = 0.51 (EtOAc/AcOH/MeOH/H_2O 6/3/3/2). $[\alpha]_D^{20}$ = - 3.8 (c = 1.06, $CHCl_3$). IR:

1614 cm^{-1} (acid, C=O stretch), 1277 cm^{-1} (SO_2 asym. stretch), 1129 cm^{-1} (SO_2 sym. stretch). **^{1}H NMR** (400 MHz, $CDCl_3$): δ 3.76 - 3.69 (m, 1H, -C*H*OH), 3.10 - 2.96 (m, 4H, -CH_2SO_2), 2.93 -2.77 (m, 2H, -CH_2N(Me)$_2$), 2.54 (s, 6H, -N(CH_3)$_2$), 2.40 - 2.34 (m, 1H, -C*H*COOH), 2.20 - 2.07 (m, 2H), 1.98 - 1.75 (m, 2H), 1.71 - 1.17 (m, 22H), 0.87 (t, *J* = 6.8, 3H, -CH_3). **^{13}C NMR** (100 MHz, $CDCl_3$): δ 180.3, 71.9, 55.8, 52.3 (2C), 49.6, 43.1 (2C), 32.9, 31.9, 29.8, 29.7, 29.6, 29.6, 29.3, 28.1, 27.8, 24.3, 22.7, 22.1, 18.9, 14.1. HRMS (ESI) calc. for $C_{22}H_{45}NO_5S$ $[M+H]^+$ 436.3091, found $[M+H]^+$ 436.3085. LCMS (ESI) found 436.32 for $[M+H]^+$.

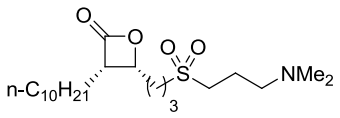

(*3S,4R*)-4-(3-(3-(dimethylamino)propylsulfonyl)propyl)-3-decyloxetan-2-one (**76**). Compound **76** was synthesized following the general procedure for β-lactonization using 0.37 mmol of β-hydroxyacid **72.** Reaction uncomplete, with a ratio *trans/cis* β-lactone 1:1. Purification by flash chromatography using 1-5 % MeOH/DCM, followed by several recrystalization in EtOAc/pentane. Yield = 23 % (yield low due to a ratio 1:1 *cis*/*trans* β-lactone). White solid. R_f = 0.52 (10% MeOH/DCM). mp = 54.8°C- 55.3°C. $[\alpha]_D^{20}$ not measured as final product not enantiopure (*cis*/*trans* β-lactone 1:0.2). IR: 1814 cm^{-1} (β-lactone, C=O stretch), 1279 cm^{-1} (SO_2 asym. stretch), 1118cm^{-1} (SO_2 sym. Stretch). **^{1}H NMR** (400 MHz, $CDCl_3$): δ 4.53 (ddd, *J* = 3.0, 6.4, 9.7, 1H, -C*H*OCOR), 3.67 (ddd, *J* = 6.9, 6.9, 8.9, 1H, -C*H*CO), 3.19 - 2.98 (m, 4H, -CH_2SO_2), 2.72 - 2.57 (m, 2H, -CH_2NMe$_2$), 2.39 (s, 6H, -N(CH_3)$_2$), 1.21 - 1.43 (m, 8H), 1.45 - 1.20 (m, 16H), 0.87 (t, *J* = 6.8, 3H, -CH_3). **^{13}C NMR** (100 MHz, $CDCl_3$): δ 171.4, 74.8, 56.7, 53.1, 52.5, 49.9, 43.9 (2C), 31.9, 29.5, 29.5, 29.3, 29.3 (2C), 28.9, 27.5, 23.9, 22.7, 18.7, 18.4, 14.1. HRMS (ESI) calc. for $C_{21}H_{41}NO_4S$ $[M+H]^+$ 404.2829, found $[M+H]^+$ 404.2822. LCMS (ESI) found 404.09 for $[M+H]^+$.

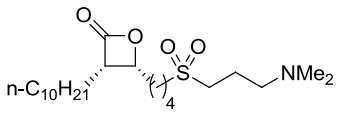

(*3S,4R*)-4-(4-(3-(dimethylamino)propylsulfonyl)butyl)-3-decyloxetan-2-one (77). Compound **77** was synthesized following the general procedure for β-lactonization using 0.82 mmol of β-hydroxyacid **73.** Reaction uncomplete, with *cis* β-lactone as main product. Purification by flash chromatography using 1-5 % MeOH/DCM, followed by several recrystalization in EtOAc/hexane. Yield = 46 % (slight yellow solid). R_f = 0.58 (10% MeOH/DCM). mp = 36.5°C-36.8°C. $[\alpha]_D^{20}$ not measured as final product not enantiopure (*cis*/*trans* β-lactone 1: 0.1). IR: 1811 cm^{-1} (β-lactone,

C=O stretch), 1272 cm^{-1} (SO_2 asym. stretch), 1126 cm^{-1} (SO_2 sym. Stretch). **^{1}H NMR** (400 MHz, $CDCl_3$): δ 4.53 (ddd, *J* = 3.9, 6.4, 9.7, 1H, -C*H*OCOR), 3.62 (ddd, *J* = 6.6, 6.6, 8.1, 1H, -C*H*CO), 3.05 (t, *J* = 7.7, 2H, -CH_2SO_2), 2.98 (t, *J* = 8.0, 2H, -CH_2SO_2), 2.43 (t, *J* = 6.5, 2H, -CH_2NMe_2), 2.24 (s, 6H, -N(CH_3)$_2$), 2.08 - 1.42 (m, 10H), 1.40 - 1.17 (m, 16H), 0.87 (t, *J* = 7.0, 3H, -CH_3). **^{13}C NMR** (100 MHz, $CDCl_3$): δ 171.7, 74.9, 57.4, 52.9, 52.7, 50.7, 45.1 (2C), 31.8, 29.7, 29.5, 29.5, 29.3, 29.3, 29.3, 27.6, 24.7, 23.9, 22.6, 21.6, 19.7, 14.1. HRMS (ESI) calc. for $C_{22}H_{43}NO_4S$ $[M+H]^+$ 418. 2986, found $[M+H]^+$ 418.2980. LCMS (ESI) found 418.11 for $[M+H]^+$.

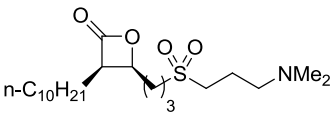

(*3R,4S*)-4-(3-(3-(dimethylamino)propylsulfonyl)propyl)-3-decyloxetan-2-one (**78**). Compound **78** was synthesized following the general procedure for β-lactonization using 0.98 mmol of β-hydroxyacid **74.** Reaction uncomplete, with *cis* β-lactone as main product. Purification by flash chromatography using 1-5 % MeOH/DCM, followed by several recrystalization in EtOAc/hexane. Yield = 55 % (slight yellow solid). R_f = 0.55 (10% MeOH/DCM). mp = 61.9°C-62.2°C. $[\alpha]_D^{20}$ not measured as final product not enantiopure (*cis*/*trans* β-lactone 1:0.2). IR: 1808 cm^{-1} (β-lactone, C=O stretch), 1270 cm^{-1} (SO_2 asym. stretch), 1127 cm^{-1} (SO_2 sym. Stretch). **^{1}H NMR** (400 MHz, $CDCl_3$): δ 4.52 (ddd, *J* = 3.1, 6.4, 9.9, 1H, -C*H*OCOR), 3.62 (ddd, *J* = 6.9, 6.9, 9.1, 1H, -C*H*CO), 3.11 - 2.91 (m, 4H, -CH_2SO_2), 2.36 (t, *J* = 6.8, 2H, -CH_2NMe_2), 2.17 (s, 6H, -N(CH_3)$_2$), 2.07 -1.39 (m, 8H), 1.38 - 1.15 (m, 16H), 0.83 (t, *J* = 7.0, 3H, -CH_3). **^{13}C NMR** (100 MHz, $CDCl_3$): δ 171.4, 74.6, 57.2, 52.9, 51.9, 50.6, 44.9 (2C), 31.7, 29.4, 29.3, 29.2, 29.1 (2C), 28.8, 27.3, 23.8, 22.5, 19.6, 18.6, 13.9. HRMS (ESI) calc. for $C_{21}H_{41}NO_4S$ $[M+H]^+$ 404.2829, found $[M+H]^+$ 404.2822. LCMS (ESI) found 404.07 for $[M+H]^+$.

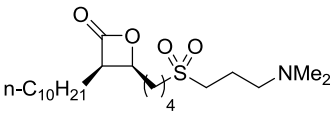

(*3R,4S*)-4-(4-(3-(dimethylamino)propylsulfonyl)butyl)-3-decyloxetan-2-one (**79**)**.** Compound **79** was synthesized following the general procedure for β-lactonization using 1.17 mmol of β-hydroxyacid **75**. Reaction uncomplete, with a ratio *trans/cis* β-lactone 1:1. Purification by flash chromatography using 1-5 % MeOH/DCM followed by several recrystalization in EtOAc/pentane. Yield = 13 % (yield low due to a ratio 1:1 *cis*/*trans* β-lactone).White solid. R_f = 0.52 (10% MeOH/DCM). mp = 34.9-35.2°C. $[\alpha]_D^{20}$ not measured as final product not enantiopure (*cis*/*trans*

β-lactone 1:0.2). IR: 1812 cm^{-1} (β-lactone, C=O stretch), 1272 cm^{-1} (SO_2 asym. stretch), 1127 cm^{-1} (SO_2 sym. Stretch). **^{1}H NMR** (400 MHz, $CDCl_3$): δ 4.53 (ddd, *J* = 3.9, 6.4, 9.8, 1H, -C*H*OCOR), 3.62 (ddd, *J* = 7.1, 7.1, 8.5, 1H, -C*H*CO), 3.06 (t, *J* = 7.7, 2H, -CH_2SO_2), 2.99 (t, *J* = 7.7, 2H, -CH_2SO_2), 2.46 (t, *J* = 6.7, 2H, -CH_2NMe_2), 2.26 (s, 6H, -N(CH_3)$_2$), 2.05 - 1.47 (m, 10H), 1.38 - 1.16 (m, 16H), 0.87 (t, *J* = 6.7, 3H, -CH_3). **^{13}C NMR** (100 MHz, $CDCl_3$): δ 171.7, 74.9, 57.3, 52.8, 52.7, 50.6, 45.0 (2C), 31.8, 29.7, 29.5, 29.5, 29.3, 29.3, 29.2, 27.6, 24.7, 23.9, 22.6, 21.6, 19.6, 14.0. HRMS (ESI) calc. for $C_{22}H_{43}NO_4S$ $[M+H]^+$ 418.2985, found $[M+H]^+$ 418.2981. LCMS (ESI) found 418.12 for $[M+H]^+$.

2.8 Synthesis of palmostatin M-derived pull down probe 83

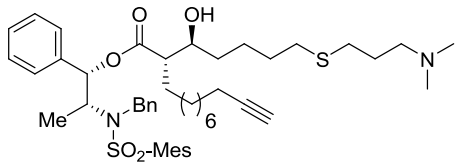

(*S*)-((*1S,2R*)-2-(*N*-benzyl-2,4,6-trimethylphenylsulfonamido)-1-phenylpropyl)2-((*S*)-5-(3-(dimethyl amino)propylthio)-1-hydroxypentyl)dodec-11-ynoate (**80**). Compound **80** was synthesized following the general procedure for the *anti*-selective aldol reaction using 10.40 mmol of aldehyde **55**, followed by purification by flash chromatography using 1-3% $MeOH/CH_2Cl_2$. Yield = 66% (yellow oil). R_f = 0.65 ($MeOH/CH_2Cl_2$ 10/90). $[\alpha]_D^{20}$ = - 38.4 (c = 0.18, $CHCl_3$). IR: 3304 cm^{-1} (C≡C-H stretch), 2116 cm^{-1} (-C≡C- stretch), 1736 cm^{-1} (ester, C=O stretch). **^{1}H NMR** (400 MHz, $CDCl_3$): δ 7.20 – 7.09 (m, 8H, Haro), 6.87 - 6.81 (m, 4H, Haro), 5.82 (d, *J* = 5.6, 1H, -C*H*OCOR), 4.69 (d, *J* = 16.4, 1H, -C*H*Ph), 4.48 (d, *J* = 16.4, 1H, -C*H*Ph), 4.13 – 4.07 (m, 1H, -C*H*N(Bn)Mes), 3.68 - 3.61 (m, 1H, -C*H*OH), 2.56 - 2.44 (m, 6H, -CH_2N(Me)$_2$, -CH_2S), 2.44 - 2.38 (m, 7H, -C*H*COOR, CH_3 (Mes)), 2.31 (s, 6H, N(CH_3)$_2$), 2.27 (s, 3H, CH_3 (Mes)), 2.14 (dt, *J* = 2.8, 7.2, 2H, -CH_2-C≡C), 1.93 (t, *J* = 2.8, 1H, -C≡C*H*), 1.78 (p, *J* = 7.2, 2H), 1.61 - 0.95 (m, 23H). **^{13}C NMR** (100 MHz, $CDCl_3$): δ 174.4, 142.5, 140.3, 138.3, 137.8, 133.1, 132.0, 128.3, 128.2, 128.0, 127.9, 127.2, 126.6, 84.6, 77.9, 71.9, 68.1, 58.3, 56.3, 51.3, 48.1, 45.0, 34.7 32.0, 29.7, 29.6, 29.4, 29.4, 29.1, 28.8, 28.6, 28.4, 27.0, 24.7, 22.8, 20.8, 18.3, 14.4. HRMS (ESI) calc. for $C_{47}H_{68}N_2O_5S_2$ $[M+H]^+$ 805.4642, found 805.4639. LCMS (ESI) found 805.29 for $[M+H]^+$.

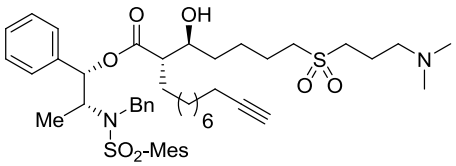

(*S*)-((*1S,2R*)-2-(*N*-benzyl-2,4,6-trimethylphenylsulfonamido)-1-phenylpropyl)2-((*S*)-5-(3-(dimethyl amino)propylsulfonyl)-1-hydroxypentyl) dodec-11-ynoate (**81**). Compound **81** was synthesized following the general procedure for oxidation into sulfone using 5.04 mmol of sulfide derivative **80**, reaction time 8 hours. Yield = quantitative (white semi-solid). R_f = 0.55 ($MeOH/CH_2Cl_2$ 10/90). $[\alpha]_D^{20}$= - 29.7 (c = 0.62, $CHCl_3$). IR: 3284 cm^{-1} (C≡C-H stretch), 2115 cm^{-1} (-C≡C- stretch), 1734 cm^{-1} (ester, C=O stretch), 1314 cm^{-1} (SO_2 asym. stretch), 1150cm^{-1} (SO_2 sym. Stretch). **^{1}H NMR** (400 MHz, $CDCl_3$): δ 7.26 - 7.11 (m, 8H, Haro), 6.89 - 6.80 (m, 4H, Haro), 5.86 (d, *J* = 5.6, 1H, -C*H*OCOR), 4.74 (d, *J* = 16.8, 1H, -C*H*Ph), 4.55 (d, *J* = 16.6, 1H, -C*H*Ph), 4.23 - 4.15 (m, 1H, -C*H*N(Bn)Mes), 3.69 - 3.61 (m, 1H, -C*H*OH), 3.02 (t, *J* = 7.6, 2H, -CH_2SO_2), 2.94 (t, *J* = 8.0, 2H, -CH_2SO_2), 2.52 (t, *J* = 7.0, 2H, -CH_2N(Me)$_2$), 2.45 - 2.39 (m, 7H, -C*H*COOR, CH_3 (Mes)), 2.31 (s, 6H, N(CH_3)$_2$), 2.26 (s, 3H, CH_3 (Mes)), 2.16 (dt, *J* = 2.4, 6.8, 2H, -CH_2-C≡C), 2.07 - 1.97 (m, 2H), 1.93 (t, *J* = 2.4, 1H, -C≡C*H*), 1.89 - 0.95 (m, 23H). **^{13}C NMR** (100 MHz, $CDCl_3$): δ 174.3, 142.5, 140.3,138.1, 137.8, 133.1, 132.0, 128.3, 128.3, 128.1, 127.9, 127.3, 126.7, 84.7, 78.1, 71.6, 68.1, 57.3, 56.4, 52.9, 51.4, 50.2, 48.1, 44.9, 34.3, 29.5, 29.4, 29.1, 28.9, 28.6, 28.4, 27.0, 24.6, 22.9, 21.9, 20.8, 19.4, 18.3, 14.4. HRMS (ESI) calc. for $C_{47}H_{68}N_2O_7S_2$ $[M+H]^+$ 837.4541, found 837.4538. LCMS (ESI) found 837.26 for $[M+H]^+$.

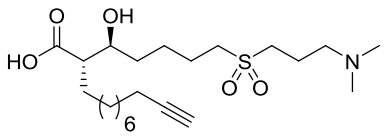

(*S*)-2-((*S*)-5-(3-(dimethylamino)propylsulfonyl)-1-hydroxypentyl) dodec-11-ynoic acid (**82**). Compound **82** was synthesized following the general procedure for saponification using 5.01 mmol of -hydroxyester **81** by reaction with 4.3 eqv. $LiOH\cdot H_2O$ at 40°C for 48 hours. Purification by flash chromatography using 10% $MeOH/CH_2Cl_2$ to remove unpolar impurities, then $MeOH/CH_2Cl_2/NEt_3$ 10/88/2 to collect compound **82** (separation monitored by TLC using EtOAc/AcOH/MeOH/H_2O 3/3/3/2 as eluent). Yield = 85% (white semi-solid). R_f = 0.28 (AcOH/ EtOAc/MeOH/H_2O 3/14/3/2). $[\alpha]_D^{20}$ not measured as contained some residual NEt_3. IR: 3306 cm^{-1} (C≡C-H stretch), 2114 cm^{-1} (-C≡C- stretch), 1628 cm^{-1} (acid, C=O stretch), 1270 cm^{-1} (SO_2 asym. stretch), 1132cm^{-1} (SO_2 sym. stretch).**^{1}H NMR** (400 MHz, $CDCl_3$): δ 3.62 - 3.55 (m, 1H, -C*H*OH), 3.10 (t, *J* = 7.4, 2H, -CH_2SO_2), 3.02 (t, *J* = 7.6, 2H, -CH_2SO_2), 2.95 - 2.87 (m, 2H, -

CH_2N(Me)$_2$), 2.57 (s, 6H, -N(CH_3)$_2$), 2.29 - 2.22 (m, 1H, -C*H*COOH), 2.20 - 2.11 (m, 2H), 2.15 (dt, *J* = 2.8, 7.2, 2H, -CH_2-C≡C), 1.92 (t, *J* = 2.8, 1H, -C≡C*H*), 1.91 - 1.77 (m, 2H), 1.74 - 1.22 (m, 18H). **^{13}C NMR** (100 MHz, $CDCl_3$): δ 181.0, 84.7, 71.8, 68.1, 55.9, 52.7, 52.1, 49.6, 43.1, 35.3, 30.1, 29.6, 29.3, 29.0, 28.7, 28.4, 27.8, 24.3, 22.2, 18.5, 18.3. HRMS (ESI) calc. for $C_{22}H_{41}NO_5S$ $[M+H]^+$ 432.2778, found 432.2770. LCMS (ESI) found 432.14 for $[M+H]^+$.

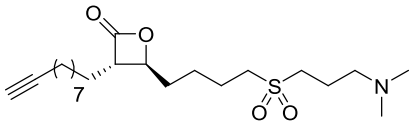

(*3S,4S*)-3-(dec-9-ynyl)-4-(4-(3-(dimethylamino)propylsulfonyl) butyl)oxetan-2-one (**83**). Compound **83** was synthesized following the general procedure for β-lactonization using 3.93 mmol of β-hydroxyacid **82**. Purification by flash chromatography using gradient 1-5% MeOH/CH_2Cl_2. Yield = 31% (yellow oil). R_f = 0.47 (MeOH/CH_2Cl_2 10/90). $[\alpha]_D^{20}$ = -23.5 (c = 0.22, $CHCl_3$). IR: 3276 cm^{-1} (C≡C-H stretch), 2115 cm^{-1} (-C≡C- stretch), 1814 cm^{-1} (β-lactone, C=O stretch), 1279 cm^{-1} (SO_2 asym. stretch), 1118cm^{-1} (SO_2 sym. Stretch).**^{1}H NMR** (400 MHz, $CDCl_3$): δ 4.15 (ddd, *J* = 4.8, 4.8, 7.4, 1H, -C*H*OCOR), 3.12 (ddd, *J* = 4.0, 6.8, 8.6, 1H,-C*H*CO), 2.96 (t, *J* = 7.8, 2H, -C$H_2$$SO_2$), 2.91 (t, *J* = 7.8, 2H, -C$H_2$$SO_2$), 2.32 (dt, *J* = 0.8, 6.8, 2H, -C$H_2$$NMe_2$), 2.14 (d, *J* = 0.8, 6H, -N(CH_3)$_2$), 2.09 (dt, *J* = 2.6, 7.1, 2H, -CH_2-C≡C), 1.95 - 1.38 (m, 13H), 1.38 - 1.14 (m,10H). **^{13}C NMR** (100 MHz, $CDCl_3$): δ 170.9, 84.4, 77.1, 68.0, 57.1, 56.0, 52.2, 50.4, 44.9, 33.6, 28.9, 28.9, 28.6, 28.3, 28.1, 27.5, 26.6, 23.9, 21.3, 19.6, 18.1. HRMS (ESI) calc. for $C_{22}H_{39}NO_4S$ $[M+H]^+$ 414.2673, found 414.2667. LCMS (ESI) found 414.01 for $[M+H]^+$.

2.9 Synthesis of palmostatin M-derived pull down probe 94

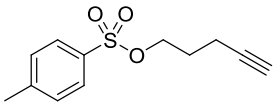

Toluene-4-sulfonic acid pent-4-ynyl ester (**85**).[40] To a solution of 4-pentyn-1-ol **84** (0.5 g, 5.94 mmol, 1.0 eqv.) and NEt_3 (0.91 ml, 6.53 mmol, 1.1 eqv.) in dry CH_2Cl_2 (5 ml) was added dropwise at 0°C (over 20 min) a solution of TsCl (1.27 g, 6.53 mmol, 1.1 eqv.) in CH_2Cl_2 (15 ml). The mixture was subsequently stirred for 20 min at 0°C, and for 20 hours at rt. The mixture was poured into ice–cold water and the separated aqueous layer was extracted with $CHCl_3$ (3x50ml). Combined organic extracts were washed with water, brine and dried over $MgSO_4$. After concentrated under reduced pressure, the residue was purified by flash chromatography (gradient 5-20%

EtOAc/cyclohexane) leading to compound **85**. Yield=71% (colorless oil). R_f = 0.41 (EtOAc/cyclohexane 20/80). IR: 3290 cm^{-1} (C≡C-H stretch), 2119 cm^{-1} (-C≡C- stretch), 660 cm^{-1} (C≡C-H bend).**^{1}H NMR** (400 MHz, CD_3CN): δ 7.79 (d, *J* = 8.4, 2H, Haro), 7.34 (d, *J* = 8.0, 2H, Haro), 4.14 (t, *J* = 6.2, 2H, -C*H*$_2$OTs), 2.44 (s, 3H, -C*H*$_3$), 2.25 (dt, *J* = 2.4, 6.8, 2H, -C*H*$_2$-C≡C), 1.87 (t, *J* = 2.4, 1H, -C≡C*H*), 1.86-1.82 (m, 2H). **^{13}C NMR** (100 MHz, $CDCl_3$): δ 144.8, 132.8, 129.8 (2C), 127.9 (2C), 82.1, 69.4, 68.7, 27.7, 21.6, 14.7. HRMS (ESI) calc. for $C_{12}H_{14}O_3S$ $[M+H]^+$ 239.0736, found 239.0737. GCMS found 238 for $[M^{+\cdot}]$. ^{1}H NMR conformed to literature [40].

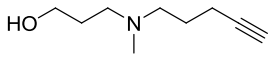

3-(Methyl(pent-4-ynyl)amino)propan-1-ol (**86**).[41] A mixture of 3-(methylamino)propan-1-ol (7.75 g, 87 mmol, 1.0 eqv.), toluene-4-sulfonic acid pent-4-ynyl ester **85** (23.1 g, 97 mmol, 1.1 eqv.) and K_2CO_3 (13.3 g, 97 mmol, 1.1 eqv.) in CH_3CN (420 ml) was heated under reflux for 20 hours under argon. The mixture was cooled to rt, filtered, concentrated under reduced pressure and purified by flash chromatography using $CHCl_3$/MeOH/NH_4OH 93/5/2 as eluent to afford compound **86**. Yield=81% (colorless oil). R_f = 0.60 (AcOH/EtOAc/MeOH/H_2O 3/3/3/2). IR: 3295 cm^{-1} (C≡C-H stretch), 2115 cm^{-1} (-C≡C- stretch), 627 cm^{-1} (C≡C-H bend). **^{1}H NMR** (400 MHz, $CDCl_3$): δ 5.19 - 5.05 (sbr, 1H, -O*H*), 3.78 (t, *J* = 5.0, 2H, -C*H*$_2$OH), 2.59 (t, *J* = 5.8, 2H, -C*H*$_2$N), 2.47 (t, *J* = 7.2, 2H, -C*H*$_2$N), 2.25 (s, 3H, -C*H*$_3$), 2.22 (dt, *J* = 2.5, 7.2, 2H, -C*H*$_2$-C≡C), 1.95 (t, *J* = 2.6, 1H, -C≡C*H*), 1.75 - 1.67 (m, 4H). **^{13}C NMR** (100 MHz, $CDCl_3$): δ 83.8, 68.6, 64.7, 58.6, 57.1, 41.9, 27.6, 26.0, 16.3. HRMS (ESI) calc. for $C_9H_{17}NO$ $[M+H]^+$ 156.1383, found 156.1379. LCMS (ESI) found 155.98 for $[M+H]^+$.

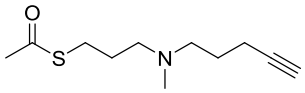

***S*-3-(Methyl(pent-4-ynyl)amino)propyl ethanethioate** (**87**). To a solution of 3-(methyl(pent-4-ynyl)amino)propan-1-ol **86** (11 g, 70 mmol, 1.0 eqv.) in dry CH_2Cl_2 (450 ml) was added $SOCl_2$ (6.2 ml, 85 mmol, 1.2 eqv.) at 0°C. The mixture was stirred for 4 hours at rt and was concentrated under reduced pressure leading to a chlorinated intermediate: R_f = 0.62 (MeOH/CH_2Cl_2 10/90). IR: 3288 cm^{-1} (C≡C-H stretch), 2111 cm^{-1} (-C≡C- stretch), 704 cm^{-1} (C≡C-H bend). **^{1}H NMR** (400 MHz, $CDCl_3$): δ 2.90 (t, *J* = 7.2, 2H, -C*H*$_2$Cl), 2.41 (t, *J* = 6.8, 2H, -C*H*$_2$N), 2.39 (t, *J* = 7.0, 2H, -C*H*$_2$N), 2.31 (s, 3H, -C*H*$_3$N), 2.22 (dt, *J* = 2.4, 6.8, 2H, -C*H*$_2$-C≡C), 1.93 (t, *J* = 2.4, 1H, -C≡C*H*), 1.77 - 1.68 (m, 4H). **^{13}C NMR** (100 MHz, $CDCl_3$): δ 81.2, 70.7, 55.2, 54.0, 41.6, 40.3, 26.7, 22.3, 15.9. HRMS (ESI) calc. for $C_9H_{16}ClN$ $[M+H]^+$ 174.1044, found 174.1041. LCMS (ESI) found 173.98 for $[M+H]^+$. The

chlorinated intermediate was taken into $CHCl_3$ (330 ml) and NEt_3 (29 ml, 210 mmol, 3.0 eqv.) followed by thioacetic acid (6 ml, 84 mmol, 1.2 eqv.) were added dropwise (over 30 min) to the reaction mixture which was subsequently heated under reflux for 18 hours. The mixture was poured into a separatory funnel and washed several times with cold 1N NaOH, followed by water. The combined organic extracts were washed with brine, dried over anhydrous $MgSO_4$, concentrated under reduced pressure and purified by flash chromatography (2% $MeOH/CH_2Cl_2$) leading to compound **87** as a brown oil. Yield = 80% over two steps. R_f = 0.64 (MeOH/DCM 10/90). IR: 3295 cm^{-1} (C≡C-H stretch), 2116 cm^{-1} (-C≡C- stretch), 622 cm^{-1} (C≡C-H bend), 1688 cm^{-1} (C=O). **^{1}H NMR** (400 MHz, $CDCl_3$): δ 2.90 (t, *J* = 7.2, 2H, -CH_2S), 2.40 (t, *J* = 7.2, 2H, -CH_2N), 2.38 (t, *J* = 7.2, 2H, -CH_2N), 2.32 (s, 3H, -CH_3N), 2.22 (dt, *J* = 2.5, 7.2, 2H, -CH_2-C≡C), 2.18 (s, 3H, -CH_3CO), 1.94 (t, *J* = 2.5, 1H, -C≡C*H*), 1.72 (p, *J* = 7.2, 2H), 1.69 -1.63 (m, 2H). **^{13}C NMR** (100 MHz, $CDCl_3$): δ 196.0, 84.3, 68.3, 56.3, 56.2, 42.0, 30.6, 27.2, 27.0, 26.2, 16.2. HRMS (ESI) calc. for $C_{11}H_{19}NOS$ $[M+H]^+$ 214.1260, found 214.1258. LCMS (ESI) found 213.94 for $[M+H]^+$.

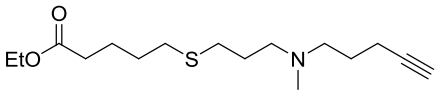

Ethyl-5-(3-(methyl(pent-4-ynyl)amino)propylthio)pentanoate (**88**).[42] To a solution of *S*-3-(methyl(pent-4-ynyl)amino)propyl ethanethioate **87** (0.9 g, 4.25 mmol, 1.0 eqv.) in absolute EtOH (35 ml) was added t-BuOK (0.5 g, 4.46 mmol, 1.05 eqv.). The reaction mixture was stirred for 30 min at rt and a solution of ethyl 5-iodopentanoate **49** (1.1 g, 4.25 mmol, 1.0 eqv.) in EtOH (15 ml) was added dropwise to the reaction mixture which was then stirred at rt for 20 hours. After concentration under reduced pressure, the residue was diluted with H_2O/EtOAc 1/5 (200ml) and the two layers separated. The aqueous layer was extracted with EtOAc and combined organic layers were concentrated under reduced pressure leading to compound **88**, which was used directly in the next step. Yield = 90% (yellow oil). R_f = 0.64 ($MeOH/CH_2Cl_2$ 10/90). IR: 3293 cm^{-1} (C≡C-H stretch), 2116 cm^{-1} (-C≡C- stretch), 629 cm^{-1} (C≡C-H bend), 1731 cm^{-1} (ester, C=O stretch). **^{1}H NMR** (400 MHz, $CDCl_3$): δ 4.12 (q, *J* = 7.2, 2H, -OCH_2CH$_3$), 2.52 (t, *J* = 7.2, 2H, -CH_2N), 2.51 (t, *J* = 7.2, 2H, -CH_2N), 2.41 (t, *J* = 7.0, 2H, -CH_2S), 2.40 (t, *J* = 7.2, 2H, -CH_2S), 2.31 (t, *J* = 7.4, 2H, -CH_2CO), 2.22 (dt, *J* = 2.4, 7.2, 2H, -CH_2-C≡C), 2.19 (s, 3H, -CH_3N), 1.94 (t, *J* = 2.8, 1H, -C≡C*H*), 1.76 - 1.57 (m, 8H), 1.25 (t, *J* = 7.2, 3H, -OCH$_2$CH_3). **^{13}C NMR** (100 MHz, $CDCl_3$): δ 173.4, 84.3, 68.3, 60.3, 56.6, 56.3, 42.2, 33.8, 31.7, 29.9, 29.0, 27.3, 26.2, 24.2, 16.2, 14.2. HRMS (ESI) calc. for $C_{16}H_{29}NO_2S$ $[M+H]^+$ 300.1992, found 300.1992. LCMS (ESI) found 299.98 for $[M+H]^+$.

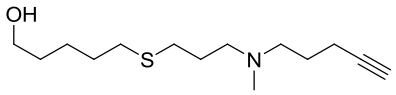

5-(3-(Methyl(pent-4-ynyl)amino)propylthio)pentan-1-ol (**89**). To an oven dried 250 ml round bottom flask was added $LiAlH_4$ (0.67 mmol, 17.7 mmol, 1.05 eqv.), followed by a large egg-shaped stirring bar. The flask was flushed with argon, set under positive argon pressure and subsequently cooled to 0°C. Dry Et_2O (30 ml) was added under rapid stirring and the resulting suspension was stirred at 0°C for 15 min. A solution of compound **88** (5.04 g, 16.8 mmol, 1.0 eqv.) in dry Et_2O (20 ml) was added dropwise over 10 min to the reaction mixture at such a rate that the temperature was kept around 0°C. The mixture was stirred for 1 hour at 0°C followed by 2 hours at rt and was quenched at 0°C by dropwise addition of H_2O (1.1 ml) (caution, gas evolution), followed by 1N NaOH (2.2 ml) and 1.1 ml H_2O. The thick suspension gets thinner upon aging and was diluted with further 50 ml Et_2O. Two spoons of Celite were added and the mixture was allowed to age for another 30 min at rt. The resulting free running suspension was filtered over Celite in a sintered funnel. The filter cake was re-suspended in Et_2O/MeOH 10/1 (50 ml) and was refluxed for 10 min in order to dissolve all products. After hot filtration over Celite, the combined organic extracts were evaporated under reduced pressure. Al-salt traces remaining were removed by suspending the residue in 6 N NaOH (20 ml) and CH_2Cl_2 (100 ml). The organic layer was isolated, extracted with CH_2Cl_2 (3x30 ml), washed with brine and dried over over Na_2SO_4. After concentration under reduced pressure, the compound **89** was obtained, which was used directly in the next step. Yield = 73 % (yellow oil). R_f = 0.42 (MeOH/CH_2Cl_2 10/90). IR: 3295 cm^{-1} (C≡C-H stretch), 2116 cm^{-1} (-C≡C- stretch), 629 cm^{-1} (C≡C-H bend). **^{1}H NMR** (400 MHz, $CDCl_3$): δ 3.62 (t, *J* = 6.4, 2H, -C*H*$_2$OH), 3.52 - 3.47 (bs, 1H, -O*H*), 2.52 (t, *J* = 7.4, 2H, -C*H*$_2$N), 2.51 (t, *J* = 7.4, 2H, -C*H*$_2$N), 2.40 (t, *J* = 7.2, 2H, -C*H*$_2$S), 2.41 (t, *J* = 7.2, 2H, -C*H*$_2$S), 2.21 (dt, *J* = 2.4, 6.8, 2H, -C*H*$_2$-C≡C), 2.19 (s, 3H, -C*H*$_3$N), 1.94 (t, *J* = 2.8, 1H, -C≡C*H*), 1.76 - 1.54 (m, 8H), 1.50 - 1.41 (m, 2H). **^{13}C NMR** (100 MHz, $CDCl_3$): δ 84.3, 68.3, 62.5, 56.5, 56.3, 42.2, 32.2, 32.0, 29.9, 29.4, 27.3, 26.1, 25.0, 16.2**.** HRMS (ESI) calc. for $C_{14}H_{27}NOS$ $[M+H]^+$ 258.1886, found 258.1886. LCMS (ESI) found 257.97 for $[M+H]^+$.

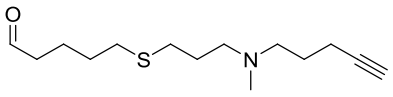

5-(3-(Methyl(pent-4-ynyl)amino)propylthio)pentanal (**90**)**.** Compound **90** was synthesized following the general procedure for Swern oxidation using 5.4 mmol of alcohol **89**. Yield = 91% (brown oil). R_f = 0.51 (AcOH/ EtOAc/MeOH/H_2O 3/3/3/2). IR: 3289 cm^{-1} (C≡C-H stretch), 2115 cm^{-}

[1] (-C≡C- stretch), 631 cm^{-1} (C≡C-H bend), 1721 cm^{-1} (C=O) .**^{1}H NMR** (400 MHz, $CDCl_3$): δ 9.76 (t, *J* = 1.6, 1H, -C*H*O), 2.53 (t, *J* = 7.2, 2H, -CH_2N), 2.52 (t, *J* = 7.2, 2H, -CH_2N), 2.45 (dt, *J* = 1.6, 7.2, 2H, -CH_2CHO), 2.45 - 2.38 (m, 4H, -CH_2S), 2.22 (dt, *J* = 2.4, 7.2, 2H, -CH_2-C≡C), 2.20 (s, 3H, -CH_3N), 1.93 (t, *J* = 2.4, 1H, -C≡C*H*), 1.78 - 1.57 (m, 8H). **^{13}C NMR** (100 MHz, $CDCl_3$): δ 202.2, 77.2, 68.6, 56.3, 56.1, 45.7, 43.4, 41.9, 31.7, 29.8, 28.9, 21.2, 16.2, 8.8. HRMS (ESI) calc. for $C_{14}H_{25}NOS$ $[M+H]^+$ 256.1730, found 256.1732. GCMS found 254 for $[M^{+\cdot}]$.

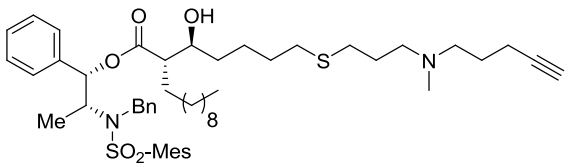

(*S*)-((*1S,2R*)-2-(*N*-benzyl-2,4,6-trimethylphenylsulfonamido)-1-phenylpropyl)2-((*S*)-1-hydroxy-5-(3-(methyl(pent-4-ynyl)amino)propylthio) pentyl) dodecanoate (**91**). Compound **91** was synthesized following the general procedure for the *anti*-selective aldol reaction using 7.11 mmol of aldehyde **90** followed by purification by flash chromatography using 1-3% $MeOH/CH_2Cl_2$. Yield = 68 % (white–beige semi solid). R_f = 0.54 ($MeOH/CH_2Cl_2$ 10/90). $[\alpha]_D^{20}$ = -32.3 (c = 0.19, $CHCl_3$). IR: 1733 cm^{-1} (ester, C=O stretch), alkyne not apparent. **^{1}H NMR** (400 MHz, $CDCl_3$): δ 7.31 - 7.11 (m, 8H, Haro), 6.87 - 6.81 (m, 4H, Haro), 5.98 – 5.89 (brs, 1H, -O*H*), 5.80 (d, *J* = 5.2, 1H, -C*H*OCOR), 4.75 (d, *J* = 16.8, 1H, -C*H*Ph), 4.59 (d, *J* = 16.5, 1H, -C*H*Ph), 4.13 – 4.07 (m, 1H, -C*H*N(Bn)Mes), 3.73 - 3.60 (m, 1H, -C*H*OH), 2.60 - 2.49 (m, 4H, -CH_2NMe), 2.45 - 2.40 (m, 7H, -C*H*COOR, CH_3 (Mes)), 2.28 (s, 3H, CH_3 (Mes)), 2.27 (s, 3H, -NCH_3), 2.07 - 1.91 (m, 5H, -CH_2S, -CH_2-C≡C, -C≡C*H*), 1.69 - 1.35 (m, 12H, including -CH_2S), 1.33 - 0.96 (m, 21H), 0.88 (t, *J* = 6.8, 3H, -CH_3). **^{13}C NMR** (100 MHz, $CDCl_3$): δ 174.6, 142.6, 140.3, 138.4, 137.9, 133.2, 132.1, 128.3, 128.2, 128.0, 127.9, 127.2, 126.6, 78.1, 77.2, 72.1, 63.7, 62.6, 56.5, 53.4, 51.4, 48.2, 34.7, 31.9, 29.6, 29.5, 29.5, 29.4, 29.3, 29.3, 27.8, 27.2, 24.7, 24.1, 22.9, 22.7, 21.6, 20.9, 14.2, 14.1 (signal at 84 pm for quaternary alkyne not visible). HRMS (ESI) calc. for $C_{51}H_{76}N_2O_5S_2$ $[M+H]^+$ 861.5268, found 861.5268. LCMS (ESI) found 861.28 for $[M+H]^+$.

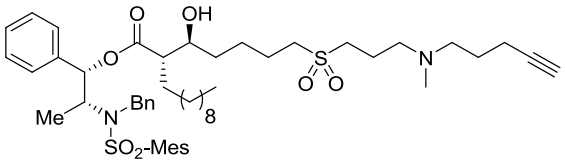

(*S*)-((*1S,2R*)-2-(*N*-benzyl-2,4,6-trimethylphenylsulfonamido)-1-phenylpropyl)2-((*S*)-1-hydroxy-5-(3-(methyl(pent-4-ynyl)amino) propylsulfony) pentyl)dodecanoate (**92**)**.** Compound **92** was synthesized following the general procedure for oxidation into sulfone using 4.36 mmol of sulfide derivative **91**, reaction time 8 hours (no purification needed). Yield = 90% (white solid). R_f = 0.57 (MeOH/CH_2Cl_2 10/90). $[\alpha]_D^{20}$ = - 24.0 (c = 0.82, $CHCl_3$). IR: 3309 cm^{-1} (C≡C-H stretch), 2115 cm^{-1} (-C≡C- stretch), 1735 cm^{-1} (ester, C=O stretch), 1315 cm^{-1} (SO_2 asym. stretch), 1151cm^{-1} (SO_2 sym. Stretch). **^{1}H NMR** (400 MHz, $CDCl_3$): δ 7.27 - 7.11 (m, 8H, Haro), 6.89 - 6.80 (m, 4H, Haro), 5.85 (d, *J* = 5.6, 1H, -C*H*OCOR), 4.72 (d, *J* = 16.4, 1H, -C*H*Ph), 4.52 (d, *J* = 16.5, 1H, -C*H*Ph), 4.23 - 4.14 (m, 1H, -C*H*N(Bn)Mes), 3.70 - 3.57 (m, 1H, -C*H*OH), 3.02 (t, *J* = 7.6, 2H, -CH_2SO_2), 2.94 (t, *J* = 8.0, 2H, -CH_2SO_2), 2.67 - 2.50 (m, 4H, -CH_2NMe), 2.86 - 2.70 (m, 1H, -C*H*COOR), 2.42 (s, 6H, CH_3 (Mes)), 2.28 (s, 3H, CH_3 (Mes)), 2.27 (s, 3H, -NCH_3), 2.23 (dt, *J* = 2.4, 6.8, 2H, -CH_2-C≡C), 1.96 (t, *J* = 2.8, 1H, -C≡C*H*), 1.91 - 1.36 (m, 10H), 1.33 - 0.95 (m, 21H), 0.88 (t, *J* = 6.8, 3H, -CH_3). **^{13}C NMR** (100 MHz, $CDCl_3$): δ 174.4, 142.5, 140.3, 138.2, 137.8, 133.0, 132.1, 128.3, 128.3, 128.1, 127.9, 127.3, 126.6, 78.1, 77.2, 71.6, 69.2, 56.4, 55.7, 55.4, 53.0, 51.4, 50.2, 48.1, 44.5, 34.3, 31.9, 29.7, 29.6, 29.5, 29.5, 29.3, 29.3, 27.1, 24.6, 22.9, 22.7, 22.5, 22.3, 21.8, 20.9, 16.04, 14.1 (signal at 84 pm for quaternary alkyne not visible). HRMS (ESI) calc. for $C_{51}H_{76}N_2O_7S_2$ $[M+H]^+$ 893.5167, found 893.5167. LCMS (ESI) found 893.27 for $[M+H]^+$.

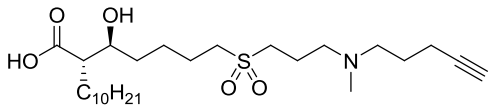

(*S*)-2-((*S*)-1-hydroxy-5-(3-(methyl(pent-4-ynyl)amino) propyl sulfonyl)pentyl) dodecanoic acid (**93**). Compound **93** was synthesized following the general procedure for saponification using 0.174 mmol of β-hydroxyester **92** by reaction with 5.5 eqv. $LiOH{\cdot}H_2O$ at 40°C for 24 hours. Purification by flash chromatography using MeOH/CH_2Cl_2 10/90 to remove unpolar impurities, then MeOH/CH_2Cl_2/ NEt_3 10/88/2 to elute compound **93** (separation monitored by TLC using EtOAc/AcOH/MeOH/ H_2O 3/3/3/2). Yield = 30% (white semi-solid). R_f = 0.5 (AcOH/EtOAc/MeOH/ H_2O 3/14/3/2). $[\alpha]_D^{20}$ not measured as contained some residual NEt_3. IR: 3311 cm^{-1} (C≡C-H stretch), 1714cm^{-1} (acid, C=O stretch), 1272 cm^{-1} (SO_2 asym. stretch), 1131cm^{-1} (SO_2 sym. Stretch). **^{1}H NMR** (400 MHz, $CDCl_3$): δ 3.56 - 3.49 (m, 1H, -C*H*OH), 3.02 (t, *J* = 8.0, 2H, -CH_2SO_2), 2.96 (t, *J* = 8.0, 2H, -CH_2SO_2), 2.60 (t, *J* = 7.0, 2H, -CH_2N), 2.56 (t, *J* = 7.4, 2H, -CH_2N), 2.28 (s, 3H, -

NC*H*$_3$), 2.25 - 2.18 (m, 3H, -C*H*COOH, -C*H*$_2$-C≡C), 2.07 - 1.98 (m, 2H), 1.96 (t, *J* = 2.6, 1H, -C≡C*H*), 1.89 - 1.42 (m, 8H), 1.37 - 1.17 (m, 18H), 0.85 (t, *J* = 6.8, 3H, -C*H*$_3$). **^{13}C NMR** (100 MHz, $CDCl_3$): δ 181.4, 83.4, 71.7, 68.9, 55.6, 55.3, 52.9, 51.9, 50.2, 41.0, 35.9, 31.8, 30.6, 29.7, 29.6, 29.6, 29.3, 27.8, 25.1, 24.9, 22.6, 22.1, 19.3, 16.0, 14.0. HRMS (ESI) calc. for $C_{26}H_{49}NO_5S$ $[M+H]^+$ 488.3404, found 488.3396. LCMS (ESI) found 488.21 for $[M+H]^+$.

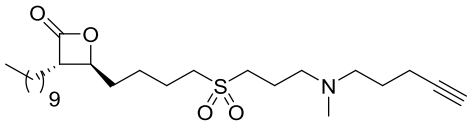

(*3S,4S*)-3-decyl-4-(4-(3-(methyl(pent-4-ynyl)amino)propyl-sulfonyl)butyl) oxetan -2-one (**94**). Compound **94** was synthesized following the general procedure for β-lactonization using 0.49 mmol β-hydroxyacid **93** (reaction monitored by TLC using MeOH/CH_2Cl_2 10/90). Purification by flash chromatography using gradient 1-5% MeOH/CH_2Cl_2. Yield=30% (yellow oil). R_f = 0.41 (MeOH/CH_2Cl_2 10/90). $[\alpha]_D^{20}$ = -22.1 (c = 0.1, $CHCl_3$). IR: 3308 cm^{-1} (C≡C-H stretch), 2116 cm^{-1} (-C≡C- stretch), 1799 cm^{-1} (β-lactone, C=O stretch), 1265 cm^{-1} (SO_2 asym. stretch), 1120cm^{-1} (SO_2 sym. Stretch). **^{1}H NMR** (400 MHz, $CDCl_3$): δ 4.22 (ddd, *J* = 4.1, 5.6, 7.3, 1H, -C*H*OCOR), 3.19 (ddd, *J* = 4.0, 6.6, 8.6, 1H, -C*H*CO), 3.07 (t, *J* = 8.0, 2H, -C*H*$_2$$SO_2$), 2.98 (t, *J* = 7.8, 2H, -C*H*$_2$$SO_2$), 2.52 – 2.41 (m, 4H, -C*H*$_2$N), 2.23 (td, *J* = 2.6, 7.0, 2H, -C*H*$_2$-C≡C), 2.22 (s, 3H, -NC*H*$_3$), 2.06 - 1.97 (m, 2H), 1.95 (t , *J* = 2.8, 1H, -C≡C*H*), 1.94 - 1.55 (m, 8H), 1.47 - 1.18 (m, 18H), 0.88 (t, *J* = 7.0, 3H, -C*H*$_3$). **^{13}C NMR** (100 MHz, $CDCl_3$): δ 171.1, 84.1, 77.2, 68.6, 56.3, 55.8, 55.7, 52.4, 50.7, 41.6, 33.9, 31.8, 29.5, 29.4, 29.3, 29.3, 27.7, 26.9, 25.9, 24.3, 22.6, 21.5, 19.7, 16.0, 14.1. HRMS (ESI) calc. for $C_{26}H_{47}NO_4S$ $[M+H]^+$ 470.3299, found 470.3291. LCMS (ESI) found 470.05 for $[M+H]^+$.

2.10 Synthesis of the trifunctional fluorophore reporter dye TrifN_3 (103)

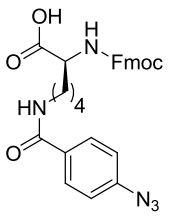

Fmoc-L-Lys (4-azidobenzoyl)-OH (**97**).[43] Into a round-bottom flask was added Fmoc-LysOH (2.27 g, 6.13 mmol, 1.0 eqv.) in 25% aqueous K_2CO_3/dioxane 1/1 (50 ml). 4-Azidobenzoyl chloride (6.13 mmol, 1 eqv., obtained quantitatively following the literature [44]) as a solution in dioxane (5 ml)

was added dropwise to the reaction mixture which was stirred at rt for 2 days. The reaction was monitorated by TLC using MeOH/DCM 1/9. The reaction was quenched with water and extracted with tert-butylmethylether. The aqueous layer was acidified to approx. pH 2.0 using concentrated HCl and was extracted with several portions of $CHCl_3$. The combined organic extracts were dried over anhydrous $MgSO_4$, concentrated under reduced pressure and purified by flash chromatography (gradient 1-10% MeOH/DCM) leading to compound **97** as yellow oil. Yield =70% over 2 steps from 4-azidobenzoic acid. R_f = 0.3 (10% MeOH/DCM). **^{1}H NMR** (400 MHz, $CDCl_3$): δ 7.78 - 7.63 (m, 4H, Haro), 7.58 - 7.42 (m, 2H, Haro), 7.39 - 7.29 (m, 2H, Haro), 7.29 - 7.15 (m, 2H, Haro), 6.96 - 6.81 (m, 2H, Haro), 6.75 - 6.52 (brs, 1H, N*H*), 5.95 - 5.74 (brs, 1H, N*H*), 4.50 - 4.02 (m, 4H), 3.52 - 3.22 (m, 2H), 2.04 - 1.14 (m, 6H). **^{13}C NMR** (100 MHz, $CDCl_3$): δ 167.1, 156.4, 143.7, 143.5, 143.1, 141.1, 130.7, 128.7, 127.6, 126.9, 124.9, 119.9, 118.7, 66.9, 53.4, 47.0, 39.5, 32.1, 29.6, 28.5, 22.4. HRMS (ESI) calc. for $C_{28}H_{27}N_5O_5$, $[M+H]^+$= 514.2085, $[M+Na]^+$= 536.1905; found $[M+H]^+$= 514.2079, $[M+Na]^+$= 536.1897. LCMS (ESI) found 511.99 for $[M-H]^-$, found 1024.93 for $[2M-H]^-$, found 1537.12 for $[3M-H]^-$.

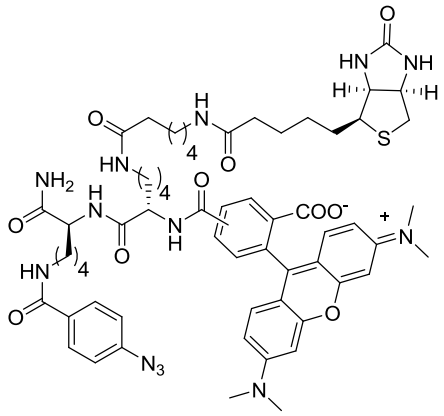

Trifunctional dye containing biotin-rhodamine-azide functionality (103, TrifN$_3$). [37] Compound **103** was synthesized on Sieber Amide resin **95** (Novabiochem, loading = 0.69 mmol/g) using a standard Fmoc solid phase strategy. Fmoc protected resin (500 mg) was deprotected with 20% piperidine/NMP (3*10 ml, 5 min) and washed (NMP, 2*10 ml, 5 min; DCM, 2*10 ml, 5 min; DMF, 3*10 ml, 5 min) to remove excess reagents. Fmoc-L-Lys (4-azidobenzoyl)-OH **97** (354 mg, 0.69 mmol, 2 eqv.)[43,44] was coupled to the resin for 1 hour at rt using HATU (262 mg, 0.69 mmol, 2 eqv.), HOBT (114 mg, 0.69 mmol, 2 eqv.) and DIPEA (178 mg, 0.239 ml, 1.38 mmol, 4 eqv.) in DMF (4 ml). The resin was washed (DMF, 7*10 ml, 5 min; DCM, 3*10 ml, 5 min) and dried under reduced pressure for 1 hour. The loading of the resin was determined by absorbance 0.49 mmol/g. Unreacted free amino groups were protected as *N*-acetamide by treatment of the resin for 30 min at rt with pyridine/acetic anhydride/ DCM 1/1/4 (12 ml). After washing the resin

(DCM, 7*10 ml, 5 min), Fmoc protected groups were deprotected using 4% DBU/DMF (6*10 ml, 10 min) and the excess of reagent washed away (DMF, 5*10 ml, 5 min; DCM, 3*10 ml, 5 min; DMF, 2*10 ml, 5 min). Commercially available Fmoc-Lys(biotinyl-ε-aminocaproyl)-OH (350 mg, 0.495 mmol, 2 eqv.) was coupled as described above in DMF for 7 hours. The resin was washed (DMF, 5*10 ml, 5 min; DCM, 3*10 ml, 5 min) and the remaining free amino groups protected as previously. After Fmoc deprotection with 4% DBU/DMF (6*10 ml, 10 min), the rhodamine was appended to the free amine upon reaction with 5/6 TAMRA-SE (178 mg, 0.33 mmol, 1.35 eqv.) using NEt_3 (0.280 ml, 1.98 mmol, 6 eqv.) in NMP (10 ml). The resin was washed with NMP (3*10 ml, 10 min), followed by DCM (3*10 ml, 10 min), MeOH (3*10ml, 10 min), and DCM/MeOH 1/1. The compound was cleaved from the resin using 1% TFA/DCM (5*3ml, 10 min). Toluene (20 ml) was added to the obtained red solution and the solvent evaporated under reduced pressure. The trifunctional dye **103** was obtained in 60% overall yield, after purification on reverse phase C_{18} cartridge as a dark red solid. R_f= 0.43 (AcOH/EtOAc/MeOH/H_2O 3/6/3/2), fluorescent as a single spot. HRMS (ESI) calc. for $C_{60}H_{75}N_{13}O_{10}S$ $[M+H]^+$ 1170.5553, found $[M+H]^+$ 1170.5561. LCMS (ESI) found 1170.40 for $[M+H]^+$.

2.11 Synthesis of C16-ω-alkynyl fatty acid (106)

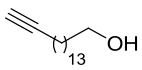

Hexadec-15-yn-1-ol (**105**).[2] Compound **105** was synthesized using a Alkyne Zipper reaction decribed in literature. Sodium Hydride (60% in mineral oil, 2.0 g, 50 mmol, 6.0 eqv.) was added to a 100 ml round bottom flask, together with a magnetic stirring bar. The flask was back-filled with argon and sodium hydride was washed with dry hexane (2x30 ml), taking care to remove as much of the hexane as possible. Diaminopropane (50 ml) was added via a cannula, and the resulting suspension was stirred at rt until gas evolution ceased (10 min). The temperature was slowly raised to 50°C and kept there until most of the NaH went into solution (30 min), temperature was then raised to 70°C for 30 min in order to complete dissolution. The resulting clear brown solution was allowed to cool to rt and 7-hexadecyn-1-ol **104** (2.0 g, 8.4 mmol, 1.0 eqv.) dissolved in diaminopropane (10 ml) was added via a syringe. The resulting mixture was stirred at 50°C for 16 hours. After cooling to 0°C, water (20 ml), was slowly added over 5 min and the reaction mixture was aged for 20 min at 0°C. Subsequently, the reaction mixture was poured into 200 ml ice water under stirring, follow by addition of ice (100 g) to lower the temperature to

10°C. The reaction mixture was extracted with MTBE (3x100 ml), and the combined organic extracts were washed with water (2x100 ml), saturated NH_4Cl (100 ml), water (100 ml) and brine (200 ml), followed by drying over Na_2SO_4. After evaporation to dryness, the residue was purified by filtration through a pad of silica (3 cm diameter, 5 cm long), eluting with EtOAc-Hexane 1:1, yielding compound **105** in 90% yield (yellow oil which solidifies upon standing). R_f = 0.48 (EtOAc/cyclohexane 1/1). Analysis in accordance with data reported in literature. **^{1}H NMR** (400 MHz, $CDCl_3$): δ 3.65 (t, *J* = 5.2, 2H, -C*H*$_2$OH), 2.17 (dt, *J* = 2.0, 5.6, 2H, -C*H*$_2$-C≡C), 1.93 (t, *J* = 2.1, 1H, -C≡C*H*), 1.62 - 1.47 (m, 4H), 1.45 – 1.18 (m, 20H). **^{13}C NMR** (100 MHz, $CDCl_3$): δ 84.8, 68.0, 63.1, 32.8, 29.6 (2C), 29.5 (3C), 29.4, 29.4, 29.1, 28.7, 28.5, 25.7, 18.4.

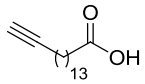

Hexadec-15-ynoic acid (**106**).[2] Hexadec-15-yn-1-ol **105** (1.6 g, 6.3 mmol, 1.0 eqv.) was dissolved in 30 ml acetone and added to a 100 ml round bottom flask, equipped with a large egg-shaped stirring bar. The flask was cooled to 0°C and Jones reagent (18.9 mmol, 3.0 eqv., prepared from CrO_3 (1.87g, 18.9 mmol) and conc. H_2SO_4 (1.6 ml) in 3 ml water at 0°C) was added dropwise over 5 min. The resulting solution was subsequently allowed to stir for 10 min at 0°C, then at rt for 20 min. A TLC-sample indicated complete dissaperance of the starting material **105** (R_f = 0.48 (EtOAc/cyclohexane 1/1) and the absence an aldehyde product (R_f = 0.7 (EtOAc/cyclohexane 1:1). The reaction was cooled to 0°C in ice-bath and isopropanol (5 ml) was added slowly. The color changes from orange-brown to deep green and a thick precipitate is formed. Additional 30 ml acetone was added, followed by some Celite 545. The resulting slurry was filtered on a sintered funnel and washed with additional 2x30 ml acetone. The combined filtrates were evaporated to a small volume under reduced pressure at 30 °C, yielding a greenish semi-solid residue which was dissolve with 0.05 N HCl (30 ml) and EtOAc (50 ml). The organic layer was subsequently washed with further 0.05 N HCl (2x30 ml) followed by brine. After concentration under reduced pressure, the residue was purified by filtration through a short pad of silica gel (diameter 3 cm, length 8 cm), eluting with a gradient from 10% EtOAc in cyclohexane to 100% EtOAc leading to compound **106**. Yield = 94% (white solid). R_f = 0.51 (EtOAc/cyclohexane 1/1). **^{1}H NMR** (400 MHz, $CDCl_3$): δ 2.34 (t, *J* = 6.0, 2H, -C*H*$_2$COOH), 2.18 (dt, , *J* = 2.4, 6.0, 2H, -C*H*$_2$-C≡C), 1.93 (t, *J* = 2.1, 1H, -C≡C*H*), 1.58 -1.68 (m, 2H), 1.55 -1.47 (m, 2H), 1.45- 1.26 (m, 18H). **^{13}C NMR** (100 MHz, $CDCl_3$): δ 179.4, 84.8, 68.0, 33.9, 29.6, 29.5, 29.5, 29.4, 29.4, 29.2, 29.1, 29.0, 28.7, 28.5, 24.7, 18.4.

2.12 Synthesis of α-keto amide candidate inhibitors

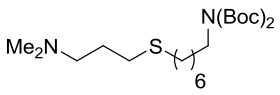

Di-tert-butyl 7-(3-(dimethylamino)propylthio)heptylcarbamate (**110**).[45] Alcohol **109** (206 mg, 0.86 mmol, 1.0 eqv.), triphenylphosphine (916 mg, 3.48 mmol, 4.06 eqv.) and di-tert-butylimino dicarboxylate (792 mg, 3.48 mmol, 4.06 eqv.) were placed under argon and dissolved into dry DCM (12 ml). The obtained mixture was stirred at 0°C for 10 min before adding di-tert-butyl azodicarboxylate (DBAD, 590 mg, 2.56 mmol, 2.96 eqv.) to the reaction mixture which was subsequently stirred for 45 min at 0°C. The avancement of the reaction was monitorated by TLC using MeOH/DCM 20/80 (less polar compound formed). The reaction mixture was diluted with water and EtOAc, and the aqueous layer was extrated with EtOAc (2*20 ml). The combined organic layers were washed with brine (20 ml), dried over anhydrous $MgSO_4$, and concentrated under reduced pressure. The residue (m =3.1g) was purified by flash chromatography using 2-10% MeOH/DCM leading to *N*-Boc-protected amine **110** in 42% yield (slight yellow oil). R_f =0.68 (10% MeOH/DCM). **^{1}H NMR** (400 MHz, $CDCl_3$): δ 3.54 - 3.48 (m, 2H, -C*H*$_2$NBoc$_2$), 2.55 - 2.44 (m, 4H, C*H*$_2$S), 2.41 (t, *J* = 7.4, 2H, -C*H*$_2$NMe$_2$), 2.27 (s, 6H, -N(C*H*$_3$)$_2$), 1.82 – 1.71 (m, 2H), 1.59 – 1.49 (m, 4H), 1.47 (2*s, 18H, C*H*$_3$ Boc), 1.39 - 1.20 (m, 6H). **^{13}C NMR** (125 MHz, $CDCl_3$): δ 152.7 (CO, 2C), 81.9 (C_{IV} Boc, 2C), 58.5, 45.4, 45.1 (2C), 32.1, 29.8, 29.5, 28.9, 28.9, 28.8, 28.05 (6C), 27.2, 26.7. HRMS (ESI) calc. for $C_{22}H_{44}N_2O_4S$ $[M+H]^+$ 433.3094, found 433.3092. LC-MS (ESI) found 433.19 for $[M+H]^+$.

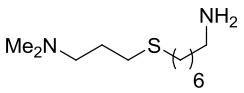

7-(3-(Dimethylamino)propylthio)heptan-1-amine (**111**).[45] Alcohol **109** (104 mg, 0.42 mmol, 1.eqv), triphenylphosphine (459 mg, 1.74 mmol, 4.06 eqv.) and di-tert-butylimino dicarboxylate (396 mg, 1.74 mmol, 4.06 eqv.) were placed under argon and dissolved into dry DCM (6 ml). The obtained mixture was stirred at 0°C for 10 min before adding di-tert-butyl azodicarboxylate (DBAD, 294 mg, 1.27 mmol, 2.96 eqv.) to the reaction mixture which was subsequently stirred for 30 min at 0°C. After addition of trifluoro acetic acid (TFA, 1.5 ml) to the mixture, the later was stirred at rt for 1H30. Then the reaction was acidified to pH = 1 using 1M HCl, and subsequently extracted with EtOAc. The organic layer was discarded and the aqueous layer was

basified to pH=12 using NaOH, and subsequently extracted with several portions of EtOAc. Combined organic layers were washed with brine, dried over anhydrous $MgSO_4$ and concentrated under reduced pressure. The residue (89 mg) was then purified through filtration using a sintered funnel (Ø 2 cm) containing in 1cm silica). Unpolar impurities were eluted using 15% MeOH/DCM, and the silica subsequently washed with 100% MeOH to collect the amine **111**. As most of the compound was aborbed on the silica, the silica was dissolved in water/EtOAc and the compound extracted with EtOAc (4*100 ml). After $MgSO_4$ treatment and concentratration under reduced pressure, the primary amine **111** was obtained in 14% yield (yellow oil). R_f = 0.36 (AcOH/EtOAc/MeOH/H_2O 3/3/3/2). ^1H and ^{13}C NMR identical to the one decribed previously using the procedure for reduction of the azide to the amine.

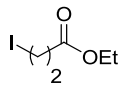

Ethyl-3-iodopropanoate (**112**). Compound **112** was synthesized following the general procedure for Finkelstein reaction on 138 mmol of ethyl-3-bromopropanoate. Yield = 92% (yellow oil). R_f= 0.42 (EtOAc/cyclohexane 5/95). IR: 1731 cm^{-1} (ester, C=O stretch). **^{1}H NMR** (400 MHz, $CDCl_3$): δ 4.16 (q, *J* = 7.2, 2H, -C*H*$_2$CH$_3$), 3.31 (t, *J* =7.0, 2H, -C*H*$_2$COOR), 2.94 (t, *J* = 7.2, 2H, -C*H*$_2$I), 1.26 (t, *J* = 7.0, 3H, -CH$_2$C*H*$_3$). **^{13}C NMR** (125 MHz, $CDCl_3$): δ 170.9, 60.9, 38.6, 14.1, - 3.8. HRMS (EI) calc. for $C_5H_9IO_2$ [$M^{+\cdot}$] 227.9642, found [$M^{+\cdot}$] 227.9640. GCMS found 228 for [$M^{+\cdot}$].

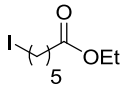

Ethyl-6-iodohexanoate (**113**). Compound **113** was synthesized following the general procedure for Finkelstein reaction on 111 mmol of ethyl-6-bromohexanoate. Yield = 98% (yellow oil). R_f= 0.42 (EtOAc/cyclohexane 5/95). IR: 1730 cm^{-1} (ester, C=O stretch). **^{1}H NMR** (400 MHz, $CDCl_3$): δ 4.11 (q, *J* = 7.2, 2H, -C*H*$_2$CH$_3$), 3.17 (t, *J* = 7.0, 2H, -C*H*$_2$COOR), 2.29 (t, *J* = 7.4, 2H, -C*H*$_2$I), 1.82 (p, *J* = 7.2, 2H), 1.63 (p, *J* = 7.6, 2H), 1.49 - 1.35 (m, 2H), 1.24 (t, *J* = 7.2, 3H, -CH$_2$C*H*$_3$). **^{13}C NMR** (125 MHz, $CDCl_3$): δ 173.3, 60.2, 34.0, 33.0, 29.9, 23.8, 14.4, 6.4. HRMS (ESI) calc. for $C_8H_{15}IO_2$ [M+Na]$^+$ 293.0009, found [M+Na]$^+$ 293.0010. GCMS found 225 for [M-OEt$^{+\cdot}$]. GCMS found 225 for [M-OEt$^{+\cdot}$].

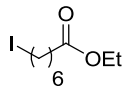

Ethyl-7-iodoheptanoate (**107**). Compound **107** was synthesized following the general procedure for Finkelstein reaction on 98 mmol of ethyl-7-bromoheptanoate. Yield = 98% (slight orange oil). R_f = 0.48 (EtOAc/cyclohexane 5/95). IR: 1731 cm^{-1} (ester, C=O stretch). **^{1}H NMR** (400 MHz, $CDCl_3$): δ 4.10 (q, *J* = 7.2, 2H, -C*H*$_2$CH$_3$), 3.16 (t, *J* = 7.0, 2H, -C*H*$_2$COOR), 2.27 (t, *J* = 7.4, 2H, -C*H*$_2$I), 1.80 (p, *J* = 7.2, 2H), 1.61 (p, *J* = 7.4, 2H), 1.45 – 1.30 (m, 4H), 1.23 (t, *J* = 7.0, 3H, -CH$_2$C*H*$_3$).**^{13}C NMR** (125 MHz, $CDCl_3$): δ 173.3, 60.0, 34.0, 33.1, 29.9, 27.8, 24.5, 14.1, 6.7. HRMS (ESI) calc. for $C_9H_{17}IO_2$ $[M+Na]^+$ 307.0165, found $[M+Na]^+$ 307.0168. GCMS found 239 for $[M\text{-}OEt^{+\cdot}]$.

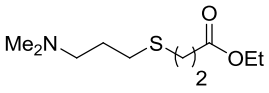

Ethyl 3-(3-(dimethylamino)propylthio)propanoate (**114**). Compound **114** was synthesized following the general procedure for *S*-alkylation using 87 mmol of thioacetate **47** (no purification needed). Yield = 94% (colorless oil). R_f = 0.45 (AcOH/EtOAc/MeOH/H_2O 3/3/3/2). IR: 1733 cm^{-1} (ester, C=O stretch). **^{1}H NMR** (400 MHz, $CDCl_3$): δ 4.02 (q, *J* = 7.2, 2H, -COC*H*$_2$CH$_3$), 2.64 (t, *J* = 7.0, 2H, -C*H*$_2$COOEt), 2.45 (t, *J* = 7.6, 2H, -C*H*$_2$S), 2.43 (t, *J* = 7.4, 2H, -C*H*$_2$S), 2.20 (t, *J* = 7.2, 2H, -C*H*$_2$NMe$_2$), 2.07 (s, 6H, N(C*H*$_3$)$_2$), 1.65 – 1.55 (m, 2H), 1.12 (t, *J* = 7.2, 3H, COCH$_2$C*H*$_3$). **^{13}C NMR** (125 MHz, $CDCl_3$): δ 171.4, 60.2, 58.2, 45.1, 34.6, 29.6, 27.3, 26.7, 13.9. HRMS (ESI) calc. for $C_{10}H_{21}NO_2S$ $[M+H]^+$ 220.1366, found 220.1368. GCMS found 219 for $[M^{+\cdot}]$.

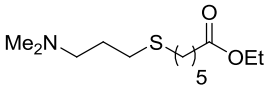

Ethyl 6-(3-(dimethylamino)propylthio)hexanoate (**115**). Compound **115** was synthesized following the general procedure for *S*-alkylation using 74 mmol of thioacetate **47**. Yield = 77% (slight yellow oil). R_f = 0.56 (AcOH/EtOAc/MeOH/H_2O 3/3/3/2). IR: 1733 cm^{-1} (ester, C=O stretch). **^{1}H NMR** (400 MHz, $CDCl_3$): δ 4.01 (q, *J* = 7.2, 2H, -COC*H*$_2$CH$_3$), 2.40 (t, *J* = 7.4, 2H, -C*H*$_2$S), 2.39 (t, *J* = 7.4, 2H, -C*H*$_2$S), 2.21 (t, *J* = 7.2, 2H, -C*H*$_2$COOEt), 2.17 (t, *J* = 7.4, 2H, -C*H*$_2$NMe$_2$), 2.09 (s, 6H, N(C*H*$_3$)$_2$), 1.65 – 1.57 (m, 2H), 1.55 – 1.43 (m, 4H), 1.34 – 1.24 (m, 2H), 1.13 (t, *J* = 7.2, 3H, -COCH$_2$C*H*$_3$). **^{13}C NMR** (125 MHz, $CDCl_3$): δ 173.2, 59.9, 58.4, 45.2, 33.9, 31.7, 29.7, 29.0, 28.1, 27.5, 24.3, 14.0. HRMS (ESI) calc. for $C_{13}H_{27}NO_2S$ $[M+H]^+$ 262.1835, found 262.1837. GCMS found 261 for $[M^{+\cdot}]$.

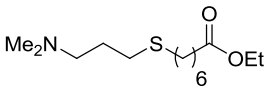

Ethyl 7-(3-(dimethylamino)propylthio)heptanoate (**108**). Compound **108** was synthesized following the general procedure for *S*-alkylation using 52 mmol of thioacetate **47**. Yield = 75% (slight yellow oil). R_f = 0.56 (AcOH/EtOAc/MeOH/H_2O 3/3/3/2). IR: 1734 cm^{-1} (ester, C=O stretch). **^{1}H NMR** (400 MHz, $CDCl_3$): δ 4.10 (q, *J* = 7.2, 2H, -COCH_2CH$_3$), 2.52 (t, *J* = 7.2, 2H, -CH_2S), 2.49 (t, *J* = 7.4, 2H, -CH_2S), 2.39 (t, *J* = 7.6, 2H, -CH_2COOEt), 2.27 (t, *J* = 7.6, 2H, -CH_2NMe$_2$), 2.25 (s, 6H, N(CH_3)$_2$), 1.76 – 1.66 (m, 2H), 1.65 – 1.50 (m, 4H), 1.41– 1.20 (m, 4H), 1.22 (t, *J* = 7.2, 3H, -COCH$_2$CH_3). **^{13}C NMR** (125 MHz, $CDCl_3$): δ 173.6, 60.1, 58.7, 45.4, 34.2, 32.1, 30.0, 29.4, 28.7, 28.5, 27.7, 24.8, 14.2. HRMS (ESI) calc. for $C_{14}H_{29}NO_2S$ $[M+H]^+$ 276.1992, found 276.1992. GCMS found 275 for $[M^{+\cdot}]$.

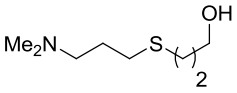

3-(3-(Dimethylamino)propylthio)propan-1-ol (**116**). Compound **116** was synthesized following the general procedure for ester reduction on 28.1 mmol ethyl ester **114**. Yield =92% (slight yellow oil). R_f = 0.28 (AcOH/EtOAc/MeOH/H_2O 3/3/3/2). **^{1}H NMR** (400 MHz, $CDCl_3$): δ 3.70 (t, *J* = 6.0, 2H, -CH_2OH), 3.04 - 2.76 (brs, 1H, -O*H*), 2.61 (t, *J* = 7.0, 2H, -CH_2S), 2.54 (t, *J* = 7.2, 2H, -CH_2S), 2.35 (t, *J* = 7.2, 2H, -CH_2NMe$_2$), 2.20 (s, 6H, N(CH_3)$_2$), 1.85 – 1.78 (m, 2H), 1.76 – 1.70 (m, 2H). **^{13}C NMR** (125 MHz, $CDCl_3$): δ 61.2, 58.4, 45.3 (2C), 32.1, 29.9, 28.7, 27.3. HRMS (ESI) calc. for $C_8H_{19}NOS$ $[M+H]^+$ 178.1260, found 178.1257. LC-MS (ESI) found 177.95 for $[M+H]^+$.

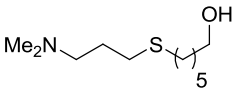

6-(3-(Dimethylamino)propylthio)hexan-1-ol (**117**). Compound **117** was synthesized following the general procedure for ester reduction on 2.29 mmol ethyl ester **115**. Yield = 87% (slight yellow oil). R_f = 0.38 (AcOH/EtOAc/MeOH/H_2O 3/3/3/2). **^{1}H NMR** (400 MHz, $CDCl_3$): δ 3.59 (t, *J* = 6.6, 2H, -CH_2OH), 2.50 (t, *J* = 7.0, 2H, -CH_2S), 2.48 (t, *J* = 7.2, 2H, -CH_2S), 2.31 (t, *J* = 7.4, 2H, CH_2NMe$_2$), 2.19 (s, 6H, N(CH_3)$_2$), 1.76 – 1.66 (m, 2H), 1.61 – 1.48 (m, 4H), 1.43 – 1.28 (m, 4H). **^{13}C NMR** (125 MHz, $CDCl_3$): δ 62.6, 58.7, 45.4 (2C), 32.6, 32.0, 30.0, 29.5, 28.5, 27.6, 25.3. HRMS (ESI) calc. for $C_{11}H_{25}NOS$ $[M+H]^+$ 220.1729, found 220.1726. LC-MS (ESI) found 220.02 for $[M+H]^+$.

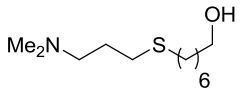

7-(3-(Dimethylamino)propythio)heptan-1-ol (**109**). Compound **109** was synthesized following the general procedure for ester reduction on 28.4 mmol ethyl ester **108**. Yield=87% (slight yellow oil). R_f = 0.42 (AcOH/EtOAc/ MeOH/H_2O 3/3/3/2). **^{1}H NMR** (400 MHz, $CDCl_3$): δ 3.54 (t, *J* = 6.6, 2H, -C*H*$_2$OH), 2.47 (t, *J* = 7.0, 2H, -C*H*$_2$S), 2.45 (t, *J* = 7.2, 2H, -C*H*$_2$S), 2.30 (t, *J* = 7.4, 2H, -C*H*$_2$NMe$_2$), 2.17 (s, 6H, N(C*H*$_3$)$_2$), 1.74 – 1.64 (m, 2H), 1.56 - 1.44 (m, 4H), 1.37 – 1.26 (m, 6H). **^{13}C NMR** (125 MHz, $CDCl_3$): δ 62.3, 58.5, 45.2 (2C), 32.6, 32.0, 29.8, 29.4, 28.8, 28.6, 27.4, 25.5. HRMS (ESI) calc. for $C_{12}H_{27}NOS$ $[M+H]^+$ 234.1886, found 234.1885. LC-MS (ESI) found 234.02 for $[M+H]^+$.

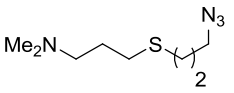

3-(3-Azidopropylthio)-*N,N*-dimethylpropan-1-amine (118). Compound **118** was synthesized following the general procedure for azide formation on 1.12 mmol alcohol **116**. Yield = 57% (brown oil). R_f = 0.48 (10% MeOH/DCM). IR: 2092 cm^{-1} (N_3). **^{1}H NMR** (400 MHz, $CDCl_3$): δ 3.38 (t, *J* = 6.6, 2H, -C*H*$_2$N$_3$), 2.57 (t, *J* = 7.2, 2H, -C*H*$_2$S), 2.52 (t, *J* = 7.4, 2H, -C*H*$_2$S), 2.34 (t, *J* = 7.2, 2H, -C*H*$_2$NMe$_2$), 2.21 (s, 6H, N(C*H*$_3$)$_2$), 1.87 – 1.79 (m, 2H), 1.77 – 1.69 (m, 2H). **^{13}C NMR** (125 MHz, $CDCl_3$): δ 58.4, 50.0, 45.3 (2C), 29.9, 28.9, 28.6, 27.4. HRMS (ESI) calc. for $C_8H_{18}N_4S$ $[M+H]^+$ 203.1325, found 203.1320. LC-MS (ESI) found 202.92 for $[M+H]^+$.

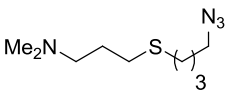

3-(4-Azidobutylthio)-*N,N*-dimethylpropan-1-amine (119). Compound **119** was synthesized following the general procedure for azide formation on 10.3 mmol alcohol **52**. Yield = 61% (brown oil). R_f = 0.42 (10% MeOH/DCM). IR: 2091 cm^{-1} (N_3).**^{1}H NMR** (400 MHz, $CDCl_3$): δ 3.28 (t, *J* = 6.2, 2H, -C*H*$_2$N$_3$), 2.53 – 2.49 (m, 4H, -C*H*$_2$S), 2.36 (t, *J* = 7.4, 2H, -C*H*$_2$NMe$_2$), 2.22 (s, 6H, N(C*H*$_3$)$_2$), 1.79 - 1.57 (m, 6H). **^{13}C NMR** (125 MHz, $CDCl_3$): δ 58.4, 50.9, 45.3 (2C), 31.5, 29.8, 27.9, 27.4, 26.5. HRMS (ESI) calc. for $C_9H_{20}N_4S$ $[M+H]^+$ 217.1481, found 217.1480. LC-MS (ESI) found 216.94 for $[M+H]^+$.

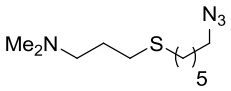

3-(6-Azidohexylthio)-*N,N*-dimethylpropan-1-amine (120). Compound **120** was synthesized following the general procedure for azide formation on 8.8 mmol alcohol **117**. Yield = 54% (brown oil). R_f = 0.51 (10% MeOH/DCM). IR: 2092 cm^{-1} (N_3). **^{1}H NMR** (400 MHz, $CDCl_3$): δ 3.19 (t, *J* = 6.8, 2H, -C*H*$_2$N$_3$), 2.48 – 2.42 (m, 4H, -C*H*$_2$S), 2.28 (t, *J* = 7.2, 2H, -C*H*$_2$NMe$_2$), 2.16 (s, 6H, N(C*H*$_3$)$_2$), 1.73 – 1.64 (m, 2H), 1.57-1.48 (m, 4H), 1.38 -1.25 (m, 4H). **^{13}C NMR** (125 MHz, $CDCl_3$): δ 58.5, 51.1, 45.3 (2C), 31.8, 29.8, 29.2, 28.5, 28.2, 27.5, 26.1. HRMS (ESI) calc. for $C_{11}H_{24}N_4S$ $[M+H]^+$ 245.1794, found 245.1794. LC-MS (ESI) found 244.97 for $[M+H]^+$.

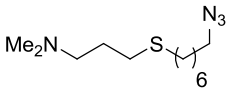

3-(7-Azidoheptylthio)-*N,N*-dimethylpropan-1-amine (121). Compound **121** was synthesized following the general procedure for azide formation on 0.86 mmol alcohol **109**. Yield = 68% (brown oil). R_f = 0.52 (10% MeOH/DCM). IR: 2091 cm^{-1} (N_3). **^{1}H NMR** (400 MHz, $CDCl_3$): δ 3.20 (t, *J* = 6.8, 2H, -C*H*$_2$N$_3$), 2.55 – 2.44 (m, 6H, -C*H*$_2$S, -C*H*$_2$S, -C*H*$_2$NMe$_2$), 2.35 (s, 6H, N(C*H*$_3$)$_2$), 1.85 – 1.75 (m, 2H), 1.63 - 1.49 (m, 4H), 1.37 - 1.19 (m, 6H). **^{13}C NMR** (125 MHz, $CDCl_3$): δ 58.0, 51.2, 44.6 (2C), 31.9, 29.5, 29.2, 28.6, 28.6, 28.5, 26.5, 26.4. HRMS (ESI) calc. for $C_{12}H_{26}N_4S$ $[M+H]^+$ 259.1951, found 259.1949. LC-MS (ESI) found 258.99 for $[M+H]^+$.

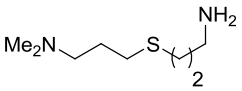

3-(3-Aminopropylthio)-*N,N*-dimethylpropan-1-amine (122). Compound **122** was synthesized following the general procedure for reduction azide into amine on 7.66 mmol azide **118**. Yield= 99% (brown oil). R_f = 0.36 (AcOH/EtOAc/MeOH/H_2O 3/3/3/2). **^{1}H NMR** (400 MHz, $CDCl_3$): δ 2.79 (t, *J* = 6.8, 2H, -C*H*$_2$NH$_2$), 2.59 – 2.51 (m, 4H, -C*H*$_2$S), 2.36 – 2.31 (m, 2H, -C*H*$_2$NMe$_2$), 2.21 (s, 6H, N(C*H*$_3$)$_2$), 1.88 – 1.80 (m, 2H), 1.78 – 1.68 (m, 2H). **^{13}C NMR** (125 MHz, $CDCl_3$): δ 58.6, 45.4 (2C), 41.0, 33.0, 29.9, 29.4, 27.6. HRMS (ESI) calc. for $C_8H_{20}N_2S$ $[M+H]^+$ 177.1420, found 177.1418. LC-MS (ESI) found 176.97 for $[M+H]^+$.

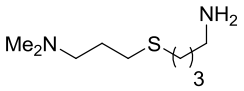

4-(3-(Dimethylamino)propylthio)butan-1-amine (123). Compound **123** was synthesized following the general procedure for reduction azide into amine on 5.94 mmol azide **119**. Yield = 86% (brown oil). R_f = 0.28 (AcOH/EtOAc/MeOH/H_2O 3/3/3/2). **^{1}H NMR** (400 MHz, $CDCl_3$): δ 2.71 (t, *J* = 6.8, 2H, -C*H*$_2$NH$_2$), 2.55 – 2.49 (m, 4H, -C*H*$_2$S), 2.43 – 2.38 (brs, 2H, N*H*$_2$), 2.34 (t, *J* = 7.4, 2H, -C*H*$_2$NMe$_2$), 2.21 (s, 6H, N(C*H*$_3$)$_2$), 1.78 – 1.68 (m, 2H), 1.66 -1.50 (m, 4H). **^{13}C NMR** (125 MHz, $CDCl_3$): δ 58.6, 45.4 (2C), 41.5, 32.4, 31.9, 29.9, 27.6, 26.9. HRMS (ESI) calc. for $C_9H_{22}N_2S$ $[M+H]^+$ 191.1576, found 191.1575. LC-MS (ESI) found 191.04 for $[M+H]^+$.

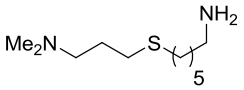

6-(3-(Dimethylamino)propylthio)hexan-1-amine (124). Compound **124** was synthesized following the general procedure for reduction azide into amine on 4.25 mmol azide **120**. Yield = 96% (brown oil). R_f = 0.33 (AcOH/EtOAc/MeOH/H_2O 3/3/3/2). **^{1}H NMR** (400 MHz, $CDCl_3$): δ 2.69 (t, *J* = 7.0, 2H, -C*H*$_2$NH$_2$), 2.52 – 2.46 (m, 4H, -C*H*$_2$S), 2.32 (t, *J* = 7.2, 2H, -C*H*$_2$NMe$_2$), 2.19 (s, 6H, N(C*H*$_3$)$_2$), 1.76 – 1.66 (m, 2H), 1.61 – 1.51 (m, 2H), 1.48 – 1.25 (m, 6H). **^{13}C NMR** (125 MHz, $CDCl_3$): δ 58.6, 45.4 (2C), 41.9, 33.1, 32.0, 29.9, 29.5, 28.6, 27.7, 26.4. HRMS (ESI) calc. for $C_{11}H_{26}N_2S$ $[M+H]^+$ 219.1889, found 219.1889. LC-MS (ESI) found 219.03 for $[M+H]^+$.

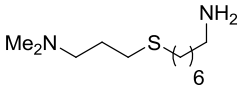

7-(3-(Dimethylamino)propylthio)heptan-1-amine (111). Compound **111** was synthesized following the general procedure for reduction azide into amine on 2.75 mmol azide **121**. Yield = 94% (brown oil). R_f =0.37 (AcOH/EtOAc/MeOH/H_2O 3/3/3/2). **^{1}H NMR** (400 MHz, $CDCl_3$): δ 2.69 (t, *J* = 7.2, 2H, -C*H*$_2$NH$_2$), 2.65 - 2.56 (brs, 2H, N*H*$_2$), 2.52 (t, *J* = 7.2, 2H, -C*H*$_2$S), 2.49 (t, *J* = 7.4, 2H, -C*H*$_2$S), 2.34 (t, *J* = 7.4, 2H, -C*H*$_2$NMe$_2$), 2.21 (s, 6H, N(C*H*$_3$)$_2$), 1.78 – 1.68 (m, 2H), 1.61 – 1.51 (m, 2H), 1.51 - 1.41 (m, 2H), 1.41 - 1.22 (m, 6H). **^{13}C NMR** (125 MHz, $CDCl_3$): δ 58.6, 45.4 (2C), 41.8, 32.8, 32.1, 29.9, 29.5, 28.9, 28.7, 27.6, 26.6. HRMS (ESI) calc. for $C_{12}H_{28}N_2S$ $[M+H]^+$ 233.2046, found 233.2046. LC-MS (ESI) found 233.03 for $[M+H]^+$.

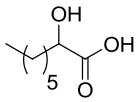

2-Hydroxyoctanoic acid (**126**).[46] To a solution of 2-bromooctanoic acid **125** (2 g, 8.9 mmol, 1.0 eqv.) in water (35 ml) was added NaOH (2.9 g, 72 mmol, 8.0 eqv.). The reaction mixture was stirred at 80°C for 24 hours and quenched at 0°C by addition of diluted HCl. The mixture was then extracted with Et_2O and the combined organic layers were washed with H_2O followed by brine and dried over anhydrous $MgSO_4$. Concentration under reduced pressure leaded to 2-hydroxyoctanoic acid **126** which was used directly in the next step. Yield= 94% (white solid). R_f = 0.76 (AcOH/EtOAc/MeOH/H_2O 3/14/3/2). IR: 1704 cm^{-1} (C=O). **^{1}H NMR** (400 MHz, $CDCl_3$): δ 4.27 (ddd, *J* = 4.0, 3.4, 3.6, 1H, -C*H*(OH)R), 1.91 - 1.79 (m, 1H, -CH_2CH(OH)R), 1.76 - 1.64 (m, 1H, -CH_2CH(OH)R), 1.55 - 1.23 (m, 8H), 0.88 (t, *J* = 6.8, 3H, -CH_3). **^{13}C NMR** (125 MHz, $CDCl_3$): δ 179.2, 70.2, 34.2, 31.6, 28.9, 24.7, 22.5, 14.0. HRMS (ESI) calc. for $C_8H_{16}O_3$ $[M-H]^-$ 159.1027, found 159.1024. LC-MS (ESI) found 159.07 for $[M-H]^-$.

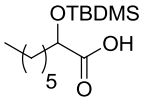

2-(Tert-butyldimethylsilyloxy)octanoic acid (**127**).[46,47] To 2-hydroxyoctanoic acid **126** (300 mg, 1.91 mmol, 1.0 eqv.) in DMF (0.8 ml) was added at 0°C imidazole (265 mg, 3.82 mmol, 2.0 eqv.) followed by TBDMSCl (1.11 g, 7.25 mmol, 3.8 eqv.) to the reaction mixture which was subsequently stirred at rt for 24 hours. The reaction mixture was then diluted with petrolum ether/EtOAc 1/1 (50ml) and washed with 10% citric acid (35 ml) followed by H_2O and saturated aqueous Na_2SO_4 solution. The organic layer was concentrated under reduced pressure and the residue finally dissolved in ice-cold MeOH (20 ml). K_2CO_3 (690 mg, 5 mmol, 2.6 eqv.) as a solution in H_2O (6 ml) was added to the reaction mixture which was then stirred at rt for 4 hours. After concentration under reduced pressure, the residue was diluted with ice-cold water and slowly acidified with 10% citric acid to approx. pH 4.0. After several extractions with EtOAc (3*40 ml), the organic layer was dried over anhydrous $MgSO_4$ and concentrated under reduced pressure leading to the TBDMS protected carboxylic acid **127** which was used directly in the next step. Yield= 76% (white solid). R_f = 0.67 (AcOH/EtOAc/MeOH/H_2O 3/3/3/2). IR: 1704 cm^{-1} (C=O). **^{1}H NMR** (400 MHz, $CDCl_3$): δ 4.28 (dd, *J* = 5.2, 5.4, 1H, -C*H*(OTBDMS)R), 1.87 - 1.62 (m, 2H, -CH_2CH(OTBDMS)R), 1.53 - 1.19 (m, 8H), 0.99 (s, 9H, -C(CH_3)$_3$, TBDMS), 0.87 (t, *J* = 7.0, 3H, -CH_3), 0.12 (s, 6H, 2* -CH_3, TBDMS). **^{13}C NMR** (125 MHz, $CDCl_3$): δ 178.9, 72.2, 34.7, 31.6, 28.9, 25.6 (-C(*C*H_3)$_3$, TBDMS), 24.1, 22.5, 18.1 (C_{IV}, TBDMS), 14.0, -4.8 (-*C*H_3, TBDMS), -5.2 (-*C*H_3,

TBDMS). HRMS (ESI) calc. for $C_{14}H_{30}O_3Si$ $[M-H]^-$ 273.1891, found 273.1891. LC-MS (ESI) found 273.11 for $[M-H]^-$.

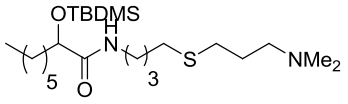

2-(Tert-butyldimethylsilyloxy)-N-(4-(3-(dimethylamino)propylthiobutyl)octanamide (**128**). To TBDMS protected α-hydroxyacid **127** (73 mg, 0.26 mmol, 1.0 eqv.) in dry THF (1 ml) was added dropwise at -10°C N-Methylmorpholine (NMM, 24 µl, 0.21 mmol, 0.8 eqv.) followed by isobutyl chloroformate (28 µl, 0.21 mmol, 0.8 eqv.). The reaction mixture was stirred at -10°C for 10 minutes. Amine **123** (60 mg, 0.31 mmol, 1.2 eqv.) in dry THF (1 ml) was subsequently added to the reaction mixture which was stirred for 1 hour at -10°C followed by 16 hours at rt. After concentration under reduced pressure, the residue was taken in EtOAc and the organic layer was washed with brine, dried over anhydrous $MgSO_4$ and concentrated to dryness. After purification by flash chromatography (eluent: gradient 1-6% MeOH/DCM) compound **128** was obtained. Yield = 57% (yellow oil). R_f = 0.85 (AcOH/EtOAc/MeOH/H_2O 3/3/3/2). IR: 1666 cm^{-1} (amide, C=O). **^{1}H NMR** (400 MHz, $CDCl_3$): δ 6.60 (t, *J* = 5.8, 1H, N*H*), 4.12 (dd, *J* = 4.6, 5.6, 1H, -C*H*(OTBDMS)CONHR), 3.37 - 3.17 (m, 2H, -CH_2NHCOR), 2.57 - 2.51 (m, 4H, -CH_2S, -CH_2S), 2.49 - 2.43 (m, 2H, -CH_2NMe_2), 2.31 (s, 6H, -N(CH_3)$_2$), 1.90 - 1.55 (m, 8H), 1.40 - 1.20 (m, 8H), 0.92 (s, 9H, -C(CH_3)$_3$, TBDMS), 0.86 (t, *J* = 7.0, 3H, -CH_3), 0.09 (s, 3H, -CH_3, TBDMS), 0.07 (s, 3H, -CH_3, TBDMS). **^{13}C NMR** (125 MHz, $CDCl_3$): δ 173.8, 73.6, 58.4, 45.0 (2C), 38.3, 35.3, 31.7, 29.8, 29.2, 28.9, 26.8, 25.7 (-C(*C*H_3)$_3$, TBDMS), 24.1, 22.6, 18.0 (C_{IV}, TBDMS), 14.0, -4.8 (-*C*H_3, TBDMS),, -5.2 (-*C*H_3, TBDMS),. HRMS (ESI) calc. for $C_{23}H_{50}N_2O_2SSi$ $[M+H]^+$ 447.3429, found 447.3430. LC-MS (ESI) found 447.25 for $[M+H]^+$.

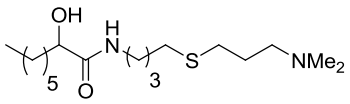

***N*-(4-(3-(dimethylamino)propylthio)butyl)-2-hydroxyoctanamide** (**129**).[46,47] To a solution of TBDMS protected α-hydroxyamide **128** (60.7 mg, 0.136 mmol, 1.0 eqv.) in dry THF (4 ml) was added dropwise TBAF (1.0M in THF, 0.8 ml, 0.8 mmol, 6.0 eqv.) at 0°C to the reaction mixture which was stirred at rt overnight. The reaction mixture was subsequently poured into brine and extracted with several portion of $CHCl_3$. Combined organic layers were washed with water followed by brine, dried over anhydrous $MgSO_4$, and concentrated under reduced pressure. Purification by flash chromatography (eluent: gradient 1-6% MeOH/DCM) lead to compound

129. Yield = 68% (yellow semi-solid). R_f= 0.71 (AcOH/EtOAc/MeOH/H_2O 3/3/3/2). IR: 1610 cm^{-1} (amide, C=O). **^{1}H NMR** (400 MHz, $CDCl_3$): δ 6.75 (t, *J* = 5.6, 1H, N*H*), 4.02 (ddd, *J* = 3.8, 4.2, 4.1, 1H, -C*H*(OH)CONHR), 3.52-3.41 (m, 1H, -CH_2NHCOR), 3.22-3.11 (m, 1H, -CH_2NHCOR), 2.60-2.47 (m, 4H, -CH_2S, -CH_2S), 2.44-2.33 (m, 2H, -CH_2NMe_2), 2.25 (s, 6H, -N(CH_3)$_2$), 190-1.50 (m, 8H), 1.48-1.21 (m, 8H), 0.87 (t, *J* = 6.8, 3H, -CH_3). **^{13}C NMR** (125 MHz, $CDCl_3$): δ 174.5, 72.0, 58.6, 45.3 (2C), 38.1, 34.9, 32.1, 31.7, 30.0, 29.1, 28.3, 27.9, 26.6, 25.3, 22.6, 14.0. HRMS (ESI) calc. for $C_{17}H_{36}N_2O_2S$ $[M+H]^+$ 333.2570, found 333.2571. LC-MS (ESI) found 333.20 for $[M+H]^+$.

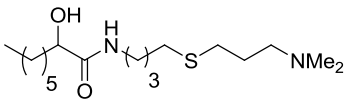

***N*-(4-(3-(dimethylamino)propylthio)butyl)-2-hydroxyoctanamide** (**129**).[48] To a solution of amine **123** (100 mg, 0.52 mmol, 1.0 eqv.) and unprotected α–hydroxyacid **126** (106 mg, 0.66 mmol, 1.27 eqv.) in dry DCM (5 ml) was added EDC·HCl (330 mg, 1.72 mmol, 3.3 eqv.) followed by HOBT (84 mg, 0.62 mmol, 1.2 eqv.) at 0° to the reaction which was stirred at 0°C for 1h and then at rt overnight. The reaction mixture was extracted with brine and the combined organic layers were dried over anhydrous $MgSO_4$ and concentrated under reduced pressure. The residue was subsequently purified by flash chromatography using a gradient of MeOH/DCM 1-10% leading to compound **129**. Yield= 76%. Similar characterization reported before after TBDMS deprotection.

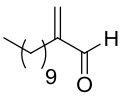

2-Methylenedodecanal (**132**).[49] In a round bottom flask was added aldehyde **131** (169 mmol, 1.0 eqv.), dimethylamine hydrogen chloride (16.75g, 203 mmol, 1.2 eqv.) followed by 37% aqueous formalin (15 ml, 203 mmol, 1.2 eqv.). The mixture was stirred at 70°C for 24 hours with progress monitorated by TLC (EtOAc/cyclohexane 1/1, formation of a less polar compound). Organic and aqueous layers were separated and the aqueous layer was extracted with several portions of hexane. Combined organic layers were dried over anhydrous $MgSO_4$, concentrated under reduced pressure and purified by short filtration over silica, leading to compound **132**. Yield= 76% (slight yellow oil). R_f = 0.79 (EtOAc/cyclohexane 3/7). IR: 1697 cm^{-1} (C=O). **^{1}H NMR** (400 MHz, $CDCl_3$): δ 9.51 (s, 1H, -C*H*O), 6.21 (d, *J* = 0.8, 1H, -C=CH_2), 5.95 (d, *J* = 0.8, 1H, -C=CH_2), 2.21 (t, *J* = 7.4, 2H), 1.45 - 1.36 (m, 2H), 1.31 - 1.18 (m, 14H), 0.85 (t, *J* = 6.8, 3H, -CH_3). **^{13}C NMR** (125 MHz, $CDCl_3$): δ 194.8, 150.5, 133.8, 31.9, 29.6, 29.5, 29.4, 29.3, 27.8, 27.7, 26.9, 22.7, 14.1.

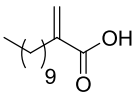

2-Methylenedodecanoic acid (**133**).[50] In a round bottom flask was added aldehyde **132** (105 mmol, 1.0 eqv.), sodium chlorite $NaClO_2$ (27.2 g, 241 mmol, 2.3 eqv.), sodium dihydrogenphosphate NaH_2PO_4 (25.45 g, 210 mmol, 2.0 eqv.) followed by 2-methyl-2-butene ($MeCH=CMe_2$, 37ml, 315 mmol, 3.0 eqv.) in t-BuOH (375 ml). Water (150 ml) was added dropwise over 10 min to the reaction mixture which was stirred at rt for 4 hours. The mixture was concentrated under reduced pressure and the residue subsequently resuspended in 2M NaOH and hexane (100 ml). The two layers were separated and the organic layer was discarded. The basic aqueous layer was re-acidified to pH 2.0 using concentrated HCl and subsequently extracted with EtOAc (4*200 ml). Combined organic layers were dried over anhydrous $MgSO_4$ and concentrated under reduced pressure leading to the carboxylic acid **133,** which was used directly in the next step.Yield = 86% (white semi-solid). R_f = 0.54 (EtOAc/cyclohexane 3/7). IR: 1693 cm^{-1} (C=O). **^{1}H NMR** (400 MHz, $CDCl_3$): δ 6.28 (d, *J* = 1.2, 1H, -C=C*H*$_2$), 5.64 (d, *J* = 1.2, 1H, -C=C*H*$_2$), 2.29 (t, *J* = 7.6, 2H, -C*H*$_2$C=C), 1.52 - 1.42 (m, 2H), 1.38 -1.20 (m, 14H), 0.88 (t, *J* = 6.8, 3H, - C*H*$_3$). **^{13}C NMR** (125 MHz, $CDCl_3$): δ 172.8, 140.3, 126.8, 31.9, 31.4, 29.6, 29.5, 29.4, 29.3, 29.2, 28.4, 22.7, 14.1. HRMS (ESI) calc. for $C_{13}H_{24}O_2$ $[M-H]^-$ 211.1704, found 211.1704. GCMS found 212 for $[M^{+\cdot}]$.

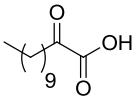

2-Oxododecanoic acid (**134**).[51-53] In a round bottom flask containing α-methylenated carboxylic acid **133** (0.94 mmol, 1.0 eqv.) in dioxane/water 3/1 (28 ml) was added catalytic OsO_4 (2.5 wt% in t-BuOH, 0.75 ml, 6.2 mol %). The dark brown mixture was stirred at rt for 45 min and sodium periodate $NaIO_4$ (603 mg, 2.82 mmol, 3.0 eqv.) was added. The reaction mixture was stirred at rt overnight until completion of the reaction visible by TLC (eluent EtOAc/cyclohexane 3/7, more polar compound formed). After evaporation under reduced pressure, the residue was diluted with DCM and 1M HCl. The aqueous layer was extracted with several portion of DCM and combined organic layers were finally dried over anhydrous $MgSO_4$ and concentrated under reduced pressure at low temperature (30°C) to prevent polymerisation or degradation of the product. The last traces of dioxane were removed by co-evaporation with several portions of n-BuOH, leading to the expected α-keto acid **134** which was used directly in the next step.Yield= 87% (slight brown semi-solid). R_f = 0.26 (20% MeOH/DCM). IR: 1713 cm^{-1} (C=O). **^{1}H NMR** (400

MHz, $CDCl_3$): δ 2.94 (t, *J* = 7.4, 2H, -C*H*$_2$CO), 1.71-1.56 (m, 2H), 1.39 - 1.18 (m, 14H), 0.88 (t, *J* = 6.8, 3H, -C*H*$_3$). **^{13}C NMR** (125 MHz, $CDCl_3$): δ 196.0, 159.5, 37.3, 31.8, 29.5, 29.3, 29.2, 29.2, 28.9, 23.1, 22.6, 14.1. HRMS (ESI) calc. for $C_{12}H_{22}O_3$ $[M-H]^-$ 213.1496, found 213.1495. LC-MS (ESI) found 426.93 for 2* $[M-H]^-$.

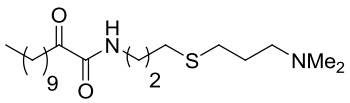

***N*-(3-(3-(dimethylamino)propylthio)propyl)-2-oxododecanamide** (**135**). Compound **135** was synthesized following the general procedure for amide formation (method A) on 1.19 mmol amine **122**. Yield = 23% (slight yellow oil). R_f = 0.24 (5% MeOH/DCM). IR: 1718 cm^{-1} (ketone, C=O), 1675 cm^{-1} (amide, C=O). **^{1}H NMR** (400 MHz, $CDCl_3$): δ 7.12 (t, *J* = 6.0, 1H, N*H*), 3.39 (ddd, *J* = 6.8, 6.8, 6.2, 2H, -C*H*$_2$NHCOR), 2.89 (t, *J* = 7.4, 2H, -C*H*$_2$CO), 2.55 (t, *J* = 7.2, 2H, -C*H*$_2$S), 2.54 (t, *J* = 7.4, 2H, -C*H*$_2$S), 2.37 (t, *J* = 7.2, 2H, -C*H*$_2$NMe$_2$), 2.23 (s, 6H, -N(C*H*$_3$)$_2$), 1.88- 1.79 (m, 2H), 1.78 - 1.70 (m, 2H), 1.64-1.54 (m, 2H), 1.35 - 1.19 (m, 14H), 0.87 (t, *J* = 6.8, 3H, -C*H*$_3$). **^{13}C NMR** (125 MHz, $CDCl_3$): δ 199.3, 160.3, 58.4, 45.3 (2C), 38.3, 36.7, 31.8, 29.9, 29.5, 29.5, 29.4, 29.3, 29.2, 29.0, 28.8, 27.4, 23.2, 22.6, 14.1. HRMS (ESI) calc. for $C_{20}H_{40}N_2O_2S$ $[M+H]^+$ 373.2883, found 373.2885. LC-MS (ESI) found 373.16 for $[M+H]^+$.

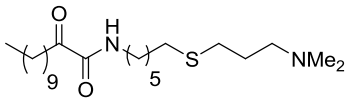

***N*-(6-(3-(dimethylamino)propylthio)hexyl)-2-oxododecanamide** (**136**). Compound **136** was synthesized following the general procedure for amide formation (method A) on 1.16 mmol amine **124**. Yield = 40% (light brown solid). R_f = 0.27 (5% MeOH/DCM). IR: 1718 cm^{-1} (ketone, C=O), 1674 cm^{-1} (amide, C=O). **^{1}H NMR** (400 MHz, $CDCl_3$): δ 6.97 (t, *J* = 5.8, 1H, N*H*), 3.28 (ddd, *J* = 6.8, 6.8, 6.2, 2H, -C*H*$_2$NHCOR), 2.90 (t, *J* = 7.2, 2H, -C*H*$_2$CO), 2.53 (t, *J* = 7.2, 2H, -C*H*$_2$S), 2.54 (t, *J* = 7.4, 2H, -C*H*$_2$S), 2.38 (t, *J* = 7.2, 2H, -C*H*$_2$NMe$_2$), 2.20 (s, 6H, -N(C*H*$_3$)$_2$), 1.85 -1.76 (m, 2H), 1.62 - 1.50 (m, 6H), 1.45 - 1.20 (m, 18H), 0.87 (t, *J* = 6.8, 3H, -C*H*$_3$). **^{13}C NMR** (125 MHz, $CDCl_3$): δ 199.5, 160.2, 58.6, 45.4 (2C), 39.2, 36.7, 32.1, 31.9, 30.0, 29.5, 29.4 (2C), 29.3, 29.3, 29.2, 29.1, 28.4, 27.6, 26.5, 23.2, 22.7, 14.1. HRMS (ESI) calc. for $C_{23}H_{46}N_2O_2S$ $[M+H]^+$ 415.3352, found 415.3347. LC-MS (ESI) found 415.21 for $[M+H]^+$.

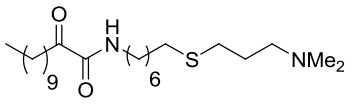

***N*-(7-(3-(dimethylamino)propylthio)heptyl)-2-oxododecanamide** (**137**). Compound **137** was synthesized following the general procedure for amide formation (method B) on 0.21 mmol amine **111**. Yield = 33% (light brown solid). R_f = 0.27 (5% MeOH/DCM). IR: 1720 cm^{-1} (ketone, C=O), 1657 cm^{-1} (amide, C=O). **^{1}H NMR** (400 MHz, $CDCl_3$): δ 6.94 (t, *J* = 5.8, 1H, N*H*), 3.27 (ddd, *J* = 6.8, 6.8, 6.0, 2H, -CH_2NHCOR), 2.90 (t, *J* = 7.2, 2H, -CH_2CO), 2.53 (t, *J* = 7.4, 2H, -CH_2S), 2.49 (t, *J* = 7.4, 2H, -CH_2S), 2.45 (t, *J* = 7.4, 2H, -C$H_2$$NMe_2$), 2.29 (s, 6H, -N(C$H_3$)$_2$), 1.84 -1.75 (m, 2H), 1.64 - 1.48 (m, 6H), 1.43 - 1.18 (m, 20H), 0.87 (t, *J* = 6.8, 3H, -CH_3). **^{13}C NMR** (125 MHz, $CDCl_3$): δ 199.5, 160.1, 58.4, 45.1 (2C), 39.2, 36.7, 32.1, 31.8, 29.9, 29.5, 29.5, 29.4, 29.3, 29.3, 29.2, 29.0, 28.8, 28.7, 27.2, 26.7, 23.2, 22.6, 14.1. HRMS (ESI) calc. for $C_{24}H_{48}N_2O_2S$ $[M+H]^+$ 429.3509, found 429.3503. LC-MS (ESI) found 429.23 for $[M+H]^+$.

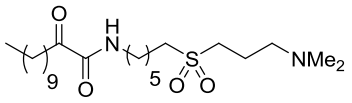

***N*-(6-(3-(dimethylamino)propylsulfonyl)hexyl)-2-oxododecanamide** (**138**)**.** Compound **138** was synthesized following the general procedure for oxidation into sulfone using 0.06 mmol of sulfide derivative **136**, reaction time 24 hours. Purification by reverse phase chromatography using RPC_{18} column (eluent 0 – 100 % MeOH). Yield= 52% (white semi-solid). R_f = 0.57 (EtOAc/AcOH/ MeOH/H_2O 3/3/3/2)**.** IR: 1717 cm^{-1} (ketone, C=O), 1659 cm^{-1} (amide, C=O), 1293 cm^{-1} (SO_2, asym. strectch), 1122 cm^{-1} (SO_2, sym. strectch). **^{1}H NMR** (400 MHz, $CDCl_3$): δ 6.96 (t, *J* = 5.8, 1H, N*H*), 3.28 (ddd, *J* = 6.8, 6.8, 6.0, 2H, -CH_2NHCOR), 3.05- 2.99 (m, 2H, -C$H_2$$SO_2$), 2.98 - 2.93 (m, 2H, -C$H_2$$SO_2$), 2.90 (t, *J* = 7.4, 2H, -CH_2CO), 2.47 (t, *J* = 6.8, 2H, -C$H_2$$NMe_2$), 2.26 (s, 6H, -N(C$H_3$)$_2$), 2.06 - 1.97 (m, 2H), 1.89 - 1.79 (m, 2H), 1.65 -1.16 (m, 22H), 0.87 (t, *J* = 6.8, 3H, -CH_3). **^{13}C NMR** (125 MHz, $CDCl_3$): δ 199.4, 160.1, 57.2, 52.8, 50.4, 44.7 (2C), 38.9, 38.7, 31.9, 29.5, 29.4, 29.3, 29.3, 29.0, 28.9, 28.0, 26.2, 23.1, 22.6, 21.8, 19.4, 14.1**.** HRMS (ESI) calc. for $C_{23}H_{46}N_2O_4S$ $[M+H]^+$ 447.3251, found 447.3246, $[M+Na]^+$ 469.3070, found 469.3062. LC-MS (ESI) found 447.28 for $[M+H]^+$.

2.13 Synthesis of α-keto CF_2CF_3/CF_3 candidate inhibitors

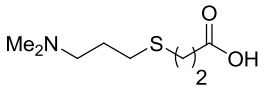

3-(3-(Dimethylamino)propylthio)propanoic acid (**139**). Compound **139** was synthesized following the general procedure for ester saponification on 11.4 mmol of ethyl ester **114.** White solid. R_f = 0.51 (AcOH/EtOAc/MeOH/H_2O 3/3/3/2). IR: 1721 cm^{-1} (C=O). **^{1}H NMR** (400 MHz, $CDCl_3$): δ 3.21 – 3.15 (m, 2H, -CH_2COOH), 2.89 - 2.86 (m, 2H, -CH_2NMe_2), 2.85 (s, 6H, N(CH_3)$_2$), 2.74 – 2.64 (m, 4H, -CH_2S), 2.20 – 2.10 (m, 2H). **^{13}C NMR** (125 MHz, $CDCl_3$): δ 174.1, 56.8, 43.3 (2C), 35.2, 29.2, 27.6, 24.2. HRMS (ESI) calc. for $C_8H_{17}NO_2S$ $[M+H]^+$ 192.1052, found 192.1052. LC-MS (ESI) found 192.00 for $[M+H]^+$.

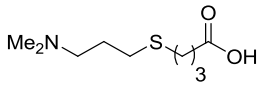

4-(3-(Dimethylamino)propylthio)butanoic acid (**140**). Compound **140** was synthesized following the general procedure for ester saponification on 6.5 mmol of ethyl ester **50**. White solid. R_f = 0.54 (AcOH/EtOAc/MeOH/H_2O 3/3/3/2). IR: 1715 cm^{-1} (C=O). **^{1}H NMR** (400 MHz, $CDCl_3$): δ 3.20 – 3.15 (m, 2H, -CH_2COOH), 2.85 (s, 6H, N(CH_3)$_2$), 2.63 (t, *J* = 6.8, 2H, -CH_2S), 2.62 (t, *J* = 7.0, 2H, -CH_2S), 2.48 (t, *J* = 7.0, 2H, -CH_2NMe_2), 2.20 – 2.11 (m, 2H), 1.97 – 1.87 (m, 2H). **^{13}C NMR** (125 MHz, $CDCl_3$): δ 175.8, 56.9, 43.2, 32.7, 30.5, 28.3, 24.2, 23.8. HRMS (ESI) calc. for $C_9H_{19}NO_2S$ $[M+H]^+$ 206.1209, found 206.1209. LC-MS (ESI) found 206.01 for $[M+H]^+$.

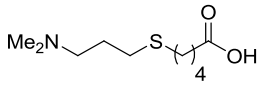

5-(3-(Dimethylamino)propylthio)pentanoic acid (**141**). Compound **141** was synthesized following the general procedure for ester saponification on 2.65 mmol of ethyl ester **51**. Yellow solid. R_f = 0.58 (AcOH/EtOAc/MeOH/H_2O 3/3/3/2). IR: 1722 cm^{-1} (C=O). **^{1}H NMR** (400 MHz, $CDCl_3$): δ 3.23 – 3.14 (m, 2H, -CH_2COOH), 2.86 (s, 6H, N(CH_3)$_2$), 2.61 (t, *J* = 6.6, 2H, -CH_2S), 2.57 (t, *J* = 6.8, 2H, -CH_2S), 2.38 (t, *J* = 6.8, 2H, -CH_2NMe_2), 2.19 – 2.08 (m, 2H), 1.82 – 1.74 (m, 2H), 1.71 – 1.63 (m, 2H). **^{13}C NMR** (125 MHz, $CDCl_3$): δ 176.5, 57.2, 43.4 (2C), 33.4, 31.4, 28.9, 28.6, 24.2, 23.2. HRMS (ESI) calc. for $C_{10}H_{21}NO_2S$ $[M+H]^+$ 220.1365, found 220.1365. LC-MS (ESI) found 220.03 for $[M+H]^+$.

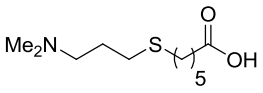

6-(3-(Dimethylamino)propylthio)hexanoic acid (**142**). Compound **142** was synthesized following the general procedure for ester saponification on 5.7 mmol of ethyl ester **115**. Yellow solid. R_f = 0.61 (AcOH/EtOAc/MeOH/H_2O 3/3/3/2). IR: 1729 cm^{-1} (C=O). **^{1}H NMR** (400 MHz, $CDCl_3$): δ 3.19 – 3.13 (m, 2H, -CH_2COOH), 2.84 (s, 6H, N(CH_3)$_2$), 2.61 (t, *J* = 6.8, 2H, -CH_2S), 2.55 (t, *J* = 7.0, 2H, -CH_2S), 2.36 (t, *J* = 7.0, 2H, -CH_2NMe_2), 2.19 – 2.10 (m, 2H), 1.73 – 1.57 (m, 4H), 1.52 – 1.44 (m, 2H). **^{13}C NMR** (125 MHz, $CDCl_3$): δ 176.9, 57.1, 43.2 (2C), 33.7, 31.8, 28.7, 28.7, 27.7, 24.2, 24.0. HRMS (ESI) calc. for $C_{11}H_{23}NO_2S$ $[M+H]^+$ 234.1522, found 234.1522. LC-MS (ESI) found 234.05 for $[M+H]^+$.

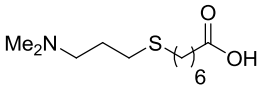

7-(3-(Dimethylamino)propylthio)heptanoic acid (**143**). Compound **143** was synthesized following the general procedure for ester saponification on 5.6 mmol of ethyl ester **108**. Yellow solid. R_f = 0.71 (AcOH/EtOAc/MeOH/H_2O 3/3/3/2). IR: 1722 cm^{-1} (C=O). **^{1}H NMR** (400 MHz, $CDCl_3$): δ 3.22 – 3.16 (m, 2H, -CH_2COOH), 2.88 (s, 6H, N(CH_3)$_2$), 2.62 (t, *J* = 7.0, 2H, -CH_2S), 2.56 (t, *J* = 7.4, 2H, -CH_2S), 2.37 (t, *J* = 6.8, 2H, -CH_2NMe_2), 2.25 – 2.23 (m, 2H), 1.71 - 1.59 (m, 4H), 1.51 - 1.36 (m, 4H). **^{13}C NMR** (125 MHz, $CDCl_3$): δ 176.9, 57.2, 43.4 (2C), 33.7, 30.8, 28.6, 28.2, 27.5, 27.2, 24.1, 23.9. HRMS (ESI) calc. for $C_{12}H_{25}NO_2S$ $[M+H]^+$ 248.1678, found 248.1679. LC-MS (ESI) found 248.04 for $[M+H]^+$.

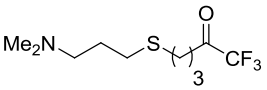

5-(3-(Dimethylamino)propylthio)-1,1,1-trifluoropentan-2-one (**145**). Compound **145** was synthesized following the general procedure for keto-CF_3 formation on 0.77 mmol of carboxylic acid **140**. Yield = 52% (over 2 steps, starting from ester **50**, as yellow oil). R_f = 0.71 (AcOH/EtOAc/MeOH/H_2O 3/3/3/2). IR: 1762 cm^{-1} (C=O). **^{1}H NMR** (400 MHz, $CDCl_3$): δ 2.86 (t, *J* = 6.8, 2H, -CH_2COCF_3), 2.57 (t, *J* = 6.8, 2H, -CH_2S), 2.52 (t, *J* = 7.4, 2H, -CH_2S), 2.37 (t, *J* = 7.4, 2H, -CH_2NMe_2), 2.24 (s, 6H, N(CH_3)$_2$), 2.02 – 1.93 (m, 2H), 1.79 – 1.70 (m, 2H). **^{13}C NMR** (125 MHz, $CDCl_3$): δ 191.0 (q, CO, J^2 (C-F) = 35Hz), 115.5 (q, CF_3, J^1 (C-F)= 290Hz), 58.4, 45.3 (2C), 34.9, 30.8, 29.5, 27.2, 21.9. **^{19}F NMR** (377 MHz, $CDCl_3$): δ -79.6 (s). HRMS (ESI) calc. for $C_{10}H_{18}F_3NOS$ $[M+H]^+$ 258.1134, found 258.1135. GCMS found 257 for $[M^{+\cdot}]$.

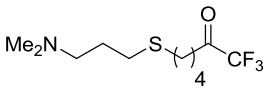

6-(3-(Dimethylamino)propylthio)-1,1,1-trifluorohexan-2-one (**146**). Compound **146** was synthesized following the general procedure for keto-CF_3 formation on 0.68 mmol of carboxylic acid **141**. Yield = 53% (over 2 steps, starting from ester **51**, as yellow oil). R_f = 0.72 (AcOH/EtOAc/MeOH/H_2O 3/3/3/2). IR: 1762 cm^{-1} (C=O). **^{1}H NMR** (400 MHz, $CDCl_3$): δ 2.74 (t, *J* = 7.2, 2H, -CH_2COCF_3), 2.53 (2*t, *J* = 7.2, 4H, -CH_2S), 2.35 (t, *J* = 7.2, 2H, -CH_2NMe_2), 2.22 (s, 6H, N(CH_3)$_2$), 1.84 -1.70 (m, 6H), 1.67 - 1.60 (m, 2H). **^{13}C NMR** (125 MHz, $CDCl_3$): δ 191.1 (q, CO, J^2(C-F) = 34.7 Hz), 115.4 (q, CF_3, J^1 (C-F)= 290 Hz), 58.5, 45.3 (2C), 35.8, 31.5, 29.9, 28.4, 27.4, 21.4. **^{19}F NMR** (377 MHz, $CDCl_3$): δ - 79.7 (s, CF_3). HRMS (ESI) calc. for $C_{11}H_{20}F_3NOS$ $[M+H]^+$ 272.1290, found 272.1292. GCMS found 271 for $[M^{+\cdot}]$.

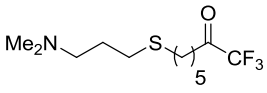

7-(3-(Dimethylamino)propylthio)-1,1,1-trifluoroheptan-2-one (**147**). Compound **147** was synthesized following the general procedure for keto-CF_3 formation on 0.67 mmol of carboxylic acid **142**. Yield = 52% (over 2 steps, starting from ester **115**, as yellow oil). R_f = 0.67 (AcOH/EtOAc/MeOH/H_2O 3/3/3/2). IR: 1762 cm^{-1} (C=O). **^{1}H NMR** (400 MHz, $CDCl_3$): δ 2.72 (t, *J* = 7.4, 2H, -CH_2COCF_3), 2.54 (t, *J* = 7.2, 2H, -CH_2S), 2.52 (t, *J* = 7.2, 2H, -CH_2S), 2.37 (t, *J* = 7.2, 2H, -CH_2NMe_2), 2.24 (s, 6H, N(CH_3)$_2$), 1.81 – 1.57 (m, 6H), 1.49 - 1.39 (m, 2H). **^{13}C NMR** (125 MHz, $CDCl_3$): δ 191.3 (q, CO, J^2(C-F) = 34.7 Hz), 115.48 (q, CF_3, J^1 (C-F)= 290 Hz), 58.5, 45.2 (2C), 36.2, 31.7, 29.9, 29.1, 27.8, 27.4, 21.9. **^{19}F NMR** (377 MHz, $CDCl_3$): δ - 79.7 (s, CF_3). HRMS (ESI) calc. for $C_{12}H_{22}F_3NOS$ $[M+H]^+$ 286.1447, found 286.1449. GCMS found 285 for $[M^{+\cdot}]$.

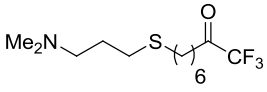

8-(3-(Dimethylamino)propylthio)-1,1,1-trifluorooctan-2-one (**148**). Compound **148** was synthesized following the general procedure for keto-CF_3 formation on 0.63 mmol of carboxylic acid **143**. Yield = 45% (over 2 steps, starting from ester **108**, as yellow oil). R_f = 0.73 (AcOH/EtOAc/MeOH/H_2O 3/3/3/2). IR: 1762 cm^{-1} (C=O). **^{1}H NMR** (400 MHz, $CDCl_3$): δ 2.70 (t, *J* = 7.2, 2H, -CH_2COCF_3), 2.53 (t, *J* = 7.4, 2H, -CH_2S), 2.51 (t, *J* = 7.4, 2H, -CH_2S), 2.35 (t, *J* = 7.4, 2H, -CH_2NMe_2), 2.23 (s, 6H, N(CH_3)$_2$), 1.79 – 1.53 (m, 6H), 1.46 - 1.26 (m, 4H). **^{13}C NMR** (125 MHz, $CDCl_3$): δ 191.4 (q, CO, J^2(C-F) = 34.6Hz), 115.5 (q, CF_3, J^1 (C-F)= 290 Hz), 58.5, 45.2 (2C), 36.2,

31.9, 29.9, 29.2, 28.3, 28.2, 27.3, 22.1. **^{19}F NMR** (377 MHz, $CDCl_3$): δ - 79.7 (s, CF_3). HRMS (ESI) calc. for $C_{13}H_{24}F_3NOS$ $[M+H]^+$ 300.1603, found 300.1606. GCMS found 299 for $[M^{+\cdot}]$.

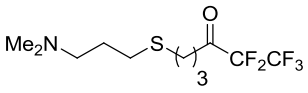

6-(3-(Dimethylamino)propylthio)-1,1,1,2,2-pentafluorohexan-3-one (**150**). Compound **150** was synthesized following the general procedure for keto-CF_2CF_3 formation on 0.77 mmol of carboxylic acid **140**. Yield = 46% (over 2 steps, starting from ester **50,** as a yellow-brown oil). R_f = 0.74 (AcOH/EtOAc/MeOH/H_2O 3/3/3/2). IR: 1753 cm^{-1} (C=O). **^{1}H NMR** (400 MHz, $CDCl_3$): δ 2.89 (t, *J* = 7.0, 2H, -C*H*$_2$COCF$_2$CF$_3$), 2.56 (t, *J* = 7.0, 2H, -C*H*$_2$S), 2.52 (t, *J* = 7.4, 2H, -C*H*$_2$S), 2.38 (t, *J* = 7.2, 2H, -C*H*$_2$NMe$_2$), 2.25 (s, 6H, N(C*H*$_3$)$_2$), 2.02 – 1.91 (m, 2H), 1.81 – 1.70 (m, 2H). **^{13}C NMR** (125 MHz, $CDCl_3$): δ 193.9 (t, CO, *J* = 26.4), 117.7 (q of t, CF_3, *J*=34Hz, *J*=283 Hz), 106.8 (t of q, CF_2, *J*=265 Hz, *J*=37.8 Hz), 58.3, 45.1(2C), 35.9, 30.7, 29.4, 27.0, 21.9. **^{19}F NMR** (377 MHz, $CDCl_3$): δ -82.3 (s, CF_3), -123.5 (s, CF_2). HRMS (ESI) calc. for $C_{11}H_{18}F_5NOS$ $[M+H]^+$ 308.1102, found 308.1104. GCMS found 307 for $[M^{+\cdot}]$.

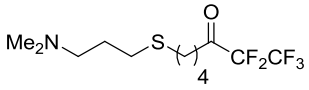

7-(3-(Dimethylamino)propylthio)-1,1,1,2,2-pentafluoroheptan-3-one (**151**)**.** Compound **151** was synthesized following the general procedure for keto-CF_2CF_3 formation on 0.68 mmol of carboxylic acid **141**. Yield = 51% (over 2 steps, starting from ester **51**, as yellow oil). R_f = 0.72 (AcOH/EtOAc/MeOH/H_2O 3/3/3/2). IR: 1754 cm^{-1} (C=O). **^{1}H NMR** (400 MHz, $CDCl_3$): δ 2.78 (t, *J* = 7.0, 2H, -C*H*$_2$COCF$_2$CF$_3$), 2.54 (t, *J* = 7.4, 2H, -C*H*$_2$S), 2.53 (t, *J* = 7.2, 2H, -C*H*$_2$S), 2.36 (t, *J* = 7.2, 2H, -C*H*$_2$NMe$_2$), 2.23 (s, 6H, N(C*H*$_3$)$_2$), 1.84 -1.71 (m, 4H), 1.67 - 1.59 (m, 2H). **^{13}C NMR** (125 MHz, $CDCl_3$): δ 193.9 (t, CO, *J* = 26.4Hz), 117.7 (q of t, CF_3, *J* = 33.9 Hz, *J* = 285 Hz), 106.8 (t of q, CF_2, *J* = 265Hz, *J* = 37.9 Hz), 58.5, 45.3, 36.8, 31.5, 29.9, 28.4, 27.4, 21.4. **^{19}F NMR** (377 MHz, $CDCl_3$): δ -82.3 (s, CF_3), -127.7 (s, CF_2). HRMS (ESI) calc. for $C_{12}H_{20}F_5NOS$ $[M+H]^+$ 322.1258, found 322.1261. GCMS found 321 for $[M^{+\cdot}]$.

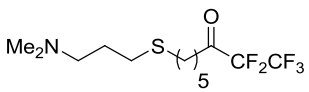

8-(3-(Dimethylamino)propylthio)-1,1,1,2,2-pentafluorooctan-3-one (**152**). Compound **152** was synthesized following the general procedure for keto-CF_2CF_3 formation on 0.67 mmol of

carboxylic acid **142**. Yield = 46% (over 2 steps, starting from ester **115**, as yellow oil). R_f = 0.74 (AcOH/EtOAc/MeOH/H_2O 3/3/3/2). IR: 1754 cm^{-1} (C=O). **^{1}H NMR** (400 MHz, $CDCl_3$): δ 2.75 (t, *J* = 7.0, 2H, -CH_2COCF_2CF_3), 2.53 (t, *J* = 7.2, 2H, -CH_2S), 2.51 (t, *J* = 7.2, 2H, -CH_2S), 2.36 (t, *J* = 7.2, 2H, -CH_2NMe_2), 2.23 (s, 6H, N(CH_3)$_2$), 1.79 – 1.56 (m, 6H), 1.46 - 1.38 (m, 2H). **^{13}C NMR** (125 MHz, $CDCl_3$): δ 194.2 (t, CO, *J* = 26.2Hz), 117.7 (q of t, CF_3, *J* = 34 Hz, *J* = 285 Hz), 106.8 (t of q, CF_2, *J* = 37.8 Hz, *J* = 265Hz), 58.5, 45.2 (2C), 37.2, 31.7, 29.9, 29.1, 27.8, 27.4, 21.9. **^{19}F NMR** (377 MHz, $CDCl_3$): δ - 82.3 (s, CF_3), -123.7 (s, CF_2). HRMS (ESI) calc. for $C_{13}H_{22}F_5NOS$ $[M+H]^+$ 336.1415, found 336.1416. GCMS found 335 for $[M^{+\cdot}]$.

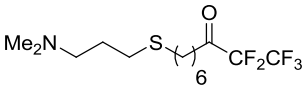

9-(3-(Dimethylamino)propylthio)-1,1,1,2,2-pentafluorononan-3-one (**153**). Compound **153** was synthesized following the general procedure for keto-CF_2CF_3 formation on 0.63 mmol of carboxylic acid **143**. Yield = 45% (over 2 steps, starting from ester **108**, as yellow oil). R_f = 0.80 (AcOH/EtOAc/MeOH/H_2O 3/3/3/2). IR: 1754 cm^{-1} (C=O). **^{1}H NMR** (400 MHz, $CDCl_3$): δ 2.75 (t, *J* = 7.0, 2H, -CH_2COCF_2CF_3), 2.54 (t, *J* = 7.4, 2H, -CH_2S), 2.51 (t, *J* = 7.2, 2H, -CH_2S), 2.36 (t, *J* = 7.4, 2H, -CH_2NMe_2), 2.23 (s, 6H, N(CH_3)$_2$), 1.80 – 1.54 (m, 6H), 1.45 - 1.28 (m, 4H). **^{13}C NMR** (125 MHz, $CDCl_3$): δ 194.3 (t, CO, *J* = 26.1 Hz), 117.7 (q of t, CF_3, *J* = 34 Hz, *J* = 285 Hz), 106.8 (t of q, CF_2, *J* = 37.8 Hz, *J* = 265 Hz), 58.6, 45.3 (2C), 37.2, 31.9, 29.9, 29.2, 28.3, 28.2, 27.5, 22.1. **^{19}F NMR** (377 MHz, $CDCl_3$): δ -82.3 (s, CF_3), -123.7 (s, CF_2). HRMS (ESI) calc. for $C_{14}H_{24}F_5NOS$ $[M+H]^+$ 350.1571, found 350.1573. GCMS found 349 for $[M^{+\cdot}]$.

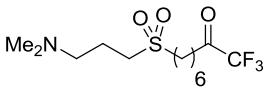

8-(3-(Dimethylamino)propylsulfonyl)-1,1,1-trifluorooctan-2-one (**154**). Compound **154** was synthesized following the general procedure for oxidation into sulfone using 0.104 mmol of the sulfide derivative **148**, reaction time 24 hours. Purification by reverse phase chromatography using RPC_{18} column (eluent 0 – 100 % MeOH). Yield = 35% (light brown semi-solid). R_f = 0.48 (AcOH/EtOAc/MeOH/H_2O 3/3/3/2). IR: 1763 cm^{-1} (C=O), 1278 cm^{-1} (SO_2 asym. stretch), 1130 cm^{-1} (SO_2 sym. stretch). **^{1}H NMR** (400 MHz, $CDCl_3$): δ 3.06 – 3.00 (m, 2H, -C$H_2$$SO_2$), 2.98 – 2.92 (m, 2H, -C$H_2$$SO_2$), 2.72 (t, *J* = 7.2, 2H, -CH_2COCF_2CF_3), 2.41 (t, *J* = 6.8, 2H, -CH_2NMe_2), 2.23 (s, 6H, N(CH_3)$_2$), 2.04 - 1.95 (m, 2H), 1.90 -1.81 (m, 2H), 1.76 – 1.63 (m, 2H), 1.53 - 1.34 (m, 4H). **^{13}C NMR** (125 MHz, $CDCl_3$): δ 191.3 (q, CO, *J* = 34.8 Hz), 115.5 (q, CF_3, *J* = 290Hz), 57.4, 52.8, 50.4, 45.0 (2C),

36.1, 28.2, 28.1, 21.9, 21.7, 19.6. **^{19}F NMR** (377 MHz, $CDCl_3$): δ - 79.7 (s, CF_3). HRMS (ESI) calc. for $C_{13}H_{24}F_3NO_3S$ $[M+H]^+$ 332.1502, found 332.1505. GCMS found 331 for $[M^{+\cdot}]$.

2.14 Synthesis of α-keto oxazole candidate inhibitors

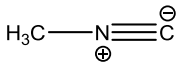

Methyl isocyanide (**157**).[54] In a four neck round bottom flask equipped with a 100 ml pressure – equalizing dropping funnel, a egg-shaped stirring bar, a thermometer and a receiver trap, was added quinoline (413 ml, 3.43 mol, 4.0 eqv.) and p-toluenesulfonyl chloride (250 g, 1.29 mol, 1.5 eqv.). The solution was heated at 85°C and the system evacuated to a pressure of 20 mbar. The receiver was cooled in a bath of liquid nitrigen. While the solution was vigorously stirred and maintained at 85°C, N-methylformamide (51 ml, 85 mmol, 1.0 eqv.) was added dropwise in order to keep a smooth distillation rate. The addition was completed in 25 minutes. The material which was collected in the receiver was distilled through a 15 cm vigreux column at atmospheric pressure. Methyl isocyanide **157** was collected, as a slight yellow liquid at 62°C in a 76% yield. **^{1}H NMR** (400 MHz, $CDCl_3$): δ 3.05, 3.045, 3.04 (3s, 3H). **^{13}C NMR** (125 MHz, $CDCl_3$): δ 156.9, 156.8, 156.8 (3C), 21.2, 27.1, 27.0 (3C).

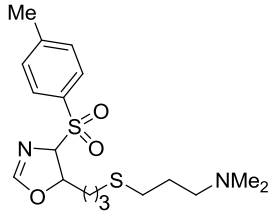

***N,N*-dimethyl-3-((4-tosyl-4,5-dihydrooxazol-5-yl)methylthio)propan-1-amine** (**155**).[55] To a 3 ml sealed glass-vial of equipped with a stirring bar was added aldehyde **54** (55.6 mg, 0.29 mmol, 1.0 eqv.) and K_2CO_3 (124.5 mg, 0.88 mmol, 3.0 eqv.) in acetonitrile (1.5 ml). TosMIC (61 mg, 0.29 mmol, 1.0 eqv.) was subsequently added to the reaction mixture which was heated under reflux (T=85°C) for 8 hours. After concentration under reduced pressure, compound **155** was obtained in 45% yield. **^{1}H NMR** (400 MHz, $CDCl_3$): δ 7.81 (d, *J* = 8.3, 2H), 7.37 (d, *J* = 7.9, 2H), 6.97 (d, *J* = 1.6, 1H), 5.05 (dd, *J* = 5.9, 12.6, 1H), 4.77 (dd, J = 1.7, 5.8, 1H), 2.59-2.49 (m, 2H), 2.45 (s, 3H, -C*H*$_3$), 2.37- 2.28 (m, 4H), 2.21 (s, 6H), 1.84 – 1.62 (m, 6H). **^{13}C NMR** (125 MHz, $CDCl_3$): δ 159.3, 145.4, 133.0, 129.7, 129.4, 89.7, 78.5, 58.4, 45.3 (2C), 33.9, 31.4, 29.8, 27.5, 24.4, 21.6.

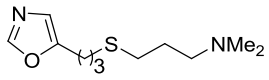

***N,N*-dimethyl-3-(3-(oxazol-5-yl)propylthiol)propan-1-amine** (**156**).[56] In a two neck round bottom flask equipped with a egg-shaped stirring bar was dissolved aldehyde **54** (203.3 mg, 1.07 mmol, 1.0 eqv.) into dry MeOH (10 ml). Tosylmethyl isocyanide (215.4 mg, 1.08 mmol, 1.0 eqv.) followed by K_2CO_3 (156.6 mg, 1.11 mmol, 1.0 eqv.) were added to the reaction mixture which was heated 1 hour under reflux (T=85°C). A solution of KOH (1.0459 g, 15.84 mmol, 14.8 eqv.) in MeOH (14 ml) was subsequently added to the reaction mixture which was stirred under reflux for 3 hours (T= 85°C). The reaction was cooled to rt and diluted with water (100 ml) and EtOAc (100 ml). The aqueous layer was extracted with EtOAc (2×100 ml) and the combined organic extracts were dried over anhydrous $MgSO_4$ and concentrated under reduced pressure. The residue was purified by flash chromatography using as eluent 10/90 MeOH/DCM. Yield = 16% (clear yellow oil). R_f= 0.43 (EtOAc/AcOH/MeOH/H_2O 3/3/3/2). **^{1}H NMR** (400 MHz, $CDCl_3$): δ 7.76 (s, 1H, *H*-C=N), 6.78 (t, *J* = 0.8, 1H, *H*-C=C), 2.79 (dt, *J* = 7.4, 0.8, 2H, -CH_2-C=C), 2.56 (t, *J* = 7.2, 2H, -CH_2S), 2.55 (t, *J* = 7.4, 2H,-CH_2S), 2.38 (t, *J* = 7.2, 2H, -CH_2NMe_2), 2.25 (s, 6H, N(CH_3)$_2$), 1.96 - 1.88 (m, 2H), 1.79 - 1.70 (m, 2H). **^{13}C NMR** (125 MHz, $CDCl_3$): δ 152.3, 145.1, 122.5, 58.7, 45.5 (2C), 31.5, 30.1, 27.7, 27.6, 24.5. HRMS (ESI) calc. for $C_{11}H_{20}N_2OS$ $[M+H]^+$ 229.1369, found 229.1368. GCMS found 228 for $[M^{+\cdot}]$.

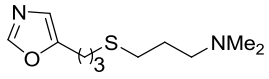

***N,N*-dimethyl-3-(3-(oxazol-5-yl)propylthiol)propan-1-amine** (**156**).[55,57] To a two neck round bottom flask equipped with a egg-shaped stirring bar was added aldehyde **54** (201.3 mg, 1.05 mmol, 1.0 eqv.) into dry MeOH (10 ml). A solution of NaOMe (6.48 mmol, 149 mg in 7.5 ml of dry MeOH, 6.2 eqv.) followed by tosylmethyl isocyanide (256.2 mg, 1.28 mmol, 1.2 eqv.) was added to the reaction mixture which was heated under reflux (T=110°C) for 12 hours. The reaction was cooled to rt and concentrated under reduced pressure. The residue was diluted with water (10 ml) and extracted with several portion of $CHCl_3$ (2×10 ml). The combined organic layers were dried over anhydrous $MgSO_4$, and concentrated under reduced pressure. The residue was purified by flash chromatography using as eluent 10/90 MeOH/DCM. Yield = 30% (clear yellow oil). R_f= 0.43 (EtOAc/AcOH/MeOH/H_2O 3/3/3/2). **^{1}H NMR** (400 MHz, $CDCl_3$): δ 7.75 (s, 1H, *H*-C=N), 6.77 (t, *J* = 0.8, 1H, *H*-C=C), 2.78 (dt, *J* = 7.4, 0.8, 2H, -CH_2-C=C), 2.55 (t, *J* = 7.4, 2H, -CH_2S), 2.55 (t, *J* = 7.4, 2H,-CH_2S), 2.38 (t, *J* = 7.4, 2H, -CH_2NMe_2), 2.24 (s, 6H, N(CH_3)$_2$), 1.96 - 1.88 (m, 2H), 1.79 - 1.70 (m, 2H). Characterization conformed to the one obtained using the previous method.

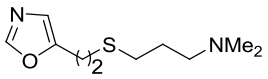

***N,N*-dimethyl-3-(2-(oxazol-5-yl)ethylthio)propan-1-amine** (**158**). Compound **158** was synthesized following the general procedure for the C5-substituted oxazole formation on 4.3 mmol of ester **114**. Yield = 84% (yellow oil). R_f= 0.42 (EtOAc/AcOH/MeOH/H_2O 3/3/3/2). **^{1}H NMR** (400 MHz, $CDCl_3$): δ 7.71 (s, 1H, *H*-C=N), 6.77 (t, *J* = 0.8, 1H, *H*-C=C), 2.81 - 2.97 (m, 2H, -CH_2-C=C), 2.76 - 2.71 (m, 2H, -CH_2S), 2.49 (t, *J* = 7.4, 2H, -CH_2S), 2.26 (t, *J* = 7.2, 2H, -C$H_2$$NMe_2$), 2.14 (s, 6H, N(C$H_3$)$_2$), 1.67 (dd, *J* = 7.4, 7.2, 2H). **^{13}C NMR** (125 MHz, $CDCl_3$): δ 150.9, 150.1, 122.6, 58.3, 45.3, 29.9, 29.4, 27.5, 26.1. HRMS (ESI) calc. for $C_{10}H_{18}N_2OS$ $[M+H]^+$ 215.1213, found 215.1211. GCMS found 214 for $[M^{+\cdot}]$.

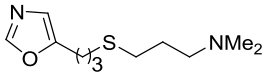

***N,N*-dimethyl-3-(3-(oxazol-5-yl)propylthiol)propan-1-amine** (**156**). Compound **156** was synthesized following the general procedure for the C5-substituted oxazole formation on 5.8 mmol of ester **50** (no purification needed). Yield = 95% (yellow oil). R_f = 0.43 (EtOAc/AcOH/MeOH/H_2O 3/3/3/2). **^{1}H NMR** (400 MHz, $CDCl_3$): δ 7.73 (s, 1H, *H*-C=N), 6.74 (t, *J* = 0.8, 1H, *H*-C=C), 2.75 (dt, *J* = 7.4, 0.8, 2H, -CH_2-C=C), 2.55 (t, *J* = 7.2, 2H, -CH_2S), 2.54 (t, *J* = 7.2, 2H,-CH_2S), 2.30 (t, *J* = 7.2, 2H, -C$H_2$$NMe_2$), 2.17 (s, 6H, N(C$H_3$)$_2$), 1.96 - 1.84 (m, 2H), 1.79 - 1.65 (m, 2H). **^{13}C NMR** (125 MHz, $CDCl_3$): δ 151.7, 149.8, 121.8, 58.1, 45.0 (2C), 30.8, 29.5, 27.3, 27.0, 23.9. HRMS (ESI) calc. for $C_{11}H_{20}N_2OS$ $[M+H]^+$ 229.1369, found 229.1368. GCMS found 228 for $[M^{+\cdot}]$.

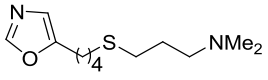

***N,N*-dimethyl-3-(4-(oxazol-5-yl)butylthio)propan-1-amine** (**159**). Compound **159** was synthesized following the general procedure for the C5-substituted oxazole formation on 14 mmol of ester **51** (no purification needed). Yield = 94% (orange oil). R_f = 0.47 (EtOAc/AcOH/MeOH/H_2O 3/3/3/2). **^{1}H NMR** (400 MHz, $CDCl_3$): δ 7.74 (s, 1H, *H*-C=N), 6.75 (t, *J* = 0.8, 1H, *H*-C=C), 2.66 (dt, *J* = 7.6, 0.8, 2H, -CH_2-C=C), 2.52 (t, *J* = 7.2, 2H, -CH_2S), 2.51 (t, *J* = 7.4, 2H, -CH_2S), 2.32 (t, *J* = 7.2, 2H, -C$H_2$$NMe_2$), 2.20 (s, 6H, N(C$H_3$)$_2$), 1.74 – 1.64 (m, 4H), 1.62 – 1.54 (m, 2H). **^{13}C NMR** (125 MHz, $CDCl_3$): δ 152.5, 149.9, 121.9, 58.5, 45.3 (2C), 31.6, 29.9, 28.8, 27.6,

26.6, 24.8. HRMS (ESI) calc. for $C_{12}H_{22}N_2OS$ $[M+H]^+$ 243.1526, found 243.1526. GCMS found 242 for $[M^{+\cdot}]$.

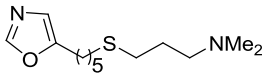

***N,N*-dimethyl-3-(5-(oxazol-5-yl)pentylthio)propan-1-amine** (**160**). Compound **160** was synthesized following the general procedure for the C5-substituted oxazole formation on 3.9 mmol of ester **115**. Yield = 90% (orange oil). R_f= 0.50 (EtOAc/AcOH/MeOH/H_2O 3/3/3/2). **^{1}H NMR** (400 MHz, $CDCl_3$): δ 7.73 (s, 1H, *H*-C=N), 6.73 (t, *J* = 0.8, 1H, *H*-C=C), 2.64 (dt, *J* = 7.6, 0.8, 2H, -CH_2-C=C), 2.51 (t, *J* = 7.6, 2H, -CH_2S), 2.49 (t, *J* = 7.6, 2H, -CH_2S), 2.32 (t, *J* = 7.4, 2H, -C$H_2$$NMe_2$), 2.19 (s, 6H, N(C$H_3$)$_2$), 1.74 – 1.51 (m, 6H), 1.45 - 1.34 (m, 2H). **^{13}C NMR** (125 MHz, $CDCl_3$): δ 152.7, 149.8, 121.7, 58.5, 45.3 (2C), 31.9, 29.9, 29.1, 28.1, 27.6, 27.0, 25.1. HRMS (ESI) calc. for $C_{13}H_{24}N_2OS$ $[M+H]^+$ 257.1682, found 257.1682. GCMS found 256 for $[M^{+\cdot}]$

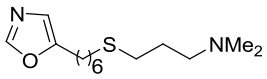

***N,N*-dimethyl-3-(6-(oxazol-5-yl)hexylthio)propan-1-amine** (**161**) **.** Compound **161** was synthesized following the general procedure for the C5-substituted oxazole formation on 9.8 mmol of ester **108** (no purification needed). Yield = 92% (orange oil). R_f = 0.50 (EtOAc/AcOH/MeOH/H_2O 3/3/3/2). **^{1}H NMR** (400 MHz, $CDCl_3$): δ 7.70 (s, 1H, *H*-C=N), 6.69 (t, *J* = 0.8, 1H, *H*-C=C), 2.59 (dt, *J* = 7.6, 0.8, 2H, -CH_2-C=C), 2.47 (t, *J* = 7.4, 2H, -CH_2S), 2.45 (t, *J* = 7.4, 2H, -CH_2S), 2.29 (t, *J* = 7.2, 2H, -C$H_2$$NMe_2$), 2.16 (s, 6H, N(C$H_3$)$_2$), 1.73-1.47 (m, 6H), 1.40 – 1.25 (m, 4H). **^{13}C NMR** (125 MHz, $CDCl_3$): δ 152.9, 149.8, 121.7, 58.6, 45.4 (2C), 32.0, 29.9, 29.4, 28.5, 28.4, 27.7, 27.3, 25.2. HRMS (ESI) calc. for $C_{14}H_{26}N_2OS$ $[M+H]^+$ 271.1839, found 271.1840. GCMS found 270 for $[M^{+\cdot}]$.

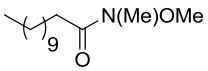

***N*-methoxy-*N*-methyldodecanamide** (**162**)**.** Compound **162** was synthesized following the general procedure for Weinreb amide synthesis using 115 mmol of acyl chloride (dodecanoyl chloride). Yield = 98% (colorless oil). R_f= 0.71 (EtOAc/cyclohexane 1/1). IR: 1668 cm^{-1} (amine C=O stretch), 2922 -2853 cm^{-1} (amine N-H stretch). **^{1}H NMR** (400 MHz, $CDCl_3$): δ 3.64 (s, 3H, OCH_3), 3.16 (s, 3H, -NCH_3), 2.37 (t, *J* = 7.4, 2H, -CH_2CO), 1.62 – 1.56 (m, 2H), 1.34 - 1.13 (m, 16H), 0.83 (t, *J* = 6.6, 3H, CH_3). **^{13}C NMR** (125 MHz, $CDCl_3$): δ 174.7, 61.0, 31.8, 29.5 (4C), 29.4, 29.3 (2C), 29.2,

24.5, 22.6, 13.9. HRMS (ESI) calc. For $C_{14}H_{29}NO_2$ $[M+H]^+$ 244.2271, found 244.2270. GCMS found 243 for $[M^{+\cdot}]$.

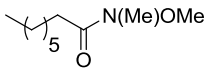

N-methoxy-N-methyloctanamide (**163**). Compound **163** was synthesized following the general procedure for Weinreb amide synthesis using 164 mmol of acyl chloride (octanoyl chloride). Yield = 94% (colorless oil). R_f = 0.67 (EtOAc/cyclohexane 1/1). IR: 1665 cm^{-1} (amine C=O stretch), 2955-2855 cm^{-1} (amine N-H stretch). **^{1}H NMR** (400 MHz, $CDCl_3$): δ 3.64 (s, 3H, OCH_3), 3.14 (s, 3H, -NCH_3), 2.37 (t, *J* = 7.6, 2H, -CH_2CO), 1.62 – 1.55 (m, 2H), 1.34 – 1.19 (m, 8H), 0.84 (t, *J* = 7.4, 3H, CH_3). **^{13}C NMR** (125 MHz, $CDCl_3$): δ 174.7, 61.1, 32.1, 31.8, 31.6, 29.3, 29.0, 24.5, 22.5, 13.9. HRMS (ESI) calc. for $C_{10}H_{21}NO_2$ $[M+H]^+$ 188.1645, found 188.1641. GCMS found 187 for $[M^{+\cdot}]$.

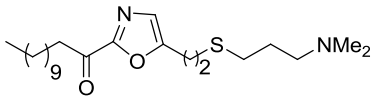

1-(5-(2-(3-(Dimethylamino)propylthio)ethyl)oxazol-2-yl)dodecan-1-one (**164**). Compound **164** was synthesized following the general procedure for oxazole C2-functionalization using 9.8 mmol of Weinreb amide **162**. Yield = 24% (orange oil). R_f = 0.74 (EtOAc/AcOH/MeOH/H_2O 3/3/3/2). IR: 1699 cm^{-1} (ketone C=O stretch). **^{1}H NMR** (400 MHz, $CDCl_3$): δ 7.01 (t, *J* = 0.8, 1H, *H*-C=C), 2.99 (t, *J* = 7.0, 2H, -CH_2CO), 2.98 (t, *J* = 6.8, 2H, -CH_2S), 2.83 (dt, *J* = 7.4, 0.8, 2H, -CH_2-C=C), 2.56 (t, *J* = 7.2, 2H, -CH_2S), 2.34 (t, *J* = 7.2, 2H, -CH_2NMe_2), 2.22 (s, 6H, N(CH_3)$_2$), 1.78- 1.66 (m, 4H), 1.39 – 1.14 (m, 16H), 0.86 (t, *J* = 6.8, 3H, -CH_3). **^{13}C NMR** (125 MHz, $CDCl_3$): δ 188.5, 157.4, 154.6, 125.5, 58.3, 45.3 (2C), 38.8, 31.9, 30.0, 29.7, 29.5 (2C), 29.4, 29.3, 29.3, 29.1, 27.4, 26.4, 24.0, 22.6, 14.1. HRMS (ESI) calc. for $C_{22}H_{40}N_2O_2S$ $[M+H]^+$ 397.2883, found 397.2873. LC-MS (ESI) found 397.23 for $[M+H]^+$.

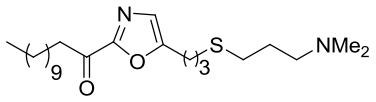

1-(5-(3-(3-(Dimethylamino)propylthio)propyl)oxazol-2-yl)dodecan-1-one (**165**). Compound **165** was synthesized following the general procedure for oxazole C2-functionalization using 8.6 mmol of Weinreb amide **162**. Yield = 37% (yellow oil). R_f = 0.64 (EtOAc/AcOH/MeOH/H_2O 3/3/3/2). IR: 1698 cm^{-1} (ketone C=O stretch). **^{1}H NMR** (400 MHz, $CDCl_3$): δ 6.96 (t, *J* = 0.8, 1H, *H*-C=C), 3.00 (t, *J* = 7.6, 2H, -CH_2CO), 2.85 (dt, *J* = 7.2, 0.8, 2H, -CH_2-C=C), 2.55 (t, *J* = 7.2, 2H, -CH_2S), 2.54 (t, *J* = 7.2, 2H, -CH_2S), 2.39 (t, *J* = 7.2, 2H, -CH_2NMe_2), 2.25 (s, 6H, N(CH_3)$_2$), 2.01 – 1.92 (m,

2H), 1.82 – 1.75 (m, 2H), 1.74 – 1.67 (m, 2H), 1.43 - 1.16 (m, 16H), 0.85 (t, *J* = 6.8, 3H, -C*H*$_3$). **^{13}C NMR** (125 MHz, $CDCl_3$): δ 188.5, 157.4, 155.8, 124.9, 58.3, 45.1 (2C), 38.8, 31.8, 31.2, 29.8, 29.5 (2C), 29.4, 29.3, 29.3, 29.1, 27.3, 27.1, 24.6, 24.0, 22.6, 14.1. HRMS (EI) calc. for $C_{23}H_{42}N_2O_2S$ [$M^{+\cdot}$] 410.2962, found 410.2951. GCMS found 410 for [$M^{+\cdot}$].

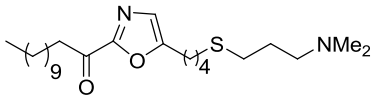

1-(5-(4-(3-(Dimethylamino)propylthio)butyl)oxazol-2-yl)dodecan-1-one (**166**). Compound **166** was synthesized following the general procedure for oxazole C2-functionalization using 8.4 mmol of Weinreb amide **162**. Yield = 29% (yellow oil). R_f= 0.71 (EtOAc/AcOH/MeOH/H_2O 3/3/3/2). IR: 1699 cm^{-1} (ketone C=O stretch). **^{1}H NMR** (400 MHz, $CDCl_3$): δ 6.95 (t, *J* = 0.8, 1H, *H*-C=C), 3.01 (t, *J* = 7.6, 2H, -C*H*$_2$CO), 2.75 (dt, *J* = 7.6, 0.8, 2H, -C*H*$_2$-C=C), 2.55 (t, *J* = 7.2, 2H, -C*H*$_2$S), 2.54 (t, *J* = 7.4, 2H, -C*H*$_2$S), 2.43 (t, *J* = 7.0, 2H, -C*H*$_2$NMe$_2$), 2.28 (s, 6H, N(C*H*$_3$)$_2$), 1.84 – 1.59 (m, 8H), 1.39 – 1.18 (m, 16H), 0.87 (t, *J* = 6.8, 3H, -C*H*$_3$). **^{13}C NMR** (125 MHz, $CDCl_3$): δ 188.5, 157.3, 156.4, 124.7, 58.4, 45.1 (2C), 38.8, 31.8, 31.6, 29.9, 29.5 (2C), 29.4, 29.3, 29.3, 29.1, 28.9, 27.3, 26.5, 25.4, 24.0, 22.6, 14.1. HRMS (ESI) calc. for $C_{24}H_{44}N_2O_2S$ $[M+H]^+$ 425.3196, found 425.3191. LC-MS (ESI) found 425.23 for $[M+H]^+$.

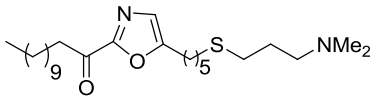

1-(5-(5-(3-(Dimethylamino)propylthio)pentyl)oxazol-2-yl)dodecan-1-one (**167**). Compound **167** was synthesized following the general procedure for oxazole C2-functionalization using 7.6 mmol of Weinreb amide **162**. Yield = 34% (yellow oil). R_f= 0.71 (EtOAc/AcOH/MeOH/H_2O 3/3/3/2). IR: 1699 cm^{-1} (ketone C=O stretch). **^{1}H NMR** (400 MHz, $CDCl_3$): δ 6.93 (t, *J* = 0.8, 1H, *H*-C=C), 3.00 (t, *J* = 7.4, 2H, -C*H*$_2$CO), 2.72 (dt, *J* = 7.4, 0.8, 2H, -C*H*$_2$-C=C), 2.52 (t, *J* = 7.4, 2H, -C*H*$_2$S), 2.50 (t, *J* = 7.4, 2H, -C*H*$_2$S), 2.39 (t, *J* = 7.4, 2H, -C*H*$_2$NMe$_2$), 2.25 (s, 6H, N(C*H*$_3$)$_2$), 1.80 – 1.65 (m, 6H), 1.64 – 1.55 (m, 2H), 1.49 – 1.39 (m, 2H), 1.37 – 1.19 (m, 16H), 0.86 (t, *J* = 6.8, 3H, -C*H*$_3$).**^{13}C NMR** (125 MHz, $CDCl_3$): δ 188.5, 157.2, 156.6, 124.6, 58.3, 45.0 (2C), 38.8, 31.9, 31.8, 29.9, 29.5 (2C), 29.4, 29.3, 29.3, 29.1, 29.1, 28.2, 27.2, 26.9, 25.6, 24.0, 22.6, 14.1. HRMS (ESI) calc. for $C_{25}H_{46}N_2O_2S$ $[M+H]^+$ 439.3353, found 439.3346. LC-MS (ESI) found 439.26 for $[M+H]^+$.

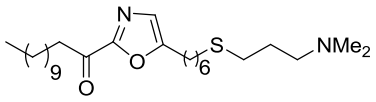

1-(5-(6-(3-(Dimethylamino)propylthio)hexyl)oxazol-2-yl)dodecan-1-one (**168**). Compound **168** was synthesized following the general procedure for oxazole C2-functionalization using 5.7 mmol of Weinreb amide **162**. Yield = 36% (yellow oil). R_f= 0.75 (EtOAc/AcOH/MeOH/H_2O 3/3/3/2). IR: 1698 cm^{-1} (ketone C=O stretch). **^{1}H NMR** (400 MHz, $CDCl_3$): δ 6.91 (t, *J* = 0.8, 1H, *H*-C=C), 2.99 (t, *J* = 7.4, 2H, -CH_2CO), 2.70 (dt, *J* = 7.6, 0.8, 2H, -CH_2-C=C), 2.52 (t, *J* = 7.2, 2H, -CH_2S), 2.48 (t, *J* = 7.2, 2H, -CH_2S), 2.45 (t, *J* = 7.6, 2H, -CH_2NMe_2), 2.29 (s, 6H, N(CH_3)$_2$), 1.82 – 1.62 (m, 6H), 1.60 – 1.50 (m, 2H), 1.43 – 1.17 (m, 20H), 0.85 (t, *J* = 6.6, 3H, -CH_3). **^{13}C NMR** (125 MHz, $CDCl_3$): δ 188.5, 157.2, 156.8, 124.6, 58.2, 44.8 (2C), 38.7, 32.0, 31.8, 29.8, 29.5(2C), 29.4, 29.3, 29.3, 29.2, 29.1, 28.6, 28.3, 27.2, 26.9, 25.6, 24.0, 22.6, 14.0. HRMS (ESI) calc. for $C_{26}H_{48}N_2O_2S$ $[M+H]^+$ 453.3509, found 453.3502. LC-MS (ESI) found 453.32 for $[M+H]^+$.

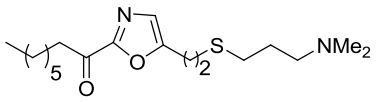

1-(5-(2-(3-(Dimethylamino)propylthio)ethyl)oxazol-2-yl)octan-1-one (**169**). Compound **169** was synthesized following the general procedure for oxazole C2-functionalization using 9.1 mmol of Weinreb amide **163**. Yield = 25% (orange oil). R_f= 0.71 (EtOAc/AcOH/MeOH/H_2O 3/3/3/2). IR: 1698 cm^{-1} (ketone C=O stretch). **^{1}H NMR** (400 MHz, $CDCl_3$): δ 6.96 (t, *J* = 0.8, 1H, *H*-C=C), 2.96 (t, *J* = 7.2, 2H, -CH_2CO), 2.94 (t, *J* = 7.4, 2H, -CH_2S), 2.77 (dt, *J* = 7.4, 0.8, 2H, -CH_2-C=C), 2.49 (t, *J* = 7.4, 2H, -CH_2S), 2.27 (t, *J* = 7.2, 2H, -CH_2NMe_2), 2.14 (s, 6H, N(CH_3)$_2$), 1.70 – 1.61 (m, 4H), 1.37 – 1.16 (m, 8H), 0.79 (t, *J* = 7.0, 3H, -CH_3). **^{13}C NMR** (125 MHz, $CDCl_3$): δ 188.4, 157.3, 154.6, 125.4, 58.2, 45.2 (2C), 38.8, 31.5, 30.0, 29.6, 29.0, 28.9, 27.3, 26.4, 23.9, 22.5, 13.9. HRMS (ESI) calc. for $C_{18}H_{32}N_2O_2S$ $[M+H]^+$ 341.2257, found 341.2258. LC-MS (ESI) found 341.15 for $[M+H]^+$.

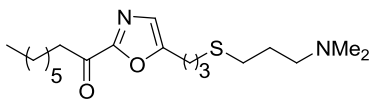

1-(5-(3-(3-(Dimethylamino)propylthio)propyl)oxazol-2-yl)octan-1-one (**170**). Compound **170** was synthesized following the general procedure for oxazole C2-functionalization using 8.5 mmol of Weinreb amide **163**. Yield = 34% (yellow oil). R_f = 0.65 (EtOAc/AcOH/MeOH/H_2O 3/3/3/2). IR: 1698 cm^{-1} (ketone C=O stretch). **^{1}H NMR** (400 MHz, $CDCl_3$): δ 6.95 (t, *J* = 0.8, 1H, *H*-C=C), 2.99 (t, *J* = 7.4, 2H, -CH_2CO), 2.84 (dt, *J* = 7.4, 0.8, 2H, -CH_2-C=C), 2.54 (t, *J* = 6.8, 2H, -CH_2S), 2.52 (t, *J* = 7.2, 2H, -CH_2S), 2.36 (t, *J* = 7.2, 2H, -CH_2NMe_2), 2.22 (s, 6H, N(CH_3)$_2$), 1.93 - 1.85 (m,

2H), 1.72 – 1.58 (m, 4H), 1.34 – 1.12 (m, 8H), 0.85 (t, *J* = 7.0, 3H, -C*H*$_3$). **^{13}C NMR** (125 MHz, $CDCl_3$): δ 188.5, 157.3, 155.8, 124.9, 58.3, 45.2 (2C), 38.7, 31.6, 31.2, 29.8, 29.1, 28.9, 27.3, 27.0, 24.6, 24.0, 22.5, 14.0. HRMS (EI) calc. for $C_{19}H_{34}N_2O_2S$ [$M^{+\cdot}$] 354.2336, found 354.2330. LC-MS (ESI) found 355.16 for $[M+H]^+$.

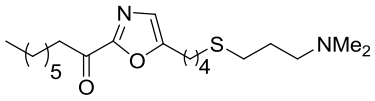

1-(5-(4-(3-(Dimethylamino)propylthio)butyl)oxazol-2-yl)octan-1-one (**171**)**.** Compound **171** was synthesized following the general procedure for oxazole C2-functionalization using 8.7 mmol of Weinreb amide **163**. Yield = 32% (yellow oil). R_f= 0.74 (EtOAc/AcOH/MeOH/H_2 3/3/3/2). IR: 1698 cm^{-1} (ketone C=O stretch). **^{1}H NMR** (400 MHz, $CDCl_3$): δ 6.96 (t, *J* = 0.8, 1H, *H*-C=C), 3.02 (t, *J* = 7.6, 2H, -C*H*$_2$CO), 2.76 (dt, *J* = 7.4, 0.8, 2H, -C*H*$_2$-C=C), 2.56 (t, *J* =7.2, 2H, -C*H*$_2$S), 2.55 (t, *J* = 7.2, 2H, -C*H*$_2$S), 2.36 (t, *J* = 7.2, 2H, -C*H*$_2$NMe$_2$), 2.22 (s, 6H, N(C*H*$_3$)$_2$), 1.90 – 1.77 (m, 4H), 1.76 – 1.61 (m, 4H), 1.42 – 1.21 (m, 8H), 0.87 (t, *J* = 7.0, 3H, -C*H*$_3$). **^{13}C NMR** (125 MHz, $CDCl_3$): δ 188.5, 157.3, 156.4, 124.7, 58.5, 45.3 (2C), 38.7, 31.6, 31.6, 30.0, 29.1, 28.9, 28.8, 27.5, 26.4, 25.3, 24.0, 22.5, 14.0. HRMS (ESI) calc. for $C_{20}H_{36}N_2O_2S$ $[M+H]^+$ 369.2570, found 369.2571. LC-MS (ESI) found 369.19 for $[M+H]^+$.

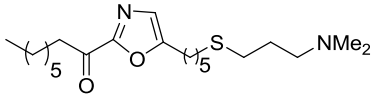

1-(5-(5-(3-(Dimethylamino)propylthio)pentyl)oxazol-2-yl)octan-1-one (**172**). Compound **172** was synthesized following the general procedure for oxazole C2-functionalization using 8.5 mmol of Weinreb amide **163**. Yield = 28% (yellow oil). R_f = 0.77 (EtOAc/AcOH/MeOH/H_2O 3/3/3/2). IR: 1698 cm^{-1} (ketone C=O stretch). **^{1}H NMR** (400 MHz, $CDCl_3$): δ 6.92 (t, *J* = 0.8, 1H, *H*-C=C), 2.99 (t, *J* = 7.6, 2H, -C*H*$_2$CO), 2.71 (dt, *J* = 7.4, 0.8, 2H, -C*H*$_2$-C=C), 2.51 (t, *J* = 7.4, 2H, -C*H*$_2$S), 2.49 (t, *J* = 7.4, 2H, -C*H*$_2$S), 2.35 (t, *J* = 7.2, 2H, -C*H*$_2$NMe$_2$), 2.21 (s, 6H, N(C*H*$_3$)$_2$), 1.80 – 1.66 (m, 6H), 1.64 – 1.55 (m, 2H), 1.48 – 1.39 (m, 2H), 1.37 – 1.19 (m, 8H), 0.85 (t, *J* = 7.0, 3H, -C*H*$_3$). **^{13}C NMR** (125 MHz, $CDCl_3$): δ 188.5, 157.2, 156.6, 124.6, 58.5, 45.2 (2C), 38.7, 31.9, 31.6, 29.9, 29.0 (2C), 28.9, 28.2, 27.4, 26.9, 25.6, 24.0, 22.5, 14.0. HRMS (ESI) calc. for $C_{21}H_{38}N_2O_2S$ $[M+H]^+$ 383.2727, found 383.2733. LC-MS (ESI) found 383.22 for $[M+H]^+$.

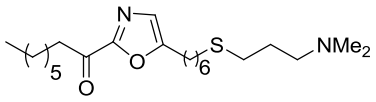

1-(5-(6-(3-(Dimethylamino)propylthio)hexyl)oxazol-2-yl)octan-1-one (**173**)**.** Compound **173** was synthesized following the general procedure for oxazole C2-functionalization using 6.6 mmol of Weinreb amide **163**. Yield = 32% (yellow oil). R_f = 0.73 (EtOAc/AcOH/MeOH/H_2O 3/3/3/2). IR: 1699 cm^{-1} (ketone C=O stretch). **^{1}H NMR** (400 MHz, $CDCl_3$): δ 6.92 (t, *J* = 0.8, 1H, *H*-C=C), 2.99 (t, *J* = 8.0, 2H, -CH_2CO), 2.76 (dt, *J* = 7.6, 0.8, 2H, -CH_2-C=C), 2.51 (t, *J* = 7.2, 2H, -CH_2S), 2.50 (t, *J* = 7.0, 2H, -CH_2S), 2.41 (t, *J* = 7.4, 2H, -CH_2NMe_2), 2.26 (s, 6H, N(CH_3)$_2$), 1.81 – 1.62 (m, 6H), 1.61-1.50 (m, 2H), 1.45 – 1.17 (m, 12H), 0.85 (t, *J* = 7.0, 3H, -CH_3). **^{13}C NMR** (125 MHz, $CDCl_3$): δ 188.5, 157.2, 156.8, 124.6, 58.4, 45.1(2C), 38.8, 32.0, 31.6, 29.9, 29.3, 29.1, 28.9, 28.6, 28.3, 27.2 (2C), 25.6, 24.0, 22.5, 14.0. HRMS (ESI) calc. for $C_{22}H_{40}N_2O_2S$ $[M+H]^+$ 397.2883, found 397.2873. LC-MS (ESI) found 397.24 for $[M+H]^+$.

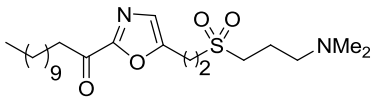

1-(5-(2-(3-(Dimethylamino)propylsulfonyl)ethyl)oxazol-2-yl)dodecan-1-one (**174**). Compound **174** was synthesized following the general procedure for oxidation into sulfone using 0.42 mmol of sulfide derivative **164**, reaction time 60 hours. Purification by reverse phase chromatography using RPC_{18} column (eluent 0 – 100 % MeOH). Yield = 76% (white semi-solid). R_f= 0.54 (EtOAc/AcOH/MeOH/H_2O 3/3/3/2). IR: 1694 cm^{-1} (ketone C=O stretch), 1304 cm^{-1} (SO_2 asym. stretch), 1112 cm^{-1} (SO_2 sym. stretch). **^{1}H NMR** (400 MHz, $CDCl_3$): δ 7.10 (t, *J* = 0.8, 1H, *H*-C=C), 3.42 – 3.27 (m, 4H, -C$H_2$$SO_2$), 3.18 – 3.11 (m, 2H, -CH_2CO), 3.04 - 2.98 (m, 2H, -CH_2-C=C), 2.70 - 2.61 (m, 2H, -CH_2NMe_2), 2.39 (s, 6H, N(CH_3)$_2$), 2.16 – 2.07 (m, 2H), 1.76 – 1.66 (m, 2H), 1.41 – 1.15 (m, 16H), 0.87 (t, *J* = 6.8, 3H, -CH_3). **^{13}C NMR** (125 MHz, $CDCl_3$): δ 188.5, 157.7, 151.8, 126.1, 56.9, 50.8, 50.3, 44.5 (2C), 38.9, 31.9, 29.6, 29.4, 29.3 (2C), 29.1, 23.9, 22.7, 19.1, 18.7, 14.1. HRMS (ESI) calc. for $C_{22}H_{40}N_2O_4S$ $[M+H]^+$ 429.2782, found 429.2776. LC-MS (ESI) found 429.22 for $[M+H]^+$.

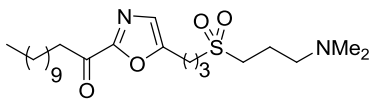

1-(5-(3-(3-(Dimethylamino)propylsulfonyl)propyl)oxazol-2-yl)dodecan-1-one (**175**). Compound **175** was synthesized following the general procedure for oxidation into sulfone using 0.43 mmol of sulfide derivative **165**, reaction time 60 hours. Purification by reverse phase chromatography

using RPC_{18} column (eluent 0 – 100 % MeOH). Yield = 75% (white semi-solid). R_f= 0.53 (EtOAc/AcOH/MeOH/H_2O 3/3/3/2). IR: 1699 cm^{-1} (ketone C=O stretch), 1318 cm^{-1} (SO_2 asym. stretch), 1129 cm^{-1} (SO_2 sym. stretch). **^{1}H NMR** (400 MHz, $CDCl_3$): δ 7.03 (t, *J* = 0.8, 1H, *H*-C=C), 3.20 – 3.14 (m, 2H, -CH_2SO_2), 3.11 – 3.05 (m, 2H, -CH_2SO_2), 3.02 (t, *J* = 7.6, 2H, -CH_2CO), 2.96 (dt, *J* = 7.4, 0.8, 2H, -CH_2-C=C), 2.83 - 2.74 (m, 2H, -CH_2NMe_2), 2.49 (s, 6H, N(CH_3)$_2$), 2.30 – 2.20 (m, 2H), 2.16 – 2.07 (m, 2H), 1.76 – 1.66 (m, 2H), 1.41 – 1.15 (m, 16H), 0.87 (t, *J* = 7.0, 3H, -CH_3). **^{13}C NMR** (125 MHz, $CDCl_3$): δ 188.5, 157.6, 154.3, 125.5, 57.0, 51.8, 50.6, 44.6 (2C), 38.9, 31.9, 29.6(2C), 29.5, 29.3, 29.3, 29.2, 24.4, 24.0, 22.7, 20.1, 19.1, 14.1. HRMS (ESI) calc. for $C_{23}H_{42}N_2O_4S$ $[M+H]^+$ 443.2938, found 443.2936. GCMS found 442 for $[M^{+\cdot}]$.

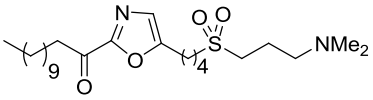

1-(5-(4-(3-(Dimethylamino)propylsulfonyl)butyl)oxazol-2-yl)dodecan-1-one (**176**). Compound **176** was synthesized following the general procedure for oxidation into sulfone using 0.38 mmol of sulfide derivative **166**, reaction time 60 hours. Purification by reverse phase chromatography using RPC_{18} column (eluent 0 – 100 % MeOH). Yield = 73% (white semi-solid). R_f= 0.53 (EtOAc/AcOH/MeOH/H_2O 3/3/3/2). IR: 1701 cm^{-1} (ketone C=O stretch), 1274 cm^{-1} (SO_2 asym. stretch), 1111 cm^{-1} (SO_2 sym. stretch). **^{1}H NMR** (400 MHz, $CDCl_3$): δ 6.99 (t, *J* = 0.8, 1H, *H*-C=C), 3.22 – 3.16 (m, 2H, -CH_2SO_2), 3.11 – 3.05 (m, 2H, -CH_2SO_2), 3.01 (t, *J* = 7.4, 2H, -CH_2CO), 2.97 – 2.90 (m, 2H, -CH_2-C=C), 2.83 - 2.76 (m, 2H, -CH_2NMe_2), 2.61 (s, 6H, N(CH_3)$_2$), 2.30 - 2.19 (m, 2H), 1.97 - 1.81 (m, 4H), 1.75 – 1.66 (m, 2H), 1.41 - 1.18 (m, 16H), 0.87 (t, *J* = 6.8, 3H, -CH_3). **^{13}C NMR** (125 MHz, $CDCl_3$): δ 188.6, 157.4, 155.5, 125.1, 56.7, 52.5, 50.0, 43.9 (2C), 38.8, 31.9, 29.6 (2C), 29.4, 29.3, 29.3, 29.1, 26.2, 25.2, 24.0, 22.6, 21.3, 18.4, 14.1. HRMS (ESI) calc. for $C_{24}H_{44}N_2O_4S$ $[M+H]^+$ 457.3095, found 457.3087. LC-MS (ESI) found 457.26 for $[M+H]^+$.

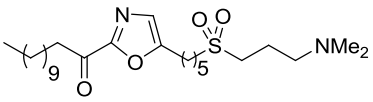

1-(5-(5-(3-(Dimethylamino)propylsulfonyl)pentyl)oxazol-2-yl)dodecan-1-one (**177**). Compound **177** was synthesized following the general procedure for oxidation into sulfone using 0.38 mmol of sulfide derivative **167**, reaction time 60 hours. Purification by reverse phase chromatography using RPC_{18} column (eluent 0 – 100 % MeOH). Yield =74% (white semi-solid). R_f= 0.58 (EtOAc/AcOH/MeOH/H_2O 3/3/3/2). IR: 1701 cm^{-1} (ketone C=O stretch), 1320 cm^{-1} (SO_2 asym. stretch), 1127 cm^{-1} (SO_2 sym. stretch). **^{1}H NMR** (400 MHz, $CDCl_3$): δ 6.95 (t, *J* = 0.8, 1H, *H*-C=C),

3.10 – 3.05 (m, 2H, -C*H*$_2$SO$_2$), 3.01 (t, *J* = 7.4, 2H, -C*H*$_2$CO), 2.99 – 2.96 (m, 2H, -C*H*$_2$SO$_2$), 2.76 (dt, *J* = 7.4, 0.8, 2H, -C*H*$_2$-C=C), 2.56 (t, *J* = 6.8, 2H, -C*H*$_2$NMe$_2$), 2.33 (s, 6H, N(C*H*$_3$)$_2$), 2.12 – 2.02 (m, 2H), 1.94 - 1.83 (m, 2H), 1.80 - 1.68 (m, 4H), 1.58 - 1.48 (m, 2H), 1.42 - 1.17 (m, 16H), 0.87 (t, *J* = 6.8, 3H, -C*H*$_3$). **^{13}C NMR** (125 MHz, $CDCl_3$): δ 188.6, 157.4, 156.1, 124.8, 57.2, 52.8, 50.4, 44.7 (2C), 38.8, 31.9, 29.6 (2C), 29.4, 29.3, 29.3, 29.2, 27.9, 26.9, 25.4, 24.0, 22.7, 21.6, 19.3, 14.1. HRMS (ESI) calc. for $C_{25}H_{46}N_2O_4S$ $[M+H]^+$ 471.3251, found 471.3243. LC-MS (ESI) found 471.27 for $[M+H]^+$.

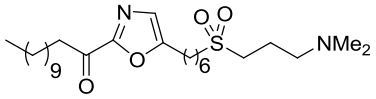

1-(5-(6-(3-(Dimethylamino)propylsulfonyl)hexyl)oxazol-2-yl)dodecan-1-one (**178**). Compound **178** was synthesized following the general procedure for oxidation into sulfone using 0.35 mmol of sulfide derivative **168**, reaction time 60 hours. Purification by reverse phase chromatography using RPC_{18} column (eluent 0 – 100 % MeOH). Yield = 69% (white semi-solid). R_f=0.62 (EtOAc/AcOH/MeOH/H_2O 3/3/3/2). IR: 1703 cm^{-1} (ketone C=O stretch), 1276 cm^{-1} (SO_2 asym. stretch), 1109 cm^{-1} (SO_2 sym. stretch). **^{1}H NMR** (400 MHz, $CDCl_3$): δ 6.94 (t, *J* = 0.8, 1H, *H*-C=C), 3.08 – 3.05 (m, 2H, -C*H*$_2$SO$_2$), 3.01 (t, *J* = 7.4, 2H, -C*H*$_2$CO), 2.99 – 2.96 (m, 2H, -C*H*$_2$SO$_2$), 2.73 (dt, *J* = 7.4, 0.8, 2H, -C*H*$_2$-C=C), 2.61 - 2.52 (m, 2H, -C*H*$_2$NMe$_2$), 2.33 (s, 6H, N(C*H*$_3$)$_2$), 2.12 – 2.02 (m, 2H), 1.90 – 1.79 (m, 2H), 1.77 – 1.67 (m, 4H), 1.54 - 1.19 (m, 20H), 0.87 (t, *J* = 7.0, 3H, -C*H*$_3$). **^{13}C NMR** (125 MHz, $CDCl_3$): δ 188.6, 157.3, 156.5, 124.7, 57.3, 53.0, 50.3, 44.8 (2C), 38.8, 31.9, 29.6 (2C), 29.5, 29.3, 29.3, 29.2, 28.5, 28.1, 27.0, 25.6, 24.1, 22.7, 21.8, 19.3, 14.1. HRMS (ESI) calc. for $C_{26}H_{48}N_2O_4S$ $[M+H]^+$ 485.3408, found 485.3399. LC-MS (ESI) found 485.30 for $[M+H]^+$.

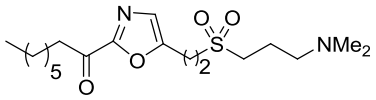

1-(5-(2-(3-(Dimethylamino)propylsulfonyl)ethyl)oxazol-2-yl)octan-1-one (**179**)**.** Compound **179** was synthesized following the general procedure for oxidation into sulfone using 0.48 mmol of sulfide derivative **169**, reaction time 60 hours. Purification by reverse phase chromatography using RPC_{18} column (eluent 0 – 100 % MeOH). Yield = 79% (white semi-solid). R_f = 0.51 (EtOAc/AcOH/MeOH/H_2O 3/3/3/2). IR: 1694 cm^{-1} (ketone C=O stretch), 1287 cm^{-1} (SO_2 asym. stretch), 1111 cm^{-1} (SO_2 sym. stretch). **^{1}H NMR** (400 MHz, $CDCl_3$): δ 7.10 (t, *J* = 0.8, 1H, *H*-C=C), 3.40 – 3.29 (m, 4H, -C*H*$_2$SO$_2$), 3.16 – 3.10 (m, 2H, -C*H*$_2$CO), 3.04 - 2.99 (m, 2H, -C*H*$_2$-C=C), 2.56 (t, *J* = 6.8, 2H, -C*H*$_2$NMe$_2$), 2.33 (s, 6H, N(C*H*$_3$)$_2$), 2.13 – 2.03 (m, 2H), 1.76 – 1.66 (m, 2H), 1.40 – 1.22

(m, 8H), 0.87 (t, *J* = 6.8, 3H, -C*H*$_3$). **^{13}C NMR** (125 MHz, $CDCl_3$): δ 188.5, 157.7, 151.8, 126.1, 57.0, 51.0, 50.3, 44.7 (2C), 38.9, 31.6, 29.0, 28.9, 23.9, 22.5, 19.3, 18.7, 14.0. HRMS (ESI) calc. for $C_{18}H_{32}N_2O_4S$ $[M+H]^+$ 373.2156, found 373.2157. LC-MS (ESI) found 373.16 for $[M+H]^+$.

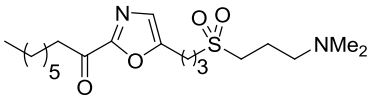

1-(5-(3-(3-(Dimethylamino)propylsulfonyl)propyl)oxazol-2-yl) octan -1-one (**180**). Compound **180** was synthesized following the general procedure for oxidation into sulfone using 0.46 mmol of sulfide derivative **170**, reaction time 60 hours. Purification by reverse phase chromatography using RPC_{18} column (eluent 0 – 100 % MeOH). Yield = 69% (white semi-solid). R_f= 0.50 (EtOAc/AcOH/MeOH/H_2O 3/3/3/2). IR: 1701 cm^{-1} (ketone C=O stretch), 1318 cm^{-1} (SO_2 asym. stretch), 1130 cm^{-1} (SO_2 sym. stretch). **^{1}H NMR** (400 MHz, $CDCl_3$): δ 7.04 (t, *J* = 0.8, 1H, *H*-C=C), 3.19 – 3.12 (m, 2H, -C*H*$_2$$SO_2$), 3.11 – 3.05 (m, 2H, -C*H*$_2$$SO_2$), 3.01 (t, *J* = 7.4, 2H, -C*H*$_2$CO), 2.97 (dt, *J* = 7.4, 0.8, 2H, -C*H*$_2$-C=C), 2.74 (t, *J* = 7.0, 2H, -C*H*$_2$$NMe_2$), 2.46 (s, 6H, N(C*H*$_3$)$_2$), 2.33 – 2.22 (m, 2H), 2.20 – 2.10 (m, 2H), 1.77 – 1.67 (m, 2H), 1.40 – 1.16 (m, 8H), 0.87 (t, *J* = 6.8, 3H, -C*H*$_3$). **^{13}C NMR** (125 MHz, $CDCl_3$): δ 188.5, 157.6, 154.3, 125.5, 56.9, 51.8, 50.4, 44.4 (2C), 38.8, 31.6, 29.1, 29.0, 24.3, 23.9, 22.5, 20.1, 18.9, 14.0. HRMS (EI) calc. for $C_{19}H_{34}N_2O_4S$ $[M^{+\cdot}]$ 386.2239, found 386.2227. GCMS found 386 for $[M^{+\cdot}]$.

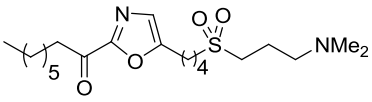

1-(5-(4-(3-(Dimethylamino)propylsulfonyl)butyl)oxazol-2-yl)octan-1-one (**181**). Compound **181** was synthesized following the general procedure for oxidation into sulfone using 0.45 mmol of sulfide derivative **171**, reaction time 60 hours. Purification by reverse phase chromatography using RPC_{18} column (eluent 0 – 100 % MeOH). Yield = 76% (white semi-solid). R_f = 0.51 (EtOAc/AcOH/MeOH/H_2O 3/3/3/2). IR: 1692 cm^{-1} (ketone C=O stretch), 1277 cm^{-1} (SO_2 asym. stretch), 1110 cm^{-1} (SO_2 sym. stretch). **^{1}H NMR** (400 MHz, $CDCl_3$): δ 6.98 (t, *J* = 0.8, 1H, *H*-C=C), 3.15 – 3.09 (m, 2H, -C*H*$_2$$SO_2$), 3.06 – 3.02 (m, 2H, -C*H*$_2$$SO_2$), 3.01 (t, *J* = 7.4, 2H, -C*H*$_2$CO), 2.83 - 2.77 (m, 2H, -C*H*$_2$-C=C), 2.69 (t, *J* = 7.0, 2H, -C*H*$_2$$NMe_2$), 2.43 (s, 6H, N(C*H*$_3$)$_2$), 2.17 – 2.09 (m, 2H), 1.96 – 1.81 (m, 4H), 1.76 -1.67 (m, 2H), 1.41- 1.19 (m, 8H), 0.87 (t, *J* = 6.8, 3H, -C*H*$_3$). **^{13}C NMR** (125 MHz, $CDCl_3$): δ 188.6, 157.4, 155.4, 125.1, 57.0, 52.5, 50.3, 44.5 (2C), 38.8, 31.6, 29.1, 28.9, 26.3, 25.2, 24.0, 22.6, 21.4, 19.0, 14.0. HRMS (ESI) calc. for $C_{20}H_{36}N_2O_4S$ $[M+H]^+$ 401.2469, found 401.2460. LC-MS (ESI) found 401.21 for $[M+H]^+$.

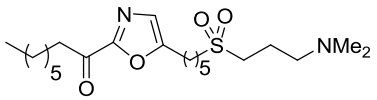

1-(5-(5-(3-(Dimethylamino)propylsulfonyl)pentyl)oxazol-2-yl)octan-1-one (**182**)**.** Compound **182** was synthesized following the general procedure for oxidation into sulfone using 0.42 mmol of sulfide derivative **172**, reaction time 60 hours. Purification by reverse phase chromatography using RPC_{18} column (eluent 0 – 100 % MeOH). Yield = 74% (yellow semi-solid). R_f=0.54 (EtOAc/AcOH/MeOH/H_2O 3/3/3/2). IR: 1696 cm^{-1} (ketone C=O stretch), 1278 cm^{-1} (SO_2 asym. stretch), 1118 cm^{-1} (SO_2 sym. stretch). **^{1}H NMR** (400 MHz, $CDCl_3$): δ 6.96 (t, *J* = 0.8, 1H, *H*-C=C), 3.24 – 3.18 (m, 2H, -C*H*$_2$$SO_2$), 3.10 – 2.97 (m, 6H, -C*H*$_2$$SO_2$, -C*H*$_2$CO, -C*H*$_2$-C=C), 2.75 (t, *J* = 7.4, 2H, -C*H*$_2$$NMe_2$), 2.71 (s, 6H, N(C*H*$_3$)$_2$), 2.35 – 2.23 (m, 2H), 1.93 – 1.81 (m, 2H), 1.80 – 1.66 (m, 4H), 1.57 – 1.47 (m, 2H), 1.39 – 1.19 (m, 8H), 0.87 (t, *J* = 7.0, 3H, -C*H*$_3$). **^{13}C NMR** (125 MHz, $CDCl_3$): δ 188.6, 157.3, 156.2, 124.8, 56.5, 52.9, 49.8, 43.7 (2C), 38.8, 31.6, 29.1, 29.0, 27.8, 26.9, 25.3, 24.0, 22.5, 21.4, 18.0, 14.0. HRMS (ESI) calc. for $C_{21}H_{38}N_2O_4S$ $[M+H]^+$ 415.2625, found 415.2619. LC-MS (ESI) found 415.21 for $[M+H]^+$.

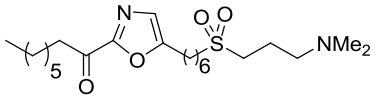

1-(5-(6-(3-(Dimethylamino)propylsulfonyl)hexyl)oxazol-2-yl)octan-1-one (**183**). Compound **183** was synthesized following the general procedure for oxidation into sulfone using 0.38 mmol of sulfide derivative **173**, reaction time 60 hours. Purification by reverse phase chromatography using RPC_{18} column (eluent 0 – 100 % MeOH). Yield = 84% (white semi-solid). R_f= 0.56 (EtOAc/AcOH/MeOH/H_2O 3/3/3/2). IR: 1694 cm^{-1} (ketone C=O stretch), 1278 cm^{-1} (SO_2 asym. stretch), 1110 cm^{-1} (SO_2 sym. stretch). **^{1}H NMR** (400 MHz, $CDCl_3$): δ 6.95 (t, *J* = 0.8, 1H, *H*-C=C), 3.34 – 3.25 (m, 4H, -C*H*$_2$$SO_2$), 3.09 – 2.97 (m, 4H, -C*H*$_2$CO, -C*H*$_2$-C=C), 2.84 (s, 6H, N(C*H*$_3$)$_2$), 2.73 (t, *J* = 7.6, 2H, -C*H*$_2$$NMe_2$), 2.50 – 2.41 (m, 2H), 1.90 -1.81 (m, 2H), 1.77 – 1.66 (m, 4H), 1.55 – 1.22 (m, 12H), 0.87 (t, *J* = 6.8, 3H, -C*H*$_3$). **^{13}C NMR** (125 MHz, $CDCl_3$): δ 188.6, 157.3, 156.5, 124.7, 56.3, 53.5, 49.3, 43.2 (2C), 38.8, 31.6, 29.1, 28.9, 28.4, 27.9, 26.9, 25.5, 24.0, 22.6, 21.7, 17.4, 14.0. HRMS (ESI) calc. for $C_{22}H_{40}N_2O_4S$ $[M+H]^+$ 429.2782, found 429.2776. LC-MS (ESI) found 429.24 for $[M+H]^+$.

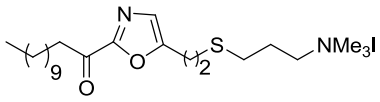

***N,N,N*-trimethyl-3-(2-(2-dodecanoyloxazol-5-yl)ethylthio)propan-1-ammonium iodide** (**184**). Compound **184** was synthesized following the general procedure for amine quaternization using 0.071 mmol of oxazole **164**. Yield = 71% (yellow semi-solid). R_f= 0.38 (EtOAc/AcOH/MeOH/H_2O 3/3/3/2). IR: 3450 cm^{-1} (quaternary amine), 1696 cm^{-1} (ketone C=O stretch). **^{1}H NMR** (400 MHz, DMSO): δ 7.29 (s, 1H, *H*-C=C), 3.34 – 3.30 (m, 2H, -C$H_2$$NMe_3^+$), 3.08 – 3.06 (m, 2H, -CH_2-C=C), 3.05 (s, 9H, N(CH_3)$_3^+$), 2.97 (t, *J* = 7.4, 2H, -CH_2CO), 2.87 (t, *J* = 7.2, 2H, -CH_2S), 2.57 (t, *J* = 7.0, 2H, -CH_2S), 2.02 – 1.90 (m, 2H), 1.65 -1.53 (m, 2H), 1.34 - 1.16 (m, 16H), 0.85 (t, *J* = 7.0, 3H, -CH_3)**. ^{13}C NMR** (125 MHz, DMSO): δ 187.7, 156.7, 154.8, 125.6, 64.3, 52.2 (3C), 38.0, 31.2, 28.9 (2C), 28.8, 28.7, 28.6, 28.4, 28.3, 27.5, 25.4, 23.3, 22.3, 22.0, 13.9**.** HRMS (ESI) calc. for $C_{23}H_{43}N_2O_2S$ $[M]^+$ 411.3040, found 411.3036. LCMS (ESI) found 411.27 for $[M]^+$.

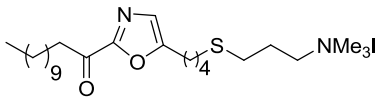

***N,N,N*-trimethyl-3-(4-(2-dodecanoyloxazol-5-yl)butylthio)propan-1-ammonium iodide** (**185**). Compound **185** was synthesized following the general procedure for amine quaternization using 0.060 mmol of oxazole **166**. Yield = 70% (white semi-solid). R_f= 0.53 (EtOAc/AcOH/MeOH/H_2O 3/3/3/2). IR: 3470 cm^{-1} (quaternary amine), 1696 cm^{-1} (ketone C=O stretch). **^{1}H NMR** (400 MHz, DMSO): δ 7.22 (s, 1H, *H*-C=C), 3.37 – 3.28 (m, 2H, -C$H_2$$NMe_3^+$), 3.05 (s, 9H, N(C$H_3$)$_3^+$), 2.96 (t, *J* = 7.2, 2H, -CH_2CO), 2.78 (t, *J* = 7.4, 2H, -CH_2-C=C), 2.57 (t, *J* = 7.2, 2H, -CH_2S), 2.52 (t, *J* = 7.2, 2H, -CH_2S), 2.01 – 1.88 (m, 2H), 1.76 – 1.64 (m, 2H), 1.64 - 1.52 (m, 4H), 1.34 - 1.14 (m, 16H), 0.85 (t, *J* = 6.6, 3H, -CH_3)**. ^{13}C NMR** (125 MHz, DMSO): δ 187.7, 156.7, 156.3, 124.8, 64.3, 52.2 (3C), 37.9, 31.2, 30.3, 28.9 (2C), 28.8, 28.7, 28.6, 28.4, 28.1, 27.5, 25.9, 24.3, 23.3, 22.3, 22.0, 13.9**.** HRMS (ESI) calc. for $C_{25}H_{47}N_2O_2S$ $[M]^+$ 439.3353, found 439.3351. LCMS (ESI) found 439.28 for $[M]^+$.

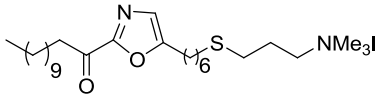

***N,N,N*-trimethyl-3-(6-(2-dodecanoyloxazol-5-yl)hexylthio)propan-1-ammonium iodide** (**186**). Compound **186** was synthesized following the general procedure for amine quaternization using 0.072 mmol of oxazole **168**. Yield = 64% (white solid). R_f= 0.69 (EtOAc/AcOH/MeOH/H_2O 3/3/3/2). IR: 3491 cm^{-1} (quaternary amine), 1695 cm^{-1} (ketone C=O stretch). **^{1}H NMR** (400 MHz, DMSO): δ 7.21 (s, 1H, *H*-C=C), 3.38 – 3.28 (m, 2H, -C$H_2$$NMe_3^+$), 3.05 (s, 9H, N(C$H_3$)$_3^+$), 2.96 (t, *J* =

7.2, 2H, -C*H*$_2$CO), 2.74 (t, *J* = 7.6, 2H, -C*H*$_2$-C=C), 2.57 – 2.50 (m, 4H, -C*H*$_2$S), 2.01 – 1.90 (m, 2H), 1.67 - 1.45 (m, 6H), 1.41 - 1.17 (m, 20H), 0.85 (t, *J* = 6.8, 3H, -C*H*$_3$). **^{13}C NMR** (125 MHz, DMSO): δ 187.8, 156.7, 156.6, 124.8, 64.5, 52.3 (3C), 38.0, 31.3, 30.8, 28.9 (2C), 28.8, 28.7 (2C), 28.7, 28.4, 27.9, 27.8, 27.7, 26.7, 24.8, 23.4, 22.4, 22.1, 13.9. HRMS (ESI) calc. for $C_{27}H_{51}N_2O_2S$ $[M]^+$ 467.3666, found 467.3666. LCMS (ESI) found 467.25 for $[M]^+$.

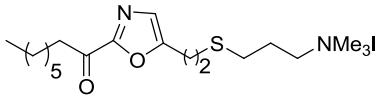

***N,N,N*-trimethyl-3-(2-(2-octanoyloxazol-5-yl)ethylthio)propan-1-ammonium iodide** (**187**). Compound **187** was synthesized following the general procedure for amine quaternization using 0.067 mmol of oxazole **169**. Yield = 72% (yellow oil). R_f= 0.45 (EtOAc/AcOH/MeOH/H_2O 3/3/3/2). IR: 3456 cm^{-1} (quaternary amine), 1695 cm^{-1} (ketone C=O stretch). **^{1}H NMR** (400 MHz, DMSO): δ 7.29 (t, *J* = 0.8, 1H, *H*-C=C), 3.36 – 3.30 (m, 2H, -C*H*$_2$NMe$_3^+$), 3.10 – 3.06 (m, 2H, -C*H*$_2$-C=C), 3.06 (s, 9H, N(C*H*$_3$)$_3^+$), 2.98 (t, *J* = 7.2, 2H, -C*H*$_2$CO), 2.88 (t, *J* = 7.4, 2H, -C*H*$_2$S), 2.58 (t, *J* = 7.0, 2H, -C*H*$_2$S), 2.03 – 1.92 (m, 2H), 1.67 – 1.58 (m, 2H), 1.34 - 1.19 (m, 8H), 0.85 (t, *J* = 6.8, 3H, -C*H*$_3$)**. ^{13}C NMR** (125 MHz, DMSO): δ 187.7, 156.7, 154.8, 125.6, 64.3, 52.3 (3C), 38.0, 31.0, 28.4 (2C), 28.3, 27.4, 25.4, 23.3, 22.3, 21.9, 13.9**.** HRMS (ESI) calc. for $C_{19}H_{35}N_2O_2S$ $[M]^+$ 355.2414, found 355.2412. LCMS (ESI) found 355.18 for $[M]^+$.

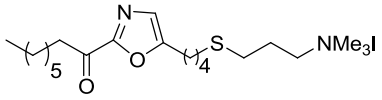

***N,N,N*-trimethyl-3-(4-(2-octanoyloxazol-5-yl)butylthio)propan-1-ammonium iodide** (**188**). Compound **188** was synthesized following the general procedure for amine quaternization using 0.105 mmol of oxazole **171**. Yield = 71% (yellow semi solid). R_f= 0.51 (EtOAc/AcOH/MeOH/H_2O 3/3/3/2). IR: 3468 cm^{-1} (quaternary amine), 1695 cm^{-1} (ketone C=O stretch). **^{1}H NMR** (400 MHz, DMSO): δ 7.22 (t, *J* = 0.8, 1H, *H*-C=C), 3.37 – 3.31 (m, 2H, -C*H*$_2$NMe$_3^+$), 3.06 (s, 9H, N(C*H*$_3$)$_3^+$), 2.97 (t, *J* = 7.2, 2H, -C*H*$_2$CO), 2.78 (dt, *J* = 7.4, 0.8, 2H, -C*H*$_2$-C=C), 2.58 (t, *J* = 7.2, 2H, -C*H*$_2$S), 2.52 (t, *J* = 7.2, 2H, -C*H*$_2$S), 2.01 – 1.90 (m, 2H), 1.76 - 1.67 (m, 2H), 1.64 - 1.54 (m, 4H), 1.34 - 1.17 (m, 8H), 0.85 (t, *J* = 7.0, 3H, -C*H*$_3$)**. ^{13}C NMR** (125 MHz, DMSO): δ 187.7, 156.7, 156.3, 124.8, 64.3, 52.2 (3C), 37.9, 31.0, 30.3, 28.4 (2C), 28.1, 27.5, 25.9, 24.4, 23.3, 22.3, 21.9, 13.9**.** HRMS (ESI) calc. for $C_{21}H_{39}N_2O_2S$ $[M]^+$ 383.2727, found 383.2732. LCMS (ESI) found 383.20 for $[M]^+$.

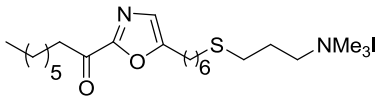

***N,N,N*-trimethyl-3-(6-(2-octanoyloxazol-5-yl)hexylthio)propan-1-ammonium iodide (189).** Compound **189** was synthesized following the general procedure for amine quaternization using 0.088 mmol of oxazole **173**. Yield = 60% (white solid). R_f= 0.43 (EtOAc/AcOH/MeOH/H_2O 3/3/3/2). IR: 3456 cm^{-1} (quaternary amine), 1695 cm^{-1} (ketone C=O stretch). **^{1}H NMR** (400 MHz, DMSO): δ 7.21 (s, 1H, *H*-C=C), 3.37 – 3.28 (m, 2H, -C$H_2$$NMe_3^+$), 3.05 (s, 9H, N(C$H_3$)$_3^+$), 2.96 (t, *J* = 7.2, 2H, -CH_2CO), 2.74 (t, *J* = 7.4, 2H, -CH_2-C=C), 2.56 - 2.51 (m, 4H, -CH_2S), 1.99 – 1.87 (m, 2H), 1.65 - 1.48 (m, 6H), 1.43 - 1.17 (m, 12H), 0.85 (t, *J* = 6.8, 3H, -CH_3)**. ^{13}C NMR** (125 MHz, DMSO): δ 187.7, 156.7, 156.5, 124.7, 64.3, 52.2 (3C), 37.9, 31.0, 30.8, 28.7, 28.4 (2C), 27.9, 27.7, 27.6, 26.7, 24.7, 23.3, 22.3, 21.9, 13.9**.** HRMS (ESI) calc. for $C_{23}H_{43}N_2O_2S$ $[M]^+$ 411.3040, found 411.3037. LCMS (ESI) found 411.26 for $[M]^+$.

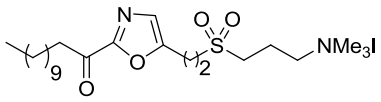

***N,N,N*-trimethyl-3-(2-(2-dodecanoyloxazol-5-yl)ethylsulfonyl)-propan-1-ammonium iodide (190).** Compound **190** was synthesized following the general procedure for amine quaternization using 0.070 mmol of oxazole **174**. Yield = 45% (yellow salt). R_f= 0.34 (EtOAc/AcOH/MeOH/H_2O 3/3/3/2). IR: 3409 cm^{-1} (quaternary amine), 1694 cm^{-1} (ketone C=O stretch), 1283 cm^{-1} (SO_2 asym. stretch), 1114 cm^{-1} (SO_2 sym. stretch). **^{1}H NMR** (400 MHz, DMSO): δ 7.35 (s, 1H, *H*-C=C), 3.65 -3.56 (m, 2H, -C$H_2$$SO_2$), 3.44 – 3.34 (m, 2H, -C$H_2$$NMe_3^+$), 3.28 – 3.21 (m, 4H, -C$H_2$$SO_2$, -C$H_2$-C=C), 3.08 (s, 9H, N(C$H_3$)$_3^+$), 2.98 (t, *J* = 7.4, 2H, -CH_2CO), 2.23 - 2.08 (m, 2H), 1.67 - 1.51 (m, 2H), 1.35 - 1.11 (m, 16H), 0.85 (t, *J* = 7.2, 3H, -CH_3)**. ^{13}C NMR** (125 MHz, DMSO): δ 187.7, 156.8, 152.9, 125.8, 63.3, 52.2 (3C), 48.8, 48.5, 38.0, 31.2, 28.9 (2C), 28.8, 28.7, 28.6, 28.4, 23.3, 22.0, 18.1, 15.8, 13.9**.** HRMS (ESI) calc. for $C_{23}H_{43}N_2O_4S$ $[M]^+$ 443.2938, found 443.2933. LCMS (ESI) found 443.29 for $[M]^+$.

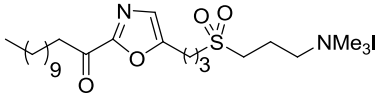

***N,N,N*-trimethyl-3-(3-(2-dodecanoyloxazol-5-yl)propylsulfonyl)-propan-1-ammonium iodide (191).** Compound **191** was synthesized following the general procedure for amine quaternization using 0.070 mmol of oxazole **175**. Yield = 50% (white solid). R_f= 0.36 (EtOAc/AcOH/MeOH/H_2O 3/3/3/2). IR: 3414 cm^{-1} (quaternary amine), 1690 cm^{-1} (ketone C=O stretch), 1265 cm^{-1} (SO_2 asym. stretch), 1129 cm^{-1} (SO_2 sym. stretch). **^{1}H NMR** (400 MHz, DMSO):

δ 7.28 (s, 1H, *H*-C=C), 3.44 – 3.34 (m, 2H, -C*H*$_2$NMe$_3^+$), 3.28 - 3.20 (m, 4H, -C*H*$_2$SO$_2$), 3.08 (s, 9H, N(C*H*$_3$)$_3^+$), 3.02 – 2.91 (m, 4H, -C*H*$_2$CO, -C*H*$_2$-C=C), 2.21 – 1.97 (m, 4H), 1.66 – 1.52 (m, 2H), 1.35 – 1.08 (m, 16H), 0.85 (t, *J* = 7.0, 3H, -C*H*$_3$)**.** **^{13}C NMR** (125 MHz, DMSO): δ 187.7, 156.8, 154.9, 125.2, 63.4, 52.2 (3C), 50.7, 48.2, 38.0, 31.2, 28.9 (2C), 28.8, 28.7, 28.6, 28.4, 23.5, 23.2, 22.0, 19.6, 15.7, 13.9**.** HRMS (ESI) calc. for $C_{24}H_{45}N_2O_4S$ $[M]^+$ 457.3094, found 457.3086. LCMS (ESI) found 457.36 for $[M]^+$.

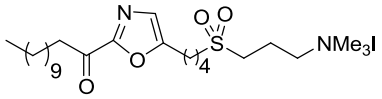

***N,N,N*-trimethyl-3-(4-(2-dodecanoyloxazol-5-yl)butylsulfonyl)-propan-1-ammonium iodide** (**192**). Compound **192** was synthesized following the general procedure for amine quaternization using 0.065 mmol of oxazole **176**. Yield = 68% (yellow solid). R_f= 0.34 (EtOAc/AcOH/MeOH/H_2O 3/3/3/2). IR: 3432 cm^{-1} (quaternary amine), 1701 cm^{-1} (ketone C=O stretch), 1282 cm^{-1} (SO_2 asym. stretch), 1120 cm^{-1} (SO_2 sym. stretch). **^{1}H NMR** (400 MHz, DMSO): δ 7.23 (s, 1H, *H*-C=C), 3.43 -3.35 (m, 2H, -C*H*$_2$NMe$_3^+$), 3.27 -3.12 (m, 4H, -C*H*$_2$SO$_2$), 3.08 (s, 9H, N(C*H*$_3$)$_3^+$), 2.97 (t, *J* = 7.4, 2H, -C*H*$_2$CO), 2.85 - 2.77 (m, 2H, -C*H*$_2$-C=C), 2.20 – 2.08 (m, 2H), 1.82 - 1.67 (m, 4H), 1.65 – 1.54 (m, 2H), 1.35 - 1.14 (m, 16H), 0.85 (t, *J* = 6.8, 3H, -C*H*$_3$)**.** **^{13}C NMR** (125 MHz, DMSO): δ 187.7, 156.8, 155.9, 124.9, 63.4, 52.2 (3C), 51.0, 48.3, 37.9, 31.2, 28.9 (2C), 28.8, 28.7, 28.6, 28.4, 25.5, 24.3, 23.3, 22.0, 20.6, 15.7, 13.9**.** HRMS (ESI) calc. for $C_{25}H_{47}N_2O_4S$ $[M]^+$ 471.3251, found 471.3250. LCMS (ESI) found 471.28 for $[M]^+$.

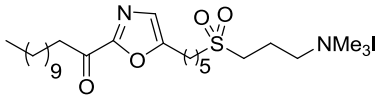

***N,N,N*-trimethyl-3-(5-(2-dodecanoyloxazol-5-yl)pentylsulfonyl)-propan-1-ammonium iodide** (**193**)**.** Compound **193** was synthesized following the general procedure for amine quaternization using 0.064 mmol of oxazole **177**. Yield = 44% (yellow solid). R_f= 0.36 (EtOAc/AcOH/MeOH/H_2O 3/3/3/2). IR: 3477 cm^{-1} (quaternary amine), 1697 cm^{-1} (ketone C=O stretch), 1286 cm^{-1} (SO_2 asym. stretch), 1115 cm^{-1} (SO_2 sym. stretch). **^{1}H NMR** (400 MHz, DMSO): δ 7.22 (s, 1H, *H*-C=C), 3.42 -3.35 (m, 2H, -C*H*$_2$NMe$_3^+$), 3.21 – 3.12 (m, 4H, -C*H*$_2$SO$_2$), 3.08 (s, 9H, N(C*H*$_3$)$_3^+$), 2.96 (t, *J* = 7.2, 2H, -C*H*$_2$CO), 2.76 (t, *J* = 7.4, 2H, -C*H*$_2$-C=C), 2.20 – 2.06 (m, 2H), 1.77 - 1.54 (m, 6H), 1.51 - 1.40 (m, 2H), 1.35 - 1.16 (m, 16H), 0.85 (t, *J* = 6.8, 3H, -C*H*$_3$)**.** **^{13}C NMR** (125 MHz, DMSO): δ 187.7, 156.7, 156.4, 124.8, 63.4, 52.2, 51.2 (3C), 48.2, 37.9, 31.2, 28.9 (2C), 28.8, 28.7, 28.6, 28.4, 27.0,

26.2, 24.6, 23.3, 22.0, 20.8, 15.7, 13.9**.** HRMS (ESI) calc. for $C_{26}H_{49}N_2O_4S$ $[M]^+$ 485.3408, found 485.3408. LCMS (ESI) found 485.30 for $[M]^+$.

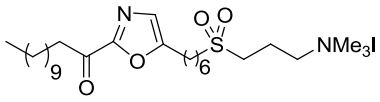

***N,N,N*-trimethyl-3-(6-(2-dodecanoyloxazol-5-yl)hexylsulfonyl)-propan-1-ammonium iodide** (**194**)**.** Compound **194** was synthesized following the general procedure for amine quaternization using 0.052 mmol of oxazole **178**. Yield = 62% (yellow solid). R_f= 0.41 (EtOAc/AcOH/MeOH/H_2O 3/3/3/2). IR: 3455 cm^{-1} (quaternary amine), 1697 cm^{-1} (ketone C=O stretch), 1282 cm^{-1} (SO_2 asym. stretch), 1131 cm^{-1} (SO_2 sym. stretch). **^{1}H NMR** (400 MHz, DMSO): δ 7.21 (t, *J* = 0.8, 1H, *H*-C=C), 3.41 – 3.35 (m, 2H, -C*H*$_2$NMe$_3^+$), 3.18 – 3.12 (m, 4H, -C*H*$_2$SO$_2$), 3.08 (s, 9H, N(C*H*$_3$)$_3^+$), 2.96 (t, *J* = 7.2, 2H, -C*H*$_2$CO), 2.75 (dt, *J* = 7.4, 0.8, 2H, -C*H*$_2$-C=C), 2.19 – 2.04 (m, 2H), 1.73 - 1.50 (m, 6H), 1.47 -1.14 (m, 20H), 0.85 (t, *J* = 6.8, 3H, -C*H*$_3$). **^{13}C NMR** (125 MHz, DMSO): δ 187.7, 156.7, 156.5, 124.8, 63.4, 52.2 (3C), 51.4, 48.2, 37.9, 31.2, 28.9 (2C), 28.8, 28.7, 28.6, 28.4, 27.8, 27.2, 26.4, 24.7, 23.3, 22.0, 20.9, 15.7, 13.9**.** HRMS (ESI) calc. for $C_{27}H_{51}N_2O_4S$ $[M]^+$ 499.3564, found 499.3565. LCMS (ESI) found 499.29 for $[M]^+$.

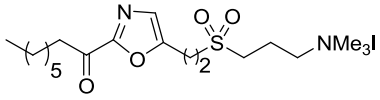

***N,N,N*-trimethyl-3-(2-(2-octanoyloxazol-5-yl)ethylsulfonyl)propan-1-ammonium iodide** (**195**). Compound **195** was synthesized following the general procedure for amine quaternization using 0.068 mmol of oxazole **179**. Yield = 79% (yellow semi-solid). R_f= 0.33 (EtOAc/AcOH/MeOH/H_2O 3/3/3/2). IR: 3451 cm^{-1} (quaternary amine), 1693 cm^{-1} (ketone C=O stretch), 1298 cm^{-1} (SO_2 asym. stretch), 1122 cm^{-1} (SO_2 sym. stretch). **^{1}H NMR** (400 MHz, DMSO): δ 7.35 (s, 1H, *H*-C=C), 3.64 – 3.57 (m, 2H, -C*H*$_2$SO$_2$), 3.43 – 3.36 (m, 2H, -C*H*$_2$NMe$_3^+$), 3.34 – 3.20 (m, 4H, -C*H*$_2$SO$_2$, -C*H*$_2$-C=C), 3.09 (s, 9H, N(C*H*$_3$)$_3^+$), 2.98 (t, *J* = 7.2, 2H, -C*H*$_2$CO), 2.22 – 2.11 (m, 2H), 1.66 - 1.55 (m, 2H), 1.35 - 1.15 (m, 8H), 0.85 (t, *J* = 6.8, 3H, -C*H*$_3$)**.** **^{13}C NMR** (125 MHz, DMSO): δ 187.7, 156.8, 152.9, 125.8, 63.3, 52.2 (3C), 48.8, 48.5, 38.0, 31.0, 28.3 (2C), 23.3, 21.9, 18.1, 15.8, 13.8**.** HRMS (ESI) calc. for $C_{19}H_{35}N_2O_4S$ $[M]^+$ 387.2312, found 387.2316. LCMS (ESI) found 387.17 for $[M]^+$.

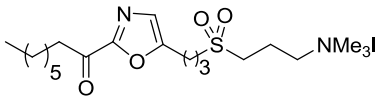

***N,N,N*-trimethyl-3-(3-(2-octanoyloxazol-5-yl)propylsulfonyl)propan-1-ammonium iodide** (**196**). Compound **196** was synthesized following the general procedure for amine quaternization using 0.085 mmol of oxazole **180**. Yield = 85% (yellow oil). R_f= 0.34 (EtOAc/AcOH/MeOH/H_2O 3/3/3/2). IR: 3447 cm^{-1} (quaternary amine), 1695 cm^{-1} (ketone C=O stretch), 1285 cm^{-1} (SO_2 asym. stretch), 1120 cm^{-1} (SO_2 sym. stretch). **^{1}H NMR** (400 MHz, DMSO): δ 7.27 (t, *J* = 0.8, 1H, *H*-C=C), 3.42 – 3.35 (m, 2H, -C$H_2$$NMe_3^+$), 3.28 -3.17 (m, 4H, -C$H_2$$SO_2$), 3.08 (s, 9H, N(C$H_3$)$_3^+$), 2.97 (t, *J* = 7.4, 2H, -CH_2CO), 2.93 (dt, *J* = 7.2, 0.8, 2H, -CH_2-C=C), 2.19 – 2.00 (m, 4H), 1.66 – 1.56 (m, 2H), 1.35 – 1.19 (m, 8H), 0.85 (t, *J* = 6.8, 3H, -CH_3)**. ^{13}C NMR** (125 MHz, DMSO): δ 187.7, 156.8, 154.9, 125.2, 63.4, 52.2 (3C), 50.7, 48.2, 38.0, 31.0, 28.4 (C2), 23.5, 23.3, 22.0, 19.6, 15.7, 13.9**.** HRMS (ESI) calc. for $C_{20}H_{37}N_2O_4S$ $[M]^+$ 401.2469, found 401.2463. LCMS (ESI) found 401.20 for $[M]^+$.

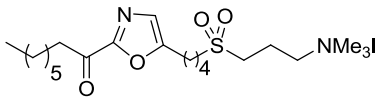

***N,N,N*-trimethyl-3-(4-(2-octanoyloxazol-5-yl)butylsulfonyl)propan-1-ammonium iodide** (**197**)**.** Compound **197** was synthesized following the general procedure for amine quaternization using 0.084 mmol of oxazole **181**. Yield = 87% (brown oil). R_f= 0.35 (EtOAc/AcOH/MeOH/H_2O 3/3/3/2). IR: 3447 cm^{-1} (quaternary amine), 1694 cm^{-1} (ketone C=O stretch), 1285 cm^{-1} (SO_2 asym. stretch), 1119 cm^{-1} (SO_2 sym. stretch). **^{1}H NMR** (400 MHz, DMSO): δ 7.23 (t, *J* = 0.8, 1H, *H*-C=C), 3.43 – 3.35 (m, 2H, -C$H_2$$NMe_3^+$), 3.26 -3.21 (m, 2H, -C$H_2$$SO_2$), 3.19 3.13 (m, 2H, -C$H_2$$SO_2$), 3.08 (s, 9H, N(C$H_3$)$_3^+$), 2.97 (t, *J* = 7.2, 2H, -CH_2CO), 2.86 – 2.78 (m, 2H, -CH_2-C=C), 2.20 – 2.09 (m, 2H), 1.82 – 1.69 (m, 4H), 1.67 -1.54 (m, 2H), 1.35 -1.16 (m, 8H), 0.85 (t, *J* = 7.0, 3H, -CH_3). **^{13}C NMR** (125 MHz, DMSO): δ 187.7, 156.8, 155.9, 124.9, 63.4, 52.2 (3C), 51.0, 48.3, 37.9, 31.0, 28.4 (2C), 25.5, 24.3, 23.3, 21.9, 20.6, 17.7, 13.9. HRMS (ESI) calc. for $C_{21}H_{39}N_2O_4S$ $[M]^+$ 415.2625, found 415.2621. LCMS (ESI) found 415.22 for $[M]^+$.

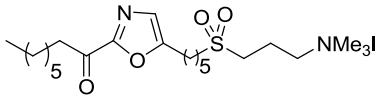

***N,N,N*–trimethyl-3-(5-(2-octanoyloxazol-5-yl)pentylsulfonyl)propan-1-ammonium iodide** (**198**)**.** Compound **198** was synthesized following the general procedure for amine quaternization using 0.060 mmol of oxazole **182**. Yield = 66% (brown oil). R_f= 0.34 (EtOAc/AcOH/MeOH/H_2O 3/3/3/2). IR: 3448 cm^{-1} (quaternary amine), 1696 cm^{-1} (ketone C=O stretch), 1282 cm^{-1} (SO_2 asym. stretch),

1118 cm^{-1} (SO_2 sym. stretch). **^{1}H NMR** (400 MHz, DMSO): δ 7.22 (s, 1H, *H*-C=C), 3.41 - 3.34 (m, 2H, -C*H*$_2$NMe$_3^+$), 3.21 – 3.11 (m, 4H, -C*H*$_2$SO$_2$), 3.07 (s, 9H, N(C*H*$_3$)$_3^+$), 2.96 (t, *J* = 7.2, 2H, -C*H*$_2$CO), 2.76 (t, *J* = 7.2, 2H, -C*H*$_2$-C=C), 2.19 – 1.96 (m, 2H), 1.78 - 1.55 (m, 6H), 1.51 - 1.40 (m, 2H), 1.34 - 1.19 (m, 8H), 0.85 (t, *J* = 6.8, 3H, -C*H*$_3$)**. ^{13}C NMR** (125 MHz, DMSO): δ 187.7, 156.7, 156.5, 124.9, 64.3, 53.0, 52.9, 49.3, 38.7, 31.6, 29.0, 28.9, 27.6, 26.8, 25.3, 23.9, 22.5, 21.4, 21.3, 17.4, 16.7, 14.0. HRMS (ESI) calc. for $C_{22}H_{41}N_2O_4S$ $[M]^+$ 429.2782, found 429.2778. LCMS (ESI) found 429.23 for $[M]^+$.

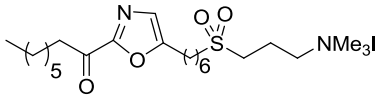

***N,N,N*-trimethyl-3-(6-(2-octanoyloxazol-5-yl)hexylsulfonyl)propan-1-ammonium iodide** (**199**). Compound **199** was synthesized following the general procedure for amine quaternization using 0.056 mmol of oxazole **183**. Yield = traces (white solid). R_f= 0.34 (EtOAc/AcOH/MeOH/H_2O 3/3/3/2). IR: 3441 cm^{-1} (quaternary amine), 1695 cm^{-1} (ketone C=O stretch), 1281 cm^{-1} (SO_2 asym. stretch), 1111 cm^{-1} (SO_2 sym. stretch). **^{1}H NMR** (400 MHz, DMSO): δ 7.21 (s, 1H, *H*-C=C), 3.35 – 3.25 (m, 2H, -C*H*$_2$NMe$_3^+$), 3.19 – 3.09 (m, 4H, -C*H*$_2$SO$_2$), 3.08 (s, 9H, N(C*H*$_3$)$_3^+$), 2.96 (t, *J* = 7.4, 2H, -C*H*$_2$CO), 2.75 (t, *J* = 7.4, 2H, -C*H*$_2$-C=C), 2.10 – 1.98 (m, 2H), 1.73 – 1.54 (m, 6H), 1.47 – 1.16 (m, 12H), 0.85 (t, *J* = 7.0, 3H, -C*H*$_3$)**. ^{13}C NMR** (125 MHz, DMSO): δ 187.7, 156.7, 156.5, 124.7, 64.3, 52.2 (3C), 37.9, 35.6, 31.0, 30.7, 28.7, 28.4, 27.9, 27.7, 27.6, 26.7, 24.7, 23.3, 22.3, 21.9, 13.9**.** HRMS (ESI) calc. for $C_{23}H_{43}N_2O_4S$ $[M]^+$ 443.2938, found 443.2930. LCMS (ESI) found 443.25 for $[M]^+$.

REFERENCES

(1) Boettcher, T.; Sieber, S. A. *Angew. Chem., Int. Ed.* **2008**, *47*, 4600.
(2) Hannoush, R. N.; Arenas-Ramirez, N. *ACS Chem. Biol*. **2009**, *4*, 581.
(3) Schmitt, M.; Lehr, M. *J. Pharm. Biomed. Anal.* **2004**, *35*, 135.
(4) Devedjiev, Y.; Dauter, Z.; Kuznetsov, S. R.; Jones, T. L. Z.; Derewenda, Z. S. *Structure* **2000**, *8*, 1137.
(5) Dekker, F. J.; Rocks, O.; Vartak, N.; Menninger, S.; Hedberg, C.; Balamurugan, R.; Wetzel, S.; Renner, S.; Gerauer, M.; Schoelermann, B.; Rusch, M.; Kramer, J. W.; Rauh, D.; Coates, G. W.; Brunsveld, L.; Bastiaens, P. I. H.; Waldmann, H. *Nat. Chem. Biol.* **2010**, *6*, 449.
(6) Sparks, S. M.; Chow, C. P.; Zhu, L.; Shea, K. J. *J. Org. Chem.* **2004**, *69,* 3025.
(7) Inoue, T.; Liu, J.-F.; Buske, D. C.; Abiko, A. *J. Org. Chem.* **2002**, *67*, 5250.
(8) Abiko, A.; Liu, J.-F.; Masamune, S. *J. Am. Chem. Soc.* **1997**, *119*, 2586.
(9) Abiko, A. *Org. Synth.* **2002**, *79*, No pp. given.
(10) Abiko, A. *Org. Synth.* **2003**, *79*, 116.
(11) Yadav, J. S.; Reddy, M. S.; Prasad, A. R. *Tetrahedron Lett.* **2006**, *47,* 4995.

(12) Black, T. H.; DuBay, W. J., III; Tully, P. S. *J. Org. Chem.* **1988**, *53*, 5922.
(13) Al-Masoudi, N.; Al-Soud, Y.; Schuppler, T. *J. Carbohydr. Chem.* **2005**, *24*, 237.
(14) Hanessian, S.; Ducharme, D.; Masse, R.; Capmau, M. L. *Carbohydr. Res*. **1978**, *63*, 265.
(15) Koshi, Y.; Nakata, E.; Miyagawa, M.; Tsukiji, S.; Ogawa, T.; Hamachi, I. *J. Am. Chem. Soc.* **2008**, *130*, 245.
(16) Bedia, C.; Triola, G.; Casas, J.; Llebaria, A.; Fabrias, G. *Org. Biomol. Chem*. **2005**, *3*, 3707.
(17) Constantinou-Kokotou, V.; Peristeraki, A.; Kokotos, C. G.; Six, D. A.; Dennis, E. A. *J. Pept. Sci*. **2005**, *11*, 431.
(18) Reeves, J. T.; Song, J. J.; Tan, Z.; Lee, H.; Yee, N. K.; Senanayake, C. H. *J. Org. Chem.* **2008**, *73*, 9476.
(19) Wenkert, D.; Chen, T.-F.; Ramachandran, K.; Valasinas, L.; Weng, L.-l.; McPhail, A. T. *Org. Lett*. **2001**, *3*, 2301.
(20) Vedejs, E.; Naidu, B. N.; Klapars, A.; Warner, D. L.; Li, V.-s.; Na, Y.; Kohn, H. *J. Am. Chem. Soc.* **2003**, *125*, 15796.
(21) Ohba, M.; Izuta, R.; Shimizu, E. *Tetrahedron Lett.* **2000**, *41*, 10251.
(22) Trost, B. M.; Lee, C. *J. Am. Chem. Soc.* **2001***, 123,* 12191.
(23) Nahm, S.; Weinreb, S. M. *Tetrahedron Lett.* **1981**, *22,* 3815.
(24) Pippel, D. J.; Mapes, C. M.; Mani, N. S*. J. Org. Chem.* **2007**, *72*, 5828.
(25) Veleiro, A. S.; Pecci, A.; Monteserin, M. C.; Baggio, R.; Garland, M. T.; Lantos, C. P.; Burton, G. *J. Med. Chem.* **2005**, *48*, 5675.
(26) Tamayo, A.; Lodeiro, C.; Escriche, L.; Casabo, J.; Covelo, B.; Gonzalez, P. *Inorg. Chem.* **2005**, *44*, 8105.
(27) Sun, W.-C.; Gee, K. R.; Klaubert, D. H.; Haugland, R. P. *J. Org. Chem.* **1997**, *62*, 6469.
(28) Russell, A.; Frye, J. R. *Org. Synth.* **1941**, *21*, 22.
(29) Brun, M.-P.; Bischoff, L.; Garbay, C. *Angew. Chem., Int. Ed*. **2004**, *43*, 3432.
(30) Sun, W.-C.; Gee, K. R.; Haugland, R. P. *Bioorg. Med. Chem. Lett.* **1998**, *8*, 3107.
(31) Khatyr, A.; Maas, H.; Calzaferri, G. *J. Org. Chem.* **2002**, *67,* 6705.
(32) Csuk, R.; Niesen, A. Z. *Naturforsch., B: Chem. Sci.* **2004**, *59*, 934.
(33) Gilpin, R. K.; Gangoda, M. E. *J. Labelled Compd. Radiopharm.* **1984**, *21*, 299.
(34) Zakhrkin, L. I.; Churilova, I. M. *Izv. Akad. Nauk SSSR, Ser. Khim.* **1984**, 2635.
(35) Campbell, K. N.; Campbell, B. K. *Org. Synth.* **1950**, *30*, 72.
(36) Bergel'son, L. D.; Molotkovskii, Y. G.; Shemyakin, M. M. *Zh. Obshch. Khim*. **1962**, *32*, 58.
(37) Speers, A. E.; Cravatt, B. F. *Chem. Biol.* **2004**, *11*, 535.
(38) Vercillo, O. E.; Andrade, C. K. Z.; Wessjohann, L. A. *Org. Lett.* **2008**, *10*, 205.
(39) Ritschel, J.; Sasse, F.; Maier, M. E. *Eur. J. Org. Chem.* **2007**, *78*.
(40) Tashima, T.; Toriumi, Y.; Mochizuki, Y.; Nonomura, T.; Nagaoka, S.; Furukawa, K.; Tsuru, H.; Adachi-Akahane, S.; Ohwada, T. *Bioorg. Med. Chem.* **2006**, *14*, 8014.
(41) Boyle, G. A.; Kruger, H. G.; Maguire, G. E. M.; Singh, A. *Struct. Chem.* **2007**, *18*, 633.
(42) Pettersson, L.; *Innoventus Project AB, Swed. .* **2005**, p 80 pp.
(43) Mehlmann, H.; Olschewski, D.; Olschewski, A.; Feigel, M. Z. *Naturforsch., B: Chem. Sci.* **2002**, *57*, 343.
(44) Lanza, T.; Leardini, R.; Minozzi, M.; Nanni, D.; Spagnolo, P.; Zanardi, G. Angew. *Chem., Int. Ed*. **2008**, *47*, 9439.
(45) Sun, W.; Pelletier, J. C. *Tetrahedron Lett*. **2007**, *48*, 7745.
(46) Masuda, Y.; Yoshida, M.; Mori, K. *Biosci., Biotechnol., Biochem.* **2002**, *66*, 1531.
(47) Diez, E.; Dixon, D. J.; Ley, S. V.; Polara, A.; Rodriguez, F. *Helv. Chim. Acta* **2003**, *86*, 3717.
(48) Dixon, D. J.; Ley, S. V.; Lohmann, S.; Sheppard, T. D. *Synlett* **2005**, 481.
(49) Nakatsuji, Y.; Nakamura, T.; Yonetani, M.; Yuya, H.; Okahara, M. *J. Am. Chem. Soc*. **1988**, *110*, 531.
(50) Hon, Y.-S.; Liu, Y.-W.; Hsieh, C.-H. *Tetrahedron* **2004**, *60*, 4837.
(51) Pappo, R.; Allen, D. S., Jr.; Lemieux, R. U.; Johnson, W. S. *J. Org. Chem.* **1956**, *21*, 478.

(52) Iwata, C.; Takemoto, Y.; Doi, M.; Imanishi, T. *J. Org. Chem.* **1988**, *53*, 1623.
(53) Mori, Y.; Kohchi, Y.; Suzuki, M.; Carmeli, S.; Moore, R. E.; Patterson, G. M. L. *J. Org. Chem.* **1991**, *56*, 631.
(54) Schuster, R. E.; Scott, J. E., Jr.; Casanova, J., Jr. *Org. Synth*. **1966**, *46*, 75.
(55) Kalai, T.; Bognar, B.; Jeko, J.; Hideg, K. *Synthesis* **2006**, 2573.
(56) Lee, J. C.; Cha, J. K. *J. Am. Chem. Soc*. **2001**, *123*, 3243.
(57) Anderson, B. A.; Becke, L. M.; Booher, R. N.; Flaugh, M. E.; Harn, N. K.; Kress, T. J.; Varie, D. L.; Wepsiec, J. P. *J. Org. Chem*. **1997**, *62*, 8634.

Summary

Palmitoylated proteins constitute an important class of signaling components controlling various cellular processes, such as cell proliferation and apoptosis, both frequently deregulated in carcinogenesis. The reversible character of palmitate lipid anchoring is of utmost importance for maintaining steady-state protein localization and subsequent signaling. Therefore, targeting protein depalmitoylation by inhibiting depalmitoylating enzymes might be a valid therapeutical strategy for modulating aberrant cell signaling.

Targeting Ras depalmitoylation

Design, Synthesis of acyl protein thioesterase 1 (APT1) inhibitors

Given the importance of Ras mutations in carcinogenesis (33% of all cancers), targeting Ras protein depalmitoylation by inhibiting Ras depalmitoylating enzymes have been considered as an attractive anti-cancer target. In particular, efforts to inhibit the serine hydrolase acyl protein thioesterase 1 (APT1) have led to the development of the β-lactone inhibitor palmostatin B (**1**) based on the Protein Structure Similarity Clustering approach. A cell permeable TAMRA-labeled palmostatin B analogue (**2**) was subsequently synthesized and used to confirm the direct interaction between palmostatin B and APT1 in cells using Fluorescence Lifetime Imaging Microscopy (Figure 1A).

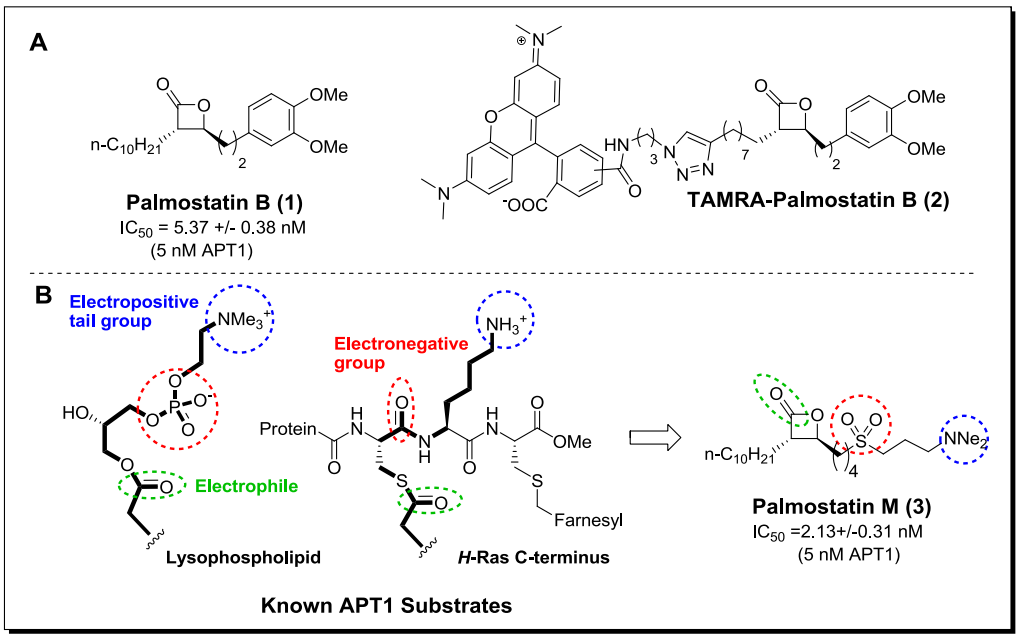

Figure 1. Designed APT1 inhibitors (1st and 2nd generation). A) Structure of palmostatin B (1st generation) and of its fluorescent analogue TAMRA-palmostatin B. B) Structure of palmostatin M (2nd generation) based on natural substrate considerations.

Subsequently, a 2nd generation of β-lactones inhibitors was developed based on native APT1 substrates leading to palmostatin M (**3**), found more potent compared to palmostatin B in the biochemical assay (IC_{50}= 2.13 +/-0.31 nM versus 5.37 +/-0.38 nM using 5nM APT1) and in cellular assays (Figure 1B).

Application of acyl protein thioesterase 1 (APT1) inhibitors

To confirm APT1 as a cellular target of the β-lactone inhibitors and to identify additional target proteins relevant to Ras depalmitoylation such as the close APT1 homologue known as APT2, *in-cellulo* Activity-Based Proteome Profiling (ABPP) experiments were performed. Several cell permeable ABPP-alkyne probes derived from palmostatin B and M were synthesized, including two regioisomeric palmostatin M-derived probes, designed to maximize the accessibility of the alkyne group for the click ligation when covalently bound into enzyme active sites (Figure 2).

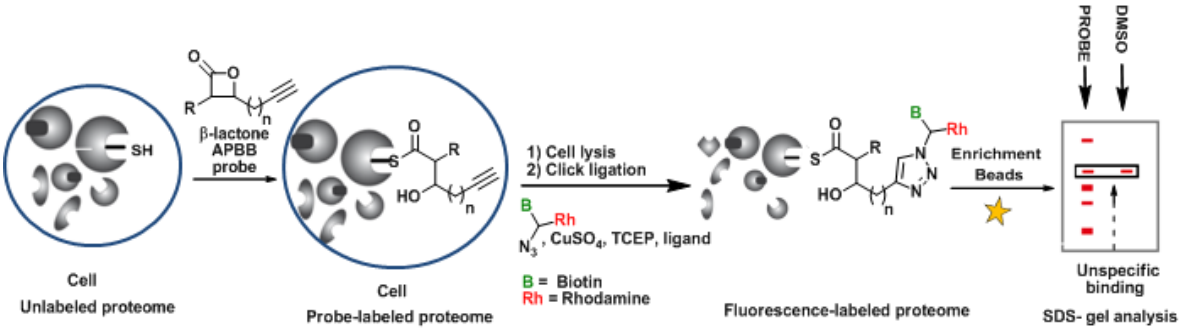

Figure 2. Principle of Activity-Based Proteome Profiling experiments. Incubation of the alkyne probe with HeLa cells allows its covalent binding to its target proteins through its reactive β-lactone group. After cell lysis, target proteins are tagged through click ligation with a trifunctional fluorescent reporter group allowing their enrichment using biotin/streptavidin affinity. After isolation and separation by SDS-gel electrophoresis, target proteins are detected by fluorescence read-out and are subsequently digested with trypsin to allow their identification by mass spectrometry.

In conclusion, the strong discrimination observed between the two regioisomeric palmostatin M-derived probes in their ability to label APT1, have confirmed the binding mode for the β-lactone inhibitors in the APT1 active site, which was found in accordance with their substrate-based design. More importantly, proteomic analyses have allowed not only to identify APT1 among the cellular targets of palmostatin B and M, but also the close homologue of APT1 called acyl protein thioesterase 2 (APT2). Subsequently, the ability of APT1 and APT2 to depalmitoylate biologically active semi-synthetic *N*-Ras proteins was demonstrated *in vitro* by an ADIBAF assay (Kristina Görmer), thereby providing the first experimental proof that both enzymes are thioesterases relevant to Ras depalmitoylation. Taken as a whole, these findings suggest that no further hydrolases in general are involved in Ras depalmitoylation in cells.

Targeting Fas depalmitoylation

Recently, the lipase inhibitor orlistat and later the APT1 inhibitor palmostatin B were shown to restore Fas-mediated apoptotic signaling in Chronic Lymphocytic Leukaemia (CLL) cells, without affecting healthy peripheral blood mononuclear cells. With the reported importance of Fas palmitoylation for Fas–mediated death signaling, absence or dysfunction of Fas palmitoylation may account for the accumulation of malignant B cells characteristic for this disease. In this context, a similar chemical proteomic approach was employed in collaboration with Wendtner et al. (academic hospital of Cologne) to rationalize the observed apoptotic effect. Experiments conducted in human cells from leukaemia and healthy patients respectively, have allowed the identification of few hydrolases possibly involved in CLL pathogenesis such as APT1, APT2, ABHDA, ABHEB and ESTD. Wendtner and co-workers are currently investigating their possible involvement in Fas depalmitoylation. Although plenty of work still remains to be done, APT1 and APT2 represent good Fas depalmitoylating enzyme candidates given their Ras depalmitoylating activity and the overexpression of APT1 in CLL cells in comparison to healthy B-cells.

Targeting all palmitoylated proteins

Subsequently, SILAC experiments employing an inert alkynylated palmitate analogue in double metabolic labelling were performed in order to evaluate the effect of palmostatin B on the complete palmitome. Although, these experiments have not permitted so far any quantification, this strategy may allow the systematic evaluation of the effect of palmostatin B on all palmitoylated proteins. This would permit to discover new interesting applications for β-lactones in general and thioesterase-mediated processes in particular.

Discovery of potent fatty acid amide hydrolase (FAAH) inhibitors

With the discovery of APT1 and APT2 as Ras depalmitoylating enzymes, targeting both proteins constitute a viable anti-cancer approach to interfere with aberrant *H*- and *N*-Ras signaling. In this context, various APT1/2 inhibitor candidates such as α-keto-amides, α-keto-CF_3, α–keto-CF_2CF_3 and α-keto oxazoles were synthesized, which would, in contrast to the previous β-lactone inhibitors, be regarded as stable transition state mimics of the depalmitoylation process. Although no or weaker inhibitors were obtained in comparison to the β-lactones, some of the α-keto oxazoles turned out to be potent and selective FAAH inhibitors. In particular, this work revealed the importance of a short C5-side chain, of a long aliphatic chain, and of electrostatic stabilizing interactions for the FAAH inhibitory activity of α-keto oxazoles substituted at the C5 position with non-aromatic substituents.

Zusammenfassung

Palmitoylierte Proteine stellen eine wichtige Klasse von Signalkomponenten dar, die unterschiedliche zelluläre Prozesse, darunter Zellproliferation und Apoptose, kontrollieren, die beide in der Karzinogenese als missreguliert gelten. Der reversible Charakter der palmitatabhängigen Membranverankerung ist von höchster Wichtigkeit für die Aufrechterhaltung von Proteinlokalisation und –Signalweiterleitung. Aus diesen Gründen kann die Beeinflussung der Proteindepalmitoylierung durch Inhibierung der entsprechenden Enzyme als eine vielversprechende therapeutische Strategie angesehen werden, korrigierend in Zellsignaltransduktionwege einzugreifen.

Targeting der Ras-Depalmitoylierung

Design und Synthese von Acyl protein thioesterase (APT1)-Inhibitoren

Aufgrund der Wichtigkeit von Ras-Mutationen in der Karzinogenese (33% in allen Fällen von Krebs) wird das Targeting der Ras-Depalmitoylierung durch Inhibierung von Ras-depalmitoylierenden Enzymen als attraktive Anti-Krebs-Strategie angesehen. Insbesondere Anstrengungen, die Serinhydrolase Acyl protein thioesterase 1 (APT1) zu inhibieren, haben zu der *Protein Structure Similarity Clustering approach*-basierten Entwicklung des β-Lacton-Inhibitors Palmostatin B geführt. Ein zellgängiges, TAMRA-markiertes Palmostatin B-Analogon (2) wurde synthetisiert und dazu genutzt, um die direkte Interaktion zwischen Palmostatin B und APT1 mittels *Fluorescence Lifetime Imaging Microscopy* (Figure 1A) nachzuweisen.

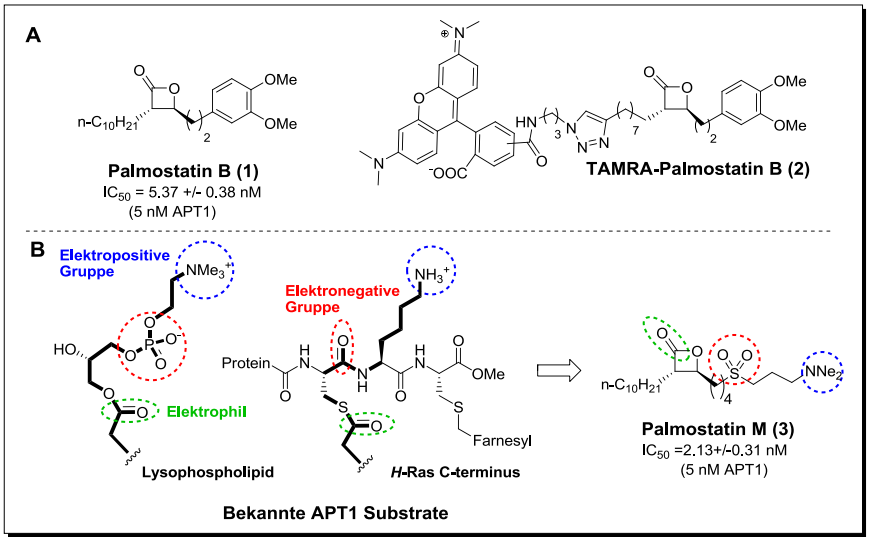

Figure 1. APT1-Inhibitoren-Design (1. und 2. Generation) A) Struktur von Palmostatin B (1. Generation) und seinem fluoreszierendem Analog TAMRA-Palmostatin B. B) Struktur von Palmostatin M (2. Generation), an das natürliche Substrat angelehnt.

Im Folgenden wurde eine 2. Generation von β-Lacton-Inhibitoren synthetisiert, die auf nativen APT1-Substraten basieren. Dies führte zur Entwicklung von Palmostatin M (3), ein im Vergleich zu Palmostatin B potenterer Inhibitor, was sowohl biochemisch (IC_{50}= 2.13 +/-0.31 nM verglichen mit 5.37 +/-0.38 nM, mit 5 nM APT1), als auch in zellbasierten Versuchen nachgewiesen werden konnte (Figure 1B).

Anwendung von Acyl protein thioesterase 1 (APT1)-Inhibitoren

Um APT1 als zelluläres Target der β-Lacton-Inhibitoren nachzuweisen und um weitere Proteine zu identifizieren, die für die Ras-Depalmitoylierung relevant sind (wie z.B. das APT1-Homolog APT2), wurden *in-cellulo* Activity-Based Proteome Profiling (ABPP)-Experimente durchgeführt. Es wurden mehrere zellpermeable ABPP-Alkin-Sonden synthetisiert (Palmostatin B und M-Derivate, darunter zwei Regioisomere (von Palmostatin M abgeleitete Sonden). Diese Sonden wurden entworfen, um die Zugänglichkeit der Alkingruppe bei Bindung an das aktive Zentrum des Enzyms für die Click-Ligation zu maximieren (Figure 2).

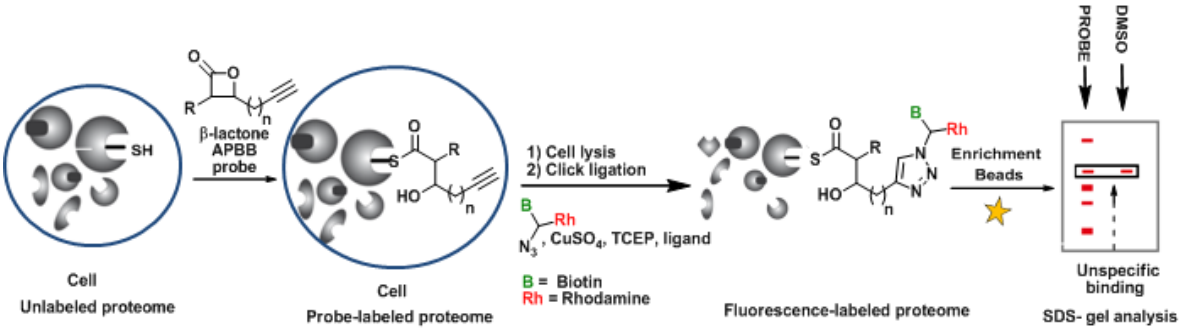

Figure 2. Prinzip der Activity-Based Proteome Profiling-Experimente. Inkubation der Alkylprobe mit HeLa-Zellen ermöglicht die kovalente Bindung an das Zielprotein durch die reaktive β-Lacton-Gruppe. Nach dem Zellaufschluss wurden die Zielproteine mittels click-Ligation mit einer trifunkionalen, fluoreszierenden Reportergruppe markiert, welche eine Bindung mittels des Biotin/Streptavidin-Systems ermöglicht. Nach der Isolation und Trennung der Proben mittels SDS-PAGE wurden die Zielproteine durch Fluoreszenzdetektion ausgelesen, im Folgenden mit Trypsin verdaut und schließlich mittels Massenspektrometrie identifiziert.

Durch den beobachteten, erheblichen Unterschied zwischen beiden regioisomeren Sonden in ihrer Fähigkeit, APT1 zu markieren, konnte der Bindungsmodus der β-Lacton-Inhibitoren im aktiven Zentrum bestätigt werden, was sich in Einklang mit ihrem substratbasierten Design befindet. Darüber hinaus konnten Proteomanalysen nicht nur dazu beitragen, APT1 als zelluläres Target für Palmostatin B und M zu identifizieren, sondern auch das nahe Homolog Acyl protein thioesterase 2 (APT2). Im Folgenden wurde die Fähigkeit von APT1 und APT2, semisynthetisches N-Ras zu depalmitoylieren, in vitro in einem ADIFAB-Assay demonstriert (Kristina Görmer). Dies stellt einen ersten experimentellen Beweis für die Relevanz beider Enzyme für die Ras-

Depalmitoylierung dar. Zusammengenommen zeigen diese Ergebnisse, dass keine weiteren Hydrolasen in die Ras-Depalmitoylierung involviert sind.

Targeting der Fas-Depalmitoylierung

Es konnte kürzlich gezeigt werden, dass der Lipase-Inhibitor Orlistat und der APT1-Inhibitor Palmostatin B den Fas-vermittelten Signalweg in Chronic Lymphocytic Leukaemia (CLL)-Zellen wiederherstellen, ohne gesunde periphere mononukleare Blutzellen zu beeinflussen. Aufgrund der Wichtigkeit von Fas könnte die Fehlfunktion seiner Depalmitoylierung zur Akkumulation von bösartigen B-Zellen, was für diese Krankheit charakteristisch ist, beitragen. In diesem Zusammenhang wurde gemeinsam mit Wendtner et al ein Ansatz entwickelt, um den apoptotischen Effekt zu untersuchen. Experimente, die in humanen Leukämiezellen und vergleichsweise in Zellen von gesunden Probanden durchgeführt wurden, haben zur Identifikation einiger Hydrolasen geführt, die in der CLL-Pathogenese überexprimiert werden, darunter APT1, APT2, ABHDA, ABHEB und ESTD. Wendtner und seine Mitarbeiter untersuchen zurzeit die mögliche Verwicklung dieser Proteine in die Fas-Depalmitoylierung. Obwohl es noch viel Arbeit zu tun gibt, sind APT1 und APT2 vernünftige Kandidaten für Fas-depalmitoylierende Enzyme, wenn man ihre Ras-Depalmitoylierungsaktivität und die Überexpression von APT1 in CLL-Zellen im Vergleich zu gesunden B-Zellen in Betracht zieht.

Targeting von neuen palmitoylierten Proteinen

Im Folgenden wurden SILAC-Experimente durchgeführt, die den Effekt von Palmostatin B auf das Protom mittels eines inert alkynylierten Palmitatanalogons untersucht haben. Obwohl diese Experimente noch keine Quantifizierung hervorgebracht haben, könnte diese Strategie eine systematische Evaluierung des Effekts von Palmostatin B auf alle palmitoylierten Proteine ermöglichen. Dies würde die Entwicklung neuer interessanter Anwendungen für β-Lactone im Allgemeinen als auch für Thioesterase-vermittelter Prozesse im Speziellen ermöglichen.

Entdeckung potenter Fatty acid amide hydrolase (FAAH)-Inhibitoren

Nach der Entdeckung von APT1 und APT2 als Ras-depalmitoylierende Enzyme stellt das Targeting dieser beiden Proteine einen wesentlichen Anti-Krebs-Ansatz dar, um gestörte H- und N-Ras-Signalwege zu beeinflussen. In diesem Zusammenhang wurden unterschiedliche APT1/2-Inhibitoren synthetisiert (α-keto-amide, α-keto-CF_3, α–keto-CF_2CF_3 und α-keto oxazole), die im

Gegensatz zu den reversiblen β-Lacton-Inhibitoren den Übergangszustand der Depalmitoylierungsreaktion nachahmen. Obwohl keine oder im Vergleich zu den β-Lactonen nur schwächere Inhibitoren gefunden wurden, erwiesen sich einige der α-keto-Oxazole als potente und selektive FAAH-Inhibitoren. Diese Arbeit stellt die Wichtigkeit einer kurzen C5-Seitenkette, einer langen aliphatischen Kette, sowie von elektrostatisch stabilisierenden Interaktionen für die inhibitorische Aktivität der α-keto-Oxazole heraus, bei denen die C5-Position durch nichtaromatische Teile substituiert wurden.

Curriculum Vitae

Name: Marion Rusch
Date of Birth: 04.08.1983
Nationality : French
Diplom: M.Sc /Engineer CPE LYON

Education

Sept. 2007 - Sept. 2011	**Ph.D. thesis "Design, Synthesis and Application of Small Molecule Acyl Protein Thioesterase inhibitors"** under the supervision of Prof. Herbert Waldmann at the Max Planck Institute of molecular physiology in Dortmund and in Dortmund university (Germany).
Sept. 2006 – June 2007	**5th Year of higher education at CPE Lyon & MSc level**, University Claude Bernard Lyon I (France) - Specialized in organic chemistry and bioactive molecule chemistry.
Sept. 2003 – June 2005	**3rd and 4th Year of higher education at CPE Lyon** (Chemistry, Physics and Electronics) - Specialized in organic chemistry and process engineering.
Sept. 2001 – June 2003	**Preparatory classes** - two years full-time higher education in mathematics, Sciences and general studies, in preparation for selective admission to CPE Lyon.
June 2000	**Higher leaving certificate** (Baccarauréat)

Publications

- *Small-molecule inhibition of APT1 affects Ras localization and signalling.* Dekker, F. J.; Rocks, O.; Vartak, N.; Menninger, S.; Hedberg, C.; Balamurugan, R.; Wetzel, S.; Renner, S.; Gerauer, M.; Schoelermann, B., Rusch, M.; Kramer, J. W.; Rauh, D.; Coates, G.W.; Brunsveld, L.; Bastiaens, P. I. H.; Waldmann, H., *Nat. Chem. Biol.***, 2010**, *6*, 449-456.

- *Development of Highly Potent Inhibitors of the Ras-Targeting Human Acyl Protein Thioesterases Based on Substrate Similarity Design.* Hedberg, C.; Dekker, F.J.; Rusch, M.; Renner, S.; Wetzel, S.; Vartak, N.; Gerding-Reimers, C.; Bon, R.S.; Bastiaens, P.I.; Waldmann, H., *Angew. Chem. Int. Ed.,* **2011**, in press.

- *Identification of Acyl Protein Thioesterases 1 and 2 as the Cellular Targets of the Ras-Signalling Modulators Palmostatin B and M.* Rusch, M.; Zimmermann, T.J.; Bürger, M.; Dekker, F.J.; Görmer, K.; Triola, G.; Brockmeyer, A.; Janning, P.; Böttcher, T.; Sieber, S.A.; Vetter, I.R.; Hedberg, C., Waldmann, H., *Angew. Chem. Int. Ed*., **2011**, in press.

- *Design, Synthesis and Evaluation of Polar Head Group 2-Keto-Oxazole Inhibitors of fatty acid amide hydrolase (FAAH)*. Rusch, M.; Zahov. S.; Vetter, I.R.; Lehr, M.; Hedberg, C., *Bioorg. Med. Chem*., **2011**, submitted.

- *Pd-catalyzed heteroannulation approach to 2,3-disubstituted furo[3,2-c]coumarins.* Raffa, G.; Rusch,M. ; Balme, G.; Monteiro, N., *Org. Lett*. **2009**, *11*, 5254-5257